Baoan Song
Song Yang
Linhong Jin
Pinaki S. Bhadury

Environment-Friendly Antiviral Agents for Plants

Chemical Industry Press

Springer

Baoan Song
Song Yang
Linhong Jin
Pinaki S. Bhadury

Environment-Friendly Antiviral Agents for Plants

Baoan Song
Song Yang
Linhong Jin
Pinaki S. Bhadury

Environment-Friendly Antiviral Agents for Plants

With 110 figures

Authors

Baoan Song
Center for R&D of Fine Chemicals,
Guizhou University
Guiyang 550025, China
E-mail: songbaoan22@yahoo.com

Song Yang
Center for R&D of Fine Chemicals,
Guizhou University
Guiyang 550025, China
E-mail: yangsdqj@gmail.com

Linhong Jin
Center for R&D of Fine Chemicals,
Guizhou University
Guiyang 550025, China
E-mail: linhong.j@gmail.com

Pinaki S. Bhadury
Center for R&D of Fine Chemicals,
Guizhou University
Guiyang 550025, China
E-mail: bhadury@gzu.edu.cn

Cover design: Frido Steinen-Broo, EStudio Calamar, Spain

Printed on acid-free paper

Springer is a part of Springer Science+Business Media (www.springer.com)

Foreword

Plant virus is often referred to as "plant cancer" which is considered to be a serious threat to agricultural production. For example, the breakout of tobacco mosaic virus (TMV) and cucumber mosaic virus (CMV) could cause billion dollars of agricultural loss world-wide. Viruses such as the genus *Tospovirus* of the family *Bunyaviridae* and the genus *Begonovirus* of family *Geminiviridae* are also destructive to vegetable plantation. Since the mechanism of parasitism and invasion into plant cell of virus is not clear yet, it poses a difficult problem for us to study the prevention and control of plant viral diseases. In the recent innovation program of environmental friendly green pesticides initiated in China, the novel virucide research seems to be lagging behind from other areas such as herbicide, fungicide and insecticide.

During the last decade, professor Baoan Song of Guizhou University, China, has led his research group, starting from a natural lead structure, to carry out persistently a project in discovering novel virucide by studying its related molecular design, bioassay technology, mode of action, formulation, with which a new plant immune activation phenomenon was discovered and its mechanism postulated. After intensive synthesis and bio-screening practices, Song's group has finally discovered a novel bio-active structure, which was named later as Dufulin and been granted as a new pesticide approved by the Ministry of Agriculture of China for further development. Professor Song has also pushed forward his related R&D of Dufulin to the industrialization stage. It is expected that Dufulin will play its significant role in combating the plant viral diseases in China.

In tackling such a rather difficult project conducted by professor Song's group, this monograph has been well documented to compile all the original research data as well as its methodology throughout the whole R&D procedures of Dufulin. The monograph is hereby highly recommended to our colleagues, which will bring us an insight into the discovery of a novel virucide, deepen our

understanding to the related inter-disciplinary work, enrich our expertise and experience in our innovation of research work.
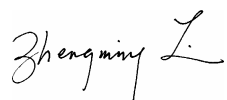
<div align="right">

Zhengming Li

Zhengming Li
Professor
Nankai University
Tianjin, China
CAE member
IUPAC Fellow
Feb. 2009

</div>

Preface

Plant viruses, generally known as "cancer of plant", are responsible for the most common diseases occurring in the main agriculture crops as well as vegetable and tobacco that lead to serious damage and enormous economic loss. In order to protect the plant from the virus disease, various methods have been developed, including crop rotation, virus eradication, mild strain cross protection (MSCP), virus transmission control, application of antivirus agents and newly emerging genetically antivirus modified crops. However, damage from plant virus cannot be avoided effectively despite taking reasonable measures. The use of traditional chemical pesticides, on the other hand, may bring about a disastrous impact on our environment. Thus, the continuous research and development of environment-friendly antivirus agents for field application have become an important endeavor for the scientists engaged in plant protection. The authors carried out ten years of research aiming at discovering novel green antiviral agents for plants and successfully found some new compounds with excellent antivirus bioactivity. After completing systematic R&D work, one brand of new compound was industrialized and applied in the field with excellent protection effect thus avoiding huge economic loss due to the great damage caused by plant virus. Interestingly enough, it was found to exert its function through new mechanism of activating plant immune system.

As mimics of natural amino acids, the synthesis and biological studies of aminophosphonic acids and their ester derivatives have attracted wide attention in recent years. Previous research demonstrated that some aminophosphonates are associated with antiviral, growth-regulatory and antifungal activities. Taking amino phosphonic acid as the lead compound for optimization studies, more than one thousand compounds were designed and synthesized by us among which Dufulin (Bingduxing) was identified as one of the potential structures with outstanding antiviral activity. Systematic researches were conducted from basic lab research to field trial as well as field application including lab bioassay, compound synthesis optimization, field bioassay trial, residual analysis, toxicity evaluation, and environmental behavior studies that finally paved the way to the registration of new pesticide Dufulin as a new molecular antivirus agent approved
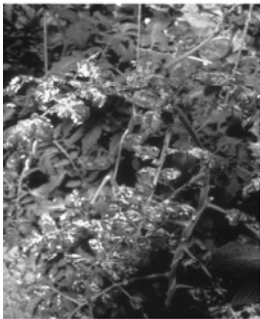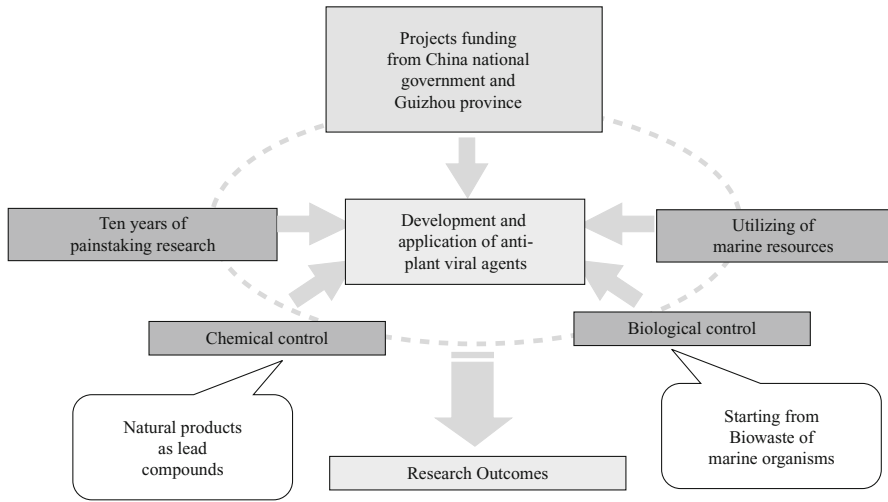
Tomato mosaic virus

Capsicum annuum Virus disease

Cucumber Mosaic disease

Tobacco mosaic disease

Rice ragged stunt disease

Rice stripe disease

by the Ministry of Agriculture. The intellectual property of Dufulin as well as its usage was approved by State Intellectual Property Office of China (SIPO). Besides studying its application, basic research on the mode of action of Dufulin was also carried out and it was found that Dufulin exerts its function through a new mechanism by activating the plant immune system. The observations were:(1) It is associated with the tobacco resistance enzymes and could cause aggregation of the virus particle thereby reducing the infecting ability of the virus.(2) This antiviral agent can also upregulate the expression of tobacco pathogenesis-related proteins PR-1 and PR-5. (3) The anti-TMV bioactivity of Dufulin is associated with the induction of cysteamine acid synthase in chloroplast, followed by activating the salicylic acid signaling pathway and thus conferring the plant the systematically acquired resistance.

Cyanoacrylates, included in our studies, have been traditionally considered as herbicides acting as Photosystem Ⅱ Inhibitors. Our research showed that these compounds also have good anti-TMV activities and are worth investigating for their potential to be employed as green anti viralagents in future. In addition, some more promising results were obtained from the research of chiral thioureas and hetercyclic compounds carried out in our center.

Although there is no dearth with regard to the scientific information or availability in terms of text books in the field of synthetic pesticides and their role in crop protection, none of them deals with the chemistry of green antiviral agents for plants.

In the context of the present inadequacy of professional book available on the anti-viral agents, we made best effort to investigate this relatively unexplored area and summarize our findings in the form of a comprehensive textbook. The present edition of Environment-Friendly Antiviral Agents for Plants has been written with an idea to keep up pace with the recent progress made in the field of environmentally benign antiviral agents for plants and encompasses five specific directions that could open new avenues for the treatment of plant virus diseases.

There are five chapters in this book. Chapter 1 describes the synthesis and antiviral activity of α-aminophosphonates. Chapter 2 introduces the synthesis and antiviral activity of cyanoacrylates. Chapter 3 talks about chiral thiourea antiviral agents. Chapter 4 discusses the heterocyclic antiviral agents, and Chapter 5 introduces the innovation and application of environment-friendly antiviral agent for plants, especially the novel antiviral chemical for plants entity Dufulin, a new antiviral agent that was granted the temporary registration by the Ministry of Agriculture of China. We made best possible effort to introduce the research progress and the research method for every kind of antivirus agent. In addition, development of green pesticides with characteristics such as high selectivity, efficiency, low toxicity and easy degradability poses enormous challenge to both synthetic chemists and biologists and we hope the book can provide some valuable

information on the chemistry of potentially novel chemicals that may be termed as green agents for the control of plant virus diseases. It would be a great comfort for the authors if this book can serve to the improvement of novel antiviral agents R&D for plants as well as their applications in plant virus disease control.

The research work introduced in this book was carried out in Key Laboratory of Green Pesticide and Agricultural Bioengineering (Guizhou University), Ministry of Education, Center for Research and Development of Fine Chemicals of Guizhou University, and was accomplished by the author together with his group members which include Xia Zhou, Song Yang, Linhong Jin, Deyu Hu, Zhuo Chen, Wei Xue, Pinaki S. Bhadury, Guiping OuYang, Rongmao Huang, Song Zeng, Yuping Zhang, etc. The scientific research results provided in this book and the publication of this book are also based on the support received from several of my master and doctoral students *e.g.* Guiping OuYang, Gang Liu, Caijun Chen, Xinwen Gao, but the names of about forty master students who made significant contribution cannot be listed here. Their experimental results, Ph. D. dissertations and master thesis, as well as the journal publications achieved by them and me are the basis of this book. The whole book was written and organized by me, Xia Zhou, Song Yang and Linhong Jin, and was finally organized by me, Xia Zhou and Dr. Pinaki who gave contributions to Chapter 5.

Finally, I would like to thank Prof. Zhengming Li to write the foreward for

this book. I also strongly appreciate the efforts of my colleagues and students and thank them for their support in this research work. I sincerely hope that this book would be helpful for the teachers, students in the field of pesticide science, plant protection, organic chemistry, fine chemicals and applied chemistry as well as environment chemistry and agriculture science, and the researchers from both industry and academia.

Baoan Song
Feb. 2009

Contents

Introduction

Plant viruses are pathogens which are composed mainly of a nucleic acid (genome) normally surrounded by a protein shell. They can replicate only in compatible cells, usually with the induction of symptoms in the affected plant. Symptoms are the result of an alteration in cellular metabolism and are most obvious in newly developing tissues. Over 800 plant viruses have been recognized and characterized. The genomes of most of them, such as the tobacco mosaic virus (TMV), are infective single-stranded RNAs whereas some RNA viruses have double-stranded RNA genomes. Cauliflower mosaic virus and bean golden mosaic virus are typical examples of viruses having double-stranded and single-stranded deoxyribonucleic acid (DNA), respectively. The genome of many plant viruses is a single polynucleotide and is contained in a single particle, whereas the genomes of brome mosaic and some other viruses are segmented and distributed between several particles. There are also several low-molecular-weight RNAs (satellite RNAs) which depend on helper viruses for their replication.

The natural hosts of plant viruses are widely distributed throughout the higher-plant kingdom. Some viruses *e.g.* TMV and cucumber mosaic virus are able to infect over a hundred species in many families, whereas others, such as wheat streak mosaic virus, are restricted to a few species in the grass family. The replication of single-stranded RNA viruses involves release of the virus genome from the coat protein; the association of the RNA with the ribosomes of the cell; translation of the genetic information of the RNA into specific proteins, including subunits of the coat protein and possibly viral RNA-synthesizing enzymes; transmission by vectors and diseases induction; synthesis of noninfective RNA using parental RNA as the template; and assembly of the protein subunits and viral RNA to form complete virus particles.

In some plants, depending on the virus, the initial infection does not spread because cells surrounding the infected cells die, resulting in the formation of necrotic lesions. The size and shape of leaves and fruit may be adversely affected, and in some instances plants may be killed. Examples of plant viruses that contribute to significant losses in crop productivity are cucumber mosaic virus, tobacco mosaic virus and zucchini mosaic virus. Although, in most of the host-virus combinations it is difficult to assess the exact amount of damage, plant

viral disease losses worldwide have been estimated to be as high as sixty billion dollars per year. Once a plant becomes infected it becomes virtually impossible to free it from infection. Furthermore, the infected plant can become a potential source of infection for the remaining healthy plants. Virus infection of perennial crops is particularly of great concern as the infected ones have to be discarded and replaced with young ones requiring a long period that ensues before the crop again reaches maturity. There is, therefore, a great need for the chemicals which could prevent or cure a virus infection in the same way as the fungicides can for the prevention and cure of fungal infections. Unfortunately, according to the published literature there are no effective economic antiviral chemicals available for agricultural use. The control methods that are generally followed involve the use of pesticides to prevent the vector of the virus (in most cases, insects) from feeding on and infecting the crop. These methods are ineffective and far from universal for practical application. In order to be effective, virtually complete control of vectors would be necessary-a situation that imposes severe constraints on the environment. On the other hand, due to their inherent chemical structures (genome surrounded by a protein coat), plant viruses are heavily dependent upon the normal plant metabolism and upon some of the enzymes of the plant for replication. Thus, to identify a chemical that will interfere with virus multiplication but not with the host metabolism, or the one that blocks a metabolic pathway when only the virus is able to use it, is indeed a challenging task. Despite these difficulties, chemicals should play a major role not only in terms of effectiveness but also in reducing undesirable side effects. As a matter of fact, the development of "intelligent" and environment-friendly antiviral agents for plants assumes enormous significance in plant protection particularly for raising and guaranteeing yields and product quality without causing unacceptable negative effects for users, consumers and nature. It must be mentioned here that plant breeding for virus resistance despite being commercially preferred due to the introduction of stable resistant varieties that avoid recurring treatment cost, has so far made less contribution possibly because of practical problems involved and lesser economic importance of plant virus diseases and lower priority in policy making. Consequently, chemical control continues to enjoy its importance; the unceasing demand for the increase in the productivity of crop production cannot be fulfilled without chemical plant protection. Thus, plant virus disease, considered as plant cancer in most places, can be treated by plant antiviral chemotherapy, the concept of which was largely derived from studies on compounds synthesized by animal virologists.Cell-surface virus receptor sites have been proposed as a target for animal antiviral chemicals, but no such sites seem to exist for plant viruses. If such a specific site existed, it could be a potential site for selective antiviral action. Chemical antiviral agents can inhibit virus replication, suppress virus symptoms or induce host defense mechanisms. In this context, potential of benzimidazoles and ribavirin (a triazole-β-D-riboside) has been extensively studied by previous workers for their antiviral activity in plant system. They are amongst the best

known antiviral chemicals to emerge out of synthetic studies. Other anti-meta-bolites which are physiologically active against plant virus diseases such as 2-thiouracil, 5-fluorouracil, 8-azaguanidine, dihydro-1,3,5-triazine-2,4-dione (DHT) and related derivatives, have been shown to be incorporated into viral nucleic acid and to modify its biological activity. DHT can selectively inhibit viral RNA synthesis in TMV-infected tobacco leaves and combination of DHT with ribavirin has been recommended for better result. The phytotoxicity of these compounds, however, appears to preclude their practical use. Amongst the substituted nucleic acid bases associated with selective antiviral activity are compounds, such as 5-bromo-2′-deoxyuridine, which are mutagenic. Incorporation of such agents into viruses without nucleic acid repair mechanisms could critically damage genome function. However, all these agents have high residue level and detrimental effects on the environment and are far from satisfactory.
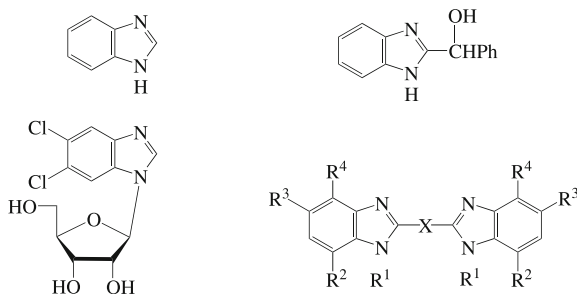
Structures of representative benzimidazoles
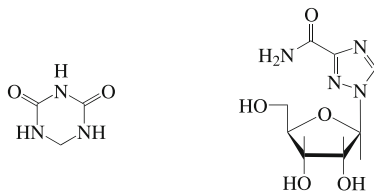
DHT   **Ribavirin**

In usage, more targeted deployment of the agent needs to be practiced and for this purpose environmentally safe spray techniques have been developed in certain cases to use minimal chemical inputs and apply them only when and where needed with reduced losses to the environment.

To sum up, the criteria determining the potential success of an anti-patho-genic composition in preventing or controlling plant viral diseases, include: whether the composition damages the plant; whether the composition affords systemic protection to the plant; whether the composition retains its activity for a reasonable length of time; whether the composition may be produced on a large scale at an economic price; and whether the composition would pass, or not be subject to, food and drug environmental protection regulations. The present book

entitled "Environment-friendly chemicals as antiviral agents for plants", which deals with direct chemical control of virus diseases of plants by anti-plant pathogen compositions, has been written to fulfill the foregoing criteria. Due to the lack of reliable data in this field, we made conscientious effort to summarize the research results emanating from our own laboratory. As a matter of fact, the book is unique in its approach and the main hallmark is the way in which the methods are described for each synthetic or biological protocol. The investigation for the discovery of environmentally benign antiviral agent for plants was financially supported by several core agencies *e.g.* National Key Basic Research Project (973 Plan), National Key Project for International Cooperation of Science and Technology, National Nature Science Foundation of China and the National Key Technologies R&D Program. In recognition to our contributions towards enhancement of basic understanding on plant protection and economic benefit for the society, a series of outstanding awards such as the top Prize of Science and Technology Progress Award of Chinese Universities and the top Prize of Science and Technology Progress Award of Guizhou Province were granted in the year 2008.

In order to tackle the existing problem in this field, we undertook a project to design new chemical structures as potent anti-viral agents based on some theoretical model and biomimetic considerations. A large number of different classes of compounds which include novel α-aminophosphonate derivatives, chiral α-aminophosphonates, chiral cyanoacrylates, heterocyclic derivatives from pyrazole and quinazoline scaffolds, and chiral thiourea derivatives were investigated in our research. The results of these studies which are described in the first four chapters involved molecular design, optimization of synthetic routes for chiral products and green technology, antiviral biological test, structure and activity relationship (SAR), environmental behavior and related action mechanism aspects. Several novel structures such as α-aminophosphonate derivative Dufulin (Bingduxing), chiral cyanoacrylates, and GU188 with good antiviral bioactivity were discovered. The antiviral bioactivities of these compounds were attributed to tobacco resistance enzymes and aggregation of the virus particles rendering them ineffective to spread the disease. These synthetically prepared agents could also upregulate the expression of tobacco pathogenesis-related proteins PR-1 and PR-5. It was noted for the first time that the anti-TMV bioactivity of Dufulin was associated with the induction of cysteamine acid synthase in chloroplast, followed by activation of the salicylic acid signaling pathway conferring the plant the necessary systematically acquired resistance to fight the viral attack. These findings led to the registration and industrialization of Dufulin as a new antiviral agent for platns. The anti-TMV bioactivities and mechanism of action in gene level of chiral 2-cyanoacrylate derivatives were also studied in detail which confirmed that these potent agents could adjust TMV induced upregulation of tobacco RNA synthesis in related genes and thus inhibit the self-replication of TMV by employing the host RNA synthesis machinery. The last chapter of the

book has systematically introduced the research achievements by the author and his group on the discovery, development, and application of novel antiviral agents for plants *e.g.* highly active α-aminophosphonate antiviral agent Dufulin (Bingduxing) and the potentially useful cyanoacrylate derivative GU188. In this context, synthetic route optimization, formulation, bioassay, field trial, pesticide residue analysis, environmental behavior, and action mechanism studies pertaining to these compounds were undertaken; the mode of action of plant immune activator was investigated and the activator structure as well as the structure activity relationships was ascertained. The outcome of the research on the mechanistic of plant immune system activation eventually guided to the development of three new antiviral agents for plants which are safe to environment and human beings with extremely low residual level.

This monograph systematically describes the underlying principles, novel ideas, new methodologies, and the strategic discovery of novel antiviral agents through the research on plant immune activation. This book introduces the cutting-edge research technology and progress on novel antiviral agent innovation. To the best of our knowledge, this is the first book introducing the innovation of new environmentally friendly antiviral agents for plants. It should also be noted that emphasis has throughout been laid on the need of green technology and development of safer and systemic new antiviral agents for plants. This book can be used as a textbook or reference book for the teachers, students in the filed of pesticide, organic chemistry, fine chemicals, applied chemistry, plant protection as well as environment chemistry and agriculture science, and the researchers from both industry and academia.

Chapter 1
Studies on α-Aminophosphonates with Antiviral Activity

1.1 Organocatalytic Synthesis and Antiviral Activity of Asymmetric α-Aminophosphonates

1.1.1 Introduction

As a kind of natural amino acid analogue, α-aminophosphonates constitute an important class of compounds with diverse biological activities and potential to be employed as enzyme inhibitors, antibiotics, and anticancer agents. They also have a wide range of antiviral and antifungal properties and are extensively used as insecticides and herbicides.[1−6] The importance of chiral α-aminophosphonates emanates from their increased industrial applications and evident from overwhelming rise in the number of reports on enantioenriched α-aminophosphonic acid derivatives.[7−9] Some racemic α-aminiophosphonates containing fluorine or heterocycle moieties such as thiophene, pyrrole, 1,3,4-thiadiazole and benzothiazole are reported to have potential anticancer properties, with the later one displaying excellent fungicidal activity in addition to antitumour activity.[10−13] However, further studies are necessary to identify chiral α-aminiophosphonates containing fluorine or heterocycle moieties with potent antitumour activities. Although, diasteroselective addition of phosphite derivatives to chiral imines, enantioselective addition of phosphites to imines in the presence of chiral metal complexes and other methods have been reported for the preparation of optically active α-aminiophosphonates,[14−25] the need to develop a general practical asymmetric route for their synthesis from achiral acyclic imine and simple dialkyl phosphites still remains.

Numerous techniques in asymmetric synthesis have been developed by chemists over the last few years. Recently, there has been enormous interest in the use of small organic molecules as catalysts instead of using asymmetric catalysts containing metals.[26−27] In contrast to metal oriented chiral catalysts, which are

generated *in situ* from metal complexes and chiral ligands, organocatalysts can generally tolerate aerobic conditions and do not require rigorous exclusion of water. On the other hand, they possess a wider substrate scope than enzymes and can be used in a variety of organic solvents.[28−33] It is further well known that incorporation of fluorine into an organic moiety markedly influences the bioactivity of the molecule.[34] Our earlier studies on fluorinated α-aminophosphonates showed that the racemate possessed good antiviral and antitumor activities.[35−39] As different chiral aminophosphonates and their derivatives display varying bioactivities, we reasoned that screening of fluorine derivatives bearing α-amiophosphonate moieties might lead to new antiviral agent with more potent antiviral activities. Keeping these considerations in mind, a series of new fluorine containing bioactive chiral α-aminophosphonates **1.5** were asymmetrically synthesized using chiral Bronsted acid organocatalyst **1.4**[40−45] derived from (*R*)-or (*S*)-BINOL[46] in a typical hydrophosphonylation reaction of aldimines obtained from cinnamaldehyde and fluorinated aromatic amine with dialkyl phosphites (Scheme 1.2, Table 1.2). The method was found to be suitable with different kinds of dialkyl phosphites and moderate to high ee values of the target compounds were obtained. In the half-leaf method test, the chiral compound **1.5g** was found to possess high antiviral activity against TMV *in vivo*.

1.1.2   Materials and Methods

1.1.2.1   General

The melting points of the products were determined on a XT-4 binocular microscope (Beijing Tech Instrument Co., China) and were not corrected. The IR spectra were recorded on a Bruker VECTOR22 spectrometer in KBr disks. NMR spectra were recorded on a JEOL-ECX 500 instrument (500MHz for ^{1}H,125MHz for ^{13}C, 200MHz for ^{31}P, 470 MHz for ^{19}F) using Acetone-d_6/CDCl$_3$ as a solvent, unless otherwise mentioned. Tetramethylsilane (δ=0) served as an internal standard for ^{1}HNMR and CDCl$_3$ was used as an internal standard (δ=77.0) for ^{13}C NMR. H$_3$PO$_4$ was used as an internal standard (δ=0) for ^{31}P NMR. CF$_3$COOD was used as an external standard (δ=−76.5) for ^{19}F NMR. Elemental analysis was performed on an Elementar Vario-Ⅲ CHN analyzer. The reagents were all of analytical grade or chemically pure. Analytical TLC was performed on silica gel GF$_{254}$. Organic solvents used were dried by standard methods when necessary. Purification of the products was performed by chromatographic operation on silica gel Qingdao GF$_{254}$ under normal pressure. Reaction experiments were performed under argon atmosphere using standard double-line pipe.

The analytical HPLC of the compounds was performed on Agilent 1100 series Apparatus composed of a quaternary pump, an auto sampler, a DAD detector, a vacuum degasser, a column oven and Agilent Chemstation software. The

two columns employed were Chiralpak AD-H-amylose tri-(3,5-dimethyl- phenyl-carbamate) coated on 5 μm silica-gel and Chiralpak IA-amylose tri-(3,5- dime-thylphenylcarbamate) immobilized on silica-gel (each of 250 mm×4.6 mm i.d., Daicel Chemical Industries Ltd).

1.1.2.2   Synthesis and Characterization of Chiral Bronsted Catalyst 1.4 and Intermediates

(R)-2,2′-dimethoxy-1,1′-dinaphthyl 1.7.
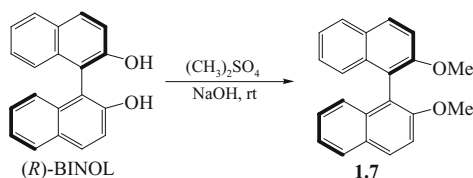
White powder, mp 231-232℃. $[\alpha]_D^{20}$ −76.5 (c 0.9, THF lit.[46] $[\alpha]_D^{20}$ −79.5 (c 1.0, THF)). ^{1}H NMR (500 MHz, CDCl$_3$): δ 7.96 (d, J=9.2 Hz, 2H), 7.85 (d, J=8.05 Hz, 2H), 7.45(d, J=9.15 Hz,2H), 7.30(t, J=7.45 Hz, 2H), 7.20(t, J=7.45 Hz,2H), 7.10(d, J=8.60 Hz,2H), 3.75(s, 6H). ^{13}C NMR (125 MHz, CDCl$_3$): δ 155.1, 129.5, 128.0, 126.4, 125.4, 123.6, 119.7, 114.4, 57.0. Anal. Calcd for C$_{22}$H$_{18}$O$_2$: C, 84.05; H, 5.77; Found: C, 84.35; H, 5.45.

(R)-3,3′-bis(dihydroxyborane)-2,2′-dimethoxy-1,1′-dinaphthyl 1.8.
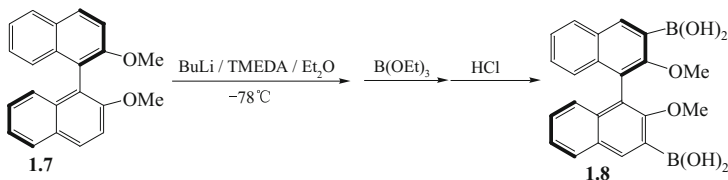
White solid, 1.5g(80%). mp>250℃. $[\alpha]_D^{20}$ −151.1 (c 1.0, CHCl$_3$; lit.[47] $[\alpha]_D^{20}$ −159.0 (c 1.05, CHCl$_3$)). ^{1}H NMR (500 MHz, acetone-d_6): δ 8.54(s, 2H), 8.05(d, J=7.5 Hz, 2H), 7.45(t, J=7.4 Hz, 2H), 7.34 (t, J=4.3 Hz, 2H), 7.11 (d, J=8.6 Hz, 2H), 3.41 (s, 6H). ^{13}C NMR (125 MHz, acetone-d$_6$): δ 160.4, 138.2, 135.7, 130.6, 128.8, 128.2, 127.3, 125.5, 124.8, 60.9. Anal. Calcd for C$_{22}$H$_{20}$B$_2$O$_6$: C, 65.73; H, 5.01; Found: C, 65.56; H, 5.15.

(R)-3,3′-bis (3,5-bis (trifluoromethyl) phenyl)[1,1′]binaphthalenyl-2,2′-diol 1.9.

Ar: 3,5-bis(trifluoromethyl)phenyl
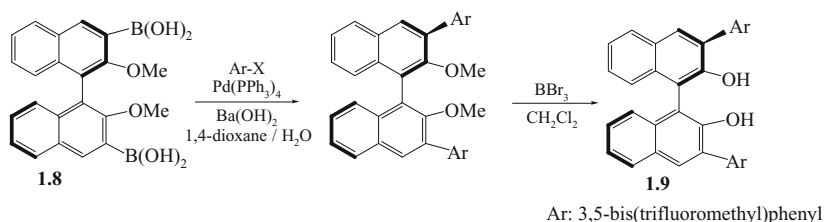
Grey solid, mp 214-215℃. $[\alpha]_D^{20}$ −47.1 (c 0.9, CHCl$_3$ lit.[44] $[\alpha]_D^{20}$ −45.3 (c 1.1, CHCl$_3$)).^{1}H NMR (500 MHz, CDCl$_3$): δ 8.24 (s, 4H), 8.11 (s, 2H), 8.00 (d, J=8.00 Hz, 2H), 7.91 (s,2H), 7.40-7.49 (m,4H), 7.22-7.25 (m,2H), 5.38 (s, 2H). ^{13}C NMR (125 MHz, CDCl$_3$): δ, 149.9, 139.5, 133.3, 132.4, 131.5, 129.9, 129.5, 128.9, 128.7, 127.7, 125.2, 124.0, 122.4,121.3, 111.8.^{19}F NMR (470 MHz, CDCl$_3$, CF$_3$COOD): δ 62.5. Anal. Calcd for C$_{36}$H$_{18}$F$_{12}$O$_2$: C, 60.86; H, 2.55; Found: C, 61.05; H, 2.58.

(R)-3,3′-[3,5-bis(trifluoromethyl)phenyl]$_2$-1,1′-binaphthylphosphate-(R)-(1.4).

Ar: 3,5-bis(trifluoromethyl)phenyl
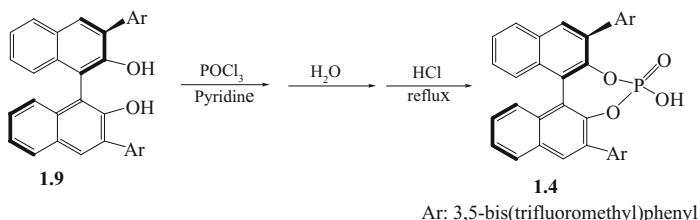
To a solution of **1.9** (0.37 g, 0.52 mmol) in pyridine (3 mL) was added slowly POCl$_3$ (0.07 mL, 0.75 mmol) at room temperature. The reaction mixture was stirred for 5 h, 1mL H$_2$O was added at 0℃ and the resulting suspension was further stirred for 3h. After removal of pyridine, the residue was added into 15 mL 6M HCl, refluxed for 2 h, filtered to afford a grey solid which was dissolved in CH$_2$Cl$_2$, dried over Na$_2$SO$_4$ and purified by preparative chromatography (Petrolium ether: ethyl acetate=1:2, R_f=0.5) to get the title chiral catalyst (0.36 g, yield 90%)as white solid. mp >250℃. $[\alpha]_D^{20}$ −195.1 (c 0.9, CHCl$_3$ lit.[48] $[\alpha]_D^{20}$ −197.5 (c 0.97, CHCl$_3$)). ^{1}H NMR (500 MHz, CDCl$_3$): δ 8.24 (s,4H), 7.94-7.98 (m,4H), 7.81 (s,2H), 7.47 (t, J=7.15 Hz,2H), 7.26-7.33 (m,4H), ^{13}C NMR (125MHz, CDCl$_3$): δ 145.5, 140.2, 132.8, 131.5, 131.2, 130.9, 130.7, 130.3, 128.5, 127.2, 126.9, 126.7, 125.9, 124.5, 123.3, 122.4, 120.8, 120.2.^{31}P NMR (200 MHz, CDCl$_3$, H$_3$PO$_4$): δ 5.77.^{19}F NMR (470 MHz, CDCl$_3$, CF$_3$COOD): δ 62.7. Anal. Calcd for C$_{36}$H$_{17}$F$_{12}$O$_4$P: C, 55.97; H, 2.22; Found: C, 55.86; H, 2.53.

1.1.2.3   General Procedure for Aldimines **1.2**

To a 25 mL three-necked round-bottomed flask containing p-or-m-(trifluoro-methyl) aniline (1.61 g, 10 mmol) dissolved in methylene chloride (15 mL) were added slowly the unsubstituted (1.38 g, 10.5 mmol) or fluorinated cinnamaldehyde (1.58 g, 10.5 mmol) and freshly distilled dry triethylamine(0.2 mL). The reaction mixture was first stirred for 5 min. at room temperature and then anhydrous Na$_2$SO$_4$(3 g) was added and refluxed for the indicated time shown in the Table 1.1. The reaction mixture was filtered and the solvent was removed under reduced pressure. The crude product obtained was recrystallized from ethanol to yield the corresponding imine as yellow needle.[65]

1.1.2.4   General Procedure for Fluorinated Asymmetric α-aminophosphonates **1.5**

To a 50 mL flame dried single-necked round bottomed flask were added the appropriate aldimine (1 mmol) and the organocatalyst **1.4** (772 mg, 0.1 mmol) in xylene (15 mL) and the mixture was stirred at room temperature for 5 min. when a yellow suspension resulted. The appropriate dialkyl phosphite **1.3** (2 mmol) was then added to the above suspension and the reaction mixture was further stirred at room temperature for the required time indicated in the Table **1.2**. The course of the reaction was followed by TLC, reaction was stopped by the addition of saturated NaHCO$_3$ solution, and organic phase was separated by extraction with ethyl acetate. The combined extracts were treated with brine, dried over anhydrous Na$_2$SO$_4$, and concentrated under reduced pressure, the residue was purified by preparative chromatography (petroleum ether:ethyl acetate=2:1) to afford the corresponding title α-aminopohosphonate. The reperesentative data for **1.5c** is shown below, while data for **1.5d-1.5d** can be found in the reference.[65]

Diethyl 1-[N-(4-trifluoromethylphenyl)amino]-3-phenyl-2-propenylphospho-nate **(1.5c).** A yellow oil. yield 58%. $[\alpha]_D^{20}$ $-$51.1(c 0.9, CHCl$_3$). IR (KBr): v_{max} 3284.7 (N-H), 2983.9 (C-H), 1616.4 (C=C), 1539.2 (C=C), 1331.2 (C-F), 1232.5 (P=O), 1161.1 (P-O-C). ^{1}H NMR (500 MHz, CDCl$_3$): δ 6.60-7.45 (m, 10H, Ar-H+=CH-Ar), 6.23 (tt, J=5.45, 5.45 Hz, 1H,-CH=), 4.50 (tt, J=7.15, 7.15 Hz, 1H, CH-P), 4.12-4.16 (m, 4H, CH$_2$O), 1.23-1.28 (m, 6H, CH$_3$).^{13}C NMR (125 MHz, CDCl$_3$): δ 149.4, 136.1, 133.4, 128.7, 128.1, 127.8, 126.5, 125.6, 122.6, 113.0, 112.9, 63.6, 54.1, 53.9, 16.5, 16.2.^{31}P NMR(200 MHz, CDCl$_3$, H$_3$PO$_4$): δ 22.3.^{19}F NMR (470 MHz, CDCl$_3$, CF$_3$COOD): δ 61.1. Anal. Calcd for C$_{20}$H$_{23}$F$_3$NO$_3$P: C, 58.11; H, 5.61; N, 3.39. Found: C, 58.35; H, 5.45; N, 3.48; HPLC analysis: Daicel Chiralpak IA (hexane:EtOH=95:5/v:v), Flow rate=1.0 mL/min, UV=254 nm, t_R(minor)=7.70 min(R), t_R(major)=8.40 min(S). ee: 76.8%.

1.1.2.5   Antiviral Biological Assay

Purification of tobacco mosaic virus. Using Gooding's method,[49,50] the upper leaves of *Nicotiana tabacum L* inoculated with TMV were selected and were ground in phosphate buffer, then filtered through double layer pledget. The filtrate was centrifuged at 10,000 g, treated twice with PEG and centrifuged again. The whole experiment was carried out at 4℃. Absorbance values were estimated at 260 nm using an ultraviolet spectrophotometer. Virus concn=(A_{260}×dilution ratio)/$E_{1cm}^{0.1\%, 260nm}$

Protective effects of compounds on TMV in vivo. The compound solution was smeared on the left side while solvent was served as control on the right side of growing *Nicotiana tabacum*. *L* leaves of the same ages. The leaves were then inoculated with the virus after 12 hours. A brush was dipped in tobacco mosaic virus of 6×10^{-3}mg/mL to inoculate the leaves, which were previously scattered with silicon carbide. The leaves were then washed with water and rubbed softly

along the nervature once or twice. The local lesion numbers appearing 3-4 days after inoculation were counted.[50]

Inactivation effect of compounds on TMV in vivo. The virus was inhibited by mixing with the compound solution at the same volume for 30 minutes. The mixture was then inoculated on the left side of the leaves of *Nicotiana tabacum. L.*, while the right side of the leaves was inoculated with the mixture of solvent and the virus for control. The local lesion numbers were recorded 3-4 days after inoculation.[49−50]

Curative effect of compounds on TMV in vivo. Growing leaves of *Nicotiana tabacum. L* of the same ages were selected. The tobacco mosaic virus (concentration of 6×10^{-3} mg/mL) was dipped and inoculated on the whole leaves. Then the leaves were washed with water and dried. The compound solution was smeared on the left side and the solvent was smeared on the right side for control. The local lesion numbers were then recorded 3-4 days after inoculation.[49−50] The experiments were repeated three times for each compound in order to ensure the reliability of the results, which were measured according to the following formula:

$$\text{Inhibition rate (\%)} = \frac{\text{av local lesion numbers of control} - \text{av local lesion numbers smeared with drugs}}{\text{av local lesion numbers without drugs}}$$

1.1.3   Results and Discussion

The preparation of cinnamaldehyde imines, known for their antibacterial bioactivities,[35] are difficult owing to the presence of free olefinic functionality in cinnamaldehyde rendering it susceptible to 1,4 Michael attack by a nucleophile. The condition of preparation of aldimines from cinnamaldehyde is highly substrate specific and although there are few reports on the preparation of non fluorinated imines from cinnamaldehyde and aromatic amine derivatives,[36−38] a practical synthetic method for the preparation of their fluorinated analogs still needs to be developed. The reaction scheme for the preparation of fluorinated imine **1.2** is shown in Scheme 1.1 and the results are given in Table 1.1.

$$R-NH_2 + R^1-CHO \xrightarrow[\text{CH}_2\text{Cl}_2, \text{ reflux}]{\text{Et}_3\text{N}} R-N=C-R^1$$

1.1   **1.2**
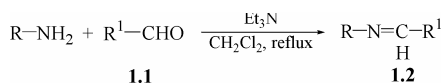
Scheme 1.1   Synthetic route to fluorinated aldimines **1.2**

Various solvents including benzene, toluene, methanol, ethanol and methylene chloride were selected for our study. It was observed that in alcoholic solvents and in aromatic hydrocarbons yield was lower and the product was accompanied by side reaction products. While the reaction was too sluggish in these solvents at low temperature presumably due to poor reactivity of fluorinated

Table 1.1   Synthesis of fluorinated aldimines **1.2** in methylene chloride [a]

Entry	R	R¹	Time (h)	Yield (%)[b]
1	F₃C—⟨benzene⟩—	⟨phenyl⟩—C=C— (H, H)	10	65
2	F₃C—⟨benzene⟩— (meta)	⟨phenyl⟩—C=C— (H, H)	8	70
3	F₃C—⟨benzene⟩— (meta)	F—⟨phenyl⟩—C=C— (H, H)	5	75
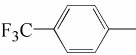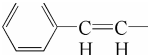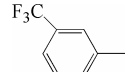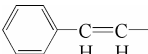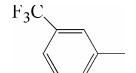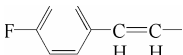
[a]Reaction conditions:aniline (10 mmol), aldehyde (10.5 mmol), triethylamine(0.2 mL),

CH₂Cl₂ (15 mL), 40℃; [b] Yields refer to isolated pure compounds.

amine, at the elevated reflux temperature Michael adducts started arising. Activation of the amine by a weak organic base *e.g.* triethylamine and addition of anhydrous sodium sulfate were found advantageous to improve the yield of the imine. The best result was achieved under reflux condition in low boiling methylene chloride which restricts the formation of side products. Under the optimal conditions, new fluorinated aldimines **1.2** were obtained in 65%-75% yield from different cinnamaldehyde and fluorinated aromatic amine (Table 1.1). The presence of electron withdrawing trifluoromethyl group at the para position of aromatic amine (entry 1) largely inhibits the nucleophilic activity and it takes longer time for the reaction to complete but the 4-fluoro substituent in cinnamaldehyde ring greatly activates the carbonyl group towards nucleophilic attack (entry 3). The results on the asymmetric hydrpohosphonylation of these achiral imines **1.2**   with dialkyl phosphites **1.3**   in the presence of 10 mol% of bifunctional Bronsted acid chiral organocatalyst **1.4** in xylene to yield new bioactive fluorinated α-aminophosphonates **1.5**   are shown in Table 1.2. The synthetic route to the novel asymmetric α-aminophosphonates is depicted in Scheme 1.2. The preparation of the chiral catalyst **1.4**   in a step-wise sequence starting from commercially available (*R*)- or (*S*)-BINOL using a modified procedure as described by us recently,[43]is shown in Scheme 1.3.

Table 1.2   Synthesis of new fluorinated asymmetric α-aminophosphonates
1.5a-1.5p using chiral catalyst **1.4**[a]

Entry	R	R¹	R²	Product[b]	Time(h)	ee[c](%) Yield[d][%]
1	*p*-CH₃C₆H₄	C₆H₅CH=CH	*n*-C₃H₇	**1.5a**	40	(22.8)/[51]
2	*p*-CH₃C₆H₄	C₆H₅CH=CH	C₂H₅	**1.5b**	40	(36.4)/[54]
3	*p*-CF₃C₆H₄	C₆H₅CH=CH	C₂H₅	**1.5c**	28	(76.8)/[58]
4	*m*-CF₃C₆H₄	C₆H₅CH=CH	C₂H₅	**1.5d**	28	(83.6)/[64]
5	*m*-CF₃C₆H₄	*p*-FC₆H₄CH=CH	C₂H₅	**1.5e**	28	(87.6)/[66]
6	*p*-CF₃C₆H₄	C₆H₅CH=CH	*n*-C₃H₇	**1.5f**	26	(82.8)/[65]
7	*m*-CF₃C₆H₄	C₆H₅CH=CH	*n*-C₃H₇	**1.5g**	26	(88.8)/[68]

Continued

Entry	R	R^1	R^2	Product[b]	Time(h)	ee[c](%) Yield[d][%]
8	$m\text{-}CF_3C_6H_4$	$p\text{-}FC_6H_4CH{=}CH$	$n\text{-}C_3H_7$	**1.5h**	26	(86.4)/[63]
9	$p\text{-}CF_3C_6H_4$	$C_6H_5CH{=}CH$	$n\text{-}C_4H_9$	**1.5i**	24	(83.7)/[71]
10	$m\text{-}CF_3C_6H_4$	$C_6H_5CH{=}CH$	$n\text{-}C_4H_9$	**1.5j**	24	(90.0)/[73]
11	$m\text{-}CF_3C_6H_4$	$p\text{-}FC_6H_4CH{=}CH$	$n\text{-}C_4H_9$	**1.5k**	24	(90.6)/[73]
12	$p\text{-}CF_3C_6H_4$	$C_6H_5CH{=}CH$	$i\text{-}C_3H_7$	**1.5l**	30	(64.6)/[58]
13	$m\text{-}CF_3C_6H_4$	$C_6H_5CH{=}CH$	$i\text{-}C_3H_7$	**1.5m**	30	(73.4)/[61]
14	$m\text{-}CF_3C_6H_4$	$p\text{-}FC_6H_4CH{=}CH$	$i\text{-}C_3H_7$	**1.5n**	30	(71.6)/[60]
15	$m\text{-}CF_3C_6H_4$	$p\text{-}FC_6H_4CH{=}CH$	C_2H_4OMe	**1.5o**	24	(78.2)/[66]
16	$m\text{-}CF_3C_6H_4$	$p\text{-}FC_6H_4CH{=}CH$	C_2H_4OEt	**1.5p**	24	(84.6)/[70]

[a]10 mol% of chiral catalyst **1.4** was employed;The chiral catalyst configuration was (R) for entry 2, 4, 9, 10, 13, 15 and 16 and (S) for the rest. [b]Reaction conditions:. aldimine (1 mmol), catalyst **1.4**   (772 mg, 0.1 mmol), xylene (15 mL), dialkyl phosphite **1.3** (2 mmol); room. temp. [c] Determined by chiral HPLC; [d] Yields refer to isolated pure compounds.
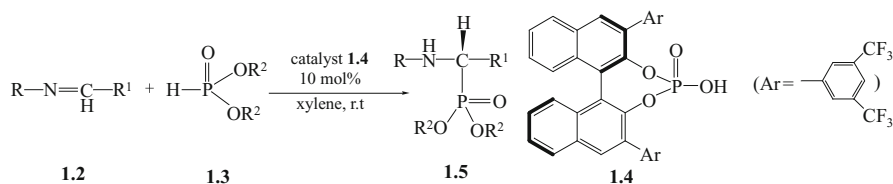
Scheme 1.2   Synthetic route to enantioenriched fluorinated α-aminophosphonates **1.5** using chiral catalyst **1.4**
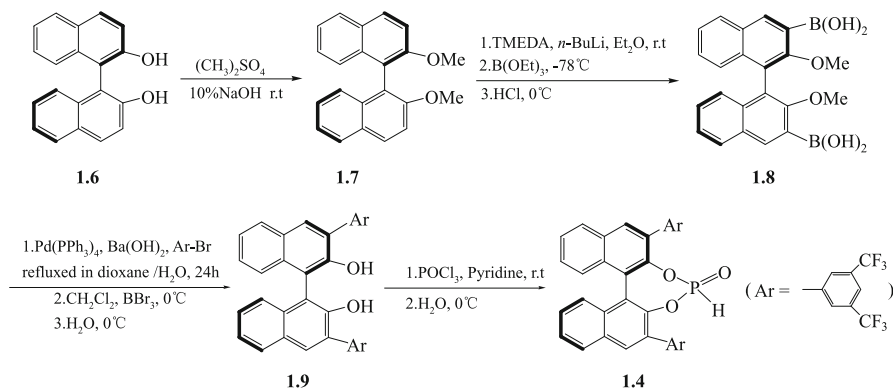
Scheme 1.3   Synthetic route to the chiral catalyst **1.4**

The (R)-2,2′-dimethoxy-1,1′-dinaphthyl **1.7** could be easily obtained by the methylation of (R)-1,1′-bi-naphthol **1.6** using dimethyl sulfate which was then converted into (R)-3,3′-bis(dihydroxyborane)-2,2′-dimethoxy-1,1′-dinaphthyl **1.8** as the nucleophilic coupling partner of Suzuki coupling. The coupling with the electrophilic bromide 3,5-bis(trifluoromethyl)bromobenzene followed by deme-

thylation with boron tribromide yields (*R*)-3,3′-bis(3,5-bis(trifluoromethyl) phenyl)[1,1′] binaphthalenyl-2,2′-diol **1.9** which was further subjected to pohosphorylation using POCl₃ to generate the desired chiral catalyst (*R*)-1,1′-binaphthyl-2,2′-diyl-3,3′-bis(3,5-bis(trifluoromethyl) phenyl) hydrogen phosphate **1.4**.

　　We assumed that the presence of fluorinated moiety in the aromatic amine part *R* (second column, Table 1.2) of the aldimine would not only facilitate the nucleophilic attack at the imine carbon by the phosphite, but would also assist in the molecular recognition of the fluorinated catalyst **1.4**. Indeed, to our delight, by employing various fluorinated Schiff's bases derived from cinnamaldehyde, a more facile and general route to the preparation of a series of new enantioenriched α-aminophosphonates (entry 3-16) from different dialkyl phosphites could be developed. The two new non fluorinated analogs **1.5a** and **1.5b** of α-aminophosphonates (entry 1 and 2) derived from cinnamaldehyde revealed much lower reactivity and enantioselectivity under similar condition. Optimization of the reaction condition was carried out with model compound **1.5h** to study the role of solvent, temperature and catalyst amount on the enantioselectivity. The results are shown in Table 1.3.

Table 1.3　Optimization of reaction parameters for enantioselective
synthesis of **1.5h** using chiral catalyst **1.4**

Entry	Solvent	Temp (℃)	Cat (mol%)	ee(%)
1	acetonitrile	r.t	10	30.6
2	methylene chloride	r.t	10	78.4
3	toluene	r.t	10	82.8
4	xylene	r.t	10	86.4
5	xylene	r.t	20	87.1
6	xylene	r.t	5	36.8
7	xylene	r.t	2	1.2
8	xylene	0	10	87.2
9	xylene	40	10	71.4
10	xylene	60	10	32.1

　　Under optimal condition, the best result was obtained in solvent xylene with 10 mol% catalyst at room temperature (entry 4, Table 1.3). The reaction in xylene showed higher eantioselectivity than those in toluene, acetonitrile and methylene chloride. The ee at higher temperature was lower than that at room temperature and did not show much improvement with 20 mol% of catalyst **1.4.** The reaction at 0℃ took much longer time to complete without beneficial effect on enantioselectivity. The unsubstituted control chiral catalyst (*R*)-binaphthylphosphoric acid derived from (*R*)-BINOL, quite expectedly, afforded lower enantioselectivity (data not shown). The ee in the presence of chiral catalyst **1.4** was found to be significant when fluorinated Schiff's bases derived from cinnamaldhydes were reacted with various dialkyl phosphites e.g diethyl, diisopropyl, di-*n*-butyl, di-

n-propyl, di-(2-methoxyethyl) and di-(2-ethoxyethyl) (Table 1.2). The enantio-selectivity and reactivity in alkyl phosphites for preparing fluorinated α-amino-phosphonates were generally found to follow the order *n*-Bu>*n*-Pr>Et> *i*-Pr. The amine bearing a similar *m*-CF$_3$ substitent as the host chiral catalyst **1.4** proved more active than the corresponding amine with a *p*-CF$_3$substituent. Comparison has been made among different groups of imines using various dialkyl phosphites (entry 3-14, Table 1.2). Aldimines were derived either from *p*-or *m*-(trifluoro-methyl) aniline and unsubstituted cinnamaldehyde (except entry 5,8,11 and 14 with *p*-F derivative). With diethyl phosphite (entry 3 and 4), *p*-CF$_3$ afforded an ee of 76.8% against 83.6% with *m*-CF$_3$, while with di-*n*-propyl phosphite (entry 6 and 7) similar substituents at *p* and *m*-positions gave 82.8% and 88.8% ee respectively. It could be noted that while with di-*n*-butyl phosphite (entry 9 and 10) high ee of 83.7% and 90% could be achieved from *p* and *m*-(trifluoromethyl) anilines, enantioselectivity was reduced considerably to 64.6% and 73.4% respectively using similar derivatives with diisopropyl phosphite (entry 12 and 13). In all these examples no significant change in terms of yield and enantioselectivity were observed with the aldimine derived from *p*-fluoro-cinnamaldehyde (com-pare entry 4 vs.5,7 vs.8,10 vs.11, and 13 vs.14) in accordance with our assume-ption that a fluorine atom in the aromatic ring of cinnamaldehyde, unlike in the aryl ring of amine, does not influence the hydrophosphonylation reaction to a great extent.

Finally, with an idea to prepare more promising and potentially bioactive enantiopure α-aminophosphonates, hydrophosphonylation reaction was executed with di (2-methoxyethyl) and di (2-ethoxyethyl) phosphites affording 78.2% and 84.6% ee respectively (entry 15 and 16). The corresponding racemic α-aminophosphonates used as standards in HPLC analysis for determining enan-tiomeric purity of asymmetric α-aminophosphonates were obtained by employing a one pot synthesis involving the aldehyde, amine and the phosphite. In order to ascertain the absolute configurations of the title α-aminophosphonates **1.5**, the sign of optical rotation of the title products was compared with those reported by Davis et al.[51]These authors made extensive studies on the absolute configurations of asymmetric α-aminophosphonates and assigned a positive value of optical rotation to the (*R*)-enantiomer and a negative value to the (*S*)-enantiomer respectively. For the purpose of unequivocal assignment of absolute configu-rations to our title products, another non fluorinated analog of α-aminophos-phonate **1.5q**(entry 17, Table 1.2) was prepared in the presence of the chiral catalyst (*R*)-**1.4**. The sign of optical rotation for this product was found positive (Table 1.2) revealing the presence of an (*R*) configuration. Thus, the absolute configurations of α-aminophosphonates derived from (*R*)-and (*S*)-**1.5** were assigned as (*R*) and (*S*) respectively by comparison with the literature data. Studies on antifungal, antiviral and anticancer bioactivities of individual enantiomers are in progress. Typical chiral HPLC chromatograms of the title α-aminophos-phonates are shown in Fig 1.1.
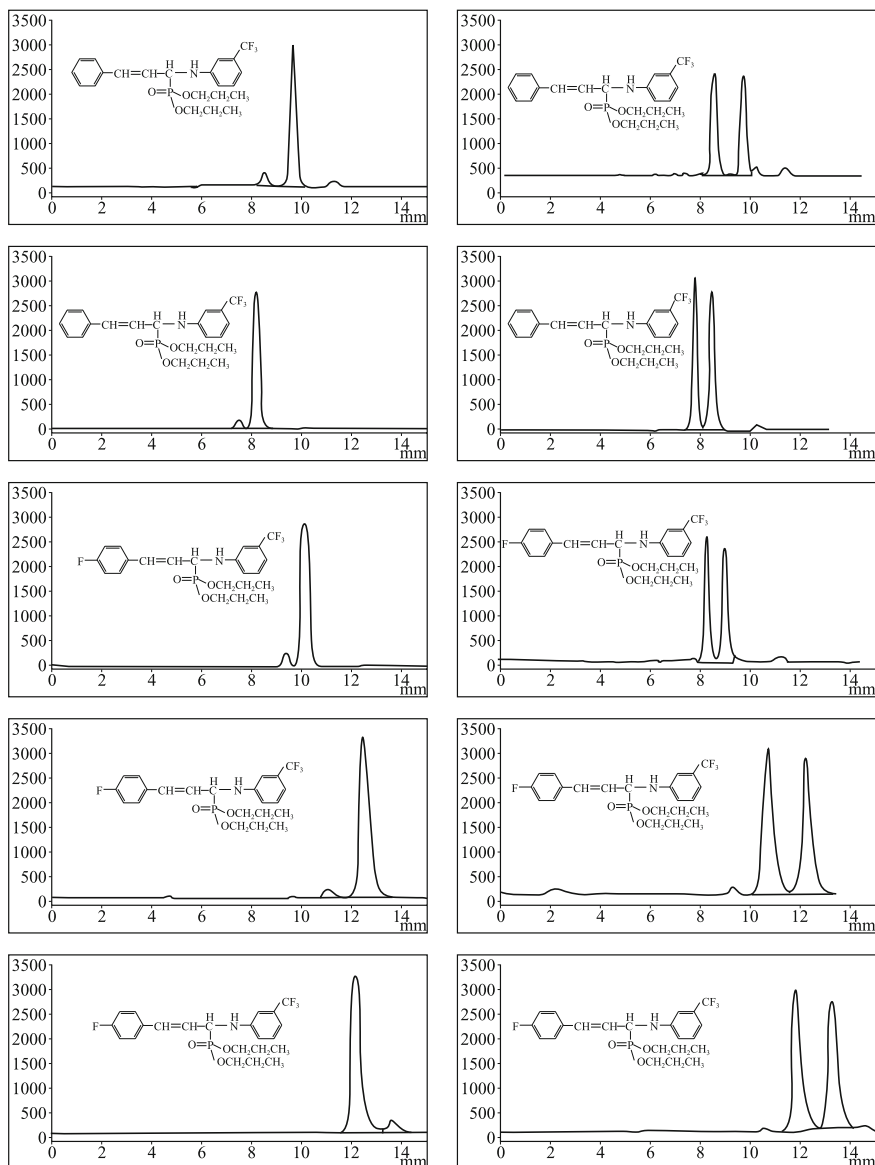
Fig 1.1   Chiral HPLC chromatograms of the title α-aminophosphonates

The observed high enantioselectivity of this catalyst in asymmetric hydro-phosphonylation of fluorinated aldimines derived from cinnamaldehyde is presumably attributed to the enhanced electrophilic reactivity of the imine carbocation due to resonance stabilization through conjugation and the presence of electron withdrawing-CF$_3$ group in the aryl ring attached to the nitrogen atom. The phosphoric acid hydrogen activates the imine as a Bronsted acid. It is further well

known that the nucleophilic phosphite form bearing Bronsted acidic-OH group is the reactive tautomer and it is likely that it coordinates with the phosphoryl oxygen of the catalyst **1.4** causing the activation of the P nucleophile. The shielding of the phosphite moiety by the bulky non coplanar aryl groups at 3,3′ positions of the catalyst facilitates its preferential binding subsequently with the imine from one side. As mentioned before, trifluoromethyl group present in the aromatic ring of the imine, could result in significant cohesive molecular interaction with the chiral catalyst due to close proximity effect.

The results of the *in vivo* activity against TMV bioassays are given in Table 1.4. Ningnanmycin was used as reference antiviral agent. The preliminary bioassay showed that some of the chiral analogues exhibited good *in vivo* antiviral activities against TMV at the dosage of 500 μg/mL. Three compounds, **1.5a**, **1.5g** and **1.5i** had good inactivation effects against TMV, with an inhibition rates of 72.5%,70.2% and 70.1% respectively compared to Ningnanmycin (inhibition rate 90.2%), **1.5g** was found to display good curative effects against TMV (inhibitroy rate: 52.2%) and the values were comparable to Ningnanmycin (inhibitroy rate: 56.9%).**1.5f** could protect TMV up to 49.6% at 500 μg/mL. All other chiral compounds have relatively lower curative activity than **1.5g.**

Table 1.4   Inhibitory activity of title compounds **1.5a-1.5n** against TMV

Compd.	Curative effect(%)	Protective effect(%)	Inactivative effect(%)
1.5a	43.8	43.4	72.5
1.5b	44.2	42.3	58.0
1.5c	46.6	48.3	61.2
1.5d	41.4	42.4	59.4
1.5e	32.7	25.1	32.5
1.5f	45.1	49.6	46.3
1.5g	52.2	41.2	70.2
1.5h	43.5	31.8	70.1
1.5i	31.6	18.8	44.1
1.5j	29.0	28.1	30.2
1.5k	27.7	27.0	47.6
1.5l	10.8	20.1	33.6
1.5m	13.1	25.3	34.4
1.5n	31.6	18.8	44.1
Ningnanmycin	56.9	58.3	90.2

1.1.4   Conclusions

In conclusion, a general route to asymmetric hydophosphonylation of fluo-rinated aldimines derived from cinnamaldehyde with various dialkyl phosphites in

presence of a chiral phosphoric acid derivative is developed. Further studies on the preparation of potential new chiral organocatalysts for asymmetric synthesis of bioactive α-aminiophosphonates are currently underway. The half-leaf method was used to determine the curative and inactivation efficacy *in vivo* of the chiral title compounds against tobacco mosaic virus. It was found that three compounds, **1.5a**, **1.5g** and **1.5h** had good inactivation effects against TMV. The inhibition rate of **1.5g** displayed good curative effect of 52.2% against TMV. To our knowledge, this is the first report on the syntheses and antiviral activity of chiral 3-[*N*-(substituent-phenyl)amino]-3-(substituent-phenyl)-2-propenylphosphonates.

1.2 Synthesis & Bioactivity of α-Aminophosphonates Containing Amide Moiety

1.2.1 Introduction

A variety of reports on the synthetic studies of amide derivatives are recently encountered in various litertature due to their wide spectrum of biological activities.[52−57] Some derivatives of amide can serve not only as agrochemicals such as fungicide, insecticide, and plant virucide, but also as medicines such as antitumor agent. α-Aminophosphonates, as stated in preceding sections, are known
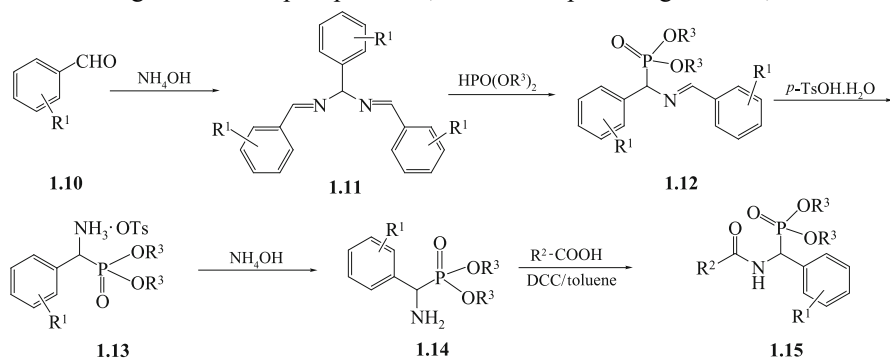
1.15a:R^1= H, R^2= 3,4,5-tri-$CH_3OC_6H_2$-, R^3 = Et; 1.15b:R^1= 2-F, R^2= 3,4,5-tri-$CH_3OC_6H_2$-, R^3 = Et;
1.15c:R^1=H, R^2=C_6H_5-, R^3 = Et; **1.15d**:R^1=F, R^2=C_6H_5-, R^3 = Et; **1.15e**:R^1=F, R^2= 2-FC_6H_5-, R_3 = Et;
1.15f:R^1=H, R^2= 2-FC_6H_5-, R^3 = Et; **1.15g**:R^1=H, R^2= 4-FC_6H_5-, R^3 = Et; **1.15h**:R^1=H, R^2= 3-FC_6H_5-, R^3 = Et; **1.15i**:R^1=H, R^2= 2-$CF_3C_6H_5$-, R^3 = Et; **1.15j**:R^1= 2-F, R^2= 3-FC_6H_5-, R^3 = Et; **1.15k**:R^1= 2-F, R^2= 2-$CF_3C_6H_5$-, R^3 = Et;**1.15l**:R^1= H, R^2= 2-ClC_6H_5-, R^3 = Et;**1.15m**:R^1= 2-F, R^2= 2-ClC_6H_5-, R^3 = Et;**1.15n**:R^1=H, R^2= C_6H_5CH=CH-, R^3 = Et;**1.15o**:R^1=2-F, R^2= C_6H_5CH=CH-, R^3 = Et;**1.15p**:R^1= H, R^2= 2-$CF_3C_6H_5$-, R^3 = *n*-Pr;**1.15q**:R^1= H, R^2= 3-FC_6H_5-, R^3 = *n*-Pr;**1.15r**:R^1= 2-F, R^2= 3,4,5-tri-$CH_3OC_6H_2$-,R^3 = *n*-Pr;**1.15s**:R^1=H, R^2=C_6H_5-, R^3 = *n*-Pr

Scheme 1.4   Synthesis of amide analogues containing α-aminophosphonate **1.15**

for their great biological and chemical relevance. Some derivatives of α-amino-phosphonic acids are used as fungicide, plant virucide and herbicide. Among these compounds, studies are mainly concentrated on those containing heterocyclic moieties such as thiophene, furan, pyrole, 1,3,4-thiadiazole and benzothiazole which serve as representative compounds with excellent bioactivities.[28,58−62] However, only a very few reports exsist on the incorporation of phosphonate moiety into the parent amide unit.

In order to extend our research work of amide as fungicide and antiviral agent, we designed and synthesized some novel amide derivatives **1.15**. The synthetic route is shown in Scheme 1.4. The structures of **1.15** were established by well defined IR, NMR and elemental analysis. The bioassay test identified these new compounds **1.15** possessing weak to good antifungal and antiviral activities. To the best of our knowledge, this is the first report on the synthesis, antifungal and antiviral activity of amide derivatives containing α-aminophosphonate moiety.

1.2.2   Materials and Methods

The materials and instruments for determination of the structure and physical data of new compounds are basically similar to the procedure described in Chapter 1.1.2. Diethyl phosphite and di-*n*-propyl phosphite were prepared according to literature method as described.[63] Intermediates **1.14a-1.14c** were prepared according to the reported methods.[64]

Preparation of Intermediates **1.14a-1.14c.** The benzaldehyde **1.10**(15 mmol) was added to ammonium hydroxide (30％, 15 mL) and the solution was stirred for 1h at reflux. During this time, a white precipitate **1.11** was formed which was removed by filtration and dried. Dialkyl phosphite (6 mmol) was added to this solid and the resulting solution was stirred for 2 h at 70℃. The intermediate **1.12** was produced in this process and then *p*-toluenesulfonic acid (6 mmol) in 50 mL tetrahydrofuran (THF) was added to the reaction mixture and stirred for 2h at 0℃. The precipitate **1.13** was removed by filtration and washed with THF (20 mL). The precipitate was added to 30 mL aqueous ammonium hydroxide (10％) and stirred for 30min at room temperature. The impurity was removed by extraction with ether (2×50 mL) and then the aqueous phase was extracted with EtOAc (2×50 mL). Evaporation of the solvent followed by chromatography on silica gel with EtOAc/*n*-hexane (9:1) gave the pure products **1.14** as oils in 40.5%-55.1% yields. The reperesentative data for **1.14a** is shown below, while data for **1.14b-1.14c** can be found in the Supporting Information of Reference.[66]

Data for diethyl amino(phenyl)methylphosphonate (**1.14a**). colorless liquid; $[\alpha]_D^{20}$ 1.4950; yield 40.5%; IR (KBr): ν_{max} 3379.1, 3200.1, 2981.3, 1238.6, 1026.4; ^{1}H NMR (500MHz, DMSO-d_6): δ 1.18 (t, 3H, J=6.85 Hz, CH$_3$), 1.28 (t, 3H, J=7.15 Hz, CH$_3$), 2.01 (s, 2H, NH$_2$), 3.83-4.06 (m, 4H, 2×CH$_2$), 4.26 (d, H,

J=17.15 Hz, CH), 7.29-7.46 (m, 5H, Ar-H); ^{13}C NMR (125 MHz, DMSO-d_6): δ 137.32, 128.53, 128.51, 127.96, 127.80, 127.75, 62.98, 62.85, 54.63, 54.57, 16.51, 16.33; ^{31}P NMR (200 MHz, DMSO-d_6): δ 25.29.

***General Procedure for the Preparation of Title Compounds* 1.15a-1.15s.** A solution of aromatic acid (1 mmol) in toluene (10 mL) was stirred, followed by the addition of intermediate **1.14**(1mmol), and then the reaction system was cooled down to 0℃. 1,3-Dicyclohexyl-carbodiimide (DCC) (1 mmol) in toluene (10 mL) was then added and the mixture was further stirred for 10~24h at 25℃. The resulting 1,3-dicyclohexylurea (DCU) was filtered, the solvent toluene was evaporated to yield the crude product, which was purified by chromatography on silica using a mixture of petroleum ether and ethyl acetate (4:1) as an eluant to give the target compounds in 40.5%-90.6% yields. The representative data for **1.15a** is shown below, while data for **1.15b-1.15s** can be found in the Supporting Information of Reference.[66]

Data for diethyl phenyl (3,4,5-trimethoxybenzamido)methylphosphonate (1.15***a***). white crystal; mp 149-151℃; yield 40.5%; IR (KBr):ν_{max} 3246.2, 2995.5, 1649.1, 1246.0, 1031.9; ^{1}H NMR (500 MHz, DMSO-d_6): δ 1.10 (t, J=7.45 Hz, 3H, CH$_3$), 1.32 (t, J=7.15 Hz, 3H, CH$_3$), 3.72-4.19 (m, 13H, 3OCH$_3$+ 2OCH$_2$), 5.69-5.73 (m, 1H, CH), 7.04-7.53 (m, 7H, Ar-H+NH); ^{13}C NMR (125 MHz, DMSO-d_6): δ 166.53, 153.19, 141.30, 135.17, 129.13, 128.24, 28.19, 104.74, 63.57, 63.51, 60.90, 56.36, 51.33,50.12, 16.45, 16.15; ^{31}P NMR (200 MHz, DMSO-d_6): δ 22.18; Anal. Calcd for C$_{21}$H$_{28}$NO$_7$P: C, 57.66; H, 6.45; N, 3.20. Found: C, 57.84; H, 6.62; N, 3.17.

Antifungal activity bioassay. The antifungal activities of all synthesized compounds were tested against three pathogenic fungi namely *Gibberella zeae*, *Botrytis cinerea*, *Sclerotina sclerotiorum*.[67] Compounds were dissolved in 1 mL acetone before being mixed with 90 mL potato dextrose agar (PDA). The final concentration of compounds in the medium was fixed at 100 µg/mL. All kinds of fungi were incubated in PDA at 25±1℃ for 4 days to get new mycelium for antifungal assay. Then a mycelia dish of approximately 4mm diameter cut from culture medium was picked up with a sterilized inoculation needle and inoculated in the center of PDA plate. The inoculated plates were incubated at 25±1℃ for 5 days. Acetone in sterile distilled water served as control, while hymexazole severed as positive control. Three replicates were conducted for each experiment. The radial growth of the fungal colonies was measured and the data were statistically analyzed. The inhibiting effects of the test compounds *in vitro* on these fungi were calculated by the formula $I = \dfrac{C-T}{C} \times 100$, where C represents the diameter of fungi growth on untreated PDA, and T represents the diameter of fungi on treated PDA while I means inhibiting rate.

Antiviral biological assay. The method for evaluating anti-TMV activity of title compounds **1.15** is similar to the procedure described in Chapter 1.1.2.[49, 50]

1.2.3   Results and Discussion

Synthesis. Amides can be synthesized by the treatment of amine on acyl chloride. However, the liberated HCl as the side product is harmful to the current reaction as the ester phosphonate is susceptible to acidolysis. Thus, amide compounds containing phosphonate were synthesized by the coupling reaction of dialkyl amino (substitutedphenyl)-methylphosphonate and aromatic acid in the presence of catalyst DCC. The reaction temperature during the drop wise addition of DCC is crucial in this exothermic reaction. When DCC was added into the reactants, the reaction temperature increased rapidly and side reactions became significant. Thus, the reaction temperature during the slow addition of DCC was controlled at $0{}^{\circ}\!C$.

Antifungal activity. Inhibition effect of sulfone derivatives on phytopathogenic fungi: The three fungi used in the fungicidal bioassay, *G.zeae*, *F.oxysporum* and *V. mali*, belong to the group of field fungi and were isolated from corresponding crops. The results of preliminary bioassays were compared with that of a commercial agricultural fungicide, hymexazol. As indicated in Table 1.5, all the compounds **1.15a-1.15s** showed weak antifungal activities against all the tested fungi.

Table 1.5   Fungicidal activities of amide derivatives **1.15**[a] at 100 μg/mL

Compd.	inhibitory rate (%)		
	F.oxysporum	*G.zeae*	*V.mali*
1.15a	4.56±1.21	9.37±0.56	9.59±8.69
1.15b	3.54±0.69	4.41±0.72	13.43±0.90
1.15c	1.53±0.68	4.41±1.08	5.76±0.51
1.15d	2.53±0.80	4.13±0.66	7.19±0.55
1.15e	4.05±0.75	9.37±1.10	16.31±0.63
1.15f	19.20±4.56	12.11±5.52	4.67±0.99
1.15g	13.45±2.32	9.90±0.67	8.89±5.42
1.15h	21.48±7.80	21.00±4.67	31.89±8.99
1.15i	20.09±6.66	10.09±3.33	21.00±8.09
1.15j	19.80±7.77	21.11±2.90	11.00±8.11
1.15k	15.55±9.90	12.22±7.89	39.00±9.00
1.15l	4.56±0.26	4.00±1.09	9.09±7.00
1.15m	19.30±9.51	14.00±8.80	29.50±10.00
1.15n	6.77±2.22	5.55±3.21	20.87±9.91
1.15o	11.09±8.54	12.00±9.53	28.70±7.99
1.15p	18.89±9.00	10.90±7.44	5.22±1.00
1.15q	4.00±0.23	3.41±0.20	9.51±8.00
1.15r	15.43±4.55	10.77±8.66	10.00±7.09
1.15s	0.97±0.16	0	5.55±1.72
hymexazol	57.22±0.75	57.85±0.40	52.52±0.48

[a]Growth inhibition expressed as a percentage of the control (mean±SD, *n*=3).

Antiviral activity. The antiviral activity of compound **1.15a-1.15s** against TMV is assayed by the reported method.[49,50] The results of bioassay *in vivo* against TMV are given in Table 1.6. Ningnanmycin was used as reference antiviral agent. The data provided in Table 1.6 indicate that the introduction of dialkyl-phosphonyl in amide might improve their protective activities. The title compounds **1.15a-1.15s** showed protection rate of 39.1%-58.8%. The compound **1.15h** (R^1 is 3-FC_6H_4, R^2 is H and R_3 is Et), **1.15l** (R^1 is 2-ClC_6H_4, R^2 is H and R^3 is Et), **1.15n** (R^1 is $C_6H_5CH=CH$, R^2 is H and R^3 is Et) and **1.15r** (R^1 is 3,4,5-tri-$MeOC_6H_2$, R^2 is H and R^3 is *n*-Pr) have the same protection activity (56.0,58.0,58.7 and 58.8%, respectively) as that of the reference (60.2%). Highest protective activity was achieved when R^1 is 4-FC_6H_4, R^2 is H and R^3 is Et (**1.15g**). A protective rate of 65.7% equivalent to Ningnanmycin against TMV at 500 μg/mL was recorded in this case. From the data in Table 1.6, it may be observed that the title compounds **1.15a-1.15s** possess potential inactivation bioactivities, with values of 45.6%, 33.7%, 42.4%, 70.0%, 80.0%, 78.0%, 99.1%, 82.1%, 45.3%, 70.7%, 62.2%, 90.6%, 39.0%, 88.2%, 51.5%, 80.0%, 86.6%, 83.4% and 78.9% at

Table 1.6   The Protection, inactivation and curative effect of the new compounds against TMV *in vivo* at 500 μg/mL

Agents	Protection effect(%)	Inactivation effect (%)	Curative effect(%)
1.15a	$42.0^*\pm1.9$	$45.6^{**}\pm1.1$	$35.6^*\pm0.6$
1.15b	$41.2^*\pm4.4$	$33.7^*\pm0.8$	$17.1^*\pm1.2$
1.15c	$39.1^*\pm1.2$	$42.4^*\pm2.0$	8.7 ± 0.6
1.15d	$43.1^*\pm0.9$	$70.0^{**}\pm3.1$	$32.2^*\pm2.0$
1.15e	$50.0^*\pm1.4$	$80.0^*\pm2.9$	$20.8^*\pm1.2$
1.15f	$42.0^*\pm2.1$	$78.0^{**}\pm1.1$	$53.6^*\pm0.4$
1.15g	$65.7^*\pm4.9$	$99.1^{**}\pm2.0$	$19.2^*\pm0.5$
1.15h	$56.0^*\pm2.9$	$82.1^*\pm1.7$	$24.6^*\pm1.0$
1.15i	41.1 ± 3.9	$45.3^*\pm1.6$	2.4 ± 0.9
1.15j	$41.0^*\pm5.9$	$70.7^*\pm0.8$	6.2 ± 0.8
1.15k	$39.2^*\pm1.0$	$62.2^*\pm0.6$	2.1 ± 0.2
1.15l	$58.0^*\pm3.3$	$90.6^*\pm1.3$	$20.0^*\pm1.9$
1.15m	$40.9^*\pm0.5$	$39.0^*\pm1.8$	$19.7^*\pm15$
1.15n	58.7 ± 6.6	$88.2^{**}\pm2.2$	$50.0^*\pm0.5$
1.15o	$39.0^*\pm2.2$	$51.5^*\pm0.6$	$22.4^*\pm1.2$
1.15p	$44.0^*\pm1.9$	$80.0^*\pm2.0$	53.7 ± 0.9
1.15q	$50.9^*\pm1.9$	$86.6^*\pm2.9$	44.1 ± 2.0
1.15r	$58.8^*\pm4.5$	$83.4^*\pm1.6$	$55.0^*\pm0.7$
1.15s	$49.9^*\pm2.2$	$78.9^{**}\pm2.2$	$45.3^*\pm2.6$
Ningnamycin	$60.2^*\pm1.6$	$100^{**}\pm1.2$	$55.4^*\pm1.9$

All results are expressed as mean$\pm$SD; *n*=3 for all groups; * $P<0.05$, $^{**}P<0.01$.

500 μg/mL, respectively. Among these compounds, **1.15g** was far more active against TMV than the rest, with an inactivation rate of 99.1% equivalent to Ningnanmycin (100%) against TMV at 500 μg/mL. The data also indicated that a change in the substituent might also affect the curative activity of title compounds **1.15a-1.15s**. Compound **1.15f**(R^1 is 2-FC_6H_4, R^2 is H and R^3 is Et), **1.15p** (R^1 is 2-$CF_3C_6H_4$, R^2 is H and R^3 is *n*-Pr) and compound **1.15r** (R^1 is 3,4,5-tri-$MeOC_6H_2$, R^2 is H and R^3 is *n*-Pr) could curate TMV up to 53.6%, 53.7% and 55.0% at 500 μg/mL. The other compounds showed relatively lower curative activities than those of **1.15f**, **1.15p** and **1.15r**.

In addition, as shown in Table 1.6, compounds **1.15f**, **1.15g**, **1.15l**, **1.15n**, **1.15p**, **1.15q**, **1.15r** and **1.15s** with good antiviral activities were selected for further test. Ningnanmycin was used as a control for making a judgment on the antiviral potency of these compounds. As shown in Table 1.7, the curative effects of compounds **1.15f**   and **1.15r** aganist TMV showed remarkable effect, the EC_{50} values on TMV were 255.6 and 250.1 μg/mL, respectively. Compounds **1.15g**, **1.15l**   and **1.15n** showed high inactivation effects against TMV and their EC_{50} values were 54.8, 60.0 and 65.2 μg/mL, respectively. Compound **1.15g** had more potent antiviral activity against TMV than the rest, the same as that of Ningnanmycin against TMV.

Table 1.7   Antiviral activities *in vivo* (%) of compounds **1.15a-1.15s**

TMV	Curative effect(%)				Inactivation effect(%)			
Concentration (μg/mL)	500	250	125	EC_{50} (μg/mL)	250	125	62.5	EC_{50} (μg/mL)
1.15f	56.0	49.0	34.0	255.6	70.9	47.2	36.7	119.1
1.15g	22.0	—	—		100.0	76.1	70.0	54.8
1.15l	19.0	—	—		82.2	60.9	59.0	60.0
1.15n	51.0	39.9	32.3	438.8	79.9	61.2	49.1	65.2
1.15p	54.0	38.0	31.6	421.9	60.0	39.2	31.2	198.9
1.15q	43.0	21.0	12.9	545.5	65.0	46.0	40.1	149.9
1.15r	56.7	50.6	40.9	250.1	61.0	30.3	28.8	210.0
1.15s	42.0	23.9	14.0	559.8	51.0	23.0	10.0	278.9
Ningnamycin	60.0	51.0	40.9	245.9	100.0	78.4	69.0	55.6

1.2.4   Conclusions

A series of novel amide derivatives containing α-aminophosphonates was synthesized by the treatment of 1-amino-arylmethylphosphonates and aromatic acid with 1,3-dicyclohexylcarbodiimide in toluene. This method is easy, rapid and moderate-yielding for preparing title compounds **1.15**. The structures of new compounds were verified by spectroscopic data. In the antifungal bioassay, the

title compounds **1.15a-1.15s** were found to possess weak antifungal activities against three kinds of fungi *in vitro*. The preliminary bioassay showed that some of the amide analogues exhibited good *in vivo* antiviral activities against TMV at the dosage of 500 μg/mL. Three of these compounds, **1.15g**, **1.15l** and **1.15n** had the same range inactivation effects (EC_{50}=54.8, 60.0 and 65.2 μg/mL) as that of Ningnanmycin (EC_{50}=55.6μg/mL) against TMV.**1.15f** and **1.15r** were found to display good curative effects against TMV (EC_{50}=255.6 μg/mL for **1.15f**; EC_{50}=250.1 μg/mL for **1.15r**) and the values were again comparable to Ningnanmycin (EC_{50}=245.9 μg/mL). To our knowledge, this is the first report on the syntheses and antiviral activity of amide-based α-aminophosphonate derivatives. Further studies on structural optimization and antiviral activities of the amide analogues are currently under progress.

1.3   Green Synthesis & Bioactivity of α-Aminophosphonates Containing an Alkoxyethyl Moiety

1.3.1   Introduction

α-Aminophosphonate derivatives have received considerable attention over the past two decades in medicine and pesticide chemistry due to their biological activities. As stated earlier, α-aminophosphonats and their derivatives are widely used as potent enzyme inhibitors,[68]antimicrobial,[69] antitumor [28]and antiviral agents.[70] In order to find potential new plant antiviral agents, we had designed and synthesized a series of α-aminophosphonate compounds, among which some compounds were found to possess moderate to good bioactivity[71,72] Recently, attention has been focused on these promising antiviral agents after the discovery of the compounds containing methoxyethyl moiety.[73,74] The traditional method of synthesizing α-aminophosphonate involves treatment of Schiffs base with dialkyl phosphite, but this method is uneconomic, inconvenient and low yielding. In this report we designed and synthesized a series of α-aminophosphonate compounds containing alkoxyethyl moieties and investigated their bioactivities. The synthetic route is shown in Scheme 1.5. The structures of compounds 1.19 were firmly estab-

R^1 = 3, 4, 5-trimethoxy, H, 2-F, 4-F, 2-CF_3, 3-CF_3;
R^2=4-$CF_3C_6H_4$-, 6-CH_3O-benzothiazol-2-yl-, 3-$NO_2C_6H_4$- ;
R^3=Me, Et
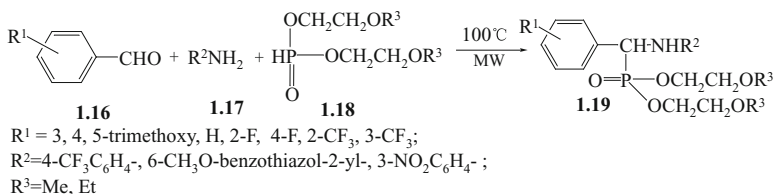
Scheme 1.5   Synthetic route to the title compounds

lished by well defined IR, ^{1}H NMR, ^{13}C NMR and elemental analysis. The X-ray crystallographic data of compound **1.19l** is provided. Preliminary bioassay tests showed that some compounds displayed antiviral activities against TMV at 500 μg/mL *in vivo*.

1.3.2   Materials and Methods

The materials and instruments for determination of the structure and physical data of new compounds are basically similar to the procedure described in Chapter 1.1.2. Microwave reaction was performed on a Focused Microwave Synthesizer (with a power of 50W). Dialkyoxyethyl phosphites were synthesized according to the literature method.[63]

Preparation of α-aminophosphonate derivatives containing alkyloxyethyl moieties **1.19a-1.19l**. Substituted benzaldehyde (5 mmol), substituted aniline (5 mmol) and bis(2-methoxyethyl) phosphite or bis(2-ethoxyethyl) phosphite were placed in a microwave tube, which was then sealed and then placed in the Discovery^{TM} synthesizer and irradiated at 100℃ and 50 W for 10 min. Completion of the reaction was checked by TLC. The reaction mixture was cooled and the crude product was recrystallized from 95% ethanol to give title compounds **1.19a-1.19l**. The repereentative data for **1.19a** is shown below, while data for **1.19b-1.19l** can be found in the Supporting Information of Reference.[72]

N-(4-trifluoromethylphenyl)-α-amino-α-(2-fluorophenyl)-O,O-bis(2-metho xyethyl)phosphonate **(1.19a)**. White crystals; yield 83.5%; mp 67-68℃; IR (KBr): v_{max} 3273.2, 1537.3, 1238.3, 1064.7; ^{1}H NMR (500 MHz CO$_3$COCD$_3$): δ 3.07 (s,1H, N-H), 3.28 (s, 6H, 2CH$_3$O), 3.44-4.27(m, 8H, 4CH$_2$), 5.37 (d, *J*=25.2 Hz, 1H, CH), 6.89-7.68(m, 8H, Ar-H); ^{13}C NMR (125 MHz CO$_3$COCD$_3$): δ 47.74, 49.01, 58.69, 58.72, 66.67, 66.73, 72.06, 75.15, 113.68, 115.90, 116.06, 125.41, 127.16, 127.20, 130.24, 150.74, 150.86, 160.73, 162.73; ^{31}P NMR (200 MHz CO$_3$COCD$_3$, H$_3$PO$_4$): δ 22.19, 22.21; *Anal*. Calcd for C$_{20}$H$_{24}$F$_4$NO$_5$P: C, 51.62; H, 5.20; N, 3.01. Found: C, 51.92; H, 5.17; N, 3.15.

Bioassays:*antifungal bioassays*. The method for evaluating antifungal activity of title compounds **1.19** is similar to the procedure described in Chapter 1.2.2.[74]

Antiviral bioassays. The method for evaluating anti-TMV activity of title compounds is similar to the procedure described in Chapter 1.1.2.[49, 50]

Crystal structure determination. For the structure determination of the single crystal of **1.19l**, X-ray intensity data were recorded on a Rigaku Raxis-IV diffraction meter using graphite monochromated MoKα radiation (λ=0.71073Å). In the range of 2.14°≤θ≤25.01°, 3641 independent reflections were obtained. Intensities were corrected for Lorentz and polarization effects and empirical absorption, and all data were corrected using SADABS[75]program. The structure

was solved by direct methods SHELXS-97 program.[76] All the non-hydrogen atoms were refined on $F2$ anisotropically by full-matrix least squares method. The hydrogen atoms were located from the difference Fourier map, but their positions were not refined. The contributions of these hydrogen atoms were included in structure-factor calculations. The final least-square cycle gave wR=0.1254, R=0.0511 for 5779 reflection with $I>2\sigma(I)$; the weighting scheme, w=1/[$S^2(F_o^2)$+(0.0603P)^2+0.7083P], where P=[(F_o^2) + 2F_c^2]/3. The max and min difference peaks and holes are 0.337 and $-$0.348 e. A^{-3}, respectively. S=1.038. Atomic scattering factors and anomalous dispersion corrections were taken from International Table for X-ray Crystallography.[77] Crystallographic data (excluding structure factors) for the structure have been deposited with the Cambridge Crystallographic Data Center as supplementary publication No. CCDC-616465.

1.3.3　Results and Discussion

In order to optimize the reaction conditions, the synthesis of **1.19a** was carried out under a variety of conditions. First, it was ascertained that microwave irradiation was beneficial, as the normal reactions without microwave irradiation were much slower, for example, the product was obtained in 64.9% yield after 4h of reaction as compared with the yield of 83.5% obtained in 10 min. under microwave irradiation (Table 1.8, entry 2, 11). In addition, we also examined the effects of reaction time on the preparation of Mannich-addition products. When the reaction time was increased from 5 min. to 10 min.,15 min. and 20 min., **1.19a** could be obtained in 78.9%, 83.5%, 82.7% and 81.8%, respectively (Table 1.8, entry 1-4). When the reaction time was prolonged further to 25 min, no improvement was noted (82.8%, entry 5), as compared to that obtained after 10 min. (83.5%, entry 2). The effect of reaction temperature was also studied and it is seen that the yield was relatively lower when the reactions were carried out at 60 or 80℃ (Table 1.8, entry 6, 7) than at 100℃ (entry 2). A lower yield was observed when the reaction system was heated to 120℃, and practically negligible yield was noticed when the reaction system was heated to 140℃ (Table 1.8, entries 9, 10). Consequently, it is practical to perform the reaction at 100℃ than at a lower or higher temperature.

Using the optimized condition, the best result was obtained when bis (2-methoxyethyl) phosphite or bis(2-ethoxyethyl) phosphite was treated with 1 equiv. of substituted benzaldehyde and 1 equiv. of aniline under microwave conditions without solvent or catalyst at 100℃ for 10 min. Under these reaction conditions, the Mannich reactions proceeded smoothly, and the results are summarized in Table 1.9.

Table 1.8   Different reaction conditions for the microwave irradiation synthesis of **1.19a**

Entry	Reaction time (min)	Power(W)	Reaction temp (℃)	Yield[c] (%)
1[a]	5	50	100	78.9
2[a]	10	50	100	83.5
3[a]	15	50	100	82.7
4[a]	20	50	100	81.8
5[a]	25	50	100	82.8
6[a]	10	50	60	5.0
7[a]	10	50	80	51.2
8[b]	10	—	100	0
9[a]	10	50	120	65.7
10[a]	10	50	140	0
11[b]	240	—	100	64.9

[a]Reaction conditions: stirred under microwave irradiation in a Discover Synthesis instrument at 50W;
[b]stirred without microwave irradiation; [c]Yields of isolated products.

Table 1.9   Yields of the title compounds **1.19**[a]

Compd.	R^1—	R^2—	R^3—	Yields (%)[b]
1.19a	2-F	$4\text{-}CF_3C_6H_4$	CH_3	83.5
1.19b	H	$4\text{-}CF_3C_6H_4$	CH_3	81.3
1.19c	2-F	6-methoxybenzothiazol-2-yl	CH_3	76.5
1.19d	2-F	$3\text{-}NO_2C_6H_4$	CH_3	79.8
1.19e	3,4,5-trimethoxy	$4\text{-}CF_3C_6H_4$	CH_3	70.6
1.19f	4-F	$4\text{-}CF_3C_6H_4$	CH_3	73.6
1.19g	$2\text{-}CF_3$	$4\text{-}CF_3C_6H_4$	CH_3	56.8
1.19h	$3\text{-}CF_3$	$4\text{-}CF_3C_6H_4$	CH_3	79.2
1.19i	3,4,5-trimethoxy	$4\text{-}CF_3C_6H_4$	C_2H_5	78.6
1.19j	2-F	$4\text{-}CF_3C_6H_4$	C_2H_5	81.6
1.19k	H	$4\text{-}CF_3C_6H_4$	C_2H_5	82.8
1.19l	2-F	$3\text{-}NO_2C_6H_4$	C_2H_5	80.5

[a]Reaction conditions: stirred under microwave irradiation in a Discover Synthesis instrument at 50W;
[b]Yields of isolated products.

The structures of title compounds **1.19a-1.19l** were established on the basis of their spectroscopic data. They showed IR absorption bands at 3200-3500 (NH) and 1520-1616 cm^{-1}(C=C) (skeleton vibration of aromatic ring), the absorption at 1220-1250 cm^{-1} was assigned to the P=O stretching absorption bands and that at 990-1100 cm^{-1}was attributed to the C-O stretching absorption bands in the P-O-C group. In the ^{1}H NMR, all phenyl protons showed multiplets at 6.19-7.78 ppm. The chemical shifts of the ester PCH were centered around 4.85-6.17 ppm.

Antifungal activity bioassay. The antifungal bioassay results are given in Table 1.10. It can be seen that these newly synthesized derivatives exhibit weak

antifungal activities. At 500 µg/mL, α-aminophosphonates containing alkoxyethyl moiety **1.19a-1.19l** exhibited weak activities on *Fusarium oxysporum*, *Valsa mali* and *Gibberella Zeae*, which are obviously lower than that of hymexazol standard.

Table 1.10 Inhibitory effects on phytopathogenic fungi at 500 µg/mL

Compd.	*Fusarium oxysporum*	*Gibberella zeae*	*Valsa mali*
1.19a	51.2	42.8	50.3
1.19b	36.7	30.2	33.5
1.19c	8.4	11.8	8.9
1.19d	12.4	17.9	15.5
1.19e	6.1	10.7	5.7
1.19f	2.1	6.9	3.2
1.19g	0	0	0
1.19h	12.1	23.1	11.0
1.19i	10.0	0	2.0
1.19j	23.1	9.0	30.9
1.19k	33.0	2.9	40.1
1.19l	20.0	1.0	43.4
hymexazol	100	90.0	82.3

Antiviral activity bioassay. The results of the *in vivo* bioassay against Tobacco Mosaic Virus (TMV) are given in Table 1.11. Ningnanmycin was used as the reference antiviral agent. The results indicated that the change of substituents affected the antiviral activity. When R^1 is H, R^2 is a 4-trifluoromethyl group and R^3 is CH_3, compound **1.19b** showed curative rate of 56.5% against TMV at 500 µg/mL, slightly higher than that of reference (53.8%). The inhibitory rates of compounds **1.19i**, **1.19d**, **1.19e**, **1.19c** and **1.19g** at the same concentration were 53.1%, 51.6%, 51.3%, 49.2% and 46.0%, respectively. These compounds have slightly lower antiviral activities than that of the reference compound. The other compounds **1.19a**, **1.19k**, **1.19f**, **1.19h**, **1.19j** and **1.19l** exhibited weak anti-TMV bioactivities, with the inhibitory rates of 38.8%, 34.3%, 34.2%, 25.0%, 16.2% and 13.8%, respectively, at 500 µg/mL.

Crystal Structure Analysis. As it can be seen from the X-ray single crystal structure of **1.19l** (Fig 1.2), the dihedral angle between the C(8)-C(7)-N(2)-C(5)

Table 1.11 The curative effects of the new compounds **1.19** against TMV *in vivo*

Agents	Ningnanmycin	**1.19a**	**1.19b**	**1.19c**	**1.19d**	**1.19e**	**1.19f**
Concentration (mg/L)	500	500	500	500	500	500	500
Inhibition rate (%)	53.8	38.8	56.5	49.2	51.6	51.3	34.2

Agents	**1.19g**	**1.19h**	**1.19i**	**1.19j**	**1.19k**	**1.19l**	
Concentration (mg/L)	500	500	500	500	500	500	
Inhibition rate (%)	46.0	25.0	53.1	16.2	34.3	13.8	
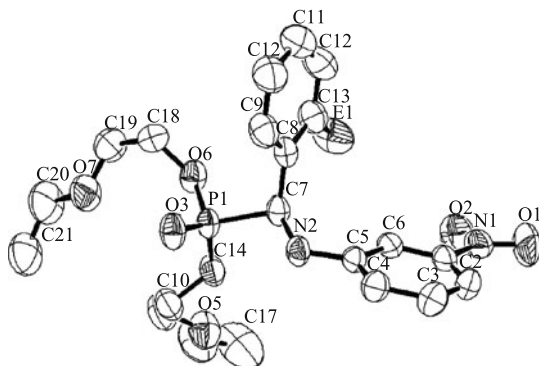
Fig 1.2 X-ray single crystal structure of **1.19l**

plane is −72.3(2)°. The N-H···O type of intermolecular interaction plays a major role in stabilizing the molecules in the unit cell. As shown in the packing diagram of the unit cell of compound **1.19l** (Fig 1.3), there is an intermolecular hydrogen bond in the form of N(2)-H(2)···O(3) (symmetry code-*x*,-*y*+1/2,-*z*+1/2) with N(2)-H(2)=0.860Å, H(2). O(2)=2.1866, N(2))···O(3)=2.892(3)Å, N(2)-H(2)···O(3)= 139.81°. In the solid state, the above hydrogen bonds connecting the molecules via hydrogen bond networks are responsible for imparting stabilization to the crystal structure.
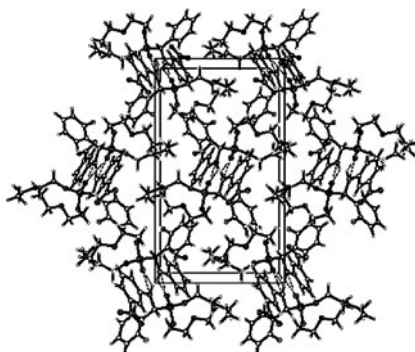
Fig 1.3 Packing diagram of the unit cell

1.3.4 Conclusions

In summary, the described novel method of the formation of α-aminophos-phonates containing alkoxyethyl moieties under microwave irradiation offers several advantages. The synthetic route is facile and affords the product in good yields under environment-friendly conditions. It was also found that title compounds **1.19b**, **1.19i**, **1.19d**, and **1.19e** displayed good antiviral activities.

1.4   Green Synthesis & Bioactivity of Brominated α-Amino-phosphonates

1.4.1   Introduction

α-Aminophosphonates, as discussed earlier, structural analogues of natural amino acids, have received wide attention in medicinal, bioorganic and organic chemistry. The applications of α-aminophosphonates have ranged from agriculture to medical science as anti-cancer agents,[78] enzyme inhibitors,[79] peptide mimetics,[80] antibiotics and pharmacological agents.[81,82] To the best of our knowledge, only a few α-aminophosphonates containing bromo and 3,4,5-trimethoxybenzyl groups have been reported. As a typical halogen, bromine has high electronegativity and is also known for its steric and lipophilic effects. As an active group, bromine is often introduced in the design of bioactive compounds. Many pesticides containing bromine are widely used commercially, and have a broad spectrum of activity, high efficiency and low toxicity, associated with their easy decomposition and minimal residues.[83] On the other hand, gallic acid derivatives are of considerable biological and pharmaceutical significance.[84, 85] Among them, 3,4,5-trimethoxybenzaldehyde (TMB) is an important pharmaceutical intermediate, which is employed, among other examples, in the synthesis of trimethoprim, tretoquinol and podophyllotoxin.[86,87]

Therefore, a series of α-aminophosphonates containing bromo and 3,4,5-trimethoxybenzyl groups were designed and synthesized in our laboratory for the purpose of exploring them as potential bioactive compounds. Substituted α-aminophosphonates are often synthesized in an organic solvent via a traditional Kabachnik-Fields reaction,[88] but the use of organic solvents has a serious impact on the environment, whereas in contrast, solvent free reactions are benign and do not call for any drastic work-ups.

An easy one pot synthesis of new α-aminophosphonates **1.22a-1.22g** by Kabachnik-Fields reaction of equimolar mixtures of 3,4,5-trimethoxybenzaldehyde (TMB) and p-or m- bromoaniline with dialkyl phosphite under solvent-free conditions has been explored in our laboratory (Scheme 1.6).

R[1] = m-Br, p-Br   R[2] = Et, i-Pr, n-Pr, n-Bu
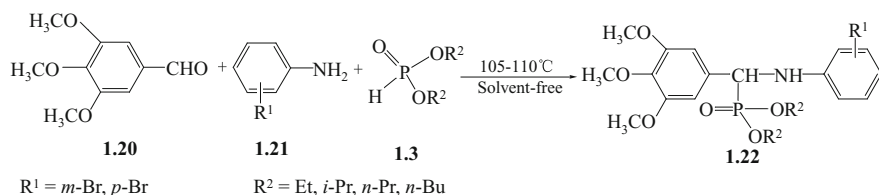
Scheme 1.6   Synthesis of compounds **1.22a-1.22h** by the Kabachnik-Fields reaction

The TMB, the starting material **1.20**, was prepared in turn in high yield from gallic acid (abundant in plant gallnut) in four steps: etherification, esterification, hydrazidation and potassium ferricyanide oxidation (Scheme 1.7).
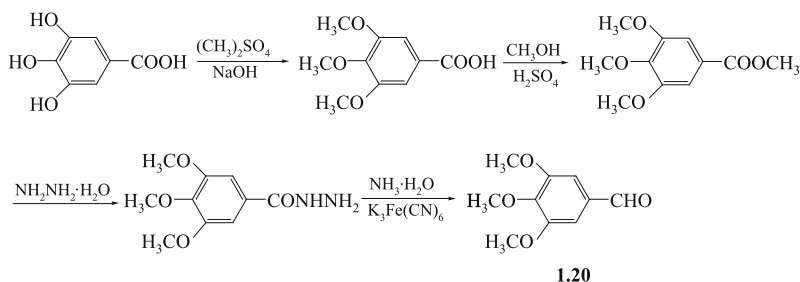
Scheme 1.7   Synthesis of the starting material **1.20** from gallic acid

1.4.2   Materials and Methods

The materials and instruments for determination of the structure and physical data of new compounds are basically similar to the procedure described in Chapter 1.1.2. TMB was prepared from gallic acid according to literature methods.[88−90] *O,O*-Dialkyl phosphites were prepared as described in the literature.[63]

General procedure for the preparation of products **1.22a-1.22h.** A mixture of 3,4,5-trimethoxybenzaldehyde (3 mmol), *p*-(or *m*-) bromoaniline (3 mmol) and dialkyl phosphite (3 mmol) was stirred in silicone oil bath at 108℃ for 2 h. The reaction was followed and monitored by TLC (petroleum: ether-ethyl acetate= 1:2, *v/v*). The resultant viscous liquid was dissolved in ether and then washed, first with saturated aqueous $NaHCO_3$ followed by distilled water. The organic layer was separated and then the aqueous layer was extracted with ethyl acetate (3×10 mL). The combined organic layers were dried over $MgSO_4$ and concentrated under reduced pressure. The residue was purified by recrystallization from petroleum ether to give compounds **1.22a-1.22h** as white crystals. At the same time, compounds **1.22a-1.22h** were also synthesized using BF_3 •Et_2O as catalyst by a similar procedure. The represervative data for **1.22a** is shown below, while data for **1.22b-1.22h** can be found in the Supporting Information of Reference.[163]

O,O′-diethyl-α-(4-bromophenylamino)-3,4,5-trimethoxybenzylphosphonate. (1.22a). mp 123-124℃; IR (KBr): v_{max} 3398.6, 1591.3, 1242.2, 1055.1, 1029.9; ^1H NMR (500 MHz, CD_3COCD_3): δ 6.82-7.18 (m, 6H, Ar-H), 4.65 (d, *J*=24.0 Hz, 1H, CH-P), 3.95-4.15 (m, 4H, 2OCH_2), 3.69-3.79 (m, 9H, 3OCH_3), 3.06 (br s, 1H, NH), 1.12-1.27 (m, 6H, 2CH_3); ^{13}C NMR (125 MHz, CD_3COCD_3): δ 16.75, 55.30, 56.42, 56.52, 60.49, 63.59, 106.71, 109.51, 116.53, 132.34, 132.75, 138.63, 147.60, 154.23; ^{31}P NMR (200MHz, CD_3COCD_3, H_3PO_4): δ 22.78; Anal. Calcd. for $C_{20}H_{27}BrNO_6P$ (488.31): C, 49.19; H, 5.57; N, 2.87. Found C, 49.28; H, 5.54;

N, 3.09.

X-Ray diffraction experiment. The experiment and method for X-ray diffraction data of compound **1.22g** are similar to the procedure described in Chapter 1.3.2.[75−77] Crystallographic data for the structure **1.22g** have been deposited with the Cambridge Crystallographic Data Center as supplementary publication No. CCDC-616465.

Antiviral Bioassay. The method for evaluating anti-TMV activity of title compounds is similar to the procedure described in Chapter 1.1.2.[49,50]

1.4.3   Results and Discussion

A systematic study of the effect of reaction parameters on the process, including reaction temperature, the molar ratios of reagents and the amount of catalyst, was undertaken for optimization of the reaction. For this purpose, compound **1.22g** was synthesized under different conditions.

In the beginning, the effect of reaction temperature was investigated. When the reaction temperature was increased from 85-90℃ to 95-100℃ and then to 105-110℃, the yields obtained were 37.5%, 61.2% and 65.6%, respectively (Table 1.12, entry 1-3). When the temperature was further increased to 115-120℃, no improvement was noticed (56.3%, Table 1.12, entry 4), compared to the results obtained in the temperature range 105-110℃ (entry 3). Next, the effect of molar ratio of the reagents was investigated in the range 105-110℃. As the molar ratio of the reagents (dialkyl phosphate/amine/aldehyde) was varied from 1:1:1, 1.2:1:1 to 2:1:1, no significant changes were observed in the yields (65.6%, 61.8%, 60.3%, respectively Table 1.12, entry 3, 5 and 6).

Table 1.12   The influence of the molar ratio of reagents (dialkyl phosphate: amine: aldehyde) and the reaction temperature on the synthesis of compound **1.22a**

Entry	molar ratio	Reaction temp(℃)	Reaction time(h)	Yield(%)
1	1:1:1	85-90	2	37.5
2	1:1:1	95-100	2	61.2
3	**1:1:1**	**105-110**	**2**	**65.6**
4	1:1:1	115-120	2	56.3
5	1.2:1:1	105-110	2	61.8
6	2:1:1	105-110	2	60.3

The yield of the product was found to be significantly lower under otherwise similar conditions when no catalyst was used (Table 1.13, entry 2). The yield was improved as the amount of catalyst was increased from 5 mol% to 10 mol% (Table 1.13, entry 3, 4), but no noteworthy change was observed when the amount of catalyst used was increased to 15 mol% (Table 1.13, entry 5). Based on these

results, the optimal conditions for the synthesis were established with the use of equivalent molar concentrations of the reactants and 10 mol% $BF_3 \cdot Et_2O$ at a reaction temperature of 105-110℃ and a reaction time of 30 min.

Table 1.13   The influence of the amount of catalyst $BF_3 \cdot Et_2O$
on the synthesis of compound **1.22a**

Entry	Catalyst	Amount of catalyst(mol %)	Reaction time(min)	Yield(%)
1	—	—	120	65.6
2	—	—	30	41.0
3	$BF_3 \cdot Et_2O$	5	30	66.6
4	**$BF_3 \cdot Et_2O$**	**10**	**30**	**76.0**
5	$BF_3 \cdot Et_2O$	15	30	71.7

As may be seen from Table 1.14, using optimal conditions and with 10 mol% $BF_3 \cdot Et_2O$ catalyst, the compounds **1.22a-1.22h** could be obtained in high yields (70.6%-83.5%) in much shorter reaction time (30 min). The compounds **1.22a-1.22h** were obtained in 61.3%-74.2% yield when the reaction was conducted for longer periods of time (2 h), but without the use of a catalyst.

Table 1.14   Yields of compounds **1.22a-1.22h.**

Compd.	Substitutents		With Catalyst		Without Catalyst	
	R^2	R^1	Reaction time (min)	Yield (%)	Reaction time(h)	Yield (%)
1.22a	Et	*p*-Br	30	76.0	2	65.6
1.22b	Et	*m*-Br	30	75.9	2	61.5
1.22c	*i*-Pr	*p*-Br	30	82.0	2	67.8
1.22d	*i*-Pr	*m*-Br	30	81.0	2	71.0
1.22e	*n*-Bu	*p*-Br	30	76.1	2	62.5
1.22f	*n*-Bu	*m*-Br	30	70.6	2	61.4
1.22g	*n*-Pr	*p*-Br	30	83.5	2	74.2
1.22h	*n*-Pr	*m*-Br	30	75.8	2	61.3

The structures of compounds **1.22a-1.22h** were identified by elemental analysis, IR, ^1H, ^{13}C and ^{31}P NMR spectral data. Taking compound **1.22g** as an example, the absorption band at 3400 cm^{-1}(s) in its IR spectrum corresponds to an N-H stretch, the absorption bands at 1240 cm^{-1}(s) and 1001 cm^{-1}(s) correspond to P=O and P-O-C stretching, respectively. The ^1H NMR spectra of **1.22g** showed well-resolved doublets at δ 4.64 (J_{P-H}=24.05 Hz) for the P(O)CH proton, while a singlet at δ 3.04 was due to the presence of the NH proton. In the ^{31}P NMR spectra, the phosphonate group resonance appeared at δ_P 22.69. The structure of compound **1.22g** was further confirmed by X-ray diffraction analysis.

Crystal Structure Analysis of **1.22g**. The crystal belongs to the tetragonal system with space group P 2(1)/c, *a*=12.7429(14) nm, *b*=14.1740(16) nm, *c*=4.2643(15) nm, α=90.00°, β=107.360(6)°, γ=90.00°, *V*=2459.0(5) nm³, *Z*=4,

Dc=1.395 mg/m^3, μ=1.77 mm^{-1}, F (000)=1072.0. The molecular structure and cell packing of the compound are presented in Fig 1.4 and Fig 1.5, respectively. As shown in Table 1.15, there is one N-H⋯O hydrogen bond intermolecular interaction. The N(1)-O(4) bond distance is 2.960 nm and N(1)-H(1)⋯O(4) bond angle is 165.94° (Table 1.15). In the solid state, the hydrogen bonds form a two-dimensional network to stabilize the crystal structure.

Antiviral activity bioassays. The results of the *in vivo* activity against TMV bioassays are given in Table 1.16. Ningnanmycin was used as reference antiviral
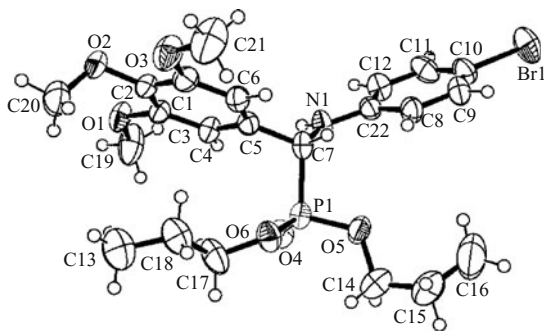
Fig 1.4   Molecular structure of compound **1.22g**
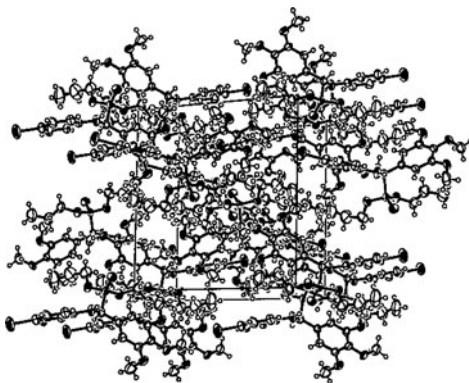
Fig 1.5   Cell packing of the compound **1.22g**

Table 1.15   Hydrogen bonds for compound **1.22g**

D-H⋯A	d(D-H)/nm	d(H-A)/nm	d(D-A)/nm	∠DHA(°)
N(1)-H(1)⋯O(4)	0.860	2.118	2.960	165.94

[*]Symmetry transformations used to generate equivalent atoms: #1: −x+1, −y, −z+2

Table 1.16   The curative effect of title compounds **1.22a-1.22h** at 500 μg/mL against TMV

Compd.	1.22a	1.22b	1.22c	1.22d	1.22e	1.22f	1.22g	1.22h	Ningnamycin
Inhibition rate (%)	35.0	23.8	28.0	26.2	22.5	11.7	44.3	54.5	57.5

agent. The data indicate that a change in the substituent might also affect the curative activity of title compounds **1.22a-1.22h**. Compound **1.22h**(R^1=*n*-Pr, R^2=3-Br) and compound **1.22g**(R^1=*n*-Pr, R^2=4-Br) could cure TMV up to 54.5% and 44.3% at 500 μg/mL. All other compounds have relatively lower curative activities than **1.22h** and **1.22g**.

1.4.4   Conclusions

A series of α-aminophosphonates **1.22a-1.22h** containing bromo and 3,4,5-trimethoxybenzyl group was synthesized by Kabachnik-Fields reaction under solvent-free conditions. The procedure offers a great alternative to existing methodologies due to its ease of work up, faster reaction rates and high yields. The method is clean, free of any significant byproducts, environmental friendly and does not employ any solvent. A half-leaf method was used to determine the curative efficacy *in vivo* of the eight title products against tobacco mosaic virus (TMV). It was found that compound **1.22h** had a good curative effect *in vivo* against TMV, with an inhibition rate of 54.5%.

1.5   Synthesis & Bioactivity of α-Aminophosphonates Containing Trifluorinated Methyl Moiety

1.5.1   Introduction

The importance of 1-aminoalkylphosphonic acids and their derivatives is well known.[91,92] Compounds of this type are widely used in agrochemistry as plant growth regulators,[93] antibacterial agents[94,95] and herbicides.[96] Some representatives find application in therapy and diagnostics medicine.[97,98] According to recent data, α-aminoalkylphosphonate derivatives have great potential for the design of therapeutic agents, including antitumor drugs.[99−101] In order to find new plant virucides, we had earlier designed and synthesized a series of 1-(4-trifluoromethyl-phenyl)-1-aminoalkylphosphonates, some of which displayed good anti-TMV activity.[102,104] Fluorinated compounds in general and fluorinated heterocycles in particular, are of enormous interest in modern medicinal chemistry. Pharmacological agents bearing a trifluoromethyl group are of great demand as they exhibit broad biological properties[105,106], and are often employed as herbicides,[107] antihyperglycemic agent,[108] insecticides,[109] antipyretic agents,[110] and inhibitors for platelet aggregation.[111] Recently, much attention has been focused on their application as antiviral and antitumor agents after the discovery of the trifluoromethyl-sub-

stituted pyrazole C-glycoside pyrazofurin.[112,113] Considering the wide application of these compounds and potential to serve as antiviral and anticancer agents, we decided to reserve the bioactive unit and replace the phenyl group by 4-trifluoromethylphenyl or 3-fluorophenyl in dialkyl (phenylamino)-(fluorophenyl) methylphosphonate. Thus, we designed a series of novel dialkyl (4-trifluoromethyl phenylamino)-(4-trifluoromethyl or 3-fluorophenyl) methylphosphonates.

A typical method for the synthesis of substituted α-aminoalkylphosphonate is the three component reaction of aldehydes, amine and dialkyl phosphite by one pot Mannich type method.[114]However, the reported methods generally involved high reaction temperature, harmful solvents and expensive reagents along with limitations such as long reaction time, low yields and complex handling. To avoid these disadvantages, a couple of modifications including using montmorillonite clay[115] and alumina[116] in dry media under microwave irradiation have recently been reported. Using montmorillonite clay and alumina catalyst in accordance with the reported method,[115,116] the reaction of fluorobenzaldehydes and 4-trifluoromethylaniline with dialkyl phosphite under microwave irradiation was often unpredictable and resulted in low yield of the title compound. As a part of our green technology program, we studied a practical green alternative to synthesize α-aminoalkylphosphonate by a three-component condensation of aldehydes, amine and dialkyl phosphite at 75-80 ℃ under microwave irradiation using $BF_3 \cdot Et_2O$ catalyst without any solvent. The synthetic route is shown in Scheme 1.8. The advantages of the procedure are short reaction period, high yield and simple work up.

R¹=4-CF₃, 2-F, 3-F, 4-F, 4-Cl, H; R²=Me, Et, *i*-Pr, *n*-Pr, *n*-Bu
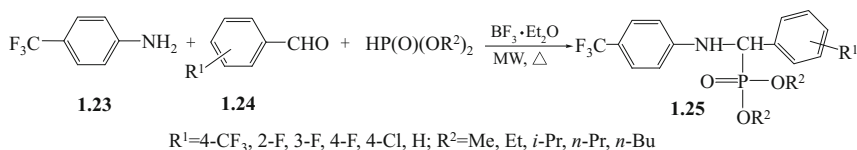
Scheme 1.8   Synthetic route to substituted α-aminoalkylphosphonate

The structures of **1.25** were firmly established by well defined IR, ¹H NMR, ¹³C NMR, ¹⁹F NMR and elemental analysis. The anticancer activity was assayed by the MTT method for all products. Some of the compounds displayed moderate antiviral activities in vivo and good anticancer activities for two cells (PC3 and A431) *in vitro*.

1.5.2   Materials and Methods

1.5.2.1   Instruments

The materials and instruments for determination of the structure and physical data of new compounds are basically similar to the procedure described in Chapter

1.1.2. Microwave reaction was performed on a Beijing XH-100A microwave catalysis synthesis and extracts appearance (with a power of 750-900 W).

1.5.2.2   General procedure for the preparation of products 1.25a-1.25i

A mixture of 4-trifluoromethylaniline (5 mmol), 3-fluorobenzaldehyde (5 mmol), and dialkyl phosphite[63] (5 mmol) and $BF_3 \cdot Et_2O$ (0.2 mmol) was irradiated in the microwave catalysis synthesis and extracts appearance at 78-80℃ for 20 min. The reaction was followed and monitored by TLC (petroleum ether + ethyl acetate=2+1 by volume). After the reaction was completed (1h), the residue was washed with water, filtered, dried, then the crude solid was purified by column chromatography on silica gel using petroleum ether/ethyl acetate ($v:v$=2:1) as eluent to give **1.25a-1.25e**. The reperesentative data for **1.25a** is shown below, while data for **1.25b-1.25e** can be found in the Supporting Information of Reference.[29]

Di-i-propyl(4-Trifluoromethylphenylamino)-(3-fluorophenyl)-methylphosp honate. (1.25a). Colorless crystals; yield 89.0%, mp 113-114℃. IR (KBr): v_{max} 3275.1 (NH), 1616.3 (C=O), 1282.6 (P=O), 1062.7 (P-O-C); ^{1}H NMR (400 MHz, CDCl$_3$): δ 6.60-7.35 (m, 8H, Ar-H), 5.34 (b, 1H, NH), 4.70-4.77 (m, 1H, OCH), 4.67 (s, 1H, CH-P), 4.47-4.55 (m, 1H, OCH), 0.97-1.34 (m, 12H, $4 \times$ CH$_3$); ^{13}C NMR (125 MHz, CDCl$_3$): δ 164.43, 162.00, 149.31, 149.18, 138.77, 138.67, 130.42, 130.39, 130.33, 126.86, 126.33, 123.91, 123.88, 123.85, 123.64, 120.49, 120.16, 115.42, 115.39, 115.26, 115.21, 115.03, 114.98, 113.23, 72.86, 72.79, 72.65, 72.59, 56.80, 55.29, 24.44, 24.41, 24.06, 24.01, 23.52, 23.46, 14.46; ^{19}F NMR (CDCl$_3$, TFA): δ $-$62.12, $-$121.01; Anal. Calcd. for $C_{20}H_{24}F_4NPO_3$: C, 55.43; H, 5.58; N, 3.23. Found: C, 55.40; H, 5.45; N, 3.20.

General method for the preparation of dialkyl (4-trifluoromethylphenyla-mino)-(4-trifluoromethylphenyl)-methylphosphonate **(1.25f-1.25i).** A mixture of 4-trifluoromethylaniline (5 mmol), 4-trifluoromethylbenzaldehyde (5 mmol), and dialkyl phosphite[63] (5 mmol) and $BF_3 \cdot Et_2O$ (0.2 mmol) was irradiated in the microwave catalysis synthesis and extracts appearance at 78-80℃ for 20 min. The reaction was followed and monitored by TLC (petroleum ether:ethyl acetate= 5:1 by volume). After the reaction was completed, the residue was washed with water, filtered, dried, then the crude solid was purified by recrystallization from ethanol three times to give **1.25f-1.25i** as a colorless solid. The reperesentative data for **1.25f** is shown below, while data for **1.25g-1.25o** can be found in the Supporting Information of Reference.[29]

Dimethyl(4-trifluoromethylphenylamino)-(4-trifluoromethylphenyl)-methyl phos-phonate (1.25f). Colorless crystals; yield 65.8%, mp 121-123℃. IR (KBr): v_{max} 3292.4 (NH), 1614.4 (C=O), 1240.2 (P=O), 1064.7 (P-O-C); MS: 427 (M$^+$), 318, 298, 248, 172, 145, 127, 109, 95, 81, 79, 63, 45, 31, 18; ^{1}H NMR (400 MHz, CDCl$_3$): δ 6.58-7.64 (m, 8H, Ar-H), 5.21 (t, 1H, J=7.8 Hz, NH), 4.96 (dd, 1H, J=24.8, 7.2 Hz, CH-P), 3.81 (d, 3H, J=10.8 Hz, CH$_3$), 3.55 (d, 3H, J=10.8 Hz,

CH$_3$); ^{13}C NMR (125 MHz, CDCl$_3$): δ 148.34, 148.20, 139.22, 128.01, 127.96, 126.69, 126.66, 125.84, 120.79, 113.03, 55.75, 54.26, 54.05, 53.98; ^{19}F NMR (470 MHz, CDCl$_3$, TMS): δ $-$118.90, $-$120.09; Anal. Calcd. for C$_{17}$H$_{16}$F$_6$NPO$_3$: C, 47.78; H, 3.77; N, 3.27. Found: C, 47.69; H, 3.60; N, 3.12.

1.5.2.3   MTT assay against cell proliferation

All compounds tested were dissolved in DMSO (1-100 μM) and subsequently diluted in the culture medium before treatment of the cultured cells. Tested cells were plated in 96-well plates at a density of 3×10^3 cells/well/100 μL of the proper culture medium and treated with the compounds at concentration of 1-100 μM for 48h. In parallel, the cells were treated with 0.1% of DMSO as control. An MTT [3-(4, 5-dimethylthiazol-2-yl)-2,5-diphenyltetrazolium bromide] assay (Roche Molecular Biochemicals) was performed according to the instructions provided by Roche. This assay is based on the cellular cleavage of the tetrazolium salt, MTT, into a formazan that is insoluble in the cell culture medium and is directly measured at 550 nm in 96-well assay plates. Absorbance is directly proportional to the number of living cells in culture. The two types of cells used in these studies, PC3 (prostate cancer) and A431 (uterus cancer) cell lines (provided by Cell Bank of Committee on Type Culture Collection of Chinese Academy of Science) were cultivated in F-12 medium (for PC3) or RPMI 1640 medium (for A431) supplemented with 10% fetal bovine serum (provided by TBD & HY Bio. Co.) and 2 mM of L-glutamine. Tissue culture reagents were obtained from Gibco Co.[117,118]

1.5.2.4   Antiviral Bioassay

The method for evaluating anti-TMV activity of title compounds is similar to the procedure described in Chapter 1.1.2.[49,50]

1.5.3   Results and Discussion

1.5.3.1   Chemistry

In order to optimize the reaction conditions, the synthesis of **1.25e** was carried out under several conditions. In the beginning, attempt was made to confirm the utility of microwave irradiation compared to conventional method. In the normal reaction conditions without microwave irradiation, the reaction was much slower and the yield of the product **1.25e** was poor, for example, when the time was prolonged to 14 h compound **1.25e** could be obtained in 87.8% yields as compared with the yield of 92.1% in 20 min under microwave irradiation (Table 1.17, entry 5). In addition, we also examined the effects of reaction temperature and reaction time on the Mannich addition reactions (Table 1.17, entry 1-3, 9-14). When the reaction time was prolonged from 5 min to 30 min, the yield of **1.25e**

was increased from 83.1% to 93.5% (Table 1.17, entry 1-4). On extending the reaction time further to 30 min under microwave irradiation, tiny improvement of yield (93.5%, Table 1.17, entry 4) was obtained compared to that of 20 min (92.1%, Table 1.17, entry 3). As for the reaction temperature, it could be seen that the yield was relatively lower when the reaction was carried out at room temperature (Table 1.17, entry 9) than that at 80℃ (Table 1.17, entry 3). No substantial improvement was observed when the reaction system was heated to 90℃ (Table 1.17, entry 14). Hence, it is convenient to perform the reaction at 80℃ than at a lower or higher temperature. As for the reaction power of microwave irradiation, it could be observed that when the reaction power was increased from 500 to 600, 750, 800 and 900 W, the yield of **1.25e** was 56.1%, 63.3%, 92.1%, 91.3% and 87.8%, respectively (Table 1.17, entry 3,5-8). Hence, optimal power for the reaction was selected at 750W and no noticeable improvement was observed when the reaction power varied from 800 to 900 W under microwave irradiation (Table 1.17, entry 7 and 8).

Table 1.17   Different conditions used for the microwave assisted synthesis of **1.25e**

Entry	Reaction time (min)	Power (W)	Reaction temp (℃)	Yeild^a (%)
1	5	750	80	83.1
2	10	750	80	85.5
3	20	750	80	92.1
4	30	750	80	93.5
5	20	500	80	56.1
6	20	600	80	63.3
7	20	800	80	91.3
8	20	900	80	87.8
9	20	750	25	33.1
10	20	750	40	50.1
11	20	750	50	61.1
12	20	750	60	69.9
13	20	750	70	80.5
14	20	750	90	82.2

^{a}Yields of isolated products; Reaction condition: stirred under microwave irradiation by 4% BF$_3$ • Et$_2$O in a Model XH-100C microwave synthesis instrument at 750-900 W.

In our experiment, we also screened BF$_3$ • Et$_2$O, Sc(TfO)$_3$ and TsOH catalysts. The results demonstrated that the presence of BF$_3$ • Et$_2$O can accelerate the addition reaction. Moreover, when TsOH and Sc(TfO)$_3$ instead of BF$_3$ • Et$_2$O were used as catalysts in the present reaction, no remarkable improvement of the yield of product was observed. For instance, with Sc(TfO)$_3$, **1.25e** was obtained in 75.1% yield within 20 min (Table 1.18, entry 3), while for TsOH, the yield of **1.25e** was 79.7% (Table 1.18, entry 1). When BF$_3$ • Et$_2$O was used as catalyst and the reaction was induced by microwave irradiation, great improvement in the yield,

approximately by 20%, was realized (Table 1.18, entry 2 Vs entry 8). When the reaction was catalyzed by $BF_3 \cdot Et_2O$ alone without microwave, the yield was only 38.0% (Table 1.18, entry 9), approximately 56% lower compared to that with microwave irradiation (Table 1.18, entry 2). Further, the effect of the amount of catalyst on the reaction was studied (Table 1.18, entry 2, 4-7). It could be seen from Table 1.18 that when the amount of catalyst was decreased from 10% to 8,6,4, and 2%, the yield of **1.25e** was 94.1%, 93.7%, 93.2%, 92.2% and 80.1%, respectively (entry 2,4-7). The product was obtained in 92.2% yield when 4% catalyst was employed (entry 6), indicating it as the ideal catalyst amount for this reaction.

Table 1.18   Effect of catalyst type and the catalyst amount on the synthesis of **1.25e**[a].

Entry	Catalyst	Catalyst amount (mol%)	Yield (%) [b]	Entry	Catalyst	Catalyst amount (mol%)	Yield (%) [b]
1	TsOH	10	79.7	6	$BF_3 \cdot Et_2O$	4	92.2
2	$BF_3 \cdot Et_2O$	10	94.1	7	$BF_3 \cdot Et_2O$	2	80.1
3	$Sc(T_fO)_3$	10	75.1	8	$BF_3 \cdot Et_2O$	0	74.4
4	$BF_3 \cdot Et_2O$	8	93.7	9[c]	$BF_3 \cdot Et_2O$	10	38.0
5	$BF_3 \cdot Et_2O$	6	93.2				

[a]All reactions were carried out at 78-80℃ for 20 min under microwave irradiation at 750 W; [b]Isolated yields; [c] The reactions were carried out at 78-80℃ for 20 min without microwave irradiation.

As shown in Table 1.19, with the fluorine substitution at 3-position of benzaldehyde, the reaction of 4-trifluoromethylaniline and dialkyl phosphite in the presence of $BF_3 \cdot Et_2O$ under microwave irradiation afforded the desired α-aminoalkylphosphonate products in excellent yields. Among the same class of compounds, the yield of products **1.25a-1.25e** obviously depended on the nature of alkyl substituents on the phosphite *e.g.* with the aldehyde R^1=3-F, the reaction at 78-80℃ gave **1.25e** and **1.25b** in high yields. The yields of the title compounds decreased in the order **1.25e>1.25b>1.25a>1.25c>1.25d**.

Table 1.19   Yields[a] and reaction conditions used for the microwave assisted synthesis of **1.25a-1.25i**

Entry	Product	Microwave method[b]		Classical method[c]	
		Reaction time	Yield(%)	Reaction time	Yield(%)
1	**1.25a**	20min	89.0	14h	78.3
2	**1.25b**	20min	90.9	14h	79.0
3	**1.25c**	20min	86.2	14h	68.9
4	**1.25d**	20min	83.1	14h	67.1
5	**1.25e**	20min	92.1	14h	87.8
6	**1.25f**	20min	65.8	14h	50.1
7	**1.25g**	20min	80.0	14h	66.1
8	**1.25h**	20min	75.9	14h	61.8

Continued

Entry	Product	Microwave method[b]		Classical method[c]	
		Reaction time	Yield(%)	Reaction time	Yield(%)
10	**1.25j**	20min	83.9	14h	68.1
11	**1.25k**	20min	79.4	14h	65.1
12	**1.25l**	20min	75.0	14h	64.9
13	**1.25m**	20min	57.1	14h	40.1
14	**1.25n**	20min	52.1	14h	39.7
15	**1.25o**	20min	58.9	14h	42.1

[a]Yields of isolated products; [b] Reaction condition: 4% $BF_3 \cdot Et_2O$, 78-80℃, with stirring under microwave irradiation in a Model XH-100C microwave synthesis instrument at 750 W; [c] Reaction condition: First reaction step: A mixture of 4-trifluoromethylaniline (5mmol) and 4-trifluoromethylbenzaldehyde (5mmol) and TsOH (0.2 mmol) in toluene (15 mL) was refluxed for 7h. Second reaction step: A mixture of N-(4 trifluoromethylphenyl)-2-(4-trifluoromethyl phenyl)imine (5 mmol), toluene (20 mL), and dialkyl phosphite (5 mmol) and 4-dimethylamino pyridine (DMAP, 0.15 mmol) was heated at 110-115℃ for 7 h.

The related analogues **1.25f-1.25i** for the same R^1=4-CF_3 were obtained with appropriate dialkyl phosphites by one pot method. Unfortunately, our trials on typical method turned out unsuccessful with low isolated yields of the products **1.25f-1.25i.** In our experiment, we also found the reactivity of Mannich addition for the dialkyl phosphite with 4-trifluoromethylaniline and 4-trifluoromethyl-benzaldehyde to decrease with incrasing number of carbon atoms in the dialkyl phosphite *e.g.* reactivity was lowered along the series dimethyl phosphite, diethyl phosphite, di-*n*-propyl phosphite and di-isopropyl phosphite under the same reaction conditions. The yields of the title products decreased in the order **1.25g**>**1.25h** >**1.25i**>**1.25f**. The effect could probably be explained by the steric demands imposed by the bulky substituents of alkyl groups of phosphite that could reduce their nucleophilic reactivity on 4-trifluoromethylaniline and 4-trifluorome-thylbenzaldehyde. Besides this, thermal stability factor may also play an important role, for example dimethyl phosphite is highly active but unstable at high tem-perature for longer reaction time. In conclusion, we have explored the addition reaction of dimethyl phosphite with 4-trifluoromethylaniline and 4-trifluorome-thylbenzaldehyde to obtain dimethyl (4-trifluoromethyl-phenylamino)-(4-trifluoro-methylphenyl)methylphosphonate in moderate yield. Under microwave irradiation using $BF_3 \cdot Et_2O$ catalyst, great improvement in the yield was achieved to afford **1.25** in 65.8%-92.1% yield within a shorter reaction time (20 min) than those conducted with $BF_3 \cdot Et_2O$ as catalyst without microwave irradiation (without $BF_3 \cdot Et_2O$ as catalyst). The best result was obtained when 4-trifluoromethylaniline was reacted with 1 equiv. of dialkyl phosphite and 0.04 equiv. $BF_3 \cdot Et_2O$ and 1 equiv. of 4-trifluorobenzaldehye or 3-fluorobenzaldehyde in solvent-free condition at 78-80℃ for 20 min. Under these conditions, Mannich-addition reaction proceeded smoothly.

The structures of all the products were confirmed by ^{1}H NMR, ^{13}C NMR, elemental analysis, IR, and mass spectrometry. The IR spectra of products **1.25** exhibited bands around 3275.1 (s)-3358.0 (s) cm^{-1}, indicating the presence of NH. The signals at 1609.2-1618.2 cm^{-1} were assigned to C=O vibrations. While the absorption at 1240.2 (s)-1286.7 (s) cm^{-1} was assigned to be P=O stretching absorption bands, 1062.7 (s)-1086.7 (s) cm^{-1} was due to the C-O stretching absorption bands in the P-O-C group. In ^{1}H NMR spectra, all phenyl protons showed multiplet at 6.577-7.642 ppm. The chemical shift of PCH of ester was observed near 4.512-5.122 ppm, the H atom at the α-C exhibited a singlet or doublet or dd peak due to the coupling with the P atom. The NH protons appeared at 5.206 and 5.356 ppm as a broad singlet or triplet due to the existence of hydrogen bond between P=O of phosphonate and NH of trifluoromethylphen-ylamino group in the molecular structure of **1.25** which moved the chemical shift of NH to the lower field region. All the carbon atoms in the compounds have been identified and the total number of protons calculated from the integration curve corresponds to the expected structure. The MS spectra revealed that the molecular ion peaks and fragmentation peaks were in accordance with the given structures of product **1.25**.

1.5.3.2 Biological Activity

The antitumor activity was assayed by the MTT method and listed in Table 1.20.[117,118] The results showed that these compounds exhibit certain activities against the two cancer cells *in vitro*. The compounds **1.25f-1.25i** have relatively higher antitumor activities than **1.25a-1.25e**. The antitumor data given in Table 1.20 indicates that the nature of fluorine and alkyl substitation affects antitumor activity of the compounds. For example, the inhibition rate of compound **1.25g** with R^1 as 4-CF$_3$, R^2 as Et attains 70.1% to PC3, and the inhibition rate of **1.25g** attains 65.2% to A431 at 10 μM.

The antiviral results are listed in Table 1.21. The preliminary biological tests showed that antiviral activities of the products are moderate or good. For example, the extent of inhibition of compound **1.25m** against TMV was 60.2% at a concentration of 500 mg/L.

Table 1.20   Inhibition ratio (%) (10 μM) of **1.25a-1.25i**[*]

Compd.	PC3 cells	A431 cells	Compd.	PC3 cells	A431 cells
1.25a	39.6	33.7	**1.25f**	49.7	48.2
1.25b	46.4	39.9	**1.25g**	70.1	65.2
1.25c	42.1	47.2	**1.25h**	59.2	58.1
1.25d	41.2	32.0	**1.25i**	55.2	50.2
1.25e	33.2	31.2			

[*]Inhibition ratio (%)=(A$_1$−A$_2$)/A$_1$100%. A$_1$: the mean optical densities of untreated cells, A$_2$: the mean optical densities of drug treated cells.

Table 1.21   The curative effects of title compounds **1.25a-1.25o**
against TMV at 500 μg/mL

Compd.	1.25a	1.25b	1.25c	1.25d	1.25e	1.25f	1.25g	1.25h
Inhibition rate (%)	30.1	28.2	15.1	30.1	25.1	40.1	34.2	37.1
Compd.	1.25i	1.25j	1.25k	1.25l	1.25m	1.25n	1.25o	
Inhibition rate (%)	30.9	41.6	40.7	15.1	60.2	41.0	18.0	

1.5.4   Conclusions

A series of novel dialkyl (4-trifluoromethylphenylamino)-(4-trifluoromethyl or 3-fluorophenyl) methylphosphonate was synthesized under microwave irradiation in one step. This one-pot method is an easy, rapid, and good-yielding reaction for the synthesis of α-aminophosphonates. The structures were verified by spectroscopic methods. The results of bioassay showed that the title compounds exhibit certain activity against PC3 and A431 cancer cells *in vitro* and anti-TMV activities. Diethyl (4-trifluoromethylphenylamino)-(4-trifluoromethyl-phenyl) methylphosphonate **1.25g** has better biological activity than its structurally related analogues **1.25a**, **1.25b**, **1.25c**, **1.25d**, **1.25e**, **1.25f**, **1.25h**, **1.25i**. against PC3 and A431 cancer cells.

Di-*i*-propyl (4-Trifluoromethylphenylamino)-(4-fluorophenyl) methylphosphonate **(1.25m)** has better biological activity than its structurally related analogaes **1.25a-1.25l**, **1.25n** and **1.25o.** The inhibitory rate of compound **1.25m** against TMV was 60.2% at 500 μg/mL.

1.6   Synthesis & Bioactivity of Chiral α-Aminophosphonates Containing Fluorine Moiety

1.6.1   Introduction

As evident from the discussions in the previous sections, α-aminophos-phonates and derivatives are used as plant growth regulators,[120] fungicides,[121] plant virucides[49] and herbicides,[69] and so on. A large volume of research on their synthesis and biological activities have been reported in the recent years.[14, 122-125] We had earlier designed and synthesized α-aminophosphonates containing fluo-rine and heterocyclic moiety, which exhibited moderate antiviral bioactivity agai-nst TMV and antitumor activity.[28, 69] It is not surprising that the absolute con-

figuration of the α carbon strongly influences the biological properties of **1.28**. For example, the *S*, *R* diastereomer of the antibiotic alafosfalin **1.29** offers considerably greater potency than the other three isomers against both Gram positive and Gram-negative bacteria.[126,127]
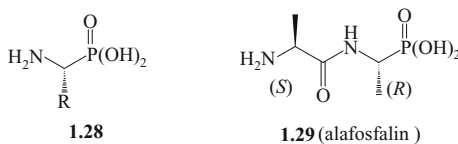
1.28   **1.29** (alafosfalin)

Recently organic reactions irradiated by microwave have been developed as safe and convenient method for the synthesis of α-aminophosphonates.[128] The application of microwave energy to accelerate organic reaction is of growing interest and offers several advantages over conventional techniques.[124] In view of these facts and in continuation to our interest on the chemistry of α-aminophosphonates, we designed and synthesized chiral α-aminophosphonates in moderate to high yields from (*R*) or (*S*)-1-phenylethylamine at 80℃ under microwave irradiation (Scheme 1.9).

The structures of **1.27** were firmly established by well defined IR, ^{1}H NMR, ^{19}F NMR, MS and elemental analysis. The bioassay tests showed that some of these chiral compounds exhibited good antifungal activity *in vitro*. All the compounds displayed week to moderate antiviral activities *in vivo*. To the best of our knowledge, this is the first report on antifungal and antiviral bioactivity of chiral α-aminophosphonates containing fluorine moiety.

1.6.2   Materials and Methods

The materials and instruments for determination of the structure and physical data of new compounds are basically similar to the procedure described in Chapter 1.1.2.

General procedure for the synthesis of title chiral compounds (**1.27**). A mixture of 2-fluoro or 2-trifluoromethylbenzaldehyde (15 mmol), dialkyl phosphite (15 mmol) and $BF_3 \cdot Et_2O$ (1.5 mmol) and (*R*) or (*S*)-1-phenylethanamine (15 mmol) was irradiated by 60 W microwave at 80℃ for 10 min. The mixture was poured into water and extracted by ether. The combined ether layer was dried with Na_2SO_4 and concentrated. The crude products were purified by column chromatography on a silica gel using ethyl acetate/petroleum ether (*v/v*, 1/4) as eluent to obtain the chiral compounds (*R*)-**1.27** and (*S*)-**1.27**. The reperesentative data for (*R*)-**1.27** is shown below, while data for the other chiral title compounds (**1.27b-j**) can be found in the reference.[129]

Diethyl[(R)-1-phenylethylamino]-(2-fluorophenyl)methylphosphonate[(R)-1.27a]. Colorless liquid; n_D^{20} 1.5170, yield 71.2%, $[\alpha]_D^{20}$ +28.05 (*c* 0.8804,

acetone). IR (KBr): ν_{max} 3296, 3065, 3030, 2980, 2940, 1614, 1585, 1487, 1393, 1244, 1230, 1165, 1096, 1053, 966.^{1}H NMR (400 MHz, CDCl$_3$): δ 1.03-1.11 (m, 3H, CH$_3$), 1.25-1.38 (m, 6H, 2$\times$CH$_3$), 2.42 (br, 1H, NH), 3.52-4.31 (m, 5H, 2$\times$ CH$_2$O$+$CH-Ar), 4.53 (d, 1H, J=24.0 Hz, CH-P), 6.98-7.56 (m, 9H, Ar-H); ^{19}F NMR (470 MHz, CDCl$_3$, CF$_3$COOH): δ 62.21; MS (EI, 70 eV) m/z: 365 (M$^+$). Anal. Calcd. for C$_{19}$H$_{25}$FNO$_3$P: C 62.46, H 6.90; N 3.83. Found: C 62.32, H 6.72, N 3.92.

　　Antifungal activity bioassay. The method for evaluating antifungal activity of title compounds **1.27** is similar to the procedure described in Chapter 1.2.2.[130]

　　The hyphal morphology observation of Fusarium graminearum. The plant pathogen of *F. graminearum* was cultured for 3 days on potato dextrose agar (PDA; 20% potato extract, 2% dextrose, 2% agar) media (27℃), which contained 100 μg/mL of compound 05223. Hyphal morphology of *F. graminearum* cultured on PDA plate was examined under the light microscope (400$\times$) (Olympus B100; Japan). Control was untreated.

　　Preparation of the crude extract of mycelium. The six mycelial discs (40 mm diameter) taken from a starting colony growing on PDA were placed in Erlenmeyer flask containing 80 mL of sterilized Czapek media (0.2% NaNO$_3$, 0.131% K$_2$HPO$_4$ · 3H$_2$O, 0.05% KCl, 0.05%, MgSO$_4$ · 7H$_2$O, 0.00183% FeSO$_4$ · 7H$_2$O, 3% sucrose, pH 6.8).[272] The discs were then incubated in a whirly shaker (120 r/m, 27℃). After 15 days, compound *R*-4h was dripped into the culture media to the final concentration of 300 μg/mL. Then mycelium was filtered, collected, and washed orderly at 1, 3, 6, 9, 12 and 24 h. After soaking with filter paper, the dried mycelium was weighed and then preserved at 0℃.

　　The dry mycelium (0.5 g) in cold mortar was mixed with Tris-HCl buffer (3.0 mL, 0.05 M, pH7.5), triturated quickly into paste, and then centrifuged at 15000 g for 30 min. The top clear layer was preserved at 4℃. Every treatment was repeated there times.[131]

　　Detection of mycelial glucose content. The 200 μL of top clear layer of mycelial extract was mixed with 3,5-dinitrosalicylic acid (DNS; 400 μL), and then the mixture was boiled for 5 min. After cooling to room temperature, it was diluted to 2.5 mL with distilled water. Absorbence value of the mixture measured at 540 nm was converted into the value of glucose content (mg) by the standard curve of glucose. Tris-HCl buffer served as control.[132]

　　Detection of mycelial chitosan content. The top clear layer (200 μL) of mycelial extract was mixed with K$_2$B$_4$O$_7$ solution (100 μL), and then the mixture was boiled for three minutes. After quickly cooling to room temperature, the mixture was added into 3 mL of 1% DMAB. Subsequently, it was incubated for 20 min (36℃), and then cooled down to room temperature again. The absorbence value of the mixture was measured immediately at 544 nm.[133] Tris-HCl buffer served as the control.

Detection of mycelial chitinase activity. The 400 μL of top clear layer of mycelial extract mixed with chitin colloid (200 μL) was dripped into a clear centrifugal tube. The tube was incubated for 1 h (37℃), and then boiled for 5 min. After being centrifuged at 5000 r/m for 10 min, the mixture (400 μL) mixed with $K_2B_4O_7$ solution (200 μL, 0.8M) was boiled, and then cooled down quickly. Then 3 mL of 1% 3,2′-dimethyl-4-aminobiphenyl (DMAB) was added, the cooling mixture was kept at 36℃ for 20 min, and then cooled down to room temperature. The absorbence value of the mixture was measured immediately at 544 nm.[134] The control was boiled before incubating.

Detection of mycelial soluble protein content. The coomassie brilliant blue G-250 dye-binding technique was adopted to observe the changes of protein content.[135] The 100 μL of top clear layer of mycelial extract was mixed with 3 mL of coomassie brilliant blue G-250 solution, and then the mixture was kept still for 5 min. The absorbence value of the mixture was measured at 595 nm. Tris-HCl buffer served as control.

Antiviral Bioassay. The method for evaluating anti-TMV activity of title compounds is similar to the procedure described in Chapter 1.1.2.

1.6.3   Results and Discussion

In order to shorten the reaction time and increase the yields of chiral compounds, the microwave technology was applied in the Mannich-addition reaction. As expected, when the mixture of (R) or (S)-1-phenylethylamine, 2-fluoro or 2-trifluoromethyl-benzaldehyde, dialkyl phosphite and $BF_3 \cdot Et_2O$ was irradiated under microwave radiation, the reaction was completed in 10 min with yields higher than conventional heating. We optimized reaction conditions for the synthesis of (R)-**1.27b**. The influence of different catalysts, reaction time and microwave irradiation was investigated and the results are shown in Table 1.22 and Table 1.23. As shown in Table 1.22, when the reaction time was prolonged from 5 to 10 min at 80℃, the yield of (R)-**1.27b** increased from 61.5% to 77.9% (entry 1 and 2). When the reaction time was further extended to 20 min, the yield of (R)-**1.27b**(78.3%, entry 3) was slightly increased with compared to that of 10 min. In Table 1.22, $BF_3 \cdot Et_2O$ was found to be the best catalyst for the present reaction. No product (R)-**1.27b** was obtained when $Sc(OTf)_3$, acidic Al_2O_3, molecular sieves (4Å) and TiO_2/H_2SO_4 were used as catalysts (Table 1.22, entry 4-7). Product (R)-**1.27b** was obtained in 62.3% and 43.2% respectively with $AlCl_3 \cdot 6H_2O$ and molecular sieves (4Å)/$AlCl_3$ as catalysts. This reaction was performed at 80℃ and catalyzed by 10% $BF_3 \cdot Et_2O$ at 60 W microwave irradiation for 10 min. It is obvious that the microwave accelerates the reaction and improves the yields.

R[1]: 4-F, H; R[2]: Et, *n*-Pr, *i*-Pr, *n*-Bu; R[3]: 2-F, 2-CF$_3$

Scheme 1.9 Synthesis of chiral α-aminophosphonates containing fluorine moiety **1.27**

Table 1.22 Different reaction conditions for synthesis of (*R*)-**1.27b**

Entry	Catalyst	Aatalyst amount(mol%)	Time (min)	Yield [b](%)
1[a]	BF$_3$·Et$_2$O	10	5	61.5%
2[a]	BF$_3$·Et$_2$O	10	10	77.9%
3[a]	BF$_3$·Et$_2$O	10	20	78.3%
4[a]	Sc(OTf)$_3$	10	10	0
5[a]	acidic Al$_2$O$_3$	200	10	0
6[a]	TiO$_2$/H$_2$SO$_4$	10	10	0
7[a]	Molecular sieves (4 Å)	200	10	0
8[a]	Molecular sieves (4 Å)/AlCl$_3$	200	10	43.2%
9[a]	AlCl$_3$· 6H$_2$O	100	10	62.3%

[a]The reactions were carried out under microwave irradiation of 60 W at 80℃; [b]Isolated yields.

The new method for the synthesis of chiral α-aminophosphonates **1.27** under microwave irradiation offers several advantages including faster reaction rates, fewer byproducts and higher yields, as compared with the one without irradiation which involves a long process (5 h) and gives low yields. It is easy to observe from Table 1.23 that the average yields of products obtained with the microwave method are 10%-20% higher than those obtained without microwave irradiation and the average reaction ratio is 1:7.5 between the two methods.

Table 1.23 Comparison of yields of compounds **1.27** obtained with or without microwave irradiation

Entry	Compound	Yield [a](%)	
		Microwave assisted[b]	Without microwave[c]
1	(*R*)-**1.27a**	71.2	54.3
2	(*S*)-**1.27a**	76.3	60.2
3	(*R*)-**1.27b**	77.9	61.4
4	(*S*)-**1.27b**	80.9	62.3
5	(*R*)-**1.27c**	70.0	59.8
6	(*S*)-**1.27c**	76.9	62.8
7	(*R*)-**1.27d**	68.0	50.3

Continued

Entry	Compound	Yield ^{a}(%)	
		Microwave assisted^b	Without microwave^c
8	(S)-**1.27d**	75.9	63.7
9	(R)-**1.27e**	70.0	55.8
10	(S)-**1.27e**	69.9	55.6
11	(R)-**1.27f**	68.8	49.2
12	(R)-**1.27f**	79.4	62.9
13	(R)-**1.27g**	69.2	52.2
14	(R)-**1.27h**	61.8	44.9
15	(R)-**1.27i**	61.8	45.9

^{a}Yields of isolated products. ^{b} Reactions were conducted at 80℃ for 10 min at 60 W microwave irradiation catalyzed by 10% BF$_3$ · Et$_2$O. ^{c}Reaction mixture was stirred at 80℃ for 5 h catalyzed by 10% BF$_3$ · Et$_2$O without microwave irradiation.

The antifugal activity results are given in Table 1.24. It could be seen that these newly synthesized chiral α-aminophosphonates exhibit promising antifungal activities. At 50 μg/mL, chiral compounds (R)-**1.27b**, (S)-**1.27c**and (R)-**1.27h** inhibited growth of *Phytophthora infestans* at 62.08%, 61.52% and 53.85%, respectively. Compounds (R)-**1.27h**, (S)-**1.27b**, (S)-**1.27c**, (R)-**1.27d**, (S)-**1.27d**, (R)-**1.27f** exhibit good activities on *Piricularia oryzae* at 54.30%, 55.03%, 56.61%, 51.32%, 50.53%, 53.97%, respectively, which are obviously higher than that of hymexazol (13.23%). Compounds (R)-**1.27h**, (S)-**1.27b**, (S)-**1.27c**, (R)-**1.27d**, (R)-**1.27f** showed activities against *Pellicularia sasakii* at 59.28%, 54.90%, 55.93%, 50.52%, 53.87%, respectively, which are little higher than Hymexozole (47.68%). Compound (R)-**1.27h** and Hymexozole showed activities against *Fusarium oxysporum* at 56.25% and 55.44% respectively. Interestingly, these chiral α-aminophosphonates have extensive antifungal activities.

In Table 1.24, the antifungal data indicate that the nature of substituent R^3 and configuration (R) or (S) of the compound are the two major reasons for the observed antifungal bioactivity. When R^1 is fluro and R^2 is *n*-propyl and configuration is (R), chiral compound (R)-**1.27h** has higher antifungal activity than other compounds.

The morphology changes of hyphal: After 3 days of inocualtion, the colony diameter of *F. graminearum* was 5.6-6.0 cm and its color was amaranth in the middle and white on the verge. When treated with 100 μg /mL of compound (R)-**1.27h**, the hypha grew slowly with ramification and tridimensional hypha increased and the amaramth color of mycelium in the middle faded. The colony diameter was only 1.5-1.6 cm, increased 26.8% higher than that of the control.

The hypha of the control was even and slippy and ramified normally. Also the septum of hypha was clear and the endosome was abundant. When treated with 100 μg/mL of compound (R)-**1.27h**, the hypha of *Fusarium graminearum* bulged irregularly, slimmed and twisted, and the space of ramification shortened (Fig 1.6).

Table 1.24   Inhibition effect of chiral α-aminophosphonates on phytopathogenic fungi.

Compd (50 μg/mL)	Inhibition rate (%)					
	Fusarium Oxysporum	Gibberella Zeae	Phytophthor a Infestans	Piricularia oryzae	Pellicular i a Sasakii	Rhizocton ia Solani
(R)-**1.27a**	10.89	9.35	27.25	15.11	8.51	5.47
(S)-**1.27a**	16.20	10.30	41.85	16.67	13.14	8.81
(R)-**1.27b**	27.85	16.80	62.08	25.93	23.45	33.89
(S)-**1.27b**	21.77	35.50	40.73	55.03	54.90	15.20
(R)-**1.27c**	11.39	28.46	27.81	42.86	47.16	5.17
(S)-**1.27c**	23.04	35.23	61.52	56.61	55.93	21.88
(R)-**1.27d**	30.89	18.16	36.52	51.32	50.52	19.45
(S)-**1.27d**	25.82	19.78	49.16	50.53	46.91	33.13
(R)-**1.27e**	33.16	33.60	37.64	43.65	40.46	20.67
(S)-**1.27e**	29.62	26.56	26.12	31.75	32.73	25.23
(R)-**1.27f**	31.65	33.88	33.85	53.97	53.87	41.34
(S)-**1.27f**	31.14	19.24	33.43	35.19	38.92	35.71
(R)-**1.27g**	20.52	42.12	30.36	20.39	24.70	26.04
(R)-**1.27h**	56.25	60.47	53.85	54.31	59.28	59.07
(R)-**1.27i**	14.30	17.03	13.65	17.57	20.81	32.69
hymexazol	55.44	50.41	69.66	13.23	47.68	22.49
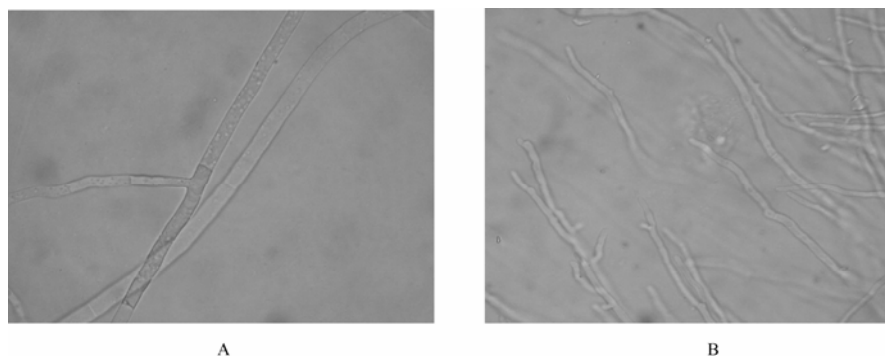
Fig 1.6   Microphtograph of hyphal morphology of *Fusarium graminearum* treated with 0 μg/mL (A) and 100 μg /mL (B) of (R)-**1.27h** under the microscope (400×)

Changes of mycelial glucose content. The mycelial glucose content of *F.graminearum* increased to its peak value in 6 h after treatment with compound (R)-**1.27h**(300 μg/mL), and then decreased (Fig 1.7). The mycelial glucose content was 8.41×10^{-2} μg /mL at 1 h after being treated, then increased by 21.1% and rose to 1.019×10^{-1} μg/mL at 6 h, which was 17.3% higher than that of the control. The glucose content then declined rapidly in 9-12 h and finally dropped to the low level, which was 88.7% of the control content in 24 h.
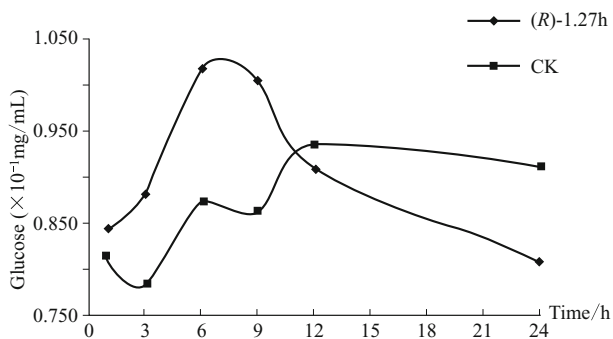
Fig 1.7   Change of mycelial glucose content

Changes of mycelial chitosan content. It could be seen from Fig 1.8 that mycelial chitosan content of *F.graminearum* increased obviously in 1-3 h after treatment with compound (*R*)-**1.27h** (300 μg/mL). The mycelial glucose content was 0.232×10^{-1} μg/mL at 1 h after treatment, and then increased by 21.2% in 3 h with the level of 0.281×10^{-1} μg/mL. The mycelial chitosan content peak appeared in 3 h, then drepped in 3-9 h, after which no obvious changes were observed in 9-24 h.
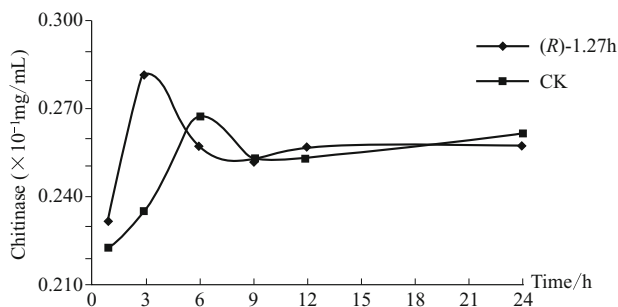
Fig 1.8   Change of mycelial chitosan content

Changes of mycelial chitinase content. It could be seen from Fig 1.9 that the changes of mycelial chitinases content were similar to that of the control. After being treated with (*R*)-**1.27h** (300 μg/mL), the mycelial chitinase content was 5.72×10^{-2} μg/mL at 3 h after inoculation and increased by 343.3% than the control. Then it dropped rapidly within 3-9 h after inoculation. Little changes were observed in 9-24 h.

Changes of mycelial soluble protein content. The mycelial soluble protein content increased in the beginning and decreased afterwards (Fig 1.10). After being treated, the content changed a little in 3 h, and then rose rapidly. Also it was higher throughout than that of control in 3-9 h. The content at 9 h was 1.465×10^{-1} μg /mL which was 19.9% higher than that of control at 1 h. Within 9-24 h after inoculation, the content dropped sharply. At 24 h after inoculation, the content
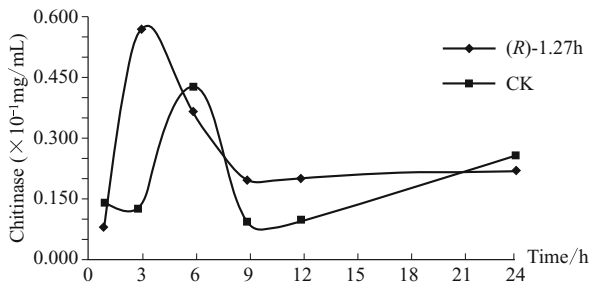
Fig 1.9　Change of mycelial chitinase content
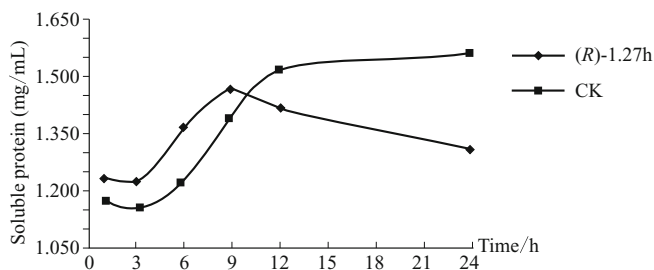
Fig 1.10　Change of mycelial soluble protein content

was $1.306 \times 10^{-1} \mu g/mL$ and was 15% lower than that of the control, which was $1.561 \times 10^{-1} \mu g/mL$.

After being treated with compound (*R*)-**1.27h**, both the soluble protein and glucose in mycelium climbed up initially and dropped later (Fig 1.10 & Fig 1.7). Possibly the compound (*R*)-**1.27h** induced the increase of the Pathogenesis-related Proteins (Pr-P), which resisted the damage to the fungal cell from the exterior. The change of mycelial soluble protein showed an increasing trend over a short period of time. However, when the time was prolonged, the soluble protein obviously began to drop. It indicated that the compound (*R*)-**1.27h** may inhibit the protein biosynthesis and the increase of enzymes in fungal cell, which interrupted the metabolism and transportation of substance and caused the fungus to die of its own due to the lack of nutrient.

At the same time, compound (*R*)-**1.27h** stimulated the mycelium to absorb the glucose in the incubated environment so as to reduce the damage to fungal cell due to the increase of compound concentration. With the lapse of time after being treated, the glucose content fell sharply, which implied that the compound disturbed the process of mycelial glucide metabolism and influenced the normal physiological action, including inhibition of the protein synthesis due to lack of energy. Therefore, from 6 h after treatment with the compound (*R*)-**1.27h**, the mycelial glucose content declined, followed by the decrease of the soluble protein content. In the present study, compound (*R*)-**1.27h** was α-aminophosphonate, which is a structural analogue to amino acid. Thus, it could be visualized as the

self-component mixing synthesis of protein by error so that the normal protein synthesis was blocked.

From the results, it could be seen that the chitinase activity increases during 1-3 h after being treated (Fig 1.10). At the same time, the chitosan also increased accordingly (Fig 1.9). However, the chitinase activity and chitosan content continually decreased in 3-9 h. They all declined to the level of control at 9 h and changed a little in 9-24 h. The decrease of glucose did not induce the increase of the chitinase activity. It could be explained by the interference of the compound with the synthesis of biological macromolecules, resulting in the decrease of the chitinase content.

The results of the in vivo bioassay against Tobacco Mosaic Virus are given in Table 1.25. Ningnanmycin was used as the reference antiviral agent. The data indicate that a change in the substituent and configration might also affect the curate activity of title chiral compounds. The chiral compounds (R)-**1-27e**, (R)-**1-27h**, (R)-**1-27i** exhibit moderate curative rate of 40.1, 41.7, 43.7% against TMV at a concentration of 500 µg/mL. The oher chiral compounds (R)-**1-27a**, (S)-**1-27a**, (R)-**1-27b**, (S)-**1-27b**, (R)-**1-27c**, (S)-**1-27c**, (R)-**1-27d**, (S)-**1-27d**, (S)-**1-27e**, (R)-**1-27f**, (S)-**1-27f** and (R)-**1-27g** exhibited weak anti-TMV bioactivities, with the inhibitory rates of 23.7%, 0%, 30.1%, 12.7%, 28.7%, 22.1%, 30.9%, 33.2%, 27.1%, 39.7%, 35.1% and 34.2%, respectively, at 500 µg/mL.

Table 1.25   The curative effects of the new chiral compounds against TMV *in vivo*

Compd.	Inhibition rate (%)	Compd.	Inhibition rate (%)
(R)-**1-27a**	23.7	(R)-**1-27e**	40.1
(S)-**1-27a**	0	(S)-**1-27e**	27.1
(R)-**1-27b**	30.1	(R)-**1-27f**	39.7
(S)-**1-27b**	12.7	(S)-**1-27f**	35.1
(R)-**1-27c**	28.7	(R)-**1-27g**	34.2
(S)-**1-27c**	22.1	(R)-**1-27h**	41.7
(R)-**1-27d**	30.9	(R)-**1-27i**	43.7
(S)-**1-27d**	33.2	Ningnanmycin	58.7

1.6.4   Conclusions

In summary, we described a practical and efficient procedure for the preparation of chiral aminophosphonates through the reaction of 2-fluoro or 2-trifluoromethylbenzaldehyde with (R) or (S)-1-phenylethylamine and dialkyl phosphite at 80℃ for 10 min under microwave irradiation using $BF_3 \cdot Et_2O$ as catalyst. In general, the reactions were fast, efficient and high yielding. By screening of antifungal activities, the chiral compound (R)-**1.27h** was found to

possess higher antifungal activity against six kinds of fungi *in vitro* than other compounds. All the compounds displayed weak to moderate antiviral activities.

1.7 Green Synthesis of α-Aminophosphonates Containing Bromine and Fluorine under Ultrasonic Irradiation

1.7.1 Introduction

A considerable work has been done on the synthesis and biological activities of α-aminophosphonates in recent years.[136−143] In order to find new plant virucides, we had earlier designed and synthesized a series of 1-(4-trifluoromethylphenyl)-α-aminophosphonates, some of which displayed good anti-TMV activity.[102-103] In continuation to our research for the development of new anticancer agents, some *N*-(4-bromo-2-trifluoromethylphenyl)-1-(2-fluorophenyl)-*O*,*O*-dialkyl-α-aminoph osphonates (**1.31**) bearing the title functional groups were synthesized.

A typical method for the synthesis of substituted α-aminophosphonate is the three component reaction of aldehydes, amine and dialkyl phosphite by one pot Mannich type method.[69] However, the reported method involved high reaction temperature, harmful solvents and expensive reagents, long reaction time, low yields and complex handling. To avoid these disadvantages, a couple of modifications including, the use of montmorillonite clay[115] and alumina[116] in dry media under microwave irradiation have been reported recently. As a part of our green technology program, we explored the potential of a new practical green alternative for the synthesis of α-aminophosphonate by a threecomponent condensation of aldehydes, amine and dialkylphosphite at 75-80 ℃ under ultrasonic irradiation without any solvent. The method was easy to operate and the condition was mild and environment-friendly. The synthetic route is shown in Scheme 1.10. The structures of the compounds were established by IR, ^{1}H NMR, ^{13}C NMR and elemental analysis. Preliminary bioassays indicated that some of these compounds exhibit moderate antitumor activity to PC3 cell *in vitro* by MTT method.
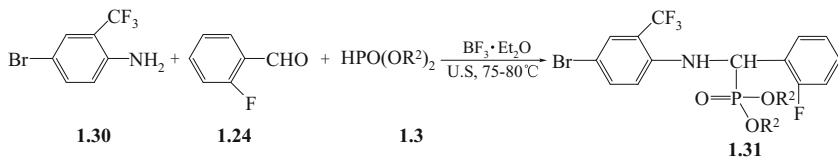
Scheme 1.10 Synthsis of α-aminophosphonate by reaction of aldehydes, amine and dialkyl phosphite

1.7.2   Materials and Methods

1.7.2.1   Apparatus and analysis

The materials and instruments for determination of the structure and physical data of new compounds are basically similar to the procedure described in Chapter 1.1.2. Sonication was performed on a Shanghai Branson-CQX ultrasonic cleaner (at 25 kHz frequency and a nominal power of 500W).

1.7.2.2   General procedure

2-Bromo-4-trifluoromethylaniline (3 mmol), 2-fluorobenzaldehyde (3 mmol), dialkyl phosphite (3 mmol) and boron trifluoride diethyl etherate (0.3 mmol) were added into an oven-dried three-necked 50 mL round-bottom flask. The mixture was irradiated in the ultrasonic cleaning bath at 78-80℃ for 0.5 hour. The mixture was washed with water, filtered, dried; then the crude solid was recrystallized from ethanol and water (1:1, v/v) to give **1.31** as a white solid. The physical data, yields and the nature of the substituents for the target compounds **1.31** are provided in the Table 1.26. The reperesentative data **for 1.31a** is shown below, while data for **1.31b-1.31e** can be found in the reference.[121]

1.31a: white solid; yield 94.7%, mp 80-81℃; IR (KBr): ν_{max} 3462.2, 2958.8, 1608.6, 1508.3, 1489.0, 1473.6, 1417.6, 1319.3, 1269.3, 1247.9, 1145.7, 1114.8, 1076.2, 1060.8, 827.4, 756.1; ^{1}H NMR (500 MHz, CDCl$_3$): δ 7.560 (s, 1H, NH), 7.298-7.555 (m, 3H, 2-CF$_3$Ar-H), 6.457-7.293 (m, 4H, 2-F-Ar-H), 5.456 (t, 1H, CHP, J=17.2 Hz), 3.558-3.857 (m, 6H, 2CH$_3$); ^{13}C NMR (125 MHz, CDCl$_3$): δ 161.81, 161.75, 159.37, 159.30, 142.33, 142.20, 135.80, 130.17, 130.14, 130.09, 130.06, 129.51, 129.45, 129.39, 129.34, 128.38, 128.34, 128.31, 127.89, 125.17, 124.94, 124.89, 124.87, 122.46, 122.15, 122.02, 116.60, 116.29, 115.59, 115.57, 115.37, 115.35, 114.34, 109.33, 54.19, 54.12, 54.00, 53.93, 48.42, 46.87, 46.84. Anal. Calcd. for C$_{16}$H$_{15}$BrF$_4$NO$_3$P: C, 42.13; H, 3.31; N, 3.07. Found: C, 42.11; H, 3.46; N, 3.00.

Antiviral Bioassay. The method for evaluating anti-TMV activity of title compounds is similar to the procedure described in Chapter 1.1.2.

1.7.3   Results and Discussion

In an effort to explore the effects of the substituents of dialkyl phosphite, we have screened the reactions of dialkyl phosphite **1.3**, aldehyde **1.24** and aniline **1.30** in the presence of boron trifluoride diethyl etherate (10%mol) under sonic waves. The results are listed in Table 1.26. It was found that the yields depend on the nature of the substituents. The yields of the products **1.31a**, **1.31d**, and **1.31e** obtained after 0.5h were 94.5, 93.0 and 92.1%, respectively (Table 1.26, entries 1,

4 and 5). It is noted that dimethyl phosphite exhibits the best reactivity, affording **1.31a** in the highest yield of 94.5% (Table 1.26, entry 1).

Table 1.26　The structure and physical data of **1.31a-1.31d** [a]

Entry	Compd.	R^2	Yield [b] (%)	Mp (℃)
1	**1.31a**	CH_3	94.5	80-81
2	**1.31b**	C_2H_5	84.2	86-87
3	**1.31c**	$n\text{-}C_3H_7$	82.9	75-77
4	**1.31d**	$i\text{-}C_3H_7$	93.0	98-99
5	**1.31e**	$n\text{-}C_4H_9$	92.1	73-75

[a] All reactions were carried out at 75-80℃ for 0.5h under ultrasonic irradiation without solvent employing 10 mol% boron fluoride-ether; [b] Isolated yields.

As shown in Table 1.27, the synthesis of **1.31** was carried out in good yields at 75-80℃ in the presence of boron trifluoride diethyl etherate under ultrasound irradiation. The dramatic improvement observed above was expressed by reaction time and yields. In the reaction catalyzed by boron trifluoride diethyl etherate, **1.31a** was obtained in 80.1% yield at 75-80℃ in the silent reaction (magnetically stirred) for 0.5 h (Table 1.27, entry 2). On the other hand, under the ultrasound irradiation **1.31a** was achieved in 94.5% yield under the same conditions (Table 1.27, entry 1). For the reactions without any catalyst, **1.31a** was obtained in 75.4% and 78.2% yields at 75-80℃ under conventional stirring for 0.5 h and 5 h respectively (Table 1.27, entries 3 and 4), while the corresponding data for **1.31a** were 88.2% and 88.7% yields within 0.5 h and 1h respectively under ultrasound irradiation (Table 1.27, entry 5,6). Apparently, the present Mannich-type reaction could be completed in short time and gave good yields under the co-effect of the catalyst boron trifluoride diethyl etherate. More importantly, under ultrasound

Table 1.27　Synthesis of compound **1.31a** under ultrasound irradiation and different catalysts [a]

Entry	Solvent	Reaction temp (℃)	Catalyst	Time(h)	Yield [b] (%)
1	—	75-80	$BF_3 \cdot Et_2O$	0.5	94.5
2[c]	—	75-80	$BF_3 \cdot Et_2O$	0.5	80.1
3[c]	—	75-80	—	0.5	75.4
4[c]	—	75-80	—	5	78.2
5	—	75-80	—	0.5	88.2
6	—	75-80	—	1	88.7
7	—	75-80	HOAc	0.5	32.1
8	—	75-80	TsOH	0.5	84.3
9	acetonitrile	75-80	$BF_3 \cdot Et_2O$	2	90.3
10	toluene	115-120	—	5	80.1

[a] All reactions were carried out at the temperature mentioned above with catalyst content of 10 mol%; [b] Isolated yields; [c] Stirring without ultrasound irradiation.

irradiation 20% higher yield was obtained compared to the reactions without catalyst and ultrasound (Table 1.27, entry 1 and 3).

Besides boron trifluoride etherate, several other catalysts were also screened, and boron trifluoride etherate was found to be the best one for the present reaction. Product **1.31a** was obtained only in 32.1% and 84.3% yields when HOAc and TsOH were used as catalyst, respectively (Table 1.27, entry 7 and 8). The effect of solvent on the reaction was also studied and it was found that the best result was achieved without any solvent (Table 1.27, entry 9 and 10). Therefore, under optimal conditions, when 2-trifluoromethyl-4-bromoaniline (**1.31**) was reacted with 1 equiv of *O,O*-dialkylphosphite and 2-fluorobenzaldehyde under ultrasound irradiation with boron trifluoride diethyl etherate as catalyst at 75-80℃ for 0.5h, the Mannich-type reaction proceeded smoothly, and the results are summarized in Table 1.27.

The antitumor activities of the title compounds were assayed by the MTT method.[117,118] It was found that these compounds exhibit certain activities against PC3 cell line *in vitro*. The results are listed in Table 1.28. It could be seen that the nature of the substituent affects bioactivity to a great extent. For example, the antiproliferation activities of compound **1.31c** to PC3 cells at the concentration of 10 μM at 48h and 72h were 52.4% and 86.5%, respectively, which are relatively higher than the others.

Table 1.28 Inhibition rate of compound **1.31a-1.31e** to PC3 cells at 10 μM (%)

Compd.	Inhibition rate (%)[a]		Compd.	Inhibition rate (%)[a]	
	48h	72h		48h	72h
1.31a	7.8	32.1	**1.31d**	32.8	54.8
1.31b	8.1	33.4	**1.31e**	34.6	52.3
1.31c	52.4	86.5			

[a] Inhibition rate (%)=(A$_1$－A$_2$)/A$_1$✕100%. A$_1$: the mean optical densities of untreated cells, A$_2$: the mean optical densities of drug treated cells.

The antiviral activities of the title compounds were tested by the half-leaf method.[273] Ningnarmycin was used as the reference antiviral agent. The preliminary biological tests showed that antiviral activities of the title compounds are weak to moderate. For example, the extent of inhibition of the compound **1.31b** against TMV was 42.1% at a concentration of 500 μg/mL.

1.7.4 Conclusions

In summary, we described a practical and efficient procedure for the preparation of *N*-(4-bromo-2-trifluoromethylphenyl)-1-(2-fluorophenyl)-*O,O*-dialkyl-α-aminophosphonate through the three-component reaction of 2-trifluoro-

methyl-4-bromoaniline, *O,O*-dialkylphosphite and 2-fluorobenzaldehyde under ultrasonic irradiation, catalyzed by boron trifluoride diethyl etherate for 0.5h at 78-80℃ without solvent. The reactions were, in general, fast, clean and atom-economic. No side product has been isolated thereby restricting the waste to a bare minimum. The products obtained after recrystallization are of high purity and do not require any chromatographic purification. It avoids use of large quantities of volatile solvent in many existing procedures.

1.8   Synthesis & Bioactivity of *α*-Aminophosphonates Containing Isoxazole Moiety

1.8.1   Introduction

As evident from the descriptions in the preceding sections, considerable number of *α*-aminophosphonate derivatives are known to be bioactive. They display antiviral, antibacterial, antifungal, antimicrobial, and antitumor activities[3] In this context, we had prepared some promising derivatives with excellent virucidal activities by modifying the parent structure of *α*-aminophosphonate through replacement of phenylamino substituent by 4-trifluoromethylphenylamino group. We found that some of them showed excellent virucidal activities.[69, 102, 104] At the same time, we noticed that the compounds having herterocyclic moieties are known to possess a wide range of biological and pharmacological activities.[113,144] In addition, fluorine containing compounds have been extensively widely used as new pharmaceuticals and agrochemicals.[111,145-147] Keeping these considerations in mind, in continuation of our efforts to synthesize heterocyclic compounds containing fluorine moiety, the present work has been directed towards the design of new aminophosphonate derivatives containing isoxazole and fluorine moiety. In order to find new anticancer agent, we designed and synthesized a series of 1-[(5-methyl-isoxazol-3-yl)amino]-1-(2 or 4-fluorophenyl)-methanephosphonate **1.33**.

The general method for synthesis of substituted *α*-aminophosphonate is the three components reaction of aldehydes, amine and dialkyl phosphite in organic solvent by one pot Mannich-type method.[114] Since the synthetic methods and control of reactivity of different substituted heterocyclic amines are not easy and often variable, the synthesis of target compounds by Mannich-type reaction can be laborious and unpredictable. The one-pot Mannich-type method developed by us involves the reaction of 3-amino-5-methylisoxazole and *O,O*-dialkylphosphite with 2 or 4-fluorobenzaldehyde under ultrasonic irradiation to access corresponding *α*-aminophosphonate derivatives. The advantages of the procedure are short reaction period, high yield and simple work up.

The structures of **1.33** were firmly established by well defined IR, ^{1}H NMR, ^{13}C NMR, ^{19}F NMR and elemental analysis. The structure of **1.33c** was clearly characterized by a single-crystal X-ray diffraction study. The anticancer activity was assayed by the MTT method for all products. Preliminary antitumor experiments *in vitro* showed that some of them displayed moderate anticancer activity for two cells (PC3 and A431) at 10 μM. The preliminary antiviral tests dispalyed that the bioactivities of the title compounds are weak to moderate. The reaction route is shown in Scheme 1.11.

R[1]:2-F, 4-F;   R[2]: Me, Et, *n*-Pr, *i*-Pr, *n*-Bu
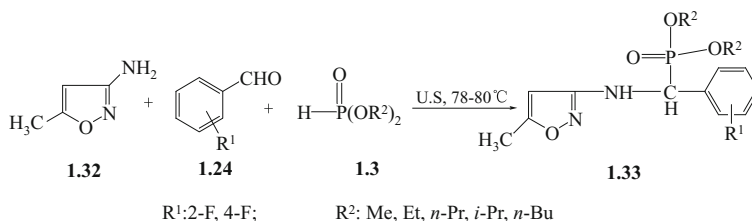
Scheme 1.11   Synthesis of compound **1.33** through one pot Mannich-type reaction.

1.8.2   Materials and Methods

The materials and instruments for determination of the structure and physical data of new compounds are basically similar to the procedure described in Chapter 1.1.2.

***General procedure for the preparation of products* 1.33a-1.33j.** A mixture of 3-amino-5-methylisoxazole (4 mmol), 2 or 4-fluorobenzaldehyde (4 mmol), and dialkyl phosphite (4 mmol) was irradiated in the ultrasonic cleaning bath at 78-80℃ for 1 h. The reaction was followed and monitored by TLC (petroleum ether + ethyl acetate =2+1, by volume). After the reaction was completed (1 h), the solvent was removed under reduced pressure and the residue washed with water, filtered, dried, then the crude solid was purified by column chromatography on silica gel using petroleum ether/ethyl acetate (*v:v*=2:1) as eluent to give **1.33a-1.33j**. The reperesentative data for **1.33a** is shown below, while data for **1.33b-1.33j** can be found in the reference.[148]

1-[(5-methylisoxazol-3-yl)amino]-1-(2-fluorophenyl)-*O,O*-dimethyl-methane phosphonate (**1.33a**). White crystal; yield 85.2%; mp171-173℃. IR (KBr): v_{max} 3271, 1625, 1537, 1514, 1490, 1232, 1062, 1026, 841, 769, 636, and 576.^{1}H NMR (500 MHz, CDCl$_3$): δ 7.05-7.54(m, 4H, Ar-H), 5.54(s, 1H, hetero-H), 5.32 (dd, *J*=23.2 Hz, 6.8 Hz, 1H, CH-P), 5.18(b, 1H, NH), 3.83 (d, *J*=10.8 Hz, 3H, OCH$_3$), 3.52 (d, *J*=10.8 Hz, 3H, OCH$_3$), and 2.24(s, 3H, CH$_3$). ^{13}C NMR (125 MHz, CDCl$_3$): δ 169.27, 163.17, 129.85, 128.93, 124.48, 122.88, 115.66, 93.25, 54.01, 53.94, 48.91, 47.35, and 12.49.^{19}F NMR (470 MHz, CDCl$_3$): δ 119.01. Anal. Calcd. for C$_{13}$H$_{16}$FN$_2$PO$_4$: C, 49.69; H, 5.13; N, 8.91. Found: C, 49.75; H, 5.00; N, 8.79.

Crystal structure determination. The experiment and method for X-ray diffraction data of compound **1.33c** are similar to the procedure described in Chapter 1.3.2.[75-77] Crystallographic data for the structure **1.33c** have been deposited with the Cambridge Crystallographic Data Center as supplementary publication No. CCDC-243914.

MTT assay against cell proliferation. The experiment and method for evaluating antitumor activity of all compounds are similar to the procedure described in Chapter 1.5.2.3 [117,118]

Antiviral Bioassay. The method for evaluating anti-TMV activity of title compounds is similar to the procedure described in Chapter 1.1.2. [49,50]

1.8.3   Results and Discussion

The reaction of 3-amino-5-methylisoxazole, *O,O*-diethylphosphite with 2 or 4-fluorobenzaldehyde under sonic waves was investigated. The results are listed in Table 1.29. It could be seen that the presence of ultrasonic irradiation could accelerate the reaction (Table 1.29, entry 1-10). Without ultrasound, the reaction was relatively slow and low yields of product were obtained within 5h at 115-120℃ in toluene. Under the condition A of using ultrasonic irradiation, great improvement was achieved to afford **1.33** in 77.6%-91.2% yields within a shorter reaction time (1 h) than those conducted under condition B (refer Table 1.29). The best result was obtained when 3-amino-5-methylisoxazole was reacted with 1 molar equiv. of dialkyl phosphite and 1 molar equiv of 2 or 4-fluorobenzaldehyde under ultrasonic irradiation without solvent and catalyst at 78-80℃ for 1 h.

Table 1.29   Mannich-type addition of 3-amino-5-methylisoxazole and
O,O-dialkylphosphite with 2 or 4-fluorobenzaldehyde

Entry	Compd.	R^1	R^2	Yield(%)^a	Yield(%)^b
1	**1.33a**	2-F	Me	85.2	68.2
2	**1.33b**	2-F	Et	87.4	69.8
3	**1.33c**	2-F	*n*-Pr	91.2	71.6
4	**1.33d**	2-F	*i*-Pr	89.1	70.7
5	**1.33e**	2-F	*n*-Bu	87.3	67.9
6	**1.33f**	4-F	Me	77.6	57.2
7	**1.33g**	4-F	Et	83.3	66.7
8	**1.33h**	4-F	*n*-Pr	85.1	68.3
9	**1.33i**	4-F	*i*-Pr	84.2	67.7
10	**1.33j**	4-F	*n*-Bu	79.3	61.7

^{a}The reactions were carried out at 78-80℃ under ultrasound irradiation for 1 h;^{b} The reactions were stirred for 5 h at 115-120℃ in toluene without ultrasound irradiation (classical heating condition).

It can be seen from Table 1.29 that the yields of product **1.33** are obviously dependent on the position of the substituent on the benzene ring of aldehyde. For the same fluorine substituent, the yield decreases in the order of *para-*, *ortho-*. For **1.33a-1.33e**, due to the intramolecular hydrogen bond formation between the hydrogen of CH=N of imine and the fluorine atom at 2-position of the benzene ring, the carbon atom of imine becomes more electrophilic making it more susceptible to be attacked by the phosphorus atom of dialkyl phosphite. Therefore, the formation of the transition state (Scheme 1.12) is proposed to account for the observed acceleration of the reaction.
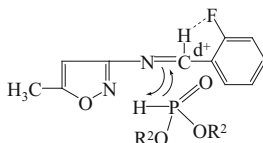
Scheme 1.12   Proposed transition state for the formation of **1.33a-1.33e**

Five kinds of different catalysts, *e.g.* boron trifluoride etherate, DMAP (*N,N*-dimethyl-4-aminopyridine), TsOH, AlCl$_3$ and aniline, were also screened. The results are listed in Table 1.30 which demonstrated that no remarkable improvement of the yield of product was observed with the catalysts.

Table 1.30   Different catalysts mediated Mannich-type reaction of
2-fluorobenzaldehyde and 3-amino-5-methylisoxazole
with diethylphosphite under ultrasound irradiation

Entry	Catalyst	Time(h)	Yield(%)	Entry	Catalyst	Time(h)	Yield(%)
1	BF$_3$ ·Et$_2$O	1	84.2	4	DMAP	1	77.2
2	AlCl$_3$	1	86.1	5	aniline	1	52.2
3	*p*-TsOH	1	76.1	6	—	1	87.4

The structures of compounds **1.33** were confirmed by IR, ^{1}H NMR, ^{13}C NMR and elemental analysis. The infrared spectra of **1.33a-1.33j** were recorded in the range of 400-4000 cm^{-1}. For **1.33a**, 3271cm^{-1}(s) corresponds to an N-H stretching absorption band, the signals at 1625-1499 cm^{-1} were assigned to C=N and C=C vibration. While the absorption at 1232cm^{-1} (s) was assigned to P=O stretching absorption bands, 1062cm^{-1}(s) was due to P-O-C stretching absorption bands. In ^{1}H NMR and ^{13}C NMR data of **1.33a-1.33j**, all the protons were identified and the total number of protons calculated from the integration curve corresponded to the expected structure. For **1.33a-1.33j**, all aromatic protons showed multiplet at δ 6.963-7.533. Due to the coupling with the phosphorus atom, the proton of P(O)CH exhibited doublet at about δ 4.899-5.322 with coupling constants (*J*) of 22.4-25.0 Hz. In ^{13}C NMR spectra, all CH(P) peaks appeared at δ 47.31-53.91, the carbon atom of CH$_2$O appeared near δ 63.42-68.79 and the CH$_3$ carbon at δ 12.45-16.72.

1.8.3.1   Crystal structure of 1.33c

The molecular structure of the title compound **1.33c** is shown in Fig 1.11. The packing diagram of the unit cell of compound **1.31c** is shown in Fig 1.12. Selected bond lengths and angles are presented in Table 1.31. The benzene ring [C(2), C(3), C(4), C(5), C(6), C(7), F(1)] and the adjacent carbon atom C(1) are fairly planar, and the deviation from the least squares plane through the ring atom is less than 0.032(3) nm. The plane equation is $3.7023x+6.747y+14.217z=5.1221$. All atoms in isoxazole group are also fairly planar and the largest deviation from the least squares planes is 0.0428(3) nm. The plane equation is $7.5203x+4.8039y+4.0296z=8.2319$. The dihedral angle between the plane of isoxazole group and the plane of the benzene is 77.27° . In the crystal lattice, there is an N-H¨O hydrogen bond intermolecular interaction. The donor and acceptor distance is N(2)-O(1)
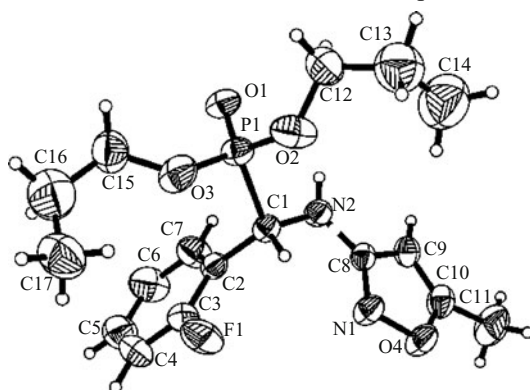
Fig 1.11   Molecular structure of compound **1.33c**
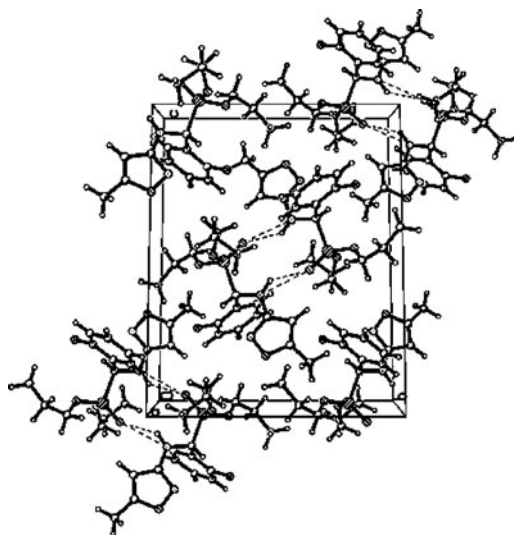
Fig 1.12   Packing diagram of the unit cell

Table 1.31   Selected bond distance (nm) and angles (°) for compound **1.33c**

P(1)-O(1)	0.1449(3)	O(1)-P(1)-O(3)	116.7 (18)
P(1)-C(1)	0.1807(4)	O(2)-P(1)-C(1)	102.6(19)
N(1)-C(8)	0.1311(5)	C(8)-N(1)-O(4)	103.8(3)
N(1)-O(4)	0.1429(4)	C(10)-O(4)-N(1)	108.0(3)
N(2)-C(8)	0.1364(5)	C(8)-N(2)-C(1)	119.3(3)
C(1)-C(2)	0.1502(5)	C(1)-C(2)-C(3)	121.3(4)
N(2)-C(1)	0.1444(4)	C(1)-N(2)-C(8)	119.3(3)
C(8)-C(9)	0.1404(5)	N(2)-C(8)-C(9)	126.1(4)
F(1)-C(3)	0.1311(5)	N(2)-C(8)-N(1)	121.2(3)

Table 1.32   Hydrogen bond for compound **1.33c**

D-H···A	d(D-H)	d(H···A)	d(D···A)	∠(DHA)
N(1)-H(1)···O(1)	0.860	2.250	2.943	137.7

0.2943nm (symmetry code: $-x+1$, $-y+2$, $-z$) and the bond angle is 137.72°   (Table 1.32). The crystal packing is stabilized by these extensive hydrogen bonds.

1.8.3.2   Bioassay Activity

The antitumor activity was assayed by the MTT method.[117,118] The result listed in Table 1.33 showed that these compounds exhibit certain activities against the two cancer cells *in vitro*. The compounds **1.33f-1.33j** have relatively higher antitumor activities than those of **1.33a-1.33e**. The antitumor data indicates that the nature of fluorine and alkyl affects antitumor activity. For example, when R_1 was 4-F and R_2 was *i*-Pr, compound **1.33i** exhibited a strong antitumor bioactivity with the anti-proliferation rates of 78.3% and 69.0% against PC3 cell and A431 cell at 10μM, respectively.

Table 1.33   Inhibition rate (%) of compounds **1.33a-1.33j** against PC3 and A431 cell proliferation at the concentration of 10 μM for 72h[*]

Compd.	PC3 cells	A431 cells	Compd.	PC3 cells	A431 cells
1.33a	22.1	10.9	**1.33f**	50.2	27.9
1.33b	40.7	29.8	**1.33g**	60.0	34.5
1.33c	47.8	34.5	**1.33h**	70.0	65.8
1.33d	58.9	48.0	**1.33i**	78.3	69.0
1.33e	65.1	55.3	**1.33j**	66.8	67.3

[*]Inhibition rate (%)=(A_1-A_2)/$A_1\times100$%. A_1：the mean optical densities of untreated cells, A_2：the mean optical densities of drug treated cells.

The preliminary biological tests showed that the antiviral activities of the products are weak to moderate. The extent of inhibition of all compounds **1.33a-j** against TMV was 12.4%-32.2% at a concentration of 500 mg/L.

1.8.4   Conclusions

A series of α-aminophosphonates（**1.33**）containing isoxazole and fluorine moiety was synthesized under ultrasonic irradiation in one step. This method is an easy, rapid, one-pot, and good-yielding reaction for the synthesis of α-aminophosphonates. The structures were verified by spectroscopic method. In the MTT bioassay, these new compounds were found to possess moderate antitumor activities against PC3 and A431 cells. The preliminary biological tests showed that the antiviral activities of the products are weak to moderate. As far as we know, it is the first report with the title compounds having anti-cancer and antiviral bioactivity.

1.9   Synthesis & Bioactivity of α-Aminophosphonates Containing Benzothiazole Moiety

1.9.1   Introduction

As isosteres of aminocarboxylic acids, α-aminophosphonate derivatives have a high potential for biological activity, possessing a wide range of antitumor, antiviral and antifungal properties. Some of them have been extensively used as insecticides and herbicides.[127] Among these compounds, the studies with heterocyclic moieties are mainly concentrated on thiophene, furan, pyrole,1,3,4-thiadiazole and benzothiazole as the active group.[147,149] For example, the compounds containing benzothiazole moiety serve as representatives due to their excellent fungicidal activity. α-Aminophosphonates containing benzothiazole moiety have been suggested as antitumor agents, although no data about antitumor activities are reported. This work is the first indication that this kind of compound may possess potential antitumor activity and we tried to explore the possibility of improving antitumour activity by making structural variation.

A typical method for the synthesis of substituted α-aminophosphonates is the three-component reaction of aldehydes, amine and dialkyl phosphite by one pot Mannich type method in organic solvent system at high temperature. However, the reported method involved harmful solvent and expensive catalyst, longer reaction times, low yields of products and complex handling. Recently, ionic liquids, a kind of ion solvent, which combine the advantages of both traditional molecular solvents and melt salts, have been considered as promising new reaction media, and have found wide use in catalytic and non-catalytic reactions.[116] As a part of our green technology program, we studied a more practical green alternative for a novel synthesis of α-aminophosphonate by a three-component condensation

of aldehydes, aminobenzothiazole and dialkyl phosphite at 100-102℃ in ionic liquids. The method provides high yields and is very easy and environmental-friendly. The synthetic route is shown in Scheme 1.13. The results are summarized in Table1.34-1.37. The structures of the compounds were confirmed by IR,^{1}H NMR, ^{13}C NMR and elemental analysis and X-ray analysis (Fig 1.13 and Fig 1.14). Preliminary bioassays indicated that the compound **1.35c** exhibits good antitumor activity against PC3 cell in vitro by MTT method.
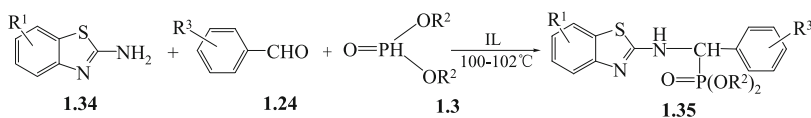
Scheme 1.13　Synthesis of the compound **1.35**

1.9.2　Materials and Methods

The materials and instruments for determination of the structure and physical data of new compounds are basically similar to the procedure described in Chapter 1.1.2. Dialkyl phosphite was prepared according to literature method. [63]

General experimental procedure for the synthesis of α-aminophophonates with benzothiazole moiety. 2-Amino-6-methylbenzothiazole or 2-amino-6-methoxybenzo-thiazole (5 mmol), 2-or 4-fluoro or 4-trifluorobenzaldehyde (5 mmol), dialkyl phosphite (5 mmol) and 4 mL ［Bmim］［PF_6］ were added into an oven-dried three-necked 25 mL round-bottom flask. The mixture was stirred at 100-102℃ for 1.5h. The resulting mixture was quenched with a few drops of water followed by extraction with Et_2O (3×6 mL). After removal of the ether solvent in vacuum, the crude solid was recrystallized from ethanol and water (1:1, *v/v*) to give **1.35a-1.35m** as white solids. The reperesentative data for **1.35a** is shown below, while data for **1.35b-1.35m** can be found in the reference.[28]

Compound **1.35a**：yield 87.0%, m.p. 147-148℃, IR (KBr)：v_{max} 3211.4, 1591.2, 1539.2, 1487.12, 1236.3, 1213.2, 1049.2, 1028.0.^{1}H NMR (400 MHz, CDCl₃)：δ 1.12-1.34 (m, 6H, 2CCH₃), 2.52 (s, 3H, Ar-CH₃), 3.80-4.06 (m, 2H, OCH₂), 4.21-4.29 (m, 2H, OCH₂), 5.83 (d, *J*=25.4 Hz,1H, CHP), 6.95-7.38 (m, 7H, Ar-H), 7.62 (t, *J*=7.2 Hz, 1H, NH).^{13}C NMR (125 MHz, CDCl₃):δ164.56, 130.83, 129.804, 129.34, 129.27, 126.49, 124.40, 123.11, 122.97, 121.76, 118.12, 115.39, 115.18, 63.70, 63.63, 63.56, 49.95, 48.36, 18.15, 16.44, 16.39, 16.14, 16.09. Anal. Calcd. for C₁₉H₂₂FN₂O₃PS:C, 55.87, H, 5.43, N, 6.86. Found: C, 55.80, H, 5.20, N, 6.76.

Crystal data of **1.35m**. C₁₉H₂₂FN₂O₄PS, *M*=424.42, Tetragonal, *a*=21.169(3), *b*=21.169(3), *c*=18.545(6) Å, β=90°, V=8311(3) Å³, T=296(2) K, space group I4(1)/a, Z=16, Dc=1.357g/cm³, μ (Mo-K*α*)=0.269mm⁻¹, F(000)=3552.23685 reflections measured, 4265 unique (R_{int}=0.0556) which were used in all calculation. Fine

R_1=0.0566, $wR(F^2)$=0.1538 (all data). Full crystallographic details of **1.35m** have been deposited at the Cambridge Crystallographic Data Center and allocated the deposition number CCDC 284909.

Crystal data of **1.35i**. $C_{21}H_{26}FN_2O_4PS$, M=452.47, Triclinic, a=9.601(3), b=10.547(4), c=11.894(4) Å, β=105.5°, V=1146.5(7)) Å^3, T=293(2) K, space group P-1, Z=2, Dc=1.311g/cm^3, μ(Mo-Kα)=0.248 mm^{-1}, F(000)=476.6029 reflections measured, 4035 unique (R_{int}=0.0179) which were used in all calculation. Fine R_1=0.0710, wR (F^2)=0.2290(all data). Full crystallographic details of **1.192i** have been deposited at the Cambridge Crystallographic Data Center and allocated the deposition number CCDC 234280.

MTT Assay Against Cell Proliferation. The experiment and method for evaluating antitumor activity of all compounds are similar to the procedure described in Chapter 1.5.2.3 [117,118].

Antiviral Bioassay. The method for evaluating anti-TMV activity of title compounds is similar to the procedure described in Chapter 1.1.2.

1.9.3   Results and Discussion

In order to optimize the reaction conditions, the Mannich addition reactions were carried out under several conditions. First, the benefit of the reaction from using four kinds of ionic liquids was confirmed. We chose a reaction of 1 equiv 2-amino-6-methoxybenzothiazole, 1 equiv diethyl phosphite and 1 equiv 2-fluoro-benzaldehyde as a model reaction to test the catalytic activity of these ionic liquids (ILs) and no other solvents were added as initial explorations. The results are shown in Table 1.34; the first three ILs can catalyze the reaction efficiently (Table 1.34, entry 1-3) and [Bmim] [PF$_6$] shows the highest catalytic activity for the above reaction. However, [Bmim][HSO$_4$] reacts readily with   the amine due to its strong acidity and the product was obtained in low yield (Table 1.34, entry 4). The results demonstrated that the presence of [Bmim] [PF$_6$] can accelerate the Mannich addition reaction. When we used other solvents instead of [Bmim] [PF$_6$], no remarkable improvement of the yield of product was observed (Table 1.34, Entry 2 and 3). We also examined the effects of reaction temperature and reaction time as shown in Table 1.34. As for the reaction temperature, it could be seen that the yield was relatively lower when the reaction was conducted at room temperature (Table 1.34, entry 5) than that at 100-102℃ (Table 1.34, entry 10). No substantial improvement was observed when the reaction system was heated to 105℃ (Table 1.34, entry 11). Hence, the reaction should be conducted at 100-102℃ than performing at a lower or higher temperature. When the reaction time was prolonged from 0.5 to 1.0h, the yield of **1.35m** was increased from 77.8% to 82.1% (Table 1.34, entry 15,16). On extending the reaction time further to 2.0h, tiny improvement of yield (92.4%, Table 1.34, entry 17) was obtained compared to that of 1.5h (91.0%, entry 10).

Table 1.34   synthesis of **1.35m** under different reaction conditions

Entry	Compd.	Solvent	Time (h)	Temp (℃)	Yield (%)
1[a]	1.35m	［Bmim］［PF$_6$］	1.5	100-102	90.2
2[a]	1.35m	［Bmim］［H$_2$PO$_4$］	1.5	100-102	74.3
3[a]	1.35m	［Bmim］［BF$_4$］	1.5	100-102	79.0
4[a]	1.35m	［Bmim］［HSO$_4$］	1.5	100-102	42.2
5[a]	1.35m	［Bmim］［PF$_6$］	1.5	20-25	23.4
6[a]	1.35m	［Bmim］［PF$_6$］	5	20-25	44.5
7[a]	1.35m	［Bmim］［PF$_6$］	15	20-25	68.9
8[a]	1.35m	［Bmim］［PF$_6$］	1.5	50-55	66.2
9[a]	1.35m	［Bmim］［PF$_6$］	1.5	80-85	70.9
10[a]	1.35m	［Bmim］［PF$_6$］	1.5	100-102	91.0
11[a]	1.35m	［Bmim］［PF$_6$］	1.5	105-110	92.0
12[b]	1.35m	toluene	1.5	100-105	45.6
13[b]	1.35m	toluene	10	100-105	76.2
14[b]	1.35m	—	1.5	100-102	66.0
15[a]	1.35m	［Bmim］［PF$_6$］	0.5	100-102	77.8
16[a]	1.35m	［Bmim］［PF$_6$］	1.0	100-102	82.1
17[a]	1.35m	［Bmim］［PF$_6$］	2.0	100-102	92.4
18[a]	1.35m	［Bmim］［PF$_6$］	3.0	100-102	92.0

[a]The reaction was carried out in ionic liquids (4 mL) under stirring;[b] The reaction was carried out in toluene under stirring.

The amount of [Bmim][PF$_6$] was investigated for the synthesis of **1.35m**. The results are summarized in Table 1.35. As can be seen from Table 1.35, the best result was obtained when 4 mL [Bmim][PF$_6$] was used (Table 1.35, entry 2). On increasing the amount of [Bmim][PF$_6$] to 5-8 mL, no remarkable improvement of the yield was observed (Table 1.35, entry 3-6).

Table 1.35   Effect of the amount of ［Bmim］［PF$_6$］ on the synthesis of **1.35m**

Entry	［Bmim］［PF$_6$］ (mL)	Yield (%)	Entry	［Bmim］［PF$_6$］(mL)	Yield (%)
1	2	82.1	4	6	90.4
2	4	91.0	5	7	91.2
3	5	90.9	6	8	89.0

Subsequently, we investigated the catalytic activity of recycled [Bmim][PF$_6$] in the reaction of 2-amino-6-methoxybenzothiazole and diethyl phosphite and 2-fluorobenzaldehyde. As shown in Table 1.36, [Bmim][PF$_6$] could be reused for at least four times without significant loss of activity.

Table 1.36   Recycling of ［Bmim］［PF$_6$］ in the synthesis of compound **1.35m**
(1.5h, IL 4.0 mL, 100-102℃)

Entry	Cycle times	Yield（%）	Entry	Cycle times	Yield（%）
1	1	90.5	3	3	91.4
2	2	89.0	4	4	88.7

Using the above optimal condition, the compounds **1.35a-1.35m** were prepared by condensation of 2-amino-6-methoxybenzothiazole or 2-amino-4-methylbenzothiazole with 2-flurobenzaldehyde or 4-fluorobenzaldehyde or 4-trifluoromethyl-benzaldehyde and dialkyl phosphite in ionic liquids as shown in Table 1.37.

Table 1.37   Synthesis of α-aminophosphonates **1.35a-1.35m** with
benzothiazole moiety

Entry	Compd.	R^1	R^3	R^2	Yield^a(%)
1	**1.35a**	4-CH$_3$	2-F	Et	87.0
2	**1.35b**	4-CH$_3$	2-F	n-Pr	85.6
3	**1.35c**	4-CH$_3$	2-F	n-Bu	68.2
4	**1.35d**	4-CH$_3$	4-CF$_3$	Me	70.8
5	**1.35e**	4-CH$_3$	4-CF$_3$	Et	84.1
6	**1.35f**	4-CH$_3$	4-CF$_3$	i-Pr	76.3
7	**1.35g**	4-CH$_3$	4-CF$_3$	n-Bu	72.3
8	**1.35h**	6-OCH$_3$	2-F	Me	66.1
9	**1.35i**	6-OCH$_3$	2-F	Et	85.6
10	**1.35j**	6-OCH$_3$	2-F	n-Pr	85.6
11	**1.35k**	6-OCH$_3$	2-F	i-Pr	84.2
12	**1.35l**	6-OCH$_3$	2-F	n-Bu	72.1
13	**1.35m**	6-OCH$_3$	4-F	Et	84.2

^{a}All reactions were carried out at 100-102℃ for 1.5h in ionic liquids (4mL).

The single-crystal structure of **1.35m** was determined by X-ray crystallography. The molecular structures of **1.35i** and **1.35m** are illustrated in Fig 1.13 and Fig 1.14. In **1.35m**, the P atom exhibits a distorted tetrahedral configuration because the bond angles of O(1)-P(1)-O(2) (114.6°) and O(2)-P(1)-O(3)(116.6°) are significantly larger than that of O(2)-P(1)-O(3) (102.5°). The bond length of P(1)-C(1)(1.804 Å) is a little shorter than normal P-C single bond length (1.850 Å) and a benzothiazole ring exists through the atom N(2) which is linked to the α-C restricting the free rotation of P(1)-C(1) bond. The bond length of C(8)-N(2)(1.358 Å) is remarkably shorter than normal C-N(1.47 Å) and close to the C=N double bond distance(1.34 Å), which is indicative of significant double bond character. The bond length of C(8)-N(1) is 1.290(4), close to that of typical C=N. The single bond lengths of C(9)-C(10), N(1)-C(9), C(8)- S(1), C(10)-S(1) are 1.384,
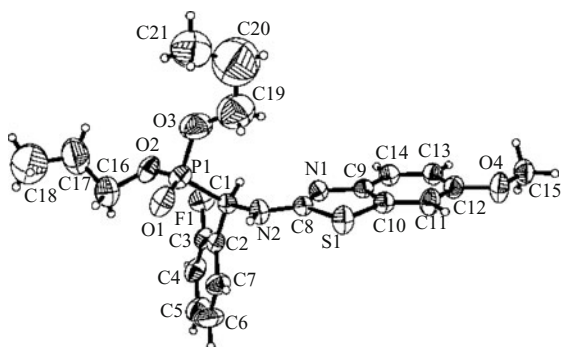
Fig 1.13   ORTEP drawing of **1.35i**
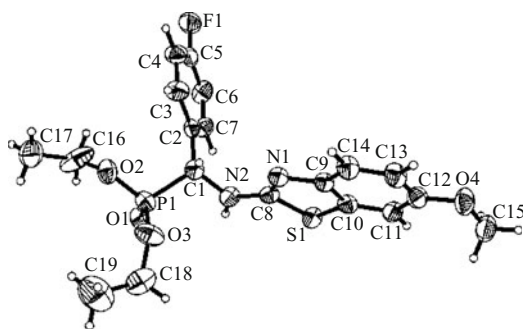
Fig 1.14   ORTEP drawing of **1.35m**

1.396, 1.758, 1.749 Å, respectively, which are shorter than typical C-C(1.54 Å), and C-S(1.85 Å). There is an intermolecular hydrogen bond in the form of N(2)-H(2)···O(1)(symmetry code,$-x+1$, $-y+1/2$, z), with N(2)-H(2)=0.860 Å, H(2)···O(1)=2.053, N(2)···O(1)=2.814 Å, and N(2)-H(2)···O(1)=147.2° .

Anticancer activity. The antitumor activities *in vitro* for these compounds were evaluated by the MTT method for PC3, A375, A431 and Bcap-37 cells.[260]The results are summarized in Table 1.38 and Table 1.39. Usually, when the concentration of the compound solution is 1μM and the inhibition ratio of the solution to cancer cell growth is more than 50%, or when the concentration of the compound solution is 10μm, and the inhibition ratio of the solution to cancer cell growth is more than 85%, the compound is considered strongly effective. According to this standard, it can be found from Table 1.38 and Table 1.39 that the compound **1.35c** has a strong affinity for PC3 cells. The data given in Table 1.38 indicates that the nature of substituent affects the antitumor activities. For example, the antiproliferation activities of compound **1.35c** at the concentration of 1μM and 5μM against PC3 cells are 52.1% and 86.0%, respectively.

Table 1.38   Inhibition rate (%)1,5,10μM of compounds **1.35a-1.35m** to PC3 and A431 in 72h

Compd.	PC3 cells			A431 cells		
	1	5	10	1	5	10
1.35a	3.51	22.9*	41.9*	17.7*	23.3*	35.3*
1.35b	21.7*	29.4*	43.3*	15.9*	27.3*	31.7*
1.35c	52.1*	86.0*	89.1**	32.1*	49.0*	72.1*
1.35d	4.0	4.6	8.9	22.1*	26.0*	47.3*
1.35e	12.6	13.5	49.3*	0.36	2.06	16.9*
1.35f	6.3	15.3	25.9*	17.3	20.5*	29.5*
1.35g	5.0	31.6	36.0*	37.7*	40.8*	57.4*
1.35h	21.4*	26.6	33.3*	1.9	7.9	8.64
1.35i	16.8	22.5	38.9	4.5	12.3	22.1*
1.35j	5.0	15.8	28.7*	35.3*	49.2*	58.1*
1.35k	−8.5	2.1	18.5*	−7.4	7.5	16.7*
1.35l	−6.6	5.3	13.2*	−3.7	5.4	28.8*
1.35m	32.1*	41.0*	49.5*	11.2	20.9*	31.2*

*Inhibition rate (%)=$(A_1-A_2)/A_1 \times 100\%$. A_1: the mean optical densities of untreated cells, A_2: the mean optical densities of drug treated cells; *$P<0.05$, **$P<0.01$.

Table 1.39   Inhibition rate(%) 1,5,10μM of compounds **1.35a-1.35m** to A375 and Bcap37 in 72h

Compd.	A375 cells			Bcap-37 cells		
	1	5	10	1	5	10
1.35a	−13.9	−6.1	9.2	35.8*	42.6*	58.9*
1.35b	−0.2	4.8	4.3	−18.9	0.8	21.7
1.35c	11.2	25.6	32.1*	10.0	29.0*	38.1*
1.35d	1.8	19.2*	20.8*	−13.2	−0.8	2.5
1.35e	−10.2	1.6	14.2*	−5.2	9.8	16.7*
1.35f	−1.3	8.6	9.1	−0.7	11.2*	22.7*
1.35g	−3.2	21.6*	31.5*	0.1	9.2	20.3
1.35h	4.3	10.1	11.4	11.9	17.8*	25.1*
1.35i	7.5	7.9	15.7*	20.5*	34.5*	49.4*
1.35j	10.3	13.9	23.8*	21.3*	25.1*	27.1*
1.35k	−4.3	1.7	2.8	39.7*	43.2*	50.4*
1.35l	−6.2	3.5	17.4*	23.6*	38.2*	44.2*
1.35m	8.0	10.9	34.5*	10.0	39.0*	49.9*

*$P<0.05$.

Antiviral activity. The antiviral activity in vivo for these compounds were assayed by the reported methods.[49,50] It could be seen from Table 1.40 that these newly synthesized compounds exhibit promising antiviral activities against TMV in vivo. Apparently and interestingly, the antiviral data indicate that the nature of substituents on the R^1, R^2, R^3 groups affects the antviral activity substatially. The inhibition effect of **1.35a** to TMV *in vivo* is marginally better than that of Ningnanmycin.

Table 1.40   The curative effects of the new compounds against TMV *in vivo*

Compd.	1.35a	1.35b	1.35c	1.35d	1.35e	1.35f	1.35g
Inhibition rate(%)	69.7	41.3	31.9	10.1	44.2	29.7	11.2
Compd.	1.35h	1.35i	1.35j	1.35k	1.35l	1.35m	
Inhibition rate(%)	22.2	45.1	30.1	21.7	30.7	42.2	

1.9.4   Conclusions

In summary, we described a practical and efficient procedure for the preparation of α-aminophosphonates with benzothiazole moiety through the three-component reaction of 2-aminobenzothiazole, O,O-dialkylphosphite and 2-or 4-fluoro-benzaldehyde or 4-trifluorobenzaldehyde in ionic liquids for 1.5h at 100-102℃. The reactions were, in general, very fast, clean and atom-economic. Compound **1.35c** is highly effective against PC3 cells and moderately effective against A431 cells, and **1.35a** has good inhibition activity to TMV *in vivo*. These identified α-aminophosphonates with benzothiazole moiety can serve as new lead structures in antitumor and antiviral chemotherapy . These molecules can be very useful for further optimization work in antitumor chemotherapy.

1.10   Chiral Separation & Bioactivity of α-Aminophosphonates Containing Benzothiazole Moiety

1.10.1   Introduction

α-Aminophosphonic acids, bioisosteres of natural amino acids, have been found to exhibit a wide range of biological activities. Some derivatives of α-amino-phosphonic acid are used as plant growth regulators, fungicides, plant virucides and herbicides, and so on. In our previous work, we designed and synthesized α-aminophosphonates containing fluorine and heterocyclic moiety,

which exhibited moderate antiviral bioactivity against the tobacco mosaic virus (TMV) and antitumor activity[28,102,148]. The stereoisomers of these compounds contain a chiral carbon atom center which has strong relevance with regard to biological activity. Therefore, determination of absolute configuration and enantioseparation of α-aminophosphonate esters have received extensive attention. Researchers have resolved some α-aminophosphonate esters with Pircle-type chiral stationary phases (CSPs)[150,152] and cyclodextrine CSPs.[153–155] Recently, polysaccharide-derived CSPs have been recognized as the most powerful materials for the enantioseparation in analytical and preparative applications due to their broad application and remarkable loading capacity.[156–160] Of late, our group has been involved in the study of enantioseparation of α-aminophosphonate esters on polysaccharide CSPs. After ensuring the best separation conditions on polysaccharide- derived CSPs, we thought to carry out semi-preparative preparations of these compounds by HPLC in order to obtain some pure enantiomers to study the bioactivities. In this report, ten novel α-aminophosphonate esters containing substituted benzoyl moiety were separated. The enantiomers were separated on coated amylose-based (Chiralpak AD-H) and immobilized amylose-based (Chiralpak IA) CSPs. Chiralpak IA is a new immobilized CSP based on (3,5-dimethyl phenylcarbamate) of amylose, which was commercialized by Daicel Chemical company in 2004. The changes in enantioselectivity and retention were observed using two organic modifiers. All the α-aminophosphonate esters were semipreparatively separated on Chiralpak IA column. Optimization of enantioselective conditions for semipreparative separation was performed. The bioassay tests showed that some of these title compounds exhibit weak to moderate antiviral activity in vivo. To the best of our knowledge, this is the first report on the chiral separation and antiviral bioactivity of α-aminophosphonate esters containing substituted benzoyl moiety.

1.10.2   Materials and Methods

1.10.2.1   Chemicals

Racemic α-aminophosphonates were synthesized in our own laboratory, the structures are shown in Table 1.41.[28] n-Hexane, ethanol, ethyl acetate (EtOAc), tetrahydrofuran (THF) and dichloromethane (CH_2Cl_2) of chromatographic grade, were purchased from Nanjing Hanbang Chemicals Co. Ltd (Jiangsu, China).

1.10.2.2   Equipments

The analytical HPLC of the compounds was performed on Agilent 1100 series Apparatus composed of a quarternary pump, an autosampler, a DAD detector, a vacuum degasser, a column oven and Agilent Chemstation software. The two columns employed were Chiralpak AD-H-amylose tris-(3,5-dimethylphenyl carbamate) coated on 5μm silica-gel and Chiralpak IA-amylose tris-(3,5-dimethylphenylcarbamate) immobilized on silica-gel (both the columns of 250mm×4.6 mm i.d., Daicel Chemical

Table 1.41   Chemical structures of the chiral α-aminophosphonate.
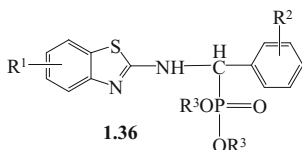
No.	R^1	R^2	R^3
1.36.1	4-CH$_3$	o-F	CH$_2$CH$_3$
1.36.2	4-CH$_3$	o-F	CH$_2$CH$_2$CH$_3$
1.36.3	6-OCH$_3$	o-F	CH$_2$CH$_3$
1.36.4	6-OCH$_3$	o-F	CH$_2$CH$_2$CH$_3$
1.36.5	4-CH$_3$	p-CF$_3$	CH$_3$
1.36.6	4-CH$_3$	p-CF$_3$	CH$_2$CH$_3$
1.36.7	4-CH$_3$	p-CF$_3$	CH$_2$CH$_2$CH$_3$
1.36.8	4-CH$_3$	p-CF$_3$	CH$_2$CH$_2$CH$_2$CH$_3$
1.36.9	6-OCH$_3$	p-F	CH$_2$CH(CH$_3$)$_2$
1.36.10	6-OCH$_3$	p-F	CH$_2$CH$_3$

Industries Ltd). Semipreparative HPLC was carried out by Agilent 1100 series consisting of a preparative pump, a DAD detector, a manual injector with a 10 mL sample loop. Semipreparative Chiralpak IA column (250mm×10 mm i.d., 5μm) was also purchased from Daicel Chemical Industries Ltd.

1.10.2.3   Instrumentation and Chromatographic conditions

Analytical and preparative HPLC enantioseparations were performed by using an Agilent 1100 LC system with diode array detection (DAD). The preparative LC was equipped with a Rheodyne injector and a 10 mL sample loop.Chiralpak AD-H, Chiralpak IA columns (250mm×4.6 mm i.d.,5μm) and semi-preparative Chiralpak IA column (250mm×10 mm i.d.,5μm) were all purchased from Daicel Chemical Industries Ltd., Tokyo, Japan. Optical rotations of α-aminophosphonate enantiomers, dissolved in anhydrous ethanol, were measured on a polarimeter WZZ-2A equipped with a Na lamp. The volume of the cell was 1 mL and the optical path was 10 cm. The system temperature was fixed at 20℃. CD spectra were recorded on a JASCO-810 spectropolarimeter.

Separations were performed with n-hexane/ethanol for compounds **1.36.1-1.36.9** and n-hexane/THF for compound **1.36.10**. The flow rates were 1.0 and 4.0 mL·min^{-1} for analytical and semi-preparative separations, respectively. All separations were performed at 25℃ at a wavelength of 270 nm. The dead time was estimated by employing 1,3,5-tri-tert-butylbenzene as an unretained compound.[161]

1.10.2.4   Antiviral Bioassay

The method for evaluating anti-TMV activity of title compounds is similar to the procedure described in Chapter 1.1.2.[49,50]

1.10.3   Results and Discussion

To achieve separation of enantiomers of the investigated series of α-aminophosphonates with a chiral center, a comparison between the two immobilized and coated amylose-based chiral stationary phases (Chiralpak AD and Chiralpak IA, respectively) was made. Also, the conditions of analytical and semi-preparative separations were optimized.

1.10.3.1   Analytical HPLC

The chiral resolution on amylose based chiral stationary phases is extremely sensitive to several factors such as type of columns, analyte structures, concentration of mobile phase and temperature.

Column selectivity. In our experiments, two new immobilized and conventional coated amylose tris-(3,5-dimethylphenylcarbamate) chiral stationary phases (Chiralpak IA and Chiralpak AD-H, respectively) were selected. A comparison was made between the two chiral stationary phases for enantioselective separation of isomers of racemic α-aminophosphonates by LC using the conventional organic solvent system *n*-hexane/ethanol (Table 1.42). Of all the chiral compounds investigated in this study, excellent baseline separation on both columns was achieved for compounds **1.36.2**-**1.36.9** by using the same solvent system as the mobile phase.While compounds **1.36.1** and **1.36.10** could not be separated on Chiralpak AD-H, the compound **1.36.1** showed a good baseline separation on Chiralpak IA with a separation factor α 1.27 and resolution *Rs* 5.02 (Fig 1.15). Although the stationary phase is similar in both the columns, the chiral recognition in case of Chiralpak IA is different from that of Chiralpak AD-H. It can be seen from the data that the enantioselectivity and resolutions were better on Chiralpak IA than that on Chiralpak AD-H for available compounds. Due to the strong binding force, the immobilized stationary phase becomes more stable. As a result, Chiralpak IA showed good enantioselectivity, and was selected for further optimization studies.

Compound **1.36.1**
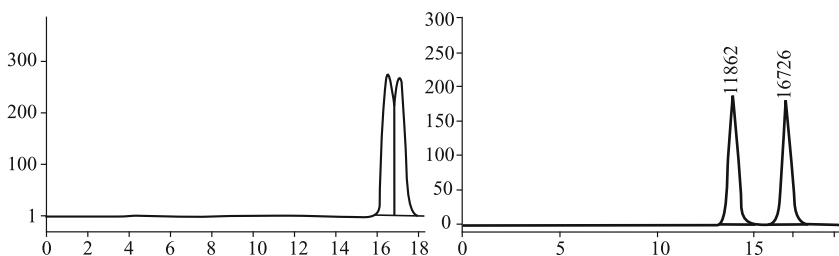
Compound **1.36.2**
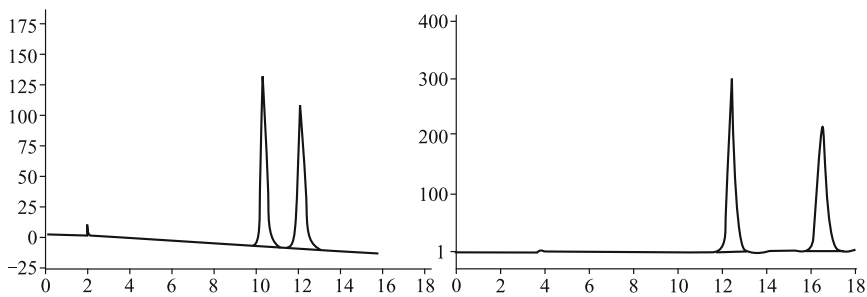
Compound **1.36.3**
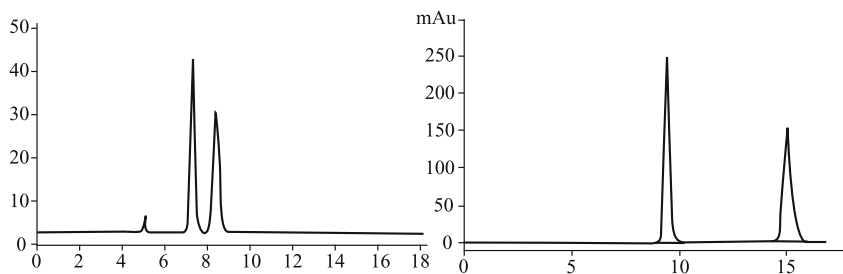
Compound **1.36.4**
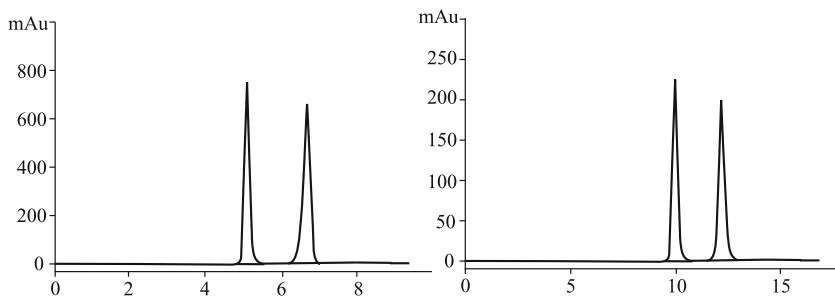
Compound **1.36.5**
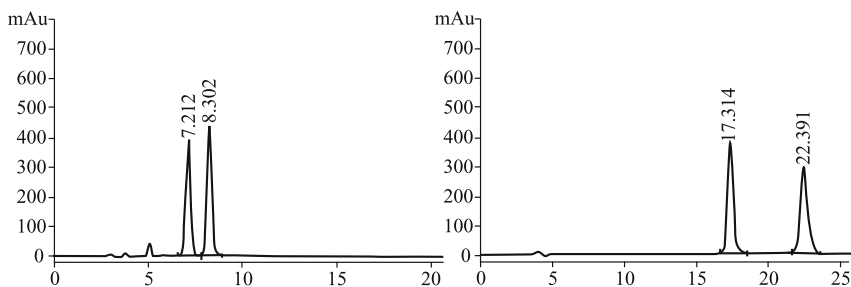
Fig1.15

Compound **1.36.6**
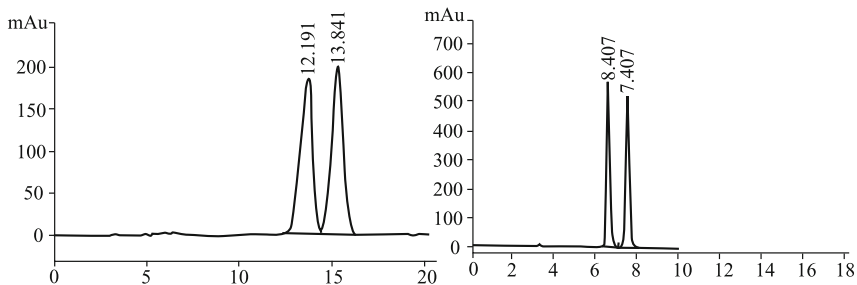
Compound **1.36.7**
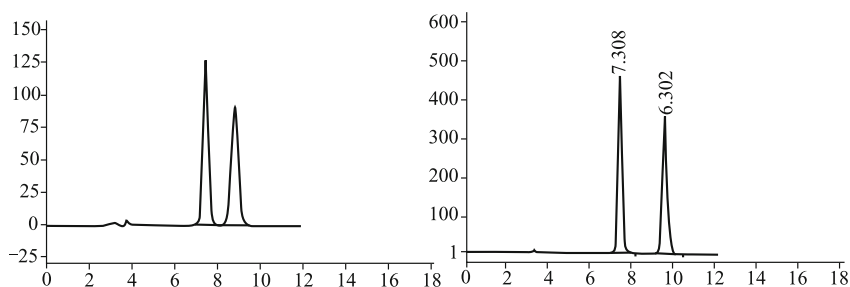
Compound **1.36.8**
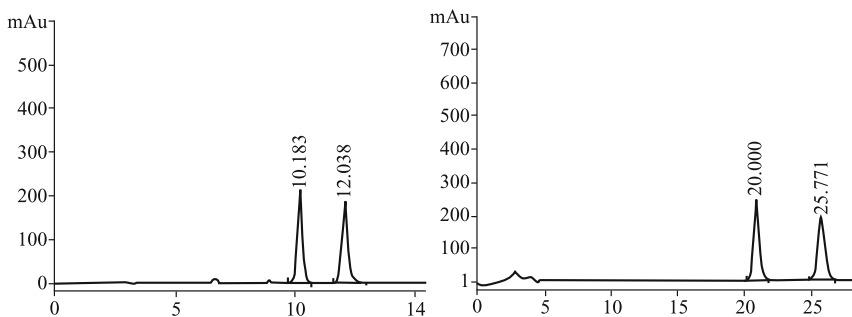
Compound **1.36.9**
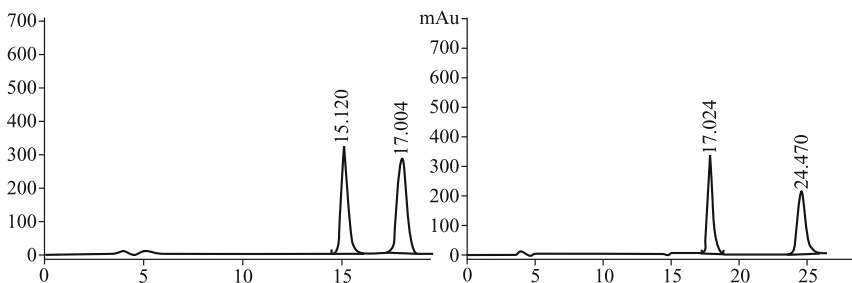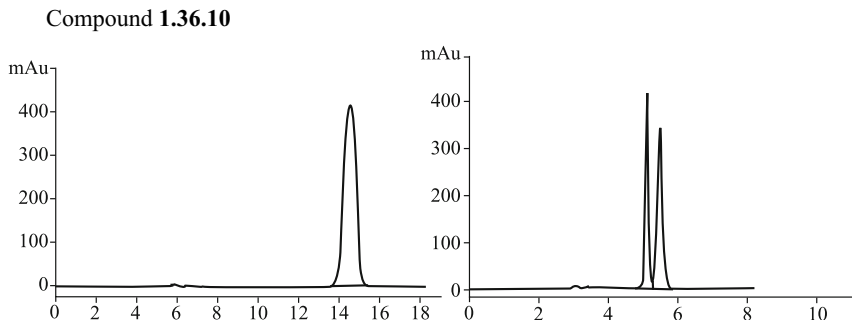
Compound **1.36.10**

Fig 1.15   Typical chromatograms showing the separation of α-aminophosphonate enantiomers **1.36.1-1.36.10** at 25℃ on Chiralpak AD (left) and Chiralpak IA (right) using *n*-hexane and ethanol (95:5, *v/v*), with λ 270 nm

Table 1.42   The compound resolution factor (*Rs*) and separation factor (α) of the simultaneous LC separation of racemic α-aminophosphonates on Chiralpak AD-H and Chiralpak IA

Compound	Chiralpak AD-H				Chiralpak IA			
	k_1	k_2	A	Rs	k_1	k_2	α	Rs
1.36.1	3.38	3.24	1.10	1.04	3.38	4.28	1.27	5.02
1.36.2	5.10	6.98	1.37	2.62	4.15	6.39	1.54	3.43
1.36.3	0.90	1.24	1.38	4.03	0.89	1.43	1.61	5.78
1.36.4	6.42	8.30	1.29	1.72	7.84	9.54	1.22	2.30
1.36.5	2.08	2.50	1.20	1.93	7.88	9.95	1.26	2.31
1.36.6	5.54	7.03	1.27	2.01	0.70	0.93	1.32	4.20
1.36.7	1.79	2.34	1.25	3.82	0.79	1.06	1.34	5.44
1.36.8	2.19	3.27	1.49	5.58	2.19	3.24	1.48	5.98
1.36.9	2.05	2.78	1.36	4.27	6.28	10.58	1.68	3.93
1.36.10	N S[a]	N S	N S	N S	2.56	3.04	1.18	1.20

Conditions：*n*-hexane: ethanol (95:5, *v/v*), λ (270 nm), rate (1.0mL·min^{-1}), temperature (25℃)

[a] N S means not separated.

Effect of concentration of the mobile phase. The selection of the mobile phase is based on the solubility and the structural characteristics of the analytes to be resolved. *n*-Hexane and ethanol in the ratio of 80:20 to 98:2(*v/v*) were employed to study their effect on resolution and selectivity, as shown in Fig 1.16. As expected, with an increase of the hydrophobicity of the mobile phase, there is a decrease of the hydrophobic interaction between the analyte and the stationary phase.

Effect of column temperature. Generally, an increase in column temperature often causes a reduction in retention and poor resolution. The influences of temperature on resolution and retention factors for enantiomers **1.36.1, 1.36.2, 1.36.3, 1.36.6, 1.36.7** and **1.36.10** were studied from 15 to 40℃ on Chiralpak IA column. As shown in Fig 1.17, the retention factors decreased as column temperature was increased.
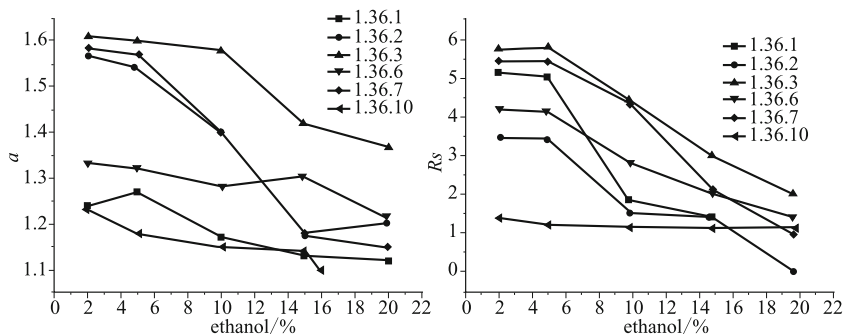
Fig 1.16 Effect of concentration of ethanol on α and *Rs* for compounds **1.36.1, 1.36.2, 1.36.3, 1.36.6, 1.36.7** and **1.36.10.**
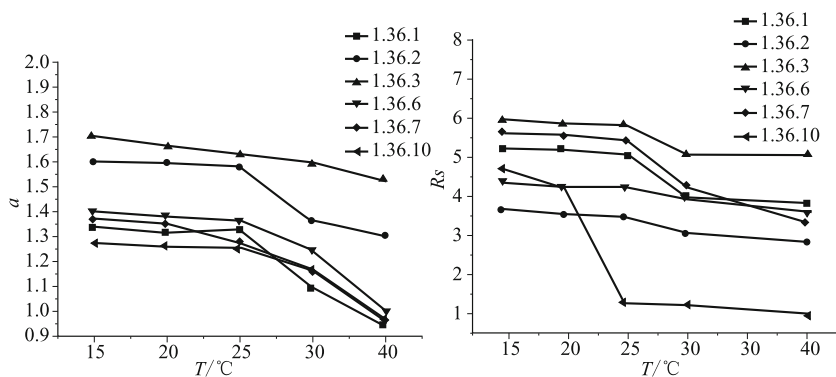
Fig 1.17 Effect of temperature on retention factor α and *Rs* for compounds **1.36.1,1.36.2, 1.36.3,1.36.6,1.36.7** and **1.36.10**.

A slightly lower resolution factor was noticed at 25℃ than that at 20℃. The temperature 25℃ was selected as optimum to perform successive analytical and semi-preparative enantioseparations with shorter run time without broadening of peaks.

Effect of the structure of the analytes. Halogens have a strong affinity for the amylose CSP, fluorine substituent in the analyte may play an important role in the enantioseparation. The enantioselectivities for compounds **1.36.6** and **1.36.7**, with higher fluorine contents, were much better than those of **1.36.1** and **1.36.2**. It is likely that the presence of a halogen could enhance interaction with the stereogenic center, leading to an improved enantioselective separation.

Comparison of results between **1.36.1** and **1.36.3**, or **1.36.2** and **1.36.4**, revealed that 4-CH_3 substituent on the benzothiazole ring could result in a lower retention time than 6-OCH_3. This might arise from strong H-bond interaction between the methoxy group and CSP.

Steric repulsion also plays an important role in chiral recognition for these α-aminophosphonates. The separation of compounds **1.36.5**-**1.36.8** shows that an increase in steric bulk near their stereogenic centers improves the separation on

the Chiralpak IA. A similar trend can be observed for compounds **1.36.1** and **1.36.2**, **1.36.3** and **1.36.4**,**1.36.9** and **1.36.10** (shown in Table 1.42). With increasing steric repulsion between alkyl substituent R^3 and the aryl group in the *α*-aminophosphonate structure, the *p-p* interaction between the solutes and CSP is decreased.

   Enantioseparation of O,O-diethyl α-[N-(6-methoxy-benzothiazol-2-yl) amino] (p-fluorobenzyl) phosphonate (compound 1.36.10) using non-standard mobile solvent. Stereoisomers of compound **1.36.10** could not be resolved at all with a conventional mobile phase consisting of *n*-hexane/ethanol (95:5, *v/v*) on the Chiralpak AD-H. However, weakly separated peaks were obtained on Chiralpak IA with *Rs* 1.20 and *α* 1.18, respectively. In some cases, both columns afforded similar enantioselectivity under the same chromatographic conditions, but often with an enhanced degree of resolution on Chiralpak IA (Table 1.43). By taking advantage of its ability to withstand prohibited LC solvents like EtOAc, THF and CH_2Cl_2, we obtained good separation of compound **1.36.10**. The use of immobilized-type IA CSP combined with nonstandard eluents allowed a dramatic enhancement of chiral recognition in terms of enantioselectivity and resolution degree. The following unconventional mobile phases were employed: *n*-hexane/ EtOAc=80:20 (*v/v*), *n*-hexane/THF= 80:20(*v/v*) and *n*-hexane/CH_2Cl_2=80:20(*v/v*). As shown in Fig 1.18, the separation of compound **1.36.10** could be achieved when EtOAc was present in the mobile phase with *Rs* 1.28. In comparison, CH_2Cl_2 and THF generally lead to higher selectivity values with *Rs* 2.32 and 8.79, respectively. Due to their varying eluting strengths, the proportions of these solvents in the mobile phase should be adjusted so that the retention factors fall within the reasonable range (k_1'>0.2 and k_2'<5.0). Based on the statistics of retention factors for this series of *α*-aminophosphonates, we chose THF as the modifier to separate compound **1.36.10** in a nonstandard solvent mode.
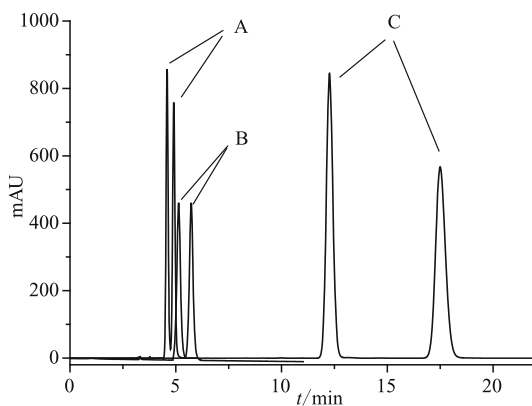
Fig 1.18   Influence of the mobile phase composition of non-standard solvent for seperation of **1.36.10** on Chiralpak IA. Eluent：n-hexane/AcOEt (*v/v*,80/20, A), *n*-hexane/ CH_2Cl_2 (*v/v*, 80/20,B), and *n*-hexane/THF (*v/v*, 80/20, C)

1.10.3.2   Semi-preparative HPLC

The preparative chromatographic resolution of racemates on CSP has emerged as a competitive approach to asymmetric synthesis in the preparation of optically pure compounds. At least during the preliminary comparative biological testing phase, chiral chromatography offers a first hand synthetic route for furnishing both the enantiopure forms. The successful development of an analytical enantioseparation essentially relies on the selection of a CSP/mobile phase combination capable of furnishing promising results in terms of resolution degree. In some cases, the solubility and resolution of the compounds are low in comparison with n-hexane/ethanol. Throughput improvements can be achieved by using different CSPs in combination with other organic solvents.

As can be seen from analytical separation, the immobilization of CSP can provide a solution to this problem. In order to evaluate the loading amount of racemic compounds that may be applied onto IA CSP at a semi-preparative level, their solubility in different eluents was examined.

The results from the study revealed a lower solubility of the compounds in n-hexane/ethanol mixtures than in nonstandard solvents, an intermediate solubility in EtOAc and CH_2Cl_2, a high solubility in THF. According to the analytical enantioseparation, good resolutions were obtained for compounds **1.36.1**-**1.36.9** with n-hexane/ethanol, but for compound **1.36.10**, due to its poor solubility, the baseline separation was not achieved successfully. Consequently, for the purpose of semi-preparative enantioseparation, we selected n-hexane/THF for compound 10 and n-hexane/ethanol for compounds **1.36.1**-**1.36.9** as the mobile phases, respectively. The optimized conditions and resolution are shown in Table 1.43.

Table 1.43   The optimized conditions of semi-preparative enantiomeric separation for the ten α-aminophosphonates

Compd.	SR/V^a (mg)	Optimized condition	Rs
1.36.1	16/3	25℃, 3% ethanol in n-hexane, 270 nm, 4.0 mL	2.94
1.36.2	9/3	25℃, 4% ethanol in n-hexane, 270 nm, 4.0 mL	4.01
1.36.3	16/3	25℃, 8% ethanol in n-hexane, 270 nm, 4.0 mL	3.51
1.36.4	16/3	25℃, 6% ethanol in n-hexane, 270 nm, 4.0 mL	5.59
1.36.5	12/3	25℃, 3% ethanol in n-hexane, 270 nm, 4.0 mL	2.36
1.36.6	16/3	25℃, 3% ethanol in n-hexane, 270 nm, 4.0 mL	3.55
1.36.7	6/3	25℃, 5% ethanol in n-hexane, 270 nm, 4.0 mL	4.67
1.36.8	9/3	25℃, 5% ethanol in n-hexane, 270 nm, 4.0 mL	3.56
1.36.9	16/3	25℃, 8% ethanol in n-hexane, 270 nm, 4.0 mL	3.18
1.36.10	10/3	25℃, 20% THF in n-hexane, 270 nm, 4.0 mL	7.46

[a] SR：semi-preparative run (mg), V：sample volume injection (mL); Column: Chiralpak IA 250 mm× 10mm i.d.

The semi-preparative HPLC enantioseparations were carried out in a single step. Purities and yields of the separated enantiomers were adjusted by setting the cut-point position for fractionation and by repeated separation (fraction recycling). Two fractions were collected; the first eluted enantiomer was collected in F1 fraction and the second eluted enantiomer was in F2 fraction. The analytical assessment of the enantiomeric excess values of the collected fractions showed *ee* >96%. The amount of racemate that could be resolved in a single pass depended on the degree of enantioselectivily and chemical purity of the sample. The practical relevance of sample solubility in the mobile phase at semipreparative level was evident in the loading study performed using compound **1.36.1** as a test solute. Injection of 16 mg of **1.36.1** dissolved in 3 mL (the maximum concentration) of *n*-hexane/ethanol 97:3 (*v/v*) afforded complete enantioseparation in one step, without peak overlapping, permitting the isolation of two fractions of the injected racemic sample as pure enantiomers. Total time for these runs was <20 min (Fig 1.19). After repeated separation, 94.2% of the initial material was collected as sepatrated enantiomers with purities of up to 98.5%. In Table 1.44, chromatographic and polarmeteric data pertinent to each collected enantiomer are reported.
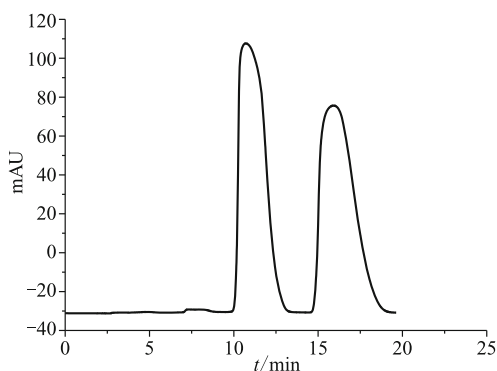
Fig 1.19   Loading study of compound **1.36.1** on a 250mm×10mm I.D.column packed with Chiralpak IA CSP. Amount injected:16 mg dissolved in 3 mL of *n*-hexane/ethanol= 97:3(*v/v*).

The assignment of the absolute configuration of the enantiomers for all the α-aminophosphonate racemates resolved on a mg-scale was performed indirectly by comparison of their circular dichroism (CD) spectra (Fig 1.20). The quantitative values of both enantiomers were measured at 20℃ in ethanol, and they are reported after subtracting the baseline value corresponding to the solvent. Each pair of enantiomers showed mirror-imagine CD spectra, confirming their enantiomeric relationships. Taking compound **1.36.1** as an example, the CD spectrum of the *R*-isomer in ethanol displayed a broad positive Cotton effect centered around 230 and 270nm , while the （*S*）-isomer presented a negative Cotton effect, as shown in Fig 1.20. These bands probably arise due to the *p-p* electronic transitions of the aromatic system directly linked to the stereogenic center.

Table 1.44　Chromatographic, quantitative and polarimetric analysis of
the first (F1) and the second fractions (F2) during enantioseparation of
α-aminophosphonates **1.36.1-1.36.10**

Comp.	F1 [(+)-R]			F2 [(−)-S]		
	Yield（%）	ee(%)	$[\alpha]_D^{20}$ /methanol	Yield（%）	ee(%)	$[\alpha]_D^{20}$ /methanol
1.36.1	94.2	98.5	84.63° (c=0.95)	93.5	97.8	−83.29° (c=0.91)
1.36.2	92.7	97.9	68.41° (c=0.89)	91.8	99.4	−59.41° (c=0.92)
1.36.3	90.2	100.0	60.75° (c=0.54)	90.6	100.0	−58.92° (c=0.70)
1.36.4	93.4	96.4	57.64° (c=0.61)	92.8	97.4	−61.76° (c=0.63)
1.36.5	95.1	98.2	67.23° (c=0.84)	93.2	97.2	−67.29° (c=0.79)
1.36.6	91.3	97.6	21.38° (c=0.23)	90.8	98.2	−21.39° (c=0.24)
1.36.7	95.5	98.1	53.42° (c=0.27)	93.4	98.7	−60.03° (c=0.18)
1.36.8	95.5	96.7	40.77° (c=0.31)	93.2	97.3	−49.02° (c=0.26)
1.36.9	92.5	98.6	79.65° (c=0.73)	90.2	98.4	−73.92° (c=0.69)
1.36.10	92.6	97.5	52.07° (c=0.29)	90.3	100.0	−60.92° (c=0.26)
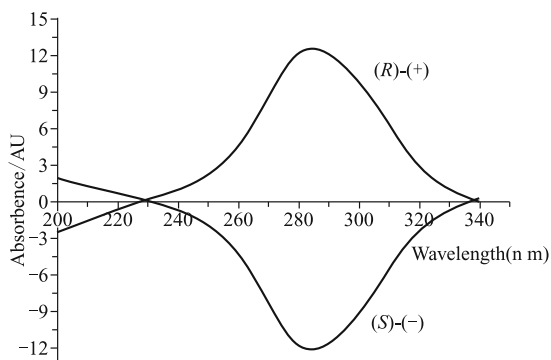
Fig 1.20　CD spectra (ethanol, 20℃) of the enantiomers obtained from the first and the
second eluted peaks.

1.10.3.3　Antiviral activity

　　The antiviral activity was assayed according to the half-leaf method.[147, 215]
The results are listed in Table 1.45. It was found that these chiral compounds and
their racemate exhibit weak activites against TMV *in vivo*. The chiral compound
(R)-**1.36** has relatively higher activity than the one with (S) configuration, and
racemate and other chiral compounds. The data given in Table 1.48 indicate that
the antiviral activity of chiral compound 1-R to TMV at 500μg/mL is 50.2%. No
substantial difference was found between the (R) and (S) configuration for
compounds **1.36.2-1.36.10** in the antiviral bioassay.

Table 1.45   The Curative, protection and incurative effect of racemic mixtures and enantiomers of analytes **1.36.1-1.36.10** against TMV in tobacoo

Compd. （500mg/L）	Activity index [a]	Inhibition (%)		
		Racemate	（R）-（＋）	（S）-（－）
1.36.1	C.E	42.53	50.22	38.52
	P.E	50.27	52.61	43.21
	I.E	41.61	51.97	47.42
1.36.2	C.E	15.22	12.00	16.07
	P.E	23.08	25.86	37.36
	I.E	43.62	42.57	52.03
1.36.3	C.E	40.23	26.23	30.00
	P.E	30.95	23.68	23.08
	I.E	53.49	55.38	53.62
1.36.4	C.E	13.33	21.52	16.35
	P.E	24.48	32.17	34.57
	I.E	34.43	15.00	18.75
1.36.5	C.E	12.90	25.32	20.90
	P.E	40.77	45.84	41.88
	I.E	9.56	33.02	38.89
1.36.6	C.E	40.78	41.00	40.23
	P.E	21.37	28.21	24.24
	I.E	31.25	48.57	46.61
1.36.7	C.E	46.66	49.35	47.50
	P.E	34.11	29.80	24.55
	I.E	42.79	40.15	49.46
1.36.8	C.E	41.86	41.87	47.89
	P.E	21.87	37.34	21.43
	I.E	46.09	48.58	45.29
1.36.9	C.E	29.85	21.79	36.26
	P.E	22.36	27.87	27.38
	I.E	44.90	49.84	47.63
1.36.10	C.E	34.69	26.67	31.18
	P.E	41.58	43.88	40.93
	I.E	41.13	48.87	40.41
Ningnanmycin	C.E		50.49	
	P.E		60.12	
	I.E		95.29	

[a] C.E means curative effect, P.E means protection effect, I.E means inactive effect.

1.10.4   Conclusions

Chiralpak AD-H and Chiralpak IA columns were compared for their recognition ability towards ten α-aminophosphonate derivatives **1.36.1-1.36.10**. Under normal-phase conditions, the new immobilized Chiralpak IA provided to create new enantioselectivity profiles by using non-standard solvents such as THF. Resolution factor values superior to 2.5 were achieved for all analytes in eluents *n*-hexane/ethanol for compounds **1.36.1-1.36.9** or *n*-hexane/THF for compound **1.36.10** as eluents. Around 200 mg of racemates could be resolved with an enantiomeric excess of >96% for isolated enantiomers. High enantiomeric purity of isolated enantiomers is suitable for chiroptical and biological trials. In the half-leaf method test, the chiral compound 1-(*R*) was found to possess high antiviral activity against TMV *in vivo*.

1.11   Crystal Structure of *O,O*-Dipropyl-α-aminophosphonate Containing Benzothiazole Moiety

1.11.1   Introduction

α-Aminophosphonic acids, bioisosteres of natural amino acids, have been found to exhibit a wide range of biological activities. Some derivatives of α-aminophosphonic acid can be used as fungicides, plant virucides and herbicides. [3] A large amount of research on their synthesis and biological activities has been reported during the last twenty years.[162–164] In order to find a new anticancer agent, we decided to synthesize and characterize *N*-(4-methylbenzothiazole-2-yl)-1-(4-trifluoromethyl phenyl)-*O,O*-dipropyl-α-aminophosphonate.

1.11.2   Materials and Methods

The title compound was prepared in the following manner. To an oven-dried three-necked 50 mL round-bottom flask was added 2-amino-4-methylbenzothiazole (3 mmol), 4-trifluoromethylbenzaldehyde(3 mmol), dipropyl phosphite (3 mmol), boron fluoride diethyl etherate (0.3 mmol), and 20 mL anhydrous acetonitrile. The mixture was irradiated in an ultrasonic cleaning bath at 78-80℃ for 2 h. The mixture was then washed with water, filtered, dried, and the crude solid was recrystallized from ethanol and water (1:1, *v/v*) to give the title compound as a white solid (1.27 g, 87.1%) with mp 127-129℃ ［Calcd.（%）: C 54.31, H 5.38, N 5.75;Found (%):C 54.41, H 5.39, N 5.61］, as shown in **1.37.**

1.37
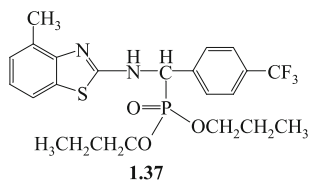
The absorption correction was semi-empirical from equivalents and the maximum and minimum transmissions were 0.966 and 0.906, respectively. The structure was solved by direct methods with the help of the SHELXS-97 package and refined on F^2 using data ($I>2\sigma(I)$) obtained by full-matrix least-square procedures from the SHELXL-97 package. The positions of hydrogen atoms were caculated based on the molecular geometry, except for H2A, which was found by different Fourier synthesis; the coordinates were refined. An ORTEP diagram of the molecule with thermal ellipsoids at 30% probability is presented in Fig 1.21.
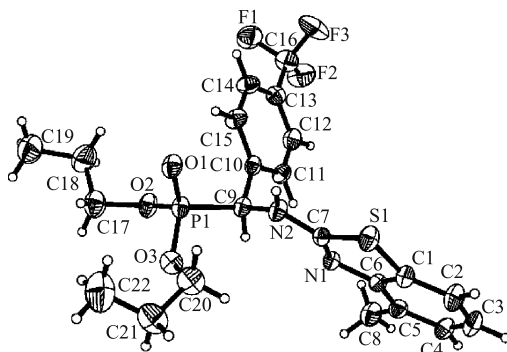
Fig 1.21 ORTEP drawing of the molecule at 30% probability

1.11.3   Results and Discussion

The P atom exhibits a distorted tetrahedral configuration because the bond angles of O(1)-P(1)-O(3) (114.0(15) °) and O(2)-P(1)-C(9) (113.0(16)°) are significantly larger than that of O(2)-P(1)-C(9) (102.7(14)°). The bond length of P(1)-C(9) (1.813 Å) is slightly shorter than the normal P-C single bond length (1.850 Å). Also, a benzothiazole ring exists through the atom N(2), which is linked to the α-C restricting the free rotation of P(1)-C(9) bond. The bond length of C(7)-N(2) (1.352(4) Å) is remarkably shorter than the normal C-N(1.47 Å) and close to the C=N double-bond distance (1.34 Å), which is indicative of a significant double-bond character. The bond length of C(7)-N(1) is 1.297(4) Å, near to that of the typical C=N. The dihedral angle between the planes of the benzothiazole ring and the benzene ring is 71.75 (0.11)° . The two propyl chains of the molecule are disordered, with C22 and C22A showing two atomic positions with occupancies of 0.83:0.17, while the other three C atoms are nearly equally

disordered across the sites, with occupancies of 0.501:0.499, for C17, C18, C19 and C17A, C18A, C19A, respectively. The three F atoms are also disordered, with F1, F2, F3 and F1A, F2A, F3A showing two atomic positions with occupancies of 0.57:0.43, respectively. In the molecule, the atoms of the major component of the disorder are labeled without a suffix, while those of the minor components have suffix A, which have been omitted from the figures. Two molecules make a hydrogen-bonded dimer around the center of symmetry, in the form of N(2)-H(2)··· O(1)(symmetry code,$-x+1$,$-y+1$,$-z$), with N(2)-H(2)=0.864 Å, H(2)···O(1)= 1.986(16), N(2)···O(1)=2.819 Å, and N(2)-H(2)···O(1)=161°

References

1.　Jaszay Z M, Nemeth G, Pham T S, *et al.* Catalytic enantioselective Michael addition in the synthesis of α-aminophosphonates. *Tetrahedron: Asymmetry*. 2005, 16(23), 3837-3840.

2.　Smith W W, Bartlett P A. Design, synthesis, and evaluation of an inhibitor bridged between P2 and P1. *J. Am. Chem. Soc*.1998,120(19), 4622-4628.

3.　Song B A, Jiang M G. Recent advances in synthesis and biological activity of α - aminophosphonic acids and their esters. *Chin. J. Org. Chem*.2004,24(8), 843-856.

4.　Yang G, Liu Z, Liu J, *et al*. Synthesis and properties of novel α-(1, 2, 4-triazolo[1, 5- α]pyrimidine-2-oxyl)phosphonate derivatives. *Heteroatom Chem*. 2000,11(4), 313-316.

5.　Yager K M, Taylor C M, Smith A B. Asymmetric synthesis of alpha- aminophosphonates via diastereoselective addition of lithium diethylphosphite to chelating imines. *J. Am. Chem. Soc*.1994,116(20), 9377-9378.

6.　Lefebvre I M, Evans S A J. Studies toward the asymmetric synthesis of α-amino phosphonic acids via the addition of phosphites to enantiopure sulfinimines. *J. Org. Chem*.1997,62(22), 7532-7533.

7.　Davis F A, Lee S, Yan H. *et al*. Asymmetric synthesis of quaternary α-amino phosphonates using sulfinimines. *Org. Lett*.2001,3(11), 1757-1760.

8.　Sasai H, Arai S, Tahara Y, *et al*. Catalytic asymmetric synthesis of α-amino phosphonates using lanthanoid-potassium-BINOL complexes. *J. Org. Chem*.1995,60(21), 6656-6657.

9.　Kobayashi S, Kiyohara H, Nakamura Y, *et al*. Catalytic asymmetric synthesis of α-aminophosphonates using enantioselective carbon-carbon bond-forming reactions. *J. Am. Chem. Soc*.2004, 126(21), 6558-6559.

10.　Groger H, Saida Y, Sasai H, *et al*. A new and highly efficient asymmetric route to cyclic α-aminophosphonates: the first catalytic enantioselective hydrophosphonylation of cyclic imines catalyzed by chiral heterobimetallic lanthanoid complexes. *J. Am. Chem. Soc*.1998, 120(13), 3089-3103.

11.　Joly G D, Jacobsen E N. Thiourea-catalyzed enantioselective hydro- phosphonylation of imines: practical access to enantiomerically enriched α-amino phosphonic acids . *J. Am. Chem. Soc*. 2004, 126(13), 4102-4103.

12.　Kobayashi S, Kiyohara H, Nakamura Y, *et al*. Catalytic asymmetric synthesis of α-aminophosphonates using enantioselective carbon-carbon bond-forming reactions. *J. Am. Chem. Soc*.2004,126(21), 6558-6559.

13.　Hammerschmidt F, Hanbauer M. Transformation of arylmethylamines into α-aminophosphonic acids via metalated phosphoramidates: rearrangement of partly configurationally stable *N*-phosphorylated α-aminocarbanions. *J. Org. Chem*. 2000, 65(19), 6121-6131.

14.　Sasai H, Arai S, Tahara Y, *et al*. Catalytic asymmetric synthesis of.alpha-amino phosphonates using lanthanoid-potassium-BINOL complexes. *J. Org. Chem*.1995,60(21), 6656-6657.

15.　Pettersen D, Marcolini M, Bernardi L, *et al*. Direct access to enantiomerically enriched α-amino phosphonic acid derivatives by organocatalytic asymmetric hydrophosphonylation of imines. *J. Org.*

Chem.2006, 71, 6269-6272.

16. Li G, Liang Y, Antilla J C. Vaulted biaryl phosphoric acid-catalyzed reduction of α-imino esters: the highly enantioselective preparation of α-amino esters. *J. Am. Chem. Soc*.2007,129 (18), 5830-5831.

17. Guo Q X, Liu H, Guo C, *et al*. Chiral brønsted acid-catalyzed direct asymmetric Mannich reaction. *J. Am. Chem. Soc*.2007,129(13), 3790-3791.

18. Hammerschmidt F, Hanbauer M. Transformation of arylmethylamines into alpha-aminophosphonic acids via metalated phosphoramidates: rearrangements of partly configurationally stable *N*-phosphorylated alpha-aminocarbanions. *J. Org. Chem*.2000,65(19), 6121-6131.

19. Dejugnat C, Etemad-Moghadam G, Rico-Lattes I. Asymmetric synthesis of (α-amino) phosphonic acid amphiphiles using chiral P–H spirophosphoranes. *Chem. Commun*. 2003, 1858-1859.

20. Gaunt M J, Johansson C C, McNally A, *et al*. Enantioselective organocatalysis. *Drug Discovery Today*.2007,12, 8-27.

21. Taylor M S, Jacobsen E N. Asymmetric catalysis by chiral hydrogen-bond donors. *Angew Chem. Int. Ed*. 2006,45(10),1520-1543.

22. Diner P, Amedjkouh M. Aminophosphonates as organocatalysts in the direct asymmetric aldol reaction, towards syn selectivity in the presence of Lewis bases. *Org. Biomol. Chem*.2006, 4(11), 2091-2096.

23. Akiyama T, Itoh J, Fuchibe K. Recent progress in chiral Brønsted acid catalysis. *Adv. Synth. Catal*., 2006, 348(9), 999-1010.

24. Connon S J. Chiral phosphoric acids: powerful organocatalysts for asymmetric addition reactions to imines. *Angew Chem.Int.Ed*. 2006, 45(24), 3909-3912.

25. Mukherjee S, List B. Chiral counteranions in asymmetric transition-metal catalysis: highly enantioselective Pd/Bronsted acid-catalyzed direct α-allylation of aldehydes. *J.Am.Chem.Soc*. 2007,129(37), 11336-11337.

26. Wang C, Zhou Z, Tang C. Novel bifunctional chiral thiourea catalyzed highly enantioselective aza-henry reaction. *Org. Lett*. 2008,10(9), 1707-1717.

27. Groger H, Hammer B. Catalytic concepts for the enantioselective synthesis of α-amino and α-hydroxy phosphonates. *Chem. Eur. J*. 2000, 6(6), 943-948.

28. Jin L H, Song B A, Zhang G., *et al*. Synthesis, X-ray crystallographic analysis, and antitumor activity of *N*-(benzothiazole-2-yl)-1-(fluorophenyl)-*O,O*- dialkyl-α-aminophosphonates. *Bioorg. & Med. Chem. Lett*. 2006, 16(6), 1537-1543.

29. Zhang G P, Song B A, Xue W, *et al*. Synthesis and biological activities of novel dialkyl (4-trifluoromethyl-phenylamino)- (4-trifluoromethyl or 3-fluorophenyl)- methylphosphonates. *J. Fluorine Chem*.2006, 127(1), 48-53.

30. Bartoszek M, Beller M, Deutsch J, *et al*. A convenient protocol for the synthesis of axially chiral Bronsted acids. *Tetrahedron*.2008, 64(7), 1316-1322.

31. Romanenko V D, Kukhar V P. Fluorinated phosphonates, synthesis and biomedical application. *Chem. Rev*. 2006, 106(9), 3868-3935.

32. Song B A, Wu Y L, Huang R M. Synthesis of α-aminoalkylphosphonates containing fluorine with antiviral activities for Agricultural plants. CN 1432573, 2003; Patent approval certificate No. ZL02113252.6. *Chem Abstr* 2005,142, 482148.

33. Song B A, Zhang G P, Hu D Y, *et al*. Preparation methods and use of *N*-substituted-benzothiazoly-l- 1-substituted-phenyl-*O,O*-dialkyl- α-aminophosphonate derivatives. CN 1687088, 2005; Patent approval certificate No. ZL0200510003041. 7. *Chem Abstr* 2006, 145, 145879.

34. Wipf P, Jung J K. Formal Total Synthesis of (+)-Diepoxin σ. J. Org. Chem.2000, 65(20), 6319-6337.

35. Wang Y, Fang X, Ye W, *et al*. Growth hormones of six new Schiff base. *J. Cent China Normal Uni*.1995, 29, 55-57.

36. Hadden M, Nieuwenhuyzen M, Osborne D, *et al*. Synthesis of the heterocyclic core of martinelline and martinellic acid. *Tetrahedron*. 2006, 62(17), 3977-3984.

37. Imhof W, Gobel A, Schweda L, *et al*. Synthesis and characterization of chiral iron carbonyl complexes

from imine ligands with carbohydrates and amino acids as substituents. *Polyhedron*. 2005, 24(18), 3082-3090.

38. Jarrahpour A A, Shekarriz M, Taslimi A.Asymmetric synthesis and antimicrobial activity of some new mono and bicyclic *β*-lactams. *Molecules*. 2004, 9(11), 939-948.

39. Flors V, Miralles C, Gonzalez-Bosch C, *et al*. Three novel synthetic amides of adipic acid protect Capsicum anuum plants against the necrotrophic pathogen Alternaria solani. *Physiol. Mol. Plant Pathol*. 2003, 63(3), 151-158.

40. Uraguchi D, Terada M. Chiral brønsted acid-catalyzed direct Mannich reactions via electrophilic activation. *J. Am. Chem. Soc*. 2004, 126(17), 5356-5357.

41. Uraguchi D, Sorimachi K, Terada M. Organocatalytic asymmetric aza-Fri- edel-Crafts alkylation of furan. *J. Am. Chem. Soc*. 2004, 126(38), 11804-11805.

42. Akiyama T, Itoh J, Yokota K, *et al*. Enantioselective Mannich-type reaction catalyzed by a chiral brønsted acid. *Angew. Chem. Int. Ed*.2004,43(12),1566-1568.

43. Bhadury P S, Song B A, Yang S, *et al*. Some potential chiral catalysts for preparation of asymmetric *α*-aminophosphonates. *Curr. Org. Syn*.2008, 5(2), 134-150.

44. Akiyama T, Morita H, Itoh J, *et al*. Chiral Bronsted acid catalyzed enantioselective hydrophosphonylation of imines: asymmetric synthesis of *α*-amino phosphonates. *Org. Lett*. 2005,7(13), 2583-2585.

45. Akiyama T. Stronger Bronsted acids. *Chem. Rev*. 2007, 107(12), 5744-5758.

46. Brunel J M. BINOL: A versatile chiral reagent. *Chem. Rev*. 2005,105(11), 857-897.

47. Lingenfalter D S, Helgeson R C, Cram D J. Host-guest complexation. 23. High chiral recognition of amino acid and ester guests by hosts containing one chiral element. *J. Org. Chem*.1981, 46(2), 393-406.

48. Lamberth C, Kempf H J, Kriz M. Synthesis and fungicidal activity of *N*-2-(3-methoxy-4-propargyloxy) phenethyl amides. Part 3, stretched and heterocyclic mandelamide oomyceticides. *Pest Manag. Sci*. 2007, 63(1), 57-62.

49. Song B A, Zhang H P, Yang S, *et al*. Synthesis and antiviral activity of novel chiral cyanoacrylate Derivatives. *J. Agric. Food Chem*.2005, 53(20), 7885-7891.

50. Gooding G V Jr, Hebert T T. A simple technique for purification of tobacco mosaic virus in large quantities. *Phytopathology*.1967, 57(11), 1285-1290.

51. Davis F A, Lee S, Yan H, *et al*. Asymmetric synthesis of quaternary *α*-aminophosphonates using sulfinimines. *Org. Lett*.2001, 3(11), 1757-1760.

52. Paula V F D, Barbosa L C D A, Demuner A J, *et al*. Synthesis and insecticidal activity of new amide derivatives of piperine. *Pest Manag. Sci*. 2000, 56(2), 168-174.

53. Jennings L D, Rayner D R, Jordan D B, *et al*. Cyclobutane carboxamide inhibitors of fugal melanin: biosynthesis and their evaluation as fungicedes. *Bioorg. Med. Chem*.2000, 8(5), 897-907.

54. Witschel M, Zagar C, Hupe E, *et al*. Synthesis of heteroaroyl-substituted serine amides for use as agricultural herbicides. WO 2006125687, 2006. *Chem. Abstr*, 2007,146, 28043.

55. Navickiene H M D, Miranda J E, Bortoli S A, *et al*. Toxicity of extracts and isobutyl amides from Piper tuberculatum: potent compounds with potential for the control of the velvetbean caterpillar, Anticarsia gemmatalis. *Pest Manag. Sci*. 2007, 63(4), 399-403.

56. Caballero F J, Navarrete C M, Hess S, *et al*. The acetaminophen-derived bioactive *N*-acylphenolamine AM404 inhibits NFAT by targeting nuclear regulatory events. *Biochem. Pharmacol*.2007, 73(7), 1013-1023.

57. Zhang H, Lemley A T. *J*. Evaluation of the performance of flow-through anodic Fenton treatment in amide compound degradation. *Agric. Food. Chem*.2007, 55(10), 4073-4079.

58. Dieltiens N, Moonen K, Stevens C V. Enyne metathesis-oxidation sequence for the synthesis of 2-phosphono pyrroles, proof of the "Yne-then-Ene" pathway. *Chem. Eur. J*. 2006, 13(1), 203-214.

59. Boukallaba K, Elachqar A, El Hallaoui A, *et al*. Synthesis of new *α*-heterocyclic- *α*-aminophosphonates. *Phosphorus, Sulfur and Silicon and the Related Elements*.2006, 181(4), 819-823.

60. Olszewski T K, Boduszek B, Sobek S, *et al*. Synthesis of thiazole aminophosphine oxides, aminophosphonic and aminophosphinic acids and Cu(II) binding abilities of thiazole aminophosphonic acids. *Tetrahedron*. 2006, 62(10), 2183-2189.

61. Kafarski P, Lejczak B. Aminophosphonic acids of potential medical importance. *Curr*. *Med*. *Chem*. *Anti-Cancer Agents*. 2001,1(3), 301-312.

62. a) Lintunen T, Yli-Kauhaluoma J T. Synthesis of aminophosphonate haptens for an aminoacylation reaction between methyl glucoside and *a*-alanyl ester. *Bioorg*. *Med*. *Chem*. *Lett*. 2000, 10(15), 1749-1750; b) Liu W, Rogers C J, Fisher A J. *et al*. Aminophosphonate inhibitors of dialkylglycine decarboxylase: Structural basis for slow, tight binding inhibition. *Biochemistry*. 2002, 41(41), 12320-12328.

63. Huang R Q, Wang H, Zhou J. Preparation of organic intermediate. Chemical industry press of China, Beijing, China, 2001, 224-225.

64. Kaboudin B, Moradi K. A simple and convenient procedure for the synthesis of 1-aminophosphonates from aromatic aldehydes. *Tetrahedron Lett*. 2005, 46(17), 2989-2991.

65. Bhadury P S, Zhang Y P, Zhang S, *et al*. An effective route to fluorine containing asymmetric α-aminophosphonates using chiral Bronsted acid catalyst. *Chirality*. 2009, 21(5), 547-557.

66. Hu D Y, Wan Q Q, Yang S, *et al*. Synthesis and antiviral activities of amide derivatives containing α-aminophosphonate moiety. *J. Agric Food Chem*. 2008, 56, 998-1001.

67. Huang W, Zhao P L, Liu C L, *et al*. Design, synthesis, and fungicidal activities of new Strobilurin derivatives. *J. Agric*. *Food Chem*. 2007, 55(8), 3004-3010.

68. Du S C, Faiger H, Belakhov V, *et al*. Towards the development of novel antibiotics, synthesis and evaluation of a mechanism-based inhibitor of Kdo8P synthase. *Bioorg*. *Med*. *Chem*. 1999,7(12), 2671-2682.

69. Zomova A M, Molodykh Zh V, Kudryavtseva L A, *et al*. Antimicrobial activity of *O,O*-diethyl N-alkylaminomethylphosphonates and *O*-ethyl *N*-alkyl-aminomethylphosphonic acids. *Pharm*. *Chem*. *J*. 1986, 20(11), 774-777.

70. Kukhar V P, Hudson H R. Aminophosphonic and aminophosphinic acids. *Chichester*. 2000, 559-577.

71. Zhang G P, Song B A, Yang S, *et al*. Crystral structrue of *N*-(4-methyl benzonthiazole-2-yl)-1-(4-trifluoromethyl-phenyl)-*O*, *O*- di-*n*-propyl-*a*-aminophosphonate. *Anal*. *Sci*. 2005, 21*x*, 105-106.

72. Xu Y S, Yan K, Song B A, *et al*. Synthesis and antiviral bioactivities of α-aminophosphonates containing alkoxyethyl moieties. *Molecules*. 2006, 11, 666-676.

73. Zideka Z, Kmoničkovaa E, Holy A. Cytotoxicity of pivoxil esters of antiviral activity nucleoside phosphonates: adefovir dipivoxil versus adefovir. *Biomed. Pap. Med. Fac. Univ. Palacky. Olomouc. Czech. Repub.* 2005, 149(2), 315–319.

74. Li S Z, Wang D M, Jiao S M. Pesticide experiment methods-fungicide sector. Agriculture Press of China, Beijing, 1991, 93-94.

75. Sheldrick G M. Program for empirical absorption correction of area detector data. *University of Gottingen*: *Gottingen*, *Germany*, 1996.

76. Sheldrick G M. SHELXTL *V*5.1, Software reference manual; Bruker AXS, Inc. Madison, Wisconsin, USA, 1997.

77. Wilson A J. International table for X-ray crystallography. Kluwer Academic Publishers, Dordrecht, 1992, vol. C, Tables 6.1.1.4 (pp.500-502) and 4.2.6.8 (pp.219-222), respectively.

78. Kafarski P, Lejczak B. Aminophosphonic acids of potential medical importance. *Curr*. *Med*. *Chem*. *Anti-Cancer Agents*. 2001, 1(3), 301-312.

79. a) Lintunen T, Yli-Kauhaluoma J T. Synthesis of aminophosphonate haptens for an aminoacylation reaction between methyl glucoside and α, β-alanyl ester. *Bioorg*. *Med*. *Chem*. *Lett*. 2000, 10(15), 1749-1750; b) Liu W, Rogers C J, Fisher A J, *et al*. Aminophosphonate inhibitors of dialkylglycine decarboxylase: Structural basis for slow, tight binding inhibition. *Biochemistry*. 2002, 41(41), 12320-12328.

80. De Lombaert S, Blanchard L, Tan J, *et al*. Non-peptidic inhibitors of neutral endopeptidase 24.11 1. Discovery and optimization of potency. *Bioorg*. *Med*. *Chem*. *Lett*. 1995, 5(2), 145-150.

81. Kafarski P, Lejczak B.Biological activity of aminophosphonic acids. *Phosphorus*, *Sulfur and Silicon and the Related Elements*.1991, 63(1&2), 193-215.

82. Atherton F R, Hassall C H, Lambert R W. Synthesis and structure-activity relationships of antibacterial phosphono-peptides incorporating (1-aminoethyl) phosphonic acid and (aminomethyl)phosphonic acid. *J. Med. Chem*. 1986,29(1), 29-40.

83. Zhang M H, Li F G. Status quo and opportunity of bromine-contained pesticide (I). *Fine Special. Chem*. 2005, 13(13), 1-4.

84. Sepulveda-Boza S, Walizei G H, Rezende M C, *et al*. The preparation of new isoflavones. *Synth. Commun*. 2001, 31(12), 1933-1940.

85. Zhao J, Song J Y, Wang Ch, J, *et al*. Synthesis of 3, 4, 5-trimethoxy- benzoylsolanesylamide. *Chin. J. Appl. Chem*. 2003,20, 95-97.

86. Li D J, Ge Zh H. Synthesis and characterization of 3, 4, 5-trimethoxyl benzylformyl-hydrazones. *Chin. J. Syn. Chem*. 2004, 12(5), 487-490.

87. Ji Y F, Zong Zh M, Wei X Y. Synthesis of 3, 4, 5- trimethoxy benzaldehyde. *Chin. J. Appl. Chem*. 2001,18(7), 581-583.

88. a) Fields E K. The synthesis of esters of substituted amino phosphonic acids. *J. Am. Chem. Soc*. 1952, 74(6), 1528-1531; b) Cherkasov R A, Galkin V I. The Kabachnik-Fields reaction: synthetic potential and the problem of the mechanism. *Russ. Chem. Rev*. 1998, 67(10), 857-882.

89. Mauthner F, Clarke H T. *Organic synthesis*; Gilman, H., Ed, Wiley: New Work, 1941, Coll. Vol 1, 537.

90. Labouta I M, Hassan, A M, Aboulwafa O M, *et al*. Synthesis of some substituted benzimidazoles with potential antimicrobial activity. *Monatsh. Chem*. 1989, 120(7), 571-574.

91. Cherkasov R A, Galkin V I. Kabachnik-Fields reaction synthetic potential and the problem of mechanism. *Usp. Khim*. 1998, 67, 940-968.

92. Maier L, Diel P J. Synthesis, physical and biological properties of the phosphorus analogues of phenylalanine and related compounds. *Phosphorus*, *Sulfur*, *and Silicon*. 1994, 90(1-4), 259-279.

93. Belciug M P, Modro A M, Modro T A, *et al*. Phosphonic systems. 6. Dimethyl 2-methylpentenylphosphonates as model for studies of the stability of unsaturated phosphonic esters. *Phosphorus*, *Sulfur*, *and Silicon*. 1991, 57 (1-2), 57-64.

94. Allen J G, Atherton F R, Hall M J, *et al*. Phosphonopeptides, a new class of synthetic antibacterial agents. *Nature*. 1978, 272(5648), 56-59.

95. Atherton F R, Hall M J, Hassel C H, *et al*. Phosphonopeptides as antibacterial agents: mechanism of action of alaphosphin. *Antimicrobiol Agents Chemother*. 1979, 15(5), 696-705.

96. Chen R Y, Dai Q. Syntheses and properties of 2-[bis-(2-chloroethyl)amino]-6-alkoxylmethyl-tetrahydro-2H-1, 3, 2-oxaza-phosphorine-2-oxide. *Sci. China. Ser. B*. 1995, 25(2), 591-594.

97. Engel R. Phosphonates as analogues of natural phosphates. *Chem. Rev*. 1977, 77 (3), 349-367.

98. Bligh S W A, Choi N, Green D S C. Transition metal complexes of dialkyl α-hydroxyiminophosphonates, a novel class of metal complexes. *Polyhedron*. 1993, 12 (23), 2887-2890.

99. Cordi P D. Novel aminophenyl phosphonic acid derivatives, process for their preparation and pharmaceutical compositions containing them. EP 754, 693, 1997.

100. Chen R Y, Mao L J. Synthesis and antitumor activity of novel α-substituted aminomethylphosphonates. *Phosphorus*, *Sulfur*, *and Silicon*. 1994, 89(1-4), 97-104.

101. Tusek-Bozíc L M, Curíc M, Balzarini J, *et al*. Biological activity of some dialkyl α-anilinobenzylphosphonates and their palladium(II) complexes. *Nucleosides Nucleotides*. 1995, 14 (3-5), 777-781.

102. Song B A, Jiang M G, Wu Y L, *et al*. Synthesis, structure and bioactivity of *N*-(*p*-trifluromethyl) phenyl- α-aminophosphonates. *Chin. J. Org. Chem*. 2003, 23(9), 967-972.

103. Yang S, Song B A, Wu Y L, *et al*. Synthesis and crystal structure of fluorine-containing α-aminophosphonates. *Chin. J. Org. Chem*. 2004, 24(10), 1292-1295.

104. Yang, S. Studies on synthesis and activities of fluorine compounds with anti-TMV activity and

anticancer Activity. Ph. Dr. Disseration, Guizhou University, Guiyang, 2004.

105. Lee L F, Schleppnik F M, Schneider R W, *et al*. Synthesis and ^{13}C NMR of (trifluoromethyl) hydroxypyrazoles. *J. Heterocycl. Chem*. 1990, 27, 243-245.

106. Bravo P, Diliddo D, Resnati G. An efficient entry to perfluoroalkyl substituted azoles starting from β-perfluoroalkyl-β-dicarbonyl compounds. *Tetrahedron*. 1994, 50(29), 8827-8836.

107. Jung J C, Watkins E B, Avery M A. Synthesis of 3-substituted and 3, 4-disubstituted pyrazolin-5-ones. *Tetrahedron*. 2002, 58(18), 3639-3646.

108. Kees K L, Fitzgerald J J, Steimer K E, *et al*. New potent antihyperglycemic agents in db/db mice: synthesis and structure-activity relationship studies of (4-substituted benzyl) (trifluoromethyl) pyrazoles and pyrazolones. *J. Med. Chem*. 1996, 39(20), 3920-3928.

109. Gregory T P, Darlene C D, David, M. S. Structure-activity relationships for the action of dihydropyrazole insecticides on mouse brain sodium channels. *Pestic. Biochem. Phys*. 1998, 60(3), 177-185.

110. Kucukguzel S G, Rollas S, Erdeniz H, *et al*. Synthesis, characterization and pharmacological properties of some 4-arylhydrazono-2-pyrazoline-5-one derivatives obtained from heterocyclic amines. *Eur. J. Med. Chem*. 2000, 35(7-8), 761-771.

111. Mutalib A E, Chen S Y, Espina R J, *et al*. P450-Mediated metabolism of 1-[3-(aminomethyl)phenyl]-*N*-[3-fluoro-2′-(methyl sulfonyl)-[1,1′-biphenyl]-4-yl] -3-(trifluoromethyl)-1*H*-pyrazole-5-carboxamide (DPC 423) and its analogues to aldoximes. characterization of glutathione conjugates of postulated intermediates derived from aldoximes. *Chem. Res. Toxicol*. 2002, 15(1), 63-75.

112. Daidone G, Maggio B, Plescia S, *et al*. Structure-activity relationships for pyrido-, imidazo-, pyrazolo-, pyrazino-, and pyrrolophenazinecarboxamides as topoisomerase-targeted anticancer agents. *Eur. J. Med. Chem*. 1998, 33(5), 375-382.

113. Gamage S A, Spicer J A, Rewcastle G W, *et al*. Structure-activity relationships for pyrido-, imidazo-, pyrazolo-, pyrazino-, and pyrrolophenazinecarboxamides as topoisomerase-targeted anticancer agents. *J. Med. Chem*. 2002, 45(3), 740-743.

114. Wang Q M, Li Z G, Hung R Q. A convenient synthesis of *N-t*-butyl-*N'*-aminocarbonyl-*N*-(substituted) benzoyl-hydrazine containing *a*-aminoalkyl phosphonate groups in a one-pot procedure. *Heteroatom Chem*. 2001, 12(2), 68-72.

115. Yadav I S, Reddy B V, Madan S C. Montmorillonite clay-catalyzed one-pot synthesis of α-aminophosphonates. *Synlett*. 2001, 7, 1131-1133.

116. Kaboudin B, Nazari R. Microwave-assisted synthesis of 1-aminoalkyl phosphonates under solvent-free conditions. *Tetrahedron Lett*. 2001, 42(46), 8211-8213.

117. Denizot F. Lang, R. Rapid colorimetric assay for cell growth and survival: Modifications to the tetrazolium dye procedure giving improved sensitivity and reliability. *J. Immunol. Methods*. 1986, 89 (2), 271-277.

118. Skehan P, Storeng R, Scudiero D A. New colorimetric cytotoxicity assay for anticancer-drug screening. *Natl. J. Cancer Inst*. 1990, 82(13), 1107-1112.

119. Mccombie H, Sauders B C, Stacey G J. Esters containing phosphorus. Part I. *J. Chem. Soc*. 1945, 380-382.

120. Kafarski P, Lejczak B, Tyka R, *et al*. Herbicidal activity of phosphonic, phosphinic, and phosphonous acid analogues of phenylglycine and phenylalanine. *Plant Growth Regulation*. 1995, 14(4), 199-203.

121. Song B A, Zhang G P, Yang S, *et al*. Synthesis of *N*-(4-bromo-2-trifluoro- methylphenyl)-1- (2-fluorophenyl)-*O*,*O*- dialkyl- α-aminophosphonates under ultrasonic irradiation. *Ultrasonics Sonochem*. 2006, 13(2), 139-142.

122. Firouzabadi H, Iranpoor N, Sobhan S I. Metal triflate-catalyzed one-pot synthesis of α-aminophosphonates from carbonyl compounds in the absence of solvent. *Synthesis*. 2004, 16, 2692-2696.

123. Manjula A, Vittal B R, Neelakantan P. One-pot synthesis of alpha-aminophosphonates: an inexpensive Approach. *Synth. Commun*. 2003, 33(17), 2963-2969.

124. Kaboudin B A. A convenient synthesis of 1-aminophosphonates from 1-hydroxyphosphonates. *Tetrhedron Lett*. 2003, 44(5), 1051-1053.

125. Ranu B C, Hajra A. A simple and green procedure for the synthesis of α-aminophosphonate by a one-pot three-component condensation of carbonyl compound, amine and diethyl phosphite without solvent and catalyst. *Green Chem*. 2002, 4(6), 551-554.

126. Allen J G, Atherton F R, Hall M J, *et al*. Phosphonopeptides, a new class of synthetic antibacterial agents. *Nature*. 1978, 272(5648), 56-59.

127. Atherton F R, Hall M J, Hassel C H, *et al*. Phosphonopeptides as antibacterial agents: mechanism of action of alaphosphin. *Antimicrobiol Agents Chemother*. 1979, 15(5), 696-705.

128. a)Bose A K, Manhas M S, Ganguly S N, *et al*. More chemistry for less pollution: Applications for process development. *Synthesis*. 2002, (11), 1578-1591; b) Varma R S. Degradtion of H-acid in aqueous solution by microwave assisted wet air oxidation using Ni-loaded GAC as catalyst. *Green Chem*. 1999, (1), 43-55.

129. Yang S, Gao X W, Diao C L, *et al*. Synthesis and antifungal activity of novel chiral α-aminophosphonates containing fluorine moiety. *Chin*. *J. Chem*. 2006, 24, 1581-1588.

130. Chattapadhyay T K, Dureja P. Antifungal Activity of 4-Methyl-6-alkyl-2*H*-pyran-2-ones. *J. Agric. Food Chem.* 2006, 54 (6), 2129-2133.

131. Fang Z D. Plant pathogen method. Beijing: China Agriculture Press, 1998, 404-407.

132. Li H S. Plant physiological and biochemical experiment theory and technology. Higher Education Press, Beijing, 2000,194.

133. Gu X Y, Hu Z J. A method of mensurating the activity of chitinase. *Chin J. Soil Sci*. 1994, 25(6), 284-285.

134. Feng J L. Zhu X F. Molecular biology of microbial chitinase. *Journal of Zhejiang University*. 2004, 130(1),102-108.

135. Zhang L X, Zhang T F, Li L Y. Biochemistry techniques and methods (Second edition). Higher Education Press, Beijing, 1997, 1-2.

136. Liu X J, Chen R Y, Liu Y Y. Synthesis and anticancer activities of novel 5-fluorouracil-1-yl phosphonotripeptides. *Chem*. *J. Chin*. *Univ*. 2002, (23), 1299-1303.

137. Li Z G, Huang R Q, Yang Z. Synthesis and biological activity of diphenyl *N*-(2-benzothiazoly1)-α-aminoalkylphosphonate. Chin. J. *Chin*. *Appl*. *Chem*. 1999 16(2), 90-92.

138. Long Y X, Zhang K S, Qin D N. Studies on synthesis and biological activity of *N*-pyrazolinyl-α-aminophosphonates. *Chem*. *J. Chin*. *Univ*. 1996, 17(8), 1247-1249.

139. Gruss U, Hägele G. Fluorinated *N*-arylaminoarylmethanephosphonic acids and bisfunctional derivatives. *Phosphorus*, *Sulfur and Silicon*. 1994, 111(1-4), 159.

140. Green D S C, Gruss U, Hägele G, *et al*. The preparation and characterization of some fluorinated α-aminoarylmethanephosphonic acids. *Phosphorus*, *Sulfur and Silicon*. 1996, 113, 179-207.

141. Huang W S, Yuan C Y. A new and convenient one-pot synthesis of α, β- unsaturated trifluoromethyl ketones. *Chem. Soc. Perkin Trans*. 1995, (1), 741-742.

142. Huang W S, Yuan C Y, Wang Z Q. Facile synthesis of 1-substituted 5-trifluoro- methylimidazole-4-carboxylates. *J. Fluorine Chem*. 1995, 74 (2), 279-282.

143. Xiao J B, Zhang X M, Yuan C Y. Synthesis of trifluoromethyltetrazoles via building block strategy. *J. Fluorine Chem*. 1999, 99(1),83-85.

144. Abdou I M, Saleh A M, Zohdi H F. Synthesis and antitumor activity of 5-trifluoromethyl-2, 4-dihydropyrazol-3-one nucleosides. *Molecules*. 2004, 9, 109-116.

145. Zhao J, Song B A, Yan K, *et al*. Synthesis, crystal structure and anti-tobacco mosaic virus activity of fluorinated *N*-phenethyl- α-aminophosphonates. *Chin J. Appl. Chem*. 2007, 24(suppl), 19-24.

146. Kenneth L K, John J F, Kurt E S, *et al*. New potent antihyperglycemic agents in db/db Mice: Synthesis and Structure-Activity Relationship Studies of (4-substituted benzyl)(trifluoromethyl)pyrazoles and

pyrazolones. *J. Med. Chem*. 1996, 39(20), 3920-3928.

147. Kucukguzel S C, Rollas S, Erdeniz H, *et al*. Synthesis, characterization and pharmacological properties of some 4-arylhydrazono-2-pyrazoline-5-one derivatives obtained from heterocyclic amines. *Eur*. *J. Med. Chem*. 2000, 35(7-8),761-771.

148. Song B A, Yang S, Hong Y P, *et al*. Synthesis and bioactivity of fluorine compounds containing isoxazolylamino and phosphonate group. *J. Fluorine Chem*. 2005, 126, 1419-1424.

149. Li Z G, Huang R Q, Yang Z. Synthesis and biological activity of diphenyl *N*-(2-benzothiazoly1)-α-aminoalkylphosphonate. *Chin. J. Appl. Chem.* 1999 16(2), 90-92.

150. Gao R Y, Yang G S, Yang H Z, *et al*. Enantioseparation of fourteen *O*-ethyl *O*-phenyl *N*-isopropyl phosphoroamidothioates by high-performance liquid chromatography on a chiral stationary phase. *J. Chromatogr*. *A*, 1997, 763(1-2), 125-128.

151. Yang G S, Huang M B, Dai Q, R, *et al*. Influence of the structure of organic phosphonate compounds on chiral separation on a pirkle type chiral stationary phase. *Chromatographia*. 2001 (53), 93-95.

152. Zhou A L, Lv X Y, Xie Y X, *et al*. Chromatographic evaluation of perphenylcarbamoylated β-cyclodextrin bonded stationary phase for micro-high performance liquid chromatography and pressurized capillary electrochromatography. *Anal Chim Acta*. 2005, 547(2), 158-164.

153. Chen H, Lv X Y, Gao R Y, *et al*. Separation of chiral phosphorus compounds on the substituted P-cyclodextrin stationary phase in normal-phase liquid chromatography. *Chin J*. *Chem*. 1999, (17), 644-650.

154. Chen H, Lv X Y, Gao R Y, *et al*. Investigation of retention and chiral recognition mechanism using quantitative structure-enantioselectivity retention relationship in high performance liquid chromatography. *Chin J Chem*. 2000, (18), 532-536.

155. Okamoto Y, Kaida Y. Resolution by high-performance liquid chromatography using polysaccharide carbamates and benzoates as chiral stationary phases. *J. Chromatogr*. *A*. 1994, 666(1-2), 403-419.

156. Yashima E, Okamoto Y. Chiral discrimination on polysaccharides derivatives. *Bull*. *Chem*. *Soc*. *Jpn*. 1995, 68(12), 3289-3307.

157. Yashima E. Polysaccharide-based chiral stationary phases for high-performance liquid chromatographic enantioseparation. *J. Chromatogr*. *A*. 2001, 906 (1-2), 105-125.

158. Tachibaba K, Ohnishi A. Covalently bonded polysaccharide derivatives as chiral stationary phases in high-performance liquid chromatography. *J. Chromatogr*. *A*, 2001, 906(1-2), 127-154.

159. Frankest E, Ahuja S. Chiral separations, ACS, Washington D C, 1997, Chapter 10, pp. 271.

160. Song B A, Wu Y L, He X Q, *et al*. Recent progress in synthesis of novel α-aminophosphonic acid and α-aminophosphonates with optical activity. *Chin*. *J. Org. Chem*. 2003, 23(9), 933-943.

161. Koller H, Rimbock K H, Mannschreck A. *J. Chromatogr*. *A*. 1983, 282, 89.

162. Wang W, Zhang G P, Song B A, *et al*. Synthesis and anti-tobacco mosaic virus activity of *O,O'*-dialkyl- α-(substituted benzothiazol-2-yl)amino-(substituted phenylmethyl)phosphonate. *Chin*. *J*. *Org. Chem*. 2007, 27(2), 279-284.

163. Li C H, Song B A, Yan G F, *et al*. One Pot Synthesis of α-aminophosphonates containing bromo and 3,4,5-trimethoxybenzyl groups under solvent-free conditions. *Molecules*. 2007, 12, 163-172.

164. Yang S, Song B A, Hong Y. *et al*. Synthesis and crystal structure of *N*-(6-methoxybenzothiazol-2-yl)-1-(4-fluorophenyl)-*O,O*-dipropyl-α-aminophosphonate. *J. Chem. Crystallography*. 2005, 35(11), 891-895. 2

Chapter 2
Synthesis, Characterization and Antiviral Activity of Cyanoacrylates and Derivatives

2.1 Synthesis and Antivival Activity of Cyanoacrylates Containing Phosphonyl Moiety

2.1.1 Introduction

Cyanoacrylates, a class of highly potent herbicidal compounds, are known to disrupt photosynthetic electron transportation at a common binding domain on the 32 kDa polypeptide of the photosystem II (PSII) reaction center[1, 2] A large number of reports on the synthesis of cyanoacrylate derivatives exist due to their wide range of biological activities.[3–6] Some derivatives can serve not only as agrochemicals such as herbicides, insecticides, fungicides and plant virucides, but also as medicines such as antitumor agents. In our previous work, we designed and synthesized some chiral cyanoacrylates with antiviral activity by replacing the methylthio moiety of some 2-cyano-3-methyl-thio-3-substituted-phenylacrylates with (*R*)-or (*S*)-1-phenylethylamine groups. The (*E*) configuration of the reported chiral products was confirmed by X-ray single-crystal structure analysis. The bioassays showed that a chiral compound containing a 4-nitrophenyl moiety ［(*E*)-ethyl 3［(*S*)-1-phenylethyl-amino］-3-(4-nitrophenylamino)-2-cyanoacrylate］ exhibited good protection activity against TMV *in vivo*. [7] On the other hand, phosphonyl compounds, in general, have received wide attention in modern medicinal and pesticide chemistry. They are ideal for use in drug design due to their good bioactivity,[8,9] low toxicity, and the ease of substitution with conventional heterocyclic ring groups. [10–12] In 2001, Chen reported an efficient method for the synthesis of ethyl 2-cyano-3-methyl-thio-3-(diethoxy phosphonyl) acrylate under microwave irradiation conditions. [13]No reports on the fungitoxicity and antiviral activity of alkyl 2-cyano-3-methylthio-3-phosphonyl-acrylates have been published in the chemical or biological literature. In order to extend our research

work on cyanoacrylates as antiviral agents and fungicides, we have designed and synthesized some novel cyanoacrylate derivatives **2.2a-2.2t** containing phosphonyl moieties. The synthetic route is shown in Scheme 2.1. Diethyl phosphite or higher homologues were employed in the reaction due to their ease of preparation. The structures of **2.2** were established by well defined IR, NMR and elemental analysis. The results of bioassay revealed that some compounds of the above series have good anti-TMV and antifungal activity.

$$CS_2 \; + \; CNCH_2CO_2R^1 \xrightarrow[Me_2SO_4]{NaOH} \quad \underset{R^1OOC}{\overset{NC}{>}}=\underset{SMe}{\overset{SMe}{<}} \xrightarrow[NaH/THF]{H-\overset{O}{\underset{OR^2}{P}}-OR^2}$$

2.1

$$\underset{R^1OOC}{\overset{NC}{>}}=\underset{\overset{|}{\underset{O}{P}}\underset{OR^2}{\overset{OR^2}{<}}}{\overset{SMe}{<}} \quad + \quad \underset{R^1OOC}{\overset{NC}{>}}=\underset{SMe}{\overset{\overset{O}{\underset{}{P}}\overset{OR^2}{\underset{OR^2}{<}}}{<}}$$

2.2　　　　　　　　　　　**2.3**

2.2a $R^1=C_2H_5$,	$R^2=C_2H_5$;	**2.2b** $R^1=C_2H_5$,	$R^2=i\text{-}C_3H_7$;
2.2c $R^1=C_2H_5$,	$R^2=n\text{-}C_3H_7$;	**2.2d** $R^1=C_2H_5$,	$R^2=n\text{-}C_4H_9$;
2.2e $R^1=C_2H_4OC_2H_5$,	$R^2=C_2H_5$;	**2.2f** $R^1=C_2H_4OC_2H_5$,	$R^2=i\text{-}C_3H_7$;
2.2g $R^1=C_2H_4OC_2H_5$,	$R^2=n\text{-}C_3H_7$;	**2.2h** $R^1=C_2H_4OC_2H_5$,	$R^2=n\text{-}C_4H_9$;
2.2i $R^1=C_2H_4OCH_3$,	$R^2=C_2H_5$;	**2.2j** $R^1=C_2H_4OCH_3$,	$R^2=i\text{-}C_3H_7$;
2.2k $R^1=C_2H_4OCH_3$,	$R^2=n\text{-}C_3H_7$;	**2.2l** $R^1=C_2H_4OCH_3$,	$R^2=n\text{-}C_4H_9$;
2.2m $R^1=C_2H_5$,	$R^2=C_2H_4OCH_3$;	**2.2n** $R^1=C_2H_5$,	$R^2=C_2H_4OC_2H_5$;
2.2o $R^1=C_2H_4OC_2H_5$,	$R^2=C_2H_4OCH_3$;	**2.2p** $R^1=C_2H_4OC_2H_5$,	$R^2=C_2H_4OC_2H_5$;
2.2q $R^1=CH_3$	$R^2=C_2H_5$;	**2.2r** $R^1=CH_3$,	$R^2=i\text{-}C_3H_7$;
2.2s $R^1=CH_3$,	$R^2=n\text{-}C_3H_7$;	**2.2t** $R^1=CH_3$,	$R^2=n\text{-}C_4H_9$;

Scheme 2.1　Synthesis of compounds **2.2a-2.2t**

2.1.2　Materials and Methods

The materials and instruments for determination of the structure and physical data of new compounds are basically similar to the procedure described in Chapter 1.1.2. Dialkyl phosphites and alkyl 2-cyano-3,3-(dimethylthio) acrylates were prepared according to literature methods.[14,15]

General procedure for the preparation of title compounds 2.2a-2.2t. A dry 100 mL round-bottom flask equipped with a magnetic stirrer and nitrogen inlet was charged with sodium hydride (0.66 g, 55%, 15.2 mmol) in THF (15 mL) at 0～5℃. Dialkyl phosphite (15.2 mmol) was then slowly added through a dropping funnel into the resulting solution over a period of 30 min followed by slow addition of alkyl 2-cyano-3,3-(dimethylthio) acrylate (5.0 mmol) dissolved in THF

(20 mL). The mixture was stirred for 16 h at room temperature. After removal of the solvent under vacuum, the residue was dissolved in ice-cold water (40 mL) and acidified with dilute hydrochloric acid (10%), extracted with ethyl acetate (3×20 mL) and the combined organic layer was dried over anhydrous magnesium sulfate, filtered, and concentrated. The residue was subjected to column chromatography using a mixture of petroleum ether and ethyl acetate (4:1) as eluent to give the title compounds **2.2a-2.2t**. The repreresentative data for 2.2a is shown below, while data for **2.2b-2.2t** can be found in the reference.[66]

Ethyl 2-cyano-3-methylthio-3-(diethoxyphosphonyl) acrylate (**2.2a**). Yellow liquid; yield 52.0%; IR (KBr)：ν_{max} 2983, 2214, 1745, 1251, 1018;^{1}H NMR (500 MHz, CDCl$_3$): δ 1.37-1.45 (m, 9H, ester CH$_3$＋$2 \times$ phosphonyl CH$_3$), 2.76 (d, J=6.8 Hz, 3H, SCH$_3$), 4.32-4.35(m, 6H, ester CH$_2$＋$2 \times$ phosphonyl CH$_2$);^{13}C NMR (125 MHz, CDCl$_3$): δ 14.1 (ester CH$_3$), 16.2 ($2 \times$ phosphonyl CH$_3$), 19.4 (SCH$_3$), 62.7 (ester OCH$_2$), 64.5 ($2 \times$ phosphonyl CH$_2$), 106.2 (C=C C-2), 114.5 (CN), 162.1 (C=C C-3), 165.7 (C=O); ^{31}P MR (200 MHz, CDCl$_3$): δ 5.1; Anal. Calcd. for C$_{11}$H$_{18}$NO$_5$PS (307.5): C, 42.93; H, 5.58; N, 4.55. Found: C, 42.99; H, 5.90; N, 4.56.

Antifungal bioassay. The method for evaluating antifungal activity of title compounds **2.2** is similar to the procedure described in Chapter 1.3.2. [16]

Hyphal morphology of F. oxysporum. Compound **2.2d** (final conc.100 μg/mL) was added to sterilized Czapek media (0.2% NaNO$_3$, 0.131% K$_2$HPO$_4$·3H$_2$O, 0.05% KCl, 0.05% MgSO$_4$·7H$_2$O, 0.00183% FeSO$_4$·7H$_2$O, 3% sucrose, pH 6.8)[17] in which *F. oxysporum* was incubated for a few days. After incubating together at 27℃ for 24 h, it was observed under microscope (Olympus $800 \times$). Acetone (0.5 mL) served as the control.

Antiviral Biological Assays . The method for evaluating anti-TMV activity of title compounds is similar to the procedure described in Chapter 1.1.2. [7, 18]

2.1.3　Results and Discussion

In order to optimize the reaction conditions for the syntheses of compounds **2.2a-2.2t**, the effects of various solvents, molar reagent ratios, reaction times and reaction temperatures on the reaction synthesis of **2.2b** were examined. The results are summarized in Table 2.1. Cyanoacrylate **2.2b** was obtained from **2.1** in poor yield (Table 2.1, entry 1-3) in solvents such as DMF, acetone and CH$_3$CN, but when tetrahydrofuran (THF) was chosen as solvent, the yield of **2.2b** increased from 11.2% to 55.0% (Table 2.1, entry1,4). Next we examined the effect of the molar ratios of the reactants on the reaction. When the molar ratio of 2-cyano-3,3-(dimethylthio)-acrylate to O, O'-di-i-propylphosphite to sodium hydride was increased from 1:1:1 to 1:3:1, 1:3:2, 1:3:3 and 1:3:4 eq, compound **2.2b** was

obtained in 0, 12.0, 20.0, 55.0 and 49.5% yields, respectively (Table 2.1, entry 4-8). With regard to the reaction time, 0, 23.0 and 55.0% yields of **2.2b** were noted after 4, 8 and 16 h, respectively (Table 2.1, entry 9,10,4). When the reaction time was prolonged further to 20 h, no significant improvement was obtained (56.0%, Table 2.1, entry 11), as compared to that seen after 16 h (55.0%, Table 2.1, entry 4). As for the reaction temperature, a lower yield was observed at lower temperature (Table 2.1, entry 12). It could also be seen that the yield was significantly lower when the reaction was performed at 40-45℃ (Table 2.1, entry 13), compared to that observed at room temperature (Table 2.1, entry 4).

Table 2.1   Synthesis of **2.2b** under different reaction conditions

Entry	Solvent	Ratio [a]	Time (h)	Reaction temp	Yield (%) [b]
1	DMF	1:3:3	16	r.t	11.2
2	acetone	1:3:3	16	r.t	19.0
3	CH$_3$CN	1:3:3	16	r.t	34.9
4	THF	1:3:3	16	r.t	55.0
5	THF	1:3:1	16	r.t	12.0
6	THF	1:3:2	16	r.t	20.0
7	THF	1:1:1	16	r.t	0
8	THF	1:3:4	16	r.t	49.5
9	THF	1:3:3	4	r.t	0
10	THF	1:3:3	8	r.t	23.0
11	THF	1:3:3	20	r.t	56.0
12	THF	1:3:3	16	0-5℃	23.0
13	THF	1:3:3	16	40-45℃	13.0

[a]Ratio of 2-cyano-3,3-dimethylthioacrylate:O,O'-di-i-propylphosphite:sodium hydride; [b]Isolated yield based on 2-cyano-3,3-dimethylthioacrylate.

Antifungal bioassay: inhibitory effects of cyanoacrylate derivatives on phytopathogenic fungi. The three fungi used in the fungicidal bioassay, *Fusarium graminearum*, *Cytospora mandshurica* and *Fusarium oxysporum*, were tested by the poison plate technique. The results of preliminary bioassays were compared with that of a commercial agricultural fungicide, hymexazol. As indicated in Table 2.2, the new compounds **2.2d** and **2.2t** exhibited promising antifungal activity, inhibiting growth of *F. graminearum* at 64.5% and 49.7%, *C. mandshurica* at 60.4% and 51.3% and *F. oxysporum* at 65.0% and 41.1%, respectively, which are little lower than that of hymexazole (73.2% against *F. graminearum*, 58.9% against *C. mandshurica*, and 65.5% against *F. oxysporum* at 50 μg/mL). Marked loss of activity was observed with other compounds such as **2.2a-2.2c** and **2.2e-2.2s**.

Table 2.2 Inhibition effects of the title compounds against fungi

Compd.	Conc.(μg/mL)	Fusarium Graminearum	Cytospora mandshurica	Fusarium oxysporum
		Inhibition rate (%)		
2.2a	50	11.14±0.21	11.00±0.25	18.21±0.11
	500	37.30±0.56	24.00±0.77	26.03±0.99
2.2b	50	4.94±0.49	1.34±0.65	8.08±0.98
	500	31.40±0.78	35.03±0.84	36.83±1.24
2.2c	50	8.31±0.57	13.10±0.78	13.47±1.24
	500	37.10±1.08	31.82±1.45	41.02±1.30
2.2d	50	64.50±0.40	60.43±0.63	65.03±1.22
	500	93.30±4.28	90.59±1.59	92.75±2.52
2.2e	50	22.04±0.90	32.01±0.78	26.71±0.90
	500	41.44±1.21	36.77±1.45	32.13±1.09
2.2f	50	35.22±1.78	41.09±3.21	46.11±3.34
	500	55.64±3.01	66.09±2.55	68.9±1.19
2.2g	50	7.79±0.57	−0.80±0.72	6.29±0.97
	500	40.0±2.15	49.47±1.01	48.80±1.33
2.2h	50	4.68±0.56	−3.21±0.85	5.99±0.87
	500	25.41±0.73	23.26±0.84	36.53±1.27
2.2i	50	5.45±0.73	−2.67±0.67	1.20±0.89
	500	16.3±0.64	8.29±0.76	20.06±0.97
2.2j	50	0.97±0.11	11.27±0.45	9.99±0.22
	500	20.00±0.21	26.78±0.44	30.99±1.09
2.2k	50	10.09±0.76	32.20±0.55	19.39±0.44
	500	31.03±0.90	36.38±1.32	40.22±1.45
2.2l	50	21.08±0.98	30.07±0.67	12.11±1.02
	500	34.01±1.67	29.51±1.02	32.00±0.69
2.2m	50	3.93±0.22	14.23±0.51	23.09±0.88
	500	27.31±0.99	16.08±0.55	41.90±2.01
2.2n	50	12.22±1.01	9.97±0.88	11.91±0.42
	500	24.04±0.62	36.09±0.55	35.69±1.90
2.2o	50	3.75±0.52	10.61±0.69	4.01±0.55
	500	21.08±0.65	48.28±0.96	29.07±0.65
2.2p	50	4.45±0.55	24.93±0.76	6.52±0.56
	500	28.10±0.69	47.21±0.95	35.59±0.69
2.2q	50	7.03±0.60	15.38±0.61	3.26±0.44
	500	42.15±0.79	57.82±1.11	33.58±0.68
2.2r	50	11.71±0.96	23.87±0.75	9.52±0.57
	500	44.03±0.81	64.72±1.26	52.13±0.84
2.2s	50	9.84±0.61	35.01±0.72	13.53±0.48
	500	53.40±0.92	65.78±1.29	56.64±0.90
2.2t	50	49.67±0.65	51.30±0.70	41.05±0.51
	500	81.97±2.91	75.33±1.71	69.42±1.23
hymexazol[a]	50	73.2±1.41	58.89±1.16	65.51±1.76
	500	100±0.66	95.33±1.87	93.18±3.76
DMSO[b]		0	0	0

[a] reference compound; [b] control.

Fig 2.1 shows the inhibition of mycelial growth of isolated hypha of *F. oxysporum* by compound **2.2d** at different concentrations (100, 50, 25, 10 and 1 μg/mL) as compared to control, when tested *in vitro*. Almost complete inhibition of mycelial growth was observed at 100 and 50 μg/mL concentrations as compared to control (full growth).
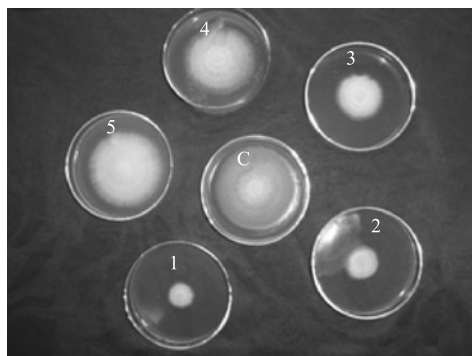
Key (μg/mL): 1, 100; 2, 50; 3, 25; 4, 5; 5, 1; and C, control

Fig 2.1   Effect of various concentrations of **2.2d** on the growth of isolated hypha of *F .oxysporum* (100,50,25,5 and 1 μg/mL)

Micro-observation results. Microphotography of the hyphal morphology of *F. oxysporum* treated with 100 μg/mL of **2.2d** (Fig 2.2) showed a series of changes, i.e. the cell of the hyphal divarication increased, hyphal knots appeared, and hypha bulged partially, compared with control.

CK

2.2d
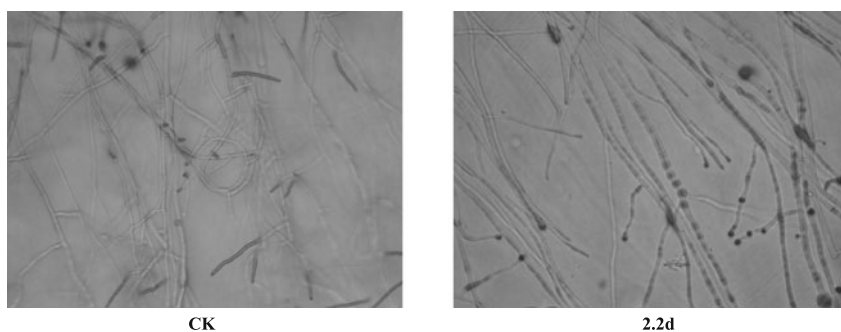
Fig 2.2   Microphotograph (800×) of hyphal morphology of *F. oxysporum* treated with **2.2d**

Preliminary antiviral activity assay. The results of the *in vivo* bioassay against TMV are given in Table 2.3. Ningnanmycin was used as reference antiviral agent. The data provided in the Table 2.3 indicate that the introduction of dialkylphosphonyl moieties in cyanoacrylates might improve their protective activities. The title compounds **2.2a-2.2t** showed protection rates of 40.8%-61.2%. When R^1 and R^2 are Et, the resulting compound **2a** displayed a lower protective activity (56.5%)

Table 2.3   The Protective, inactivation and curative effects of the new compounds against TMV *in vivo*

Agents	Concentration (mg/L)	Protective effect (%)	Inactivation effect (%)	Curative effect(%)
2.2a	500	$56.5^*\pm1.4$	$89.4^{**}\pm2.0$	$60.0^*\pm0.9$
2.2b	500	$61.2^*\pm3.2$	$84.7^{**}\pm1.0$	$64.2^*\pm1.9$
2.2c	500	$53.0^*\pm1.8$	$76.3^*\pm2.4$	$45.8^*\pm1.0$
2.2d	500	$53.4^*\pm0.7$	$80.3^{**}\pm3.4$	$41.2^*\pm2.1$
2.2e	500	$45.0^*\pm1.1$	$74.2^*\pm3.4$	$54.7^*\pm2.2$
2.2f	500	$47.9^*\pm1.7$	$79.6^{**}\pm1.6$	28.4 ± 4.4
2.2g	500	$40.8^*\pm5.4$	$73.8^*\pm3.0$	$41.8^*\pm5.5$
2.2h	500	$46.5^*\pm2.3$	$70.8^*\pm1.4$	$31.4^*\pm1.7$
2.2i	500	$50.1^*\pm3.0$	$80.0^{**}\pm2.0$	$36.6^*\pm4.4$
2.2j	500	$43.2^*\pm5.4$	$77.9^*\pm0.9$	$42.1^*\pm3.8$
2.2k	500	$45.7^*\pm1.9$	$79.0^*\pm0.7$	$44.3^*\pm6.4$
2.2l	500	$51.2^*\pm1.1$	$78.2^*\pm0.9$	$42.0^*\pm1.5$
2.2m	500	$50.0^*\pm2.0$	$81.2^*\pm1.6$	$50.0^*\pm1.0$
2.2n	500	49.7 ± 8.0	$80.2^{**}\pm1.2$	$51.2^*\pm1.0$
2.2o	500	$48.9^*\pm0.9$	$68.9^*\pm5.3$	$33.3^*\pm4.9$
2.2p	500	$47.6^*\pm1.0$	$67.3^*\pm2.4$	33.3 ± 8.9
2.2q	500	$45.6^*\pm0.4$	$60.0^*\pm3.1$	10.9 ± 6.0
2.22r	500	$50.9^*\pm1.1$	$70.0^*\pm1.9$	$36.7^*\pm6.7$
2.2s	500	$51.2^*\pm0.9$	$80.2^{**}\pm2.0$	$41.4^*\pm9.9$
2.2t	500	$46.6^*\pm5.5$	$61.0^*\pm5.1$	24.1 ± 8.7
Ningnamycin	500	$62.6^*\pm2.1$	$92.6^{**}\pm1.0$	$53.9^*\pm2.3$

All results are expressed as mean$\pm$SD; n=3 for all groups; * $P<0.05$, $^{**}P<0.01$.

than that of the reference compound (62.6%). The highest protective activity was achieved when R^1 is Et and R^2 is *i*-Pr (compound **2.2b**). A protective rate of 61.2%, equivalent to Ningnanmycin, against TMV at 500 μg/mL was recorded in this case. From the data in Table 2.3, it may be observed that the title compounds **2.2a-2.2t** possess significant potential inactivation bioactivities, with values of 89.4, 84.7, 76.3, 80.3, 74.2, 79.6, 73.8, 70.8, 80.0, 77.9, 79.0, 78.2, 81.2, 80.2, 68.9, 67.3, 60.0, 70.0, 80.2 and 61.0% at 500 μg/mL, respectively. Among these compounds, **2.2a** (R^1, R^2=Et) is much more active against TMV than the others, with an inactivation rate of 89.4%, equivalent to Ningnanmycin (92.6%) at 500 μg/mL. The data also indicate that a change in the substituent might also affect the curative activity of the title compounds **2.2a-2.2t**. Compound **2.2a** and compound **2.2b** could cure TMV up to 60.0% and 64.2% respectively at 500 μg/mL. The other compounds have relatively lower curative activities than **2.2a** and **2.2b**.

2.1.4   Conclusions

A series of novel cyanoacrylate derivatives **2.2a**-**2.2t** containing phosphonyl moieties were synthesized by treatment of alkyl 2-cyano-3,3-dimethylthioacrylates and dialkyl phosphites with NaH in THF solvent. This method is easy and generates the title compounds in moderate yields. The structures were verified by spectroscopic data. In the antifungal bioassay, the title compounds **2.2d** and **2.22t** were found to possess the highest activities against three kinds of fungi *in vitro*. The bioassay results showed that these title compounds exhibited moderate to good anti-TMV bioactivity. Title compounds **2.2a** and **2.2b** showed better biological activity than their structurally related analogues **2.2c**-**2.2t**.

2.2   Synthesis and Bioactivity of Cyanoacrylate Derivatives Containing Pyridine Moiety

2.2.1   Introduction

2-Cyanoacrylate derivatives are of considerable interests due to their potential biological properties. Various related compounds have herbicidal activity[3] and insecticidal activity. [19] It is reported that the ethoxyethyl (*Z*)-3-(4 chlorophenyl-methylamino)-2-cyano-3-isopropylacrylate (CPNPE) has the highest Hill inhibitory activity. [20,21]

As far as we are aware, the introduction of pyridinyl group into organic molecules usually results in the enhancement of the biological activity of parent compounds. [22–24] Hence, in search for new anticancer and antiviral agent, we thought that the replacement of the methylthio moiety by pyridinyl group in some 2-cyano-3,3-dimethylthioacrylate may result in the improvement of bioactivity. Therefore, several 2-cyanoacrylates containing pyridinyl moiety were synthesized and their anticancer bioactivities were evaluated. Using typical methods,[5,25] a mixture of ethyl 2-cyano-3,3-dimethylthioacrylate, 3-amino-2-chloro-4-methylpyridine, 60% sodium hydride was stirred at 10-20℃ for 10-16h in the mixed solvent system consisting of DMF and toluene. However, the method involved longer reaction time, low yield of products and complex handling. For this reaction, recently we have developed a new method to synthesize the intermediate **2.6** under ultrasonic irradiation in the mixture of solvents DMF-toluene. The method was very easy and mild and environmentally friendly. In this article we describe the preparation of 2-cyanoacrylates containing pyridinyl moiety and their antitumor bioactivities. The preliminary biological tests showed that all of them exhibit weak antiviral activities. The reaction route is shown in Scheme 2.2.
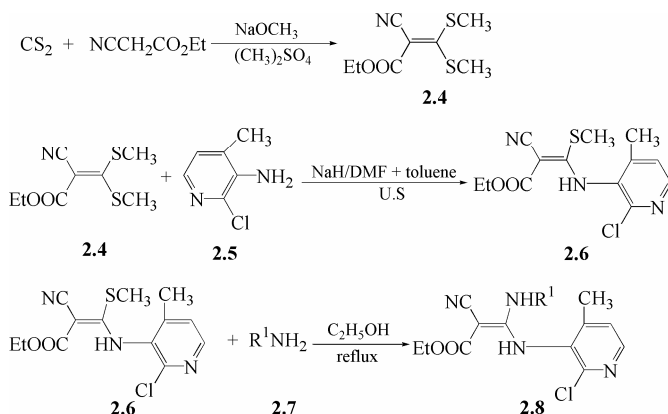
Scheme 2.2   Synthesis of the title compounds **2.8**

2.2.2   Materials and Methods

The materials and instruments for determination of the structure and physical data of new compounds are basically similar to the procedure described in Chapter 1.1.2. Sonication was performed on a Shanghai Branson-CQX ultrasonic cleaner (with frequencies of 25kHz and a nominal power of 500 W). Analytical TLC was conducted on GF_{254} plastic sheets at room temperature.

Ethyl-2-cyano-3,3-dimethylthioacrylate(**2.4**). White solid (36.7 g), yield 56.2%; mp 53.5-54.5℃ (lit.15, 30, mp 53-54℃).

3-Amino-2-chloro-4-methylpyridine(**2.5**). White solid, yield 92.1%, mp 68-69℃ (lit.37, mp 62-64℃).

(E)-Ethyl-3-(2-chloro-4-methylpyridin-3-yl-amino)-2-cyano-3-methylthio acrylate(**2.6**). To an oven-dried three-necked 50 mL round-bottom flask were added ethyl 2-cyano-3,3-dimethylthioacrylate (**2.4**) (2.17 g, 0.01 mol), 3-amino-2-chloro-4-methyl-pyridine (**2.5**) (1.43 g, 0.01 mol), 60% sodium hydride (0.80 g, 0.02 mol), DMF (3 mL) and toluene (3 mL). The resulting mixture was placed in the ultrasonic cleaning bath at 40-45℃ for 1 h. The reaction progress was monitored by TLC. The mixture was poured into ice water (100 mL) and separated. The aqueous phase was acidified with 10% HCl to pH 6-7, and filtered. The residue was dried and recrystallized from anhydrous ethanol to give a white solid, yield 73.5%, mp 113-114℃; IR (KBr): v_{max}3284.7, 2200.8, 1637.5, 1620.2, 1608.6, 1585.4, 1531.4, 1458.1, 1446.6, 1431.1, 1386.8, 1369.4, 1298.0, 1269.1, 1120.6, 1109.0, 1085.9, 779.2; ^1H NMR(400 MHz, CDCl$_3$): δ 11.17(s, 1H, NH), 7.22-8.26(m, 2H, Py-H), 4.31(q, 2H, CH$_2$), 2.55(s, 3H, SCH$_3$), 2.34(s, 3H, Py-CH$_3$), 1.38(t, 3H, CH$_3$-C, J=7.9 Hz);m/z (EI-MS): 311(M$^+$, 12.2). Anal. Calcd. for C$_{13}$H$_{14}$ClN$_3$O$_2$S:C, 50.08; H, 4.53; N, 13.48. Found: C, 50.00; H, 4.49; N, 13.48.

General procedure for the preparation of products **2.8a-2.8d.** A solution of ethyl 3-(2-chloro-4-methylpyridin-3-ylamino)-2-cyano-3-methylthioacrylate (**2.6**) (0.75 mmol) in EtOH (20 mL) was stirred, followed by the addition of amine (**2.7**) (0.82 mmol). The mixture was refluxed at 78-80℃ for 4h. The solvent was then removed under reduced pressure. The crude solid was purified by column chromatography on a silica gel (eluent: ethyl acetate /petroleum ether, 2/8 by *v/v*) to give the title compounds. The reperesentative data for 2.8a is shown below, while data for **2.8b-2.8d** can be found in the reference.[6]

(*Z*)-Ethyl-3-(2-chloro-4-methylpyridin-3-ylamino)-3-propylamino-2-cyanoa crylate(2.8a). White crystal;yield 54.7%; mp 143-145℃. IR (KBr): ν_{max} 2196.9, 1666.5, 1600.2, 1595.1, 1448.5, 1327.0, 1284.5, 1255.6, 1166.9, 1114.8, 1097.5, 1066.6; ^{1}H NMR (400 MHz, CDCl$_3$): δ 10.78(s, 1H, NH-Py), 9.37(s, 1H, NH-C), 7.17-8.23(m, 2H, Py-H), 4.21(q, 4H, NCH$_2$＋OCH$_2$), 2.66 (d, 3H, OCH$_2$, *J*=8.1Hz), 2.34 (s, 3H, Py-CH$_3$), 1.31-1.68(m, 5H, CH$_3$＋CH$_2$); 0.88 (d, 3H, CH$_3$, *J*=8.0Hz). ^{13}C NMR (125 MHz, CDCl$_3$): δ 170.63, 163.24, 148.36, 147.62, 125.11, 60.19, 18.39, 14.44; *m/z* (EI-MS): 325(M$^+$, 14.8). Anal. Calcd. for C$_{15}$H$_{19}$ClN$_4$O$_2$: C, 55.81; H, 5.93; N, 17.36. Found: C, 55.81; H, 5.89; N, 17.36.

Antiviral Biological Assays. The method for evaluating anti-TMV activity of title compounds is similar to the procedure described in Chapter 1.2.2. [7, 18]

2.2.3   Results and Discussion

In order to optimize the reaction conditions, the synthesis of **2.6** was carried out under several conditions. The effects of different solvents, reaction time, reaction temperature on the reaction, with or without ultrasonic irradiation, were studied and the results are shown in Table 2.4. It could be seen that the presence of ultrasonic irradiation could accelerate the reaction (Table 2.4, entry 1-10,18-20). Without ultrasound, the reaction was relatively slow and no product was detected within 1-4h (Table 2.4, entry 11-13). When the reaction time was prolonged to 16h, **2.6** could be obtained in 57.2% (Table 2.4, entry 16) without ultrasonic irraddition.   When the reaction was carried out from 1h to 3h under ultrasonic irradiation at room temperature, the yield of **2.6** was increased from 44.2% to 55.9% (Table 2.4, entry 1-3). Tiny improvement of the yield was obtained when the reaction time was prolonged to 4h and 5h (Table 2.4, entry 4 and 5). As for the reaction temperature, it could be seen that when the reaction was conducted at room temperature or even lower (Table 2.4, entry 1-5, and 6), the yield was lower than that at 40-45℃ (Table 2.4, entry 8). Interestingly, the yield was found to decrease when the reaction temperature was increased to 50-60℃ (Table 2.4, entry 9-10). Hence, it is recommended to conduct the rection at 40-45℃ than performing at lower or higher temperature. No substantial improvement was observed when the reaction time varied from 1h to 5h at 40-45℃ under ultrasound irradiation (Table 2.4, entry 17-20).

Table 2.4   Results at different reaction conditions for synthesizing **2.6**

Entry	Solvent	Time (h)	Temp (℃)	Yield (%) [c]
1[a]	DMF/toluene	1	20-25	44.2
2[a]	DMF/toluene	2	20-25	50.3
3[a]	DMF/toluene	3	20-25	55.9
4[a]	DMF/toluene	4	20-25	56.1
5[a]	DMF/toluene	5	20-25	59.0
6[a]	DMF/toluene	4	0-10	29.8
7[a]	DMF/toluene	4	30-35	63.4
8[a]	DMF/toluene	4	40-45	72.1
9[a]	DMF/toluene	4	50-55	64.1
10[a]	DMF/toluene	4	55-60	60.9
11[b]	DMF/toluene	1	20-25	No product
12[b]	DMF/toluene	4	20-25	No product
13[b]	DMF/toluene	1	40-45	No product
14[b]	DMF/toluene	4	40-45	34.8
15[b]	DMF/toluene	10	20-25	48.1
16[b]	DMF/toluene	16	20-25	57.2
17[a]	DMF/toluene	1	40-45	78.8
18[a]	DMF/toluene	2	40-45	76.7
19[a]	DMF/toluene	3	40-45	77.0
20[a]	DMF/toluene	5	40-45	73.5

[a] The reactions were carried out in 6 mL DMF/toluene (1/1 by v/v) under ultrasound irradiation with NaH as base; [b] The reactions were carried out in 6 mL DMF/toluene (1/1 by v/v) with stirring but without ultrasound irradiation with NaH as base; [c] Isolated yields.

The effect of the solvent amount was also investigated. It could be seen that when the amount of solvent was decreased from 12 mL to 8,6,4,2, and 0 mL, the yield of **3** was 69.7%, 73.1%, 79.2%, 68.8%, 65.0% and 31.2%, respectively (Table 2.5, entry 1-6). In conclusion, the best result was obtained when compound **2.6** was reacted with 1 equiv of amine and 2 equiv of NaH under ultrasonic irradiation with DMF-toluene as co-solvent at 40-45℃ for 1 h. Under these reaction conditions, the amination reaction proceeded smoothly and moderate yields were obtained.

Table 2.5   Effect of the amount of solvent for the synthesis of **2.6**[a]

Entry	Amount of the solvent (mL)	Yield (%) [b]	Entry	Amount of the solvent (mL)	Yield (%) [b]
1	12	69.7	4	4	68.8
2	8	73.1	5	2	65.0
3	6	79.2	6	0	31.2

[a] All reactions were carried out at 40-45℃ for 1h under ultrasound irradiation with NaH as base; [b] Isolated yields.

As shown in Table 2.6 and Scheme 2.1, the synthesis of 3-aliphatic amino-3-(2-chloro-4-methylpyridin-3-ylamino)-2-cyanoacrylate **2.8** was carried out in moderate yields at 78-80℃ in ethanol for 4 h. Dramatic improvement of the yields was obtained when the reaction temperature was increased. When the reaction was carried out at 78-80℃ in ethanol for 4h, **2.8a, 2.8b, 2.8c** and **2.8d** were obtained in 54.7%, 74.5%, 56.0% and 63.1% yields, respectively, while the corresponding figures at 40-50℃ were 34.2%, 54.2%, 34.7% and 39.6%, respectively. Hence, the aminiation reaction can be completed under reflux condition with moderate yields.

Table 2.6   Synthesis of 3-aliphatic amino-3-(2-chloro-4-methylpyridin3-ylamino)-2-cyanoacrylate **2.8** under different conditions

Entry	Compd.	R	Time（h）	Temp（℃）	Yield（%）
1	**2.8a**	*n*-Pr	4	78-80	54.7
2	**2.8b**	*n*-Bu	4	78-80	74.5
3	**2.8c**	-CH$_2$Ph	4	78-80	56.0
4	**2.8d**	*i*-Pr	4	78-80	63.1
5	**2.8a**	*n*-Pr	4	40-50	34.2
6	**2.8b**	*n*-Bu	4	40-50	54.2
7	**2.8c**	-CH$_2$Ph	4	40-50	34.7
8	**2.8d**	*i*-Pr	4	40-50	39.6

As could be seen from the structure, there could be two configurations related to compound **2.6** and **2.8**. In fact, the configuration of compound **2.6** was identified as an (*E*) configuration and was verified according to the single crystal structure determination.[5]   The attacking aliphatic amine **2.7** occupies the position of the methylthio group resulting in a (*Z*) configuration of compound **2.8**.

The antitumor activity was assayed by the MTT method.[26,27] The results presented in Table 2.7 indicate that these newly synthesized compounds exhibit promising anticancer activities against two cancer cells *in vitro*. The compound **2.8c** has higher antitumor activity than **2.8a, 2.8b** and **2.8d**. It could be seen that the nature of R affects antitumor activity to some extent. For example, when R is benzyl, compound **2.8c** has relatively higher activity against PC3 and A431 cells than its less active analogues **2.8a** and **2.8b**, in which the R groups were *n*-Pr and *n*-Bu, respectively.

Table 2.7   Bioassay of cyanoacrylates with a pyridinyl moiety against PC3 and A431 cell lines at 10μM

Compd.	R	Inhibitor rate (%)	
		PC3	A431
2.8a	*n*-Pr	34.6	52.1
2.8b	*n*-Bu	23.1	12.4
2.8c	-CH$_2$Ph	80.1	87.5
2.8d	*i*-Pr	63.2	71.3

The bioassay of all compounds showed that they have weak anti-tobacco mosaic virus (TMV) activity. For example, the inhibitory activity of all compounds to TMV at 500 μg/mL were 12.1%, 22.0%, 26.1% and 30.7%, respectively.

2.2.4   Conclusions

In summary, we described a practical and efficient procedure for the preparation of ethyl 2-cyano-3-(2-chloro-4-methylpyridin-3-ylamino)-3-methylthioacrylate through the two-component reaction of ethyl 2-cyano-3,3-dimethylthioacrylate and 2-amino-3-chloro-4-methylpyridine in presence of NaH as the base under ultrasonic irradiation and DMF-toluene as co-solvent for 1 h at 40-45℃. The reactions were, in general, fast and efficient. Subsequent amination with aliphatic amines afforded the target compounds in moderate yields.

In the MTT bioassay, these new compounds have moderate antitumor activities against PC3 and A431 cells. For example, the inhibitory activities of compound **2.8c** against PC3 and A431 cells at 10 μM were 80.1% and 87.5%, respectively. Preliminary bioassay suggests that these compounds have weak antiviral activity against TMV.

2.3   Preparation of Chiral Cyanoarylate Derivatives under Microwave Irradiation

2.3.1   Introduction

Cyanoacrylates are potent inhibitors of photosynthetic electron transport. A number of studies concerning the inhibition of photosynthetic electron flow in photosystem II (PS II) with a series of acrylate inhibitors have shown that the potency of acrylate in blocking photosynthetic electron flow is extremely sensitive to minor structural variations. [28] Among these cyanoacrylates, (Z)-ethoxyethyl-2-cyano-3-(4-chlorophenyl) methylamino-3-isopropylacrylate (CPNPE) exhibits the highest Hill inhibitory activity reported till date.[29]

There are several methods for the synthesis of 2-cyanoacrylate inhibitors. The most commonly used methods over the last decade were: (a) synthesis of 3-methylthio-3′-aminocyanoacrylate from 2-cyano-3,3-dimethylthioacrylate and benzylamine (anhydrous alcohol, room temperature, 6-11h);[15] (b) synthesis of ethyl 2-cyano-3-methylthio-3′-〔(6-chloro)-3-pyridiylmethyl〕acrylate by the reaction of 3-aminomethyl or 2-chloro-5-amino-pyridine with 2-cyano-3,3-dimethylthio

ethyl acrylate (anhydrous alcohol, reflux, 2h);[29] (c) synthesis of 3-methylthio-3′-arylamino-cyano-acrylate from 2-cyano-3,3-dimethyl- thioacrylate and 4-trifluoro-methylaniline (dimethylformamide [DMF]-toluene, 10-20℃, 40 h);[30] (d) nucleophilic substitution with 2-amino-3-chloro-4-methylpyridine under ultrasonic irradiation.[5] All these methods, however, suffer from various disadvantages. *e.g.* methods (a), (b) and (c), have slow reaction rates, low yields and complex handling, while for method (d), longer reaction time is the major issue.

Microwave-assisted rapid organic reactions constitute an emerging technology that makes experimentally and industrially important organic syntheses more effective and more eco-friendly than conventional reaction methods.[31] Recently, we have developed a new method to synthesize the title products **2.10** under microwave irradiation in a DMF-tetrahydrofuran (THF) solvent mixture. The method is very simple, mild, environmentally friendly and quick. In this article we describe the preparation of 2-cyanoacrylates containing aryl moieties and their antitumor bioactivities. The reaction route is shown in Scheme 2.3. To the best of our knowledge, it is the first report on the antivival activity and reaction of arylamines and 2-cyano-3,3-dimethylthioacrylate under microwave irradiation.
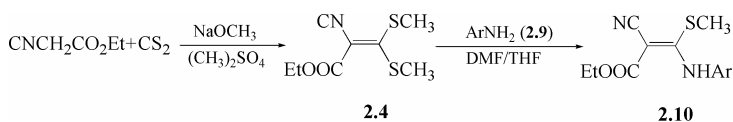
Scheme 2.3   Synthesis of the compound **2.10**

2.3.2   Materials and Methods

The materials and instruments for determination of the structure and physical data of new compounds are basically similar to the procedure described in Chapter 1.1.2. Microwave reaction was performed on a Beijing XH-100A microwave (with a power of 700W). 2,6-Dichloro-4-trifluoromethylaniline and 3-amino-2-chloro-4-methylpyridine were prepared according to a literature method.[37] 2-Cyano-3,3-dimethylthioacrylate (**2.4**) was also prepared according to literature method [30].

General method for the preparation of (*E*)-3-methylthio-3-substituted aryl amino-2-cyanoacrylate (2.10a-2.10g). 2-Cyano-3,3-dimethylthioacrylate (**2.4**, 1.736 g, 8 mmol),[30] aromatic amine (8.07 mmol), 60% sodium hydride (0.76 g, 16 mmol), DMF (3 mL) and THF (3 mL) were placed in an oven-dried three-necked 250 mL round-bottom flask fitted with a magnetic stirring bar. The resulting mixture was then stirred at 50℃ for 30 min. under microwave irradiation condition. The completion of the reaction was monitored by TLC. The mixture was poured into ice water (100 mL) and separated, then the aqueous phase was acidified with 10% HCl to pH 6-7. The mixture was then filtered and the crude

product was dried and recrystallized from ethanol to give title compounds **2.10a-2.10g**. The reperesentative data for 2.10a is shown below, while data for **2.10b-2.10g** can be found in the reference.[42]

(E)-Ethyl 3-(2,6-dichloro-4-trifluoromethylphenylamino)-2-cyano-3-methyl-thio acrylate **(2.10a)**. Colorless crystals; mp 125-126℃; IR (KBr): v_{max} 3319.0, 3300.0, 2208.0, 1625.0, 1610.1, 1571.0, 1533.0, 1492.0, 1471.0, 1452.0, 1419.0, 1244.0, 1060.0; ^{1}H NMR (400 MHz, CDCl$_3$): δ 1.38 (t, 3H, *J*=7.8 Hz, CH$_3$-C), 2.57 (s, 3H, SCH$_3$), 4.32 (dd, 2H, *J*=18.9 Hz, 8.2 Hz, OCH$_2$), 7.69 (s, 2H, Ar-H), 11.22 (s, 1H, NH); *m/z* (EI-MS): 398(M$^+$); Anal. Calcd. for C$_{14}$H$_{11}$Cl$_2$F$_3$N$_2$O$_2$S: C 42.11; H 2.76; N 7.02. Found: C 42.00; H 2.52; N 7.00.

MTT Assay Against Cell Proliferation[27]. The experiment and method for evaluating antitumor activity of all compounds are similar to the procedure described in Chapter 1.5.2.3. [27]

Antiviral Bioassay. The method for evaluating anti-TMV activity of title compounds is similar to the procedure described in Chapter 1.1.2. [7, 18]

2.3.3   Results and Discussion

In order to optimize the reaction conditions for preparing compounds **2.10**, the synthesis of (*E*)-ethyl 3-(4-trifluoromethylphenylamino)-2-cyano-3-methyl-thioacrylate (**2.10c**) was carried out under different reaction conditions. First, the importance of microwave irradiation method was established for the reaction. Under the normal reaction conditions without microwave irradiation, the reaction was much slower and the yield of the product **2.10c** was decreased, for example, when the reaction time was extended to 10h, compound **2.10c** could be obtained in 43.0% yield (Table 2.8, entry 13), as compared with the yield of 64.0% in 30 min under microwave irradiation (Table 2.8, entry 5). In addition, the effect of solvents was studied. The results demonstrated that the presence of DMF-THF could accelerate the amination reaction. Moreover, when other solvents were used instead of DMF-THF in the present reaction, no remarkable improvement of the yield was observed (Table 2.8, entry 1, 2, 3, 4). Further, we also examined the effects of reaction temperature and reaction time on the amination reactions (Table 2.8, entry 5-12). When the reaction time was prolonged from 10 min to 30 min, the yield of **2.10c** increased from 47.3% to 64.0% (Table 2.8, entry 6-7 and entry 5). When the reaction time was prolonged further to 40 min under microwave irradiation, a tiny yield improvement (65.1%, Table 2.8, entry 8) was obtained compared to that of 30 min (64.0%, entry 5). As for the reaction temperature, it could be seen that the yield was relatively lower when the reaction was carried out at room temperature (Table 2.8, entry 9) than at 50℃ (Table 2.8, entry 5). No substantial improvement was observed when the reaction system was heated to 60℃ (Table 2.8, entry 12). Hence, it is convenient for the reaction to conduct at 50℃ than to be performed at lower or higher temperature.

Table 2.8   Results at different reaction conditions for synthesizing **2.10c**
under microwave irradiation

Entry	Compd.	Substrate 2	Solvent	Time (min)	Temp (℃)	Yield (%)
1[a]	**2.10c**	4-trifluoromethylaniline	acetone	30	50	33.7
2[a]	**2.10c**	4-trifluoromethylaniline	THF	30	50	31.2
3[a]	**2.10c**	4-trifluoromethylaniline	DMF	30	50	43.4
4[a]	**2.10c**	4-trifluoromethylaniline	DMF＋PhCH$_3$	30	50	57.8
5[a]	**2.10c**	4-trifluoromethylaniline	DMF＋THF	30	50	64.0
6[a]	**2.10c**	4-trifluoromethylaniline	DMF＋THF	10	50	47.3
7[a]	**2.10c**	4-trifluoromethylaniline	DMF＋THF	20	50	51.3
8[a]	**2.10c**	4-trifluoromethylaniline	DMF＋THF	40	50	65.1
9[a]	**2.10c**	4-trifluoromethylaniline	DMF＋THF	30	25	45.5
10[a]	**2.10c**	4-trifluoromethylaniline	DMF＋THF	30	35	55.0
11[a]	**2.10c**	4-trifluoromethylaniline	DMF＋THF	30	45	53.0
12[a]	**2.10c**	4-trifluoromethylaniline	DMF＋THF	30	60	63.0
13[b]	**2.10c**	4-trifluoromethylaniline	DMF＋THF	600	50	43.0

[a]The reactions were carried out with stirring at 700W of microwave irradiation; [b] Reaction carried out in DMF-THF under stirring without microwave irradiation.

Using the optimized conditions, the best result was obtained when 2-cyano-3,3-dimethylthio ethyl acrylate **2.4** was reacted with 1 equivalent of aromatic amine or aminopyridine **2.9**   and 2 equivalent NaH under microwave irradiation with DMF-THF as co-solvent at 50℃ for 30 minutes. Under these reaction conditions, the amination reaction proceeded smoothly, and the results are summarized in Table 2.9.

Table 2.9   Yields of the title compounds **2.10**

Compd [a]	2.10a	2.10b	2.10c	2.10d	2.10e	2.10f	2.10g
Ar-							
Yields（%）[b]	83.9	85.2	64.0	77.8	76.9	93.5	70.1
Yields（%）[c]	63.8	62.1	43.0	54.1	50.9	89.2	59.0

[a]Isolated yields based on the amine;[b]All reactions were carried out in 6 mL DMF/THF (1/1, v/v) at 50℃ for 30 min under microwave irradiation with 2 equiv. of NaH used as base;[c]All reactions were carried out in 6 mL DMF/THF (1/1, v/v) at 50℃ for 600 min with 2 equiv. of NaH used as base under stirring conditions without microwave irradiation.

As can be seen from the general structure (Scheme 2.3), compounds **2.10a-2.10g** may exist in two different configurations. In practice, they have been shown to exist in the (E) configuration, as verified by single crystal structure determination.[5] The structures of all the synthesized compounds were established on the basis of their spectroscopic data. They showed IR absorption bands at 3284(s)-3367(s)(NH), 3002-3008(C=C), 2200-2265 (CN) and 1620-1673 cm^{-1} (COOR). In the ^{1}H NMR spectra, all phenyl and pyridyl protons appeared as multiplets at δ 6.85-8.21, while the peaks of the ester CH$_2$ groups were at about 4.26 and 4.32 ppm, respectively, appearing as two doublets. The NH protons of compounds **2.10** were at 10.89-11.51 ppm as a singlet, probably due to the existence of hydrogen bonding between the ester carbonyl and NH of phenylamino or aminopyridyl group which moves the chemical shift to a lower field. The MS spectra revealed that the molecular ion and fragmentation peaks were in accordance with the proposed structure of compounds **2.10**.

Biological activity. The antitumor activity was assayed by the MTT ［3-(4,5-dimethylthiazol-2-yl)-2,5-diphenyltetrazolium bromide］ method.[27] The results are listed in Table 2.10. It was found that these compounds exhibit certain activity against the two kinds of cancer cells _in vitro_. The compound **2.10f** had relatively higher antitumor activity than the other compounds. The data given in Table 2.10 indicated that the nature of substituent affects the antitumor activity. For example, the antiproliferation activities of compound **2.10f** at the concentration of 10 μg/mL against PC3 and A431 cells were 90.1% and 88.0%, respectively.

Table 2.10   Inhibition rate ($\overline{x}\pm$s) (%) (10 μg/mL) of compounds
2.10a-2.10g in 72 h ($P<0.01$)^a

Compd.	PC3 cells	A431 cells	Compd.	PC3 cells	A431 cells
2.10a	81.3±12.0	72.1±11.0	**2.10e**	41.2±10.0	31.6±7.8
2.10b	22.8±7.8	32.1±8.8	**2.10f**	90.1±20.1	88.0±19.0
2.10c	51.5±11.0	48.9±10.0	**2.10g**	67.8±12.1	72.1±14.2
2.10d	47.3±9.0	38.8±4.9			

^{a} Inhibition rate (%)=(A$_1$—A$_2$)/A$_1$×100%. A$_1$:the mean optical densities of untreated cells, A$_2$：the mean optical densities of drug treated cells.

The results of the _in vivo_ activity against TMV bioassay are given in Table 2.11. Ningnanmycin was used as reference antiviral agent. The data indicated that a change in the substituents might also affect the curative activity of the compounds **2.10a-2.10g**. Compound **2.10c** (Ar=4-CF$_3$C$_6$H$_4$-) and compounds **2.10f** (Ar=4-NO$_2$ C$_6$H$_4$-) could cure TMV up to 51.9% and 48.1% at 500 μg/mL. The other compouds have relatively lower curative activities than **2.10c** and **2.10f**.

Table 2.11   The curative effects of title compounds **2.10a-2.10g** at
500 μg/mL against TMV

Compd.	2.10a	2.10b	2.10c	2.10d	2.10e	2.10f	2.10g
Inhibition rate (%)	31.2	28.9	51.9	10.1	37.6	48.1	40.2

2.3.4   Conclusions

In summary, a mild and effective method for the preparation of (*E*)-3-methylthio-3-arylamine 2-cyanoacrylates was achieved by the amination reaction of arylamines and 3,3-dimethylthiolacrylate under microwave irradiation. We believe that this procedure will offer a better and more practical alternative to the existing methodologies. A half-leaf method was used to determine the curative efficacy *in vivo* of seven title products against tobacco mosaic virus. It was found that compound **2.10c** had a good curative effect *in vivo* against TMV, with an inhibition rate of 51.9%.

2.4   Preparation of Chiral Cyanoacylate Derivatives from Phenylethanamine

2.4.1   Introduction

2-Cyanoacrylates are of considerable importance because of their versatile biological activity and the possibility for application in agrochemistry as. herbicides that disrupt photosynthetic electron transportation at a common binding domain on the 32 KD polypeptide of the photosystem II (PSII) reaction center.[20, 28] Among these cyanoacrylates, (*Z*)-ethoxyethyl 2-cyano-3-(4-chlorophenyl) methylamino-3-isopropyl-acrylate (CPNPE) exhibits the highest Hill inhibitory activity.[1, 15, 21, 29] To the best of our knowledge, there are no reports of the antiviral activity of cyanoacrylate in the literature.[32] In our previous work, we designed and synthesized cyanoacrylates containing 4-trifluoromethylphenylamino moiety exhibiting moderate antiviral bioactivity against TMV.[33] In view of these facts and in continuation of our interest on the chemistry of cyanoacrylate, we contemplated undertaking the synthesis of an, as yet, unexplored novel chiral compounds containing cyanoacrylate moiety to obtain chiral compound with better biological activity. To explore the bioactivity of the chiral analogues of such compounds, considering the fact that chiral compounds are of primary interest in modern agricultural chemistry as the chiral isomers are always biologically more active than their racemic mixtures and they are more environmentally friendly due to their lower usage,[34] we decided to design and synthesize some chiral cyanoacrylates with antiviral activity through replacement of the methylthio moiety by the (*R*)-or (*S*)-1-phenylethanamine in some 2-cyano-3-methylthio-3-substitutedphenylaminoacrylates. Many useful methods for the preparation of cyanoacrylate have been developed including prolonged heating

of amine with 2-cyano-3-methylthio-3-aminoacrylate. However, these methods have several shortcomings such as longer reaction times accompanied by side reactions.[5] Recently organic reactions irradiated by microwave have been developed as safe and convenient method for the synthesis of phosphonyl/S-methyl ketenethioacetals.[13] The application of microwave energy to accelerate organic reaction is of increasing interest and offers several advantages over conventional techniques.[35] Those synthetic reactions normally requiring lengthy periods can be achieved conveniently and rapidly in a microwave oven. Hence, we reported herein a new method for the preparation of chiral cyanoacrylate from (R)-or (S)-1-phenylethanamine in refluxing n-propanol under microwave irradiation producing chiral cyanoacrylate with moderate or high yields (Scheme 2.4). Several ethyl 3-((R or S)-1-phenylethylamino)-3-(4-substitutedphenyl-amino)-2-cyanoacrylates were synthesized and the bioassay tests showed that some of these title compounds exhibit good antiviral activity in vivo and anticancer activity in vitro. The crystal structure of (R)-2.12a was determined by X-ray single crystal structure analysis from which an (E)-configuration of title compounds was confirmed. To the best of our knowledge, this is the first report on synthesis, anti-TMV bioactivity and antitumor bioactivity of chiral cyanoacrylate derivatives.

Scheme 2.4   Synthesis of the compounds **2.12**
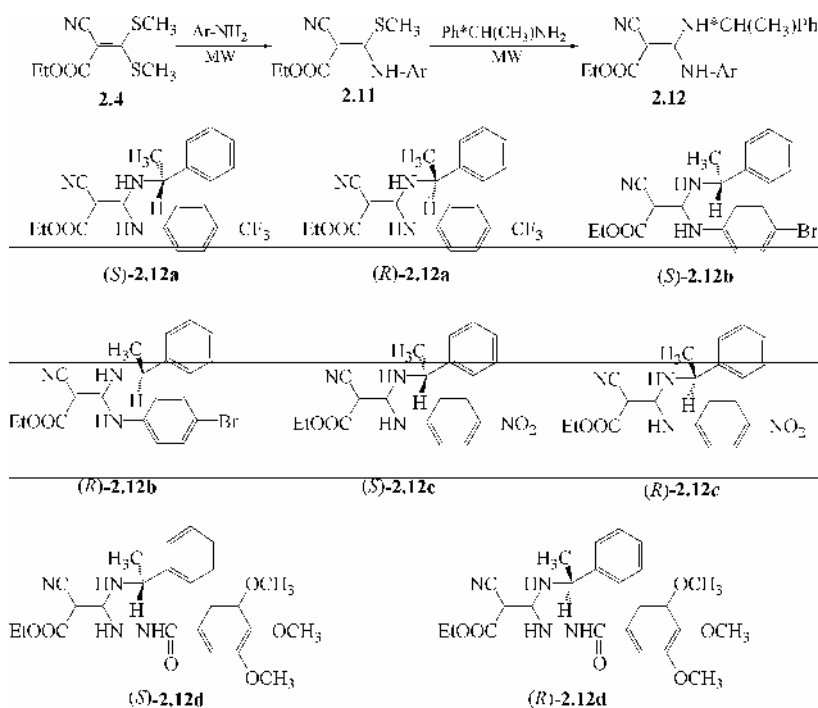
2.4.2   Materials and Methods

2.4.2.1   Synthetic Procedures

The materials and instruments for determination of the structure and physical data of new compounds are basically similar to the procedure described in Chapter 1.1.2. Microwave irradiations were carried out in a XH-100A CNC microwave-catalysis appearance at 600 W (Beijing Xianghu technical development Co., China). The reagents were of analytical grade or chemically pure. 2-Cyano-3,3- dimethylthio-acrylate was prepared according to literature method.[36]

2.4.2.2   General procedure for the preparation of intermediates 2.11a-2.11d

To an oven-dried three-necked 50 mL round-bottom flask fitted with a magnetic stirring bar were added 2-cyano-3,3-dimethylthioacrylate (2.17 g, 0.01 mol), substituted aniline (0.01 mol), 60% NaH (0.80 g, 0.02 mol), DMF (6 mL) and toluene (6 mL). The resulting mixture was irradiated in the microwave oven at 80℃ and 600 W for 15 min. The mixture was then poured into ice water (40 mL) and separated. The aqueous phase was acidified with 10% HCl to pH 6-7, and filtered. The residue was dried and recrystallized from ethanol-water to give the title compounds. The reperesentative data for **2.11a** is shown below, while data for **2.11b-2.11d** can be found in the reference.[7]

(E)-Ethyl 3-(4-(trifluoromethyl) phenylamino)-2-*cyano*-3-(methylthio) acrylate (**2.11a**). White crystal; mp 80-82℃; yield 62.1%. IR (KBr): ν_{max} 3216,2980, 2208, 1655, 1591, 1563, 1396, 1381, 1324, 1298, 1265, 11679, 1150, 1124, 1113, 1065, 1022, 779. ^{1}H NMR (400 MHz, CDCl$_3$): δ 1.27 (t, J=6.4 Hz, 3H, CH$_3$-C), 2.05 (s, 3H, S-CH$_3$), 4.54 (q, 2H, CH$_2$), 7.82-7.69 (m, 4H, Ar-H), 11.40 (s, 1H, NH). m/z (EI-MS):318 (M$^+$); Anal. Calcd. for C$_{14}$H$_{13}$F$_3$N$_2$O$_2$S: C, 50.91; H, 3.97; N, 8.48. Found: C, 50.94; H, 3.96; N, 8.34.

2.4.2.3   General procedure for the preparation of title compounds 2.12

A solution of intermediate **2.11** (0.4 mmol) in n-PrOH (20 mL) was stirred, followed by the addition of (R)-1-phenylethanamine or (S)-1-phenylethanamine (0.4 mmol). The mixture was irradiated in the microwave oven at 97℃ and 600 W for 20 minutes. The solvent was removed under reduced pressure. The crude product was purified by column chromatography on a silica gel (eluent: ethyl acetate/petroleum ether, 2/8, v/v) to give the title compounds. The reperesentative data for（R）**-2.12a** is shown below, while data for (S)-**2.12a** and (R)-**2.12b** *or* (S)-**2.12b** can be found in the reference.[7]

(E)-Ethyl 3-((R)-1-phenylethylamino)-3-(4-(trifluoromethyl) phenylamino)-2-cyanoacrylate［(R)-**2.12a**］. White crystal; mp 145-147℃; yield 53.1%; $[\alpha]_D^{25}$ －210.2 (c 0.4828, acetone). IR (KBr): ν_{max} 3258, 3125, 2980, 2195, 1666, 1620, 1595, 1327, 1284, 1115, 1067, 702.^{1}H NMR (400 MHz, CDCl$_3$): δ 1.26 (t, J=6.4 Hz, 3H,

CH$_3$-C), 1.45 (d, J=6.4 Hz, 3H, C-CH$_3$), 4.18-4.28 (br, 3H, OCH$_2$＋NCH), 7.15-7.31 (m, 9H, ArH), 9.61 (d, J=6.4 Hz, 1H, C-NH), 10.54 (s, 1H, Ar-NH). m/z (EI-MS):389 (M$^+$); Anal. Calcd. for C$_{21}$H$_{20}$F$_3$N$_3$O$_2$:C, 62.52; H, 5.00; N, 10.42. Found: C, 62.70; H, 4.96; N, 10.36.

2.4.2.4　Crystal structure determination

The experiment and method for X-ray diffraction data of compound (*R*)-**2.12a** are similar to the procedure described in Chapter 1.4.2.[38-40]. Crystallographic data for the structure (*R*)-**2.12a** have been deposited with the Cambridge Crystallographic Data Center as supplementary publication No. CCDC-271061.

2.4.2.5　Antiviral Biological Assay

The method for evaluating anti-TMV activity of title compounds is similar to the procedure described in Chapter 1.2.2.[7, 18]

2.4.2.6　Herbicidal activity bioassay

Several plants including *Brassica campestris*, *Amaranthus retroflexus L.*, *and Echinochloa crus-galli* were used to test the herbicidal activity of compounds. All the seeds were bought from the Institute of Crop, Tianjin Agriculture Science Academy, P. R. China. The seeds were planted in 6-cm-diameter plastic boxes containing artificial mixed soil. Before plant emergence, the boxes were covered with plastic film to keep moist. Plants were grown in the green house. The dosage (activity ingredient) was kept at 1500 g per hectare. Purified compounds were dissolved in 100 μL DMF with the addition of a little Tween 20, and then were sprayed using a laboratory belt sprayer delivering at 750 L/ha spray volume. The same amount of water was sprayed as control. Compounds were sprayed to treat the soil immediately after seeds planting and were sprayed to the stem and leaves after the seed germinating. The fresh weight of aerial tissues was measured 10 days after treatment. The inhibition percent of aerial tissues fresh weight is used to describe the control efficiency of compounds.

2.4.2.7　MTT Assay against Cell Viability and Proliferation

The experiment and method for evaluating antitumor activity of all compounds are similar to the procedure described in Chapter 1.5.2.3.[27]

2.4.3　Results and Discussion

2.4.3.1　Synthesis

In order to optimize the reaction conditions, the synthesis of （*R*）-**2.12a** was carried out under several conditions. The effects of different solvents, reaction

time, on the reaction with and without MW reaction, were investigated and the results are shown in Table 2.12. The results indicated that microwave irradiation can accelerate the reaction (entry 1-10). Without microwave irradiation, the reaction was relatively slow and no product was detected within 4 h (entry 11-15). When the reaction time was prolonged to 6 h to 10 h without microwave irradiation, (R) **-2.12a** could be obtained in 22.1% and 37.8% yields respectively (entry 16 and 17), while under microwave irradiation, the yield of (R)**-2.12a** increased from 24.1% to 53.1% when the reaction time was prolonged from 5 to 20 minutes in refluxing n-propanol at 97℃ (entry 1-3). When the reaction time was prolonged further to 30 minutes under microwave irradiation, tiny improvement of yield (54.1%, entry 4) was obtained compared to that of 20 minutes (53.1%, entry 3). As for the reaction temperature, it could be seen that the yield was relatively lower when the reaction was carried out at low temperature (entry 5-10, 18, 19) compared with that at 97℃ (entry 3). No substantial improvement was observed when the reaction system was heated to 105℃ (entry 20). Hence, the ideal temperature for the reaction was 97℃.

Table 2.12   Results at Different Reaction Conditions for Synthesis of (R)-**2.12a**

Entry	Solvent	Time（min）	Temp（℃）	Yield（%）[c]
1[a]	n-propanol	5	97	24.1
2[a]	n-propanol	10	97	30.3
3[a]	n-propanol	20	97	53.1
4[a]	n-propanol	30	97	54.1
5[a]	n-propanol	15	40	No product
6[a]	n-propanol	30	40	9.8
7[a]	n-propanol	20	50	21.5
8[a]	n-propanol	20	60	33.1
9[a]	n-propanol	20	70	41.2
10[a]	n-propanol	20	80	44.2
11[b]	n-propanol	20	97	No product
12[b]	n-propanol	60	97	No product
13[b]	n-propanol	120	97	No product
14[b]	n-propanol	180	97	No product
15[b]	n-propanol	240	97	No product
16[b]	n-propanol	360	97	22.1
17[b]	n-propanol	600	97	37.8
18[a]	ethanol	45	78	47.6
19[a]	methanol	45	65	31.1
20[a]	i-propanol	45	105	46.9

[a] The reaction was carried out in 20 mL solvent under microwave irradiation, power 600 W; [b] The reaction was carried out in 20 mL solvent under stirring without microwave; [c] Isolated yields.

The present new method for the synthesis of chiral cyanoacrylate **2.12** under microwave irradiation offers several advantages including faster reaction rates, fewer byproducts, and higher yields, as compared with the drawbacks of the classical method which involves a long tedious process (10h) and gives low yields. From Table 2.13, it is easy to observe that the average yields of products obtained by the microwave method are 10% higher than those obtained by the classical method. The short reaction time of the microwave method is beneficial in relation to other method; the average time ratio between the two methods is 1:30.

Table 2.13   Comparison of the Yields between the Microwave Assisted and Classical Synthesis of **2.12**

Entry	Compd.	Solvent	Yield(%)[a]	
			Microwave assisted[b]	Classical method[c]
1	(R)-**2.12a**	n-propanol	53.1	38.9
2	(S)-**2.12a**	n-propanol	54.1	38.9
3	(R)-**2.12b**	n-propanol	50.9	31.1
4	(S)-**2.12b**	n-propanol	51.1	33.3
5	(R)-**2.12c**	n-propanol	65.6	48.9
6	(S)-**2.12c**	n-propanol	71.2	56.4
7	(R)-**2.12d**	n-propanol	98.1	88.1
8	(S)-**2.12d**	n-propanol	97.8	88.8

[a]Yields of isolated products;[b]Reaction conditions: reaction under microwave irradiation in n-propanol, power 600 W, at 97℃ for 20 minutes; [c]Reaction conditions: using n-propanol as solvent, at 97℃ under stirring without microwave irradiation for 10 hours.

2.4.3.2   Antiviral Activity

The antiviral activity of compound **2.12** against TMV is assayed by the reported method.[41] It could be seen from Table 2.14, Table 2.15 that these newly synthesized chiral compounds exhibit promising antiviral activities against TMV in *vivo*. Apparently and interestingly, the antiviral data indicate that the (R)- or (S)-configuration substantially affects their bioactivity and the role of (R)-configuration is vital. For example, the bioactivities against TMV of the (R)-isomers of **2.12a,2.12b,2.12c,** and **2.12d** are all better than those of the (S)-isomers. It could be also seen that the nature of the substituent on the phenyl group affects the antiviral activity substantially. The electron withdrawing property of the substituent helps in enhancing antiviral bioactivity, as shown by the (R)-isomer of **2.12c** having a more potent antiviral activity than the other (R)- or (S)-isomers and the standard drugs (Virus A [Moroxydine Hydrochloride. copper acetate] and Antofine). The inhibition effect of (R)-**2.12c** to TMV *in vivo* is approximately equivalent to Ningnanmycin.

Table 2.14   The inhibition effect of the new chiral compounds against TMV *in vivo*

Agents	Ningnanmycin	Virus A	Antofine	(*R*)-**2.12a**	(*S*)-**2.12a**	(*R*)-**2.12b**
Concentration(mg/L)	500	500	50	500	500	500
Inhibition rate (%)	88.9	78.4	14.0	28.9	6.1	53.4

Agents	(*S*)-**2.12b**	(*R*)-**2.12c**	(*S*)-**2.12c**	(*R*)-**2.12d**	(*S*)-**2.12d**	
Concentration (mg/L)	500	500	500	500	500	
Inhibition rate (%)	0	89.1	5.3	46.4	7.5	

Table 2.15   The curative effect of the new chiral compounds against TMV *in vivo*

Agents	Ningnanmycin	Virus A	Antofine	(*R*)-**2.12a**	(*S*)-**2.12a**	(*R*)-**2.12b**
Concentration (mg/L)	500	500	50	500	500	500
Inhibitory rate (%)	28.9	14.6	29.2	39.1	15.2	12.3

Agents	(*S*)-**2.12b**	(*R*)-**2.12c**	(*S*)-**2.12c**	(*R*)-**2.12d**	(*S*)-**2.12d**	
Concentration(mg/L)	500	500	500	500	500	
Inhibitory rate (%)	3.4	43.1	13.1	26.7	12.1	

2.4.3.3   Herbicidal activity

The herbicidal bioactivity of compound **2.12** was also investigated and weak bioactivity of the compound was found, as can be seen in Table 2.16.

Table 2.16   Herbicidal Activities of Chiral Compounds at the Dose of 1.5 kg（a.i.）/ha

Compd.	*Brassica campestris*		*Amaranthus retroflexus L.*		*Echinochloa crus-galli*	
	soil treat	stem treat	soil treat	stem control	soil control	stem control
(*R*)-**2.12a**	16.07	0	0	0	11.43	2.86
(*S*)-**2.12a**	21.43	30.47	10.53	0	10.00	5.71
(*R*)-**2.12b**	5.38	10.94	0	0	4.29	0
(*S*)-**2.12**	1.29	35.26	0	0	10.00	34.29
(*R*)-**2.12c**	21.43	17.19	0	0	18.57	0
(*S*)-**2.12c**	25.00	32.13	0	0	14.29	13.33
(*R*)-**2.12d**	0	3.13	26.32	0	5.71	7.62
(*S*)-**2.12d**	0	18.75	10.53	0	7.14	0

2.4.3.4   Antiproliferation activity

The anti-cell viability and proliferation activity are assayed by the MTT method.[26, 27] The results are listed in Table 2.17. It was found that these chiral compounds exhibit weak activities against the two cancer cells *in vitro*. The compounds (*R*)-**2.12a** and (*S*)-**2.12a** have relatively higher activity than other chiral

Table 2.17   Inhibition Rate ($\bar{x}\pm$s)(%) of Compounds II to PC3 and
A431 Cells at 5μM(P<0.01)

Compd.	PC3 cells	A431 cells	Compd.	PC3 cells	A431 cells
(*R*)-**2.12a**	59.4± 4.7	43.1±9.6	(*S*)-**2.12c**	0.7±0.1	18.1±4.5
(*S*)-**2.12a**	49.1±6.0	39.9±8.1	(*R*)-**2.12d**	32.1±14.2	25.1±7.8
(*R*)-**2.12b**	1.5±0.1	16.1±8.5	(*S*)-**2.12d**	3.2±0.2	29.4±9.2
(*S*)-**2.12b**	24.7±11.3	19.3±9.1	Fluorouracil (5-Fu)	41.1±8.2	30.7±7.4
(*R*)-**2.12c**	2.9±0.3	23.6±11.2			

compounds. The data given in Table 2.17 indicate that the nature of the substituent on the phenyl ring affects the antitumor activity. For example, the antiproliferation activities of compound (*R*)-**2.12a** to PC3 and A431 cells at 5μM are 59.4% and 43.1%, respectively. No substantial difference was found between the (*R*)-or (*S*)-configuration in the antitumor bioassay.

2.4.3.5   Crystal Structure Analysis

It could be seen from the X-Ray single crystal analysis that chiral compound (*R*)-**2.12a** maintains a planar structure (Fig.2.3 & Fig.2.4). The configuration of target compound (*R*)-**2.12a** was determined to be an (*E*) by X-ray diffraction. The bond length of C(9)-C(10) (1.406 Å) is longer than normal C=C (1.34 Å), C(12)-O(1) (1.327 Å) is shorter than normal single C-O (1.44 Å), C(10)-C(12) (1.454 Å) and C(10)-C(11)(1.400 Å) are shorter than normal C-C (1.54 Å), C(9)-N(1) (1.315 Å) and C(9)-N(2) (1.365 Å) bonds are shorter than the normal C-N single bond (1.49 Å), which suggests the existence of an electron density delocalization among N(2)-C(9)-C(10)-C(12)-O(2), C(11) and N(1).
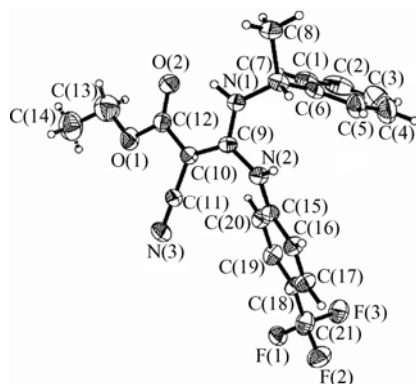
Fig 2.3   The molecular structure of compound (*R*)-**2.12a**
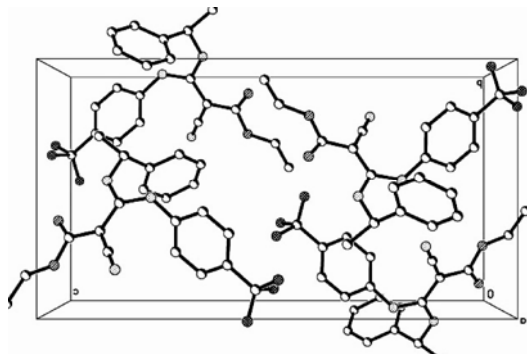
Fig 2.4   Packing diagram of the unit cell of compound (*R*)-**2.12a**

2.4.4   Conclusions

In summary, we described a practical and efficient procedure for the preparation of chiral cyanoacrylate compounds through the reaction of intermediate **2.11** with (*R*)-1-phenylethanamine or (*S*)-1-phenylethanamine under microwave irradiation in *n*-PrOH for 20 minutes at 97℃. The reactions were, in general, very fast, efficient and moderate yielding. In the half-leaf method test, the chiral compound (*R*)-**2.12c** was found to possess high antiviral activity against TMV *in vivo*.

2.5   Preparation and Antiviral Activity of Chiral Cyanoacylate Derivatives from Aryl (Heterocyclic) Amine

2.5.1   Introduction

Synthetic studies on cyanoacrylate derivatives have recently received wide attention due to their herbicidal action caused by disrupting photosynthetic electron transport.[3,20,29] Among them, (*Z*)-ethoxyethyl 2-cyano-3-(4-chlorophenyl)-methyl-amino-3-isopropylacrylate (CPNPE) has served as a model compound due to its excellent herbicidal activity.[1] In our previous work, we designed and synthesized some chiral cyanoacrylates with antiviral activity by replacing methylthio moiety with (*R*)- or (*S*)-1-phenylethylamine groups in some 2-cyano-3-methylthio-3-substituted-phenylaminoacrylates. The crystal structure of the chiral product was determined by X-ray single-crystal structure analysis which confirmed the presence of an (*E*) configuration. The bioassay showed that the chiral compound

with 4-nitrophenyl moiety had no herbicidal activity *in vivo*, but possessed good antiviral activity.[7] Viruses are unique in the deceptive simplicity of their structure. However, this simplicity leads to a greater dependence on the host and a highly intricate relationship exists between the two which complicates the strategic designs to control plant viruses and the losses caused by them.[43] Control programs depend on our understanding of the virus-host relationship, and several conventional strategies to control virus infection have been explored but without much success. In most of the modern approaches involving antiviral action, the induced resistance is very promising to a particular strain or group of viruses. PAL, the key enzyme in the phenylpropanoid pathway, which is associated with PR gene, is strongly induced after the infection of tobacco plants with viral pathogens.[44] In order to extend our research work of cyanoacrylate as antiviral agent, we designed and synthesized some novel chiral cyanoacrylates with (*E*)-configuration in which the phenylamino group was replaced by 2-nitrophenylamino, 3-nitrophenylamino, 2,4-dinitrophenylamino,4-methylbenzo-thiazol-2-amino, benzylamino groups. The synthetic route is shown in Scheme 2.5. The structures of **2.15a**-**2.15r** were established by well defined IR, NMR and elemental analysis. In the bioassay conducted by half-leaf method, these new chiral compounds were found to possess weak to good anti-TMV activities. Our previous and present studies have shown the effectiveness of chiral cyanoacrylates in protecting tobacco plant against disease caused by TMV. Their mode of action and cellular targets are however still unknown. The objective of our study is to establish the role of (*R*)-**2.15p** in inducing disease resistance in tobacco leaves against virus pathogen attack, and to study the activity of enzymes or metabolites that might be involved for resistance development. To the best of our knowledge, this is the first report on the synthesis, antiviral activity of (*E*)-ethyl 3- ［(*R*) or (*S*)-1-phenylethylamino］-3-(substituted phenylamino)-2-cyanoacrylate derivatives, and the relationship between the bioactivity of (*R*)-**2.15p** and the activity of PAL, POD and SOD enzymes and PR gene expression in tobacco. Our studies suggest that (*R*)-**2.15p** possesses antiviral activity by up-regulation of PR-1a, and PR-5 gene and enhancing activity of some defensive enzyme in defense response.

2.5.2   Materials and Methods

The materials and instruments for determination of the structure and physical data of new compounds are basically similar to the procedure described in Chapter 1.1.2. Microwave reaction was performed on a Focused Microwave Synthesizer, Disover[TM] LabMate (with a power of 50 W) according to Huang's and Zhou's methods.[61,62] 2-Cyano-3, 3-dimethylthioacrylate was prepared according to the literature method.[36]

2.5.2.1   General procedure for the preparation of intermediates **2.14a-2.14d**

A solution of Ethyl 2-cyano-3,3-dimethyl thioacrylate (0.4 mmol) in EtOH (20mL) was stirred, followed by the addition of (S)-1-(4-fluorophenylethyl amine or (R)-1-(4-fluorophenylethyl) amine (0.4 mmol). The mixture was irradiated in the microwave oven at 78℃ and 50 W for 10 min. The solvent was removed under reduced pressure. The crude product was purified by column chromatography on a silica gel (eluent, ethyl acetate/petroleum ether, 4∶1, v /v) to give the intermediates **2.14a**-**2.14d**. The structure was confirmed by ^{1}H NMR, ^{13}C NMR, IR, and elemental analysis.

2.5.2.2   General procedure for the preparation of title chiral compounds **2.15**

A solution of Ethyl intermediate **2.14** (0.72 mmol) in EtOH (10 mL) was stirred, followed by the addition of substituted phenylamine or 2-aminobenzothiazole (0.72 mmol). The resulting mixture was irradiated in the microwave at 78℃, 60 W for 20 min. The course of the reaction was followed by TLC. The mixture was poured into ice water (100 mL) and acidified with 10% HCl to a pH of 6-7, and filtered. The residue was purified by column chromatography on silica gel (eluent, ethyl acetate/ petroleum ether, 1∶4, v/v) to give title compounds **2.15**.

2.5.2.3   Crystal structure determination

The experiment and method for X-ray diffraction data of compound (R)-**2.15b** (Fig 2.5 & Fig 2.6) are similar to the procedure described in Chapter 1.4.2. [38-40] Crystallographic data for the structure (R)-**2.15b** have been deposited with the Cambridge Crystallographic Data Center as supplementary publication No. CCDC-299719.

2.5.2.4   Protection and inactivation and cure effect of compound against TMV *in vivo*

Purification of TMV was assessed by Gooding's method. [18] The bioactivity assay for protection and inactivation and cure effect was assessed according to Li's method. [41]

2.5.2.5   Determination of PAL and POD and SOD activity

The leaf samples were homogenized in the 2-mercaptoethanol-boric acid buffer (5 mM, pH 8.8) on the ice bath and centrifuged. The supernatant was used for experiment. PAL and POD and SOD activities were determined by He's method,[45] Polle's method,[46] Beauchamp's method,[47] respectively.

2.5.2.6   RT-PCR assay

Trizol kit was used according to the standard protocol for total RNA isolation. Prior to RT-PCR, the total RNA samples were treated with DNase I for 10 min and quantified by spectrophotometry and identified by agarose gel electrophoresis.[48] cDNA was synthesized with oligo $(dT)_{18}$ at the 3′ end of mRNA as a primer. Total RNA (1μg) was used for temple of first-strand cDNA synthesis using extend

reverse transcriptase. Reverse transcription was carried out at 37℃ for 1 h. The single-stranded DNA mixture was used as template in PCR. The primers for PCR amplification are shown in Table 2.18. The PCR were performed in Tris-HCl buffer (10 mM, pH 8.3), KCl (50 mM), MgCl$_2$ (1.8-2.0 μL), dNTPs (0.02 μM), primers (0.04 μM), DNA polymerase (1 U). PCR amplification steps consisted of a preliminary denaturation step at 94℃ for 1 min, followed by 35 cycles at 94℃ for 40 seconds, at 58℃ for 40 seconds and at 72℃ for 50 seconds on BioRad iCycler PCR. Products were separated on 1.5% agarose gel in 0.5×TBE buffer and visualized under UV light after staining with ethidium bromide.[49]

Table 2.18   Sequences of gene-specific primers used in RT-PCR analysis

Gene family	Accession	5′ primer	3′ primer
β-actin	U60495	5′-gacatgaaggaggagcttgc-3′	5′-atcatggatggctggaagag-3′
PR-1a	X12737	5′-caatacggcgaaaacctagctga -3′	5′-cctagcacatccaacacgaa-3′
PR-5	X03913	5′-gcttcccctttttatgccttc-3′	5′-cctggggttcacgttaatgct-3′

2.5.2.7   Semi-quantity PCR for expression of gene

In order to assess relative expression levels of target-gene in water-treated tobacco and (*R*)-**2.15p** and TMV-treated tobacco and tobacco by inoculated TMV only, semi-quantity PCR consisting of 20 cycles (within the logarithmic range of amplification of gene) with putting primer of β-actin serving as an internal reference gene was employed for the study. The amplified products were analyzed on a 1.5% agarose gel by the method of Mohamed. [50]

2.5.2.8   The relative quantification real-time PCR for expression of the target gene

The relative quantification real-time PCR was carried out with iCycler IQ according to manufacturer's protocol with primer of β-actin serving as an internal reference gene. Precautions were taken to ascertain reliable quantitative results. Log-linear dilution curves were performed with primers for the target gene as well as with primers for the β-actin. Reactions performed without reverse transcriptase or without template did not result in any product. By following PCR, 110 steps for melt curve analysis were completed in 10 seconds at temperature ranging from 40℃ to 95℃. The amplification efficiency was 95%-99% for PR-1a and PR-5 gene, respectively (The standard curve figures are not shown). Each target gene peak was assigned an arbitrary quantitative value correlated to the β-actin gene peak, according to the formula $\Delta\Delta C_T = \Delta C_{T, \text{ test}} - \Delta C_{T, \text{ calibrator}}$, C_T being the cycle threshold. Rates of stimulation of RNA expression were calculated from the ΔC_T values at various time points.[51]

2.5.2.9   Statistical analysis

All statistical analyses were performed with SPSS 10.0. Data were analyzed by one-way analysis of variance (ANOVA). Mean separations were performed

using the least significant difference method (LSD test). Each experiment had three replicates and all experiments were run three times with similar results. Measurements from all the replicates were combined and treatment effects analyzed.

2.5.3   Chemistry

2.5.3.1   Synthesis of novel chiral cyanoacrylate derivatives.

Nucleophilic Michael attack by the amine at the olefinic double bond followed by the expulsion of the leaving group SCH_3 from the conjugated system seems to generate compounds **2.14** and **2.15**, as shown in Scheme 2.5. To optimize the reaction conditions, the synthesis of chiral compound (*R*)-**2.15p** was carried out under several conditions. The effects of different solvents, reaction time and the merit of using microwave irradiation over classical reaction conditions were investigated, and the results are shown in Table 2.19. It revealed that the presence of microwave irradiation could accelerate the reaction (entry 1-5). When the reaction time was prolonged from 5 to 20 min under microwave irradiation in refluxing ethanol at 78℃, the yield of target chiral compound was increased from 39.4% to 52.5% (Table 2.19, entry 1-4). In classical method without microwave irradiation, the reaction was relatively slow and when refluxed in ethanol for 300min, 600min, 900min, and 1200min, 41.9%, 47.0%, 52.0% and 53.8% yields were obtained respectively (Table 2.19, entry 6-9). The reaction under microwave irradiation gave comparable yield with significant reduction of reaction time from 900min to just 20 min, the average time ratio for the two methods being 1:30 for similar yield.
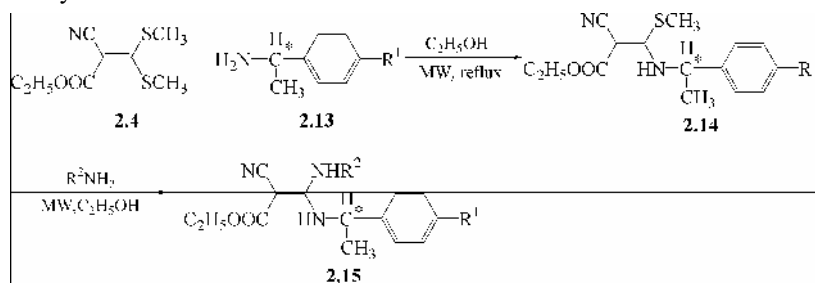
R^1=F,Br,H;R^2=benzylamino;2-nitrophenylamino;3-nitrophenylamino;2,4-dinitrophanylamino;4-trifluoromethylphenylamino;6-nirobenzothiazol-2-amino;4-methylbenzothiazole-2-amino.

Scheme 2.5   Synthesis of novel chiral cyanoacrylate derivatives with (*E*) configuration

The structures of all the compounds were confirmed by ^{1}H NMR, ^{13}C NMR, elemental analysis, IR and mass spectrometry. IR spectra of compound **2.15** show absorption band in the region 3220-3379 cm^{-1}, indicating the presence of NH. The

Table 2.19 Effect of reaction time on the synthesis of (*E*)-Ethyl-3-［(*R*)-1-(4-fluoro phenylethylamino)］-3-benzylamine-2-cyanoacrylate ［(*R*)-**2.15p**］

Entry	Power(W)	Temp(℃)	Time(min)	Solvent	Amount of the solvent（mL）	Yield[c](%)
1[a]	50	78	5	ethanol	10	39.4
2[a]	50	78	10	ethanol	10	44.2
3[a]	50	78	15	ethanol	10	49.5
4[a]	50	78	20	ethanol	10	52.5
5[a]	50	78	30	ethanol	10	53.1
6[b]	—	78	5×60	ethanol	10	41.9
7[b]	—	78	10×60	ethanol	10	47.0
8[b]	—	78	15×60	ethanol	10	52.0
9[b]	—	78	20×60	ethanol	10	53.8

[a] The reaction was conducted in 10 mL solvent under microwave irradiation, power 50 W; [b] The reaction was conducted at 78℃ in 10 mL solvent under stirring without microwave; [c] Isolated yields.

characteristic C=O stretching and strong C=C vibrations appeared in the region 1639-1672 cm^{-1} and 1539-1548 cm^{-1} respectively. A set of peaks near 2193-2212 cm^{-1} and 1113-1165(s) were assigned to C=N and C-F vibrations respectively. In ^{1}H NMR data, all phenyl protons showed a multiplet at δ 6.94-7.55. The chemical shifts of CH$_2$ ester generally appeared as a quartet in the region 4.22-4.37 ppm. The NH proton of **2.14** appeared downfield as a broad singlet around 9.02-11.12 ppm due to the existence of H-bond interaction between ester carbonyl and NH of phenylamino group. As for the ^{13}C NMR data of 2.15, all the carbon atoms were identified and the number of protons calculated from the integration curve (in ^{1}H NMR) was consistent with the molecular formula.

2.5.3.2 Crystal structure analysis.

It could be seen from the X-Ray single crystal analysis that chiral compound (*R*)-**2.15b** maintains a planar structure. The configuration of target compound (*R*)-**2.15b** was established as (*E*) by X-ray diffraction. The bond length of C(4)-C(6) (1.418 Å) is longer than normal C=C (1.34 Å), C(3)-O(2) (1.361 Å) is shorter than normal single C-O (1.44 Å), C(3)-C(4) (1.436 Å) and C(4)-C(5) (1.413 Å) are shorter than normal C-C (1.54 Å), C(6)-N(2) (1.341 Å) and C(6)-N(3) (1.362 Å) bonds are shorter than the normal C-N single bond (1.49 Å), suggesting the existence of an electron density delocalization among N(3)-C(6)-C(4)-C(3)-O(1), C(5) and N(2). As shown in the packing diagram of the title compound (Fig 2.5 & Fig 2.6), there is an intramolecular hydrogen bond interaction within N(2)-H(2)⋯O(1), in which N(2)-H(2)=0.86 Å, H(2)⋯O(1)=2.04, N(2)⋯O(1)= 2.692(3) Å, N(2)-H(2)⋯O(1)= 132.1°, -*x*, -*y*+1/2, -*z*+1/2). The N-H…O type intramolecular interaction leading to a six membered stable cyclic structure perhaps plays a major role in stabilizing the molecules in the unit cell.
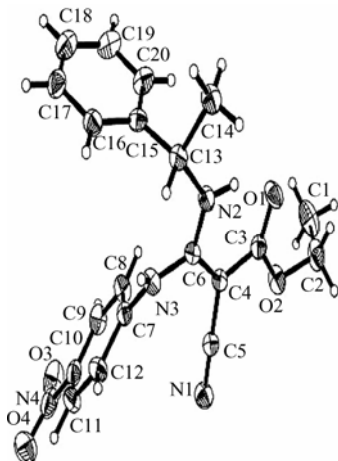
Fig 2.5   The molecular structure of compound (*R*)-**2.15b**
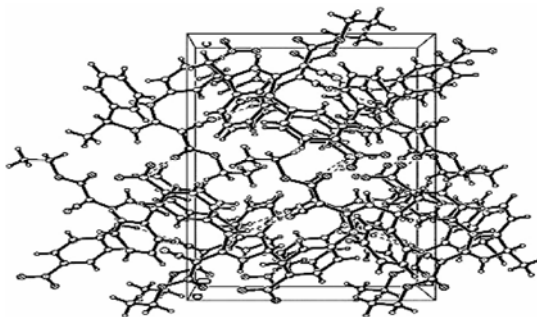
Fig 2.6   Packing diagram of the unit cell

2.5.4   Antiviral Activity

2.5.4.1   Preliminary antiviral activity assay

The results of bioassay *in vivo* against TMV are provided in Table 2.20. Ningnanmycin was used as reference antiviral agent. The results indicated that the antiviral activity is greatly dependent upon the nature of substituents. When R^1 was fluoro and R^2 was benzyl, the title compound (*R*)-**2.15p** showed higher curative rate (64.0%) than that of the reference (57.8%) and comparable inactivation rate (49.5%) with the standard Ningnanmycin (50.0%) against TMV at 500 μg/mL. It should be noted that no protection effect was observed with (*R*)-**2.15p**. The other compounds have a relatively lower antiviral activity than that of (*R*)-**2.15p**.

2.5.4.2   Effect of (R)-2.15p treatment on PAL, POD and SOD activity in tobacco.

As shown in Fig 2.7A, PAL levels in (*R*)-**2.15p**-treated tobacco rapidly increased by the end of the first day after the inoculation and reached 5.88 EU/mg

Table 2.20   The Protection, inactivation and curative effect of the new
chiral compounds against TMV *in vivo* (500 mg/L)

Agents	Protection effect(%)	Inactivation effect (%)	Curative effect(%)
(*S*)-**2.15a**	0	0	19.7
(*R*)-**2.15b**	38.1±4[*]	0	0
(*S*)-**2.15c**	10.0±4[*]	0	44.8±4[*]
(*R*)-**2.15d**	2.7±2	0	7.5±4
(*S*)-**2.15e**	16.7±4[*]	0	38.7±8[*]
(*R*)-**2.15f**	0	0	21.7±4[*]
(*S*)-**2.15g**	7.8±4[*]	23.2±[*]	9.6±2[*]
(*R*)-**2.15h**	48.1±4[*]	32.3±7[*]	20.0±5[*]
(*S*)-**2.15i**	11.0±2[*]	11.0±4	0
(*R*)-**2.15j**	51.9±7[*]	16.8±3[*]	12.3±4[*]
(*S*)-**2.15k**	0	15.4	0
(*R*)-**2.15l**	3.8±1	0	28.6±4[*]
(*S*)-**2.15m**	17.4±3[*]	4.2±2	0
(*R*)-**2.15n**	5.4±42	14.3±3[*]	0
(*S*)-**2.15o**	46.4±5[*]	46.5±4[*]	34.5±4[*]
(*R*)-**2.15p**	65.7±8[*]	49.5±5[*]	64.0±5[**]
(*S*)-**2.15q**	22.6±3[*]	32.6±4[*]	55.5±5[**]
(*R*)-**2.15r**	25.0±4[*]	5.3±1	36.9±4[*]
Ningnanmycin	100±7[**]	50.0±4[**]	57.8±6[**]

All results are expressed as mean±SD; n=3 for all groups;[*] $P<0.05$,[**]$P<0.01$.

protein on the 7th day, 37.93 times more as on the first day ([*]$P<0.05$) after inoculation. In contrast, in control and TMV, no significant increase in PAL activity was measured. The PAL activity in tobacco (control and TMV) increased marginally and reached a peak at the end of the fifth day after inoculation before starting to fall gradually thereafter.

As shown in Fig 2.7B, it could be found that SOD activity in (*R*)-**2.15**-treated tobacco gradually decreased from 1st day to the start of the 3rd day and then started to increase by the end of the 3rd day after inoculation. Similar trend in the change of SOD activity was observed with water-treated tobacco and not much difference was noticed within and among groups. It was found that the SOD activity in TMV gradually increased after the first day of inoculation, but the level was lower than that in water-treated by the first day ([*]$P<0.05$).

As shown in Fig 2.7C, it could be seen that POD activity of (*R*)-**2.15** increased and reached a peak on the 5th day after the inoculation, then gradually decreased (Fig 2.7). POD contents in (*R*)-**2.15** treated tobacco leaf were 8.42 times as large as that ([*]$P<0.05$) in water-treated tobacco leaf on the 1st day of inoculation. The POD activity of water and TMV treatments both reached their peaks on the 3rd and 1st day after the inoculation, but the peak value of POD activity corresponding to the control was lower than that of (*R*)-**2.15** treated one.
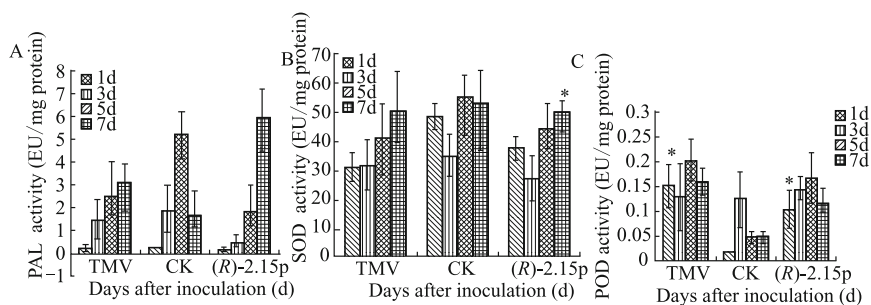
Fig 2.7   Effect of (*R*)-**2.15** treatment on PAL and SOD and POD activity in *Nicotiana tabacum*. *Nicotiana tabacum* inoculated by TMV was treated with (*R*)-**2.15** at 500ppm for 1, 3,5 and 7 days. Leaf sample extracts using homogenized and centrifuged methods were used to determine the PAL and SOD and POD activities as described in the 'Experimental'. Water treatment and TMV treatment were used for negative and positive controls. Data were expressed as the mean±SD (*n*=3) of three individual experiments. One-Way ANOVA revealed significant difference ($^{*}P<0.05$)

2.5.4.3   Gene expression analysis of PR-1a and PR-5 in (*R*)-**2.15**-treatedtobacco leaf

For the results of product of PCR in PR-1a and PR-5 and its sequence identification, see the Supporting Information. *In vitro* synthesized single-stranded cDNA from RNA samples were isolated from leaf in water-treated tobacco and the TMV-treated tobacco and the (*R*)-**2.15**-and TMV-treated tobacco. The differential expression analysis of the PR-1a and PR-5 gene was determined by the semi-quantity PCR and the relative quantification real-time PCR analysis. The mRNAs of PR-1a and PR-5 gene accumulated to detectable levels in (*R*)-**2.15**-and TMV-treated tobacco leaf, while no-detectable levels were reached in water-treated tobacco and the TMV-treated tobacco. The mRNA content of (*R*)-**2.15**-treated tobacco leaf for PR-1a gene started to increase after 12 h and reached a peak at the end of the 2nd day before falling to the normal level. In contrast, in TMV-treated tobacco leaf, no significant increase in the levels of gene expression was noticed (Fig 2.8A, Fig 2.9A). The expression levels of PR-5 gene in (*R*)-**2.15**-treated tobacco rapidly increased and reached a peak within 12 h after the inoculation and then started to decrease gradually. As depicted in Fig 2.8B and Fig 2.9B, (*R*)-**2.15** treated tobacco leaves showed significant enhancement in the levels of gene expression, almost twice as large as compared to TMV-treated tobacco leaves within 12 h after the inoculation. In contrast, in TMV-treated tobacco leaf, no significant increase in the levels of gene expression was observed.
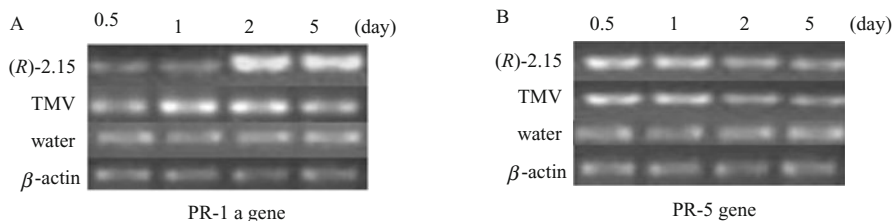
Fig 2.8   Semi-quantitative RT-PCR analysis of RNA isolated from tobacco leaf.
The figure shows that 20 cycles were performed and the amplified products
were resolved on a 1.5% agarose gel by following the RT. Parts A and B in the figures
indicate result of PR-1a and PR-5 gene expression treated by (R)-**2.15** compound
at 500 ppm for 0.5,1, 2,5 day, respectively. Lane 1-4 represents the amount of PCR
amplification at period four. β-actin gene served as an internal reference gene
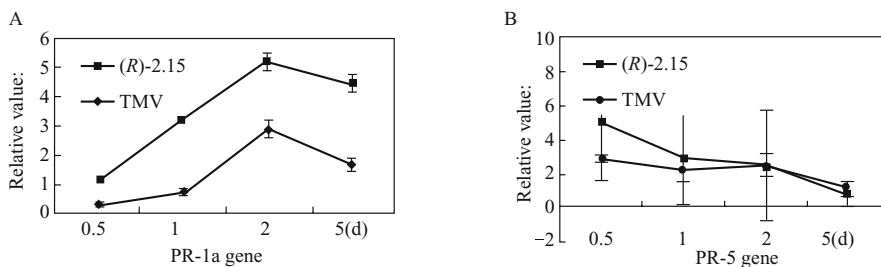
Fig 2.9   Real time PCR analysis of RNA isolated from tobacco leaf. Letters A and B in the
figures indicate the results of PR-1a and PR-5 gene expression ratio through C_T value
formula $\Delta\Delta C_T = \Delta C_{T, test} - \Delta C_{T, calibrator}$. Relative values of real time PCR between
target gene and β-actin gene were calculated, each value represents means $\pm$ SD (n=4)
and each experiment was performed in triplicate sets. The data was analyzed by
One-Way ANOVA

2.5.5   Discussion

Although the action mechanism of anti-TMV has not yet been elucidated,
some studies show that there exists requisite association between the defense
enzymes of tobacco and salicylic acid-mediated signal transduction pathway
regarding pathogenesis related proteins. PAL is a rate-limiting enzyme in the
activation of the phenylpropanoid pathway, and an increase in PAL activity is
associated with biosynthesis of active metabolites, such as salicylic acid, which is
used for molecular signal in plant SAR defense pathways.[52] POD is also a very
important enzyme in the plant defense reaction and is involved in the scavenging
of reactive oxygen species. The increase in POD activity promotes the cross-link
of lignin, strengthens the structure barrier and enhances disease resistance.[53-56]

Rasmussen has shown that SA could enhance the activity of POD and PAL.[57] PR-1a and PR-5 are regulation proteins of downstream in SA signal pathway that play a significant role in antiviral, antifungal and wound repair.[58-60] Our studies have shown that PR-1a and PR-5 gene were induced to up-regulation by compound (R)-**2.15** at 500 mg/mL on the 1st day after inoculation. Meanwhile, the activity of PAL and POD were increased from 1st day to 5th day after inoculation. These results show that there is significant association between curative effect and up-regulation of PR-1a and PR-5 gene against anti-TMV by (R)-**2.15** to enhance defense enzymes activity level. Future research would be focused on studying the action mechanism between gene regulation and anti-TMV, and the knock down technique to evaluate the antiviral effect against target gene.

2.5.6   Conclusions

In conclusion, A series of novel (E)-ethyl-3-〔(R)-or (S)-1-phenyl-ethylamino〕-3-(substituted phenylamino)-2-cyanoacrylate derivatives were synthesized by the treatment of chiral intermediate **2.14** with aryl (heterocyclic) amine under microwave irradiation. This method is easy, rapid and moderate-yielding for the synthesis of title chiral compounds (R)-**2.15**. Their structures were verified by spectroscopic data. The results of bioassay showed that these title compounds exhibited weak to good anti-TMV bioactivity. Title compounds (R)-**2.15p** showed better biological activity than their structurally related analogues (R)-**2.15a-o**, (R)-**2.15q-r**. Preliminary studies showed that treatment by compound (R)-**2.15p** can significantly enhance disease resistance of tobacco leaf, and substitute for antiviral agent control of TMV diseases in tobacco.

2.6   Preparation and Antiviral Activity of Chiral Cyanoacylate Derivatives Containing α-Aminophosphonate Moiety

2.6.1   Introduction

2-Cyanoacrylates, a class of highly potent herbicial compounds, are known to disrupt photosynthetic electron transportation at a common binding domain on the 32 kDa polypeptide of the photosystem II (PSII) reaction center.[1-2]Due to their versatile biological activities and promising application in agrochemistry, a large number of cyanoacrylate derivatives have been reported which show broad spectrum bioactivities having potential to be employed as herbicides, insecticides, fungicides, plant virucides and antitumor agents.[3, 4, 15, 63-65] In our previous work,

we designed and synthesized some chiral cyanoacrylates with antiviral activity by replacing the methylthio moiety of some 2-cyano-3-methyl-thio-3-substituted-phenylacrylates with (*R*)-or (*S*)-1-phenylethyla-mine groups. The (*E*) configuration of the reported chiral products was confirmed by X-ray single-crystal structure analysis. The bioassays showed that a chiral compound containing a 4-nitrophenyl moiety [(*E*)-ethyl 3 [(*S*)-1-phenylethylamino］-3-(4-nitrophenylamino)-2-cyanoacrylate］ exhibited good protection activity against TMV *in vivo*.[7] Some alkyl 2-cyano-3-methylthio-3-phosphonylacrylates were found to possess good *in vivo* curative, protection and inactivation effects against TMV with inhibitory rates at 500 mg/L.[66] Recently, we reported the synthesis and antiviral activity of (*E*)-ethyl 3-(*R*)-or (*S*)-1-phenylethylamino-3-(substitutedphenylamino)-2-cyanoacrylate. The objective of our study was to show the effects of (*R*)-**4p** in inducing disease resistance of tobacco leaves in response to virus pathogen attack, and on the activity of enzymes or metabolites that might be involved in induced resistance.[67] On the other hand, α-aminophosphonic acids, bioisosteres of natural amino acids, have been found to exhibit a wide range of bioactivities. Some derivatives of α-aminophosphonic acids find application as plant growth regulators, fungicide, plant virucide, herbicides and so on. [17, 68,69] A large volume of researches on their synthesis and biological activities has been reported in recent years.[70–75]

In our previous work, while many substituted aryl aminophosphonate derivatives were shown to have good antiviral activities,[76–80] carbonylamino phosphonates revealed better antiviral activities.[81] As different aminophosphonates and their derivatives display potential bioactivities, screening of cyanoacrylate derivatives bearing various α-amiophosphonate moities might produce new lead compounds with more potent antiviral activities against TMV. Keeping these considerations in mind, we herein designed and synthesized some novel cyanoacrylate derivatives containing α-aminophosphonates(Scheme 2.6). The synthetic route is shown in Scheme 2.7. The bioassay test showed that the new compounds **2.23** possessed moderate to good antiviral activities. To the best of our knowledge, this is the first report on the synthesis and antiviral activity of cyanoacrylate derivatives containing α-aminophosphonate moiety.

2.6.2   Materials and Methods

Instruments. The materials and instruments for determination of the structure and physical data of new compounds are basically similar to the procedure described in Chapter 1.1.2.

Synthetic Procedures. Diethyl phosphite and di-*n*-propyl phosphite were prepared according to literature method as described.[82] Intermediates **2.20a-2.20f, 2.21a-2.21e** and **2.22a-2.22e** were prepared according to the reported methods[83].

Preparation of Title Compounds **2.23a-2.23x.** A mixture of alkyl (imido) 2-cyano-3,3-dimethylthioacrylate (**2.22a-2.22e**) (0.1mmol) and α-aminobenzylphophonate (**2.20a-2.20e**) (0.1mmol) in ethanol (10 mL) was refluxed for 4 h. Upon completion of the reaction, the solvent was removed under reduced pressure and the residue was washed with water, filtered off and purified by silica gel column chromatography (petroleum ether-ethyl acetate, 2:1, $v:v$) to give the title compounds **2.23a-2.23x** in 25.6-70.0 yields. The reperesentative data for **2.23a** is shown below, while data for **2.23b-2.23x** can be found in the literature cited.[84]

Data for Methyl 2-cyano-3-methylthio-3-(diethyl aminobenzylphosphonyl) acrylate **(2.23a).** Colorless liquid; yield 51.3%;IR (KBr): ν_{max} 3062.9,3030.1,2983.8, 2953.0,2208.4,1643.3,1566.2,1556.5,1514.1,1494.8,1440.8,1384.8,1257.5,1161.1, 1045.4,1020.3,975.9,840.9,781.1,748.3,698.2,561.2; ^{1}H NMR (CDCl$_3$,500 MHz): δ 1.28-1.29 (m,3H, C-CH$_3$),1.31-1.32 (m,3H, C-CH$_3$),2.54 (s,3H, S-CH$_3$),3.82 (s,3H, O-CH$_3$),4.05-4.91 (m,2H, O-CH),5.59 (dd, J=21.75,9.15 Hz,1H, Ar-CH), 7.34-7.40 (m,5H, Ar-H), 10.94 (s,1H, C-NH); ^{13}C NMR (CDCl$_3$,125 MHz): δ 172.26,172.18,171.18,168.45,129.08,128.76,127.66,127.63,117.93,63.89,58.16, 56.94,52.22,18.49,16.47,16.43,16.37; ^{31}P NMR (CDCl$_3$,200 MHz): δ 19.21; Anal. Calcd. for：C$_{17}$H$_{23}$N$_2$O$_5$SP (398.11): C,51.25; H,5.82; N,7.03. Found: C,51.01; H,5.90; N,6.81.

X-ray Diffraction. Colorless blocks of **2.23v** (0.29mm×0.24mm×0.21mm) were counted on a quartz fiber with protection oil. Cell dimensions and intensities were measured at 273 K on a Bruker SMART CCD area detector diffractometer with graphite monochromated MoKa radiation (λ=0.71073 Å),θ_{max} =25.00,19767 measured reflections, and 3232 independent reflections (R_{int}=0.1763) of which 4767 had $I > 2\sigma$ (I). Data were corrected for Lorentz and polarization effects and for absorption (T_{min}=0.7680; T_{max}=0.8237). The structure was solved by direct methods using SHELXS-97; all other calculations were performed with Bruker SAINT System and Bruker SMART programs. Full-matrix leastsquares refinement based on F^2 using the weight of $1/\left[s^2(F_o{}^2)+(0.0703P)^2+0.0000P\right]$ gave final values of R=0.0558,ωR=0.1610, and GOF(F)=1.052 for 307 variables and 4767 contributing reflections. The maximum shift/error=0.001, and max/min residual electron density=0.400/$-$0.322 e Å^{-3}. Hydrogen atoms were observed and refined with a fixed value of their isotropic displacement parameter.

Antiviral Biological Assay. The method for evaluating anti-TMV activity of title compounds is similar to the procedure described in Chapter 1.1.2.[7,18]

2.6.3   Results and Discussion

Synthesis. α-Benzylphosphonates **2.20a-2.20e** were synthesized from dialkyl phosphites and benzaldehyde in accordance with Scheme 2.7. Addition of *p*-toluenesulfonic acid into the imine is highly exothermic and may cause

undesired side reaction. Controlling the reaction temperature near 0℃ during its addition is the most important factor in the synthesis of α-benzylphosphonates.

Esters **2.21a-2.21c** were prepared conveniently from cyanoacetic acid and primary alcohols in the presence of a catalytic amount of anhydrous H_2SO_4. Amides **2.21d-2.21e** were synthesized from ethyl cyanoacetate and the corresponding amine in excellent yields. Intermediate 2-cyano-3,3-dimethyl-thioacrylate **2.22a-2.22e** was achieved by treating corresponding ester (amide) **2.21a-2.21e** with carbon disulfide and two moles of dimethyl sulfate in a one-pot reaction using sodium hydroxide as alkali.
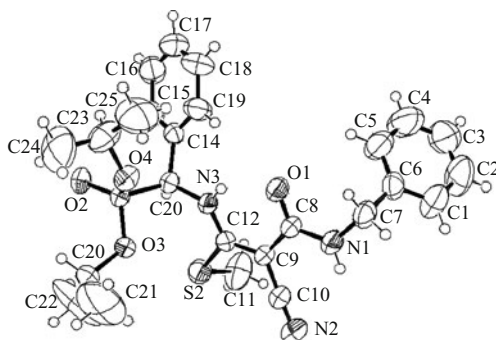
Fig 2.10   Molecular 2.23v

The desired products (**2.23a-2.23x**) were then obtained in moderate yields by a nucleophilic substitution reaction involving intermediates **2.22a-2.22e** and α-aminobenzylphosphonate **2.20a-2.20e** in refluxing ethanol. This reaction is assumed to be initiated by a nucleophilic attack followed by expulsion of SCH_3. The Michael type attack of the α-aminophosphonate at the α,β-unsaturated center presumably leads to a transition state in which the orientation of α-aminophosphonate and ester carbonyl is *cis* due to the presence of an intramolecular hydrogen bonding. The *E*-configuration of the title compounds established by X-ray single crystal structure analysis of typical **2.23v** is shown in Fig 2.10. All compounds were confirmed by elemental analyses, IR,^{1}H NMR, and ^{13}C NMR spectral data.

Antiviral Activity and Structure-Activity Relationship. To make a judgment of the antiviral potency of the synthesized compounds **2.23a-2.23x,** the commercially available plant virucide Ningnanmycin,[85] perhaps the most successful registered antiviral agents for plants available in China, was used as the control. The antiviral bioassay against TMV is assayed by the reported method [7,] [18]and the antiviral results of all the compounds against TMV are listed in Table 2.21 The results showed that most of our designed compounds had moderate antiviral activities at 500 mg/L against TMV *in vivo*.

The title compounds **2.23a-2.23x** exhibited protection activities of 29.6%-56.5% at 500 mg/L. Compounds **2.23d** (R^1 is H, R^2 is OCH_3 and R^3 is

n-Bu), **2.23h** (R^1 is H, R^2 is OC_2H_5 and R^3 is n-Bu), **2.23o**(R^1 is H, R^2 is NH_2 and R^3 is Et), **2.23q** (R^1 is H, R^2 is NH_2 and R^3 is i-Pr) and **2.23t** (R^1 is H, R^2 is $PhCH_2NH_2$ and R^3 is Et) have the same protection activity (55.9%, 56.5%, 55.6%, 54.4% and 55.1%, respectively) as that of the standard reference (59.9%). In addition, compounds **2.23b**, **2.23c**, **2.23e**, **2.23f**, **2.23i**, **2.23j**, **2.23k**, **2.23m**, **2.23n**, **2.23p**, **2.23r**, **2.23s**, **2.23u**, **2.23w** and **2.23x** showed 40.8%-48.3% potection activities at 500 mg/L. From the data presented in Table 2.21, it can be observed that the title compounds **2.23a-2.23x** possess potential inactivation bioactivities, with values of 64.1%, 47.1%, 45.7%, 92.8%, 92.1%, 71.0%, 37.8%, 84.0%, 74.1%, 46.8%, 51.5%, 55.9%, 80.6%, 70.0%, 60.8%, 63.0%, 5.7%, 9.6%, 70.7%, 51.9%, 50.0%, 51.5%, 11.0% and 73.4% at 500 μg/mL, respectively. Among these compounds, **2.23d** and **2.23e** are appreciably more active than the rest, with the inactivation rate of 92.8% and 92.1% respectively, which are similar to that of Ningnanmycin (99.5%) against TMV at 500 μg/mL. The data also indicate that a change in the substituent might also affect the curative activity of title compounds **2.23a-2.23x**. Compounds **2.23a** (R^1 is H, R^2 is OCH_3 and R^3 is Et), **2.23d** (R^1 is H, R^2 is OCH_3 and R^3 is n-Bu), **2.23e** (R^1 is 2-F, R^2 is OCH_3 and R^3 is Et), **2.23f** (R^1 is H, R^2 is OC_2H_5 and R^3 is n-Pr), **2.23h** (R^1 is H, R^2 is OC_2H_5 and R^3 is n-Bu), **2.23i** (R^1 is 2-F, R^2 is OC_2H_5 and R^3 is Et), **2.23j** (R^1 is H, R^2 is $OC_2H_5OC_2H_5$ and R^3 is Et), **2.23m** (R^1 is H, R^2 is $OC_2H_5OC_2H_5$ and R^3 is n-Bu), **2.23n** (R^1 is 2-F, R^2 is $OC_2H_5OC_2H_5$ and R^3 is Et), **2.23o** (R^1 is H, R^2 is NH_2 and R^3 is Et), **2.23p** (R^1 is H, R^2 is NH_2 and R^3 is n-Pr) and **2.23u** (R^1 is H, R^2 is $PhCH_2NH_2$ and R^3 is n-Pr) have curative activities against TMV of up to 56.7%, 60.2%, 58.4%, 55.8%, 50.7%, 55.2%, 51.8%, 52.7%, 54.4%, 53.9% and 53.8% respectively at 500 μg/mL. The other compounds have a relatively lower curative activity than those of **2.23a, 2.23d, 2.23e, 2.23f, 2.23h, 2.23i, 2.23j, 2.23m, 2.23n, 2.23o, 2.23p** and **2.23u.** Comparison of biological activities among **2.23a-2.23x,** figures out functional groups with R^2=OMe, OEt, R^3=n-Bu to be potentially more active than those with R^2=NH_2, $PHCH_2NH_2$, $OC_2H_5OC_2H_5$, R^3=n-Pr, i-Pr, Et.

Table 2.21 The Protection effect, inactivation effect and curative effect of the new compounds against TMV *in vivo*

Agents	Concentration(μg/mL)	Protection effect(%)	Inactivation effect (%)	Curative effect(%)
2.23a	500	$29.6^*\pm4.9$	$64.1^*\pm1.6$	$56.7^*\pm2.9$
2.23b	500	$44.4^*\pm4.0$	$47.1^*\pm2.2$	$37.7^*\pm4.6$
2.23c	500	$40.8^*\pm4.2$	$45.7^*\pm3.0$	$43.3^*\pm2.7$
2.23d	500	55.9 ± 3.8	$92.8^{**}\pm1.9$	$60.2^*\pm2.6$
2.23e	500	$44.0^*\pm3.3$	$92.1^*\pm1.9$	$58.4^*\pm3.4$
2.23f	500	41.6 ± 5.0	$71.0^*\pm2.8$	50.5 ± 4.3
2.23g	500	37.6 ± 3.0	$37.8^*\pm4.1$	$42.8^*\pm3.9$

Continued

Agents	Concentration(μg/mL)	Protection effect(%)	Inactivation effect (%)	Curative effect(%)
2.23h	500	56.5±3.8	84.0**±2.1	55.8*±4.2
2.23i	500	48.3*±4.0	74.1*±2.8	50.7*±3.6
2.23j	500	41.2*±3.2	46.8*±3.1	55.2*±3.1
2.23k	500	43.1±2.8	51.5*±3.5	43.2±2.7
2.23l	500	38.4±2.8	55.9*±4.9	35.1*±4.2
2.23m	500	44.4*±2.9	80.6±1.4	51.8*±2.8
2.23n	500	48.3±4.5	70.0*±1.6	52.7*±3.9
2.23o	500	55.6*±3.2	60.8*±3.7	54.4*±3.6
2.23p	500	45.8*±5.2	63.0*±2.2	53.9±5.4
2.23q	500	54.4*±4.4	5.7±2.1	28.8±4.8
2.23r	500	40.2*±2.6	9.6±2.4	25.4*±3.9
2.23s	500	42.8*±3.2	70.7*±2.3	25.4*±2.1
2.23t	500	55.1*±5.9	51.9*±3.0	55.0*±2.9
2.23u	500	42.4*±4.1	50.0*±2.9	53.8*±4.3
2.23v	500	39.0*±3.5	51.5*±2.3	52.9±5.9
2.23w	500	45.0*±2.1	11.0±0.9	28.4±2.5
2.23x	500	47.7*±3.7	73.4**±2.8	49.9*±2.2
Ningnamycin	500	59.9*±2.5	99.5**±2.9	55.8*±1.7

All results are expressed as mean±SD; n=3 for all groups; * $P<0.05$, ** $P<0.01$.

In addition, as shown in Table 2.22, compounds **2.23d, 2.23e, 2.23f, 2.23h, 2.23i, 2.23m, 2.23n, 2.23s** and **2.23x** were found to display good antiviral activities. These compounds were bioassayed further to investigate their inactivation activities at different concentrations with Ningnanmycin serving as the commercial control. As shown in Table 2.22, the inactivation effects against TMV of compounds **2.23d, 2.23e, 2.23f, 2.23h, 2.23i, 2.23m, 2.23n, 2.23s** and **2.23x** are significant. The EC$_{50}$ values were 55.5, 55.3, 159.0, 62.6, 118.2, 87.9, 167.3, 150.9 and 127.9 μg/mL, respectively. Among these compounds, **2.23d** and **2.23e** had more potent antiviral activities than the others, being similar to that of Ningnanmycin (EC$_{50}$=50.9 μg/mL) against TMV.

Table 2.22   Antiviral activities *in vivo* (%) of compounds **2.23d, 2.23e, 2.23f, 2.23h, 2.23i, 2.23m, 2.23n, 2.23s** and **2.23x**

TMV	Inactivation effect					
Concentration(μg/mL)	500	250	125	62.5	30.7	EC$_{50}$(μg/mL)
2.23d	93.6	70.2	66.9	53.7	37.6	55.5
2.23e	93.7	69.7	60.6	52.5	40.8	55.3

TMV	Inactivation effect					
Concentration(μg/mL)	500	250	125	62.5	30.7	EC_{50}(μg/mL)
2.23f	72.0	50.1	47.9	33.1	20.9	159.0
2.23h	85.1	65.7	51.6	48.5	42.6	62.6
2.23i	75.0	64.1	50.1	39.1	30.7	118.2
2.23m	80.2	62.0	53.8	42.8	27.8	87.9
2.23n	70.5	48.8	44.2	34.4	20.8	167.3
2.23s	71.1	49.0	46.2	35.8	26.9	150.9
2.23x	74.9	58.9	48.9	41.2	29.0	127.9
Ningnamycin	99.0	80.0	70.0	60.1	42.1	50.9
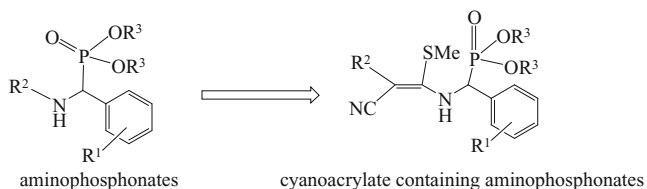
Scheme 2.6   Structural features of aminophosphonates Vs. cyanoacrylate analogues containing aminophosphonates.

2.6.4   Conclusions

In summary, a series of new cyanoacrylate derivatives containing α-amino-phosphonate moities **2.23a-2.23x** were designed and synthesized by refluxing a mixture of alkyl 2-cyano-3,3-dimethylthioacrylate or cyarylamide and α-aminobenzyl phosphonate in ethanol. The *in vivo* tests indicated that compounds **2.23d** and **2.23h** exhibited excellent protection effects against TMV and that the curative activity of compound **2.23d** against TMV is much higher than that of Ningnanmycin, while a very similar inactivation bioactivity level of compounds **2.23d** and **2.23e** and Ningnanmycin against TMV was observed. Therefore, the present work demonstrates that the antiviral activity of cyanoacrylate derivatives was significantly improved via the introduction of the α-aminophosphonates moiety. Effects of steric, hydrophobic, electrostatic and electronic parameters on structure activity relationships and structural modification studies of compounds **2.23d**,**2.23e** and **2.23h** are currently underway.

Compd.	R^1	R^2	R^3	Compd.	R^1	R^2	R^3
2.23a	H	OCH_3	Et	2.23b	H	OCH_3	n-Pr
2.23c	H	OCH_3	i-Pr	2.23d	H	OCH_3	n-Bu
2.23e	2-F	OCH_3	Et	2.23f	H	OC_2H_5	n-Pr
2.23g	H	OC_2H_5	i-Pr	2.23h	H	OC_2H_5	n-Bu
2.23i	2-F	OC_2H_5	Et	2.23j	H	$OC_2H_5OC_2H_5$	Et
2.23k	H	$OC_2H_5OC_2H_5$	n-Pr	2.23l	H	$OC_2H_5OC_2H_5$	i-Pr
2.23m	H	$OC_2H_5OC_2H_5$	n-Bu	2.23n	2-F	$OC_2H_5OC_2H_5$	Et
2.23o	H	NH_2	Et	2.23p	H	NH_2	n-Pr
2.23q	H	NH_2	i-Pr	2.23r	H	NH_2	n-Bu
2.23s	2-F	NH_2	Et	2.23t	H	$PhCH_2NH_2$	Et
2.23u	H	$PhCH_2NH_2$	n-Pr	2.23v	H	$PhCH_2NH_2$	i-Pr
2.23w	H	$PhCH_2NH_2$	n-Bu	2.23x	F	$PhCH_2NH_2$	Et

Scheme 2.7   Synthetic route to cyanoacrylate analogues **2.23** containing α-aminophosphonate

2.7   Crystal Structure elucidation of Cyanoacrylates

2.7.1   Crystal Structure of (E)-Ethyl-3-[(S)-1-phenylethylamino]-3-[4-(trifluoromethyl)-phenylamino]-2-cyanoacrylate

Cyanoacrylates have been found to exhibit a wide range of biological activities. Some derivatives of them are potent inhibitors of photosynthetic

electron transport. A number of studies on the inhibition of photosynthetic electron flow in PS II with a series of acrylate inhibitors have shown that the potency of acrylate in blocking photosynthetic electron flow is extremely sensitive to minor structural variation [20, 28] Among these cyanoacrylates, (Z)-ethoxyethyl 2-cyano-3-(4-chloro-phenyl) methyl-amino-3-isopropyl-acrylate (CPNPE) exhibits the highest Hill inhibitory activity [29]. A large volume of research on their synthesis and biological activities has been reported over the last two decades [1–8]. In order to find new anti-TMV agent, we decided to synthesize (E)-ethyl-3-［(S)-1-phenylethylamino］-3-［4-(trifluoromethyl)-phenylamino］-cyanoacrylate.

The title compound was prepared in the following manner: A mixture of (E)-Ethyl 3-(4-(trifluoromethyl) phenylamino)-2-cyano-3-(methylthio) acrylate (4mmol) and (S)-1-phenylethanamine (4mmol) in 20 mL anhydrous ethanol was added into an oven-dried three-necked 50 mL round-bottom flask. The mixture was irradiated in the microwave oven under reflux at 750W for 25 minutes. The solvent was removed under reduced pressure. The crude product was purified by column chromatography on a silica gel (eluent: ethyl acetate/petroleum ether, 2/8, v/v) to give the title compound **2.24** as a white crystal; mp 135-137℃; yield 50.1%; $[\alpha]_D^{25}$ +251.0(c 0.7970, acetone). IR (KBr): ν_{max} 3258, 3125, 2980, 2195, 1666, 1620, 1595, 1448, 1327, 1284, 1256, 1115, 1067, 845, 702, 550. ^{1}H NMR (400 MHz, CDCl$_3$): δ 1.32 (t, J=6.4 Hz, 3H, CH$_3$-C), 1.44 (d, J=6.4 Hz, 3H, C-CH$_3$), 4.24-4.35 (br, 3H, OCH$_2$＋NCH), 7.15-7.27 (m, 9H, ArH), 9.60 (d, J=6.0 Hz, 1H, C-NH), 10.53 (s, 1H, Ar-NH). m/z (EI-MS): 403 (M$^+$); Anal. Calcd. for C$_{21}$H$_{20}$F$_3$N$_3$O$_2$: C, 62.52; H, 5.00; N, 10.42. Found: C, 62.27; H, 4.99; N, 10.36. Structure is shown as in Fig 2.11.

2.24
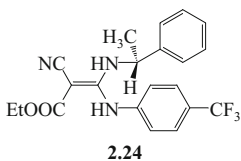
Fig 2.11　The structure of **2.24**

A colorless plate crystal of the title compound having approximate dimensions of 0.40×0.38×0.30 mm was selected for the crystallographic study. The data collection was performed at 293K using graphite mono chromated MoKa radiation (λ=0.71073 Å) and an Enraf-Nonius CAD4 four-circle diffractometer. The structure was solved by direct methods using SHELXS-976 package and refined on F2 using the data (I>2σ (I)) by full-matrix least-square procedures using SHELXL-977 package. Hydrogen atoms were allowed as riding atoms with isotropic displacement parameters related to the non-H atoms on which they were riding. The absorption correction was semi-empirical from equivalents while the maximum and minimum transmission were 0.972 and 0.960, respectively. The results of X-ray structure determination are given in Table 2.22 to Table 2.26. The ORTEP diagram and packing diagram of the unit cell for the title compound are presented in Fig 2.12 and Fig 2.13 respectively.
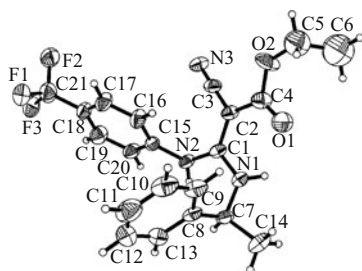
Fig 2.12 ORTEP drawing of the
molecule A at 30% probability
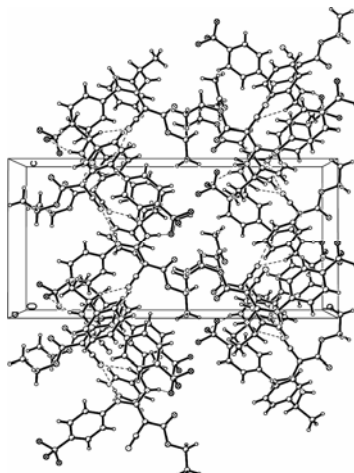
Fig 2.13 Packing diagram of
the unit cell

As shown in the X-ray analysis, there are two same conformations in one asymmetric unit cell. This could be due to the crystal packing resulting from the two different crystal environments in compound **2.24**; molecule A is composed of atoms from C1 to C21, and molecule B is composed of atoms from C22 to C44 (see Table 2.23). It could be seen from the X-Ray single crystal analysis that the chiral compound maintains a planar structure. The configuration of target compound was determined to be an (E) by X-ray diffraction. In molecule A, the bond length of C(1)-C(2) (1.417 Å) is longer than normal C=C(1.34 Å), C(4)-O(2) (1.339 Å) is shorter than normal single C-O (1.44 Å), C(2)-C(4) (1.436 Å) and C(2)-C(3) (1.406 Å) are shorter than normal C-C (1.54 Å), C(1)-N(1) (1.348 Å) and C(1)-N(2) (1.364 Å) bonds are shorter than the normal C-N single bond (1.49 Å), which suggests the existence of an electron density delocalization among N(2)-C(1)-C(2)-C(4)-O(1), C(3) and N(1). The benzene ring [C(8), C(9), C(10), C(11), C(12), C(13)] and the adjacent carbon atom C(7) are fairly planar, and the deviation from the least squares plane through the ring atom is all smaller than 0.0090nm. The equation of the plane is $5.4243x-10.5216y+7.4379z=6.3883$; All atoms in 4-trifluoromethylphenyl group are also quite planar and the largest deviation from the least squares planes is 0.0077 nm. The equation of the plane is $7.4681x+7.8457y+5.1772z=7.1534$. The dihedral angle between the plane of 4-trifluoromethylphenyl group and the plane of the benzene is 51.35°. In molecule B, The dihedral angle between the plane of 4-trifluoromethylphenyl group and the plane of the benzene is 52.70°. In the crystal lattice, intermolecular hydrogen bond among N(1)⋯O(1), N(2)⋯N(6), N(5)⋯N(3) and N(2)⋯O(6) is observed. The range of the distance between donor and acceptor is 2.692-2.952 Å. All the above interactions stabilize the crystal structure.

Table 2.23   Crystallographic Data

Formula:$C_{44} H_{43} F_6 N_6 O_5$

Formula weight:835.84

Crystal color, habit：colorless, plates

Crystal size: $0.40 \times 0.38 \times 0.30$ mm

Crystal system:monoclinic

Space group:P2(1)/c Z=2

A=9.1634(17) Å

B=22.546(4) Å   β=90.848(3)(2)°

C=11.473(2) Å

V=2370.1(7) Å^3

D_{calc}=1.171g/cm^3

F(000)=872

$2\theta_{max}$=50.0°   with $M_oKa(\lambda$=0.71073 Å)

No.of independent reflections=4294 ［R_{int}=0.0385］

No.of observed reflections=2690 ［$I>2\sigma(I)$］

No.of parameters=625

R=0.1222, Rw=0.2660

Goodness of fit=1.023

$(\Delta s)_{max}$=0.000

$(\Delta\rho)_{max}$=0.448 eA^{-3}

$(\Delta\rho)_{min}$=$-$0.342 eA^{-3}

Diffractometer: Enraf- Nonius CAD4

Program system: SAINT

Structure determination: SHELXS-97

Refinement: Full-matrix least-squares (SHELXL-97)

Table 2.24   Atomic coordinates ($\times 10^4$) and equivalent isotropic displacement parameters ($\text{Å} \times 10^3$)

Atom	x	y	z	$U_{eq}{}^a$
F1	1304(11)	5162(7)	5998(13)	93(4)
F2	$-$851(18)	4940(6)	5322(10)	93(4)
F3	$-$670(14)	5544(4)	6709(10)	90(4)
F(4)	6360(30)	1400(8)	550(15)	118(6)
F(5)	8655(13)	1106(8)	1292(16)	92(5)
F(6)	6780(20)	798(5)	1984(14)	101(5)
O1	605(9)	1337(3)	8796(6)	93(2)
O2	$-$724(8)	1440(3)	7151(6)	96(2)

Continued

Atom	x	y	z	$U_{eq}{}^a$
O(3)	6036(8)	5026(3)	3565(5)	81(2)
O(4)	7038(7)	4828(2)	1836(4)	72(2)
N1	524(7)	2256(3)	10291(5)	57(2)
N2	−338(6)	3143(3)	9574(5)	50(1)
N3	−2389(8)	2743(4)	6936(5)	71(2)
N(4)	6345(7)	4171(3)	5209(5)	60(2)
N(5)	7232(6)	3268(3)	4589(5)	54(2)
N(6)	9146(8)	3642(4)	1895(5)	71(2)
C1	−123(7)	2551(3)	9402(5)	47(2)
C2	−610(8)	2239(3)	8396(6)	52(2)
C3	−1574(8)	2516(4)	7601(6)	58(2)
C4	−166(10)	1641(4)	8162(8)	71(2)
C5	−266(17)	875(7)	6758(13)	129(5)
C6	−1130(20)	394(6)	7381(18)	200(9)
C7	1578(8)	2516(4)	11095(6)	56(2)
C8	2850(8)	2784(4)	10457(6)	58(2)
C9	3513(9)	2494(5)	9545(7)	73(2)
C10	4725(10)	2717(6)	8998(8)	88(3)
C11	5243(14)	3253(8)	9351(11)	110(4)
C12	4668(14)	3545(6)	10213(11)	98(3)
C(13)	3430(13)	3324(4)	10778(8)	84(3)
C(14)	2102(11)	2036(5)	11935(7)	83(3)
C(15)	−281(8)	3604(3)	8749(6)	49(2)
C(16)	516(9)	3549(4)	7720(7)	64(2)
C(17)	538(10)	4006(4)	6951(7)	72(2)
C(18)	−156(10)	4530(4)	7178(7)	66(2)
C(19)	−915(11)	4588(4)	8196(8)	76(2)
C(20)	−989(10)	4128(4)	8982(7)	65(2)
C(21)	−85(9)	5022(4)	6312(7)	89(3)
C(22)	6965(7)	3851(3)	4360(6)	50(2)
C(23)	7328(8)	4129(3)	3297(6)	55(2)
C(24)	8322(8)	3854(4)	2536(6)	55(2)
C(25)	6724(9)	4693(4)	2943(6)	58(2)
C(26)	6443(13)	5389(6)	1421(8)	97(3)
C(27)	6717(19)	5434(7)	135(9)	101(6)
C(28)	5314(8)	3922(4)	6034(6)	59(2)

Atom	x	y	z	$U_{eq}{}^{a}$
C(29)	3998(8)	3658(3)	5420(6)	55(2)
C(30)	3450(10)	3116(5)	5722(7)	71(2)
C(31)	2231(12)	2871(5)	5163(9)	85(3)
C(32)	1558(10)	3176(5)	4286(8)	81(3)
C(33)	2076(9)	3716(5)	3944(7)	74(2)
C(34)	3310(9)	3950(4)	4518(7)	67(2)
C(35)	4860(11)	4427(6)	6852(8)	92(3)
C(36)	7237(8)	2796(3)	3794(6)	52(2)
C(37)	6366(9)	2786(4)	2795(7)	64(2)
C(38)	6384(10)	2316(4)	2056(8)	76(3)
C(39)	7247(10)	1835(4)	2289(7)	71(2)
C(40)	8089(10)	1816(4)	3328(7)	71(2)
C(41)	8044(8)	2291(3)	4057(6)	57(2)
C(42)	7265(10)	1305(4)	1493(7)	96(3)
O(5)	6680(30)	6615(8)	3440(20)	139(8)
C(43)	6160(30)	6327(10)	5260(30)	130(11)
C(44)	5880(20)	6465(8)	4070(20)	76(6)

^{a} U_{eq} is defined as one-third of the trace of the orthogonalized U_{ij} tensor.

Table 2.25　Selected bond distances (Å) and angles (°)

C1-C2	1.417(10)	O2-C4	1.339(11)	C1-N1-C7	124.3(6)
C2-C3	1.406(11)	O1-C4	1.218(11)	C1-N2-C15	128.2(5)
N2-C1	1.364(9)	O2-C5	1.417(17)	N1-C1-N2	115.8(6)
N1-C1	1.348(8)	N1-C7	1.449(9)	N1-C1-C2	120.1(6)
N3-C3	1.178(10)	N2-C15	1.407(9)	N2-C1-C2	123.9(6)
C2-C4	1.436(12)	N1-C7-C14	108.4(7)	C3-C2-C4	118.1(7)
O2-C4-C2	112.0(8)	C16-C15-N2	121.7(6)	O1-C4-O2	122.5(9)

Table 2.26　Selected bond distances (Å) and angles (°) of the H-bonds

D-H⋯A^{a}	d(D-H)	d(H⋯A)	d(D⋯A)	∠(DHA)
N(5)-H(5)⋯N(3)	0.86($x+1, y, z$)	2.12	2.956(9)	164.6
N(4)-H(4)⋯O(3)	0.86	2.29	2.710(9)	110.4
N(2)-H(2)⋯N(6)	0.86($x-1, y, z+1$)	2.08	2.935(9)	170.2
N(1)-H(1)⋯O(1)	0.86	2.23	2.692(9)	113.4

^{a} D=donor atom; A=acceptor atom.

2.7.2 Characterization of Two Chiral Isomers of (*E*)-Ethyl-3-[(*R*) or (*S*)-1-phenylethyl amino]-3-[4-nitrophenylamino]-2-cyano-acrylate

Cyanoacrylate derivatives have received considerable attention in pesticidal and medicinal chemistry. Various related compounds have herbicidal activities [29]and antitumor activities.[5] Hence, in search for new anticancer drug, we envisioned that the judicious replacement of methylthio moiety by (*R*) or (*S*) phenylethanamino group in (*E*)-ethyl-3-[4-nitro phenylamino]-2-cyanoacrylate might lead to significant change in the bioactivity. Therefore, in this work, we report the structures of two optical isomers of (*E*)-Ethyl-3-(1-phenylethylamino)-3-[4 nitrophenylamino]-2-cyanoacrylate, (*R*)-**2.25** and (*S*)-**2.25** (Fig 2.14, Fig 2.15).

(*S*)-**2.25**   (*R*)-**2.25**

(*R*)-**2.25**   (*S*)-**2.25**
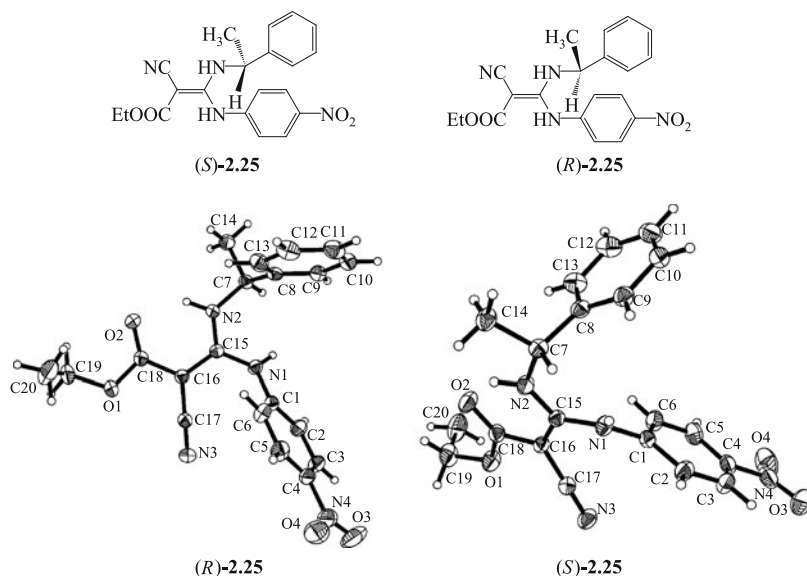
Fig 2.14   ORTEP drawing of the title compound with the atom labeling scheme and 30% probability ellipsoids

The title optical compound was prepared in the following manner: A mixture of (*E*)-Ethyl 3-(4-nitrophenylamino)-2-cyano-3-(methylthio) acrylate (4mmol) and (*R*) or (*S*)-1-phenyl-ethanamine (4mmol) in 20 mL anhydrous ethanol was added into an oven-dried three-necked 50 mL round-bottom flask. The mixture was irradiated in the microwave oven under reflux at 750W for 25 minutes. The solvent was removed under reduced pressure. The crude product was purified by column chromatography on a silica gel (eluent: ethyl acetate/petroleum ether, 2/8, *v/v*) to give the title optical compounds. (*E*)-Ethyl 3-((*R*)-1-phenylethyl- amino)-
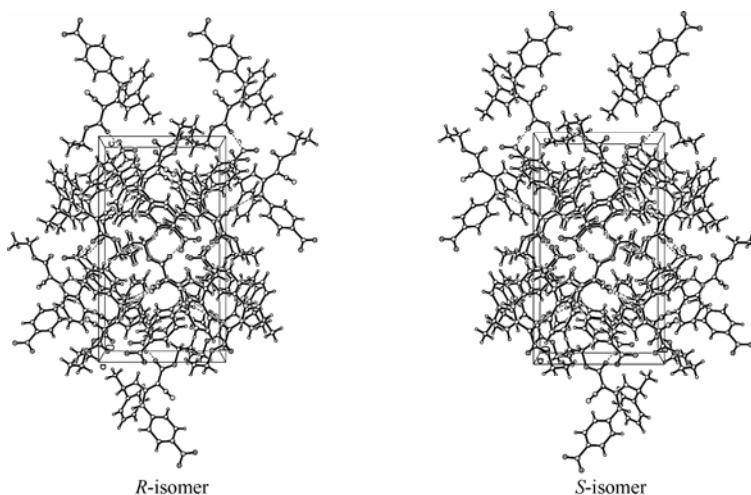
Fig 2.15   Crystals of (*R*)/(*S*)-isomer

3-(4-nitrophenylamino)-2-cyano-acrylate[（*R*）-**2.25**]; white crystal;mp 201-203℃; yield 65.6%; $[\alpha]_D^{25}$ -297.4(*c* 0.7616, acetone). IR(KBr): ν_{max} 3233, 2980, 2193, 1670, 1601, 1518, 1340, 1302, 1283, 1258, 1090, 853, 764, 700, 554.^{1}H NMR (400 MHz, CDCl3): δ 1.20 (t, *J*=6.8 Hz, 3H, CH3-C), 1.49 (d, *J*=6.4 Hz, 3H, C-CH3), 4.09-4.22 (m, 2H, OCH2), 4.87 (t, *J*=7.2 Hz, 1H, NCH), 7.20-8.14 (m, 9H, ArH), 9.44 (d, *J*=6.8 Hz,1H, C-NH), 9.75 (s, 1H, Ar-NH). *m/z* (EI-MS): 380 (M[+]); Anal. Calcd. for C20H20N4O4: C, 63.15; H, 5.30; N, 14.73. Found:C, 63.05; H, 5.25; N, 14.66.

Crystals of (*S*)-isomer were obtained as blocks by recrystallization from ethanol.

(*E*)-Ethyl 3-((*S*)-1-phenylethylamino)-3-(4-nitrophenylamino)-2-cyanoacrylate [(*S*)-**2.25**]; white crystal; mp 203-205℃; yield 71.2%; $[\alpha]_D^{25}$ +283.3(*c* 1.0140, acetone). IR (KBr)：ν_{max}3235, 3219, 2980, 2194, 1670, 1601, 1551, 1518, 1497, 1443, 1387, 1340, 1302, 1281, 1257, 1113, 1090, 853, 764, 748, 700, 553. ^{1}H NMR (400 MHz, CDCl3): δ1.20 (t, *J*=6.8 Hz, 3H, CH3-C), 1.49-1.50 (d, *J*=6.8 Hz, 3H, C-CH3), 4.09-4.22 (m, 2H, O-CH2), 4.89 (t, *J*=7.2 Hz, 1H, N-CH), 7.20-8.14 (m, 9H, ArH), 9.44 (d, *J*=6.8Hz, 1H, C-NH), 9.75 (s, 1H, Ar-NH). *m/z* (EI-MS): 380 (M[+]); Anal. Calcd. for C20H20N4O4: C, 63.15; H, 5.30; N, 14.73. Found: C, 63.15; H, 5.00; N, 14.70.

Crystal data of （*R*）**-2.25**

C20H20N4O4 Orthorhombic	MoKa radiation
Mr=380.40	Cell parameters from 11057
A=9.5478(16)	θ=2.18-26.42°
B=10.7380(17)	μ=0.093mm^{-1}
C=18.951(3)	*T*=294(2)K

V=1942.9(6)

Z=4

D_x=1.300 Mg/m^3

Data collection

Bruker SMART 1000

Diffractometer

Absorption correction: multi-scan

　[*SAINT* (Bruker,1998) and

SADABS (Sheldrick,1997)]

T_{min}=0.970, T_{max}=0.982

Refinement

Refinement on F^2

R [F^2>2$s(F^2)$] =0.0320

wR(F^2)=0.0672

s=1.067

3578 reflections

264 parameters

H-atom parameters constrained

Crystal data of **(S)-2.25**

C$_{20}$H$_{20}$N$_4$O$_4$ Orthorhombic

Mr=380.40

A=9.5340(13)

B=10.7380(14)

C=18.953(3)

V=1940.4(4)

Z=4

D_x=1.302 Mg/m^3

Data collection

Bruker SMART 1000

Diffractometer

Absorption correction: multi-scan

　[*SAINT* (Bruker,1998) and

SADABS (Sheldrick,1997)]

T_{min}=0.970, T_{max}=0.982

Refinement

Refinement on F^2

R [F^2>2$s(F^2)$] =0.0315

wR(F^2)=0.0674

Prism, colorless

0.30×0.24×0.20 mm

2277 independent reflections

3578 reflections with I>2σ(I)

θ_{max}=25.0°

h=－11→9

k=－8→13

L=－23→23

W=1/ [s^2 (F$_O^2$)+(0.0264P)^2+0.3494P]

where P=(F$_O^2$ +2 F$_e^2$)/3

$(\Delta s)_{max}$<0.0275

$(\Delta\rho)_{max}$=0.0275 eA^{-3}

$(\Delta\rho)_{min}$= －0.127 eA^{-3}

MoKα radiation

Cell parameters from 11057

θ=2.15-26.42 °

μ=0.093mm^{-1}

T=294(2)K

Prism, colorless

0.28×0.24×0.20 mm

2277 independent reflections

2270 reflections with I>2σ(I)

θ_{max}=25.0°

h=－11→11

k=－13→12

L=－16→23

W=1/ [s^2 (Fo^2) +(0.0252P)^2+0.3417P]

where P=(Fo^2+2Fc^2)/3

S=1.072　　　　　　　　　　　　　$(\Delta/s)_{max}$< 0.041

2270 reflections　　　　　　　　　　$(\Delta\rho)_{max}$=0.116 eA^{-3}

264 parameters　　　　　　　　　　$(\Delta\rho)_{min}$ =−0.120 eA^{-3}

H-atom parameters constrained

Table 2.27　Bond distances (Å) and angles (°)

（R）-2.25		（S）-2.25	
C(15)-C(16)	1.414(3)	C(15)-C(16)	1.415(3)
C(16)-C(17)	1.415(3)	C(16)-C(17)	1.413(3)
C(16)-C(18)	1.438(3)	C(16)-C(18)	1.443(3)
C(19)-C(20)	1.469(4)	C(19)-C(20)	1.466(4)
O(1)-C(18)	1.350(3)	O(1)-C(18)	1.351(2)
O(1)-C(19)	1.452(3)	O(1)-C(19)	1.457(3)
O(2)-C(18)	1.220(3)	O(2)-C(18)	1.214(2)
O(3)-N(4)	1.222(4)	O(3)-N(4)	1.217(3)
N(4)-C(4)	1.470(3)	N(4)-C(4)	1.475(3)
N(3)-C(17)	1.150(3)	N(3)-C(17)	1.147(3)
N(2)-C(7)	1.474(3)	N(2)-C(7)	1.472(3)
N(2)-C(15)	1.332(3)	N(2)-C(15)	1.328(3)
N(1)-C(1)	1.409(3)	N(1)-C(1)	1.407(3)
N(1)-C(15)	1.361(3)	N(1)-C(15)	1.365(3)
O(4)-N(4)	1.222(4)	O(4)-N(4)	1.221(3)
N(2)-C(15)-N(1)	117.1(2)	N(2)-C(15)-N(1)	117.32(19)
N(2)-C(15)-C(16)	120.94(19)	N(2)-C(15)-C(16)	121.08(17)
N(1)-C(15)-C(16)	121.9(2)	N(1)-C(15)-C(16)	121.54(19)
C(15)-C(16)-C(17)	119.6(2)	C(17)-C(16)-C(15)	119.86(18)
C(15)-C(16)-C(18)	121.7(2)	C(15)-C(16)-C(18)	121.29(18)
C(17)-C(16)-C(18)	118.1(2)	C(17)-C(16)-C(18)	118.32(19)
N(3)-C(17)-C(16)	179.7(3)	N(3)-C(17)-C(16)	179.6(2)
O(2)-C(18)-O(1)	122.1(2)	O(2)-C(18)-O(1)	122.5(2)
O(2)-C(18)-C(16)	125.6(2)	O(2)-C(18)-C(16)	125.66(19)
O(1)-C(18)-C(16)	112.3(2)	O(1)-C(18)-C(16)	111.89(18)
O(1)-C(19)-C(20)	111.2(2)	O(1)-C(19)-C(20)	110.9(2)
N(2)-C(7)-C(14)	107.67(18)	N(2)-C(7)-C(14)	107.81(17)
C(8)-C(7)-C(14)	110.9(2)	C(8)-C(7)-C(14)	110.67(19)
C(15)-N(2)-C(7)	126.33(19)	C(15)-N(2)-C(7)	126.21(17)

Table 2.28　Hydrogen-bonding geometry (Å, °) of （R）**-2.25**

D-H…A	D-H	H…A	D-A	D-H…A
N(1)-H(1)…N(3)#1	0.89(3)	2.15(3)	3.017(3)	163(2)
N(2)-H(2)…O(2)	0.91(2)	1.95(2)	2.685(2)	137(2)

Symmetry codes:#1　$[-x, y+1/2, -z+1/2]$,(ii) $[x, -y+3/2, z+1/2]$

Table 2.29　Hydrogen-bonding geometry (Å, °) of （S）**-2.25**

D-H…A	D-H	H…A	D-A	D-H…A
N（1)-H（1)…N（3）#1	0.89（2）	2.16（2）	3.013（3）	162（2）
N（2)-H（2)…O（2）	0.92（2）	1.95（2）	2.680（2）	135（2）

Symmetry codes：#1　$[-x+1, y-1/2, -z+3/2]$.

It could be seen from the X-Ray single crystal analysis that both the chiral compounds （R）**-2.25** and （S）**-2.25** maintain a planar structure (Table 2.27, Table 2.28). The configuration of target compound (R)**-2.25** or (S)**-2.25** was determined to be an （E） by X-ray diffraction. The bond length of C（15)-C（16）(1.414, 1.415 Å) is longer than normal C=C（1.34 Å）, C（19)-O（1）(1.452 Å) is longer than normal single C-O（1.44 Å）, C（18)-C（16）(1.438 Å) and C (16)-C(17) (1.415 Å) are shorter than normal C-C（1.54 Å）, C（15)-N(2) (1.332 Å) and C（15)-N（1）(1.361 Å) bonds are shorter than the normal C-N single bond (1.49 Å), which suggests the existence of an electron density delocalization among N (1)-C (15)-C (16)-C (18)-O（2）, C (17) and N (2). From the view of Fig 2.15 and Table 2.29, it is clear that the two neighboring molecules are linked by hydrogen bonds, in the form of N (1)-H (1)…N (3) #1 and N (2)-H (2)…O (2) for I-*R*. The donor and acceptor distance is N（2)-O（2)2.685（2）Å and the bond angle is 137 (2)°. The crystal packing is stabilized by these extensive hydrogen bonds. In the *R*-isomer, the benzene ring [C (8), C (9), C (10), C (11), C (12), C (13)] and the adjacent carbon atom C (7) are fairly planar, and the deviation from the least squares plane through the ring atom is all smaller than 0.0038nm. The equation of the plane is $5.4053x+7.5783y+8.0719z =10.5745$; All atoms in 4-nitrophenyl group are also fairly planar and the largest deviation from the least squares plane is 0.0115 nm. The equation of the plane is $6.6297x+ 4.5319 y-11.0457z =1.1292$. The dihedral angle between the plane of 4-nitrophenyl group and the plane of the benzene is 63.72°, whereas in *S*-isomer, the corresponding dihedral angle appears to be 63.60°.

References

1.　Mackay S P, Omalley P J Z. Molecular modelling of the interaction between DCMU and the Q(B)-binding site of photosystem-II. *Z. Naturforsch*. 1993, 48c, 191-198.

2.　Huppatz J L, Phillips J N, Rattigan B M. Cyanoacrylates. Herbicidal and photosynthetic inhibitory

activity. *Agric. Biol. Chem*. 1981, 45(12), 2769-2773.

3.　Wang Q M, Li H, Li Y H, *et al*. Synthesis and herbicidal activity of 2-cyano-3- (2-chlorothiazol-5-yl) methylaminoacrylates. *J. Agric. Food. Chem*. 2004, 52, 1918-1922.

4.　Wang L G, Wang F Y, Diao Y M, *et al*. Synthesis and fungicidal activity of ethyl 2-cyano-3-substituted-amino-3-(2-methylphenyl)propenoate. *Chin. J. Org. Chem*. 2005, 25, 1254-1258.

5.　Song B A, Yang S, Zhong H M, *et al*. Synthesis and bioactivity of 2-cyanoacrylates containing a trifluoromethylphenyl moiety. *J. Fluorine Chem*. 2005, 126, 87-92.

6.　Zhang H P, Song B A, Zhong H M, *et al*. Synthesis of 2-cyanoacrylates containing pyridinyl moiety under ultrasound irradiation. *J. Heterocyclic Chem*. 2005, 42, 1211-1214.

7.　Song B A, Zhang H P, Wang H, *et al*. Synthesis and antiviral activity of novel chiral cyanoacrylate derivatives. *J. Agric. Food Chem*. 2005, 53, 7886-7891.

8.　Boehner B, Hall R G. Preparation of pyrazolylphosphonate pestcides. *DE* 4139849, 1992.

9.　Cross H, Koeckritz A, Scheidecker S, *et al. DE* 4108345, 1992.

10.　Fouque D, About-Jaudet E, Collignon N. Alpha-pyrazolyl-alkylphosphonates. Part II: a simple and efficient synthesis of diethyl-1-(pyrazol-4-yl)-alkyl phosphonates. *Synth. Commun*. 1995, 25, 3443-3455.

11.　Huang W S, Yuan C Y. Studies on organophosphorus compounds 92: a facile synthesis of 1-substituted-5-trifluoromethylimidazole-4-phosphonates. *Synthesis*. 1996, 4, 511-513.

12.　a)Lu R J, Yang H Z. A novel approach to phosphonyl-substituted heterocyclic system (I). *Tetrahedron Lett*. 1997, 8, 5201-5204; b)Chen K, Hu F Z, Zhang J H, *et al*. Progress in the synthetic methods of phosphonyl heterocyclic compouds. *Chin. J. Org. Chem*. 2000, 20, 866-873.

13.　Chen K, Yang H Z, Liu Z, *et al*. Synthesis of novel phosphonyl/ *S*-methyl ketene thioacetals and *N*-substituted phosphonyl/*S*-methyl thiocarbonates under microwave irradiation. *Chin. J. Org. Chem*. 2001, 21, 690-692.

14.　McCombie H, Sauders B C, Stacey G J. Esters containing phosphorus Part I. *J. Chem. Soc*. 1945, 380-382.

15.　Liu H Y, Sha Y L, Dai G X. *et al*. Synthesis of novel derivatives of 2-cyano-3-methylthio-3'-benzylamino-acrylates (acryl, amides) and their biological activity. *Phosphorus*, *Sulfur Silicon.* 1999, 148, 235-241.

16.　Erwin D C, Sims J J, Borum D E, *et al*. Detection of the systemic fungicide, thiabendazole, in cotton plants and soil by chemical analysis and bioassay. *Phytopathology*. 1971, 61, 964-967.

17.　Yang S, Gao X W, Diao C L, *et al*. Synthesis and antifungal activity of novel chiral *α*-amino-phosphonates containing fluorine moiety. *Chin. J. Chem*. 2006, 24, 1581-1588.

18.　Gooding G V Jr, Hebert T T. A simple technique for purification of tobacco mosaic virus in large quantities. *Phytopathology.* 1967, 57, 1285-1290.

19.　McFadden H G, Craig D C, Huppatz J L, *et al*. X-Ray Structure analysis of a cyanoacrylate inhibitor of photosystem II electron transport. *Z. Naturforsch*. 1991, 46C, 93-98.

20.　Wang Q M, Sun H K, Cao H Y, *et al*. Synthesis and herbicidal activity of 2-cyano-3-substituted-pyridinemethylaminoacrylates. *J. Agri. Food Chem*. 2003, 17, 5030-5035.

21.　Sun H K, Wang Q M, Huang R Q, *et al*. Synthesis and biological activity of novel cyanoacrylates containing ferrocenyl moiety. *J. Organometallic Chem*. 2002, 655, 182-185.

22.　Jablonkai I. Alkylating reactivity and herbicidal activity of chloroacetamides. *Pest Manag. Sci*. 2003, 59, 443-450.

23.　a)Nizamuddin M G, Manoj K S. Synthesis and fungicidal activity of substituted pyrazolo[5,4-*b*] pyridine/pyrid-6-ones and pyrazolo[5,4-d]thiazines. *Bull. Chim. Farm*, 2001, 140(5), 311-315; b)Wang Q M, Sun H K, Huang R Q, *et al*. Synthesis and herbicidal activity of (*Z*)-ethoxyethyl 2-cyano-3-(2-methylthio-5-pyridylmethylamino) acrylates. *Heteroatom Chem*. 2004, 15(1), 67-70.

24.　Kuzmin V E, Lozitsky V P, Kamalov G L, *et al*. Analysis of the structure - anticancer activity relationship in a set of Schiff bases of macrocyclic 2, 6-bis(2- and 4-formylaryloxymethyl)pyridines. *Acta. Biochimica Polonica*. 2000, 47(3), 867-875.

25. Liu H Y, Lu R J, Chen K, *et al*. Studies on bio-rational design of photosystem Ⅱ Inhibitors(Ⅶ) synthesis and hill inhibitory activity of ethyl 2-cyano-3-methylthio-3-arylaminoacrylates. *Chem. J. Chin. Univ.* 1999, 20(3), 711-714.

26. Denizot F, Long R. *J*. Rapid colorimetric assay for cell growth and survival. *Immunol Methods*. 1986, 89(2), 271-277.

27. Skehan P, Storeng R, Scadiero D, *et al*. New colorimetric cytotoxicity assay for anticancer-drug screening. *J. Natl. Cancer Inst*. 1990, 82, 1107-1112.

28. Huppatz J L, Philips J N. Cyanoacrylate inhibitors of the hill reactions. Ⅳ. Binding characteristics of the hydrophobic domain. *Z. Naturforsch.* 1987, 42*c*, 679-683.

29. a) Huppatz J L. Quantifying the inhibitor-target site interactions of photosystem II herbicides. *Weed Sci*. 1996, (44), 743-748; b)Phillips J N, Banham W K. Hydrogen Bonding of Cyanoacrylates with the D1 peptide. *Z. Naturforsch*. 1993, 48*c*, 132-135; c)Yu S. Y, Li Z M. Synthesis and biological activities of 2-cyano-3-6-chloro-3-pyridylmethyl)amino-3-aliphatic amine acrylonitrile. *Chin. J. Pestic. Sci*. 2001, 3 (3), 18; d)Yu, S. Y. ; Li, Z. M. Synthesis of 2-cyano-3-[(6-chloro)-3-pyridylmethyl]-3-aliphatic amine ethyl acrylate. *Chin. J. Pestic. Sci*. 2002, 4(3), 79; e)Zhao Y G, Hung R Q, Cheng J R. Synthesis and biological activity of biscyano substituted acyclic ketene amines containing 2-chloro-5-pyridylmethyl group. *Chem. J. Chin. Univ*. 1998, 19(10), 1620.

30. Liu H Y, Yang G F, Lu R J, *et al*. The crystalline and molecular structure of ethyl 3-benzylamino-2-cyano-3-methylthioacrylate. *Chem. J. Chin. Univ*. 1998, 19, 899.

31. a)Bose A K, Manhas M S, Ganguly S N, *et al*. More chemistry for less pollution: Applications for process development. *Synthesis*. 2002, 11, 1578-1591; b)Varma R S. Solvent-free organic synthesis. *Green Chemistry*. 1999, 1, 43-55.

32. Jin L H, Zhong H M, Song B A, *et al*. Advance in the synthesis and biological activity of 2-cyanoacrylate. *Chin. J. Synth. Chem*. 2005, 13(2), 113-117.

33. Yang S, Jin L H, Song B A, *et al*. The preparation method and bioactivity of cyanoacrylate derivatives. CN 1603307A, 2004.

34. Charles W H, Matthew E M, Isiah M W. Separation of the insecticidal pyrethrin ester by capillary electrochromatography. *J Chromatography A*. 2001, 905, 319-327.

35. Hayes B L. Recent advances in microwave-assisted synthesis. *Aldrichimica Acta*. 2004, 37, 66-77.

36. Liu X, Huang R Q, Cheng M R, *et al*. Synthesis and bioactivity of S, N-ketene acetal containing pyridine methylene. *Chem. J. Chin. Univ*. 1999, 20, 1404-1408.

37. Grozinger K. Synthesis of 3-amino-2-chloro-4-methylpyridine from acetone and ethyl cyanoacetate. US 6136982, 2000; *Chem. Abstr*. 2000, 133, 120236.

38. Sheldrick G M. Program for empirical absorption correction of area detector data. University of Gottingen, Germany, 1996.

39. Sheldrick G M. SHELXTL V5. 1, Software reference manual, Bruker AXS, Inc., Madison, Wisconsin, USA, 1997.

40. Wilson A. J. International table for X-ray crystallography, vol. C, Kluwer Academic Publishers, Dordrecht, Tables 6. 1. 1. 4（pp. 500-502）and 4. 2. 6. 8（pp. 219-222）respectively, 1992.

41. Li S Z, Wang D M, Jiao S M. Pesticide experiment methods-fungicide sector. Agricuture Press of China, Beijing, 1991, 93-94.

42. Ouyang G P, Song B A, hang H P, *et al*. Synthesis and antiviral activity of novel chiral cyanoacrylate derivatives. *Molecules*. 2005, 10, 1351-1357.

43. Hari V, Das P. in *plant disease virus control*; Hadidi A, Khetarpal R K, Koganezawa H., Ed.; APS Press: St. Paul, 1998, 417-427.

44. Shadle G L, Wesley S V, Korth K L, *et al*. Phenylpropanoid compounds and disease resistance in transgenic tobacco with altered expression of L-phenylalanine ammonia-lyase. *Phytochemistry*, 2003, 64, 153-161.

45. He Z P. in *A guide to experiments of chemical control for crops*; He Z P., Ed.; Beijing Agricultural University Press: Beijing, 1933, 30-31.

46. Polle A, Otter T, Seifert F. Apoplastic peroxidases and lignification in needles of Norway Spruce (Picea abies L.). *Plant Physiol*. 1994, 106, 53-60.

47. Beauchamp C, Fridovich J. Superoxide dismutase. Improved assay and an assay applicable to acrylamide gels. *Anal*. *Biochem*. 1971, 444, 276-278.

48. Yamakawa H, Kamada H, Satoh M, *et al*. Spermine is a salicylate-independent endogenous inducer for both tobacco acidic pathogenesis-related proteins and resistance. *Plant Physiol*. 1998, 118, 1213.

49. Anand A, Zhou T, Trick H N, *et al*. Greenhouse and field testing of transgenic wheat plants stable expressing genes for thaumati-like protein, chitinase and glucanase against *Fusarium graminearum*. *J*. *Exp*. *Bot*. 2003, 54, 1101-1111.

50. Mohamed F, Lydia F, Masumi I. *et al*. Expression of potential defense responses of Asian and European pears to infection with *Venturia nashicola*. *Physiol*. *Mol*. *Plant Path*. 2004, 64(6), 319.

51. Yuan J S, Reed A, Chen F, *et al*. Statistical analysis of real-time PCR data. *BMC*. *Bioinform*. 2006, 7, 85.

52. Milosevic N, Slusarenko A J. Active oxygen metabolism and lignification in the hypersensitive response in bean. *Physiol Plant Pathol*. 1996, 49, 143-158.

53. Wang Y C, Hu D W, Zhang Z G, *et al*. Purification and immunocytolocalization of a novel *Phytophthora boehmeriae* protein inducing the hypersensitive response and systemic acquired resistance in tobacco and Chinese cabbage. *Physiol*. *Mol*. *Plant Path*. 2003, 63, 223-232.

54. Sticher L, Mauch-Mani B, Metraux J P. Systemic acquired resistance. *Annu Rev Phytopathol*. 1997, 35, 235-270.

55. Malamy J, Carr J P, Klessigm D, *et al*. Salilcylic acid-a likely endogenous singnal in the resistance responses of tobacco to viral infection. *Science*. 1990, 250, 1002-1004.

56. Hahlbrock K, Scheel D. Physiology and molecular biology of phenylpropanoid metabolism. *Ann*. *Rev*. *Plant*. *Physiol*. *Plant*. *Mol*. *Biol*. 1989, 40, 347-369.

57. Rusmussen J B, Hammersschmidt R, Zook M N. Systemic induction of salicylic acid accumulation in cucumber after inoculation with Pseudomonas syringae pv. Syringae. *Plant Physiol*. 1991, 97, 1342.

58. Van Loon L C. Pathogenesis-related proteins. *Plant Mol*. *Biol*. 1985, 4, 111-116.

59. Tornero P, Gadea J, Conejero V, *et al*. Two *PR1* genes from tomato are differentially regulated and reveal a novel mode of expression for a pathogenesis-related gene during the hypersensitive response and development. *Mol*. *Plant-Microbe Interact*. 1997, 10, 624-634.

60. Cheong N E, Choi Y O, Kim W Y, *et al*. Purification of an antifungal PR-5 protein from flower buds of brassica campestris and cloning of Its Gene. *Physiol Mol*. *Plant Pathol*, 1997, 101, 583-590.

61. Huang W, Yang G F. Microwave-assisted, one-pot syntheses and fungicidal activity of polyfluorinated 2-benzylthiobenzothiazo. *Bioorg*. *Med*. *Chem*. 2006, 14, 8280-8285.

62. Zhou Z Z, Yang G F. Insecticidal lead identification by screening benzopyrano[3, 4-c]pyrazol-3-one library constructed from multiple-parallel synthesis under microwave irradiation. *Bioorg*. *Med*. *Chem*. 2006, 14, 8666-8674

63. a)Liu Y, Li H, Zhao Q, *et al*. Synthesis and herbicidal activity of 2-cyano- 3-(2-fluoro-5-pyridyl) methylaminoacrylates. *J*. *Fluorine Chem*. 2005, 126, 345-348; b)Liu Y, Cai B, Li Y, Song H, *et al*. Synthesis, crystal structure, and biological activities of 2-cyanoacrylates containing furan or tetrahydrofuran moieties. *J*. *Agric*. *Food Chem*. 2007, 55, 3011-3017; c)Yang G F, Liu Z M, Liu J C, *et al*. Synthesis and properties of novel α-(1, 2, 4-triazolo-[1,5-a]pyrimidine-2-oxyl)phosphonate derivatives. *Heteroatom Chem*. 2000, 11, 313-316.

64. Liu Y X, Wei D G, Zhu Y R, *et al*. Synthesis, herbicidal activities, and 3D-QSAR of 2-cyanoacrylates containing aromatic methylamine moieties. *J*. *Agric*. *Food Chem*. 2008, 56, 204-212.

65. McFadden H G, Phillips J N. Synthesisanduseofradiolabeled cyanoacrylate probes of photosystem II herbicide binding site. *Z*. *Naturforsch*. 1990, 45*C*, 196-202.

66. Lv Y P, Wang X Y, Song B A, *et al*. Synthesis, antiviral and antifungal bioactivity of 2-cyanoacrylate

derivatives containing phosphonyl moieties. *Molecules*. 2007, 12, 965-978.

67. Chen Z, Wang X Y, Song B A, *et al*. Synthesis and antiviral activities of novel chiral cyanoacrylate derivatives with (*E*) configuration. *Bioorg*. *Med*. *Chem*. 2008, 16, 3076-3083.

68. Gioia P l, Chuah P H, Sclapari T. Herbicidal composition comprising an aminophosphate or aminophosphonate salt. WO 2007054540, 2007.

69. Kafarski P, Lejczak B. Biological activity of aminophosphonic acids. *Phosphorus Sulfur*. 1991, 63, 193-215.

70. Jin L H, Song B A, Zhang G P, *et al*. Synthesis, X-ray crystallographic analysis, and antitumor activity of *N*-(benzothiazole-2-yl)-1-(fluorophenyl)-*O* ,*O*-dialkyl - α-amino phosphonates. *Bioorg*. *Med*. *Chem*. *Lett*. 2006, 16, 1537-1543.

71. Kafarski P, Lejczak B. Aminophosphonic acids of potential medical importance. *Curr*. *Med*. *Chem*. *Anti-Cancer Agents* 2001, 1, 301-312.

72. Lintunen T, Yli-Kauhaluoma J T. Synthesis of aminophosphonate haptens for an aminoacylation reaction between methyl glucoside and a-alanyl ester. *Bioorg*. *Med*. *Chem*. *Lett*. 2000, 10, 1749-1750.

73. Liu W, Rogers C J, Fisher A J, *et al*. Aminophosphonate inhibitors of dialkylglycine decarboxylase: Structural basis for slow, tight binding inhibition. *Biochem*. 2002, 41, 12320-12328.

74. Pan W D, Ansiaux C, Vincent S P. Synthesis of acyclic galactitol- and lyxitol- aminophosphonates as inhibitors of UDP-galactopyranose mutase. *Tetrahedron Letters*. 2007, 48, 4353-4356.

75. Deng S L, Baglin I, Nour M, *et al*. Synthesis of ursolic phosphonate derivatives as potential anti-HIV agents. *Phosphorus*, *Sulfur and Silicon and the Related Elements*. 2007, 182, 951-967.

76. Zhang G P, Song B A, Xue W, *et al*. Synthesis and biological activities of novel dialkyl 1-(4-trifluoromethyl-phenylamino)- 1-(4-trifluoromethyl or 3-fluorophenyl) methylphosphonate. *J*. *Fluorine Chem*. 2006, 127, 48-53.

77. Xu Y S, Yan K, Song B A, *et al*. Synthesis and antiviral bioactivities of α-aminophosphonates containing alkoxyethyl moieties. *Molecules*. 2006, 11, 666-676.

78. Song B A, Wu Y L, Huang R M. Synthesis of plant virucidal fluorine containing α-aminophosphonates. *CN* 1432573, 2003; Patent approval certificate. No. ZL02113252. 6; *Chem*. *Abstr*. 2005, 142, 482148.

79. Song B A, Zhang G P, Hu D Y, *et al*. N-substituted benzothiazolyl-1-substituted phenyl-*O*, *O*-dialkyl-alpha-amino phosphonate ester derivatives preparation and application. *CN* 1687088, 2005; Patent approval certificate. No. ZL0200510003041. 7; *Chem*. *Abstr*. 2006, 145, 145879.

80. Li C H, Song B A, Yan K, *et al*. One Pot Synthesis of α-aminophosphonates containing bromo and 3,4,5-trimethoxybenzyl groups under solvent-free conditions. *Molecules*. 2007, 12, 163-172.

81. Hu D Y, Wan Q Q, Yang S, *et al*. Synthesis and antiviral activities of amide derivatives containing α-aminophosphonate moiety. *J*. *Agric Food Chem*. 2008, 56(3), 998-1001.

82. Huang R Q, Wang H, Zhou J. Preparation of organic intermediate; Chemical industry press of China, Beijing, China, 2001, 224-225.

83. Kaboudin B, Moradi K. A simple and convenient procedure for the synthesis of 1-aminophosphonates from aromatic aldehydes. *Tetrahedron Lett*. 2005, 46, 2989-2991.

84. Long N, Cai X J, Song B A, *et al*. Synthesis and antiviral activities of cyanoacrylate derivatives containing an alpha-aminophosphonate moiety. *J*. *Agric Food Chem*. 2008, 56(13), 5242-5246.

Chapter 3
Synthesis and Antiviral Activity of Chiral Thiourea Derivatives

3.1 Chiral Thiourea Deravatives from Primary Amine and Isocyanate

3.1.1 Introduction

Thioureas occupy an important position in pesticide chemistry due to their strong biological activities.[1,2] They possess antibacterial and antifungal activities[3–5] and can also act as herbicides and rodenticides.[6,7] Till 1960, thiourea-based fungicides *e.g*., thiophanate and thio-phanate-methyl were used extensively in agriculture.[8] These compounds possess low acute toxicity against mammals and are very effective in preventing and curing a number of crop diseases. Recently, a large number of reports on the synthetic studies of new chiral thiourea derivatives have been documented with a wide range of functional and biological activities. Some derivatives can serve not only as catalysts for the synthesis of optically active compounds, [9] but can also be employed as medicines such as anti-cancer and anti-HIV agents. Venkatachalam and his group have found that stereochemistry plays an important role in the anti-leukemic potency of halopyridyl and thiazolyl thiourea compounds. Preliminary screening indicated that the (*S*)-isomers displayed improved activity in comparison with (*R*)-enantiomers in the inhibition of tubulin polymerization and activation of caspase-3.[10–12] Venkatachalam and his group proved that certain chiral enantiomers of thiourea derivatives were associated with anti-HIV activities and also synthesized chiral naphthyl thiourea (CNT) compounds, as non-nucleoside inhibitors (NNI) of the reverse transcriptase (RT) enzyme of HIV-1.[13,14] Molecular modeling studies indicated that, due to asymmetry of the NNI binding pocket, the R stereoisomers would fit the NNI binding pocket of the HIV-1 RT much better

than the corresponding *S* stereoisomers, as reflected by their 104-fold lower values. The *R* stereoisomers of all 11 compounds inhibited the recombinant RT *in vitro* with lower IC_{50} values than their *S* enantiomers. In addition, a large number of research studies on their synthesis and application as bifunctional organocatalysts have been conducted during the last five years.[9,15–17] However, to date, most of the work has been focused on anti-cancer and anti-HIV activities in medicinal formulation while no publication concerning antiviral activity in pesticidal formulation has appeared in the literature.

In order to extend our research work of chiral thiourea as antiviral agent against tobacco mosaic virus (TMV), we designed and synthesized some novel chiral thiourea derivatives **3.3** in ionic liquid. The synthetic route is shown in Scheme 3.1. The structures of **3.3** were established by well defined IR, NMR and elemental analysis. The bioassay tests revealed that the new compounds **3.3** possessed moderate antiviral activities. Title compound **3.3i** was found to possess good *in vivo* protection, inactivation and curative effects against TMV with inhibitory activities of 57.0%, 96.4%, 55.0%, respectively at 500 μg/mL. It was found that the title chiral compound **3.3i** had the same inactivation effect against TMV (EC_{50}=50.8 μg/mL) as Ningnanmycin (EC_{50}=60.2 μg/mL). To the best of our knowledge, this is the first report on the synthesis and antiviral activity of chiral thiourea derivatives.

3.1.2   Materials and Methods

The materials and instruments for determination of the structure and physical data of new compounds are basically similar to the procedure described in Chapter 1.1.2. Isothiocyanatobenzene was prepared according to a literature method as described.[20] Unless otherwise indicated, all compounds were purchased from Aldrich and/or Alfa Aesar.

***General procedure for preparation of chiral thioureas**(**3.3a-3.3x**).* Aromatic isothiocyanate **3.1** (2 mmol) and corresponding chiral amine **3.2** (2.4 mmol) were added to ionic liquid ［Bmim］PF_6(1 mL)(Warning：although ［Bmim］BF_6 is considered as a green solvent and is non-volatile, enough care should still be paid when handling this kind of chemical), and the mixture was stirred at room temperature for 5 min (for reaction conditions see Table 3.1). The product was extracted with ether (3×10 mL). The combined ethereal phase was evaporated under reduced pressure to give the crude product, which was purified by chromatography on silica gel (100-200 mesh) using petroleum ether：ethyl acetate=2:1 to provide the corresponding chiral thiourea derivatives (**3.3a-3.3x**). After reaction, the ionic liquid was simply washed with ether, dried under vacuum

and then used again without further purification. The reperesentative data for **3.3a** is shown below, while data for **3.3b-3.3x** can be found in the reference.[36]

(*S*)-1-[1-(3-*Anisyl*)ethyl]-3-phenylthiourea.(3.3a). White crystal, yield 86.6%; mp 136.1-138.2℃; $[\alpha]_D^{25}$ +65.2° (*c* 0.55, ethyl acetate); IR(KBr)：ν_{max} 3265, 3120, 3045, 3008, 2972, 1595, 1537, 1494, 1357, 1319, 1253, 1033, 790, 711, 669, 576. ^{1}H NMR(500 MHz, DMSO-d_6)：δ 9.46(br s, 1H, ArNH), 8.15(br s, 1H, NH), 7.47-6.82(m, 9H, ArH), 5.5(br s, 1H, CH), 3.76(s, 3H, OCH$_3$), 1.44(3H, d, *J*=7.45 Hz, CH$_3$); ^{13}C NMR(125 MHz, DMSO-d_6)：δ 180.3, 159.8, 146.1, 140.0, 129.9, 129.0, 124.5, 123.3, 119.0, 112.7, 112.5, 55.5, 53.1, 22.5. Anal.Calcd for C$_{16}$H$_{18}$N$_2$OS：C, 67.10; H, 6.33; N, 9.78. Found：C, 67.05; H, 6.44; N, 9.81.

Antiviral Biological Assay. The method for evaluating anti-TMV activity of title compounds is similar to the procedure described in Chapter 1.1.2.[19,31]

3.1.3 Results and Discussion

The most common method for the synthesis of chiral thiourea derivatives is the direct reaction of isothiocyanate with chiral amine. However the application is limited due to longer reaction time, lower yield, and use of toxic solvents, such as benzene, toluene, acetonitrile, DMF, dichloromethane and THF. We have developed a simple, mild, efficient and environmentally friendly method for the synthesis of chiral thiourea derivatives in ionic liquid [Bmim]PF$_6$ (1-butyl-3-methylimidazolium hexafluorophosphate).[18] In order to optimize the reaction conditions for the preparation of chiral thiourea derivatives, the synthesis of **3.3d** was carried out under different conditions. The effects of different solvents, reaction time, reaction temperature, and the amount of the ionic liquid on the reaction were investigated. The results are summarized in Table 3.1. First, the effect of five different solvents was studied. As can be seen from Table 3.1, while the yield of the product **3.3d** reached up to 85.5% in ionic solvent [Bmim]PF$_6$, the yield was significantly lower in other solvents, particularly in DMF the yield was only 55.3%. This proved superior efficiency of the ionic solvent [Bmim]PF$_6$ compared to the rest. The percentage yield of **3.3d** in ionic liquid was however not greatly affected when the reaction time was prolonged from 5 to 10 min. As for reaction temperature, no substantial change was noticed when the temperature was raised from room temperature to 50℃. In addition, the yield of **3.3d** was not improved with increased amount of ionic liquid and finally it was observed that the reaction of isothiocyanate with 1.2 equiv chiral amine afforded improved yield compared with 1.0 equiv chiral amine. Thus, under the optimal conditions, the best result was obtained when isothiocyanatobenzene was reacted with 1.2 equiv (*R*)-1-cyclohexylethanamine in ionic liquid ［Bmim］PF$_6$ at room temperature for 5 min.
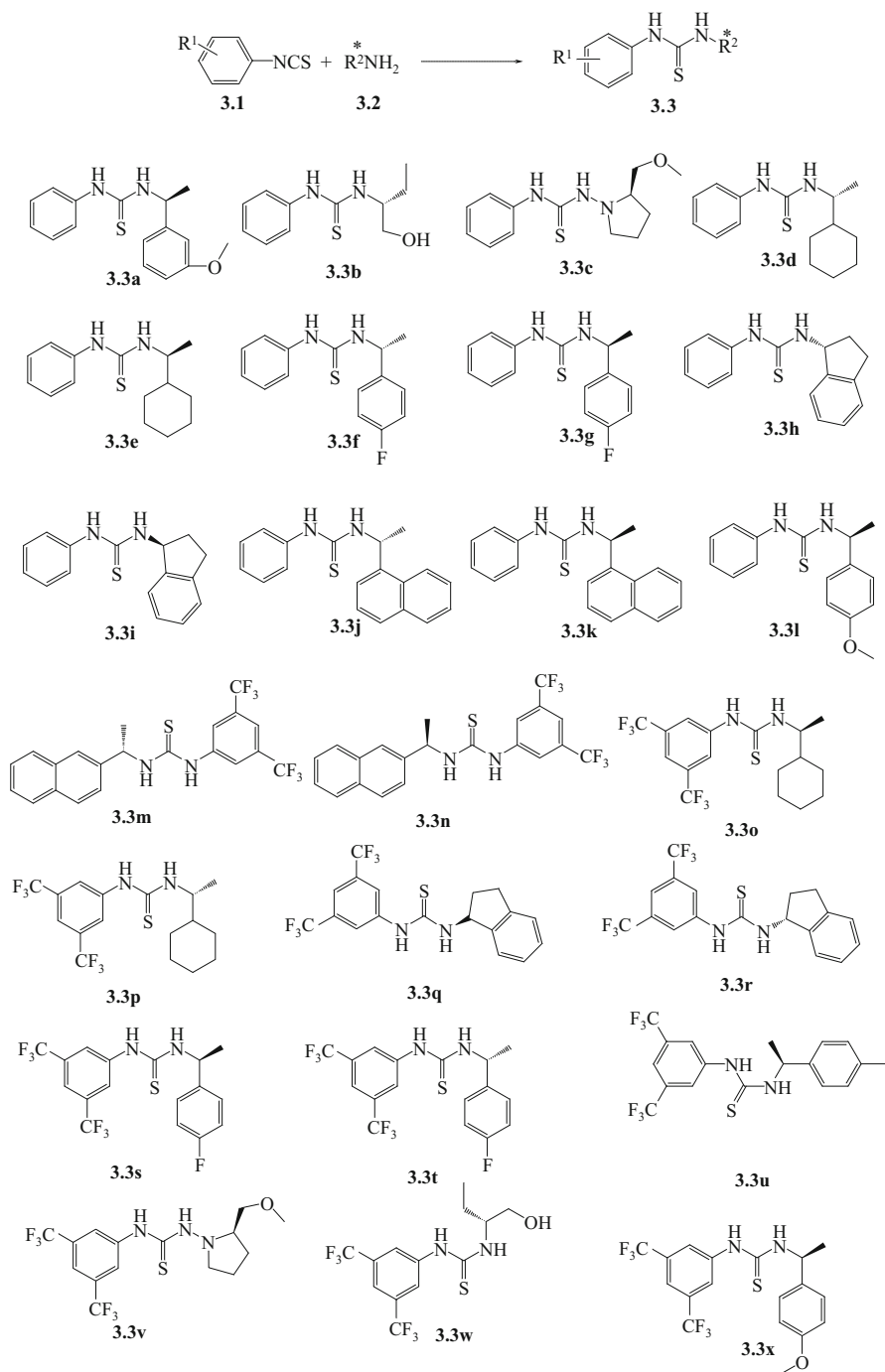
Scheme 3.1   Synthetic route to title chiral compounds **3.3** from primary amine and isocyanate

Table 3. 1 Synthesis of **3. 3d** in ionic liquids and other solvents under different reaction conditions

Entry	Isothiocyanatobenzene (equiv)	(R)-1-cyclohexyl-ethanamine(equiv)	Solvent	Volume (mL)	Time (min)	Temp (℃)	3d[a] (%)
1	1	1. 2	THF	10	30	r. t.	65. 4
2	1	1. 2	CH$_3$CN	10	30	r. t.	63. 5
3	1	1. 2	Benzene	10	30	r. t.	58. 6
4	1	1. 2	DMF	10	30	r. t.	55. 3
5	1	1. 0	［Bmim］PF$_6$[b]	1	5	r. t.	68. 7
6	1	1. 2	［Bmim］PF$_6$	1	5	r. t.	85. 5
7	1	1. 2	［Bmim］PF$_6$	2	5	r. t.	74. 4
8	1	1. 2	［Bmim］PF$_6$	1	10	r. t.	83. 5
9	1	1. 2	［Bmim］PF$_6$	1	5	50	85. 3

[a]Isolated yields after work-up;[b]reaction medium, 1-butyl-3-methylimidazolium hexafluorophosphate.

Various chiral thioureas were obtained through such optimized reactions in the ionic liquid. A wide range of chiral amines with aromatic, aliphatic and heterocyclic moieties were employed in this procedure to synthesize the corresponding chiral thioureas in good yields (70.5%-86.6%)(Table 3.2).

Table 3. 2 Yields of **3. 3a-3. 3x** from reaction of ArNCS **3.1** with chiral amines

Entry	Product	Chiral amine	Yield(%)	
			IL method[ac]	Classical method[bc]
1	**3.3a**	(S)-1-(3-anisyl)ethanamine	86.6	71.5
2	**3.3b**	(R)-2-aminobutan-1-ol	85.7	73.7
3	**3.3c**	(R)-2-(methoxymethyl)pyrrolidin-1-amine	81.7	69.5
4	**3.3d**	(R)-1-cyclohexylethanamine	85.5	65.4
5	**3.3e**	(S)-1-cyclohexylethanamine	84.5	66.1
6	**3.3f**	(R)-1-(4-fluorophenyl)ethanamine	82.3	69.2
7	**3.3g**	(S)-1-(4-fluorophenyl)ethanamine	81.8	66.6
8	**3.3h**	(R)-1-aminoindane	83.1	68.2
9	**3.3i**	(S)-1-aminoindane	82.6	68.6
10	**3.3j**	(R)-1-(2-naphthyl)ethanamine	71.4	62.5
11	**3.3k**	(S)-1-(2-naphthyl)ethanamine	70.5	61.0
12	**3.3l**	(S)-1-(4-anisyl)ethanamine	70.9	62.2
13	**3.3m**	(S)-1-(2-naphthyl)ethanamine	71.5	61.2
14	**3.3n**	(R)-1-(2-naphthyl)ethanamine	73.2	62.9
15	**3.3o**	(S)-1-cyclohexylethanamine	81.3	70.5
16	**3.3p**	(R)-1-cyclohexylethanamine	83.1	70.0
17	**3.3q**	(S)-1-aminoindane	75.1	63.5
18	**3.3r**	(R)-1-aminoindane	73.8	65.2
19	**3.3s**	(S)-1-(4-fluorophenyl)ethanamine	82.5	70.2
20	**3.3t**	(R)-1-(4-fluorophenyl)ethanamine	83.4	69.5
21	**3.3u**	(S)-1-(4-tolyl)ethanamine	80.5	68.6
22	**3.3v**	(R)-2-(methoxymethyl)pyrrolidin-1-amine	80.1	69.7
23	**3.3w**	(R)-2-aminobutan-1-ol	82.6	70.2
24	**3.3x**	(S)-1-(3-anisyl)ethanamine	80.1	67.2

[a]General conditions：**3. 1** was reacted with **1. 2** equivalent chiral amine in ionic liquid ［Bmim］PF$_6$ at room temperature for 5 minutes; [b]Reaction conditions：ArNCS **3. 1** was reacted with **1. 2** equivalent chiral amine at room temperature in THF for 30 minutes; [c]Yields of isolated products.

Furthermore, in the reaction of isothiocyanatobenzene with (*R*)-1-cyclohexylethanamine, the ionic liquid ［Bmim］PF$_6$ could be recycled and reused for at least 6 times without showing any significant decrease in the activity (Table 3.3).

Table. 3. 3   Recycling efficiency of ［Bmim］PF$_6$ for the synthesis of **3. 3d**[a]

Cycle	Yield(%)[b]	Cycle	Yield(%)
1	83. 5	4	82. 0
2	82. 9	5	81. 5
3	84. 1	6	80. 3

[a]General conditions：reactions were performed at room temperature in ionic liquid ［Bmim］PF$_6$ for 5 minutes；mole ratio：ArNCS:chiral amine＝1:1. 2; [b]Yields of isolated products.

Antiviral activity assay. The antiviral activities of compounds **3.3a-3.3l** against TMV were assayed by the reported method.[31] The results of bioassay *in vivo* against TMV are given in Table 3.4. Ningnanmycin was used as a reference antiviral agent. The data indicated that the title chiral compounds **3.3a-3.3x** showed protection rate of 15.8%-57.0%. The compounds **3.3b** ［R^1=Ph, R^2=(*S*)-(1-hydroxybut-2-yl)］, **3.3c** ［R^1=Ph, R^2=(*R*)-2-(methoxymethyl)pyrrolidin-1-yl］ and **3.3i** ［R^1=Ph, R^2=(*S*)-(indan-1-yl)］have the same protection activity (52.9%, 52.3%, 57.0%, respectively) as that of the Ninnanmycin (55.9%). The present data also show that, at 500 μg/mL, the title chiral compounds **3.3a-3.3x** possess potential inactivation bioactivities, with values of 80.8%, 30.7%, 40.9%, 63.8%, 67.8%, 66.4%, 71.9%, 60.9%, 96.4%, 61.7%, 67.4%, 71.1%, 62.0%, 60.9%, 64.4%, 64.3%, 57.7%, 54.3%, 50.7%, 68.1%, 53.6%, 70.5%, 49.0% and 71.4%, respectively. Among these chiral compounds, **3.3i** is much more active against TMV than the others, with an inactivation rate of 96.4% equivalent to that of Ningnanmycin (96.5%) against TMV at 500 μg/mL. We also observed that a change in the configuration and substituent might also affect the curative activity of the title chiral compounds **3.3a-3.3l.** The chiral compound **3.3i** could curate TMV up to 55.0% at the concentration of 500 μg/mL. The other chiral compounds have a lower curative activity than **3.3i**.

At a concentration of 500 μg/mL, compound **3.3i**［(*S*)-configuration］showed significant enhancement in anti-TMV activities compared to the compound **3.3h** ［(*R*)-configuration］from the curative, protection and inactivation effects. As shown in Table 3.4, except chiral compound **3.3i** and its enantioner **3.3h**, the other (*S*)-isomers of **3.3e** and **3.3g** did not display improved activity in comparison with (*R*)-enantiomers **3.3d** and **3.3f** against TMV. The enantiomers of **3.3d-3.3g** present little difference in the anti-TMV activity and show weak to moderate (lower than 43%.) protection and curative effects.

Since the chiral compound **3.3i** was found to display good antiviral activity, it was selected for further bioassay with commercial plant antiviral agent Ningnanmycin serving as a control. As shown in Table 3.5, the curative effects of

Table 3.4 The protection, inactivation and curative effect of the new
chiral compounds at 500 g/mL against TMV *in vivo*

Agents	Protection effect(%)	Inactivation effect(%)	Curative effect(%)
3.3a	15. 8[*]±1. 0	80. 8[**]±1. 3	25. 4[*]±0. 8
3.3b	52. 9[*]±4. 0	30. 7[*]±0. 6	32. 4[*]±1. 8
3.3c	52. 3[*]±1. 0	40. 9[*]±1. 0	6. 9±0. 4
3.3d	28. 7±0. 6	63. 8[*]±1. 1	41. 1[*]±1. 4
3.3e	39. 3[*]±2. 2	67. 8[*]±1. 9	35. 9±1. 4
3.3f	42. 2[*]±1. 1	66. 4[**]±1. 9	34. 9[*]±0. 9
3.3g	18. 9[*]±2. 3	71. 9[**]±2. 0	34. 4±0. 3
3.3h	35. 6[*]±3. 8	60. 9[*]±2. 0	40. 3[*]±1. 0
3.3i	57. 0[*] ±1. 9	96. 4[*]±1. 6	55. 0[*]±1. 2
3.3j	25. 9[*]±2. 9	61. 7[*]±1. 8	37. 4±0. 9
3.3k	20. 8[*]±1. 0	67. 4[*]±0. 9	42. 5[*]±0. 9
3.3l	22. 6[*]±3. 3	71. 1[**]±1. 9	42. 8[*]±1. 9
3.3m	26. 2[*]±1. 9	62. 0[**]±1. 2	38. 5[*]±1. 0
3.3n	21. 1[*]±1. 2	60. 9[**]±2. 1	48. 3[*]±1. 9
3.3p	46. 5[*]±1. 4	64. 4[**]±2. 3	49. 1[*]±1. 4
3.3q	40. 4[*]±1. 0	64. 3[**]±2. 0	32. 6[*]±0. 8
3.3r	43. 5[*]±1. 1	57. 7[**]±2. 0	43. 4[*]±1. 1
3.3s	40. 3[*]±1. 7	54. 3[**]±1. 3	31. 7[*]±1. 0
3.3t	36. 7[*]±0. 4	50. 7[**]±2. 0	28. 8[*]±0. 9
3.3u	44. 9[*]±1. 3	68. 1[**]±2. 0	45. 1[*]±1. 4
3.3v	25. 0[*]±1. 0	53. 6[*]±2. 9	26. 0[*]±1. 0
3.3w	17. 6[*]±1. 8	70. 5[**]±2. 0	41. 6[*]±1. 2
3.3x	34. 2[*]±1. 0	49. 0[**]±2. 1	37. 5[*]±1. 0
3.3y	42. 7[*]±1. 1	71. 4[**]±1. 9	35. 1[*]±1. 2
Ningnanmycin	55. 9[*]±2. 0	96. 5[**]±1. 8	53. 9[*]±2. 1

All results are expressed as mean±SD; *n*=3 for all groups; [*] $P<0.05$, [**] $P<0.01$.

Table 3.5 Antiviral activities in vivo (%) of the chiral compound **3.3i**

TMV	Curative effect				Inactivation effect			
Concentration(μg/mL)	500	250	125	EC_{50}(μg/mL)	250	125	62.5	EC_{50}(μg/mL)
3.3i	56.0	50.0	37.0	223.7	94.9	86.1	70.7	50.8
Ningnamycin	54.0	48.0	40.9	230.9	92.9	78.4	69.0	60.2

TMV	Protection effect			
Concentration(μg/mL)	500	250	125	EC_{50}(μg/mL)
3.3i	58.0	52.0	47.0	239.6
Ningnamycin	56.0	49.0	44.9	242.9

chiral compound **3.3i** and Ningnanmycin against TMV showed remarkable action, with the EC_{50} values being 223.7 and 230.9 μg/mL, respectively. The compound **3.3i** and Ningnanmycin also had high inactivation effects against TMV and their EC_{50} values were 50.8 and 60.2 μg/mL, respectively. The chiral compound **3.3i** and Ningnanmycin showed more potent protection effects against TMV than the others, with the EC_{50} values of 239.6 and 242.9 μg/mL, respectively.
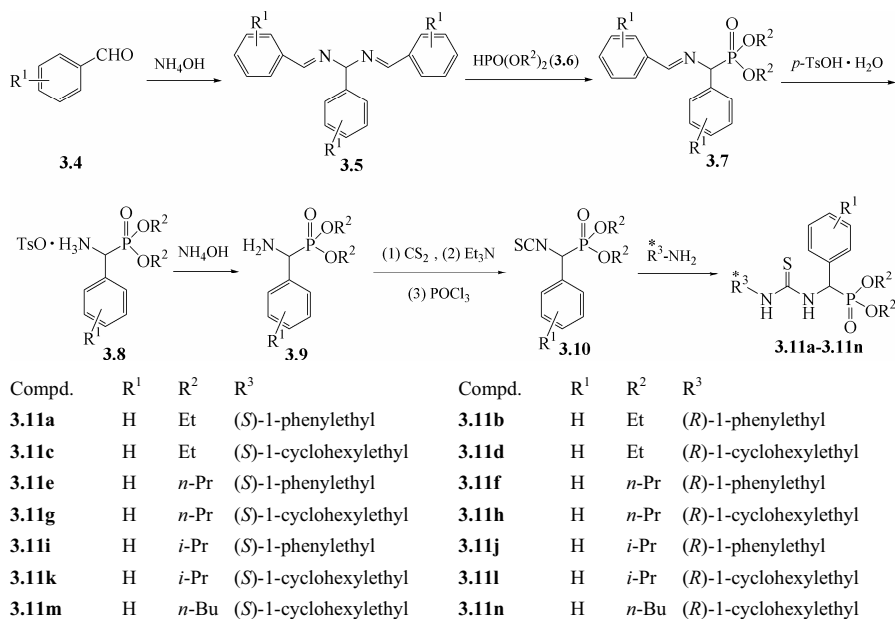
3.1.4   Conclusions

In conclusion, an eco-friendly green chemistry procedure in ionic liquid has been developed for the synthesis of novel chiral thiourea derivatives in high yields. The ionic solvent can be recovered and reused without any loss of its activity. This method is easy, rapid and good-yielding for the synthesis of title chiral compounds **3.3**. The structures of the title compounds were verified by spectroscopic data. The preliminary bioassay showed that some of the chiral thiourea analogues exhibited moderate to good *in vivo* antiviral activities against TMV at 500 μg/mL. Title chiral compound **3.3i** was found to possess good *in vivo* protection, inactivation and curative effects against TMV with inhibitory effects of 57.0%, 96.4%, 55.0% at 500 μg/mL. It was found that the title chiral compound **3.3i** had better inactivation effect against TMV(EC_{50}=50.8 μg/mL) than Ningnanmycin (EC_{50}=60.2 μg/mL). To the best of our knowledge, this is the first report on the syntheses of chiral thiourea derivatives with antiviral activity in ionic solvent. Further studies are in progress to promote structural optimization and antiviral activities of the chiral thiourea analogues.

3.2   Chiral Thiourea Derivatives Containing α-Aminophospho-nate Moiety

3.2.1   Introduction

Chiral thioureas and their derivatives are known for their wide range of functional and biological activities. Some chiral thiourea derivatives can serve not only as chiral catalysts for the synthesis of optically active compounds, [9] but also as medicines such as anti-cancer and anti-HIV agents.[10,11] In this context, Venkatachalam and his group[13,21] held-stereochemistry as the key factor responsible for anti-leukemic potency of halopyridyl and thiazolyl thiourea compounds. Preliminary screening indicated that the (*S*)-isomers displayed improved activity in comparison with (*R*)-enantiomers to inhibit tubulin polymerase and activate caspase-3. The role of stereochemistry of chiral thiourea

compounds on the anti-HIV activity was further established and confirmed by this group. Venkatachalam and his group[14] synthesized chiral naphthyl thiourea (CNT) compounds as non-nucleoside inhibitors (NNI) of the reverse transcriptase (RT) enzyme of HIV-1. The (R)-stereoisomers of all 11 compounds inhibited the recombinant RT *in vitro* with lower IC_{50} values than their enantiomers. In recent years, chiral thioureas have started to gain enormous importance due to their wide bioactivity and ability to serve as potential bifunctional organocatalysts in typical organic transformations.[9,16] However, to date, most of the reports are focused on anti-cancer and anti-HIV activity in medicinal formulation while no publication concerning antiviral activity of these compounds in pesticide formulation is encountered.

On the other hand, α-aminophosphonic acids, bioisosteres of natural amino acids, have been found to exhibit a wide range of biological activities and are widely employed as fungicide, plant virucide, herbicide, plant growth regulators, and so on.[21–26] A large number of literatures on their synthesis and biological activities have been reported during the last ten years.[27–30]

Tobacco mosaic virus (TMV) infection is very widely distributed, and can cause serious damage and large economic loss. It was found that in certain fields 90%-100% of the plants show mosaic by harvesting time. In view of the unsatisfactory curatives (30%-60%) cure rate obtained by common antiviral agent Ningnanmycin (or Virus A) and widespread economic loss of tobacco, further research needs to be conducted in this area for the development of a highly efficient, novel environmentally benign antiviral agent.

In our preliminary work, many substituted diaryl aminophosphonate derivatives containing amide or cyanoacrylate moieties were synthesized and were found to have good antiviral activities[31,32]. To extend our research work of chiral thiourea as antiviral agent against tobacco mosaic virus (TMV), we designed and synthesized some novel chiral thiourea derivatives **3.11** containing aminophosphonates moiety (Fig 3.1). The synthetic route is shown in Scheme 3.2. Preliminary bioassay tests showed that some compounds possess certain degree of antiviral activity against TMV at 500 mg/L *in vivo* as shown in Table 3.3, however with a degree of variation. The bioassay results showed that the title compounds **3.11g**, **3.11e**, **3.11k** and **3.11m** had the same curative effect against TMV (inhibitory rate=54.8%, 50.5%, 50.4% and 50.4%) as the commercial product Ningnanmycin (56.2%) and the EC_{50} values range from 227.0 to 413.9 µg/mL. To the best of our knowledge, this is the first report on the synthesis and antiviral activity of chiral thioureas containing an α-aminophosphonate moiety.

Fig 3.1 Design of the target compounds

Compd.	R^1	R^2	R^3	Compd.	R^1	R^2	R^3
3.11a	H	Et	(S)-1-phenylethyl	**3.11b**	H	Et	(R)-1-phenylethyl
3.11c	H	Et	(S)-1-cyclohexylethyl	**3.11d**	H	Et	(R)-1-cyclohexylethyl
3.11e	H	n-Pr	(S)-1-phenylethyl	**3.11f**	H	n-Pr	(R)-1-phenylethyl
3.11g	H	n-Pr	(S)-1-cyclohexylethyl	**3.11h**	H	n-Pr	(R)-1-cyclohexylethyl
3.11i	H	i-Pr	(S)-1-phenylethyl	**3.11j**	H	i-Pr	(R)-1-phenylethyl
3.11k	H	i-Pr	(S)-1-cyclohexylethyl	**3.11l**	H	i-Pr	(R)-1-cyclohexylethyl
3.11m	H	n-Bu	(S)-1-cyclohexylethyl	**3.11n**	H	n-Bu	(R)-1-cyclohexylethyl

Scheme 3.2   Synthetic route to chiral thiourea analogues **3.11** containing α-aminophosphonate moiety

3.2.2   Materials and Methods

Instruments. The materials and instruments for determination of the structure and physical data of new compounds are basically similar to the procedure described in Chapter 1.1.2.

Synthetic procedures. Dialkyl phosphite **3.6** was prepared according to literature method as described.[33] Intermediates **3.9** were prepared according to the reported methods.[34]

General procedure for the preparation of the intermediates O, O′-dialkyl isothiocyanato(phenyl)methylphosphonate **3.10.** A solution of α-aminophosphonates **3.9** (6 mmol) in ether (15 mL) was stirred, followed by the addition of triethylamine (18 mmol), and then the reaction system was cooled down to 0℃. Then, carbon disulfide (6 mmol) was added drop-wise and was stirred for 2h at 0℃, the temperature was raised to 25℃ and the reaction mixture was stirred for an additional 2h. Phosphorus-oxychloride (6 mmol) dissolved in ether (10 mL) was then added drop wise into the reaction mixture and was stirred for 4h at 25℃. The solid was filtered off, the solution was washed with saturated sodium bicarbonate, and dried on anhydrous sodium sulfate and filtered again. The solvent was removed by evaporation and the crude product resulted was purified by chromatography on silica using a mixture of petroleum ether and ethyl acetate (2:1) as the eluent to give the intermediates **3.10** in 54.2%-61.5% yields.[35] The

reperesentative data for **3.10a** is shown below, while data for **3.10b-3.10d** can be found in the reference.[37]

Data for O, O' -diethyl isothiocyanato (phenyl) methylphosphonate (**3.10a**). Light yellow liquid; $n^{25}{}_D$=1.6365; yield 60.3%; IR(KBr)：v_{max}2981.4, 2063.8, 1494.3, 1456.3, 1392.6, 1259.5, 1022.3; ^{1}H NMR(CDCl$_3$, 500 MHz)：δ 1.25-1.27(6H, m, 2CH$_3$), 4.00-4.03(4H, m, 2OCH$_2$), 5.02(1H, d, J=18.02 Hz, CH), 7.37-7.43(5H, m, ArH); ^{13}C NMR(125 MHz, CDCl$_3$)：δ 137.14, 131.78, 128.95, 128.80, 127.48, 64.32, 58.58, 16.51, 16.28; ^{31}P NMR (200 MHz, CDCl)：δ 15.99.

General procedure for the preparation of title compounds **3.11a-3.11n.** A solution of O, O' -dialkyl isothiocyanato (phenyl) methylphosphonate **3.10** (1mmol) in tetrahydrofuran (10 mL) was stirred, followed by drop-wise addition of chiral amine (1.2 mmol). The reaction mixture was stirred for 0.5h at 25℃ and then the solvent was removed by evaporation. The resulting crude product was purified by chromatography on silica using a mixture of petroleum ether and ethyl acetate (2:1) as the eluent to give the title compounds **3.11a-3.11n** in 58%-70% yields. The reperesentative data for **3.11a** is shown below, while data for **3.11b-3.11n** can be found in the reference.[37]

Data for O, O' -diethyl phenyl［3-((S)-1-phenylethyl)thioureido］methylphos phonate (**3.11a**). White crystal, mp 97-98℃; yield 70%; $[\alpha]_D^{20}$ =＋16.8° (c 1.7, acetone); IR(KBr)：v_{max} 3300, 3118, 3057, 2983, 1533, 1492, 1452, 1336, 1207, 1018, 763, 742, 698, 565, 542; ^{1}H NMR (D$_3$CCOCD$_3$, 500 MHz)：δ 8.31 (1H, br s, NH), 8.19 (1H, br d, J=74.8 Hz, NH), 7.31-7.25 (10H, m, ArH), 6.10 (1H, d, J=20.0 Hz, N-CH-P), 5.37 (1H, br s, N-CH-Ar), 3.97-3.83 (4H, m, 2OCH$_2$), 1.38-0.98 (9H, m, 3CH$_3$); ^{13}C NMR (125 MHz, DMSO-d_6)：δ 182.7, 144.5, 136.6, 128.9, 128.7, 128.4, 128.2, 127.4, 126.5, 63.2, 53.9, 53.6, 21.5, 16.0; ^{31}P NMR(200 MHz, D$_3$CCOCD$_3$)：δ 22.3, 22.1; Anal. Calcd. for C$_{20}$H$_{27}$N$_2$O$_3$PS：C, 59.10; H, 6.70; N, 6.89. Found：C, 59.01; H, 6.39; N, 6.58.

Antiviral biological assay. The method for evaluating anti-TMV activity of title compounds is similar to the procedure described in Chapter 1.2.2.[19,31]

3.2.3　Results and Discussion

Synthesis. In order to obtain intermediates **3.10** with high purity, the method reported by Kaboudin[34] was modified by employing ether as the extraction solvent and petroleum ether and ethyl acetate as the eluent for column chromatography. In order to restrict the formation of side products, the reaction was conducted at lower temperature.

To optimize the reaction conditions for the preparation of compound **3.11b**, the synthesis was carried out in different solvents, such as tetrahydrofuran (THF), acetonitrile, N, N-dimethylformamide (DMF) and toluene. A maximum yield of up to 70.0% was achieved when the reaction mixture was stirred for 0.5 h in THF. The effect of solvent system is summarized in Table **3.6**.

Table 3.6   Effect of different solvents for synthesis of **3.11b**

No.	Solvent	Volume(mL)	Reaction time(h)	Temp(℃)	Yield(%)
1	THF	10	0.5	r.t	70.0
2	CH$_3$CN	10	0.5	r.t	58.3
3	DMF	10	0.5	r.t	62.4
4	Toluene	10	0.5	r.t	51.5

The main characteristic of the **^{1}H NMR** spectra of **3.11a-3.11n** is the presence of high-frequency downfield broad singlet δ_H8.53-8.12, presumably arising due to the deshielded N-H proton of thiourea linked to the phoosphoryl moiety and benzene ring through an intervening carbon atom. The broad doublets at δ_H 8.19-7.53 are assigned to the N-H proton of thiourea directly attached to the asymmetric center R^3. The doublet at δ_H 6.63-6.16 is assigned to the C-H proton of N-C-P and the broad singlet at δ_H 5.54-4.11 is assigned to the C-H of N-C-C. The typical carbon resonance at δ_C 183.6-182.7 in the **^{13}C NMR** spectra of **3.11a-3.11n** also confirms the presence of a carbon sulfur double bond. The typical phosphorus resonance at δ_P22.6-21.1 in the **^{31}P NMR** spectra of **3.11a-3.11n** reveals the presence of phosphorus center coupled to adjacent CH.

Antiviral activity and structure-activity relationship. The antiviral activities of compounds **3.11a-3.11n** against TMV is assayed by the reported method.[31] The results of bioassay *in vivo* against TMV are given in Table 3.7. Ningnanmycin was used as reference antiviral agent. The data provided in Table 3.7 indicated that the title chiral compounds **3.11a-3.11n** showed protection rate of 30.9%-46.3%. Compounds **3.11b** 〔R^1 is H, R^2 is Et, R^3 is (*R*)-1-phenylethyl〕, **3.11e** 〔R^1 is H, R^2 is *n*-Pr, R^3 is (*S*)-1-phenylethyl〕, **3.11f** 〔R^1 is H, R^2 is *n*-Pr, R^3 is (*R*)-1-phenylethyl〕 and **3.11j** 〔R^1 is H, R^2 is *i*-Pr, R^3 is (*R*)-1-phenylethyl 〕 have moderate protection activity (42.6%, 42.7%, 45.9%, 46.3%, respectively), which is lower than that of the commercial reference (60.2%). From the data in Table 3.7, it may be observed that the title chiral compounds **3.11a-3.11n** possess moderate to good curative bioactivities, with values of 41.8%, 45.2%, 36.3%, 40.1%, 50.5%, 41.9%, 54.8%, 40.7%, 36.8%, 34.5%, 50.4%, 34.6%, 50.4% and 34.6% respectively at 500 μg/mL. The data also indicate that the curative activity of the title chiral compounds **3.11a-3.11n** is strongly dependent upon the absolute configuration of the enantiomer and the nature of substituents. The chiral enantiomer **3.11g** 〔R^1 is H, R^2 is *n*-Pr, R^3 is (*S*)-1-cyclohexylethyl〕 could curate TMV up to 54.3% at the concentration of 500 μg/mL. The other chiral compounds with different substituents and configurations have a relatively lower curative activity than that of **3.11g**. At a concentration of 500 μg/mL, compound **3.11g** 〔(*S*)-configuration〕 showed significant enhancement in anti-TMV activities compared to the compound **3.11h** 〔(*R*)-configuration〕 〔R^1 is H, R^2 is *n*-Pr, R^3 is (*R*)-1-cyclohexylethyl〕from the curative effect and inactivation effect. The same trend in terms of improved activity was noted with other (*S*)-enantiomers **3.11e**

Table 3. 7　The protection and curative effect of compounds
3. 11 against TMV *in vivo* at 500 g/mL

Agents	Protection effect (%)	Curative effect (%)	Agents	Protection effect (%)	Curative effect (%)
3.11a	37.6*	41.8*	**3.11i**	36.9*	36.8*
3.11b	42.6*	45.2*	**3.11j**	46.3*	34.5*
3.11c	36.4*	36.3*	**3.11k**	36.3*	50.4**
3.11d	33.1*	40.1*	**3.11l**	33.7*	34.6*
3.11e	42.7*	50.5*	**3.11m**	36.3*	50.4**
3.11f	45.9*	41.9*	**3.11n**	33.7*	34.6*
3.11g	30.9*	54.8**	Ningnamycin	60.6**	56.2**
3.11h	37.9*	40.7*			

n=3 for all groups; * $P<0.05$, ** $P<0.01$.

〔R^1 is H, R^2 is *n*-Pr, R^3 is (*S*)-1-phenylethyl〕 and **3.11k** 〔R^1 is H, R^2 is *i*-Pr, R^3 is (*S*)-1-cyclohexylethyl〕 and **3.11m** 〔R^1 is H, R^2 is *n*-Bu, R^3 is (*S*)-1-cyclohexylethyl〕) when compared with the activities shown by their corresponding (*R*)-enantiomers **3.11f** 〔R^1 is H, R^2 is *n*-Pr, R^3 is (*R*)-1-phenylethyl〕 and **3.11l** [R^1 is H, R^2 is *i*-Pr, R^3 is (*R*)-1-cyclohexylethyl]and **3.11n**〔R^1 is H, R^2 is *n*-Bu, R^3 is (*R*)-1-cyclohexylethyl〕) to TMV. The enantiomers of **3.11a**〔R^1 is H, R^2 is Et, R^3 is (*S*)-1-phenylethyl], **3.11b**〔R^1 is H, R^2 is Et, R^3 is (*R*)-1-phenylethyl], **3.11c** [R^1 is H, R^2 is Et, R^3 is (*S*)-1-cyclohexylethyl〕, **3.11d**〔R^1 is H, R^2 is Et, R^3 is (*R*)-1-cyclohexylethyl〕, **3.11i**〔R^1 is H, R^2 is *i*-Pr, R^3 is (*S*)-1-phenylethyl〕 and **3.11j**〔R^1 is H, R^2 is *i*-Pr, R^3 is (*R*)-1-phenylethyl〕 present little difference in the anti-TMV activity and show moderate protection and curative effect, and the values are not greater than 46%.

As the eantiomers **3.11e**, **3.11g**, **3.11k** and **3.11m** were found to display good antiviral activities, they were selected for further bioassay with commercial plant antiviral agent Ningnanmycin serving as a control, for making a judgement on the antiviral potency of these compounds. As shown in Table 3.8, the curative effect against TMV of chiral compound **3.11g** and Ningnanmycin showed remarkable effect on TMV. The EC_{50} values on TMV were 239.8 and 227.0 μg/mL, respectively. Compounds **3.11b**, **3.11e**, **3.11k** and **3.11m** were fairly effective in curating TMV, and the EC_{50} values were 399.9, 413.4 and 378.9 μg/mL, respectively.

Table 3. 8　Antiviral activities *in vivo* (%) of compounds
3. 11b, 3. 11e, 3. 11g, 3. 11k and **3. 11m**

TMV	Curative effect			
Concentration(μg/mL)	500	250	125	EC_{50}(μg/mL)
3.11e	50.5	37.7	30.9	399.9
3.11g	54.8	49.0	39.1	239.8
3.11k	50.4	36.7	29.0	413.4
3.11m	50.4	37.2	32.9	378.9
Ningnamycin	56.2	50.7	41.9	227.0

3.2.4   Conclusions

In summary, a series of new chiral thiourea derivatives containing α-aminophosphonate moiety **3.11a-3.11n** were designed and synthesized by the addition reaction of O, O' -dialkyl isothiocyanato (phenyl) methylphosphonate **3.10** with chiral amine in THF. The *in vivo* tests indicated that compounds **3.11g**, **3.11e** and **3.11k** and **3.11m** exhibited a very similar curative activity level as that of Ningnanmycin against TMV. Therefore, the present work demonstrates that the antiviral activity of chiral thiourea derivatives was significantly improved via the introduction of the *S* configuration. Effects of steric parameters on structure activity relationships and structural modification studies for identifying lead bioactive compounds are undertaken. The (*S*)-isomers for **3.11g** and **3.11e** and **3.11k** and **3.11m** display improved activity in comparison with (*R*)-enantiomers of **3.11h** and **3.11f** and **3.11l** and **3.11n** against TMV.

References

1.   Smith J, Liras J L. Solid and solution phase organic syntheses of oligomeric thioureas. *J. Org. Chem.*1996, 61, 8811-8818.

2.   a)Chalina E G, Chakarova L. Synthesis, hypotensive and antiarrhythmic activities of 3-alkyl-1-(2-hydroxy-5, 8-dimethoxy-1, 2, 3, 4-tetrahydro-3-naphthalenyl) ureas or thioureas and their guanidine analogs. *Eur. J. Med. Chem.*1998, 33, 975-983; b)Stark H, Purand K, Ligneau X, et al. Novel carbamates as potent histamine H3 receptor antagonists with high *in vitro* and oral *in vivo* activity. *J. Med. Chem.*1996, 39, 1157-1163; c)Walpole C, Ko S Y, Brown M, et al. 2-Nitrophenylcarbamo-yl-(*S*)-prolyl-(*S*)-3-(2-naphthyl)alanyl-*N*-benzyl-*N*-methyl-amide (SDZ NKT 343), a potent human NK1 tachykinin receptor antagonist with good oral analgesic activity in chronic pain models. *J. Med.Chem.* 1998, 41(17), 3159-3173.

3.   Mallams A K, Morton J B, Reichert P. Semisynthetic aminoglycoside antibacterials. Part 10. Synthesis of novel 1-*N*-aminoalkoxycarbonyl and 1-*N*-aminoalkylcarboxamido derivatives of sisomicin, gentamicin B, gentamicin C1a, and kanamycin A. *J. Chem. Soc., Perkin Trans* 1, 1981, 2186-2208.

4.   Ramadas K, Suresh G, Janarthanan N, et al. Antifungal activity of 1, 3-disubstituted symmetrical and unsymmetrical thioureas. *Pestic. Sci.*1998, 52(2), 145-151.

5.   George C, Mdrtin H, Ray R. Thiourea derivatives of 2-aminooxazoles showing antibacterial and antifungal activity. *J. Med. Chem.*1973, 16(12), 1042.

6.   Schroeder D C. Thiourea compounds are well known to possess biological activity. *Chem.Rev.*1955, 55, 181.

7.   Sarkis G Y, Faisal E D. Synthesis and spectroscopic of some new N, N'-disubstituted thiourea of potential biological interest. *J.Heterocycl.Chem.*1985, 22, 137-140.

8.   Nene Y L, Thapliyal P N. Fungicides in Plant Disease Control, 3rd.IBH Publishing Co., Oxford, 1993.

9.   Jiang L, Zheng H T, Liu T Y, et al. Asymmetric direct vinylogous carbon-carbon bond formation catalyzed by bifunctional organocatalysts. *Tetrahedron.*2007, 63, 5123-5128.

10.   Venkatachalam T K, Vassilev A O, Benyunov A, *et al*. Stereochemistry as a determinant of the anti-leukemic potency of halopyridyl and thiazolyl thiourea compounds. *Letters in Drug Design* & *Discovery*. 2007, 4, 318-326.

11. Venkatachalam T K, Sudbeck E A, Mao C, *et al*. Stereochemistry of halopyridyl and thiazolyl thiourea compounds is a major determinant of their potency as nonnucleoside inhibitors of HIV-1 reverse transcriptase. *Bioorg.Med.Chem.Lett*. 2000, 10(18), 2071-2074.

12. Venkatachalam T K, Mao C, Uckun F M. Effect of stereo and regiochemistry towards wild and multidrug resistant HIV-1 virus: viral potency of chiral PETT derivatives. *Biochem Pharmacol*.2004, 67(10), 1933-1946.

13. Venkatachalam T K, Mao C, Uckun F M. Effect of stereochemistry on the anti-HIV activity of chiral thiourea compounds. *Bioorg.Med.Chem*.2004, 12, 4275-4284.

14. Venkatachalam T K, Mao C, Uckun F M. Stereochemistry as a major determinant of the anti-HIV activity of chiral naphthyl thiourea compounds. *Antivir.Chem.Chemo-therapy*.2001, 12, 213-221.

15. Hamza A, Schubert G, Soos T, *et al*. Theoretical studies on the bifunctionality of chiral thiourea-based organocatalysts: Competing routes to C-C bond formation. *J.Amer.Chem.Soc*.2006, 128(40), 13151-13160.

16. Yalalov D A, Tsogoeva S B, Schmatz S. Chiral thiourea-based bifunctional organo-catalysts in the asymmetric nitro-Michael addition: a joint experimental- theoretical study. *Adv. Synth. Catal*. 2006, 348, 826-832.

17. Kleidernigg O P, Lindner W. Indirect separation of chiral proteinogenic α-amino acids using the fluorescence active (1*R*, 2*R*)-*N*-[(2-isothiocyanato) cyclohexyl]- 6-methoxy-4-quinolinylamide as chiral derivatizing agent: A comparison.   *J. Chromatogr. A*. 1998, 795, 251-261.

18. Zhou Z Z, Ji F Q, Cao M, *et al*. An efficient intramolecular Stetter reaction in room temperature ionic liquids promoted by microwave irradiation. *Adv. Synth. Catal*.2006, 348, 1826.

19. a)Gooding G V Jr, Hebert T T. A simple technique for purification of tobacco mosaic virus in large quantities. *Phytopathology*. 1967, 57, 1285-1290; b)Song B A, Zhang H P, Wang H, *et al*. Synthesis and antiviral activity of novel chiral cyanoacrylate derivatives. *J. Agric. Food. Chem*.2005, 53(20), 7885-7891.

20. Hodgkins J E, Reevesv W P. The Modified Kaluza synthesis: III. The synthesis of some Aromatic isothiocyanates. *J. Org Chem*.1964, 29(10), 3098-3099.

21. Kuhkar V P, Hudson H R, Eds.Synthesis of α-aminoalkanephosphonic and α-Aminophosphonic Acids; John Wiley & Sons; Chichester.2000.

22. Gioia P L, Chuah P H, Sclapari T. Herbicidal composition comprising an aminophosphate or aminophosphonate salt. WO 2007054540, 2007.

23. Yang S, Gao X W, Diao C L, *et al*. Synthesis and antifungal activity of novel chiral α-aminophos-phonates containing fluorine moiety. *Chin. J. Chem*.2006, 24, 1581-1588.

24. Kafarski P, Lejczak B. Biological activity of aminophosphonic acids. *Phosphorus Sulfur*.1991, 63, 193-215.

25. Jin L H, Song B A, Zhang G P, *et al*. Synthesis, X-ray crystallographic analysis, and antitumor activity of N-(benzothiazole-2-yl)-1 -(fluorophenyl)- *O,O*- dialkyl-α-aminophosphonates. *Bioorg. Med.Chem. Lett*. 2006, 16, 1537-1543.

26. Kafarski P, Lejczak B. Aminophosphonic acids of potential medical importance. *Curr. Med. Chem. Anti-Cancer Agents*.2001, 1, 301-312.

27. Lintunen T, Yli-Kauhaluoma J T. Synthesis of aminophosphonate haptens for an aminoacylation reaction between methyl glucoside and a-alanyl ester. *Bioorg.Med.Chem.Lett*.2000, 10, 1749-1750.

28. Liu W, Rogers C J, Fisher A J. Aminophosphonate inhibitors of dialkylglycine decarboxylase: Structural basis for slow, tight binding inhibition. *Biochem*.2002, 41, 12320-12328.

29. Pan W D, Ansiaux C, Vincent S P. Synthesis of acyclic galactitol- and lyxitol- aminophosphonates as inhibitors of UDP-galactopyranose mutase. *Tetrahedron Lett*. 2007, 48, 4353-4356.

30. Deng S L, Baglin I, Nour M, *et al*. Synthesis of ursolic phosphonate derivatives as potential anti-HIV agents. *Phosphorus,   Sulfur and Silicon and the Related Elements*. 2007, 182, 951-967.

31. Hu D Y, Wan Q Q, Yang S, *et al*. Synthesis and antiviral activities of amide derivatives containing *α*-aminophosphonate moiety. *J. Agric.Food Chem*.2008, 56(3), 998-1001.

32. Long N, Cai X J, Song B A, *et al*. Synthesis and antiviral activities of cyanoacrylate derivatives containing an *α*-aminophosphonate moiety. *J. Agric. Food Chem*.2008, 56(13), 5242-5246.

33. Huang R Q, Wang H L, Zhou J. *Preparation of Organic Intermediate*, 2001, 224-225.

34. Kaboudin B, Moradi K. A simple and convenient procedure for the synthesis of 1-aminophosphonates from aromatic aldehydes. *Tetrahedron Lett*.2005, 46, 2989-2991.

35. Wang T, Ye W F, He H W. Preparation of isocyanates, isothiocyanates and iso- selenocyanates in the laboratory. C*hemical reagents*. 2002, 24(4), 204-207.

36. Yan Z K, Cai X J, Yang S, *et al*. Synthesis and antiviral activities of chiral thiourea derivatives. *Chin J. Chem*. 2009, 27(3), 593-601.

37. Chen M H, Chen Z, Song B A, *et al*. Synthesis and antiviral activities of chiral thiourea derivatives containing *α*-aminophosphonate moiety. *J. Agric. Food Chem*.2009, 57(4), 1383-1388.

Chapter 4
The Heterocyclic Antiviral Agents

4.1   Pyrazole Derivatives Containing Oxime Ester Moiety

4.1.1   Introduction

Pyrazole and their derivatives exhibit a broad spectrum of biological activities such as antimicrobial, [1] herbicidal, [2,3] antitumor, [4,5] anti-inflammatory activities.[6-8] Among them, some are used as insecticides, herbicides and fungicides, such as fipronil (Colliot et al, 1992), topramezon (BASF, 2006), pyraelostrobin (BASF, 2001), and so on. With growing application on their synthesis and bioactivity, chemists and biologists in recent years have directed considerable attention on the research of pyrazole derivatives.

TMV infection is very widely distributed, and can cause serious damage and large economic loss. It was found that in certain fields 90%-100% of the plants show mosaic by harvesting time. Due to the unsatisfactory curative effect (30%-60%) by common antiviral agent Ningnanmycin (or Virus A) and economic loss of tobacco, a wide range of chemicals have been synthesized and tested for antiviral effects during screening for biological activity. However, since there are only a few reported economically viable antiviral chemicals available for practical application in agriculture, [9] a great deal of scope still persists for further research in this field. In view of this, we turned our attention to evaluate the modification of the biological profile induced by the change of the substituents at the 1,3,4 or 5-position in pyrazole ring.

Pyrazolaldoxime esters at 4-position are scarcely evaluated for their antiviral activities. Due to their known fungicidal activities, we reasoned that if oxime esters are linked at 4-position in the pyrazole ring, the resulting compounds will have better bioactivities. Therefore, in our pursuit to develop new class of agrochemicals, we synthesized a series of pyrazole deratives containing oxime ester moiety and studied their antiviral activities. The synthetic route is shown in Scheme 4.1. Starting from the key intermediate 1-substituted phenyl-3-methyl-5-substitutedphenylthio-4-pyrazolaldoximes **4.3**, the pyrazole oxime esters **4.4**

were synthesized in one step by reacting **4.3** with acyl chloride. The structures of **4.4** were firmly established by well-defined IR, ^{1}H NMR, ^{13}C NMR and elemental analysis. Preliminary bioassay tests showed that some compounds possess certain degree of antiviral activity against TMV at 500 mg/L *in vivo* as shown in Table 4.2, however with a degree of variation. The title compounds **4.4l** and **4.4m** had high curative and inactivation activities against TMV, and the inhibitory effects for the two treated methods ranged from 60.0% to 85.6%. The preliminary studies on action mechanism of compound **4.4l** against TMV revealed that it was capable to enhance the defense related enzyme activity within a certain period and up-regulate PR-1a gene expression. Further studies on the relationship among compound **4.4l** and TMV CP and TMV RNA showed special affinity of **4.4l** for CP, but not for RNA. The compound **4.4l** exhibited a good curative activity through induction of PR-gene expression and improvement of defense related enzyme activity access to SAR, and a good inactivation activity through special affinity for CP.

4.1.2   Materials and Methods

4.1.2.1   Analysis and Instruments

The materials and instruments for determination of the structure and physical data of new compounds are basically similar to the procedure described in Chapter 1.1.2.1-Aryl-3-methyl-1H-4-pyrazoleylformaldehydes   and   1-(4-chlorophenyl)-3-methyl-1H-4-pyrazolyl-formaldehydes   were   prepared   according   to   literature method as described.[19-21] Intermediates 1-aryl-3-methyl-5-chloro-1H-4-pyrazolyl-formaldehydes **4.1**, **4.2** and **4.3** were prepared according to the reported methods.[22]

4.1.2.2   Preparation of pyrazolaldoxime ester derivatives (4.4a-4.4n)

A 100 mL round-bottomed flask equipped with a magnetic stirrer was charged with **4.3**(1.5 mmol) and dichloromethane(50 mL) and pyridine (0.012mol). The reaction mixture was stirred at room temperature for 10 min, and then was added drop wise acyl chloride R^{3}COCl (0.012mol) dissolved in 20 mL dichloro-methane over a period of 0.5 h and refluxed for 4 h. The mixture was cooled and washed with 5% Na$_2$CO$_3$ solution and distilled water, dried over anhydrous MgSO$_4$. The solvent was removed and the crude product was purified by chromatography (petroleum ether/ethyl acetate, 2/1) and recrystallized from ethanol to give compound **4.4**. The reperesentative data for **4.4a** is shown below, while data for **4.4b-4.4n** can be found in the reference.[79]

1-phenyl-3-methyl-5-(4-methylphenylthio)-4-pyrazolaldoxime acetate (**4.4a**). White crystal, mp 90-91℃, yield 81%; IR(KBr)：v_{max} 3019(Ar-H), 2975, 923(CH$_3$＋CH$_2$), 1775(C＝O), 1616(C＝N), 1499(Ar skeleton vibration), 1194(C＝N—N), 801(*p*-disubstituded benzene), 662(C—S—C); ^{1}H NMR(500 MHz, DMSO-d_6)：δ

8.45(s, 1H, CH—H), 7.44-7.49(m, 5H, Ph—H), 7.06(d, J=8.05 Hz, 2H, S—Ph-3, 5-H), 6.88(q, J=8.00 Hz, 2H, S—Ph—2, 6—H), 6.87(t, J=8.05 Hz, J=9.16 Hz 2H, S—Ph—3, 5—H); 3.38(s, 3H, O=C—CH$_3$—H), 2.2(s, 3H, pyrazole-CH$_3$—H), 2.1(s, 3H, Ph—CH$_3$—H); ^{13}C NMR(125 MHz, DMSO-d_6)：δ 168.9, 149.8, 149.2, 138.7, 137.3, 135.2, 130.7, 130.5, 129.4, 129.2, 128.1, 126.1, 116.9, 20.9, 19.9, 14.9; Anal. Calcd. for C$_{20}$H$_{19}$N$_3$O$_2$S (365.0)：C, 65.47; H, 5.20; N, 11.50. Found：C, 66.55; H, 5.12; N, 10.54.

4.1.2.3　Crystal structure determination

The experiment and method for X-ray diffraction data of compound **4.4n** are similar to the procedure described in Chapter 1.4.2.[23-25] Crystallographic data for the structure **4.4n** have been deposited with the Cambridge Crystallographic Data Center as supplementary publication No. CCDC-696918.

4.1.2.4　Protection and inactivation and cure effect of compound against TMV *in vivo*

Purification of TMV was assessed by Gooding's method.[26] The bio-activity assay for protection and inactivation and cure effect was assessed according to Li's method.[27]

4.1.2.5　Determination of PAL and POD and SOD activity

The leaf samples were homogenized in the 2-mercaptoethanol-boric acid buffer (5 mM, pH 8.8) on the ice bath and centrifuged. The supernatant was used for experiment. PAL and POD and SOD activities were determined by He's method, [28] Polle's method, [29] Beauchamp's method, [30] respectively.

4.1.2.6　RT-PCR assay

Trizol kit was used according to the standard protocol for total RNA isolation. Prior to RT-PCR, the total RNA samples were treated with DNase I for 10 min and quantified by spectrophotometer and identified by agarose gel electro-phoresis.[31] cDNA was synthesized with Oligo (dT)$_{18}$ at the 3′ end of mRNA as a primer. Total RNA (1μg) was used for template of first-strand cDNA synthesis using extend reverse transcriptase. Reverse transcription was carried out at 37℃ for 1 h. The single-stranded DNA mixture was used as template in PCR. The primers for PCR amplification are shown in Table 4.1. The PCR was performed in Tris-HCl buffer (10 mM, pH 8.3), KCl (50 mM), MgCl$_2$ (1.8-2.0 μL), dNTPs (0.02 μM), primers (0.04 μM), DNA polymerase (1 U). PCR amplification steps consisted of a preliminary denaturation step at 94℃ for 1 min, followed by 35 cycles at 94℃ for 40 seconds, at 58℃ for 40 seconds and at 72℃ for 50 seconds on icycle of BioRad. PCR products were separated on 1.5% agarose gel in 0.5×TBE buffer and visualized under UV light after staining with ethidium bromide.[32]

Table 4. 1   Sequences of gene-specific primers used in RT-PCR analysis.

Gene family	Accession No.	5′ primer	3′ primer
β-actin	U60495	5′-gacatgaaggaggagcttgc-3′	5′-atcatggatggctggaagag-3′
PR-1a	X12737	5′-caatacggcgaaaacctagctga-3′	5′-cctagcacatccaacacgaa-3′
PR-5	X03913	5′-gcttcccctttatgccttc-3′	5′-cctgggttcacgttaatgct-3′

Semi-quantitative PCR for expression of gene. In order to assess relative expression levels of target-gene in water-treated tobacco and **4.4l** and TMV-treated tobacco and tobacco by inoculated TMV only, semi-quantitative PCR consisting of 20 cycles (within the logarithmic range of amplification of gene) with putting primer of β-actin serving as an internal reference gene was employed for the study. The amplified products were analyzed on a 1.5% agarose gel by the method of Mohamed.[33]

4.1.2.7   The relative quantification real-time PCR for expression of the target gene

The relative quantification real-time PCR was carried out with iCycler IQ according to manufacturer's protocol with primer of β-actin serving as an internal reference gene. Precautions were taken to ascertain reliable quantitative results：Log-linear dilution curves were performed with primers for the target gene as well as with primers for the β-actin. Reactions performed without reverse transcriptase or without template did not result in any product. By following PCR, 110 steps for melt curve analysis were completed in 10 seconds at temperature ranging from 40℃ to 95℃. The amplification efficiency was 95%-99% for PR-1a and PR-5 gene, respectively (The standard curve figures are not shown). Each target gene peak was assigned an arbitrary quantitative value correlated to the β-actin gene peak, according to the formula $\Delta\Delta C_T = \Delta C_{T, test} - \Delta C_{T, calibrator}$，$C_T$ being the cycle threshold. Rates of stimulation of RNA expression were calculated from the ΔC_T values at various time points.[34]

4.1.2.8   The primary spectroscopic study of compound 4.4l for TMV CP

Owing to the presence of tryptophan and tyrosine, protein can emit fluorescence. Therefore, the fluorescence method has sometimes been employed to study the interaction between protein and small drug molecules, the latter being known as fluorescence quencher[35,36] as it can quench the intrinsic fluorescence from the protein. It could be seen that TMV CP containing 3 tryptophan and 5 tyrosine is constituted from 155 amino acids from NCBI protein AAD20291. TMV CP was isolated by acetic acid methods.[37] TMV CP was dissolved in 10mM phosphate potassium buffer, pH 7.1, 50 mM NaCl. At the concentration of 0.01% of **4.4l** and 0.65 mg/mL of TMV CP, the interaction between the **4.4l** and TMV CP ceased to exist and a full spectrum scan was made for the samples with ultraviolet spectroscopy (wavelength range from 200 to 600 nm). Using fluorescence spectroscopy method, at the resolution of TMV CP 4S and 20S protein at concentration of 1.32 μM, a full spectrum scan (wavelength range from 280 to 400 nm) to the samples was made at 278 nm excitation wavelength.

4.1.2.9   The determination of quenching constants

The course of fluorescence quenching was divided into the dynamic quenching and the static quenching.[35] The dynamic quenching involves the interaction between fluorescence quencher and the excited molecular state of the substance. The action mechanisms accord to the following formulas：

Stern-Volmer equation：

$$F_0/F=1+K_q t_0[Q]=1+K_{sv}[Q]$$

Lineweaver-Burk equation：

$$(F_0 - F)^{-1}=F_0^{-1} + K_{LB}F_0^{-1}[Q]^{-1}$$

F_0：the fluorescence intensity of substance as the quencher was not added. F：the fluorescence intensity of substance as the quencher was added. $[Q]$：the concentration of quencher. K_{sv}：The dynamic quenching constants, or the constants of Stern-Volmer. K_q：the constants of collisional quenching rates. K_{LB}：the static quenching constants.

4.1.2.10   The primary spectroscopic study of compound 4.4l for TMV RNA

As RNA contained cyanine dye can emit more intensity of fluorescence than RNA-treated only, some reports employ the fluorescence method to study the interaction between RNA and small drug molecules because quencher, small drug molecules, can competitively bind with RNA, causing cyanine dye to depart from RNA. TMV RNA was dissolved in 10mM phosphate potassium buffer, pH 7.1, 50 mM NaCl. At the concentration of **4.4l** varying from 19.952 μM to 159.616 μM, the interaction between **4.4l** and TMV RNA was found to disappear as detected by fluorescence spectroscopy at the excitation and emission wavelength of TMV RNA of 495nm and 525 nm, respectively.[37]

4.1.2.11   Statistical analysis

All statistical analyses were performed with SPSS 10.0. Data were analyzed by one-way analysis of variance (ANOVA). Mean separations were performed using the least significant difference method (LSD test). Each experiment had three replicates and all experiments were run three times with similar results. Measurements from all the replicates were combined and treatment effects analyzed.

4.1.3   Chemistry

4.1.3.1   Synthesis of novel pyrazole derivatives

The synthetic route designed for the oxime ester analogues **4.4** is summarized in Scheme 4.1. Starting from 1-substituted phenyl-3-methyl-4-pyrazolone derivatives, the intermediate **4.1**, 1-substituted phenyl-3-methyl-4-
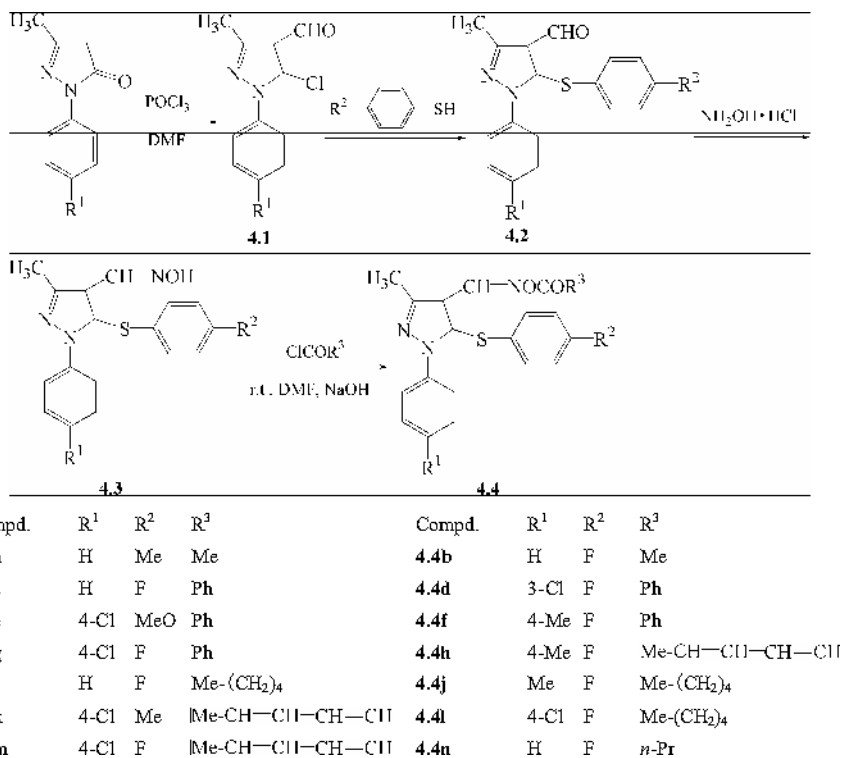
Scheme 4.1   Synthetic route to the compound **4.4**

Compd.	R^1	R^2	R^3	Compd.	R^1	R^2	R^3
4.4a	H	Me	Me	**4.4b**	H	F	Me
4.4c	H	F	Ph	**4.4d**	3-Cl	F	Ph
4.4e	4-Cl	MeO	Ph	**4.4f**	4-Me	F	Ph
4.4g	4-Cl	F	Ph	**4.4h**	4-Me	F	Me-CH—CH—CH—CH
4.4i	H	F	Me-(CH$_2$)$_4$	**4.4j**	Me	F	Me-(CH$_2$)$_4$
4.4k	4-Cl	Me	Me-CH—CH—CH—CH	**4.4l**	4-Cl	F	Me-(CH$_2$)$_4$
4.4m	4-Cl	F	Me-CH—CH—CH—CH	**4.4n**	H	F	n-Pr

formyl-5-chloropyrazole was prepared by chlorination reaction with POCl$_3$ in DMF. Then, treatment of **4.1** with substituted thiophenol afforded 1-substituted phenyl- 3-methyl-5-substituted phenylthio-4-pyrazol-aldehyde **4.2**. Reaction of **4.2** with hydroxylamine hydrochloride gave 1-substituted phenyl-3-methyl-5-substituted phenylthio-4-pyrazolaldoximes **4.3**. The title compounds, 1-substituted-5-substitutedphenylthio-4-pyrazolaldoxime ester derivatives **4.4** were synthesized by the esterification reaction of **4.3** with acyl chloride (ClCOR^3).

4.1.3.2   Crystal structure analysis

It could be seen from the X-Ray single crystal analysis that the title compound **4.4n** maintains a planar structure (Fig 4.1, Fig 4.2). The structure of target compound **4.4n** was established by X-ray diffraction. The bond lengths of C(7)-C(8)(1.389 Å) and C(8)-C(9)(1.410 Å) are longer than normal C=C(1.34 Å), C(12)-O(1)(1.365 Å) is shorter than normal single C-O(1.44 Å), C(8)-C(11) (1.458 Å) and C(12)-C(13)(1.453 Å) are shorter than normal C-C (1.54 Å), C(11)-N(3)(1.269 Å) and C(3)-N(1)(1.444 Å) bonds are shorter than the normal C-N single bond (1.49 Å), suggesting the existence of an electron density delocalization among O(1)-N(3)-C(11)-C(8)-C(7)-N(1), C(9) and S(1).
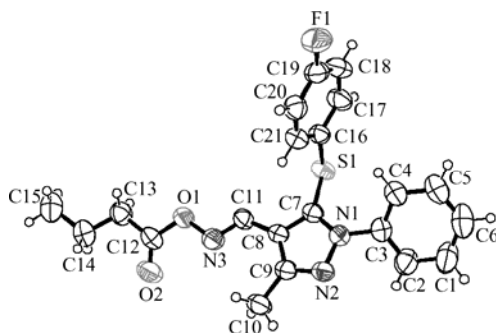
Fig 4.1 The molecular structure of compound **4.4n**
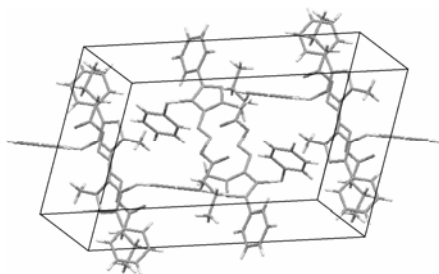
Fig 4.2 Packing diagram of the unit cell of compound **4.4n**

4.1.4 Antiviral Activity

4.1.4.1 Preliminary antiviral activity assay

The commercially available plant virucide Ningnanmycin, perhaps the most successful registered antiviral agents for plants available in China, was used as the positive control. The antiviral bioassay against TMV is assayed by the reported method and the antiviral results of all the compounds against TMV are listed in Table 4.2. The results showed that most of our designed compounds had moderate to good antiviral activities at 500 mg/L against TMV *in vivo*.

The title compounds **4.4a-4.4n** exhibited good curative activities of 30.0%-62.0% at 500 mg/L. Compound **4.4l** (R^1=4-Cl, R^2=F, and R^3=Me-$(CH_2)_4$), **4.4m** (R^1=4-Cl, R^2=F and R^3=Me-CH=CH—CHC=H) had higher activities (62.0% and 60.0%, respectively) than that of the positive control Ningnanmycin (56.0%). In addition, compounds **4.4a**, **4.4b**, **4.4f**, **4.4g**, **4.4h** and **4.4i** showed 40.8%-50.0% curative activities at 500 mg/L, with values of 47.8%, 40.4%, 50.0%, 47.7%, 46.7%, and 40.0%, respectively. From the data presented in Table 4.2, it can be observed that the title compounds **4.4a-4.4n** possess potential inactivation bioactivities, with values of 68.3%, 81.4%, 55.0%, 55.0%, 56.8%, 69.2%, 63.8%, 80.2%, 67.8%, 61.5%, 68.9%, 85.6%, 82.9% and 79.9% respectively at 500 μg/mL.

Table 4. 2   The Protection, inactivation and curative effect of the title
compounds **4.4a-4.4n** against TMV *in vivo* at 500(mg/L)

Compd.	Protection effect(%)	Inactivation effect(%)	Curative effect(%)
4.4a	33.8±1[*]	68.3±3[*]	47.8±2[*]
4.4b	36.7±4[*]	81.4±4[**]	40.4±3[*]
4.4c	28.8±3[*]	55.0±4[*]	34.9±6[*]
4.4d	41.0±8[*]	55.0±6[*]	30.2±7[*]
4.4e	27.6±5[*]	56.8±5[*]	35.0±6[*]
4.4f	48.4±7[*]	69.2±7[*]	50.0±9[*]
4.4g	35.0±5[*]	63.8±9[*]	47.7±9[*]
4.4h	26.0±6[*]	80.2±4[**]	46.4±3[*]
4.4i	28.9±5[*]	67.8±4[*]	40.2±6[*]
4.4j	40.9±5[*]	61.5±3[*]	30.0±5[*]
4.4k	50.0±7[*]	68.9±6[*]	38.9±4[*]
4.4l	31.0±6[*]	85.6±4[**]	62.0±8[**]
4.4m	28.3±5[*]	82.9±5[**]	60.0±8[*]
4.4n	25.9±6[*]	79.9±4[**]	34.0±3[*]
Ningnan mycin	68.0±5[*]	97.0±6[**]	56.0±4[*]

All results are expressed as mean±SD; n=3 for all groups; [*] $P<0.05,$ [**]$P<0.01$.

Among these compounds, **4.4b**, **4.4h**, **4.4l**, **4.4m and 4.4n** were appreciably more active than the rest, with the inactivation rates of 81.4%, 80.2%, 85.6%, 82.9% and 79.9% respectively, which were similar to that of Ningnanmycin (97%) against TMV at 500 μg/mL. The data also indicated that a change in the substituent might also affect the protection activity of title compounds **4.4a-4.4n**. Compound **4.4d** (R^1=3-Cl, R^2=F and R^3=Ph), **4.4f** (R^1=4-Me, R^2=F and R^3= Ph), **4.4j** (R^1=Me, R^2=F and R^3=Me-$(CH_2)_4$)) and **4.4k** (R^1=4-Cl, R^2=Me and R^3=Me-CH=CH—CHC=H) had moderate protection activities against TMV of up to 41.0%, 48.4%, 40.9% and 50.0% respectively at 500 μg/mL. The other compounds had a relatively lower curative activity than those of **4.4d**, **4.4f**, **4.4j**, and **4.4k**.

4.1.4.2   Effect of 4.4l treatment on PAL, POD and SOD activity in tobacco

As shown in Fig 4.3, using enzyme activity method, PAL, POD, SOD contents in **4.4l**-treated tobacco showed some definite trend within a certain period of time. POD and SOD levels in **4.4l**-treated tobacco increased by the end of the first day after the inoculation and reached up to 2.4 EU/mg and 40 EU/mg on the 7th day, respectively, 4 times greater than the first day after inoculation in enzyme levels. In contrast, in control and TMV treatment, no significant increase was detected. We found that PAL activity in **4.4l**-treated tobacco decreased from the 1st day to the 7th day after inoculation, similar trend was not observed on control and TMV.
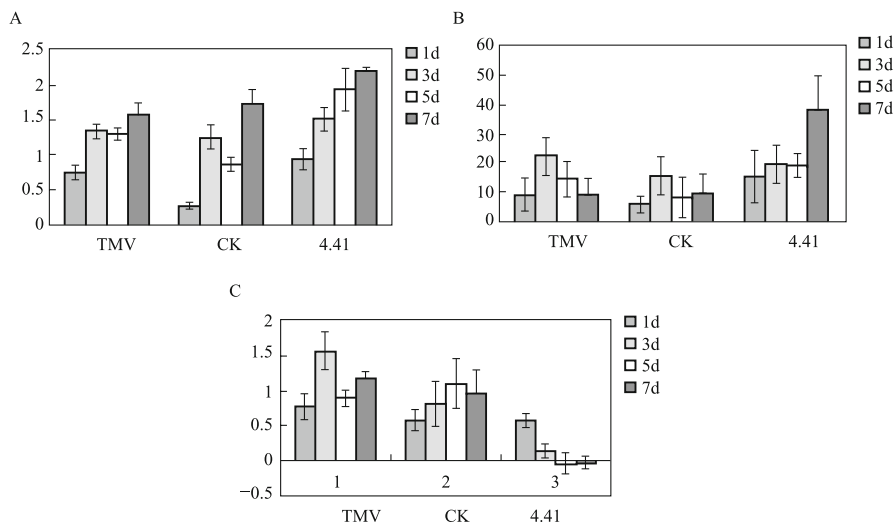
Fig 4.3   Effect of **4.4l** treatment on PAL and SOD and POD activity in *Nicotiana tabacum*. *Nicotiana tabacum* inoculated by TMV was treated with **4.4l** at 500 μg/mL for 1, 3, 5 and 7 day. Leaf sample extracts using homogenized and centrifuged methods were used to determine the PAL and SOD and POD activities as described in the 'Experimental'. Water treatment and TMV treatment were used for negative and positive controls respectively. Data were expressed as the mean $\pm$ SD(n=3) of three individual experiments. One-Way ANOVA revealed significant difference

4.1.4.3   Gene expression analysis of PR-1a and PR-5 in 4.4l-treated tobacco leaf

In vitro synthesized single-stranded cDNA from RNA samples was isolated from leaf in Ningnanmycin-treated tobacco, TMV-treated tobacco and the **4.4l** and TMV-treated tobacco. The differential expression analysis of the PR-1a and PR-5 gene was determined by the relative quantification PCR and real-time PCR analysis. As shown in Fig 4.4, the mRNAs of PR-1a gene accumulated to detectable levels in all-treated tobacco leaf, although, the gene up-regulation in **4.4l**-treated was found to be higher than the rest from the 3rd day to the 7th day. The gene expression ratio reached up to 26.6 on the 5th day, the corresponding values for Ningnanmycin and TMV treatment reached only up to 13.85 and 7.64, respectively. The values of compound **4.4l** were almost twice as large as compared to Ningnanmycin-treated tobacco.

As shown in Fig 4.5, the mRNA content of **4.4l** treated tobacco leaf for PR-5 gene slowly decreased from the 1st day to the start of the 3rd day, then gradually increased and reached a peak on the 5th day after the inoculation before showing a gradual decreasing trend again. Meanwhile, similar trends were also observed in TMV treatment tobacco leaf, although, for Ningnanmycin-treated tobacco leaf, significant increase in the levels of gene expression ratio was noticed from the 3rd day to 5th day, the value reaching up to 17.95. From above results, we found that
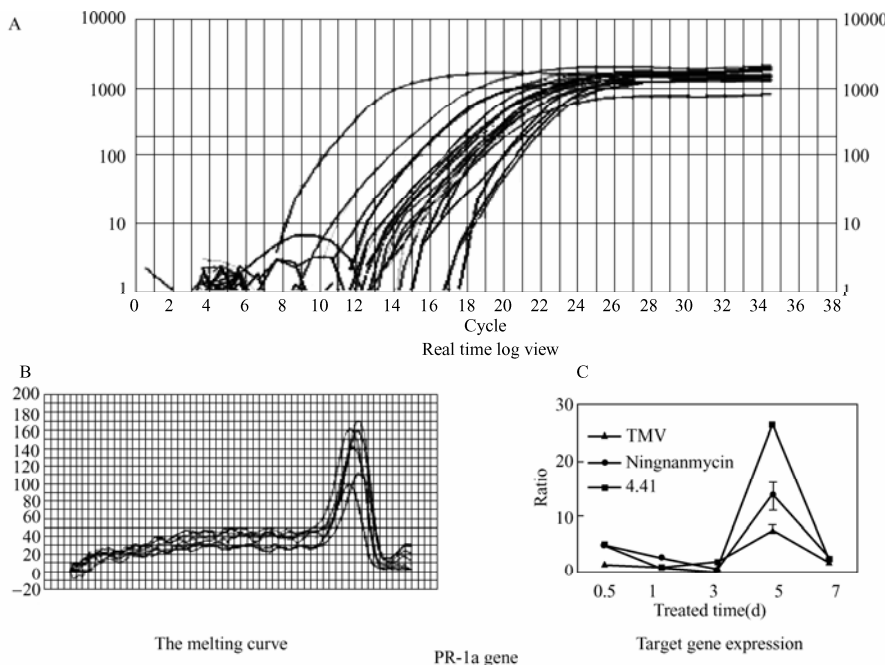
Fig 4.4　Real time PCR analysis of RNA isolated from tobacco leaf against PR-1a gene. A indicates real time log view of PR-1a gene; B in the figure indicates the melting curve of real time PCR against PR-1a gene. The temperature of the melting curve was 85℃, the results show that the PCR products were purified relatively and had no other non-specific products; C in the figure indicates the results of PR-1a gene expression ratio through C_T value formula $\Delta\Delta C_T = \Delta C_{T,test} - \Delta C_{T,calibrator}$. Relative values of real time PCR between target gene and β-actin gene were calculated, each value represents $\pm$SD(n=4) and each experiment was performed in triplicate sets. The data was analyzed by One-Way ANOVA.

compound **4.4l** could induce gene up-regulation of PR-1a without any effect in the regulation of PR-5 gene.

4.1.4.4　The primary spectroscopic study of **4.4l** for TMV CP

The ultraviolet-vis spectroscopic study of **4.4l** *for TMV CP.* The intrinsic UV-vis absorbance peak of TMV CP appeared mainly due to the presence of tryptophan and tyrosine in the CP peptide. As shown in Fig 4.6, blue line and red line correspond to the UV-Vis spectra for TMV CP and TMV CP-**4.4l** treatment, respectively. It could be seen from the red line in Fig 4.6A that the absorbance peak values were 2.726 and 0.195 at 207.0 nm and 281.0 nm respectively for 4S CP. The absorption peak values of 4S CP shifted toward the longer wavelength side as the compound **4.4l** was added and the maximum absorption peak increased from 2.726 to 3.136. In addition, the relatively smaller absorption peak value

Real time log view

The melting curve

Target gene expression
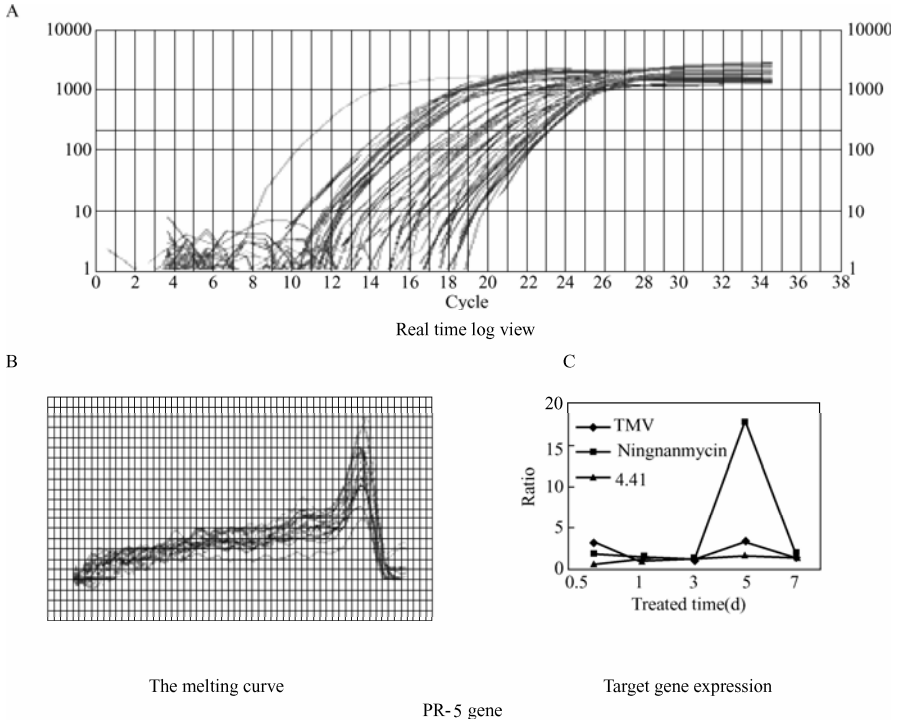
PR-5 gene

Fig 4.5   Real time PCR analysis of RNA isolated from tobacco leaf against PR-5 gene. A in the figure indicates real time log view of PR-5 gene; B in the figure indicates the melting curve of real time PCR against PR-5 gene. The temperature of the melting curve was 83℃, the results show that the PCR products were purified relatively and had no other non-specific products; C in the figure indicates the results of PR-5 gene expression ratio through C_T value formula $\Delta\Delta C_T = \Delta C_{T,test} - \Delta C_{T,calibrator}$. Relative values of real time PCR between target gene and β-actin gene were calculated, each value represents $\pm$ SD(n=4) and each experiment was performed in triplicate sets. The data was analyzed by One-Way ANOVA.
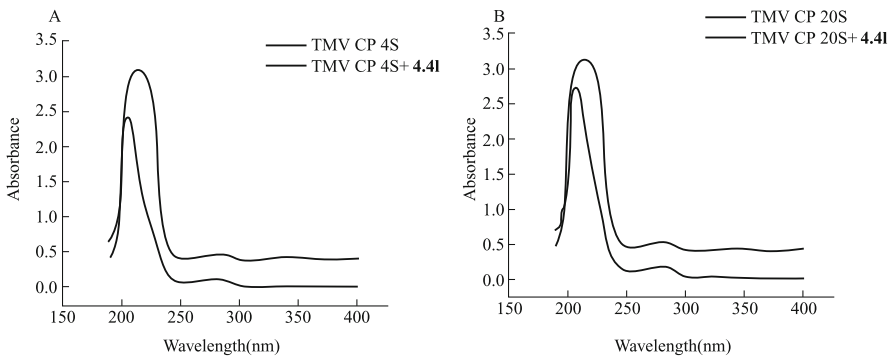
Fig 4.6   The ultraviolet spectroscopy of TMV CP 4S(A) r 20S(B) rotein and **4.4l**. TMV CP concentration was 0.65 mg/L and concentration of **4.4l** was varied from 0 to 0.01%.

shifted slightly toward the longer wavelength side as shown by the blue line in Fig 4.6A. Similar phenomenon could be observed for TMV CP 20S from Fig 4.6B. To conclude, as evident from Fig 4.6, a change in UV-Vis spectrum was noticed in the range 190-400nm as compound **4.4l** was added, red-shift-phenomenon occurred and peak value increased sharply around 207 nm and 280 nm. The results indicated that the compound **4.4l** could associate with CP.

Fluorescence spectroscopic study of **4.4l** *for TMV CP.* For studying the relationship of compound **4.4l** with TMV CP, fluorescence spectroscopic assay was used. At 278 nm excitation wavelength, emission wavelength of TMV CP revealed a maximum of emission at 325 nm. As shown in Fig 4.7A, the excitation wavelengths of TMV CP 4S shifted from 320 to 331 nm as compound **4.4l** was added, and the fluorescence intensity (a.u) of TMV CP decreased from 175 to 87. Meanwhile, from Fig 4.7B, it could be seen that the excitation wavelengths of TMV CP 20S shifted from 321.07 to 330 nm as compound **4.4l** was added, and the fluorescence intensity (a.u) of TMV CP 20S decreased from 168.14 to 87.35. From above results, red-shift of wavelengths and fluorescence quenching phenomenon for CP 4S and 20S were noticed when compound **4.4l** was added. These results also showed that the compound **4.4l** exhibited a higher affinity for TMV CP.
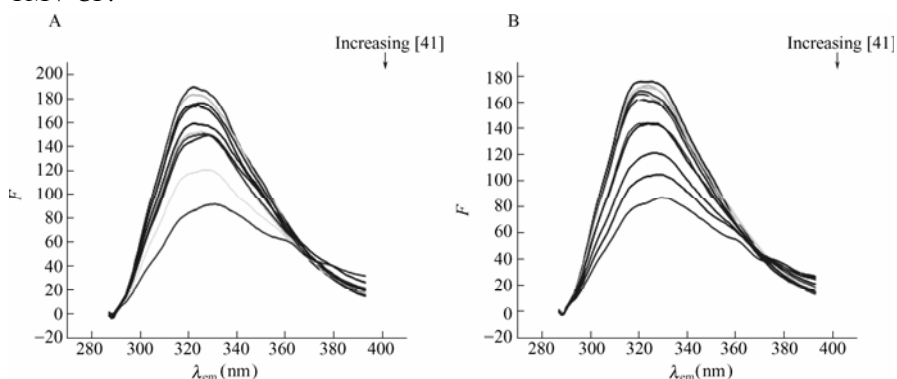
Fig 4.7   The Fluorescence quenching spectra of TMV CP 20S or 4S protein as **4.4l** is added. (1) 4.4l=0μM; (2) 4.4l=19.952 μM; (3) 4.4l=39.904 μM; (4) 4.4l=79.808 μM; (5) 4.4l=159.616μM; (6) 4.4l=203μM; (7) 4.4l=319.232 μM; (8) 4.4l=464μM; (9) 4.4l= 638μM；(10) Curves 1-10：TMV CP=1.32 μM. The data was recorded on Fluorescence Spetrophotometer (VARIAN CARY Eclipse) at 25℃. The excitation wavelength and emission wavelength of TMV CP are 278nm and 325 nm, respectively. The EX. Slit, EM. Slit and smoothing factor are 5nm, 5nm and 10, respectively.

The determination of quenching constants. The intrinsic fluorescence of TMV CP can be quenched by compound **4.4l** at 321 and 330 nm. As shown in Plot 8A, F_0/F presented a linear relationship against compound **4.4l** concentration for TMV CP 4S and 20S protein. From the plot 8A of F_0/F against compound **4.4l**

concentration, the dynamic quenching constants, K_{sv}, were easily calculated from the slope of the straight line, the values were 0.0031×10^4 and 0.0016×10^4 for TMV CP 4S and 20S protein, respectively (Table 4.3). According to the equation of the constants of collisional quenching rates (K_q), the K_q values were 31×10^8 and 16×10^8 for the above protein. The value was lower than the value of K_q, which is 2.0×10^{10} L • mol^{-1} • s^{-1} for all the fluorescence quenchers of biomacromolecule. Meanwhile, as shown in Plot 8B, the static quenching constants (K_{LB}) were 2.1681×10^{-7} and 3.9027×10^{-7} for the above protein (Fig 4.8) respeatively.

Table 4. 3 Regression equations and correlation coefficient

	Regression equations	R^2
Fig 4.7A 4S	$F_0/F=1.0231+0.0031\times10^4\,[4l]$	0.986
Fig 4.7A 20S	$F_0/F=0.9608+0.0016\times10^4\,[4l]$	0.9898
Fig 4.7B 4S	$(F_0-F)^{-1}=0.0028+2.1681\times10^{-7}\,[4l]^{-1}$	0.9997
Fig 4.7B 20S	$(F_0-F)^{-1}=0.011+3.9027\times10^{-7}\,[4l]^{-1}$	0.9728
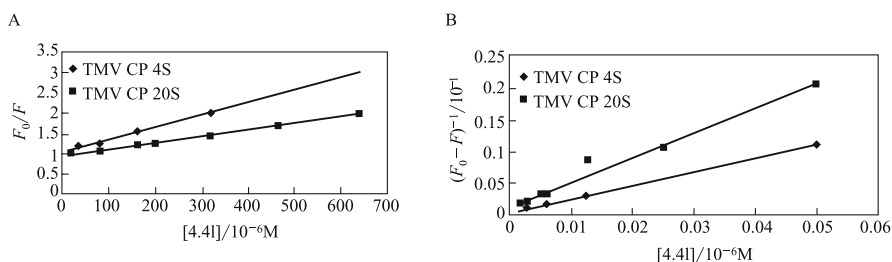
Fig 4.8 The Stern-Volmer curves(A)and the double-reciprocal curves(B)of TMV CP 4S and 20S protein.

Above results suggested a probable binding of compound **4.4l** with TMV CP mainly through dynamic quenching. The relation between **4.4l** and TMV CP is worthy of further investigation.

    Fluorescence spectroscopic study of* 4l *for TMV RNA. As shown in Fig 4.9, at 495 nm excitation wavelength, emission wavelength of TMV RNA was 525 nm, the fluorescence intensity of TMV RNA was relatively moderate, and reached up to 52.30 a • u. The fluorescence intensity was lower for cyanine dye, the value being 3.73 a • u which was close to 0 a • u. When the TMV RNA was mixed with cyanine dye, the fluorescence intensity of the system was increased suddenly, reached to 857.2 a • u at 528.95 nm for emission wavelength. When compound **4.4l** was added to the system of TMV RNA and cyanine dye, the fluorescence intensity was not significantly changed but the fluorescence intensity of the system containing compound **4.4l** was noticed to be comparatively lower. As the differences of the fluorescence intensity were not observed in every concentration group, it was believed that compound **4.4l** had no effect on TMV RNA.

4.1.5   Discussion

With the help of biochemistry and molecular biology, significant progress has been made in the antiviral action mechanism studies. At present, we have great understanding about pathogenic mechanism of plant virus and disease resistance mechanism from plant host and pharmacological mechanism of some commercially employed anti-viral reagents. Some studies have revealed that the plant defense related enzymes [10-12] and some signal transduction pathways mediated by SA and PR can correlate SAR and induce expression by anti-viral agents thereby playing an important role in anti-viral action mechanism.[13–17] Other studies showed that small natural molecules possessed inhibition activity of plant virus proliferation by specially binding with sub-components of virus such as virus nucleic acid or protein. [18]Our results indicate that compound **4.4l** induced up-regulation of PR-1a gene, the downstream molecule of SA-mediated signal transduction pathway, from 3rd day to 5th day; the corresponding ratio in **4.4l**-
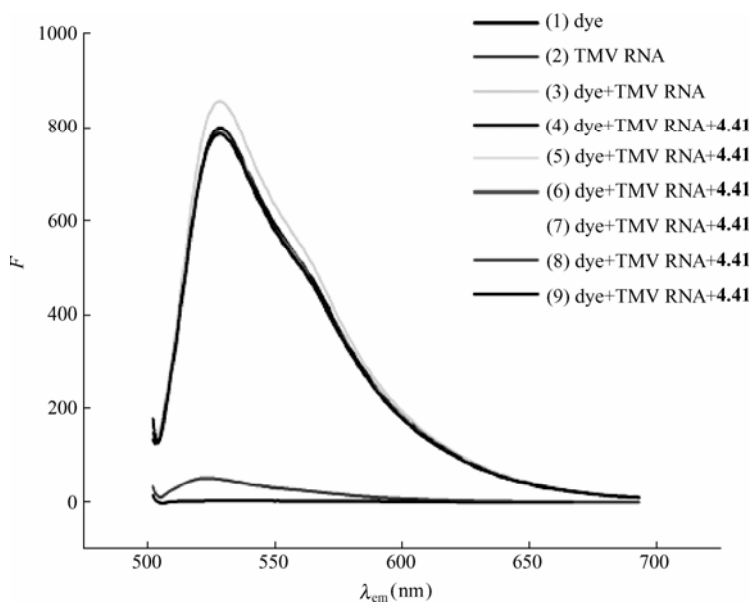
Fig 4.9   The Fluorescence quenching spectra of TMV RNA as 4l and cyanine dye are added.1. cyanine dye by treated only; 2. TMV RNA by treated only; 3. cyanine dye and TMV RNA by treated; 4-9. The resolution of cyanine dye and TMV RNA as **4.4l** was added. The concentration of **4.4l** was increased from 19.952 μmol・L^{-1} to 159.616μmol・L^{-1}. The data was recorded on Fluorescence Spetrophotometer (VARIAN CARY Eclipse) at 25℃. The excitation wavelength and emission wavelength of TMV CP are 495nm and 525 nm, respectively. The EX. Slit and EM. Slit and smoothing factor are 5nm, 5nm and 15, respectively.

treated tobacco leaf was 4 times as large as that in TMV-treated tobacco leaf on the 5th day after inoculation. Meanwhile, during the 1st day to the 7th day, the activity increase of POD and SOD was noticed in compound **4.4l** treatment, but not detected in CK and TMV treatment. So we assumed that compound **4.4l** possessed the capacity to induce disease resistance. Moreover, using ultraviolet-vis spectroscopic and fluorescence spectroscopic methods, we found that compound **4.4l** had affinity to TMV CP 4S and 20S protein by induction to red-shift and fluorescence quenching phenomenon, but not to TMV RNA. As TMV CP possessed the ability to protect TMV RNA from digestion by ribonuclease and then help the formation of normal virus particle, anti-viral activity of compound 4.4l was also thought to be associated with affinity towards TMV CP. So we infer that the anti-viral action mechanism might be through multiple action modes for compound **4.4l**. Future research would be focused on the study of gene regulation by northern blot and real-time PCR methods such as pathogenesis-related gene family member, determination of SA content by isolation, extraction and HPLC methods, studies on various molecular levels in SA signaling pathway by gene knock-out and gene knock-in technology, and ascertaining of molecular target sites. Meanwhile, capillary electrophoresition mode between compound **4.4l** and TMV CP, the site-directed mutagenesis technology was used to construct the CP peptide containing anticipated amino acids in advance, and analysis of the specific action location of the CP for compound **4.4l** was made through the single-crystal diffraction and simulation methods to further verification.

4.1.6   Conclusions

In conclusion, a series of novel pyrazole derivatives were synthesized by the treatment of 1-substituted phenyl-3-methyl-5-substituted phenylthio-4-pyrazolal-doximes **4.3** with acyl chloride. Their structures were verified by spectroscopic data. The results of bioassay showed that these title compounds exhibited weak to good anti-TMV bioactivity. Title compounds **4.4l**, **4.4m** showed better biological activity than their structurally related analogues **4.4a**-**4.4k** and **4.4n**. Preliminary studies showed that treatment by compound **4.4l** can significantly enhance disease resistance of tobacco and also show that the compound **4.4l** is structurally related to TMV by exhibiting a higher affinity for TMV CP. So, the action mechanism of curative effect by the compound **4.4l** was mainly attributed to the induced disease resistance against tobacco while the action mechanism of inactivation effect was caused by its affinity towards TMV CP. More detailed studies on mechanistic aspects are currently underway.

4.2   Pyrazole Derivatives Containing Oxime Ether Moiety

4.2.1   Introduction

Pyrazole and its derivatives are typical hererocyclic compounds which find important position in medicinal and pesticide chemistry with wide range of bioactivities. As medicines, many of them display antibacterial, [38] antimicrobial, [39] anticancer, [40] antiinflammatory, [41] selective enzyme inhibitory activities.[42] As pesticides, they are used as insecticides, [43] fungicides, [44,45] and herbicides.[46–48] As shown in **4.5-4.8**, for example, Pyrazophos, the first fungicide of this class to be commercialized, was put on the market for control of powdery mildew in vegetable by Hoechst AG in 1974 and more than 10 pyrazole derivatives are now commercially available. The advantages such as novel mode of action, wide spectrum, low toxicity toward mammalian cells and favorable profiles to human being prompted chemists to design and synthesize novel pyrazole derivatives. Recently, the pyrazole compounds such as, Penthiopyrad (Mitsui Toatsu Chemicals, 1995) and Pyraclostrobin (BASF, 2001) were found to have potential antifungal activities for the control of some plant diseases. With growing application on their synthesis and bioactivity, chemists and biologists in recent years have directed considerable attention on the research of pyrazole derivatives.[49]

4.5(pyrazophos)   **4.6**(furametpyr)

4.7(penthiopyrad)   **4.8**(pyraclostrobin)
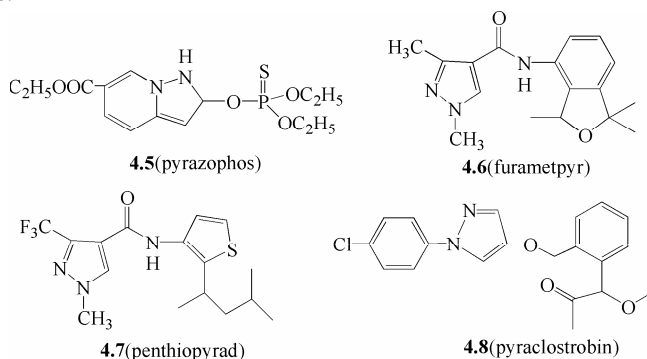
Tobacco mosaic virus (TMV) infection is widely distributed, and can cause serious damage and large economic loss. It was found that in certain fields 90%-100% of the plants show mosaic by harvesting time. In view of the unsatisfactory curatives (30%-60%) cure rate obtained by common antiviral agent Ningnanmycin (or Virus A) and widespread economic loss of tobacco, further research needs to be conducted in this area for the development of a highly efficient, novel environmentally benign antiviral agent.

Modification of structural profile by the change of substituents at the 1 or 3 or 4-position in pyrazole ring can bring about significant change in bioactivity.

However, pyrazolaldoxime ethers bearing other heterocyclic moities have been scarcely been evaluated for their activities.[50,51] It has been demonstrated that the pyridine and pyrazole groups are important pharmacophores of many fungicides. Linking the pyridine and pyrazole group with a structurally diverse side chain is an effective way to obtain new heterocyclic derivatives with high fungicidal activities.[49,52] We assumed that, if the pyridine and pyrazole pharmacophores were introduced into the pyrazole scaffold, the resulting compounds should have an interesting lead structure for antiviral agent development (Fig 4.10) due to the coexistence of two kinds of fungicidal pharmacophores with different action mechanisms. In continuation to our research program on the discovery of novel lead compounds, [53]we described herein the synthesis and antiviral activity of a series of new pyrazolaldoxime ether analogues. Meanwhile, as a control, we also synthesized and measured their antiviral activities in a series of pyrazolaldoxime ether analogues. The synthetic route is shown in Scheme 4.2. Starting from the key intermediate 1-substitutedphenyl-3-methyl-5-substituted phenylthio-4-pyrazo-laldoximes **4.11**, compounds **4.12** and **4.13** are synthesized by etherification with chloromethylated heterocyclic compound followed by potassium permangante oxidation in acetic acid. The structures of **4.12**-**4.13** were firmly established by
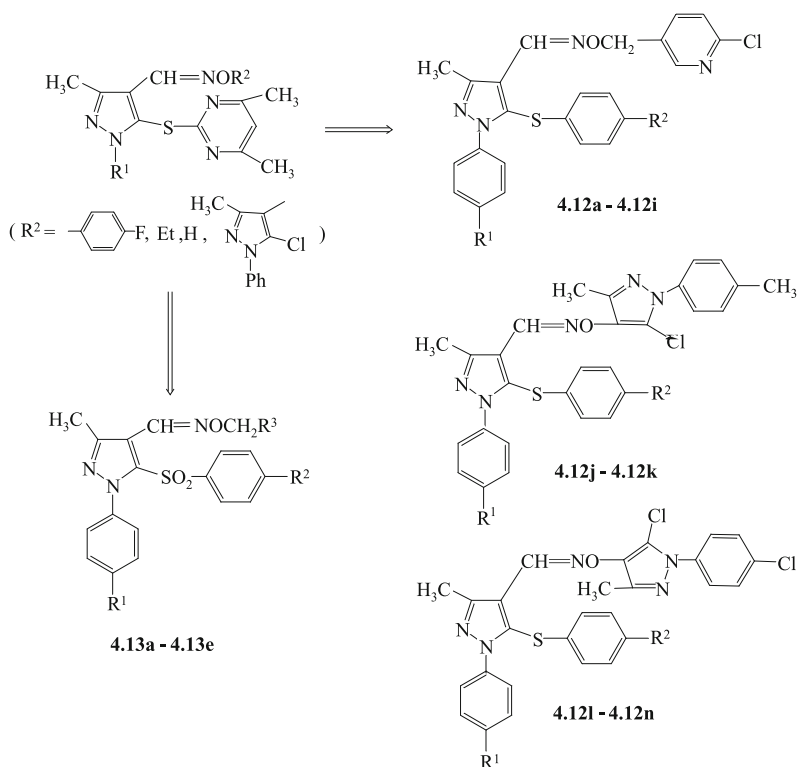
Fig 4. 10   Design of the target compounds

well-defined IR, ^{1}H NMR, ^{13}C NMR and elemental analysis. Preliminary bioassay tests showed that some compounds possess certain degree of antiviral activity against TMV at 500 mg/L *in vivo* as shown in Table 4.4 and Table 4.5, however with a degree of variation. The bioassay results showed that title compounds **4.12a** and **4.12g** possess high inactivation activities against TMV and the EC_{50} values range from 58.7 to 65.3 μg/mL.

4.2.2   Materials and Methods

Instruments. The materials and instruments for determination of the structure and physical data of new compounds are basically similar to the procedure described in Chapter 1.1.2.

Synthetic Procedures. 1-aryl-3-methyl-1H-4-pyrazolylformaldehydes and 1-(4-chlorophenyl)-3-methyl-1*H*-4-pyrazolylformaldehydes were prepared accor- ding to literature method as described.[19,20] Intermediates 1-aryl-3-methyl-5-chloro- 1*H*-4-pyrazolyl-formaldehydes **4.9**, **4.10** and **4.11** were prepared according to the reported methods.[21,22]

General Procedure for the Preparation of Title Compounds **4.12a-4.12n.** A 100 mL round-bottomed flask equipped with a magnetic stirrer was charged with **4.11** (10 mmol) and DMF (50mL) and NaOH (12 mmol). The flask was stirred at room temperature for 10 min, and then R^3CH_2Cl (0.012mol) was added dropwise over a period of 10 min and stirred at room temperature for 4 h. The mixture was poured into ice water and filtered. The white solid resulted was washed with distilled water, dried under vacuum, and recrystallized from ethanol to give the title compounds **4.12a-4.12n** in 54%-87% yields. The reperesentative data for **4.12a** is shown below, while data for **4.12b-4.12n** can be found in the reference.
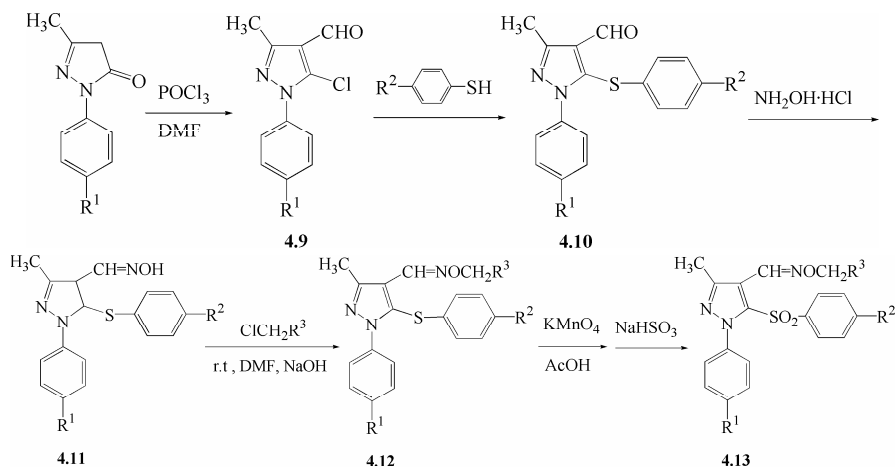
Data for 1-phenyl-3-methyl-5-(4-methylphenylthio)-4-pyrazolaldoxime-(2- chloropyridine-5-ylmethyl) ether (**4.12a**). White crystal, mp 95-96℃; yield 81%; IR(KBr, cm^{-1})：v_{max} 3063(Ar—H), 2923, 2867(CH$_3$＋CH$_2$), 1593(C＝N), 1495, 1458 (Ar skeleton vibration), 1216(C＝N—N), 845(*p*-disubstituded benzene), 655(C—S—C); ^{1}H NMR(500 MHz, DMSO-d_6)：δ 8.42(d, *J*=2.30 Hz, 1H, Py-6-H), 8.25(s, 1H, CH-H), 7.70(dd, *J*=2.30 Hz, *J*=2.30 Hz, 1H, Py-4-H), 7.38-7.40(m, 6H, 1-Ph-H, Py-3-H), 6.99(d, *J*=8.55 Hz, 2H, S-Ph-2, 6-H), 6.83(d, *J*=8.60 Hz, 2H, S-Ph-3, 5-H), 5.12(s, 2H, CH$_2$-H), 2.52(s, 3H, pyrazole-CH$_3$-H), 2.26(s, 3H, Ph-CH$_3$-H); ^{13}C NMR(125 MHz, DMSO-d_6)：δ 151.1, 149.9, 148.9, 144.0, 139.2, 138.9, 1136.9, 133.0, 132.4, 131.2, 130.2, 128.8, 128.4, 127.8, 125.6, 124.1, 118.7, 77.1, 21.0, 14.9; Anal. Calcd. for C$_{24}$H$_{21}$ClN$_4$OS(448.5)：C, 64.24; H, 4.66; N, 12.46. Found：C, 64.32; H, 4.38; N, 12.60.

General Procedure for the Preparation of Title Compounds **4.13a-4.13h.** A 50 mL round-bottomed flask equipped with a magnetic stirrer was charged with **4.12** (5 mmol) dissolved in glacial acetic acid (30 mL). The flask was stirred at

room temperature for 10 min, and then potassium permanganate (1.0g) was added and stirred at room temperature for 2 h. Sodium bisulfite was then added to turn the mixture colorless again. The reaction mixture was then filtered and the resulted white solid was washed with distilled water, dried under vacuum, and recrystallized from ethanol to give the title compounds **4.13a**-**4.13h** in 50%-58% yields. The reperesentative data for **4.13a** is shown below, while data for **4.13b**-**4.13h** can be found in the reference.[78]

Data for 1-phenyl-3-methyl-5-(4-methylphenylsulfonyl)-4-pyrazolaldoxime-(2-chloropyridine-5-ylmethyl) ether (**4.13a**). White crystal, mp 120-121℃; yield 56%; IR(KBr)：ν_{max} 3069(Ar-H), 2926, 2877(CH_3＋CH_2), 1605(C=N), 1587, 1488 (Ar skeleton vibration), 1344, 1152(SO_2 vibration), 1230(C=N-N), 845(p-disubstituded benzene)cm^{-1}; ^{1}H NMR(500 MHz, DMSO-d_6)：δ 8.75(s, 1H, CH-H), 8.46(d, J=2.35 Hz, 1H, Py-6-H), 7.60(d, J=2.30 Hz, 1H, Py-4-H), 7.48-7.38(m, 6H, 1-Ph-H, Py-3-H), 7.37(dd, J=8.60 Hz, J=8.00 Hz, 2H, SO_2-Ph-2, 6-H), 7.10(t, J=8.55 Hz, J=8.60 Hz, 2H, SO_2Ph-3, 5-H), 5.24(s, 2H, CH_2-H), 2.52(s, 3H, pyrazole-CH_3-H), 2.25(s, 3H, Ph-CH_3-H); Anal. Calcd. for $C_{24}H_{21}ClN_4O_3S$ (480.5)：C, 59.93; H, 4.37; N, 11.65. Found：C, 59.92; H, 4.39; N, 11.50.

X-ray Diffraction. Colorless blocks of **4.12b** (0.20mm×0.19mm×0.18mm) were counted on a quartz fiber with protection oil. Cell dimensions and intensities were measured at 293 K on a Bruker SMART CCD area detector diffractometer with graphite monochromated MoKa radiation (λ=0.71073 Å), θ_{max}=25.00, 19528 measured reflections, and 2498 independent reflections (R_{int}=0.1763) of which 4595 had $I > 2\sigma(I)$. Data were corrected for Lorentz and polarization effects and for absorption (T_{min}=0.7680; T_{max}=0.8237). The structure was solved by direct methods using SHELXS-97; all other calculations were performed with Bruker SAINT System and Bruker SMART programs. Full-matrix least squares refinement based on F^2 using the weight of $1/\left[s^2(F_0^2)+(0.0850P)^2+0.0458P\right]$ gave final values of R=0.0517, ωR=0.1631, and GOF(F)=1.011 for 453 variables and 4595 contributing reflections. The maximum shift/error=0.001, and max/min residual electron density=0.400/−0.322 e Å^{-3}. Hydrogen atoms were observed and refined with a fixed value of their isotropic displacement parameter.

Antiviral Biological Assay. The method for evaluating anti-TMV activity of title compounds is similar to the procedure described in Chapter 1.2.2.[26,54]

4.2.3   Results and Discussion

Synthesis. The synthetic route designed for the oxime ester analogues **4.12**-**4.13** is summarized in Scheme 4.2. Starting from 1-substituted phenyl 3-methyl-pyrazolone derivative, the intermediate **4.9**, 1-substituted phenyl-3-methyl-4-formyl-5-chloro pyrazole was prepared by chlorination reaction with POCl$_3$ in DMF. Then, treatment of **4.9** with substituted thiophenol afforded

Reaction scheme for compounds 4.9, 4.10, 4.11, 4.12, and 4.13. Steps: POCl₃/DMF; R²–C₆H₄–SH; NH₂OH·HCl; ClCH₂R³, r.t., DMF, NaOH; KMnO₄, NaHSO₃, AcOH.

Compd.	R^1	R^2	R^3	Compd.	R^1	R^2	R^3
4.12a	H	Me	(5-methyl-2-chloropyridinyl)	**4.12b**	H	OMe	(5-methyl-2-chloropyridinyl)
4.12c	H	F	(5-methyl-2-chloropyridinyl)	**4.12d**	3-Cl	F	(5-methyl-2-chloropyridinyl)
4.12e	4-Cl	Me	(5-methyl-2-chloropyridinyl)	**4.12f**	4-Cl	MeO	(5-methyl-2-chloropyridinyl)
4.12g	4-Cl	F	(5-methyl-2-chloropyridinyl)	**4.12h**	4-Me	F	(5-methyl-2-chloropyridinyl)
4.12i	4-Me	Me	(5-methyl-2-chloropyridinyl)	**4.12j**	4-Me	F	(pyrazole-4-Cl-phenyl)
4.12k	H	F	(pyrazole-4-Cl-phenyl)	**4.12l**	4-Me	Me	(pyrazole-4-CH₃-phenyl)
4.12m	4-Me	F	(pyrazole-4-CH₃-phenyl)	**4.12n**	4-Cl	Me	(pyrazole-4-CH₃-phenyl)
4.13a	H	Me	(5-methyl-2-chloropyridinyl)	**4.13b**	H	OMe	(5-methyl-2-chloropyridinyl)
4.13c	H	F	(5-methyl-2-chloropyridinyl)	**4.13d**	3-Cl	F	(5-methyl-2-chloropyridinyl)
4.13e	4-Cl	Me	(5-methyl-2-chloropyridinyl)	**4.13f**	4-Cl	MeO	(5-methyl-2-chloropyridinyl)
4.13g	4-Cl	F	(5-methyl-2-chloropyridinyl)	**4.13h**	4-Me	F	(5-methyl-2-chloropyridinyl)

Scheme 4.2   Synthetic route to pyrazole analogues **4.12**-**4.13** containing oxime

1-substituted phenyl-3-methyl-5-substituted-phenylthio-4-pyrazol-aldehyde **4.10**. Reaction of **4.10** with hydroxylamine hydrochloride gave 1-substituted phenyl-3-methyl-5-substituted phenylthio-4-pyrazolaldoximes **4.11**. Compounds **4.13**, 1-substitutedphenyl-3-methyl-5-substituted phenylthio-4-pyrazolaldoxime ethers were synthesized by the etherification reaction of **4.11** with chlorome-thylated-heterocyclic compounds (ClCH$_2$R^3). 1-Substituted phenyl-3-methyl-5-substituted phenyl-sulfonyl-4-pyrazolald-oxime ether derivatives **4.13** were then obtained from the oxidation of **4.12** with potassium permanganate in HOAc solution at room temperature. While the compounds **4.12a**-**4.12n** were obtained in high yields (54%-87%), the compounds **4.13a**-**4.13h** were obtained in good yields (50%-58%). The X-ray single crystal structure of typical **4.12b** has been shown in Fig 4.11 and all compounds were characterized unequivocally by spectroscopic data and elemental analysis as described in the section materials and methods.
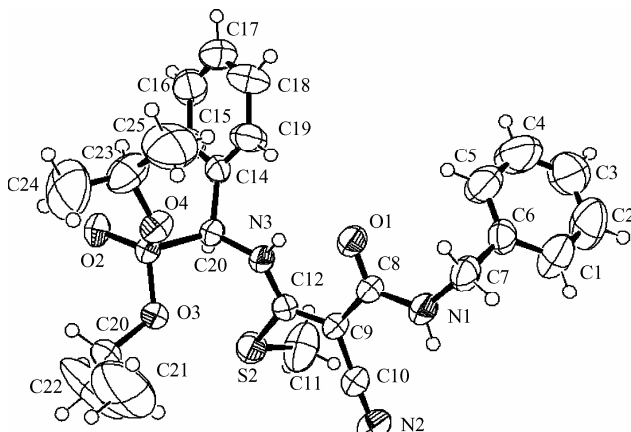
Fig 4.11   Molecular structure of **4.12b**

Antiviral Activity and Structure-Activity Relationship. To make a judgment of the antiviral potency of the synthesized compounds **4.12a**-**4.12n** and **4.13a**-**4.13h**, the commercially available plant virucide Ningnanmycin, perhaps the most successful registered antiviral agents for plants available in China, was used as the positive control. The antiviral bioassay against TMV is assayed by the reported method[26,54] and the antiviral results of all the compounds against TMV are listed in Table 4.4. The results showed that most of our designed compounds had moderate antiviral activities at 500 mg/L against TMV *in vivo*.

The title compounds **4.12a**-**4.12n** and **4.13a**-**4.13h** exhibited protection activities of 15.7%-44.8% at 500 mg/L. Compounds **4.12g** (R^1 is 4-Cl, R^2 is F and R^3 is 2-chloropyridine-5-ylmethyl), **4.12l** 〔R^1 is 4-Me, R^2 is Me and R^3 is 5-chloro-3-methyl-1-(4-methylphenyl)-pyrazol-4-ylmethyl 〕, **4.12m** (R^1 is 4-Me, R^2 is F and R^3 is 5-chloro-3-methyl-1-(4-methylphenyl)-pyrazol-4-ylmethyl), **4.13c** (R^1 is H, R^2 is F and R^3 is 2-chloropyridine-5-ylmethyl) and **4.13g** (R^1 is 4-Cl, R^2 is F and R^3 is 2-chloropyridine-5-ylmethyl) had moderate protection activities

Table 4.4   The protection, inactivation and curative effect of the new
compounds against TMV *in vivo* at 500 μg/mL

Agents	Protection effect(%)	Inactivation effect(%)	Curative effect(%)
4.12a	31.3*	90.4**	47.0*
4.12b	16.4	71.2**	26.6*
4.12c	18.9*	65.9*	24.0*
4.12d	28.6*	61.7*	34.3*
4.12e	37.7*	61.2*	26.0*
4.12f	22.0*	34.5*	12.9
4.12g	43.5*	80.6**	37.3*
4.12h	31.0*	56.6*	22.0
4.12i	15.7	61.0*	32.1*
4.12j	19.0	43.0*	31.9
4.12k	32.0*	55.9*	35.6*
4.12l	44.8*	51.2*	38.9*
4.12m	41.0*	50.9**	22.0*
4.12n	21.0	36.7*	18.9
4.13o	28.0*	45.0*	9.0 a
4.13b	29.8*	30.1**	15.6*
4.13c	40.2*	20.6	21.7
4.13d	12.9	30.0*	11.0
4.13e	31.3	33.3	9.2
4.13f	16.4	30.9	3.6
4.13g	42.2*	44.1*	7.7*
4.13h	28.2	11.0	22.0
Ningnanmycin	57.0*	98.0**	54.8*

n=3 for all groups; * $P < 0.05$, ** $P < 0.01$.

(43.5%, 44.8%, 41.0%, 40.2% and 42.2%, respectively) comparable to that of the standard reference (59.9%). In addition, the other compounds **4.12c-4.12f**, **4.12h-4.12k** and **4.13a**, **4.13b**, **4.13d-4.13f, 4.13h**, showed less than 40% protection activities at 500 mg/L. From the data presented in Table 4.4, it can be observed that compounds **4.12a-4.12n** possess potential inactivation bioactivities, with values of 90.4%, 71.2%, 65.9%, 61.7%, 61.2%, 34.5%, 80.6%, 56.6%, 61.0%, 43.0%, 55.9%, 51.2%, 50.9% and 36.7% respectively at 500 μg/mL. Among these compounds, **4.12a and 4.12g** are appreciably more active than the rest, with the inactivation rates of 90.4% and 80.6% respectively, which are similar to that of Ningnanmycin (98.0%) against TMV at 500 μg/mL. The data also indicate that all compounds have a relatively lower curative activity than that

of Ningnanmycin. However, it is difficult to provide a rational account of structure activity relationships on the basis of steric, electronic and hydrophobic effects. The diversity of the structures was limited by the availability of the reagents and the ease with which para-substituted (for R^1 and R^2 groups) products could be obtained compared to those with ortho- and meta-substituted ones. Electronic factor does not seem to play a significant role as both the compounds **4.12a** (R^1 as H and R^2 as Me) and **4.12g** (R^1 as Cl and R^2 as F) with electron rich and electron poor substituents respectively were found to display good bioactivity. Comparison of biological activities among **4.12a-4.12n and 4.12a-4.12h** confirms that the functional groups with alkylthio are potentially more active than those with sulfonyl groups at 5-position of pyrazole which is necessary for inactivation activity to occur.

In addition, as shown in Table 4.5, compounds **4.12a**, **4.12b**, and **4.12g** were found to display good antiviral activities. These compounds were bioassayed further to investigate their inactivation activities at different concentrations with Ningnanmycin serving as the commercial control. As shown in Table 4.5, the inactivation effects against TMV of compounds **4.12a**, **4.12b**, and **4.12g** are significant. The EC_{50} values were 58.7, 115.0 and 65.3 µg/mL, respectively. Among these compounds, **4.12a** displayed more potent antiviral activity than the others, being similar to that of Ningnanmycin (EC_{50}=52.7 µg/mL) against TMV.

Table 4. 5   Antiviral activities *in vivo* (%) of compounds **4. 12a, 4. 12b and 4. 12g**

TMV	Inactivation effect					
Concentration(µg/mL)	500	250	125	62.5	31.8	EC_{50}(µg/mL)
4.12a	90.4	76.0	69.2	55.1	40.1	58.7
4.12b	71.0	65.0	48.9	41.0	32.0	115.0
4.12g	80.6	65.7	53.0	51.2	40.6	65.3
Ningnanmycin	98.0	81.1	72.0	59.9	44.0	52.7

4.2.4   Conclusions

In summary, a series of new pyrazole derivatives containing oxime moities **4.12a-4.12n** were designed and synthesized by the thioetherification reaction of 1-substituted phenyl-3-methyl-5-substituted phenylthio-4-pyrazolaldoximes **4.11** with chloromethylated-heterocyclic compounds (ClCH$_2$R^3) and NaOH in DMF. The *in vivo* tests indicated that compounds **4.12a** and **4.12g** exhibited a very similar inactivation bioactivity level as that of Ningnanmycin against TMV. Therefore, this study demonstrates that the antiviral activity of pyrazole derivatives was significantly improved via the introduction of the oxime moiety.

Although, structure activity relationships could not be successfully established due to lack of structural diversity, the present work paves the way towards the synthesis and antiviral studies of new pyrazole derivatives containing oxime moieties. Effects of steric, hydrophobic, electronic, electrostatic parameters on structure activity relationships and structural modification studies for identifying lead bioactive compounds are currently underway.

4.3   Quinazolinone Derivatives

4.3.1   Introduction

4(3*H*)-Quinazolinones and their derivatives constitute an important class of heterocyclic compounds. They occupy vital position in medicinal and pesticide chemistry by presenting a wide range of bioactivities. As medicines, many of them display antifungal, [55]antimicrobial, [56]anti-HIV, [57]antitubercular, [58]anticancer, [59]antiinflammatory, [60]anticonvulsant, [61]antidepressant, [62] hypolipidemic, [63]antiulcer, [64]analgesic[65] or immunotropic activities[66], and are also known to act as thymidyalate synthase, [67] poly (ADP-ribose) polymerase (PARP), [68]and protein tyrosine kinase inhibitors[69]. As pesticides, they are used as insecticides, [70] fungicides [71]and antiviral agents [72]such as TMV, CMV inhibitors. In light of their overwhelming application, an enormous increase in the interest for the synthesis and bioactivity studies of quinazoline derivatives has been observed among biologists and chemists in recent years. In our previous work in this area, we reported that some of these compounds possessed antifungal activities.[71]Nanda and his co-workers synthesized ten 3-(arylideneamino)-2-phenylquinazoline-4 (3*H*)-ones, which were investigated for their antimicrobial activity against both Gram-positive (*Staphylococcus aureus* 6571 and *Bacillus subtilis*) and Gram-negative bacteria (*Escherichia coli* K12 and *Shigella dysenteriae* 6) using a turbidometric assay method. It was found that the incorporation of the 3-arylideneamino substituent enhanced the antibacterial activity of the quinazolone system.[73]However, no attention has been paid to the antiviral activities for 3-(arylideneamino)-2-phenylquinazoline-4(3*H*)-ones against TMV (tobacco mosaic virus).

In this report, we have designed and synthesized a series of 2-aryl-or 2-methyl-3-(substituted-benzalamino)-4(3*H*)-quinazolinone derivatives and investigated their antiviral bioactivities. The synthetic route has been shown in Scheme 4.3. The structures of 4.16 were firmly established by well defined IR, ^{1}H NMR, ^{13}C NMR data and elemental analysis. Preliminary bioassay tests showed that some compounds displayed *in vivo* antiviral activity against TMV at 500 μg/mL.

Scheme 4.3   Synthetic route of the title compounds

4.16.1：R=H, R¹=H, R²=Ph
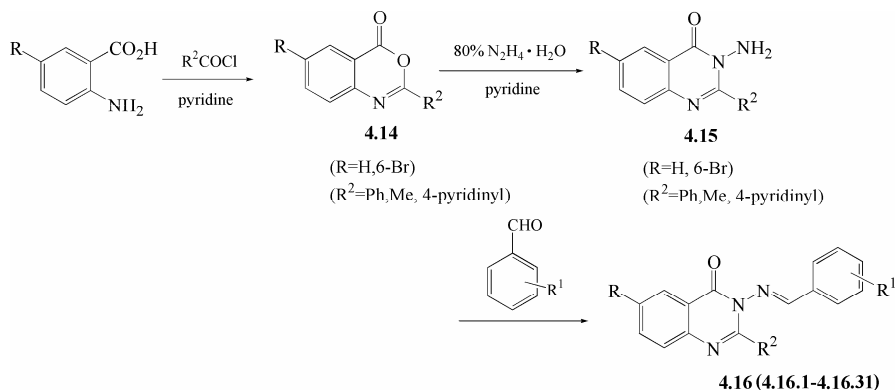
4.16.2：R=H, R¹=3-nitro-4-chloro, R²＝Ph

4.16.3：R=H, R¹=4-trifluoromethyl, R²＝Ph

4.16.4：R=H, R¹=3-chloro, R²＝Ph

4.16.5：R=H, R¹=2,3-dichloro, R²＝Ph

4.16.6：R=H, R¹=2, 6-dichloro, R²＝Ph

4.16.7：R=H, R¹=3, 4-difluoro, R²＝Ph

4.16.8：R=H, R¹=3-trifluoromethyl, R²＝Ph

4.16.9：R=H, R¹=H, R²＝4-pyridinyl

4.16.10：R=H, R¹=2-chloro, R²＝4-pyridinyl

4.16.11：R=H, R¹=4-fluoro, R²＝4-pyridinyl

4.16.12：R=H, R¹=2, 3-dichloro, R²＝4-pyridinyl

4.16.13：R=6-Br, R¹=2-fluoro, R²＝Me

4.16.14：R=6-Br, R¹=3-fluoro, R²＝Me

4.16.15：R=6-Br, R¹=4-fluoro, R²＝Me

4.16.16：R=6-Br, R¹=2-trifluoromethyl, R²＝Me

4.16.17：R=6-Br, R¹=3-chloro, R²＝Me

4.16.18：R=6-Br, R¹=2, 4-dichloro, R²＝Me

4.16.19：R=6-Br, R¹=2, 6-dichloro, R²＝Me

4.16.20：R=6-Br, R¹=3, 4-difluoro, R²＝Me

4.16.21：R=6-Br, R¹=2-chloro-5-nitro, R²＝Me

4.16.22：R=6-Br, R¹=4-chloro-3-nitro, R²＝Me

4.16.23：R=6-Br, R¹=2-fluoro-3-trifluoromethyl, R²＝Me

4.16.24：R=6-Br, R¹=3, 4-dimethoxy, R²＝Me

4.16.25：R=6-Br, R¹=2, 3-dimethoxy, R²＝Me

4.16.26：R=6-Br, R¹=2, 5-dimethoxy, R²＝Me

4.16.27：R=6-Br, R¹=3-nitro, R²＝Me

4.16.28：R=6-Br, R¹=2-hydroxy, R²＝Me

4.16.29：R=6-Br, R¹=2, 4-dimethoxy, R²＝Me

4.16.30：R=6-Br, R¹=5-chloro-2-hydroxy, R²＝Me

4.16.31：R=H, R¹=2, 3-dichloro, R²＝Me

4.3.2   Materials and Methods

The materials and instruments for determination of the structure and physical data of new compounds are basically similar to the procedure described in Chapter 1.1.2.

Preparation of 2-Aryl-4(3H)-3, 1-benzoxazinone **4.14(R=H, R²=Ph)**. To a stirred solution of anthranilic acid (0.05 mole) in pyridine (60 mL), benzoyl chloride (0.05 mole) was added dropwise, maintaining the temperature near 0-5℃ for 1 hour. Reaction mixture was stirred for another 2 hours at room temperature when a solid product was formed. The reaction mixture was neutralized with saturated sodium bicarbonate solution. A pale yellow solid separated which was filtered, washed with water and recrystallised from ethanol. Yield 83%,

mp 113-115℃(lit[74], 114℃); IR(KBr)：ν_{max} 3030(C-H, Ar-H), 1721(C=O), 1595(C=N), 1180(C-O); ^{1}H NMR(500 MHz, DMSO-d_6)：δ 7.61(m, 9H, Ar-H, Quinazolinone-H).

Preparation of 3-amino-2-aryl-4(3H)-quinazolinones **4.15.1(R=H, R^2=Ph).** To a stirred solution of 4.14 (0.05 mole) in pyridine (20 mL), 80% N_2H_4 • H_2O (0.15 mole) was added. Reaction mixture was stirred and refluxed for 20 minutes at 117℃. After cooling, a crude product was obtained after filtration which was recrystallized from ethanol to afford 4.15 as white solid, yield 88%; mp 177-178℃ (lit[75], 178-179 ℃); IR(KBr)：ν_{max} 3448(NH$_2$), 3030(C-H, Ar-H), 1685(C=O), 1598(C=N); ^{1}H NMR (500 MHz, DMSO-d_6)：δ 7.92 (m, 9H, Ar-H, Quinazolinone-H); ^{1}H NMR (500 MHz, DMSO-d_6)：δ 5.67 (s, 2H, 3-quinazo-linone-NH$_2$), 7.48-8.19 (m, 9H, Ar-H, quinazolinone-H);^{13}C NMR(125 MHz, DMSO-d_6)：δ 161.7, 156.3, 147.2, 135.4, 134.8, 130.1, 130.0, 127.9, 127.3, 126.6, 120.6.

Preparation of Schiff base derivatives **4.16.1-4.16.31.** To a solution of substituted benzaldehyde (1.0 mmol) in ethanol (15 mL), were added the appropriate 3-amino-2-aryl-4(3H)-quinazolinone (1.0 mmol) and a few drops of acetic acid (0.05mmol). The reaction mixture was refluxed for 3-24h and the course of the reaction was monitored by TLC［petroleum ether/ethyl acetate (v/v=1:2)］ for its completion. The reaction mixture was cooled. The crude product was recrystallized from 95% ethanol to give title compounds **4.16.1-4.16.31**. The reperesentative data for **4.16.1** is shown below, while data for **4.16.2-4.16.31** can be found in the reference.[80]

2-Phenyl-3-(3,5-di-chlorobenzalamino)-4(3H)-quinazolinone **4.16.1.** White solid, yield 79%; mp 218-220℃; IR(KBr)：ν_{max} 3088(quinazolinone-H, Ar-H), 1678(C=O), 1622, 1590(C=N), 1551-1489(C=C, benzene and quinazolinone ring skeleton), 875, 775, 688(1, 3, 5-substituted benzene), 748, 700(mono substituted benzene); ^{1}H NMR(500 MHz, DMSO-d_6)：δ 7.45-8.25(m, 12H, Quinazolinone-H, Ar-H), 9.35(s, 1H, N=CH); ^{13}C NMR(125 MHz, DMSO-d_6)：δ 170.0, 158.3, 153.6, 146.9, 135.2, 135.1, 133.2, 132.8, 130.4, 130.3, 129.6, 129.1, 128.2, 128.1, 127.7, 127.3, 121.6; Anal Calcd for $C_{21}H_{13}Cl_2N_3O$ (394.26)：C, 63.98; H, 3.32; N, 10.66. Found：C, 63.86; H, 3.22; N, 10.58.

Antifungal bioassays. The method for evaluating antifungal activity of title compounds **4.16.1-4.16.31** is similar to the procedure described in Chapter 1.2.2.[76]

Antiviral bioassays. The method for evaluating anti-TMV activity of title compounds **4.16** is similar to the procedure described in Chapter 1.1.2.[26,54]

Isolation of total RNA from tobacco leaf. Trizol kit was used according to the standard protocol for total RNA isolation. Prior to RT-PCR, the total RNA samples were treated with DNase I for 10 min and quantified by spectrophoto-metry and identified by agarose gel Electrophoresis.[31]

Reagents. RNA isolation kit, MMLV reverse transcriptase and RT-PCR kit were purchased from TAKARA Biotechnology (Dalian) CO., LTD. DNA Marker pUC/Msp I was purchased from MBI Company, Ltd. Primer was designed with

Beacon Designer software. Oligo $(dT)_{18}$ and primers were synthesized by Shanghai Sangon Biotechnology Company, Ltd.

RT-PCR assay. The assay was carried out as described in the section 4.1.2.6.[32]

Products of PCR sequencing. The purified PCR products were sequenced on an automated DNA sequencer by model ABI 310 DNA sequencer. The sequencer analysis was carried out using the chromas 223 software and BLAST network services at the National Center for Biotechnology Information (NCBI) Genbank.

Semi-quantity PCR for expression of gene. The procedure was similar as described in section 4.1.2.7.[33]

The relative quantification real-time PCR for expression of the target gene. The metnodology was similar as described in the section 4.1.2.10.[77]

4.3.3   Results and Discussion

Different homologues of 3-amino-2-aryl-4(3*H*)-quinazolinone **4.15** were prepared in accordance with the literature procedure.[74]The reaction conditions were non-heterogeneous and the use of an increased-amount of hydrazine hydrate did not afford successful results. The reaction conditions for the synthesis of **4.15.1**(R=H, R^1=H, R^2=Ph) were optimized in various solvents at different temperatures for different time and the results are shown in Table 4.6. An 87% yield could be obtained when the reaction mixture was heated at 116℃ for 0.5 h in pyridine.

Table 4.6   The effect of reaction conditions on the yield of intermediate **4.15.1**
(R=H, R^1=H, R^2=Ph)

Entry	Solvent	Reaction temp.(℃)	Reaction times(h)	Yield(%)
1	anhydrous ethanol	78	3	24
2	isopropanol	85	3	31
3	*n*-Butanol	117	3	35
4	-	118	3	22
5	pyridine	116	0.5	87
6	pyridine	116	3	89

In order to optimize the reaction conditions for the compounds **4.16**, the synthesis of **4.16.1** (R=H, R^1=3, 5-di-chloro, R^2=Ph) was examined under different conditions. First, the role of the catalyst (HOAc) in accelerating the reaction rate was ascertained. While in the presence of catalyst, a 72% yield of **4.16.1** was achieved in only 10 h (Table 4.7, entry 1), a yield of only 52% was obtained with a prolonged reaction period of 30 h in the absence of the catalyst (Table 4.7, entry 2). In addition, we also studied the effects of reaction time. When the reaction time was prolonged further to 20 h, no improvement in the yields

(75%) was obtained (Table 4.7, entry 3), as compared to that of 10 h (72%). It could also be observed that the yield was significantly lower at room temperature (Table 4.7, entry 4). For different substituted benzaldehydes, under optimal conditions, as depicted in Table 4.8, compounds **4.16.1**-**4.16.31** could be obtained in 53%-89% yields at 78℃in ethanol in presence of HOAc as the catalyst.

Table 4.7   The effect of reaction conditions on yield of title compound **4.16.1**

Entry	Catalyst	Reaction temp.(℃)	Reaction times(h)	Yield(%)
1	HOAc	78	10	71.9
2	-	78	30	52.4
3	HOAc	78	20	74.8
4	HOAc	r.t	10	22.1

Table 4.8   Yield of title compounds **4.16.1**-**4.16.31** under optimized conditions

Compd.	R	R^1	R^2	Yields(%)
4.16.1	H	3, 5-dichloro	Ph	79
4.16.2	H	3-nitro-4-chloro	Ph	74
4.16.3	H	4-trifluoromethyl	Ph	72
4.16.4	H	3-chloro	Ph	71
4.16.5	H	2, 3-dichloro	Ph	70
4.16.6	H	2, 6-dichloro	Ph	78
4.16.7	H	3, 4-difluoro	Ph	69
4.16.8	H	3-trifluoromethyl	Ph	74
4.16.9	H	H	4-pyridinyl	67
4.16.10	H	2-chloro	4-pyridinyl	69
4.16.11	H	4-fluoro	4-pyridinyl	89
4.16.12	H	2, 3-dichloro	4-pyridinyl	89
4.16.13	6-Br	2-fluoro	Me	59
4.16.14	6-Br	3-fluoro	Me	63
4.16.15	6-Br	4-fluoro	Me	68
4.16.16	6-Br	2-trifluoromethyl	Me	66
4.16.17	6-Br	3-chloro	Me	63
4.16.18	6-Br	2, 4-dichloro	Me	72
4.16.19	6-Br	2, 6-dichloro	Me	70
4.16.20	6-Br	3, 4-difluoro	Me	64
4.16.21	6-Br	2-chloro-5-nitro	Me	70
4.16.22	6-Br	4-chloro-3-nitro	Me	68
4.16.23	6-Br	2-fluoro-3-trifluoromethyl	Me	64
4.16.24	6-Br	3, 4-dimethoxy	Me	66
4.16.25	6-Br	2, 3-dimethoxy	Me	61
4.16.26	6-Br	2, 5-dimethoxy	Me	63
4.16.27	6-Br	3-nitro	Me	56
4.16.28	6-Br	2-hydroxy	Me	53
4.16.29	6-Br	2, 4-dimethoxy	Me	62
4.16.30	6-Br	5-chloro-3-hydroxy	Me	64
4.16.31	H	2, 3-dichloro	Me	87

Representative analysis of spectral data ： *compound 4.16.3.* The IR frequency range for **4.16.3** from 3060-3032 cm^{-1} corresponds to weak multiple absorption peaks for Qu-H and Ar-H stretching vibrations. The absorption at 1671 cm^{-1} is due to strong C=O stretching vibrations, and the moderately intense absorption at 1607 cm^{-1} corresponds to C=N stretching vibration. The absorption range at 1591～1474 cm^{-1} is due to the skeleton vibration of aryl and heterocyclic ring. The series of bands in the region 1319, 1174, 1125 cm^{-1} correspond to the C-F stretching at the para position of the imine-Ar-CF group, 843 cm^{-1} is due to methylene group linked to the benzene ring at 4-position. The absorption peaks at 766 and 696 cm^{-1} arise due to phenyl substitation at 2-position in quinazolinones.

The structure and carbon number assignment of compound **4.16.3**, with molecular formula $C_{22}H_{14}F_3N_3O$ (393.37), are shown in Fig 4.12. It can be seen from the chemical structure that different pairs of carbons *e.g.* C-11 and C15, C-12 and C-14, C-17 and C-21, C-18 and C-20 are attached to chemically equivalent protons. The proton attached at C-5 position appears as a multiplet at δ 7.46-7.58 ppm due to mutual coupling with H-4 and H-6. Chemical shift in the aromatic region with a multiplet centered at δ 7.63 ppm corresponds to H-4 and the multiplet in the region 7.80-7.94 ppm arises due to the five aromatic protons present in the phenyl ring directly attached to the quinazolinone ring. The multiplet at 7.70-7.73 ppm must be for the two equivalent protons at C-11 and C-15. The relatively downfield multiplet at 8.19-8.26 ppm which integrates up to 2H corresponds to the protons in the vicinity of trifluoromethyl group, i.e.attached to C-12 and C-14. The singlet at 9.25 ppm appears due to the proton attached to the imine carbon at C-9.
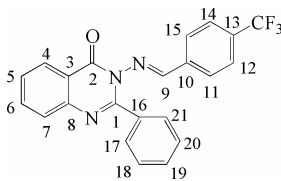
Fig 4.12　The structure of compound **4.16.3**

Representative analysis of ^{13}*C NMR spectra of compound 4.16.8.* The chemical structure of compound **4.16.8** and the assignment of carbon atoms are shown in Figure 4.13. The compound **4.16.8** with a molecular formula of $C_{22}H_{14}F_3N_3O$ (393.37) contains 22 carbon atoms. Among them, there are two equivalent pairs, C-17, C-21 and C-18, C-20. The ^{13}C chemical shift values of the 20 non equivalent carbons are assigned and shown in Table 4.9.

The compound **4.16.8** essentially has three parts. The chemical shift of carbons present in the quinazolinone ring varies from δ=167.2 to 121.6 ppm. The carbon nuclei under strong electronegative environment appear downfield *e.g.*C-2 carbonyl which is directly linked to nitrogen of the ring has a chemical shift value of δ=167.2 ppm whereas the C-1 linked to two ring nitrogen atoms appears at 158.4 ppm. The chemical shift of the annular carbon at C-8 is affected by the
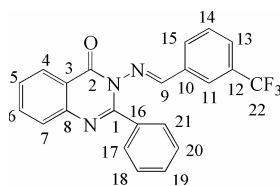
Fig 4.13   The structure of compound **4.16.8**

Table 4.9   ¹³C NMR analysis of compound 4.16.8

C No.	¹³C NMR δ(ppm)	C No.	¹³C NMR δ(ppm)
C-1	158.4	C-11	127.4
C-2	167.2	C-12	132.6
C-3	121.6	C-13	129.3
C-4	130.3	C-14	130.5
C-5	128.2	C-15	134.1
C-6	135.1	C-16	130.1
C-7	123.2	C-17	127.8
C-8	153.7	C-18	130.4
C-9	146.7	C-19	131.0
C-10	135.4	C-22	125.4

presence of directly attached ring nitrogen atom and appears at δ=153.7 ppm. The imine carbon at C-9, conjugated to the phenyl ring records a downfield chemical shift at 146.7 ppm. The carbons of the phenyl ring conjugated to the imine functionality have chemical shifts in the range 127.4 to 135.4 ppm. The trifluoromethyl carbon present at the side chain appears at 125.4 ppm under the strong electron withdrawing influence exerted by the three fluorine atoms. The carbons of unsubstituted phenyl ring directly linked to the quinazolinone ring through the intervening carbon between two ring nitrogens appear upfield (127.8 ppm-131.0 ppm) compared to those of quinazolinone ring carbons at C1, C2 and C8. The equivalent C17, C-21 and C-18, C-20 have chemical shift values δ=127.8 and 130.4 ppm respectively.

Antifungal activity. The antiviral bioassay results are given in Table 4.10. It could be seen that these newly synthesized derivatives exhibit weak to good antiviral activities. At 500 µg/mL, title compounds exhibited weak activities against *Fusarium oxysporum*, *Valsa mali* and *Gibberella Zeae*, which are lower than that of hymexazol.

Antiviral activity. The results of bioassay *in vivo* against TMV are given in Table 4.11. Ningnanmycin was used as positive control. It was found that these compounds exhibit certain activities against TMV *in vivo*. The compounds **4.16.31**, **4.16.16**, **4.16.3**, **4.16.1** and **4.16.8** have relatively higher curative effects than the

Table 4.10   Inhibition effect of 4.16 against phytopathogenic fungi

Compd.(50 µg/mL)	Fusarium Oxysporum	Gibberella zeae	Valsa mali
4.16.1	17.5±0.77	11.3±0.29	6.75±0.84
4.16.2	6.14±0.50	1.07±0.32	1.23±0.51
4.16.3	1.59±0.68	−3.23±0.54	2.45±0.37
4.16.4	2.90±0.88	3.78±0.94	2.00±0.55
4.16.5	10.2±0.62	6.45±0.52	−0.31±1.49
4.16.6	5.68±0.91	0.00±0.55	9.51±1.15
4.16.7	1.90±0.38	3.09±0.94	5.66±0.30
4.16.8	5.68±0.69	2.69±0.94	5.52±0.52
4.16.9	4.09±0.51	4.77±0.71	0.90±0.12
4.16.10	5.90±0.77	7.12±0.99	1.09±0.33
4.16.11	9.54±0.95	6.18±0.26	1.23±0.81
4.16.12	8.89±0.37	4.77±0.55	7.98±0.86
4.16.13	17.5±3.25	7.55±1.70	−0.81±1.79
4.16.14	13.9±3.92	5.03±2.06	0±1.51
4.16.15	−0.89±3.22	5.03±1.84	−1.35±2.50
4.16.16	12.4±3.69	1.41±1.74	1.89±1.59
4.16.17	14.2±3.40	3.14±1.7	4.04±1.45
4.16.18	12.4±3.80	6.60±1.53	3.50±1.60
4.16.19	16.3±3.14	11.0±1.31	2.43±1.54
4.16.20	17.0±1.42	9.00±1.0	8.09±1.09
4.16.21	20.11±2.99	15.22±2.11	6.78±2.09
4.16.22	9.00±3.11	24.21±1.99	3.09±1.01
4.16.23	19.91±2.88	26.01±6.43	10.32±4.92
4.16.24	19.00±2.77	17.70±3.44	6.77±1.99
4.16.25	16.9±1.11	19.0±1.22	4.93±1.09
4.16.26	21.1±1.89	9.99±0.77	7.68±0.96
4.16.27	26.7±7.55	3.97±1.18	4.99±1.40
4.16.28	28.8±3.09	34.1±10.1	7.77±2.10
4.16.29	39.7±3.01	22.30±1.55	6.66±1.08
4.16.30	29.4±9.99	10.4±2.90	20.5±3.33
4.16.31	12.8±1.19	3.12±0.84	3.04±2.19
hymexazol	68.7±3.59	62.2±1.86	67.4±2.06

Table 4.11   The curative effect of the new compounds 4.16 against TMV in vivo

Agents	Ninganmycin	4.16.1	4.16.2	4.16.3	4.16.4	4.16.5
Concentration(mg/L)	500	500	50	500	500	500
Inhibition rate(%)	53.5	51.1	25.3	52.9	44.7	37.9
Agents	4.16.6	4.16.7	4.16.8	4.16.9	4.16.10	4.16.11
Concentration(mg/L)	500	500	500	500	500	500
Inhibition rate(%)	37.4	49.8	50.4	27.1	9.30	50.4
Agents	4.16.12	4.16.13	4.16.14	4.16.15	4.16.16	4.16.17
Concentration(mg/L)	500	500	500	500	500	500
Inhibition rate(%)	22.1	23.4	36.6	40.4	54.0	42.8
Agents	4.16.18	4.16.19	4.16.20	4.16.21	4.16.22	4.16.23
Concentration(mg/L)	500	500	500	500	500	500
Inhibition rate(%)	45.6	41.4	24.6	26.1	34.8	39.9
Agents	4.16.24	4.16.25	4.16.26	4.16.27	4.16.28	4.16.29
Concentration(mg/L)	500	500	500	500	500	500
Inhibition rate(%)	43.2	40.0	29.9	41.0	41.8	38.9
Agents	4.16.30	4.16.31				
Concentration(mg/L)	500	500				
Inhibition rate(%)	44.6	55.4				

compounds **4.16.2**, **4.16.4**, **4.16.5**, **4.16.6**, **4.16.7**, **4.16.9-4.16.15**, **4.16.17-4.16.30**. The data listed in Table 11 indicate that antiviral activity depends on the nature of the substituents present in the title compound. When R was 4-CF$_3$, the title compounds 4.16.31 and 4.16.16 showed curative rates of 55% and 54%, respectively, which were slightly higher than that of the positive control (54%) against TMV at 500 µg/mL. The other compounds displayed a slightly lower antiviral activity than that of the reference.

   Product of PCR in PR-1a and PR-5 and its sequence identification. By following RT-PCR, the product of PCR performed in 35 cycles was resolved on a 1.5% agarose gel. The purified products of PCR were sequenced by model ABI 310 DNA sequencer and were identified as the target gene by BLAST searching in Genbank (Fig 4.14).
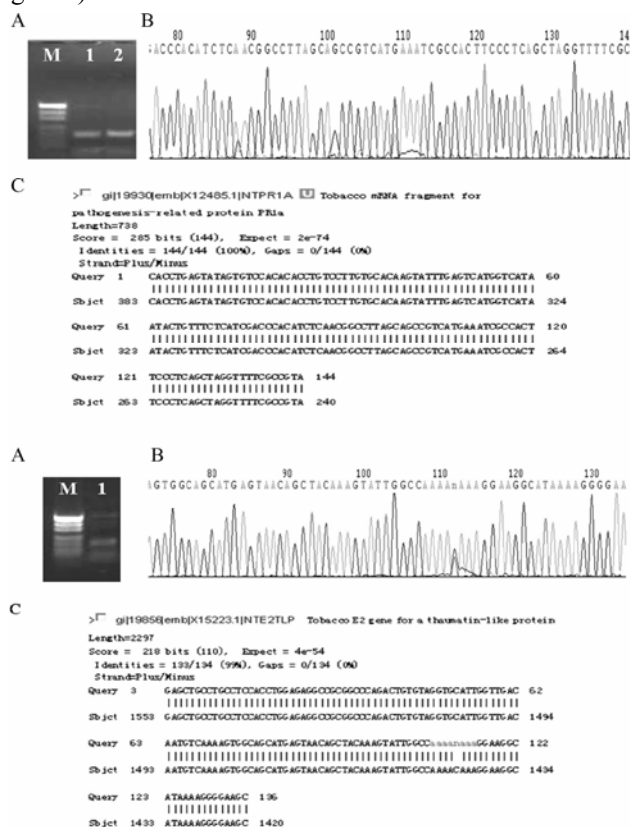
Fig 4.14   The clone of PR-1a and PR-5 genes

   Gene expression analysis of PR-1a and PR-5 in III-31-treated tobacco leaf. *In vitro* synthesized single-stranded cDNA from RNA samples was isolated from leaf in water-treated tobacco, the TMV-treated tobacco, and **4.16.31**- and TMV-treated tobacco. The differential expression analysis of the PR-1a and PR-5 gene was determined by the semi-quantitative PCR and the relative quantification real-time PCR analysis. The mRNAs of PR-1a and PR-5 gene accumulated to

detectable levels in **4.16.31**- and TMV-treated tobacco leaf, while no detectable levels were reached in water-treated tobacco and the TMV-treated tobacco. The mRNA content of **4.16.31**-treated tobacco leaf for PR-1a gene started to increase after 5 day and reached a peak at the end of the 5th day before falling to the normal level. In contrast, in TMV-treated tobacco leaf, no significant increase in the levels of gene expression was noticed(Fig 4.15A, Fig 4.16A). The expression
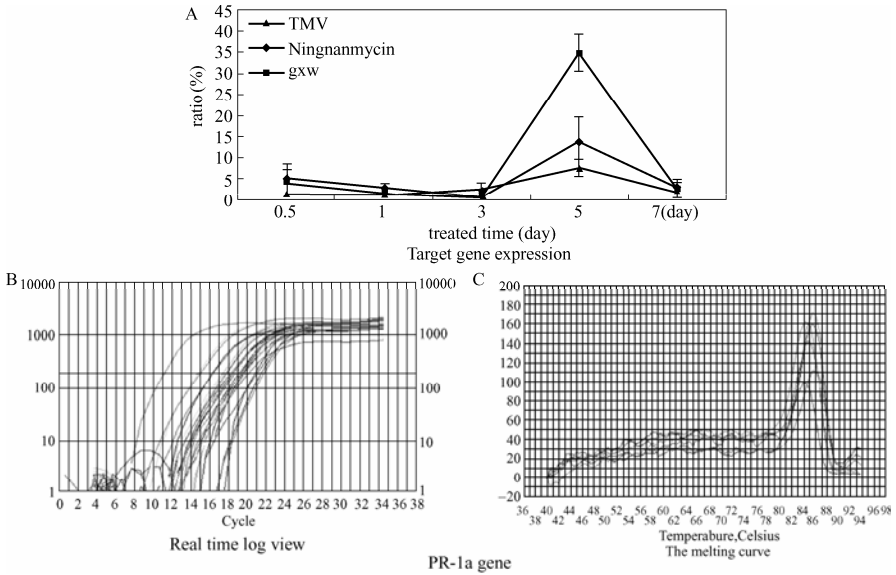
Fig 4.15 The PCR effects of PR-1a gene real time
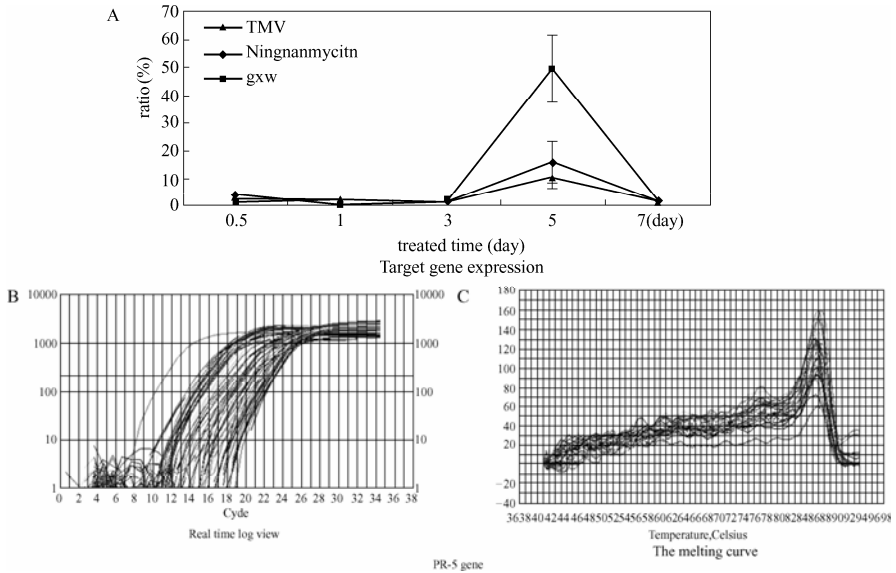
Fig 4.16 The PCR effects of PR-5 gene real time

levels of PR-5 gene in **4.16.31**-treated tobacco rapidly increased and reached a peak within 5 day after the inoculation and then started to decrease gradually. As depicted in Fig 4.14B and Fig 4.15B, **4.16.31** treated tobacco leaves showed significant enhancement in the levels of gene expression as compared to TMV- treated tobacco leaves within 5 day after the inoculation. In contrast, in TMV- treated tobacco leaf, no significant increase in the levels of gene expression was observed.

4.3.4   Conclusions

In summary, the new method of preparation of 4(3H)-quinazolinone Schiff base derivatives from appropriate 3-amino-2-aryl-4(3H)-quinazolinone and substituted benzaldehyde in ethanol is convenient, rapid and associated with moderate yield. It was also found that the title compounds **4.16.31**, **4.16.1**, **4.16.3**, **4.16.8**, **4.16.16** displayed good antiviral activities. Semi-quantitative PCR and Real time PCR assay were evaluated to ascertain the target of action of compound **4.16.31** against TMV. The studies suggest that **4.16.31** possesses antiviral activity by induction up-regulation of PR-1a, PR-5 thereby inhibiting proliferation and movement of virus by enhancing activities of some defense related enzymes.

References

1.   Boyne M, Stratton C, Johnson F, *et al*. High affinity inhibitors with activity against drug-resistant strains of mycobacterium tuberculosis. *Chem. Biol*.2006, 1(1), 43-53.

2.   Vicentini C B, Guccione S, Giurato L, *et al*. Pyrazole derivatives as photosynthetic electron transport inhibitors: new leads and structure-activity relationship. *J. Agric. Food Chem*.2005, 53, 3848-3855.

3.   Waldrep TW, Beck JR, Lynch MP, *et al*. Synthesis and herbicidal activity of 1-aryl-5-halo and 1-aryl-5-(trifluoromethyl)-1H-pyrazole-4-carboxamides. *J. Agric. Food Chem*.1990, 38(2), 541-544.

4.   Pevarello P, Brasca M G, Amici R, *et al*. 3-Aminopyrazole inhibitors of CDK2/Cyclin a as antitumor agents.1.lead finding. *J. Med.Chem*.2004, 47(13), 3367-3380.

5.   Baraldi P G, Balboni G, Pavani M G., *et al*. Design, synthesis, DNA binding, and biological evaluation of water-soluble hybrid molecule containing two pyrazole analogues of the alkylating cyclopropyl-pyrroloindole (CPI) subunit of the antitumor agent CC-1065 and polypyrrol minor groove binders. *J.Med.Chem*.2001, 44(16), 2536-2543.

6.   Fancelli D, Moll J, Varasi M, *et al*. 1,4,5,6-Tetrahydropyrrolo[3,4-c]pyrazoles: identification of a potent aurora kinase inhibitor with a favorable antitumor kinase inhibition profile. *J. Med. Chem*. 2006, 49(24), 7247-7251.

7.   Ranatunge R R, Augustyniak M, Bandarage U K, *et al*. Synthesis and selective cyclooxygenase-2 inhibitory activity of a series of novel, nitric oxide donor-containing pyrazoles. *J.Med.Chem*.2004, 47(9), 2180-2193.

8.   Goel A, Madan A K. Structure-activity atudy on antiinflammatory pyrazole carboxylic acid hydrazide analogs using molecular connectivity indices. *J. Chem. Inf. Comput. Sci*. 1995, 35(3), 510-514.

9.   Hansen A J. Antiviral chemicals for plant disease control. *Critical Reviews in Plant. Critical Reviews in*

Plant Sciences. 1989, 8, 45-88.

10. Milosevic N, Slusarenko A J. Active oxygen metabolism and lignification in the hypersensitive response in bean. *Phys*. *Plant Path*, 1996, 49, 143-158.

11. Wang Y C, Hu D W, Zhang Z G, *et al*. Purification and immuno-cytolocalization of a novel elicitor inducing SAR in plants from *Phytophthora boehmeriae*. *Phys*. *and Mol*. *Plant Path*. 2003, 63, 223-232.

12. Sticher L, Mauch-Mani B, Metraux, J.P. Systemic acquired resistance. *Annu.Rev.Phytopathol*.1997, 35, 235-270.

13. Malamy J, Carr J P, Klessig D F, *et al*. Salicylic acid-a likely endogenous signal in the resistance response of tobacco to viral infection. *Science*. 1990, 250, 1002-1004.

14. Hahlbrock K, Scheel D. Physiology and molecular biology of phenylpropanoid metabolism. *Annu.Rev.Plant.Physiol.Plant Mol.Biol*.1989, 40, 347-369.

15. Rusmussen J B, Hammersschmidt R, Zook M N. Systemic induction of salicylic acid accumulation in cucumber after inoculation with *Pseudomonas syringae pv syringae*. *Plant Physiol*. 1991, 97, 1342-1347.

16. Van Loon L C. Pathogenesis-related Proteins. *Plant Mol*. *Biol*.1985, 4, 111-116.

17. Tornero P, Gadea J, Conejero V. Two PR-1 Genes from Tomato are differentially regulated and reveal a novel mode of expression for a pathogenesis-related gene during hypersensitive response and development. *Mol*. *Plant.Microbe Interact*. 1997, 10, 624-634.

18. Xi Z, Zhang R Y, Yu Z H, *et al*. Selective interaction between tylophorine B and bulged DNA. *Bioorg*. *Med*. *Chem*. *Lett*. 2005, 15(10), 2673-2677.

19. Jin G Y, Cao C Y, Li L T, *et al*. Synthesis and biological activities of substituted pyrazolo [4,5-*e*][1,3] thiazine derivative. *Chin*. *J*. *Pestic*. *Sci*.1999, 1, 15-19.

20. Li Z G. Preparation of organic intermediates.Chemical Industry Press, Beijing, 2001, pp.8, 152, 445.

21. Xu K X. Handbook of materials and intermediates of fine organic chemical industry Chemical Industry Press, Beijing, 1998, 4-39.

22. a)Xiao H Q, Ouyang G P, Sun X D, *et al*. Synthesis of pyrazole oxime esters. *Chin*. *J*. *Syn*. *Chem*. 2005, 13(6), 600-602; b)Ouyang G. P. Ph.D. Dissertation, Guizhou University, Guiyang, China, 2008.

23. Wilson A J. International table for X-ray crystallography, Vol.C, Kluwer Academic Publishers. Dordrecht: Tables 6.1.1.4 (pp. 500-502) and 4.2.6.8 (pp.219-222). 1992.

24. Sheldrick G M. SHELXTL, V 5.1, Software Reference Manual, Bruker AXS, Inc., Madison, Wisconsin, USA, 1997.

25. Sheldrick G M. in Program for empirical absorption correction of area detector data; University of Göttingen: Germany, 1996.

26. Gooding G V Jr, Hebert T T. A simple technique for purification of tobacco mosaic virus in large quantities. *Phytopathology*. 1967, 57(11), 1285-1286.

27. Li S Z, Wang D M, Jiao S M. in *Pesticide Experiment Methods-Fungicide Sector*; Li S Z, Ed.; Agricuture Press of China: Beijing, 1991, 93-94.

28. He Z P. in *A Guide to Experiments of Chemical control for Crops*; He, Z.P., Ed.; Beijing Agricultural University Press:Beijing, 1933, 30-31.

29. Polle A, Otter T, Seifert F. Apoplastic Peroxidases and Lignificatio n in Needles of Norway Spruce. *Plant Physiol*.1994, 106, 53-60.

30. Beauchamp C, Fridovich J. Superoxide dismutase. Improved assay and an assay applicable to acrylamide gels. *J*. *Anal*. *Biochem*.1971, 444, 276-278.

31. Yamakawa H, Kamada H, Satoh M, *et al*. Spermine is a salicylate-independent endogenous inducer for both tobacco acidic pathogenesis-related proteins and resistance against tobacco mosaic virus infection. *Plant Physiol*.1998, 118, 1213-1222.

32. Anand A, Zhou T, Trick H N, *et al*. Greenhouse and field testing of transgenic wheat plants stably expressing genes for thaumatin-like protein, chitinase and glucanase against Fusarium graminearum. *J*. *Exp*. *Botany*.2003, 54, 1101-1111.

33. Mohamed F, Lydia F, Masumi I, *et al*.Expression of potential defense responses of Asian and European pears to infection with Venturia nashicola. *Physiol*. *Mole*. *Plant Path*. 2004, 64, 319-330.

34. Yuan J S, Reed A, Chen F, *et al*. Statistical analysis of real-time PCR data. *BMC.Bioinform*. 2006, 7, 85.

35. Chen G Z. Fluorescence analytical method. Beijing: Science Press, 1990, 122.

36. The National Center for Biotechnology Information (NCBI). Protein AAD20291.

37. Fraenkel-Conrat H, Williams R C. Reconstitution of active tobacco mosaic virus from its inactive protein and nucleic acid components. *Proc*. *Natl*. *Acad*. *U S A*, 1955, 41, 690.

38. Liu X H, Cui P, Song B A, *et al*. Synthesis, structure and antibacterial activity of novel 1-(5-substituted-3-substituted-4, 5- dihydropyrazol-1-yl)ethanone oxime ester derivatives. *Bioorg*. & *Med.Chem*.2008, 16, 4075-4082.

39. Velaparthi S, Brunsteiner M, Uddin R, *et al*. 5-*tert*-Butyl-*N*-pyrazol-4-yl-4, 5, 6,7-tetrahydrobenzo [*d*]isoxazole-3-carboxamide derivatives as novel potent inhibitors of *Mycobacterium tuberculosis* Pantothenate synthetase: initiating a quest for new antitubercular drugs. *J*. *Med*. *Chem*.2008, 51, 1999-2002.

40. Magedov I V, Manpadi M, Van slambrouck S, *et al*. Discovery and investigation of antiproliferative and apoptosis-inducing properties of new heterocyclic podophyllotoxin analogues accessible by a one-step multicomponent synthesis. *J*. *Med*. *Chem*. 2007, 50, 5183-5192.

41. Rovnyak G C, Millonig R C, Schwartz J, *et al*. Synthesis and antiinflammatory activity of hexahydrothiopyrano [4, 3-*c*]pyrazoles and related analogs. *J*. *Med*. *Chem*.1982, 25, 1482-1488.

42. Wachter G A, Hartmann R W, Sergejew T, *et al*. Tetrahydronaphthalenes: influence of heterocyclic substituents on inhibition of steroidogenic enzymes P450 arom and P450 17. *J*. *Med*. *Chem*.1996, 39, 834-841.

43. Colliot F, Kukorowski K, Hawkins A, *et al*. Fipronil: a new soil and foliar broad spectrum insecticide. *Brighton Crop Prot*. *Conf*. *Pests Dis*.1992, 1, 29-34.

44. Chen H S, Li Z, Han M, *et al*. Synthesis and fungicidal activity against *Rhizoctonia solani* of 2-alkyl(alkylthio)-5-pyrazolyl-1,3,4-oxadiazoles (Thiadiazoles). *J*. *Agric*. *Food*. *Chem*.2000, 48, 5312-5315.

45. Vicentini C B, Romagnoli C, Andreotti E, *et al*. Synthetic pyrazole derivatives as growth inhibitors of some phyto-pathogenic fungi. *J*. *Agric*. *Food Chem*. 2007, 55(25), 10331-10338.

46. Vicentini C B, Mares D, Tartari A, *et al*. Synthesis of pyrazole derivatives and their evaluation as photosynthetic electron transport inhibitors. *J*. *Agric*. *Food Chem*.2004, 52, 1898-1906.

47. Waldrep T W, Beck J R, Lynch M P, *et al*. Synthesis and herbicidal activity of 1-aryl-5-halo and 1-aryl-5-(trifluoromethyl)-1H-pyrazole-4-carboxamides. *J*. *Agric*. *Food Chem*.1990, 38, 541-544.

48. Clark, R.D. ynthesis and QSAR of herbicidal 3-pyrazolyl α, α, α-trifluorotolyl ethers. *J.Agric.Food Chem*.1996, 44, 3643-3652.

49. Li Y, Zhang H Q, Liu J, *et al*. Stereoselective synthesis and antifungal activities of (*E*)-α-(methoxyimino) benzeneacetate derivatives containing 1, 3, 5-substituted pyrazole ring. *J*. *Agric*. *Food*. *Chem*. 2006, 54, 3636-3640.

50. Huang R Q, Song J, Feng L. Synthesis and bioactivity of 1, 3,5-substituted pyrazol-4-methylene cyclopropane carboxylate. *Chem J*. *Chin Univer*.1996, 17, 1089-1091.

51. Liu Y, Ren J, Jin G Y. Synthesis and biological activities of 1-phenyl (methyl)-3- methyl-5-(4,6-dimethyl-2-thio)pyrimidyl-4-pyrazolyl oxime ethers (esters). *Chin*. *J*. *Pestic*. *Sci*.2001, 3, 12-16.

52. Minakata S, Hamada T, Komatsu M, *et al*. Synthesis and biological activity of 1*H*-pyrrolo [2,3-*b*] pyridine derivatives: correlation between inhibitory activity against the fungus causing rice blast and ionization potential. *J*. *Agric*. *Food Chem*.1997, 45, 2345-2348.

53. Cui P, Liu X H, Zhi L P, *et al*. Synthesis and biological activity of novel 5-aryl-*N*-pyrazole oxime ester derivatives. *Chin.J*. *Appl Chem*.2008, 25(7), 820-824.

54. Song B A, Zhang H P, Wang H, *et al*. Synthesis and antiviral activity of novel chiral cyanoacrylate

derivatives. *J. Agric.Food Chem*.2005, 53, 7886-7891.

55. Bartroli J, Turmo E, Alguero M, *et al*. New azole antifungals. 3. Synthesis and antifungal activity of 3-substituted- 4(3H)-quinazolinones. *J. Med. Chem*.1998, *48*, 1869-1882.

56. El-Sharief A M Sh, Ammar Y A, Zahran M A, *et al*. Aminoacids in the synthesis of heterocyclic systems: The synthesis of triazinoquinazolinones, triazepinoquinazolinones and triazocinoquinazolinones of potential biological interest. *Molecules*. 2001, 6, 267-278.

57. Purohit D M, Bhuva V R, Shah V H. Synthesis of 5-arylaminosulpho-*N*-acetyl-anthranilic acid, 6-arylaminosulpho-2-methyl-3-amino/3-*N*-chloroaceta mido /3-*N*-arylamino acetamido-4-(3*H*)-quina-zolones as potential anti-HIV, anticancer and antimicrobial agents. *Chemistry* (*Rajkot*, *India*), 2003, 1(4), 233-245.

58. Murav'eva K M, Arkhangel'skaya N V, Shchukina M N, *et al*. Synthesis and tuberculostatic activity of aminoquinazolines. *Khimiko-Farmatsevticheskii Zhurnal*. 1971, 5(6), 25-27.

59. Abdel-Hamid S G. Synthesis of some new heterocyclic systems bearing 2-phenyl-6-iodo-4(3*H*)-quinazolinon-3-yl moiety as antibacterial agents. *J. Indian Chem. Soc*.1997, 74, 613-618.

60. Barker A J. Quinazoline derivatives and their use as anti-cancer agents. *Eur Pat*, 635498, 1995; *Chem. Abstr*.1995, 122, 214099.

61. Aziza M A, Ibrahim M K, El-Helpy A G. Synthesis of novel-2-styryl-3- benzylidenimino-4(3*H*)-quinazolone derivatives of expected anticonvulsant activity. *Al-Azhar Pharm. Sci*.1994, 14, 193-201.

62. Ergenc N, Buyuktimkin S, Capan G, *et al*. Quinazolinones. 19. Communication [1]: synthesis and evaluation of some CNS depressant properties of 3-{2- [(5- aryl-1,3,4-oxadiazol-2-yl)amino]acetamido}-2-methyl-4(3*H*)-quinazolin ones.*Pharmazie*. 1991, 46(4), 290-291.

63. Bekhit A A, Khalil M A. Synthesis benzopyrazolyl derivatives of quinazolinones. *Pharmazie* 1998, 53, 539-544.

64. Hamel E, Lin C M, Plowman J, *et al*. Antitumor 2,3-dihydro-2-aryl-4(1*H*)-quinazolinone derivatives. Interactions with tubulin. *Biochem.Pharmacol*.1996, 51, 53-59.

65. Terashima K, Shimamura H, Kawase A, *et al*. Studies on antiulcer agents. IV: Antiulcer effects of 2-benzylthio-5, 6, 7, 8-tetrahydro- 4(3*H*)-quinazolinones and related compounds. *Chem.Pharm.Bull*. 1995, 43, 2021-2023.

66. Gursoy A, Karali N. Synthesis and anticonvulsant activity of new acylthiosemicarbazides and thiazolidones. *Farmaco*. 1995, 50, 857-866.

67. Baek D J, Park Y K, Heo H I, *et al*. Synthesis of 5-substituted quinazolinone derivatives and their inhibitory activity *in vitro*. *Bioorg Med.Chem.Lett*.1998, 8, 3287-3290.

68. Griffin R J, Srinivasan S, Bowman K, *et al*. Resistance-modifying agents.5. Synthesis and biological properties of quinazolinone inhibitors of the DNA repair enzyme poly (ADP-ribose) polymerase (PARP). *J.Med.Chem*.1998, 41, 5247-5256.

69. Balazs S, Kalman H, Tamas K. Quinazolinone-derivatives and their use for preparation of pharmaceutical compositions having parp enzyme inhibitory effect. *US Patent*. 20070042935, 2007.

70. Uehara M, Shimizu T, Fujioka S, *et al*. Synthesis and insecticidal activity of 3-amino-quinazolinone derivatives. *Pesticide Science*. 1999, 55(3), 359-362.

71. Ouyang G P, Zhang P Q, Xu G F, *et al*. Synthesis and Antifungal Bioactivities of 3-Alkylquinazolin-4-one Derivatives. *Molecules*. 2006, 11, 383-392.

72. Liu X, Huang R Q, Li H, *et al*. Synthesis and bioactivity of O-(4-quinazolinyl) hydroximic thioesters (amides). *Chin. J. Appl. Chem*.1999, 16(2), 23-26.

73. Nanda A K, Ganguli S, Chakraborty R. Antibacterial activity of some 3-(Arylideneamino)-2-phenylquinazoline-4(3*H*)-ones: synthesis and preliminary QSAR studies. *Molecules*.2007, 12, 2413-2426.

74. Ameta U, Ojha S, Bhambi D, et al. Synthetic studies on some 3-[(5- arylidene- 4-oxo-1, 3-thiazolidin-2-yliden)amino]-2-phenylquinazolin-4-(3*H*)-ones and their ethoxyphthalimide derivatives. *Arkivoc*.2006,

(xiii), 83-89.

75. Desai N C, Bhatt J J, Shah B R. Synthesis of substituted quinazolone derivatives as potential anti-HIV agents. (Part III). *Farmaco*.1996, 51(5), 361-366.

76. Song S Q, Zhou L G, Li D, *et al*. Antifungal activity of five plants from Xinjiang. *Nat*. *Prod*. *Res*. & *Dev*.2004, 16, 157-159.

77. Faize M, Faize L, Lshizaka M, *et al*. Expression of potencial defense relponse of Asian and European pears to infection with Venturia nashicola.*Phgsiol*. *Mol*. *Plant*. *Path*.2004, 64, 319-330.

78. Ouyang G P, Cai X J, Chen Z, *et al*. Synthesis and antiviral activities of pyrazole derivatives containing oxime ethers moiety. *J. Agric. Food. Chem*.2008, 56, 10160-10167.

79. Ouyang G P, Chen Z, Cai X J, *et al*. Synthesis and antiviral activities of pyrazole derivatives containing oxime esters group. *Bioorg.& Med.Chem*.2008, *16*, 9699-9707.

80. Gao X W, Cai X J, Yai K, *et al*. Synthesis and antiviral bioactivities of 2-phenyl-3-(substituted-benzalamino)-4(3H)-quinazolinone derivatives. *Molecules*, 2007, 12, 2621-2642.

Chapter 5
Innovation and Application of Environment-Friendly Antiviral Agents for Plants

In the research work described in the first four chapters, several compounds, such as Dufulin and GU188, were identified with high bioactivities against plant virus such as TMV or CMV. Afterwards, a great deal of work in this area was carried out, which included the preparation of Dufulin formulation (SC, EC, and WP), optimization of synthetic conditions, and studies on health toxicity evaluation, field trial bioassay, residue analysis, environmental behavior, systemic behaviors, as well as mode of action. Based on these work, Dufulin and its formulation were granted temporary registrations by the Ministry of Agriculture of China and were put into industrial production for large scale field application. Besides, some basic mechanicstic research on the mode of action of Dufulin was conducted which proved that Dufulin exerts its function through a new mechanism by activating the plant immune system. Extensive R&D work on cyanoacrylate derivative GU188 was also undertaken which included the synthesis optimization, bioassays, field trial, toxicity evaluation, and mode of aciton investigation. It was demonstrated that GU188 is another highly active potential antiviral agents for plants. The bioassay and mechanism of another antiviral product for plants, named "Jingtuling" (0.5% amino-oligosaccharin aqua), which was produced from the marine biowastes, were also studied.

5.1   Innovation of New Antiviral Agent Dufulin[*N*-[2-(4-methylbenzothiazol)]-2-ylamino-2-fluophenyl-*O,O*-diethyl phosphonate]

Taking natural amino acid as the lead compound, thousands of novel compounds were designed and synthesized by us. Among them a new chemical entity Dufulin, a typical aminophosphonate derivative containing fluorine, was screened out with significant anti-virus activity.

In the bioassay of protection, curation, and inactivation activities against TMV *in vitro* and *in vivo*, Dufulin showed higher anti-TMV activity than that of the commercial antiviral agent Ningnanmycin. During the R&D of Dufulin,

research on product chemistry, toxicology, field trial for biological effect, residue, environmental toxicology, environmental behavior, analysis method and action mechanism was carried out and are described as follows.

5.1.1   Product Chemistry

Dufulin (Bingduxing), chemical name:*N*-[2-(4-methylbenzothiazol)]-2-ylamino-2-fluoro-phenyl-*O,O*-diethyl phosphonate(Fig 5.1).
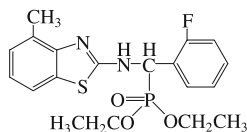
Structure：

Pesticide common chemical name：Dufulin.

Physicohemical Properties:MW:408.43; molecular formula：$C_{19}H_{22}FN_2O_3PS$; colorless crystal; mp 143-145℃.

Dissolves freely in acetone, THF, DMSO and so on. Solubilities in water, acetone, cyclohexane, cyclohexanone and dimethylbenzene at 22℃ are 0.04 g/L, 147.8 g/L, 17.28 g/L, 329.00 g/L and 73.30 g/L respectively. It is stable under light, heat and moist conditions, but slowly gets decomposed by acid or base.

Formulation of 30% Dufulin wettable powder(WP)was developed with the composition of effective ingredient of Dufulin 30%, diatomite 60%, sodium lignosulfonate 5%, LS detergent 5%, water content 0.5%, pH=7.6.

Formulation of 10% Dufulin EC was developed with the composition of 10% Dufulin, 8% E-3, and 82% solvent C.

Formulation of 30% Dufulin suspension concentrate (SC) was developed with 30% Dufulin, 1.5% emulsifier 600[#], 1.5% emulsifier 500[#], 2.0% alkylphenol ethoxylates (NP-10), 0.15% thickening agent, 3% antifreezing agent, 0.1% antifoaming agent and 62% water.

5.1.2   Formulation of Dufulin

In order to make novel virucide Dufulin usable for practical purpose, it is necessary to prepare its formulation before field trial and the subsequent field application. In this study, three different kinds of formulation, which are 30% wettable powder (WP), 10% emulsion concentrate (EC), and 30% suspension concentrate (SC) were developed. The formulations obtained by adopting simple methodologies to achieve stable performance for bioassay and under field trial and application, were optimized.
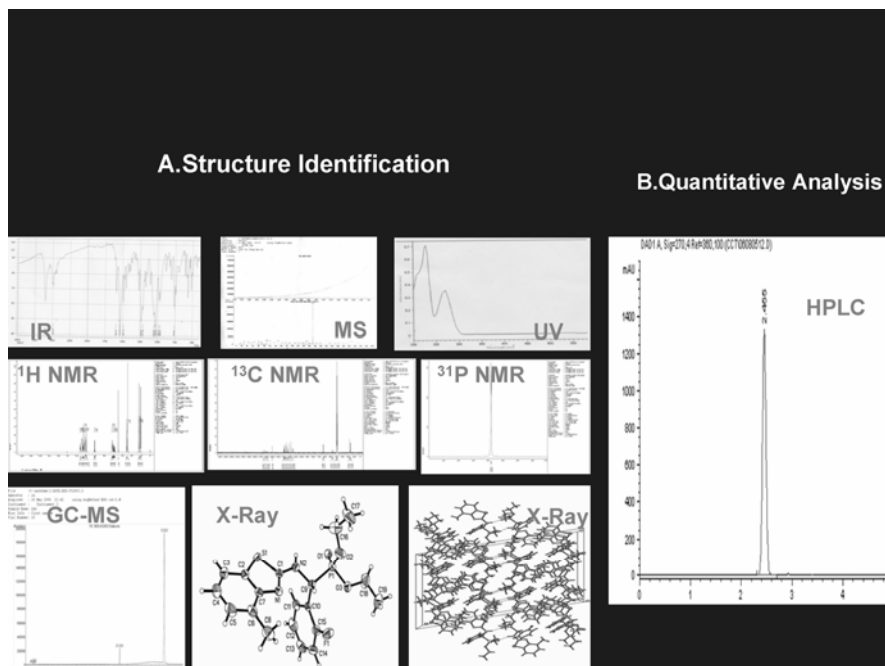
Fig 5.1   Structure elucidation and quantitative analysis for Dufulin

5.1.2.1   Formalation of 30% Dufulin suspension concentrate(SC)

(1) *Introduction*

SC, also known as water sc and enrichment suspension, was developed as a kind of new formulation in the 1970s. SC has the advantage of both WP and EC and was once considered as "epoch-making" new formulation. As the spreading medium is water, SC has several advantages such as low cost, safer production, easy storage and application. It can be mixed with water by any ratio and not affected by the water quality, water temperature. The formulation of 30% Dufulin SC was carried out through the selection and optimization of dispersing reagents and emulsifiers followed by optimization of the formulation ingredients. The technical parameters and storage stabilities of different combination were also investigated.

In order to increase the stability of the SC suspension, the addition of a certain amount of suitable surfactants is essential. Therefore, the selection of type and amount of surfactant is extremely important. For pesticide formulations, the emulsifier, dispersant, and the auxiliary reagents consist mostly of anionic and non-ionic surfactants. The synergistic effect of these surfactants can improve the suspension rate of the formulation. In this study, anonic emulsifier, emulsifier 500[#] and non-ionic emulsifier 700[#] were investigated and the type as well as the amount of the surfactant was determined by means of flow-point and viscosity

curve. Several anion and non-anion surfactants and other auxiliary to build compounded system were selected by optimization grouping method. Formula of Dufulin 30% SC was studied. The characteristics, method of manufacture and specification for quality control are also described in this chapter. This formulation has several advantages including low degradation, good storage stability and excellent suspension ratio (>90%), making it a potentially good product for agricultural applications.

(2) *Materials and Methods*

Dufulin (98% in purity), emulsifier 500[#], emulsifier 600[#], emulsifier 34[#], emulsifier 700[#], emulsifier 1601, OP-15, AEO-15, OP-40, T-20, T-80, BY-110, XG, CMC, PVA, Ethylene glycol, Octanol.

Dufulin was grinded by ball mill for 2.5-3h and screened through 325 mesh sieves. Different ingredients were weighed according to the recipes and mixed together. The mixture was then mixed with glass beads and was grinded coarsely for 30 min, followed by grinding for 2.5-3h in high-speed shearing machine (3500r/min) until the average particle size varied between 3-5μm. The liquid mixture was then filtered to give the formulation product.

Evaluation of wetting dispersant. Wetting dispersant was evaluated by flow-point. The wetting dispersant was dissolved in water to the concentration of 5%. Five gram of water was added to a 50 mL beaker and the beaker together with a stainless spoon was weighed accurately. Then the prepared wetting dispersant solution was added to the beaker dropwise and the resulting mixture was stirred. The spoon was lifted as the dropwise addition continued and the addition was stopped when a liquid droplet adhering to the spoon began to drip. The beaker, together with the stainless spoon and the liquid mixture was weighed again and then the weight of added solution can be calculated. Four replicates were carried out for each experiment and the results are listed in Table 5.1.

(3) *Results and Discussion*

Selection of wetting dispersant. The results of the wetting dispersant selection are listed in Table 5.1. As can be seen in Table 5.1, flow points of 12 kinds of surfactants on Dufulin were tested, which varied from 2.25 ± 0.13g to 4.12 ± 0.15g. Based on these results, emulsifier 600[#], emulsifier 700[#], NP-10, and OP-15 were selected for the further investigation in preparing 30% Dufulin SC.

Table 5.1   Flow point of wetting dispersant

Wetting dispersant	Flow point(g)	Wetting dispersant	Flow point(g)
Emulsifier 600[#]	2.25 ± 0.13	Emulsifier 33[#]	3.13 ± 0.17
Emulsifier 700[#]	2.58 ± 0.21	Emulsifier 34[#]	3.23 ± 0.18
BY-110	4.12 ± 0.15	T-20	2.71 ± 0.15
NP-10	2.52 ± 0.16	OP-40	2.76 ± 0.11
OP-15	2.55 ± 0.11	T-80	2.82 ± 0.14
Emulsifier 1601	2.90 ± 0.13	AEO-15	3.06 ± 0.16

Optimization of wetting dispersant dosage. After the selection of the wetting dispersant, the wetting dispersant dosage was investigated. It was found that the minimum suspension viscosity appeared with 1.5% emulsifier 600# or 1.5% NP-10. On the other hand, for emulsifier 700#and OP-15, the minimum suspension viscosity appeared at the concentration of 2% and 2.5%, respectively.However, the dosage of the minimum suspension viscosity of OP-15 was higher than the others, and emulsifier 700# was easily foamable. Therefore Emulsifier 600# and NP-10 were selected for further formulation optimization.

Selection of viscosity modifier. Adding viscosity regulator is an important method to improve suspension stability and to prevent delay flocculation, sedimentation and agglomeration of the suspension, which are important technical parameters of SC. To keep the suspension in the appropriate viscosity range is very important for maintaining quality and the application effect. As a result, the ideal viscosity of the suspension is in the range of 500-800 mPa • s. It was found that XG had good thixotropy, good tolerance against alkali and high concentration salt, and not sensitive to changes in temperature. Also taking into account various factors such as solubility, etc, XG was finally selected as the viscosity modifier of the formulation. Since the concentration of viscosity modifier has strong effect on the viscosity of the suspension, the content of XG was set as 0.15%.

Selection of antifreezing agent. For those water based formulation, antifreezing agent is essential for the production, storage and application of the formulation in north cold area. The commonly used antifreezing agents include glycol, propylene glycol, glycerin, and so on. Here, we selected ethylene glycol as the antifreezing agent with the concentration of 3% and the resulting product still possessed good fluidity at low temperature.

Optimization of Dufulin SC formulation. According to the physicochemical properties of dufulin and based on the experimental finding of mixing Dufulin with single nonionic and anionic emulsifier, it was found that the use of non-ionic and anionic emulsifier mixture should have better performance. So, non-ionic emulsifier 600# and NP-10 and Anionic emulsifier 500# were selected for further optimization and the results are listed in Table 5.2.

Storage stability test of the formulation. Five SC samples were prepared according to the best formula and were sealed in ampoule bottles and stored at $54\pm2℃$ for 14 days to test their heat storage stability.The results are listed in Table 5.3. From the heat storage stability testing results (Table 5.3), it can be seen that after heat storage the suspension decomposition rates were 1.60% to 3.74%.

The technical parameters of 30% Dufulin SC are listed in Table 5.4. It can be concluded that 30% Dufulin SC has several advantages such as easy preparation, stable performance, and reliable quality. Components for the formulation are easily obtainable and the formulation is environmentally benign. The 30% Dufulin SC is expected to be applied for industrialization.

Table 5.2   Composition and performance of 30% Duflin SC
by orthogonal design[a]

Composition (%)	Number of Formula								
	1	2	3	4	5	6	7	8	9
Dufulin	30	30	30	30	30	30	30	30	30
Emulsifier600[#]	0	1.0	1.5	1.0	1.5	0	1.5	0	2.0
Emulsifier700[#]	1.5	2.0	2.5	1.5	2.0	2.5	1.5	2.0	1.0
TX-10	1.5	2.0	2.5	2.5	1.5	2.0	2.0	2.5	1.5
XG	0	0	0	0.1	0.1	0.1	0.15	0.15	0.15
Glycol	3	3	3	3	3	3	3	3	3
Octanol	0.1	0.1	0.1	0.1	0.1	0.1	0.1	0.1	0.1
Water	63.9	61.9	60.4	61.8	61.8	62.3	61.8	62.3	62.3
Suspension rate	82.9	85.5	87.0	90.3	90.8	86.3	91.6	85.0	90.6
Sieve analysis	94.3	94.9	95.7	95.6	96.3	94.5	97.6	94.6	96.8
Dispersion	NG	NG	G	G	G	NG	G	NG	G
Heat storage stability	F	F	G$^-$	G$^+$	G	G$^-$	G	G$^-$	G
Cold storage stability	G$^-$	G$^-$	G$^-$	G$^-$	G$^-$	NG	G$^+$	G$^-$	G

[a] F stands for Fail; NG for Not Good or just fair; G for good.

It can be seen from Table 5.2 that formula 7 is associated with good suspension rate and sieve analysis.

Table 5.3   Heat storage stability test of 30% Dufulin SC[a]

No.	Sieve analysis 75μm(%)		Dufilin content(%)		Suspensibility(%)		Pourability(%)		Decomposition rate(%)
	P	A.	P	A	P	A	P	A	
01	96.3	95.6	31.6	30.9	92.6	90.2			2.22
02	97.6	97.1	30.4	29.8	91.4	90.3			1.97
03	94.5	93.2	31.5	30.6	92.8	91.4	Qualified	Qualified	2.86
04	95.8	94.4	32.1	30.9	91.7	90.2			3.74
05	97.1	94.7	31.2	30.7	92.5	90.8			1.60

[a] P represents before heat storage. A represents after the heat storage.

Table 5.4   Technical parameters of 30% Dufulin SC

Item	Dufilin content(%)	Suspension rate(%)	Sieve analysis (75μm)	Viscosity (mPa·s)	pH	Pourability	Storage stability	
							Cold	Heat
Result	30	90	95	630-790	7.1	Qualified	Qualified	Qualified

(4) *Conclusions*

After optimizing the type and amount of wetting dispersant, the selection of antifreezing agent, antifoaming agent and the composition optimization, the ingredients of the formulation are as follows：the composition consists of dufilin 30.0%, alkylphenol ethoxylates (NP-10) 2.0%, thickening agent 0.15%, emulsifier 600 0.15% and 500 2.0%, antifoaming agent 0.1%, antifreezing agent 3% and water 62%. The experimental results of the storage stability and the characteristics

of the formulation show that it has salient features such as low cost, low degradation, simple operation, economic benefits, good storage stability and excellent suspension ratio (>90%), making it a potential candidate for agricultural applications.

5.1.2.2   Formalation of 30% Dufulin wettable powder(WP)

(1) *Introduction*

Wettable powder (WP) is a kind of traditional pesticide formulation which is usually prepared by mixing the active constituent, inert fillers and a certain amount of additives. The mixture is then grinded to certain degree of fineness. There is no difference between the powder formulation and the WP from the appearance point of view. However, due to the presence of additives such as wetting agent and dispersant, WP can be wetted and suspended to suspension and thus can be sprayed for application. Compared to EC, the production cost of WP is lower. Morever, WP can be packed with paper or plastic bag and may be easily stored and transported. More importantly, it is harmless to plants compared to EC due to the absence of solvents or emulsifiers in the WP formulation. The formalation of 30% Dufulin WP was carried out through the selection and optimization of dispersing reagents and emulsifiers followed by optimization of the formulation ingredients.

(2) *Materials and Methods*

The materials used for Dufulin WP formulation preparation are as follows：Dufulin (98% in purity), precipitated calcium carbonate (325 mesh), neat lotion LS, sodium lignosulfonate (NaLS in brief)and cacium lignosulfonate (CaLS in brief).

Certain amount of active ingredient Dufulin (98% in purity), additives, and fillers were mixed and added into the experimental jet miller, and the resulting air-grinded powder was mixed thoroughly to give Dufulin WP.

Analysis of the active ingredient：The concentration of the active ingredient Dufulin was analyzed using HPLC. 2.5g of WP sample was added to 15 mL methanol and the mixture was sonicated for 5 min and then filtered. The methanol solution was collected and the volume was adjusted to 50 mL. The analysis was carried out using Waters 600 HPLC instrument equipped with a 4.6mm×250mm C18 reverse column through external standard quantification method.

Suspension rate was tested according to the National standard GB/T 14825-93 of China. The moisture content was determined according to GB/1600 using Karl. Fischer method. The pH value was tested by using the method described in National standard GB/T1601.

(3) *Results and Discussion*

Effect of different type and amount of additives on suspension rate & wetting time. In order to find the best combinations to prepare Dufulin WP, different additives together with different auxiliary agents were investigated. The effect of different types and amount of additives on the suspension rate & wetting time of WP was studied and the results are listed in Table 5.5.

Table 5.5   Effect of different additives and amount on product quality

Auxiliary 1	Auxiliary 2	Suspension rate products(%)	Product wetting time(s)
8% NNO	5% NaLS	30.8%	120
8% LS	5% CaLS	62.4%	77
6% LS	5% CaLS	51.3%	60
5% LS	5% NaLS	75.8%	34
6% LS	6% NaLS	77.8%	35
7% LS	7% NaLS	70.4%	46

It can be seen from Table 5.5 that combination of Neat lotion LS with sodium lignosulfonate (NaLS), with the concentration of 5% for each, can give good suspension rate and wetting time for 30% Dufulin WP formulation. 30% Dufulin WP made with this combination meets all the requirements of 30% Dufulin WP enterprise standard Q/GD02-2005.

The effect of moisture on product quality. Water content in 30% Dufulin WP is an important parameter since it can affect the product stability. The effect of water content on product quality was investigated and the results are listed in Table 5.6.

From Table 5.6 it can be seen that when the moisture content varies from 0.5% to 2%, the product quality does not change to a large extent after heat storage. However, when the water contents are 3% or 4%, the active ingredient content, pH value, fineness and suspension rate decrease sharply, whereas the wetting time as well as the decomposition rate increase significantly. Hence, the water content in 30% Dufulin WP should not exceed 2%, which was required in the enterprise standard of 30% Dufulin WP.

Table 5.6   The effect of moisture on product quality

Water content		0.5%	1%	2%	3%	4%
Technical parameters before heat storage	Active ingredient(%)	30.12	30.20	30.18	30.22	30.09
	pH value	7.1	6.9	7.0	6.8	6.7
	Fineness(%)(325 mesh)	97.21	96.56	96.45	96.57	96.23
	Suspension rate(%)	78.9	78.4	77.6	70.2	65.8
	Wetting time(s)	30	35	40	56	62
Technical parameters after heat storage	Active ingredient(%)	30.00	30.11	29.67	28.34	26.35
	pH value	7.0	6.8	6.9	6.5	6.3
	Fineness(%)(325 mesh)	97.16	96.34	96.04	92.32	91.87
	Suspension rate(%)	78.5	78.2	77.1	67.8	61.7
	Wetting time(s)	31	38	43	59	65
	Decomposition rate(%)	0.398	0.298	1.69	6.22	12.43

For the 30% Dufulin WP products, the water content was tested regularly and some results are listed in Table 5.7. From Table 5.7, it can be seen that water contents in 30% Dufulin WP products are centainly less than 2%, thereby meeting the enterprise standard of 30% Dufulin WP very well.

Table 5.7   Water contents of some 30% Dufulin products

No.	Moisture	Acidity	Insoluble	Content	Appearance	Content(%)	Decomposition[a] rate(%)
1	0.30	0.2	0.86	95.66	Colorless	95.63	No effect
2	0.15	0.1	0.82	95.75	Colorless	95.72	No effect
3	0.46	0.3	0.91	95.23	Colorless	95.18	No effect
4	0.87	0.4	1.24	95.53	Colorless	94.49	0.88
5	0.60	0.6	2.50	90.42	Colorless	87.58	3.14

[a] Stored at $54 \pm 2℃$ for one week.

The effect of pH value on product quality. pH value is another important parameter of 30% Dufulin that affects the stability of the product. The effect of pH value on product quality was investigated and the results are listed in Table 5.8. From Table 5.8 it can be seen that when the pH value varies from 6 to 8, the product quality does not change much after heat storage. However, when the water content is less than 6 or more than 8, the active ingredient content decreases sharply, and the wetting time as well as the decomposition rate increase noticeably. Hence, the pH value in 30% Dufulin WP should be in the range of 6～8.

(4) *Conclusions*

After the selection of the type and amount of wetting dispersant combinatoins, the ingredients of the formulation of 30% Dufulin WP were ascertained as follows：30% Dufulin, 5% neat lotion LS, 5% sodium lignosulfonate, and 60% precipitated calcium carbonate. The suspension rate of this formulation is more than 75% with the wetting time of less than 1 min.

Table 5.8   Effect of pH value on product quality

pH value		5	6	7	8	9
Technical parameters before heat storage	Active ingredient(%)	30.12	30.20	30.18	30.22	30.09
	Water content(%)	0.51	0.63	0.63	0.67	0.78
	Fineness(%)(325 mesh)	97.01	96.53	96.60	96.52	96.12
	Wetting time(s)	30	31	33	35	41
Technical parameters after heat storage	Active ingredient(%)	27.10	29.11	29.63	29.34	26.55
	Water content(%)	0.50	0.58	0.60	0.63	0.74
	Fineness(%)(325 mesh)	97.12	96.31	96.72	96.47	96.35
	Wetting time(s)	32	30	34	36	44
	Decomposition rate(%)	10.02	3.61	1.82	2.91	11.76

5.1.2.3   Formulations of 10% Dufulin Emulsion Concentrate(EC)

(1) *Introduction*

EC formulations are generally prepared in toluene, xylene or other organic solvents as the dispersion medium, with appropriate emulsifiers as additives. The physical appearance of EC is homogeneous transparent oily liquid since the active ingredients are dissolved in the solvent with the help of dispersants or emulsifiers.

In comparision with the powder formulation, EC has no dust pollution and can improve the field efficacy of the active ingredient with less damage to the crop. EC is also easy to prepare and there is no waste product during the whole production process. The active ingredient content can be very high in EC with good storage stability. It is relatively easy to use and has good effect in the field. However, since the preparation of EC requires organic solvents such as toluene and xylene, waste petroleum resources that are harmful to human health and environment are often encountered. The transportation, storage and the container selection of EC are not convenient due to the use of flammable organic solvents.

　　The preparation of 10% Dufulin EC was carried out through the selection and optimization of emulsifiers followed by optimization of the formulation ingredients. The effects of different factors such as water content and pH value on the storage stability were also investigated.

　　(2) **Materials and Methods**

　　The materials used for Dufulin WP formulation preparation include：Dufulin(98% in purity)and different emulsifiers and organic solvents that are commercially available in the market.

　　Methods. 10% Dufulin EC preparation：Certain amount of Dufulin (98% in purity), emulsifier, and solvent were added into a beaker and the resulting mixture was stirred at room temperature until completely dissolved to give 10% Dufulin EC.

　　EC dispersion：To a 1000 mL beaker was added 990 ± 1 mL of distilled water and 10 mL of hard water. The temperature was set at $30 \pm 1℃$. 1 mL EC sample was withdrawn by means of a syringe which was held 1 cm above the water surface and then the sample was added dropwise to the hard water prepared above. After completion of the addition, the mixture was stirred with a glass bar of 6-8 cm diameter at the rate of 2-3 revolutions per second. The liquid turned homogeneous and no visible oil drop was noticed.

　　Analysis of the active ingredient：The concentration of the active ingredient Dufulin was analyzed using HPLC. 2.5g of EC sample was dissolved in 15 mL methanol. The analysis was carried out using Waters 600 HPLC instrument equipped with a $4.6mm \times 250mm$ C18 reverse column through external standard quantification method.

　　EC stability was tested according to the National standard GB1603-89 of China. The acidity of EC was determined according to GB1601-93. Moisture content tests were carried out by following the method described in National standard GB1600-89.

　　(3) **Results and Discussion**

　　Selection of solvents. Different solvents such as ethanol, methanol, acetonitrile, THF, DMSO, and solvent C, etc, were investigated. The results are listed in Table 5.9. It can be seen from Table 5.9 that solvents THF, DMSO and solvent C give satisfactory results. Taking the solvent cost into account, solvent C was selected for 10% Dufulin EC preparation.

Table 5.9   Solvent optimization experiment

Solvent	Cold(0-5℃ for three days)
ethanol	crystallization
methanol	crystallization
acetonitrile	crystallization
THF	5 awarded duplicate normal
DMSO	5 awarded duplicate normal
C	5 awarded duplicate normal

Selection of emulsifier. Different emulsifiers including E-1, E-2, E-3, E-4, E-5, E-6 and E-7 were investigated and the results are listed in Table 5. 10. As can be seen from Table 5.10, 10% emulsifier E-3 afforded good quality results both in terms of dispersibility and stability. Thus E-3 was selected for further studies on amount optimization. Different concentrations of E-3 from 6% to 12% were tested and it was found that 8%-10% E-3 gave good dispersion and stability.

Effect of moisture on EC. The effect of water content on EC quality was investigated. It was found that when the water content was 0.3% and 0.5%, the EC products were transparent yellow liquid. However, when water content was 1.0%, the EC turned turbid and flocculent precipitation appeared. Hence, the water content in EC should be less than 0.5%.

Table 5.10   Test results with different emulsifiers

No.	The amount of emulsifier(%)	Determination of the performance of emulsifier	
		Dispersibility	Stability
E-1	10%	Failed	Unqualified
E-2	10%	Failed	Unqualified
E-3	10%	Qualified	Qualified
E-5	10%	Failed	Unqualified
E-6	10%	Failed	Unqualified
E-7	10%	Failed	Unqualified
E-3	6%	Failed	Unqualified
E-3	8%	Qualified	Qualified
E-3	12%	Failed	Unqualified

Effect of acidity on EC product. Acidity of EC is an important parameter of 10% Dufulin EC product. It was found that the acidity value of 10% Dufulin EC product should be less than 0.5.

Reproducible Stability test of the EC formulation. Based on the formulation obtained above, 10% Dufulin EC product was prepared for five times to check its reproducible stability. As can be seen from Table 5.11, the optimized formulations are stable under the cold and heat storage condition. After being stored at $54 \pm 2℃$ for 14 days, the decomposition rate was less than 5%.

Table 5.11　Reproducible stability test of the EC formulation

No.	Emulsifier dosage(%)	Low temperature stability	Stability	Acidity(%)	Content(%)^a	Decomposition rate(%)^b
2005-11	8	Pass	Pass	0.3	95.72	2.01
2005-12	8	Pass	Pass	0.2	95.42	1.81
2005-13	8	Pass	Pass	0.3	95.48	2.43
2005-14	8	Pass	Pass	0.3	95.71	2.19
2005-15	8	Pass	Pass	0.3	95.29	2.42
2005-16	8	Pass	Pass	0.2	95.44	1.90
Average	8	Pass	Pass	0.25	95.51	2.12

^{a} Storage before analysis of the content(%).

^{b} storage at $54\pm2℃$ for 14 days.

(4) *Conclusions*

After the selection of the type and amount of emulsifier, the ingredients of the formulation of 10% Dufulin WP are established as follows：10% Dufulin, 8% E-3, and 82% solvent C. The acidity and water content should be less than 0.5 and 0.5% respectively. With this formulation, 10% Dufulin EC is stable under both cold and heat storage.

5.1.3　Optimization of Synthetic Conditions in Lab Scale and Pilot Scale

5.1.3.1　Introduction

As described in the previous chapters, Dufulin was found to have excellent anti-TMV bioactivity. In order to obtain this product in large quantity for further development such as field trial and industrial production, the synthetic route as well as the synthetic conditions need to be optimized on both lab and pilot scales. We investigated different synthetic methods and the reaction parameters were optimized. The synthesis under solvent free condition with *p*-toluenesulfonic acid as catalyst was identified as the ideal choice. Under these reaction conditions, Dufulin could be obtained in more than 83% yield with 98% purity. A national invention patent of China has been awarded to Dufulin and this new antiviral agent was recently granted temporary registration by the Ministry of Agriculture of China. The product has been industrialized for the large scale field application (Fig.5.2-Fig.5.4).

5.1.3.2　Materials and Methods

The materials used for Dufulin synthesis include 2-fluorobenzaldehyde, 2-amino-4-methylbenzothiazole, diethyl phosphite, *p*-toluenesulfonic acid (TsOH), and some other chemical reagents and solvents that are commercially available in the market.
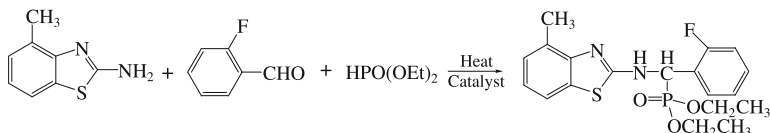
Scheme 5.1 Synthesis of Dufulin in lab scale

The synthetic route to Dufulin is shown in Scheme 5.1. To a 500 mL round bottomed flask were added 2-fluorobenzaldehyde (53.8 g), 2-amino-4-methyl-benzothiazole (71.0 g), and diethyl phosphite (59.8), with or without catalyst. The resulting mixture was stirred at 78-80 ℃ for 1-3 h. After cooling to room temperature, the mixture was filtered, and the resulted solid was recrystallized form 100 mL of ethanol to give Dufulin as white crystals, mp 143-145℃ (purity 98% according to HPLC analysis).

Synthesis of Dufulin in pilot scale. The reagent amounts under the lab scale experiments were scaled up to 700 times for pilot-scale production. Accordingly, a mixture of 49.2 kg 2-amino-4-methylbenzothiazole, 36.3 kg o-fluorobenzaldehyde, 41.4 kg diethyl phosphite and 2.1 kg of TsOH were stirred at 78-80℃ for 1 h.

5.1.3.3 Results and Discussion

In order to optimize the synthesis of Dufulin, several reaction conditions were investigated, including solvent free and catalyst free, ionic liquid as catalyst, solvent free with p-toluenesulfonic acid as catalyst, catalytic reaction by TsOH promoted by ultrasound and microwave irradiation. The results are shown in Table 5.12. From Table 5.12, it can be seen that the highest yield (90%) of Dufulin was obtained with p-toluenesulfonic acid as catalyst under the ultrasonic irradiation for 30min. Similar condition of microwave irradiation with TsOH as catalyst also afforded 89.2% yield in 20min. While the solvent free condition catalyzed by TsOH afforded 83.8% yield in 1 h, the reaction conducted in ionic liquid gave 47.8% yield in 12 h. For the solvent free reaction without involving any catalyst, 50.3% yield was obtained in 3h. Therefore, under optimized conditions of lab scale preparation, solvent free reaction with p-TsOH as catalyst is recommended.

In order to further optimize the reaction conditions, different reaction parameters such as temperature, catalyst and catalyst amount, and reaction time were investigated.

Table 5.12 The yield of the reaction under different conditions

Reaction conditions	Reactant ratio(mol)	Reaction temp.	Reaction time	Catalyst amount	Yield (%)
solvent free and catalyst free	1:1:1	78-80℃	3h	—	50.3
ionic liquid	1:1:1	Rt	12h	—	47.8
solvent free with TsOH as catalyst	1:1:1	78-80℃	1h	6%	84.2
microwave irradiation with TsOH as catalyst	1:1:1	78-80℃	20min	6%	89.2
ultrasonic irradiation with TsOH as catalyst	1:1:1	78-80℃	30min	6%	90.0

Selection of catalyst. Four kinds of different catalysts, including $AlCl_3 \cdot 6H_2O$, $SC(OTf)_3$, TsOH, $ZnCl_2$ were investigated based on the reactant ratio [fluorobenzaldehyde:2-amino-4-methylbenzothiazole:diethyl phosphite=1:1:1] and reaction temperature at 78-80℃. The molar equivalents of catalysts were 6% and the results are listed in Table 5.13. From Table 5.13, it can be seen that the highest yield of 84.2% was obtained with TsOH as catalyst, whlie the yields with other catalysts were all lower than that of TsOH.

Table 5.13　Effect of catalyst species on yield of Dufulin

Entry	Reactant ratio	Catalyst	Catalyst amount(mol)	Yield(%)
A1	1:1:1	$AlCl_3 \cdot 6H_2O$	6%	70.2
A2	1:1:1	$SC(OTf)_3$	6%	73.4
A3	1:1:1	TsOH	6%	84.2
A4	1:1:1	$ZnCl_2$	6%	65.6

Optimization of catalyst amount. After selecting TsOH as the ideal catalyst, the effect of the amount of TsOH was also invesitigated. The amount of TsOH was varied from 0.5%, 2%, 4%, 6%, to 8%, and the results are listed in Table 5.14. It can be seen that the best yield of 83.8% was obtained with the dosage of 4% TsOH. Also the yield was not improved on increasing the dosage to 8%. Therefore, the catalyst amount of 4% was selected as the optimum one.

Table 5.14　Effect of different catalyst amount on the yield of Dufulin

Entry	Reactant ratio	Amount of TsOH (mol)	Yield(%)	Entry	Reactant ratio	Amount of TsOH (mol)	Yield(%)
B1	1:1:1	0.5%	42.3	B4	1:1:1	6%	84.2
B2	1:1:1	2%	58.9	B5	1:1:1	8%	84.0
B3	1:1:1	4%	83.8				

Effect of reaction temperature on the yield. The effect of reaction temperature on the yield was also investigated. With the fixed reactant ratio(1:1:1), reaction time (1h), and the amount of TsOH (4%), the reaction temperature was varied from 38-40℃, 58-60℃, 78-80℃, 98-100℃, to 118-120℃,and the results are shown in Table 5.15. From Table 5.15, we can infer that at the optimum reaction temperature of 78-80℃, the yield of Dufulin was 83.3%, which was much higher than that obtained at 38-40℃, 58-60℃, 98-100℃, and 118-120℃. As expected, in the lower temperature range from 38-60℃, the reaction was found to be slower, low yielding and incomplete. At very high temperature, *e.g.* at 118-120℃, the reactant diethyl phosphite may get partially decomposed.

Table 5.15   Effect of different reaction temperatures on the yield of Dufulin

Entry	Reactant ratio	Amount of TsOH(mol)	Reaction temp(℃)	yield(%)
C1	1:1:1	4%	38-40	47.3
C2	1:1:1	4%	58-60	65.7
C3	1:1:1	4%	78-80	83.8
C4	1:1:1	4%	98-100	82.6
C5	1:1:1	4%	118-120	75.8

Effect of reaction time on the yield. Keeping other reaction parameters intact, the results of different reaction time were studied and are listed in Table 5.16 keeping other reaction parameters intact. It can be seen from Table 5.16 that the reaction yields were not improved significantly on prolonging the reaction time from 60 min (83.8%) to 80 and 100 min (83.6% and 84.0%, respectively). Thus, the optimum reaction time selected was 60 min.

The reproducibility of the optimum reaction conditions. In order to check the reproducibility of the optimum reaction conditions, the optimal conditions were repeated for several times and the results are shown in Table 5.17. The optimum reaction conditions were achieved with a reactant ratio of *n* (fluorobenzaldehyde):*n*(2-amino-4-methyl-benzothiazole):*n*(diethyl   phosphite):*n* (TsOH)=1:1:1:0.04(mole ratio) at 78-80℃ when reacted for 1 h.

It can be seen from Table 5.17 that the reaction conditions are reliable and the yields are reproducible. Based on these results, the technical parameters of the product standard are listed in Table 5.18.

Optimization of the reaction conditions in pilot scale. After completing the reaction optimization in lab scale, the process was enlarged in pilot scale to produce

Table 5.16   Effect of different reaction time on the yield of Dufulin

Entry	Reactant ratio(mol)	Amount of TsOH(mol)	Reaction temp	Reaction time	Yield(%)
D1	1:1:1	4%	78-80℃	20 min	23.8
D2	1:1:1	4%	78-80℃	30 min	52.3
D3	1:1:1	4%	78-80℃	50 min	76.4
D4	1:1:1	4%	78-80℃	60 min	83.8
D5	1:1:1	4%	78-80℃	80 min	83.6
D6	1:1:1	4%	78-80℃	100 min	84.0

Table 5.17   The reproducibility of the optimum reaction conditions

Entry	Yield(%)	Purity(%)	Entry	Yield(%)	Purity(%)
E1	83.42	98.58	E5	83.53	98.56
E2	83.37	98.54	E6	83.39	98.59
E3	83.28	98.63	E7	83.47	98.60
E4	83.45	98.68	E8	83.31	98.51

Table 5.18   The main technical parameters of product

Technical indicators	Content(%)
purity(m/m)	=98
Moisture content(m/m)	=0.5
Acidity content(m/m)	=0.3
Acetone insoluble substance(m/m)	=1.0

more Dufulin product. During the enlarged pilot scale experiments, the reaction parameters were optimized again as follows: the reactant ratio n(fluorobenzaldehyde):n(2-amino-4-methylbenzothiazole):n(diethyl phosphite):n(p-toluene sulfonic acid)=300:300:300:12(mol); reaction time was 1h; reaction temperature was 78-80℃.

   Under these optimized reaction conditions, the yield of Dufulin was more than 83% with purity greater than 98%. All the product parameters meet the requirements listed in Table 5.18. The process flow diagram for synthesis of Dufulin is shown in Scheme 5.2.
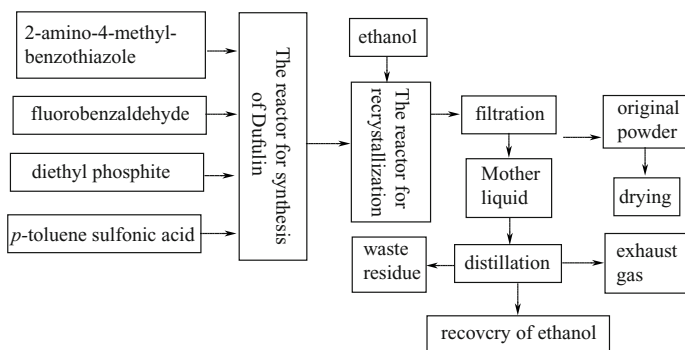
Scheme 5.2   Process flow diagram for the synthesis of Dufulin

5.1.3.4   Conclusions

   The optimum reaction parameters for the synthesis of Dufulin are obtained with a 1:1:1 molar ratio of 2-fluorobenzaldehyde, and 2-amino-4-methylbenzothiazole, and diethyl phosphite, in the presence of 0.09 molar catalytic amount of TsOH at 78-80℃ under stirring for 1 h. The yields of Dufulin are more than 83% with purity greater than 98%. The overall process for the preparation of Dufulin is quick, cheap, reproducible and easy to operate. The technology and the product quality are reliable and the production technology was easily industrialized (Fig 5.2,Fig 5.3,Fig 5.4).

Fig 5.2　Novel antiviral agent Dufulin
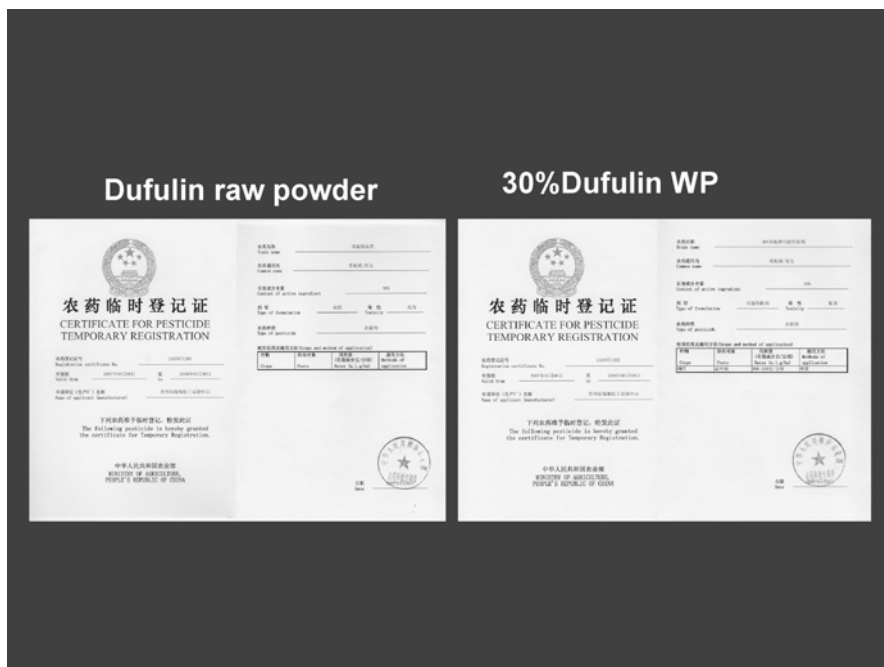
Fig 5.3　Certificate for Dufulin temporary registration

5.1.4   Toxicology Test

5.1.4.1   Introduction

It is imperative to observe the acute toxicity of Dufulin and its 30% WP formulation and provide evidence for assessment of toxicological security of Dufulin and WP. According to the requirements of pesticide registration in China, new chemical entity needs to be evaluated for its toxicology parameters which include acute oral and transdermal toxicity, skin and eye irritation, dermal allergic, bacterial reverse mutation test, Chromosome aberration test of mouse primary spermatocyte, Micronucleated Polychromatic Erythrocytes in Mice Bone Marrow, subchronic acute oral toxicity. Dufulin was also tested for all necessary test items that are required for its temporary registration. All the tests were carried out by the toxicology test institute certified by the Ministry of Health, the Ministry of Agriculture, such as China National Center for Disease Control (NCDC), China National Center for Quality Supervision & Test of Pesticides Safety (NCQSTP), and Insitution of Shenyang Chemical Industry (ISCI), Occupational Health and Evaluation Division.

Fig 5.4   Certificate for National Invention Patent of China

5.1.4.2　Methods

Based on GB15670-1995, acute toxicity tests by oral LD_{50} skin and inhalation, acute irritation toxicity test by skin and eye, skin sensitization tests were conducted. The methods for acute oral toxicity, percutaneous toxicity and eye irritation test are illustrated in this part.

Animal preparation. The animals are kept under the experimental housing and feeding conditions for certain days prior to the test. Before the test, healthy young animals are randomized and assigned to the treated and control groups.

Acute Oral Toxicity. The test compound was grinded and passed through 100 mesh sieve, followed by mixing with 3% starch slurry to make suspension solution at 250 mg/mL concentration. Tested rat was fed with only water over night before experiments, then was administered 2 mL/(100 g • d) by gavage and the final dosage was 5000 mg/(kg • d). Rats were fed normally 2 h after treatment. Rats were observed at 1, 3, 8, and 24 h on the first day and then observed on daily basis in the following two weeks. If the rat survived 3 days after treatment, this experiment was repeated again. The dead animal was dissected for pathological observation.

Percutaneous Toxicity. The test compound was grinded and passed through 100 mesh sieve, followed by mixing with distilled water to make suspension solution. The administration dosage was calculated according to the body weight of each rat based on the final dosage of 2150 mg/(kg • d). Then certain amount of the compound solution was applied on the back (ca.4cm×5cm) of male and female Wistar rat after shearing the fur. Rats were observed at 1, 3, 8 and 24 h on the first day and then observed on daily basis in the following two weeks. If the rat survived 3 days after treatment, this experiment was repeated again. The dead animal was dissected for pathological observation.

Rabbit eye irritation test. Four healthy rabbits with healthy eyes were selected. Dufulin sample was administrated into rabbit right eye conjunctival cell at the dosage of 0.1g. Then the eyelids were mandatorily closed for 1 min without any washing of the treated eye for 24 h after administration. The treated eye was observed at 1, 24, 48 and 72 h after treatment. The experiment was terminated 72 h after treatment if no irritation was noticed. The left eye was set as the control.

5.1.4.3　Results and discussion

According to the registration requirements for new pesticide, the health toxicities of Dufulin and its 30% WP formulation were tested. The test results are shown in Table 5.19, Table 5.20. It can be seen that the LD_{50} of oral toxicities of both Dufulin and its 30% WP formulation were more than 5000 mg/kg, the LD_{50} values of skin toxicities were more than 2000 mg/kg (LD_{50}>2000mg/kg). The test results of three mutagenic experiments were all negative. Subchronic acute oral toxicity test results revealed that Dufulin had no obvious effect on the animal

organs. Therefore, Dufulin is a kind of pesticide with low toxicity and is safe to human beings (Fig 5.5).

Table 5.19   Toxicology tests for Dufulin

Toxicity test items	Test objects	Toxicity	Authorized testing agency[*]
Acute Oral Toxicity Test	Male and female SD rats	Micro-pesticide(LD_{50}>5000 mg/kg)	NCDC
Acute Dermal Toxicity Test	Male and female SD rats	Low toxicity(LD_{50}>2150mg/kg)	NCDC
Acute Dermal Irritation Test	Male rabbits	No irritation	NCDC
Acute Eye Irritation Test	Male rabbits	No irritation	NCDC
Dermal Allergic Reaction	Male rats	Weak sensitization	NCDC
Subchronic Acute Oral Toxicity Test	Wistar rats	No organs changes	NCDC
Bacterial Reverse Mutation Test	Salmonella	Negative	(ISCI)
Chromosome aberration test of mouse primary spermatocyte	Male mice	Negative	NCDC
Micronucleated Polychromatic Erythrocytes in Mice Bone Marrow	Male mice	Negative	NCDC

*China National Center for Disease Control(NCDC)China National Center for Quality Supervision & Test of Pesticides Safety (NCQSTP), and Institution of shenyang Chemical Industry(ISCI), Occupational Health and Evaluation Division.

Table 5.20   Toxicology tests of 30% Dufulin WP

Toxicity test	Test objects	Toxicity	Authorized testing agency
Acute Oral Toxicity Test	Male and female SD rats	Micro-pesticide (LD_{50}> 5000mg/kg)	NCDC
Acute Dermal Toxicity Test	Male and female SD rats	Low toxicity (LD_{50}> 2000mg/kg)	NCDC
AcuteDermal Irritation Test	Male rabbits	No irritation	NCDC
Acute Eye Irritation Test	Male rabbits	No irritation	NCDC
Dermal Allergic Reaction	Male rats	Weak sensitization	NCDC

5.1.4.4   Conclusions

The acute toxicity, subchronic toxicity and mutagenicity of Dufulin were investigated and the results of the acute oral test indicated that the LD_{50} was up to 5000 mg/kg bw to male and female rats；the results of the acute dermal test indicated that the LD_{50} was up to 2150 mg/kg to male and female rats. The results of erythrocyte micronucleus assay, spermatogonial chromosomal aberrations test, and the Ames test were all negative. The NOAEL of the

subchronic toxicity on rats was 36.38 mg/(kg · d) to male rats and 40.75 mg/(kg · d) to female rats. All the health toxicology tests revealed that Dufulin is a kind of less toxic, less-irritating, less-allergic chemical and is relatively safe to mammals and human beings.
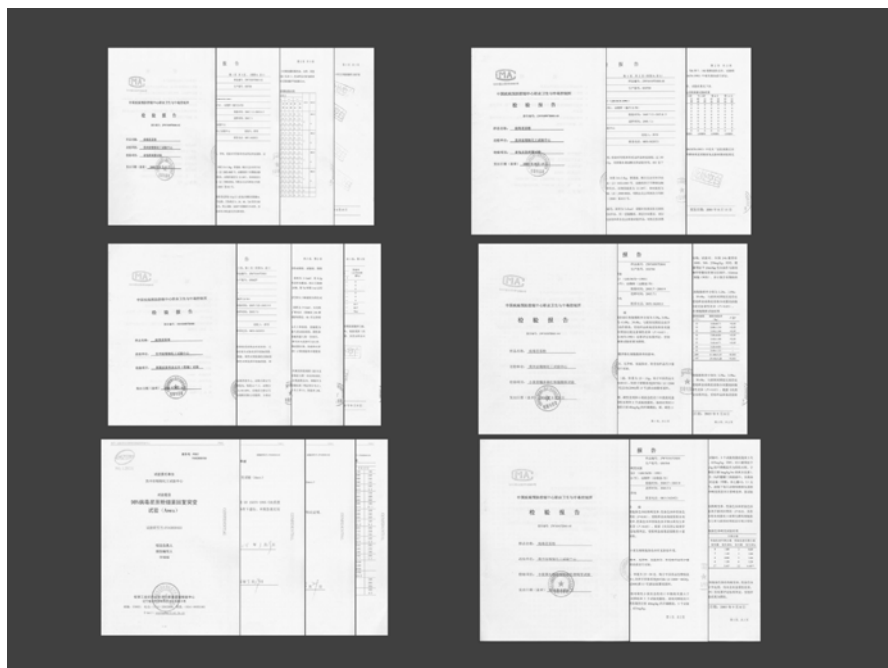
Fig 5.5   The test reports of oral toxicity, Ames, chromome aberration and erythrocyte micronucleus.

5.1.5   Field Trials

5.1.5.1   Introduction

Dufulin was found to have excellent anti-TMV bioactivity in the bioassay indoors (Fig 5.6, Fig 5.7). In order to select more effective virus inhibitors to control tobacco mosaic virus diseases and evaluate the field performance of Dufulin, series of field trials were carried out from 2005 to 2006 in different areas in China which included Guizhou, Chongqing, Henan, Shandong, Yunnan, Sichuan etc. All the field tests were approved by the pesticide administrative department of Ministry of Agiruclture of China. The results of the field trial demonstrated that the field efficacy of Dufulin is better than the commercial antiviral product agents Ningnanmycin, Virus A, etc.
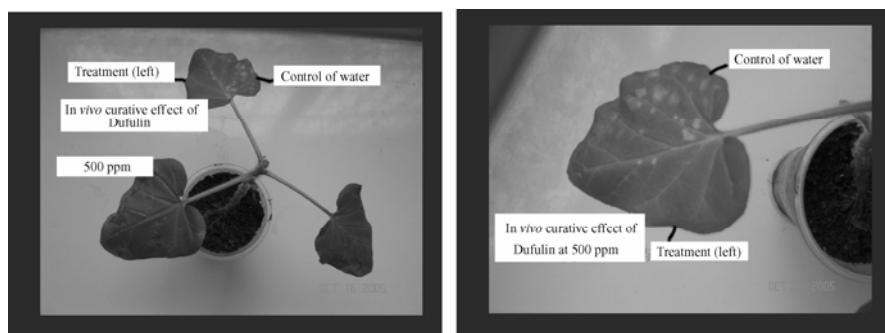
Fig 5.6   Curative effect of Dufulin in the bioassay indoors
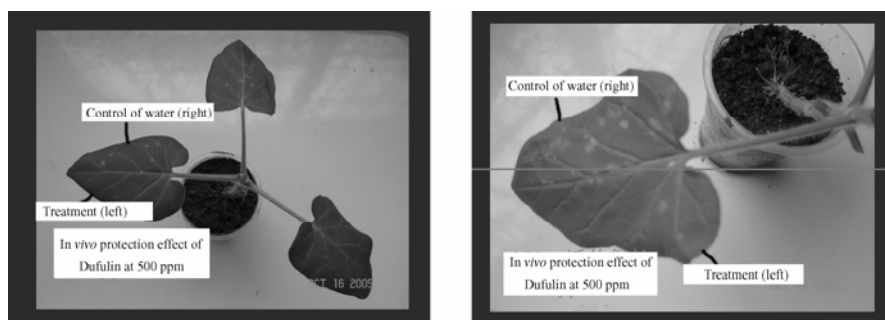
Fig 5.7   Protective effect of Dufulin in the bioassay indoors

5.1.5.2   Materials and methods

Taking the 2005 field trial in Qingdao, Shandong province as illustrative, similar methods were adopted for field trials in other provinces.

The materials and reagents used in field trials are as follows：30% Dufulin WP, 2% Ningnanmycin aqua and 20% Virus A WP. Among these experimental materials, 2% Ningnanmycin aqua and 20% Virus A WP were purchased from the market, the tested crop was tobacco.

Field trial design and district setting. The tested field was separated into several districts. Each district was treated with certain antiviral agent at certain concentrations, as can be seen from Table 5.21.

Table 5.21   Field trial design using different agents

Agent application No.	Agents	Dosage [g(a.i.)/ha]	Active ingredient[g(a.i.)/ha]
1	30% Dufulin WP	333	100
2	30% Dufulin WP	1000	300
3	30% Dufulin WP	1667	500
4	2% Ningnanmycin	4500	90
5	20% Virus A WP	3000	600
6	Control	Pure water	750 kg/ha

Each treatment had four replicates and the area of each district was 50 m^2. Table 5.22 illustrates the districts arrangement, in which the numbers are the treatments listed.

Table 5.22   District settings

2	1	3	4	6	5
3	5	2	6	1	4
4	6	5	3	2	1
6	2	4	1	5	3

Agent spraying method. The agents were dissolved or dispersed in water and the resulting solution was sparyed on the tobacoo leaves. For each field trial, agents were sprayed for three times, with ten days interval between two treatments.

Investigation and calculating methods. Investigation was carried out on the 7th day, 14th day, and 21st day after the third treatment. The disease condition of the tobacco was investigated in all plants in every district. The classification of disease conditions are described as follows.

Level 0：no disease found in the whole plant.

Level 1：leaf vein clear, with light mosaic of tobacco leaves, or the top one third leaves with mosaic but without distortion, tobacco plant is not dwarfed significantly.

Level 2：one third to half of the leaves with mosaic, or minor leaves distorting, or the leaf vein turns black, the plant dwarfed to about two thirds of the normal plant height.

Level 3：1/2 to 2/3 leaves with mosaic or distortion, or main vein necrosises, or the plant dwarfed to two thirds to half of the normal plant height.

Level 4：leaves of the whole plants with mosaic, seriously distorted or necrosed, or the plant dwarfed to one third to half of the normal plant height.

The disease index and the curative effect were calculated according to the following formula. DMRT method was applied to do variance analysis for determining the difference significance between every treatment.

Disease index=[∑(number of every level diseased plants×value of relative series)/(total number of investigated plants×9)]×100

Control effects(%)=[(disease index of CK-disease index of control district)/ disease index of CK]×100

5.1.5.3   Results and Discussion

To make a judgment of the antiviral potency of 30% Dufulin WP, the commercially available plant virucide Ningnanmycin and Virus A, the most successful registered antiplant viral agents available in China, were used as the control. The control efficacies of 30% Dufulin WP are listed in Table 5.23 and Table 5.24.

Table 5.23   Control efficacy of 30% Dufulin WP

Place	30% Dufulin WP(%)			Ningnanmycin(%)	Virus A(%)
	100[a]	300[a]	500[a]	90[a]	600[a]
Shandong	56.6	63.4	68.5	51.1	45.5
Henan	57.1	61.6	61.5	56.0	41.6
Guizhou	51.5	56.9	60.7	39.6	40.6
Yunnan	68.9	74.3	76.1	73.5	75.3
Chongqing	62.5	81.6	90.2	83.4	80.5

[a] The unit is g(a.i.)/ha.

Table 5.24   Control efficacy of 30% Dufulin WP in field test(2006)

Place	30% Dufulin WP(%)			Ningnanmycin(%)	Virus A(%)
	100[a]	300[a]	500[a]	90[a]	600[a]
Shandong	51.6	53.0	54.3	49.8	48.4
Henan	26.1	53.1	55.9	42.3	38.6
Guizhou	51.7	60.8	62.9	53.2	42.9
Yunnan	49.0	60.8	80.1	78.8	80.2
Chongqing	52.1	75.0	83.9	73.9	72.4

[a] The unit is g(a.i.)/ha.

In 2005, field trial of 30% Dufulin WP was carried out in Shandong, Henan, Guizhou, Yunnan, and Chongqing, as shown in Table 5.23. The trial treatments were 100 g(a.i.)/ha for Dufulin, 90 g(a.i.)/ha for Ninnanmycin AS, 600 g(a.i.)/ha for Virus A and CK, respectively, each treatment replicated 4 times; the control efficacies of 30% Dufulin WP were 56.6%, 57.1%, 51.5%, 68.9% and 62.5%, in Shandong, Henan, Guizhou, Yunnan, and Chongqing provinces respectively. The field trial showed that the control effects of Ninnanmycin were 51.1%, 56.0%, 39.6%, 73.5% and 83.4% in Shandong, Henan, Guizhou, Yunnan, and Chongqing respectively. At usage dose of 100 g(a.i.)/ha for Dufulin, it had the same control effect as that of the standard reference, Ninnanmycin at 90 g(a.i.)/ha. Form the data presented in Table 5.23, it can be observed that Dufulin possesses potential bioactivities, with control efficiencies of 63.4%, 61.6%, 56.9%, 74.3% and 81.6% at 300 g(a.i.)/ha, respectively. Ningnanmycin had slightly lower control efficiency than those of Dufulin and Virus A. The Virus A had relatively lower control efficiency than those of Dufulin and Ningnanmycin. During the experiment, 30% Dufulin WP exhibited better control efficacies against TMV at the dosage from 300 to 500 g(a.i.)/ha than the commercial agent Ningnanmycin and Virus A(Fig 5.8).

The five field trials for registration were conducted in 2006 and the results of 30% Dufulin WP were obtained in 2007 which can be seen from Table 5.24. The test results show that control efficacies of 30% Dufulin WP against TMV at dosage of 300, 500 g(a.i.)/ha were better than or close to 2% Ningnamycin at

dosage of 90 g(a.i.)/ha(Shandong, Henan, Guizhou, Yunnan and Chongqing). The activity of 30% Dufulin WP to TMV in Tobacco at dosage of 300, 500 g(a.i.)/ha was better than Virus A at dosage of 600 g(a.i.)/ha (Shandong, Henan, Guizhou, Yunnan and Chongqing).

Fig 5.8   Field trial of Dufulin in Guizhou

5.1.5.4   Conclusion

The field trials demonstrated that the curative effect of 30% Dufulin WP in the field is relatively better than other commercial antiviral product Virus A and Ningnanmycin for plants. The suggested dosages of 30% Dufulin WP are 300-500 g(a.i.)/ha.

5.1.6   Pesticide Residue

5.1.6.1   Introduction

Based on the requirements for registration of Ministry of Agriculture, residue tests of 30% Dufulin WP were carried out in Shandong Qinzhou Tabbaco Institution and the Center for R&D of Fine Chemicals of Guizhou University. The "two-year-two-place" residue experiments were conducted in Shandong and Guizhou. The objective of this section is to establish the residual analysis methods

for Dufulin in soil (tobacco) and evaluate its dissipation rate and residue levels in soil (tobacco) under natural outdoor conditions so as to provide the scientific evidence of environmental safety from the application of Dufulin.

5.1.6.2   Materials and Methods

HPLC (Waters 600E, USA); Waters 2487 Dual λ UV detector, S-Gel C18 RP column (5 μm, 250mm×4.6mm); Ultrasonic cleaning tank; Nitrogen blowing NG; Rotary evaporator. 30% Dufulin Powder was provided by Fine Chemicals test Center Guizhou Province; Stock solutions and dilutions were made in HPLC grade methanol. Residue analysis grade acetone, ethyl acetate, petroleum ether and sodium chloride were used. Anhydrous sodium sulfate was previously conditioned by heating at 450℃ for 4 h. Distilled water was further purified by passing it through a Milli-Q apparatus.

Preparation of soil Sample. All kinds of soil samples used were screened through 40 meshes, thoroughly mixed to ensure homogeneity, and then stored at －20℃. Dufulin standard solutions in methanol were prepared at 40, 2 and 0.8 μg/mL concentratious respectively. Aliquot (1 mL) of standard solution was added to 10 g of soil. The final concentrations of Dufilin were 4, 0.25 and 0.08 mg/kg, respectively. Quintuplicate soil samples for each fortification level were prepared.

Each of the fortified soil sample (10 g) was extracted with 50 mL of acetone for 1 h by thorough shaking. After vacuum filtration and washing three times with 10 mL of acetone. olid soil mud samples were discarded after solvent extractions. Soil extracts were combined and cleaned up using solvent partitioning; 5 mL of saturated brine and 20 mL distilled water were added to the combied soil extract and extracted three times by 30 mL ethyl acetate/petroleum ether (1:1, *v/v*). After drying on anhydrous sodium sulfate, the combined organic solvent was evaporated to 2-3 mL before subjecting to nitrogen purging. The residue was dissolved in 2 mL methanol for HPLC analysis.

Field experiments. Two field experiments were conducted in 2005 and 2006 at different locations near Huaxi, Guiyang City and Qingdao,according to"The Guidline for Pesticide Residue Field Experiments"issued by Institute of the Control of Agrochemicals, Ministry of Agriculture, the People'Republic of China. A single application of Dufulin in the field was carried out at the use rate of 500 g(a.i.)/ha and 1000 g(a.i.)/ha. They were equivalent to a maximum single and 2 times of the label use rate. Soil samples at 0-15 cm depth of soils and tobacco leaf samples(>40 leaves for every plot)were accordingly collected at different intervals for terminal residue analyses.

Extraction and cleaning. Fresh tobacco was cut up and stored for less than one month before analysis. Acetone/petroleum ether (1:1, *v/v*)(40 mL) was added to 5 g of fresh tobacco. The mixture was shaken vigorously for 15 min on a

sonicator and then filtered through a 12 cm Buchner funnel, the solid residue was treated with an additional 10 mL of the extractant. The filtrate was transferred into a 150 mL separatory funnel and then 5 mL of saturated brine and 20 mL distilled water were added. The mixture was extracted with 30 mL×3 ethyl acetate/ petroleum ether (4:1, *v/v*). The organic portion was collected, dried on anhydrous sodium sulfate, evaporated on a vacuum rotary evaporator (40℃ water bath)to a final volume of 1 mL. The concentrate was further cleaned up by passing through a Florisil-packed glass column which was previously conditioned by heating at 130℃ for 8 h. The column (17 cm×1.8 cm ID) was prepared from slurry of petroleum ether in Florisil. The column was then loaded with the sample (concentrate 1 mL), and washed with 20 mL petroleum ether and ethyl acetate (2:1, *v/v*). The Dufulin residue was then eluted by using 10 mL petroleum ether and ethyl acetate (2:3, *v/v*). Care must be taken to prevent the column from drying at any time. Subsequently, the solvent from the eluate was completely removed under nitrogen purge. The residue was dissolved in 2 mL methanol for HPLC analysis.

HPLC detection. The operating conditions were as follows：the analytical column (250 mm×4.6 mm ID) 5 μm ODS, ethanol-water (90:10, *v/v*) as mobile phase at a flow rate of 1 mL/min; injection volumn 20μL. Detection was performed at 270 nm on Chiralpak IA (250 mm×4.6 mm, 5 μm) using *n*-hexane-ethanol (95:5, *v/v*) as mobile phase at a flow rate of 1 mL/min and injection volume 20 μL.

Field experiments. Two field experiments were conducted in 2005 and 2006 at locations near Huaxi, Guiyang City and Qingdao according to"The Guidline for Pesticide Residue Field Experiments"issued by Institute of the Control of Agrochemicals, Ministry of Agriculture. A single application of Dufulin in the field was carried out at the use rate of 500 g(a.i.)/ha and 1000 g(a.i.)/ha. They were equivalent to a maximum single and 2 times of the label use rate. Soil samples at 0-15 cm depth and tobacco leave samples (>40 leaves for every plot)were accordingly collected at different intervals for final residue analyses.

5.1.6.3   Results and Discussion

Accuracy and precision. Recovery tests were performed in order to study the accuracy of the analytical results provided in Table 5.25. Average recoveries were in the range of 76.7%-120.8% (76.8%-97.1%) at three spiking levels (0.08, 0.25 and 4.00 mg/kg, five replicates for each spiking level). The results were within acceptable range laid down by the Chinese official method (The Institute for the Control of Agrochemicals, Ministry of Agriculture, China, 1995). Fig 5.9 and Fig 5.11 show the chromatograms for the blank control of soil and tobacco samples, while Fig 5.10 and Fig 5.12 show those of the spiked soil and tobacco samples, respectively.
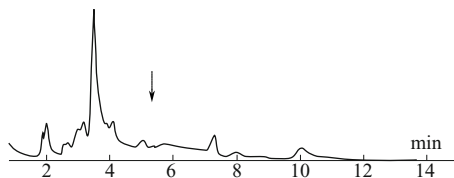
Fig 5.9   chromatogram of soil blank
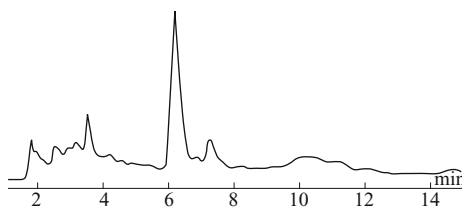
Fig 5.10   chromatogram of soil spiked with Dufulin
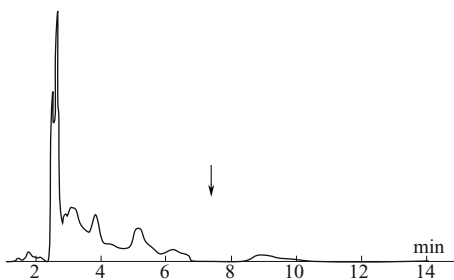
Fig 5.11   chromatogram of tobacco blank
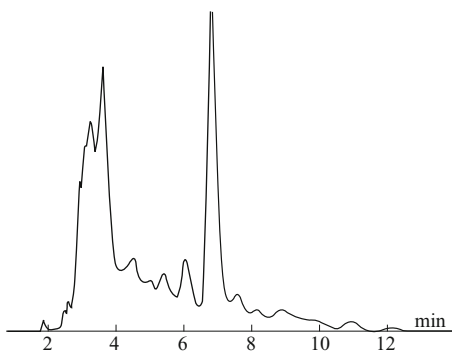
Fig 5.12   chromatogram of tobacco spiked with Dufulin

Residue analysis. The mobile phase of methanol and water was effective to obtain a good separation of Dufulin from other ingredients. Since Dufulin has maximum absorbance at 270 nm, it was selected as the detective wavelength.

Table 5.25   Method recoveries of Dufulin from soil and tobacco

Sample	Spiked concentration(mg/kg)	Recovery(%)						RSD(%)
		1	2	3	4	5	average	
Soil	0.08	76.7	89.7	100.6	85.8	120.8	94.7	13.4
	0.25	102.1	91.0	99.5	93.5	96.0	96.4	4.6
	4.00	83.0	83.5	85.5	85.0	81.5	83.7	1.6
Tobacco	0.08	79.6	81.6	97.1	83.0	85.0	83.3	9.8
	0.8	82.0	84.9	80.2	86.0	81.7	85.0.	3.2
	4.00	76.8	82.5	82.2	75.1	83.2	80.0	3.5

Sample extraction and purification performance. Acetone is the most commonly employed extractant due to its ability to extract both non-polar and polar pesticides and easy miscibility with soil and tobacco materials. However, due to its high polarity, some unwanted interfering compounds from the sample matrix are also extracted. Liquid-liquid extractions with petroleum ether and ethyl acetate and Florisil cartridges were performed for better recovery and without any significant interference from matrix components.

Degradation study. Residues of Dufulin in soil (tobacco) determined at various time intervals are given in Table 5.26, Table 5.27. From the test results obtained over the two years, the decay may be described mathematically by a pseudo-first rate equation. In Guiyang, Dufulin may dissipate up to 95% or above after 45 days from the soil, the regression line equations relating the concentration (C) and time(t)are $C=3.708e^{-0.0603t}$ ($r=-0.9564$) and $C=3.368e^{-0.0696t}$ ($r=-0.9571$), respectively, which show high correlation with the half-life times of 11.5 d and 10.0 d, respectively. In Shandong, Dufulin may dissipate up to 95% or above after 60 days in soil, dissipation regression equations are $C=14.376e^{-0.0538t}$ ($r=-0.9837$)(Fig 5.13) and $C=15.062e^{-0.0581t}$($r=-0.9629$)respectively with half-life times of 12.9 d and 11.9 d respectively.

In Guiyang, the time for the disappearance of Dufulin (>95%) is 21 days, dissipation regression equations are $C=17.97e^{-0.158t}$ ($r=0.9781$) and $C=18.69e^{-0.169t}$($r=0.9939$)respectively. The half-life times were 4.4 d and 4.1 d respectively. In Shandong, Dufulin may dissipate up to 95% or above after 30 days in tobacco, dissipation regression equations are $C=25.77e^{-0.116t}$($r=0.9911$) and $C=26.59e^{-0.123t}$ ($r=0.9932$).The half-life times were 6.0 d and 5.6 d, respectively.

Decline of the residues may be attributed primarily to growth dilution between application and sampling, as well as to the volatilization that occurs during the first days following application. In addition, weathering, heat decomposition, sunlight and UV radiation and other complex conditions may also play important role in the removal.

Degradation of Dufulin in soil is dependent on the type of soil and its character. There is no big difference in the degradation rate for the two different years and locations selected for the study. While in 2005 the half-life was 11.5-12.9 day, in 2006 it was found to be 10.0-11.9 day.

Table 5.26 Residues of Dufulin in soil (in Guiyang and Shandong) determined at various time intervals[a]

Sample	Soil							
Test place	Guiyang				Shandong			
Test time	2005		2006		2005		2006	
Interval time(d)	Residue (mg/kg)	Dissipation (%)	Residue (mg/kg)	Dissipation (%)	Residue (mg/kg)	Dissipation (%)	Residue (mg/kg)	Dissipation (%)
0	5.59	—	6.13	—	14.54	—	15.05	—
1	3.55	36.4	4.67	23.8	13.69	5.8	14.56	3.2
3	3.36	40.0	3.45	43.8	12.48	14.2	12.20	18.9
7	1.25	77.5	1.82	70.3	10.41	28.4	10.07	33.1
10	1.58	71.6	1.03	83.2	8.66	40.4	9.02	40.0
14	1.40	75.0	0.55	90.9	5.27	63.8	5.51	63.4
21	1.21	78.4	0.12	98.0	4.41	69.7	4.02	73.3
30	1.21	78.4	0.36	94.2	2.87	80.3	2.45	83.7
45	0.20	96.4	0.16	97.3	2.01	86.2	2.49	83.4
60	0.09	98.3	0.07	98.9	0.43	97.0	0.28	98.1
Regressione quation	$C=3.708e^{-0.0603t}$		$C=3.368e^{-0.0696t}$		$C=14.376e^{-0.0538t}$		$C=15.062e^{-0.0581t}$	

[a] Data were the results of three replicates.

Table 5.27 Residues of Dufulin in tobacco (in Guiyang and Shandong)determined at various time intervals[a]

Sample	Tobacco							
Test place	Guiyang				Shandong			
Test time	2005		2006		2005		2006	
Interval time(d)	Residue (mg/kg)	Dissipation (%)	Residue (mg/kg)	Dissipation (%)	Residue (mg/kg)	Dissipation (%)	Residue (mg/kg)	Dissipation (%)
0	20.32	—	21.20	—	22.64	—	23.46	—
1	10.36	49.0	11.14	47.4	21.70	4.2	21.56	8.1
3	9.10	55.2	10.10	52.4	18.87	16.6	18.84	19.7
7	8.15	59.9	6.31	70.2	9.75	56.9	10.24	56.4
10	5.94	70.8	4.58	78.4	9.53	57.9	9.79	58.4
14	2.13	89.4	1.84	91.3	6.70	70.4	6.02	74.3
21	0.37	98.2	0.57	97.3	2.37	89.5	1.93	91.8
30	0.18	99.1	<0.10	>99.95	0.66	97.1	0.59	97.5
45	0.08	99.6	<0.10	>99.95	0.92	95.9	0.87	96.6
60	<0.01	>99.99	<0.10	>99.95	0.38	98.32	0.73	96.9
Regression equation	$C=17.97e^{-0.158t}$		$C=18.687e^{-0.169t}$		$C=25.77e^{-0.116t}$		$C=26.59e^{-0.123t}$	

[a] Data were the results of three replicates.

$$C=14.376e^{-0.0538t}$$
$$r=-0.9837$$
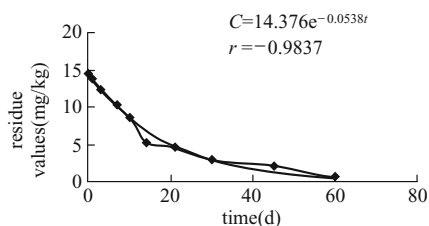
Fig 5.13   The dissipation regression equation in soil in 2005(Shandong)

There could be many other factors that affect the rate of Dufulin degradation in tobacco. The often rainy and overcast conditions prevailing in Guiyang might help in the dissipation and rapid degradation of Dufulin after the pesticide has been sprayed in experimental field. The rate of Dufulin degradation in shandong is lower, presumably due to the fact that the days are generally clear.

Terminal residue levels. When Dufulin was sprayed following the doses[1000 g(a.i)/ha]and time intervals, terminal residue levels of Dufulin in soil (tobacco) were < 0.31 mg/kg(<0.70 mg/kg)respectively after 21 d from the final application (shown in Table 5.28). No maximum residue limit (MRL) has been set by the Chinese government for Dufulin in soil(tobacco). As it is a new pesticide, further work must be done with respect to the different experimental plots and different experimental times. Combined with the toxicological literature, MRL for Dufulin should be set up by China legislation.

Table 5.28   Terminal residue levels for different samples

Sample	Locus	Dose [g(a.i.)/ha]	Times	2005			2006		
				7d	14d	21d	7d	14d	21d
Soil	Guiyang	500	2	0.31	0.17	0.11	0.21	0.15	0.07
			3	0.42	0.28	0.18	0.28	0.20	0.19
		1000	2	0.45	0.25	0.20	0.22	0.12	0.06
			3	0.57	0.33	0.21	0.34	0.25	0.23
	Shandong	500	2	2.98	0.12	0.07	3.00	0.11	0.09
			3	0.57	0.16	0.15	0.35	0.17	0.16
		1000	2	0.23	0.27	0.11	0.21	0.19	0.08
			3	1.50	0.52	0.29	1.22	0.41	0.31
Tobacco	Guiyang	500	2	2.26	0.82	0.07	2.23	0.70	0.04
			3	3.55	0.36	0.31	1.80	0.69	0.22
		1000	2	3.41	0.98	0.46	3.11	1.45	0.35
			3	4.70	1.39	0.17	4.56	1.64	0.13
	Shandong	500	2	1.10	0.75	0.50	1.00	0.79	0.57
			3	2.13	1.09	0.70	2.09	1.18	0.67
		1000	2	1.23	1.05	0.70	1.25	1.00	0.68
			3	2.67	1.26	0.55	2.61	1.60	0.66

5.1.6.4   Conclusions

A residue method for the determination of Dufulin was established and validated for soil (tobacco). The procedures are characterized by recovery >75.1%, precision < 13.4% and sensitivity of 0.01 mg/kg. Degradation study showed that the half-lives obtained for Dufulin in soil (tobacco) were 10.0-12.9 (4.1-6.0) d under the field conditions. Also, Dufulin dissipated up to 95%(>99%)in soil(tobacco)and terminal residue levels of Dufulin in soil (tobacco) at harvest were <0.31 mg/kg (<0.70 mg/kg) respectively following 2 times of the maximum recommended dose and time intervals.

5.1.7   Environmental toxicology

5.1.7.1   Introduction

Dufulin has been intensively studied for its good antiplant virus activity. However, safety evaluation on the non-target species and the effect of Dufulin on non-target species and biological systems in the associated environment need to be studied. The environmental toxicology tests of 30% Dufulin WP were conducted by commissioning to Nanjing Institute of Environmental Science of National Environmental Protection Administration. Bees, birds, silkworm, and fish were involved as test objects and the methods and results of environmental toxicology test were established. The environmental toxicology results demonstrated that 30% Dufulin WP is less toxic to the bees, birds, silkworm, and fish.

5.1.7.2   Materials and Methods

Enviromental toxicology test targets include Fish(Brachydanio rerio H.B), Bees (Apis melifera L.), birds (*Cotunix coturnix japonica*) and silkworm(*Bombyx mori L.*)

Test on fish. Water used for the test was stored and dechloridated for more than 24 h. Test vessel consisted of a 25 L glass cylinder, containing 10L solution with different concentrations of Dufulin and 10 fish. Water temperature was kept at around 25℃. Pretest was to be carried out first to determine the scope of toxicity of 30% Dufulin WP, and within this scope, a concentration gradient with a control was set. Each treatment had three repetitions. A half static method of changing agents in every 24 h was applied. The dissolved oxygen and pH value of solution were detected in every vessel. The toxic symptom and death rate of *Brachydanio rerio* H. B were recorded at 24 h, 48 h, 72 h and 96 h. The dead fish was removed at the appropriate time and then the Lethal Concentration 50(LC_{50}) of 30% Dufulin WP on *Brachydanio rerio* H.B. was calculated by probability statistics.

Test on Bees. Stomach poison method was adopted by feeding bees with honey premixed with Dufulin to test the toxicity of Dufulin on bees. Feeding

honey solution was prepared by mixing 2 mL honey with 4 mL Dufulin solutions at different concentrations. Twenty bees were transferred into each cage. Room temperature was kept at around 25-27℃. The bees were then fed with the toxic honey during the experiment period and this was followed by treatment with normal honey after the experiment was over. Each treatment had three repetitions. The death rate of *Apis melifera* L. was recorded at 24 h and 48 h. Then LC_{50} of 30% Dufulin WP on *Apis melifera* L. could be calculated by probability Statistics.

Test on birds. *Cotunix coturnix japonica* (ten male and ten female ones) were raised in a lighted and ventilated room at around 20-25℃. The birds were fed with normal feeding stuff together with drinking water. Before the experiment, birds were only fed with water over night. Pre-experiment was needed to be carried out first to determine the scope of toxicity of 30% Dufulin WP on the birds, and within this scope, a concentration gradient with a control was set. Each treatment had three repetitions. Stomach of each *Cotunix coturnix japonica* was filled at dosage of 0.5 mL/100g with different concentrations. Then birds were fed in normal way for 7 days and the toxic symptom and death rate were observed. The LD_{50} value of 30% Dufulin WP to birds could then be calculated with probability statistics.

Test on silkworm. Toxicity of 30% Dufulin WP on *Bombyx mori* L. was tested by food intake method. The testing room temperature was kept at 25-30℃. In a glass dish (9 cm), twenty silkworms of two different age groups were fed with toxic leaves, which were previously soaked with agent solution (5 g mulberry leaves dipped in 5 mL agent solution) for the entire test period；the procedure was followed by the nontoxic leaves. A group of concentration gradient and a control was set with three repetitions for each treatment. The toxic symptom and death rate at 24 h, 48 h, and the time of newly born three aged silkworms were observed and recorded. Stomach toxicity LC_{50} of 30% Dufulin WP to *Bombyx mori*. was then caculated by probability statistics.

5.1.7.3   Results

The acute toxicities of emamectin Dufulin against four representative non-target organisms *e.g.* zebra fish, bee, bird and silkworm were evaluated. The results of environmental toxicology test of 30% Dufulin WP are listed in Table 5.29. The test results suggested that 30% Dufulin WP was less toxic to fish, bee, bird and silkworm, thus it is safe to the environmental non-target organisms and the environment.

Table 5.29   Results of environmental toxicology test of 30% Dufulin WP

Test objects	Toxicity
Zebra fish	LC_{50}(96h)>12.4 mg/L
Bee	LC_{50}(48h)>5000 mg/L
Bird	LD_{50}(7d)>450 mg/kg
Slkworm	LC_{50}>5000 mg/kg mulberry leaf

5.1.7.4   Conclusion

The results of the experiment showed that the stomach toxicity caused by Dufulin for bee LC_{50}(48 h):>5000 mg/L, for bird LC_{50}(7d):>450 mg/kg, for zebra fish LC_{50}(96 h):12.4 mg/L, for silkworm LD_{50}(96h):5000 mg/kg. The pesticide was relatively harmless for bee, bird, zebra fish and completely harmless and non toxic for silkworm. This experiment provided scientific evidence for seasonable use of Dufulin.

5.1.8   Mode of Action

5.1.8.1   Introduction

The gene for an enzyme, responsible for imparting natural disease resistance in plants, was discovered by biologists at the Boyce Thompson Institute for Plant Research (BTI) and at Cornell. The researchers believe that by enhancing the activity of the enzyme they might be able to boost natural disease resistance in crop plants without resorting to pesticides or the introduction of non-plant genes.[1] Plants react to pathogen attack through a variety of active and passive defense mechanisms primarily related to the metabolism of phenolic compounds and oxidative metabolism.[2,3] Thus the activation of defensive reactions is associated with the increased expression of a great number of genes that encode enzymes involved in the biosynthetic pathway of phenolic compounds.[4,5] Similarly, activation of oxidative metabolism precedes the expression of defense genes during plant-pathogen interactions, so both metabolic processes must exert a major function in directing the mechanisms to resist disease.[6] Likewise, it has been suggested that certain fungicides and antiviral agents for plants used to mitigate or prevent pathogen attack may be involved in activating certain defensive responses of plants. However, the fact that such substances may influence the key steps of the phenolic and oxidative processes has scarcely been studied and used in application in crop protection.

Dufulin belongs to α-aminophosphonate derivatives and is a new antiviral agents for plants discovered by Center for R&D of Fine Chemicals of Guizhou University in 2003. The lab bioassay and field trial demonstrated that Dufulin is highly active against the plant virus diseases caused by TMV, CMV and PVY, [7] which prompted us to study in detail the mode of action (MOA) of Dufulin. Also this MOA investigation may in turn help researchers to understand the antiviral process and lead to the quick discovery of new antiviral agents.

Extensive research on the MOA of Dufulin was therefore conducted, including：(a) The effect of Dufulin on the activities of tobacco defense related enzymes, such as phenylalanine ammonia-lyase (PAL), peroxidase (POD), superoxide dismutase (SOD), and chlorophyll content. (b) The effect of Dufulin

on the morphology of TMV particles. (c) The effect of Dufulin on tobacco salicylic acid signaling pathway as well as the signaling pathway downstream target gene and PR-1a, PR-5 proteins. (d) The induction expression of chloroplast cysteine synthetase which is related to SA signaling pathway stimulation.

Experiments have shown that Dufulin can induce the expression of PR by enhancing the content of SA, and then increase the activity of defense related enzymes. These results show that Dufulin is most likely a kind of inducer or activator of plant immune system. Our investigation confirms that the MOA of Dufulin is involved in the activation of some defensive responses of plants. The different proteins or genes involved are considered to be within the SA signaling pathway by using 2-D gel and DDRT-PCR. Studies show that Dufulin activates chloroplast cysteine synthase 1 precursor, and thus plastid-lipid-associated protein. There is considerable evidence that plastid-lipid-associated protein and chloroplast cysteine synthase 1 are associated with plant disease resistance. Cysteine synthetase regulates the composition and expression of plastid-lipid-associated protein. These proteins interact with SA and increase the matter expression of pathway downstream.

5.1.8.2   Materials and Methods

(1) *The defense related enzymes induced by Dufulin in tobacco leaf*
Preparation and determination of enzymes extracts. After mechanical inoculation with TMV, K_{326} leaves treated by Dufulin were collected in every two days interval. 1.0 g of the treated leaves was grounded and homogenized with a little quartz sand in 2.0 mL of 0.2 M pH8.8 sodium borate buffer (containing 5 mM β-mercaptoethanol, 1 mM EDTA). The leaf homogenate was stirred for 5 min and centrifuged at 20000 g for 20 min at 4℃. The supernatant was collected and preserved at -80℃ and was used as crude enzyme extract for ready determination of PAL, and POD and SOD contents. The liquid extract was diluted 5 times with 50 mM pH 8.8 sodium borate buffer. Each sample was repeated for three times for determination of enzymes. Ningnanmycin was used as a positive control.[8]

PAL determination. According to Koukol and Conn's methods, 2 mL of sodium borate buffer (0.05 M pH8.8) and 1 mL of L-phenylalanine(pH8.8, 0.02 M, and 0.05 M sodium borate buffer)and 0.5 mL of the diluted enzymes liquid were added into 5 mL glass tube. L-phenylalanine was used as the substrate of enzymatic reaction. The solution containing 3 mL sodium borate buffer (0.05 M,pH8.8) and 0.5 mL of the diluted enzymes solution was used as the control. The OD_1 values were determined at 290 nm by ultraviolet-visible spectrophotometry. After reacting on a water bath for 5 h at 40℃, the mixture was quenched on an ice-water bath and then the OD value was determined under the same conditions. OD_2-OD_1 represented the net value added and a unit of the enzyme activity level corresponded to an increase of 0.01 of OD values per hour.

POD determination. According to Rao and Castillo's methods, 20 μL of the

diluted enzymes liquid was poured into a 15 mL test tube, then the liquid was mixed with 3 mL of the sodium phosphate buffer(0.1 M pH 5.8 Guaiacol)followed by balancing of the mixture on a water bath at 30℃ for 5 min. To initiate the enzyme reaction, 50 uL of H_2O_2 solution(v/v：2.5%)was added and mixed uniformly, Guaiacol was used as substrate and the same volume of distilled water was used as control instead of H_2O_2. Enzyme activity was represented to the net value added per minute per mg protein at 470 nm.[9, 10]

SOD determination. In the light of Dhindsa's methods, the enzyme liquid was diluted 5 times with sodium borate buffer (0.05 M, pH8.8). As shown in Table 5.30, the reaction components were poured into a 5 mL glass tube, the two for the determination and the other two for the control. One control tube was set in the dark, the other tubes were set under the sunlight for 20 min. After the reaction was completed, the dark control was set as the blank control and the absorbance values of the other tubes were determined.[11]

Table 5.30   Individual components in solution

Reagent/enzyme	Volume(mL)	Final concentration
PBS(0.05 M)	1.5	
Met solution(130 M)	0.3	13 mM
NBT(750 M)	0.3	75 M
EDTA solution(100 M)	0.3	10 M
riboflavin solution(20 M)	0.3	2.0 M
Enzyme solution	0.05	2 control tubes(buffer instead of enzyme)
double distilled H_2O	0.25	
Total volume	3.0	

One unit of the SOD activity implied that the inhibition value reduced NBT to reach at 50%. The SOD activity was calculated according to the formula：

$$\text{SOD total activity}=(A_{CK}-A_E) \cdot V/(0.5 \cdot A_{CK} \cdot W \cdot V_t)$$

In the above equation, A_{CK} means the absorption of photo contrast tube, A_E represents the absorption of sample tube, V is the total volume of sample liquid(mL), while V_t is the tested volume of sample liquid in mL and W represents sample weight in gram.

Chlorophyll content determination. The chlorophyll content of tobacco leaf was determined daily ranging from 1st day to 13th day by using Sükran and Porra's method .[12, 13] After acetone and ethanol (2:1) were added to the mixture, the rectangular tested samples (0.5 cm × 2 cm) were used to extract the chlorophyll at 4℃, and absorbance was determined at 663 nm and 645 nm by UV-visible spectrophotometer with acetone and ethanol(2:1)as control. The chlorophyll content(mg/g)was determined by using the following formulas：

$$Ca=12.7 A_{663}-2.69 A_{645}$$
$$Cb=22.9 A_{645}-4.68 A_{663}$$

(2) ***The observation of TMV treated by Dufulin under electron microscope***

The test samples of purified TMV and TMV treated by Dufulin for 30 min were dyed with staining solution-PTA (2%, pH 6.7) for 1-2 min, and dried on a pad of paper plate, and observed under an Electron microscope up to a magnification of 10000 times.

SA signal pathway in K_{326} tobacco leaf treated by Dufulin. Salicylic acid is an important signal molecule in plant defense. In the past several years, significant progress has been made in understanding the mechanism of salicylic-acid biosynthesis and signaling in plants. The SA in tobacco was extracted and analyzed by HPLC. The results showed that the SA content of Dufulin treatment is higher than that of TMV-treated and CK. It can be speculated that Dufulin can affect the SA signal pathway by activating the plant defense responses. Therefore, Real-time PCR and semi-quantitative PCR were applied to determine differential gene expression and it was found that the level of differential gene expression of Dufulin-treatment was 3 times higher than that of TMV-treatment. Subsequently DD-PCR and SDS-PAGE of tobacco leaf intercellular protein were used to confirm these results.

Determination of SA content. Ground tobacco K_{326} leaves were made into a fine powder and frozen liquid nitrogen and 3 mL 90% methanol were added. The homogenate was preserved at $-20℃$ for 5 h. Then the mixture was centrifuged at 6000g for 15 min and the supernatant was collected and stored at $-20℃$. The precipitate was mixed with methanol again and preserved at $-20℃$ for 12 h, centrifuged at 6000 g for 15 min. The supernatant was collected and combined with the early parts and centrifuged at 2000 g for 15 min. Then the resulted supernatant was subjected to HPLC (Agilent 1100) analysis using methanol: water=60:40 (pH was adjusted to 3-4 with glacial acetic acid) as the mobile phase on a C18 250mm×4.6 mm column. The detection wavelength was 234 nm and the observed retention time was 3.04 min.[14, 15]

The PR gene expression.The total RNA was isolated from tobacco leaf by Bio-rad AquaPure RNA Isolation Kit and cDNA was synthesized by RT-PCR using Bio-rad iScript cDNA Synthesis Kit. The cloning and identification of PR genes were completed by RT-PCR (Bio-rad iCycler PCR) and gene sequencing (ABI 3100 gene analyzer) and BLAST software. The gene expression was then studied by Real-time PCR and semi-quantitative PCR methods (Bio-rad iCycler PCR). The primers were designed according to Beacon Designer Probe/Primer Design Software (Bio-Rad Icycler), β-actin gene was used as an internal reference gene (Table 5.31).[16, 17]

Table 5.31   The primer of real time PCR and semi-quantitative PCR

Gene family	Accession No.	5′ primer	3′primer
β-actin	U60495	5′-gacatgaaggaggagcttgc-3	5′-atcatggatggctggaagag-3′
PR-1a	X12737	5′-caatacggcgaaaacctagctga-3′	5′-cctagcacatccaacacgaa-3′
PR-5	X03913	5′-gcttcccctttatgccttc-3′	5′-cctgggttcacgttaatgct-3′

PR analysis.Samples of K_{326}tobacco leaves were divided into three different groups by treatments of CK, TMV, and TMV-Dufulin. K_{326} tobacco was treated every one day for six days. The tobacco leaf treated at different time was placed at the bottom of the beaker filled with Double-distilled water (ddH$_2$O) and pump gas repeatedly. It can be seen that leaf colour became darker and no bubble generated. The leaf was centrifuged at 4000 g for 15 min and the intercellular liquid was collected and preserved at $-20\,^\circ\text{C}$. The SDS-PAGE method was employed and the concentrations of stacking gel and separating gel were found to be 4% and 10%, respectively. The concentrated protein sample was separated at 120 V constant voltage in Tris-glycine buffer (pH 8.3) until the bromophenol blue reached at the bottom of PAGE, and gels were stained with coomassie brilliant blue R-250. The different stained bands were cut out of the gels with a razor blade and purified and identified by the enzymolysis in gel and matrix-assisted laser-desorption/ ionization time-of-flight mass spectrometry (MALDI-TOF-MS).[18,19]

DDRT-PCR on Dufulin treated tobacco. According to Delta[®] Differential Display Kit User Manual (CLONTECH), the DDRT-PCR was completed with primer combinations containing one of the random primers (P_1-P_{10}) and/or anchor primer (T_1-T_9)(Table 5.32). The optimistic RCR system of 25 μL contained $10\times$ buffer 2.5 μL, 1.6mM dNTP, 1.0mM Primer, 1.8mM MgCl$_2$, 0.35U exTaq DNA polymerase and Hotstart Taq DNA polymerase and 20 ng template cDNA. The reaction condition consisted of 1 cycle：94℃ 5 min, 40℃ 5 min, 68℃ 5 min; 2 cycles：94℃ 30 sec, 40℃ 30 sec, 68℃ 5 min; 23 cycles：94℃ 20 sec, 60℃ 30 sec, 68 ℃ 2 min cycle. The product was observed through 5% PAGE electrophoresis and silver staining, and the primer combinations were screened according to fragment abundance and the large difference molecular weight bands. The cDNA from different treatment tobacco leaf was amplified in DDRT-PCR with dNTP containing [a-33P] dATP* with the primer combinations; the different fragments were collected by employing autoradiographic coupled image analysis method and identified by amplification by PCR with the same primers and gene sequencing (ABI 3100 gene analyzer).[20,21]

(3) *The analysis of 2-D gel electrophoresis coupled with mass spectrum*

Protein sample preparation. Tobacco protein samples were prepared from K_{326} leaf inoculated by TMV and then treated by Dufulin for 5 days. After dissolving the tobacco leaf sample at $-80\,^\circ\text{C}$, Plant Protein Extraction Kit was used to extract the total protein from the sample, and then the sample was concentrated by ultracentrifugation. The quantity of tobacco leaf total protein was determined using the Bradford assay according to the described Bio-Rad Protein Assay Kit protocol, and then protein sample was divided into 50 μL aliquots, and stored at $-80\,^\circ\text{C}$ until ready to be used.[22]

Table 5.32   The primer of DDRT-PCR

Arbitrary primers	Oligo(dT)primers
P1：5′-ATTAACCCTCACTAAATGCTGGGGA-3′	T1：5′-CATTATGCTGAGTGATATCTTTTTTTTTTAA-3′
P2：5′-ATTAACCCTCACTAAATCGGTCATAG-3′	T2：5′-CATTATGCTGAGTGATATCTTTTTTTTTTAC-3′
P3：5′-ATTAACCCTCACTAAATGCTGGTGG-3′	T3：5′-CATTATGCTGAGTGATATCTTTTTTTTTTAG-3′
P4：5′-ATTAACCCTCACTAAATGCTGGTAG-3′	T4：5′-CATTATGCTGAGTGATATCTTTTTTTTTTCA-3′
P5：5′-ATTAACCCTCACTAAAGATCTGACTG-3′	T5：5′-CATTATGCTGAGTGATATCTTTTTTTTTTCC-3′
P6：5′-ATTAACCCTCACTAAATGCTGGGGT-3′	T6：5′-CATTATGCTGAGTGATATCTTTTTTTTTTCG-3′
P7：5′-ATTAACCCTCACTAAATGCTGTATG-3′	T7：5′-CATTATGCTGAGTGATATCTTTTTTTTTTGA-3′
P8：5′-ATTAACCCTCACTAAATGGAGCTGG-3′	T8：5′-CATTATGCTGAGTGATATCTTTTTTTTTTGC-3
P9：5′-ATTAACCCTCACTAAATGTGGCAGG-3′	T9：5′-CATTATGCTGAGTGATATCTTTTTTTTTTGG-3′
P10：5′-ATTAACCCTCACTAAAGCACCGTCC-3′	

2-D gel electrophoresis and imaging. Protein samples containing one pooled standard, and TMV-treated, and TMV-Dufulin-treated were combined. Pooled sample of 1 mg was then treated by 2-D gel electrophoresis for the purpose of protein identification. Thirty milligram of protein samples were separated on 13 cm, 3-10 immobilized pH gradient (IPG) strips (Amersham Biosciences, Piscataway, NJ) using an IPGphor focusing apparatus (Amersham Biosciences, Piscataway, NJ) at constant current of 50 mA at 20℃, IPG strips were then stored at －20℃ or equilibrated in equilibration buffer (50 mM Tris-HCl, 6M urea, 30% glycerol, 2% SDS) supplemented with 1% DTT to maintain the fully reduced state of proteins, followed by 2.5% iodoacetamide to prevent reoxidation of thiol groups during electrophoresis. Protein samples were run at constant current of 15 mA for 15 min, and were then run at 30 mA on 10% Tris-glycine gels using an Ettan DALT II System, and continued until bromophenol blue reached at the lower side. Protein samples were separated in triplicate. The 2-D gel was first fixed in 30% methanol and 7.5% acetic acid, and then stained using Coomassie blue or silver staining method using classical techniques. The gels were scanned using Typhoon 9410 Variable Mode Imager and analyzed with the differential protein software to obtain the interesting protein. Protein samples were separated in triplicate. A total of 30 protein spot features were analyzed across all samples. Student's t-test and one-way ANOVA were used to calculate significant difference in relative abundances of protein spot-features in TMV-Dufulin treatment compared with TMV-treatment.[23, 24]

The identification of the interesting proteins. The interesting proteins in all samples treated by TMV and Dufulin which showed significant enhancement ($P < 0.01$) and attained an expression level of 1.5 times compared to the samples infected by TMV only, were selected for further analysis. The protein of interest was picked using the automated Ettan Spot Picker for the purpose of acquiring peptides cleaved by in-gel digestion. The gel spots of about 2 millimeter diameter were washed in mycoplasma-free double distilled H_2O for 10 min, then washed

three times in 25 mM NH$_4$HCO$_3$, 50% CH$_3$CN for 30 min, followed by dehydration in 100% CH$_3$CN for 15 min by vortex-mixing. The solution containing gel plugs was digested overnight on a water bath at 37℃ after adding 1.5 μM trypsin to the solution. The peptide solutions were centrifuged at 1000 r/min for 2 min, and supernatant was used for MALDI-TOF/MALDI-TOF/TOF analysis using 4700 Proteomics Analyzer Applied Biosystems. Protein identification was completed using Global Proteome Server Explorer software utilizing the NCBI Database.

5.1.8.3   Results and Discussion

(1) ***The effect of Dufulin on defense related enzymes and chlorophyll content***

Effect on PAL activity. It was found that on the 1st day the PAL enzyme activity in treated tobacco plants was higher than that of the control. The PAL enzyme activities in Ningnanmycin and Dufulin treatment were significantly higher than those of TMV infected tobacco plant and the negative control. This trend kept on increasing until the third day, and then gradually declined (Fig 5.14).
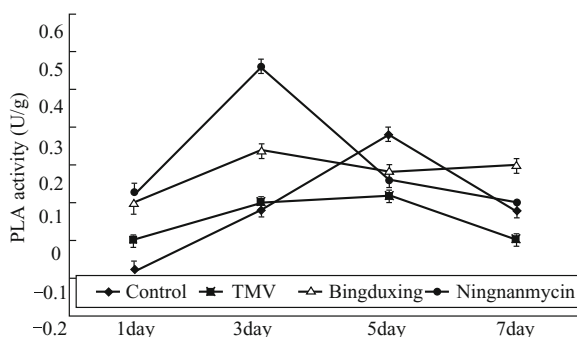
Fig 5.14   Effect of Dufulin on PAL activity in the tobacco plant.

Effect on POD activity. The POD activity on Dufulin treated was significantly higher than those of the blank control and TMV treatment. The values reached their corresponding maximum after 4 days of treatment and then decreased sharply (Fig 5.15).

Effect on SOD activity. SOD activities of tobacco induced by Dufulin and Ningnanmycin reached maximum on the first day and were much higher than those of the blank control and TMV treatment. After reaching the lowest point on the 5th day, it started to ascend again and attained a higher level on the 7th day (Fig 5.16).

Effect on chlorophyll content. During the entire detection period (14 days), the chlorophyll contents treated with Dufulin or Ningnanmycin were higher than that of TMV infected plants. The chlorophyll contents of healthy plant (control) were relatively higher than that in TMV infected tobacco. A good correlation exists between chlorophyll content and Dufulin treatment time (Fig 5.17).

(2) ***The effect of Dufulin on the morphology of TMV particles***

It can be seen that Dufulin has no influence on the size and length of TMV par-
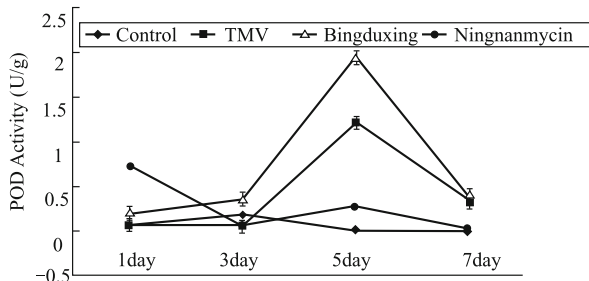
Fig 5.15 Effect on POD activity in the tobacco plant
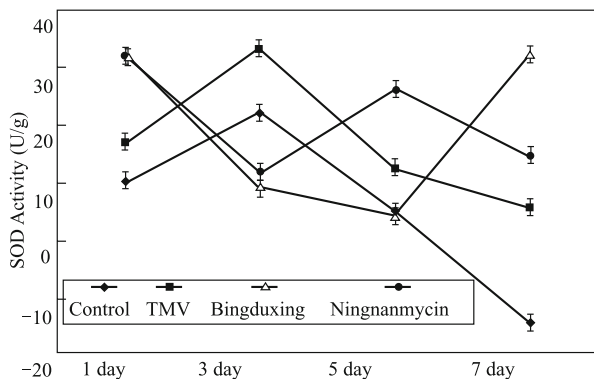
Fig 5.16 Effect of Dufulin on SOD activity in the tobacco plant
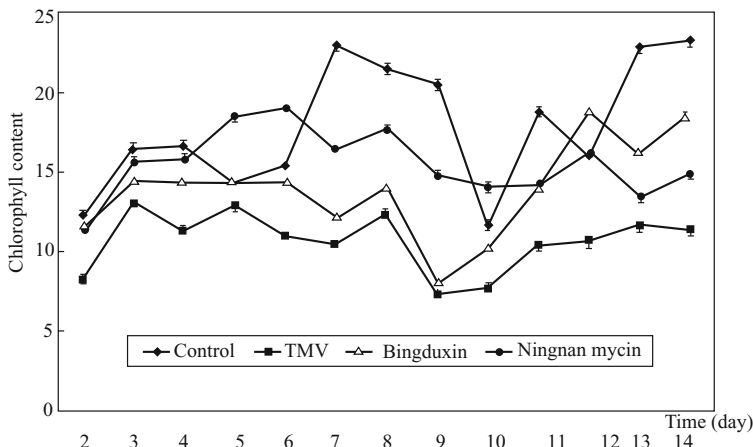
Fig 5.17 Effect on chlorophyll content in the tobacco plant

ticle, but it distorts the shape of TMV particle by aggregating them together (Fig 5.18). This phenomenon indicates that Dufulin can inactivate TMV particles. The ability of TMV to infect tobacco decreased significantly after treatment with Dufulin. The necrosis spots per tobacco leaf after TMV-treatment and TMV-Dufulin-treatment were 18.5 and 8.5 respectively, which gave an inhibition rate of 54.05% for Dufulin-treatment.
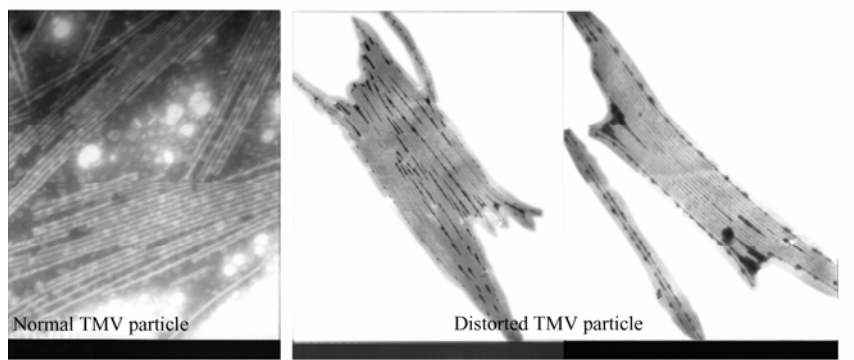
Fig 5.18   Morphology observation about TMV particles treated by DUFULIN *in vitro*.Left：normal shape of untreated TMV particles; Right：TMV particles were treated by Dufulin *in vitro* at 500 μg/mL

(3) ***The effect on tobacco salicylic acid (SA) signaling pathway***

Determination of SA. With the established HPLC methods, regression analysis generates the standard curve $Y=37.6354X-12.5222$ with the correlation coefficient of 0.99984. It is obvious that there is an excellent linear relationship between the concentrations of SA and their peak areas in the range of 8.16-40.8 μg/mL (Table 5.33, Fig 5.19).

Table 5.33   Standard curve of salicylic acid

X(μg/mL)	8.16	23.1	40.8
Peak area	27.71	276.92	480.15
Regression equation	$Y=37.6354X-12.5222$,　$\gamma=0.99984$		

It was found that the contents of SA in the leaves treated by Dufulin were much higher than that in the control. For the same treatment, SA content in lower leaves is higher than that of the upper leaves (Fig 5.20).

The induction of PR expression by Dufulin. As shown in Fig 5.21, there is no obvious band appearing in lane 1 of CK-treatment. In lane 2 (TMV-treatment), three obvious bands appear at the molecular weights of 65kDa, 55kDa and 34kDa, respectively. These proteins were speculated to be chitinase and β-1,3-glucanase.
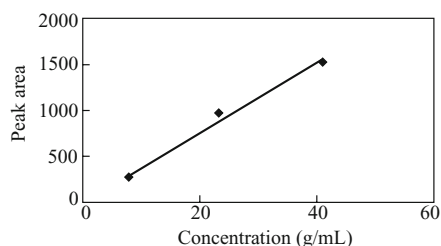
Fig 5.19   Standard curve for the determination of Salicylic acid content

A 34 kDa band appeared in the lane of Dufulin-treatment on the second day, and bands of 65kDa and 55kDa and 34kDa appeared respectively on the 4th day. Meanwhile, the contents of intercellular protein reached the peak on the 4th day, and then decreased gradually. So we concluded that the types of the intercellular protein of Dufulin-treatment were consistent with that of the TMV-treated-tobacco.
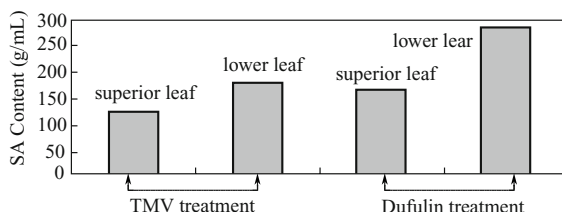
Fig 5.20   salicylic acid(SA)content of tobacco K_{326} leaf on
the 5th day after being treated by Dufulin.
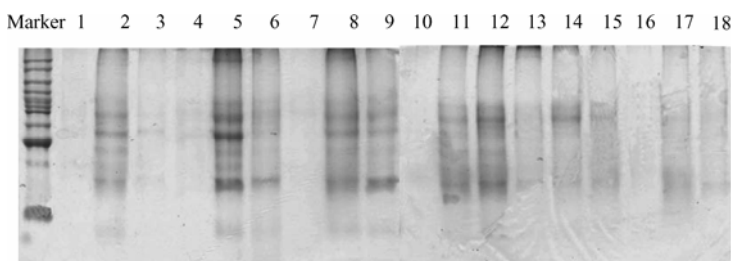
Fig 5.21   Electrophoresis band patterns dealing with the tobacco PR-induced cell.Every three line in one group, lane 123, lane 456, lane789 in the left fig represented the protein of water treatment, Dufulin treatment, TMV treatment on the 1st, 2nd, 3rd day respectively. Lane 123, lane 456, lane789 in the right fig represented the protein of water treatment, Dufulin treatment, TMV treatment on the 4th, 5th, 6th day respectively

It can be seen that Dufulin can upregualate the expression of PR-protein and protein type in tobacco. Among them, two proteins of 34kDa, 45kDa were most remarkable. In the whole process, PR-proteins finally declined after climbing to a maximum.

Effect of Dufulin on tobacco PR gene and N gene. The N gene of tobacco confers resistance to the viral pathogen, tobacco mosaic virus. It can suppress TMV movement and its reproduction. It was found that Dufulin can induce pathogenesis-related proteins gene PRs-1 PR-5 and N gene expression, which indicated that Dufulin can induce and activate the tobacco immune system.

Effect of Dufulin on PR-5 gene. The target product was acquired by the methods of PCR and agarose electrophoresis in Fig 5.22. The sequence was confirmed as thaumatin-like protein gene by gene sequencing and comparing with GenBank sequence database in Fig 5.23 and Fig 5.24. The results in Fig 5.25 showed that PR-5 gene expression of common tobacco treated by Dufulin increased on the 5th day. It can be inferred that Dufulin is able to induce PR-5 gene expression and plays a vital role in plant disease resistance against TMV.
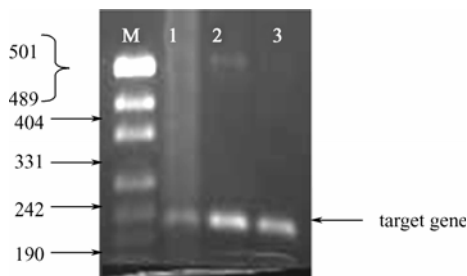
Fig 5.22   The product of like-thaumatin protein(PR-5)gene with PCR amplification. The arrow
is pointed to the product of the target gene whose size is 150bp. DNA Marker：
PUC/Msp I, its molecular weights are 501, 489, 404, 331, 242, 190, 147, 110bp
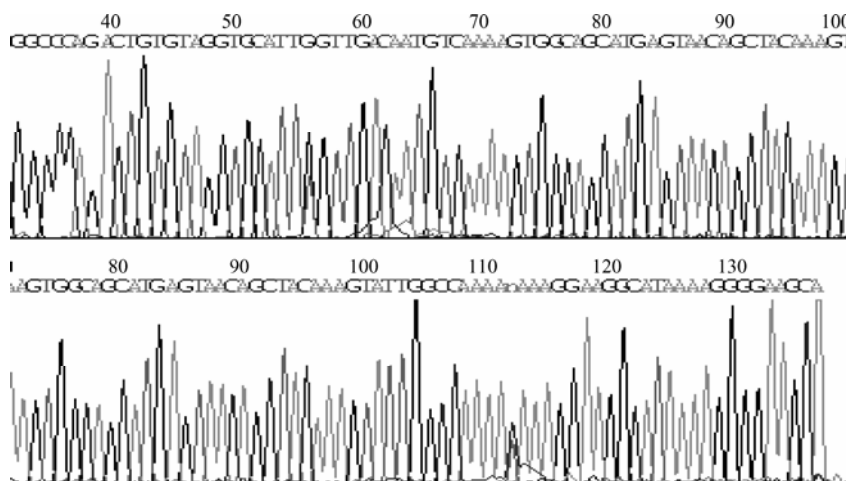
Fig 5.23   Sequencing map of the product of like-thaumatin protein with PCR
amplification(up：map 1, down：map 2)

Copy Sequence FASTA Format>GYS295_GYS295P1 sequence exported
from GYS295_GYS295P1. ab1 TcGAGCTGCCTGCCTCCACCTGGAGAGGC
CGCGGCCCAGA CTGTGTAGGTGCATTGGTTGACAATGTCAAAAGTGGC-
AGCATGAGTAACAGCTACAAAGTATTGGCCAAAAnAAAGGAAGGCATA-
AAAGGGGAAGCA

The PR-5 Gene expression of common tobacco was obviously upregulated 5
days after Dufulin treatment, which indicated that Dufulin played a key role in
inducing up-regulation of PR-5 gene expression.

Effect of Dufulin on PR-1a gene. The target product was acquired by the
methods of PCR and agarose electrophoresis in Fig 5.26. The sequence was
confirmed as PR-1a gene by gene sequencing and comparing with GenBank
sequence database in Fig 5.27 and Fig 5.28. Tobacco was infected by TMV and
followed by Dufulin treatment. The effect of Dufulin on the pathogenesis-related

Blast search

Fig 5.24   Blast search in sequence database
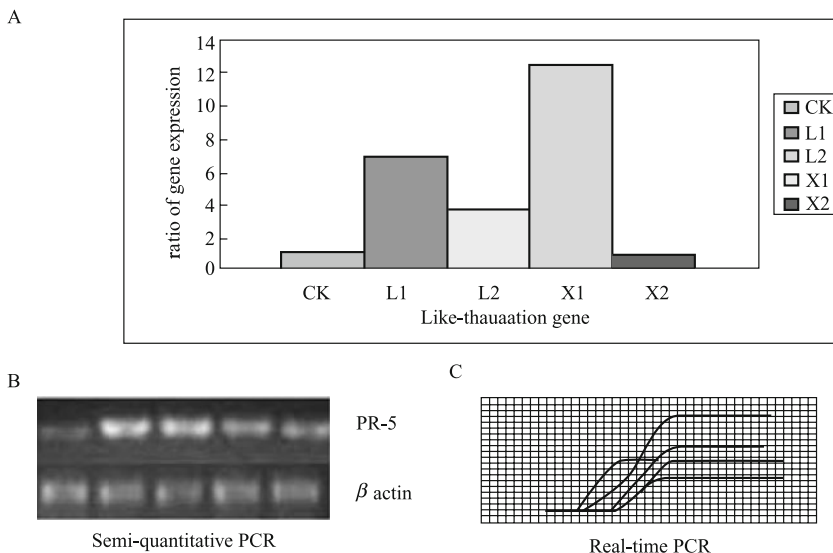
Fig 5.25   The PR-5 Gene expression of common tobacco was obviously upregulated 5 days after Dufulin treatment. A：PR-5 Gene real time PC statistical result. CK：pure water ; L：Ningnanmycin; X：dufulin 1, 1day after busing dufulin ; 2：Five days after busing dufulin. B：Semi-quantitative PCR, reference gene (actin), swim lanes are CK, L1, L2, X1, X2 from left to right. C：Real time PCR curve

proteins (PR-1a) gene expression was investigated through RNA extraction, RT-PCR, Real time PCR and so on. The results showed that Dufulin played an important part in inducing upregulation of PR-1a gene expression and can thus prevent TMV infection and distant invasion. *Nicotiana tabacum* is taken as the template in pathogenesis-related proteins(PR-1a)amplification.

Fig 5.26   Amplified products of pathogenesis-related proteins(PR-1a)gene, the size of 180bp.M：pUC/Msp I is employed as standard molecular weight, the molecular weights of amplified products are 501,489,404,331,242,190,147,110bp

  Pathogenesis-related proteins(PR-1a)Gene sequence identification.

Fig 5.27   Sequencing mapping of the product of pathogenesis-related proteins(PR-1a)gene with PCR amplification. Comparison with the genBank sequence database indicated that the sequence was pathogenesis-related proteins (PR-1a) gene

    The effect on the pathogenesis-related proteins (PR-1a) gene expression revealed that Dufulin can induce upregulation of PR-1a gene expression, and enhance the anti-TMV immune system of tobacco itself, and can prevent TMV infection and distance invasion(Fig 5.29).

Fig 5.28   Blast search in sequence database

A

CK: water

L: Ningnanmeisu

X: Bingduxing

1: 1 day

2: 5 day

B

Semi-quantity PCR

C

Real-time PCR

Fig 5.29   Upregulation of PR-1a gene expression of Nicotiana tabacum treated by Dufulin.A：The statistics of real time PCR for N gene. B：Semi-quantity PCR, β-actin served as internal reference gene.C：the figure of real time PCR

The effect of Dufulin on the N gene. TMV infected K_{236} tobacco was treated with Dufulin for three days. Then RNA extraction, RT-PCR, real time PCR, and gene sequencing methods were employed to study the expression of N gene expression as shown in Fig 5.30. The results showed that the N gene in tobacco leaves was upregulated by Dufulin, which indicated that Dufulin can induce upregulation of tobacco N gene and thus supress the reproduction and long distance movement of TMV in Fig 5.31.
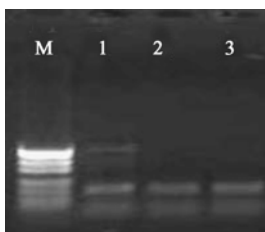
Fig 5.30   The product of N gene with PCR amplification.The arrow is pointed to the product of the target gene whose size is 150bp. DNA Marker：pUC/Msp I, Molecular weights are 501, 489, 404, 331, 242, 190, 147, 110bp
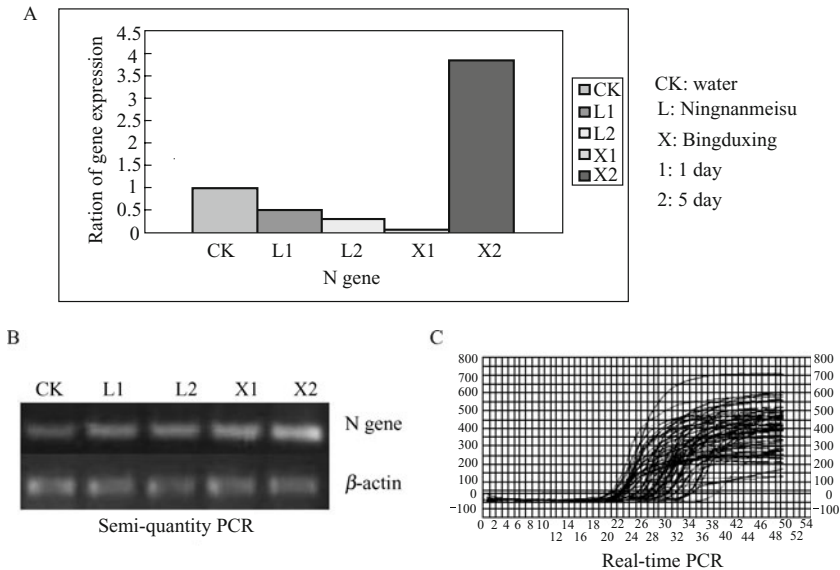
Fig 5.31 Upregulation of N Gene expression after treatment of Dufulin. A：The statistics of real time PCR about N gene. B：Semi-quantity PCR, β-actin serves as internal reference gene. C：the figure of real time PCR

mRNA differential display of tobacco after treatment with Dufulin. The leaves of common tobacco with consistent growth for 6 weeks cycle were sprayed with 500 μg/mL Dufulin, and were then inoculated with TMV 24 h later. After 6 hours treatment, tobacco leaves were collected to extract total RNA. Lane 1 (Fig 5.32) represents the control of Dufulin treatment without TMV infection, while lane 2 means both TMV and Dufulin treatment as described. The figure showed that
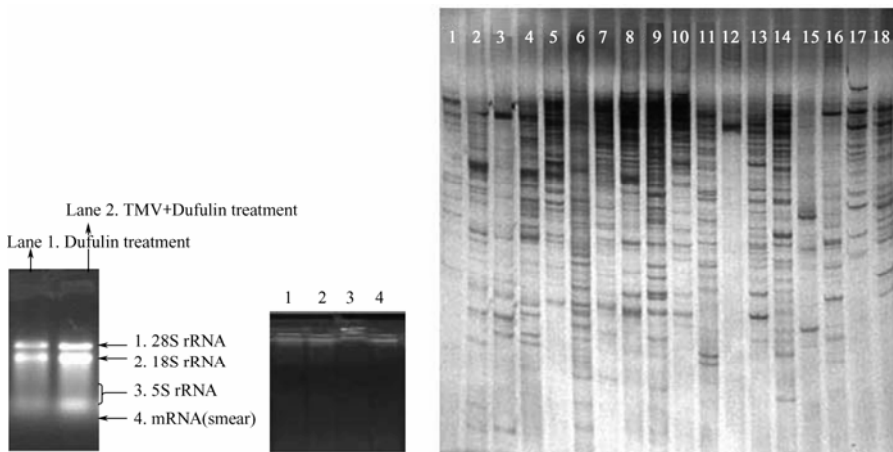
Fig 5.32 Agarose gel electrophoresis of total RNA and cDNA synthesis and mRNA differential display

luminance ratio of lane 2 was higher than lane 1, which indicated a better quality of the extracted RNA that can be used in next step. Each smear band represents synthetic cDNA.

(4) *Two-dimensional electrophoresis coupled with mass spectrum*

In our study, protein samples from *Nicotiana tabacum* K_{326} leaves inoculated by TMV were compared with that of the leaves treated by Dufulin at 500 μg/mL for 5 days. As shown in Fig 5.33, differential expression protein analysis was performed using 2-D gel electrophoresis by combining gel silver staining and imaging analysis. A total of 200 protein spot-features were analyzed across all leaf protein samples. Five spot-features of interesting protein were found to be significantly increased and the times of expression level ranged from 1.6 times to 4.2 times, as shown in Fig 5.33. All interest protein spots were digested by trypsin for overnight and submitted to MALDI-TOF/MALDI-TOF/TOF analysis for identification of the protein name as shown in Fig 5.34. The four up-regulated proteins were identified in tobacco leaf inoculated by TMV and treated by Dufulin using NCBI database. The names of different kinds of protein are shown in Table 5.34. Accession number (gi|76556492) was assigned to putative chloroplast cysteine synthase 1 precursor in Nicotiana tabacum, while chloroplast cysteine synthase [*O*-acetyl-L-serine (thiol)-iyase, EC 4.2.99.8] was responsible for the terminal step of cysteine biosynthesis that catalyzed the formation of L-cysteine from *O*-acetyl-L-serine (OAS) and hydrogen sulfide. Accession number (gi|76869447) was assigned to KP1B. 103D22F. 050725T7 KP1B cDNA clone KP1B. 103D22 in Nicotiana tabacum and till date there is no report regarding its gene structure and function. Accession number (gi|121309841) was assigned to malate dehydrogenase like-protein, and its function is still not clear. Finally, the accession number (gi|39791637) appeared in two spots and assigned to EST728893 potato callus cDNA library, and is not present in *Nicotiana tabacum*.
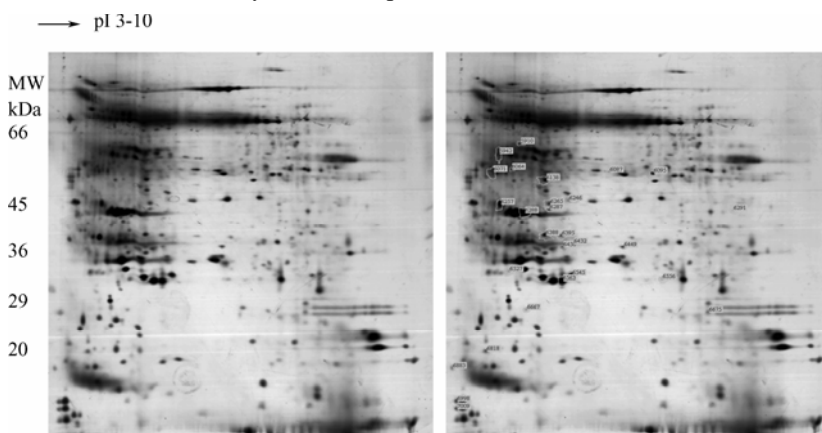
Fig 5.33   2-D gel electrophoresis image. Left part represents the tobacco leaf protein sample inoculated only by TMV, Right part stands for the tobacco leaf protein sample treated by TMV and Dufulin
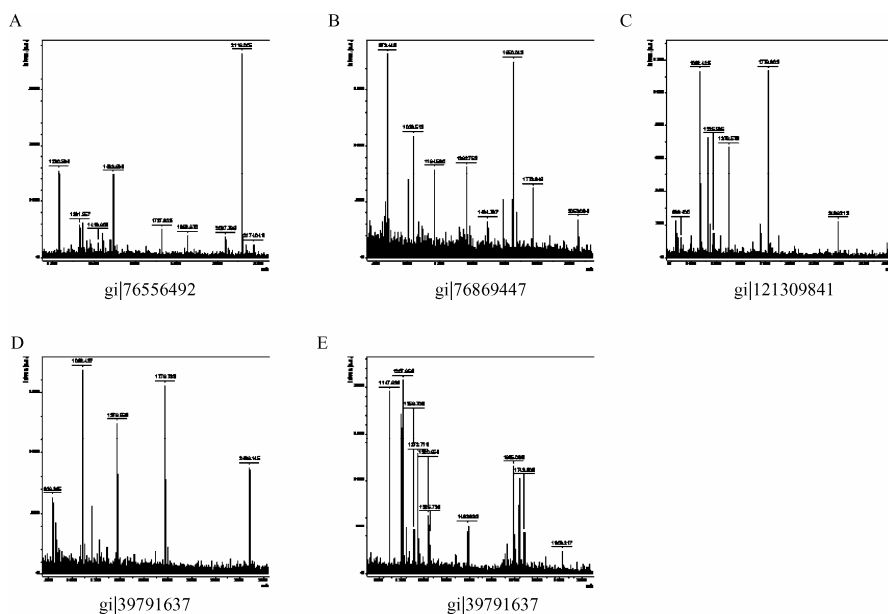
Fig 5.34   MALDI-TOF/MALDI-TOF/TOF spectrum after trypsin digestion of five protein spots. Every part ranging from A to E indicated those proteins whose accession numbers were gi|76556492, gi|76869447, gi|121309841, gi|39791637, respectively

Table 5.34   Protein name

Accession number	Protein Name	Mass spectrum type
Gi|76556492	putative chloroplast cysteine synthase 1 precursor [Nicotiana tabacum]	MALDI-TOF
Gi|76869447	KP1B.103D22F.050725T7 KP1B Nicotiana tabacum cDNA clone KP1B.103D22, mRNA sequence	MALDI-TOF
Gi|121309841	malate dehydrogenase like-protein [Iris x hollandica]	MALDI-TOF
Gi|39791637	EST728893 potato callus cDNA library, normalized and full-length Solanum` tuberosum cDNA clone POCAC92 5' end, mRNA sequence	MALDI-TOF-TOF
Gi|39791637	EST728893 potato callus cDNA library, normalized and full-length Solanum tuberosum cDNA clone POCAC92 5' end, mRNA sequence	MALDI-TOF-TOF

The protein names of gel spot were identified using Global Proteome Server Explorer software utilizing the NCBI Database.

5.1.8.4   Conclusions

From these experiments, it may be concluded that：(1) Dufulin can enhance the activities of defense related enzymes of tobacco, such as phenylalanine ammonia-lyase (PAL), peroxidase (POD), superoxide dismutase (SOD), and chlorophyll content and (2) Dufulin does not change the phenotype of TMV particles but will make them aggregated and (3) Dufulin can increase the salicylic acid level in tobacco and thus activate salicylic acid signaling pathway and the pathway downstream target genes as well as PR-1a, PR-5 proteins.

As a further support, it was also found that the protein expression level of tobacco chloroplast cysteine synthetase precursor in tobacco leaves treated by TMV and Dufulin was up-regulated and the expression level of the treatment was 4 times higher than the treatment of tobacco leaf inoculated by TMV. At the same time, the product of chloroplast cysteine synthetase which was found to be hydrogen peroxide by information retrieval in NCBI Hydrogen peroxide, could be associated with plant systemic acquired resistance (SAR) by interaction with SA.Therefore, our preliminary findings indicated that Dufulin could increase resistance of tobacco against TMV by inducing expression of chloroplast cysteine synthetase and stimulating SA signaling pathway. It is concluded that Dufulin is a novel class of inducer or activator of plant immune system through activating tobacco SA signal transduction pathway.

References

1.   Van Loon L C. Systemic induced resistance. In: Slusarenko AJ, Fraser RSS, van Loon LC, eds. Mechanisms of Resistance to Plant Diseases. *Dordrecht, The Netherlands: Kluwer Academic Publishers.* 2000, 521-574.

2.   Hammerschmidt R. Induced resistance: How do induced plants stop pathogens? *Physiol. Mol. Plant. Pathol.* 1999, 55, 77-84

3.   Ryals J, Neuenschwander U H, Willits M G, *et al*. Systemic acquired resistance. *Plant Cell*, 1996, 8, 1809-1819.

4.   Malamy J, Carr J P, Klessig D F, *et al*. Salicylic acid: a likely endogenous signal in the resistance response of tobacco to viral infection *Science.* 1990, 250, 1002-1004.

5.   Yalpani N, Silverman P, Wilson T M A, *et al*. salicylic-acid is a systemic signal and an inducer of pathogenesis-related proteins in virus-infected tobacco. *Plant Cell.* 1991, 3, 809-818.

6.   Metraux J P, Signer H, Ryals J, *et al*. increase in salicylic acid at the onset of systemic acquired resistance in cucumber. *Science.* 1990, 250, 1004-1006.

7.   Zhang G P, Song B A, Xue, W, *et al*. Synthesis and biological activities of novel dialkyl 1-(4-trifluoromethylphenylamino)-1-(4 - trifluoromethyl- or 3-fluoro-phenyl) methylphos phonate. *J. Fluorine Chem.* 2006, 127, 48-53.

8.   Koukol J, Conn E E. The metabolism of aromatic: compounds in higher plants Ⅳ.Purification and properties of the phenylalanine deaminase of Herdeum Vulagare. *J. Biol. Chem.* 1961, 23, 2692-2698.

9.   Rao M V, Paliyath G, Ormrod D P. Ultraviolet-B- and ozone-induced biochemical changes in antioxidant enzymes of *Arabidopsis thaliana*. *Plant Physiol*. 1996, 110, 125-136.

10. Castillo F J, Penel C, Greppin H. Peroxidase release induced by ozone in sedum album leaves: involvement of Ca^{2+}. *Plant Physiol*. 1984, 74, 846-851.

11. Dhindsa R A, Plumb-Dhindsa P, Thorpe T A. Leaf senescence: correlated with increased permeability and lipid peroxidation, and decreased levels of superoxide dismutase and catalase. *J. Exp. Bot*. 1981, 126, 93-101.

12. Sükran D, Tohit G, Rıdvan S. Spectrophotometric determination of chlorophyll- A, B and total carotenoid contents of some algae species using different solvents. *Annals botany*. 1998, 22, 13-17.

13. Porra R J, Grimme L H. A new procedure for the determination of chlorophylls *a* and *b* and its application to normal and regreening *Chlorella*A new procedure for the determination of chlorophylls *a* and *b* and its application to normal and regreening. *Chlorella*. 1974, 57, 255-267.

14. Achuo E A, Audenaert K, Höfte, M, *et al*. The salicylic acid-dependent defence pathway is effective against different pathogens in tomato and tobacco. *Plant Pathology*. 2004, 53, 65-72.

15. Raskin I, Turner I M, Melander W R. Regulation of heat production in the inflorescences of an Arum lily by endogenous salicylic acid. *Proc Natl Acad Sci USA*. 1989, 86, 2214-2218.

16. Wilkinson, M. F. Purification of RNA. In essential molecular biology: A practical approach (ed. Brown, T.A). *Oxford University Press New York USA*. 1991, 1, 69-86.

17. Yuan J S, Reed A, Chen F, *et al*. Statistical analysis of real-time PCR data. *BMC Bioinform*. 2006, 7, 85.

18. Paent J G, Asselin A. Detection of pathogenesis-related (PR or b) and of other proteins in the intercellular fluid of hypersentitive plants infected with tobacco mosaic virus. *Can. J. Bot*. 1984, 62, 564-569.

19. Rathmell W G, Sequeria L. Soluble peroxidase in fluid from the intercellular spaces of tobacco leaves. *Plant Physiol*. 1974, 53:317-318.

20. Bauer D, Warthoe P, Rohde M, *et al*. Detection and differential display of expressed genes by DDRT-PCR. *PCR Methods Appl Manual Supplement (Cold Spring Harbor Laboratory, USA)*. 1994, S97-S108.

21. Liang P, Pardee A. Differential display of eukaryotic messenger RNA by means of the polymerase chain reaction. *Science*. 1992, 257, 967-970.

22. Lee J, Cooper B. Alternative workflows for plant proteomic analysis. *Mol Biosyst*. 2006, 2, 621-626.

23. Florens L, Washburn M P. Proteomic analysis by multidimensional protein identification technology. *Methods Mol. Biol*. 2006, 328, 159-175.

24. Ünlü M, Morgan M E, Minden J S. Difference gel electrophoresis. A single gel method for detecting changes in protein extracts. *Electrophoresis*. 1997, 18, 2071-2077.

5.1.9   Photolysis and Hydrolysis

5.1.9.1   Introduction

Research on environmental behavior, such as photolysis and hydrolysis, can indicate the potential movements of chemicals released into the natural environment and provide reasonable forecast and theoretical basis for pollution caused by chemicals. This research provides scientific basis not only for rational application and environmental safety evaluation of Dufulin, but also lays foundation

for the registration of pesticides. This work was commissioned to China National Center for Quality Supervision & Test of Pesticides Safety (NCQSTP) to test photolysis and hydrolysis of Dufulin.

5.1.9.2   Materials and Methods

(1) *Hydrolysis*

Hydrolysis is an interactive process between a chemical compound and water molecule. The temperature and pH value are often the most important parameters that control hydrolysis. The dynamics of Dufulin hydrolysis was studied in different sterilized buffer solution and natural waters at various temperatures. During the investigation, changes of activation energy of hydrolysis (Ea), activation enthalpy (ΔH) and activation entropy (ΔS), were studied.

Main instruments. Chemical and biological incubator, cyclotron oscillator, pH meter, electronic analytical balance (ten thousandth, Sartorius); rotary evaporator (RE-52AA); Agilent 1100 HPLC(equipped with DAD).

Chemical reagents. Dufulin standard, anhydrous sodium sulfate, sodium chloride and common analytical reagent, distilled water, methanol (HPLC grade).

Preparation of the buffer solution (US EPA, 1998) and collection of natural water were performed as described below.

Buffer solution (pH=5) :230.9 mL 0.1 M sodium hydroxide +500.0 mL 0.l mol/mL potassium phosphate, add distilled water to make up the volume up to 1000.0 mL;

Buffer solution (pH=7):296.0 mL 0.l M sodium hydroxide +500.0 mL 0.l mol/mL potassium dihydrogen phosphate, add distilled water to make up the volume up to 1000.0 mL;

Buffer solution (pH=9):213.0 mL 0.1 M sodium hydroxide +500.0 mL 0.l mol/mL boric acid/potassium chloride, add distilled water to make up the volume up to 1000.0 mL.

The buffer containers used in experiments were sterilized for 1 h by high-pressure and at high-temperature (130℃, 0.15 MPa), stored in a brown bottle for backup. After sterilizing, solution was re-calibrated with the standard pH buffers (actual pH measurements were 5.04, 7.09 and 9.20).

Collection of natural water. Pond water was collected from the pond located in front of Guizhou University Library. Huaxi river water was taken from the downstream of the river in Guizhou at Huaxi District, Guiyang City. All natural waters were filtered through neutral filter paper, pH values measured (pond water: 8.80, river water: 8.04, distilled water: 6.28).

*Sample extraction.*20.0 mL water samples were transferred into a 250 mL separating funnel, added 1.0 mL brine, and extracted thrice with dichloromethane

of volume 20.0 mL, 20.0 mL, and 15.0 mL. After drying on anhydrous sodium sulfate, the combined solvent was transferred into a 100 mL pear-shaped flask for vacuum concentration at 30℃, and was finally analyzed by HPLC.

HPLC method. Agilent Eclipse XDB-C$_{18}$ (150 mm×4.6 mm i.d., 5 μm), Column temperature 25℃, mobile phase methanol/pure water=90/10 (*v/v*), flow rate 1.0 mL/min, detective wavelength 270 nm; injection volume 20 μL. The content was calculated with external standard method. The retention time was about 5.0 min under the chromatographic conditions.

Hydrolysis test in different buffer solution. A number of clean and sterilized 100 mL glass bottles were divided into different groups classified as A, B and C groups each consisting of three. 1.00 mL 0.10 g/L Dufulin methanol solution was transferred to A, B and C group flasks accurately, added 100.0 mL buffer of pH=5, pH= 7, pH= 9 respectively. In order to inhibit the growth of microorganisms, 0.1 g NaN$_3$ solid was added into each group. Medical solutions were well-mixed by oscillation. Dufulin solution of concentration 1.00 mg/L was placed in dark in the biochemical incubator for hydrolysis test at 25℃ (dark and lucifge). After a certain period of time, each group of sample was tested after extraction and concentration.

Hydrolysis test at different temperature. A number of clean and sterilized 100 mL glass bottles were divided into different groups classified as A, B, C, D, E, F, G, H, I each consisting of three.1.00 mL 0.10 g/L *Dufuin* methanol solution was transferred into A, B, C, D, E, F, G, H, I group flasks accurately, added 100.0 mL buffer of pH=5, pH=7, pH=9 respectively. Medical solutions were well-mixed by oscillation. The concentration of Dufulin thus obtained was 1.00 mg/L. It was then placed in the biochemical incubator for hydrolysis test at 25℃, 50℃, 75℃ respectively (dark and lucifuge). After a certain period of time, each group of sample was tested after extraction and concentration.

Hydrolysis test in netural water. A number of clean and sterilized 100 mL glass bottles were divided into different groups classified as J, K, L each consisting of three. After determining pH value, pond water and Huaxi river water were filtered through neutral filter paper to remove suspended matter.1.00 mL 0.10 g/L *Dufuin* methanol solution was transferred into J, K, L group flasks accurately, added 100.0 mL pond water, Huaxi river river water and distilled water respectively. Medical solutions were well-mixed by oscillation. The concentration of Dufulin thus obtained was 1.00 mg/L. Then it was cultivated in dark in the biochemical incubator at 25℃. After a certain period of time, each group of sample was tested after extraction and concentration.

(2) **Photolysis**

Photolysis of Dufulin is a complex reaction which is initiated by light energy.

The photodecomposition experiment was carried out by direct irradiation of aqueous solution and organic solvents of Dufulin with ultraviolet lamps (30W, λ=253.7 nm). The experiment provides the scientific basis for the safe and effective application of Dufulin.

Materials and sample preparation. Self-made Photolytic device: two ultraviolet lamps (30W, 253.7nm) were hung parallel in a fume hood, and a mirror was placed below the lamps to reflect the light, the distance between light source and sample was about 4 cm and the main wavelength of light was 253.7 nm.

Calculation and statistical method.

photodegradation rate (%) =

$$\frac{\text{the remain of darkness control} - \text{the remain of illumination}}{\text{the remain of darkness control}} \times 100\%$$

When the concentration of pesticides in water is very low, the pesticide photolysis reaction rate follows false first order dynamic model, $-dC/dt=kC_o$. The equation $C_t=C_o\, e^{-kt}$ is obtained by integral method, k is the hydrolysis rate constant, C_o is the initial concentration of pesticides, C_t is the instantaneous concentration of pesticides at time t. Time required for 50% of pesticide hydrolysis (C_t=1/2 C_o) is known as the photodegradation half-life, denoted as $T_{1/2}$ ($T_{1/2}$=ln2/k=0.693/k).

All test data were statistically analyzed with EXCEL2003 and the photodegradation rate constant of Dufulin (k) was calculated by direct fitting with first order dynamic equation.

Photolysis experiment in organic solvents.2.0 mL of Dufulin standard solution (1.0 g/L) was precisely transferred into a 200.0 mL volumetric flask, and methanol was evaporated by nitrogen flush. Then it was diluted to 10.0 mg/L with n-hexane, methanol and acetone respectively. 20 mL solution was subjected to photolysis test under UV light (253.7 nm) illumination at room temperature. Two parallel samples were set for each experiment, and absorption-free sample was prepared by wrapping with opaque aluminum foil. The sample after illumination was evaporated to dryness by nitrogen flush, then diluted by adding 1 mL methanol and subjected to HPLC detection.

Photolysis experiment in buffer solutions. 0.5 mL of Dufulin standard solution (1.0 g/L) was precisely transferred into a 500.0 mL volumetric flask, then added 500.0 mL sterilized buffer with pH=5, 7 and 9 respectively. Then the agent solutions were thoroughly mixed by ultrasonic agitation. Finally, the concentration of Dufulin in each buffer was 1.00 mg/L.50 mL Solution was subjected to photolysis test under UV light (253.7 nm) illumination at room temperature. Two parallel samples were set for each experiment, and absorption-free sample was prepared by wrapping with opaque aluminum foil. The sample after illumination

was evaporated to dryness by nitrogen flush, then diluted by adding 1 mL methanol and subjected to HPLC detection.

*Photolysis experiment in natural waters.*0.5 mL of Dufulin standard solution (1.0 g/L) was precisely transferred into a 500.0 mL volumetric flask, then added 500.0 mL of different waters (*e.g.* pond water, river water and distilled water) respectively. Then the agent solutions were thoroughly mixed by ultrasonic agitation. Finally, the concentration of Dufulin aqueous solution was 1.00 mg/L.50 mL solution was subjected to photolysis test under UV light (253.7 nm) illumination at room temperature. Two parallel samples were set for each experiment, and absorption-free sample was prepared by wrapping with opaque aluminum foil. The sample after illumination was evaporated to dryness by nitrogen flush, then diluted by adding 1 mL methanol and subjected to HPLC detection.

5.1.9.3   Results

(1) ***Result of Hydrolysis test***

Hydrolysis test in different buffer solution. Under acidic and alkaline conditions, the hydrolysis of Dufulin showed somewhat different trend. After being hydrolyzed for 120 d, hydrolysis rates of different samples of pH=5, pH=7 and pH=9 were 7.14%, 1.60% and 9.70% respectively (Fig 5.35).
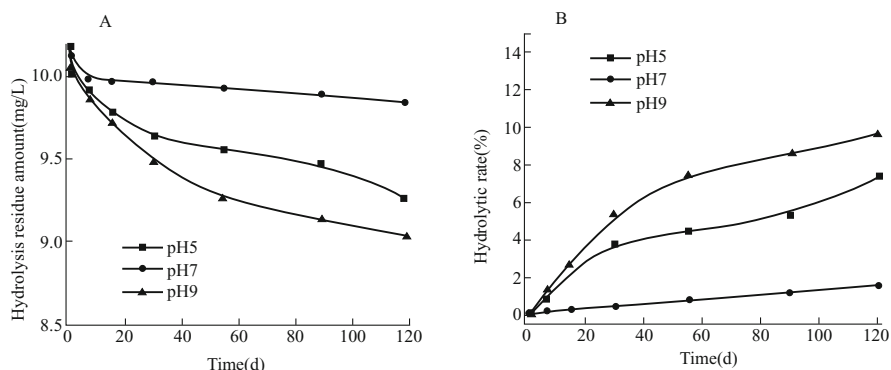
Fig 5.35 Hydrolysis dynamics curves of Dufulin in the aqueous buffer solution with different pH values at the temperature of 25℃ (A stands for the residue amount and B is the hydrolytic rate)

It is obvious that Dufulin was much stable in the neutral medium with only slight hydrolysis in 120 days. Although the hydrolysis of Dufulin takes place under both acidic and alkaline conditions, the rate is much higher in alkaline medium. Hydrolysis test data was calculated by first order dynamic equation, the results are provided in Table 5.35.

Table 5.35   Hydrolysis kinetics of Dufulin in buffer with different
pH values under the UV light[a]

Temp (℃)	pH	$C_t=C_0 \cdot e^{-kt}$	K (d^{-1})	$T_{1/2}$ (d)	R^2
25	5	$C_t=10.247e^{-0.0120t}$	0.0120	57.75	0.9843
25	7	$C_t=10.184e^{-0.0044t}$	0.0044	157.5	0.9000
25	9	$C_t=10.367e^{-0.0177t}$	0.0177	39.15	0.9827

[a]K: hydrolysis rate constant, $T_{1/2}$: half time, R^2: correlation coefficient.

It can be seen from Table 5.35, the degradation of Dufulin in water body can be well fitted with the first order kinetic equation. Half-lives of hydrolysis in buffer solutions with pH=5, pH=7 and pH=9, were 57.75 d, 157.5 d and 39.15 d, respectively.

Hydrolysis test at different temperatures. The hydrolysis dynamic curve of the new pesticide Dufulin at different temperatures can be seen from Fig 5.36 and Fig 5.37.
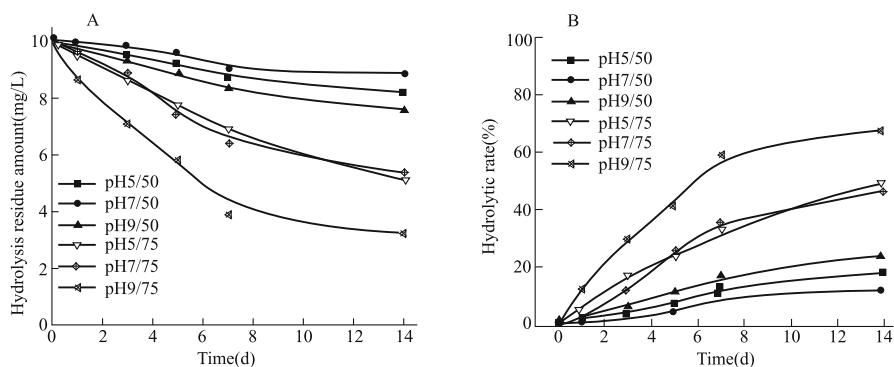
Fig 5.36   pH-temperature curves of residue and hydrolysis of Dufulin (A: residue amount, B: hydrolysis rate)

It can be seen from Fig 5.36 and Fig 5.37 that hydrolysis rate constant of Dufulin increases with temperature, and depends on the pH of the buffer solution. In alkaline medium at high temperature, the rate of hydrolysis of Dufulin is very fast. Hydrolysis test data was calculated with the first order dynamic equation, the results are given in Table 5.36.

It can be seen from Table 5.36, hydrolysis of Dufulin was in accordance with the dynamic equation at different temperatures. At 25℃, 50℃ and 75℃, half-lives of Dufulin in buffer solution (pH=5) were 57.75 d, 17.33 d and 5.33 d
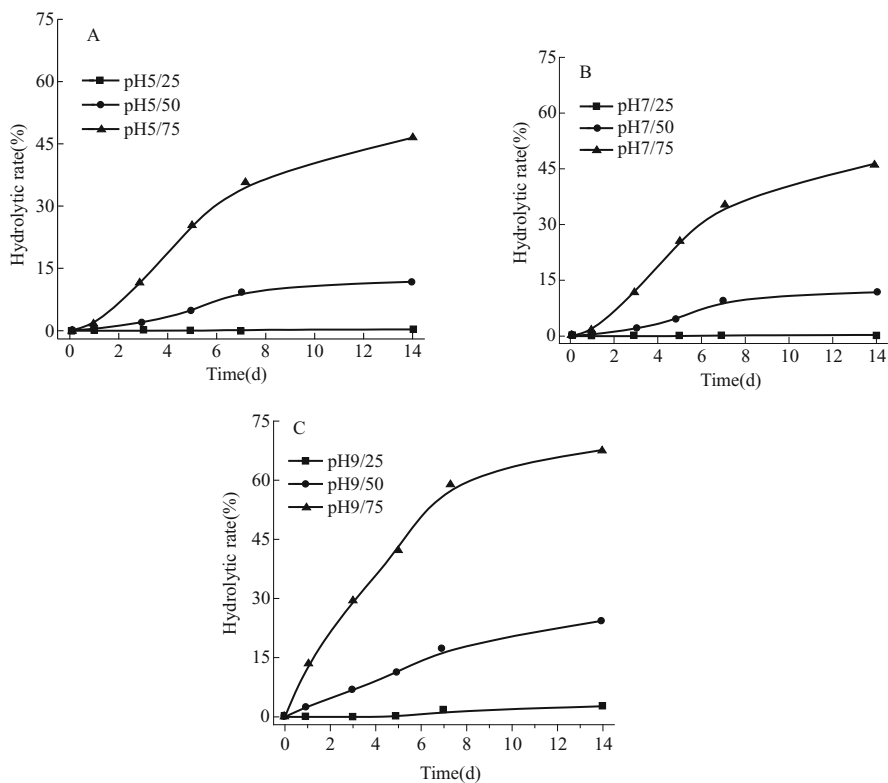
Fig 5.37 pH-temperature curves of Hydrolysis rate of Dufulin (A: in pH=5 solution, B: in pH=7 solution and C in pH=9 solution)

Table 5.36 Hydrolysis kinetics of Dufulin in the aqueous buffer solution with different pH values at the different temperatures

pH	Temp (℃)	$C_t=C_0 \cdot e^{-kt}$	$K\,(\mathrm{d}^{-1})$	$T_{1/2}$ (d)	R^2
	25	$C_t=10.247e^{-0.0120t}$	0.0120	57.75	0.9843
5	50	$C_t=10.607e^{-0.0400t}$	0.0400	17.33	0.9484
	75	$C_t=12.195e^{-0.1301t}$	0.1301	5.33	0.9141
	25	$C_t=10.184e^{-0.0044t}$	0.0044	157.5	0.9000
7	50	$C_t=10.475e^{-0.0278t}$	0.0278	24.93	0.9082
	75	$C_t=12.159e^{-0.1291t}$	0.1291	5.37	0.9607
	25	$C_t=10.367e^{-0.0177t}$	0.0177	39.15	0.9827
9	50	$C_t=10.934e^{-0.0567t}$	0.0567	12.22	0.9267
	75	$C_t=13.552e^{-0.2353t}$	0.2353	2.95	0.9779

respectively. The corresponding values at pH 7 and 9 were 157.5 d, 24.9 d, 5.37 d and 39.15 d, 12.22 d and 2.95 d, respectively.

Hydrolysis of organic compounds, including pesticides, depends on the temperature of the system. The higher the temperature, the faster is the hydrolysis rate in general. This is perhaps attributed to the presence of thermally activated molecular collisions of organic compounds that provide favorable activation energy for the reaction at higher temperature. As a matter of fact, temperature has significant effect on the hydrolysis rate of Dufulin.

Hydrolysis in neutral water. Hydrolysis dynamic curves of Dufulin in natural waters are shown in Fig 5.37. It can be seen from Fig 5.38, despite being tested under same conditions, Dufulin hydrolysis rate is different in different kinds of water. The degradation rate in all three systems increased with time and the hydrolysis rate in pond water, river water and distilled water reached up to 29.9%, 28.4% and 18.7% respectively in 120 d. Hydrolysis of Dufulin in both natural waters was faster than that in distilled water. The calculated results by means of the kinetic equation are listed in Table 5.37. We can see that the degradation rate of Dufulin in water can be well fitted with the first order kinetics equation. Hydrolysis half-lives of Dufulin in pond water, river water and distilled water were 12.58 d, 14.68 d and 21.19 d, respectively.
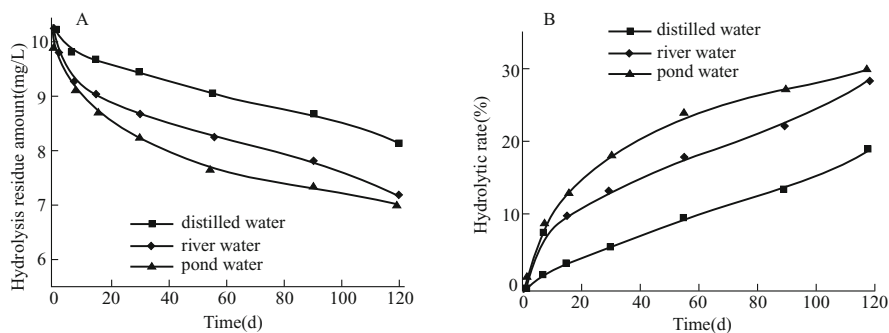
Fig 5.38 Hydrolysis dynamics curves of Dufulin in different natural waters at 25℃ (A indicates the residue amount and B the hydrolytic rate)

Table 5.37 Hydrolysis kinetics of Dufulin in different types of water at 25℃

Temp (℃)	Water	$C_t=C_0 \cdot e^{-kt}$	K (d^{-1})	$T_{1/2}$ (d)	R^2
25	dd water	$C_t=10.879e^{-0.0327t}$	0.0327	21.19	0.9545
25	River water	$C_t=10.796e^{-0.0472t}$	0.0472	14.68	0.9684
25	Pond water	$C_t=10.797e^{-0.0551t}$	0.0551	12.58	0.9924

Many studies have confirmed that pesticide hydrolysis is largely restricted by the pH value of the solution system and temperature. A variety of micro-organisms and suspended particles in natural water are found to be beneficial in the degradation of pesticides. However, anions form dissolved organic matters in

water can probably hinder degradation of pesticides. Therefore, the comparison of Dufulin degradation in natural water with ideal body of water (distilled water) appears to be complex and depends on a number of factors including the role of the components in natural water.

Discussion-The activation energy (*Ea*), activation enthalpy (Δ*H*) and the activation entropy (Δ*S*) of the hydrolysis reaction of Dufulin. The main factor that affects pesticide hydrolysis rate constant is the activation energy, the other being the activation entropy. Under the same conditions, Arrhenius empirical equation can be used to calculate pesticide hydrolysis rate at different temperatures.

$$k = A \cdot e^{-Ea/RT} \qquad (5\text{-}1)$$

In equation (5-1), k is the rate constant, Ea is the Arrhenius activation energy (kJ/mol), A is pre-exponential factor, R is the gas constant (8.314 J/K • mol), T is the absolute temperature (K). By taking logarithms on the each side of the above equation, it may be written as:

$$\ln k = \frac{-Ea}{R} \cdot \frac{1}{T} + \ln A \qquad (5\text{-}2)$$

Following the method described by Hong in 2000, activation enthalpy (Δ*H*) can be obtained by using the following equation.

$$\Delta H = Ea - RT \qquad (5\text{-}3)$$

Activation entropy (Δ*S*) is a measure of disorder in the system, thereby reflecting the degrees of freedom in terms of gains and losses between the starting compound and the transition state (activated complex). The change of the compound structure and aggregation state of the species associated with the change of entropy is expressed in terms of activation entropy by means of the following equation:

$$\Delta S = \left(\frac{\Delta H}{T} \right) + R\ln \left(\frac{hk}{k_B K T} \right) \qquad (5\text{-}4)$$

In equation (5-4), k is the rate constant, k_B is Boltzmann constant (1.381×10^{-23} J/K), K is the transfer coefficient (~ 1), h is the Planck constant (6.626×10^{-34} J•s), R is the gas constant (8.314 J/K•mol), T is the absolute temperature (K).

The hydrolysis rate constant $\ln k$ was plotted against the absolute temperature $1/T$ (K). The equations relating the temperature ($1/T$) and hydrolysis rate ($\ln k$) for Dufulin hydrolysis in the aqueous buffer solution with different pH values are shown in Fig 5.39. The equations can be expressed as follows: pH=5, $\ln k = -4.7071 \times 10^3/T + 11.522$, correlation coefficient $R^2 = 0.9882$, the straight line slope is 4.7071×10^3; pH=7, $\ln k = -6.7096 \times 10^3/T + 17.338$, correlation coefficient $R^2 = 0.9961$, the straight line slope is 6.7096×10^3; pH=9 $\ln k = -5.0723 \times 10^3/T + 13.109$, correlation coefficient $R^2 = 0.9705$, the straight line slope is 5.0723×10^3. At different temperatures, the calculated activation energy and activation entropy of Dufulin hydrolysis are shown in Table 5.38.

a: pH9 $\ln k = -5072.3 \times 1/T + 13.109$ $R^2 = 0.9705$
b: pH5 $\ln k = -4707.1 \times 1/T + 11.522$ $R^2 = 0.9882$
c: pH7 $\ln k = -6709.6 \times 1/T + 17.338$ $R^2 = 0.9961$
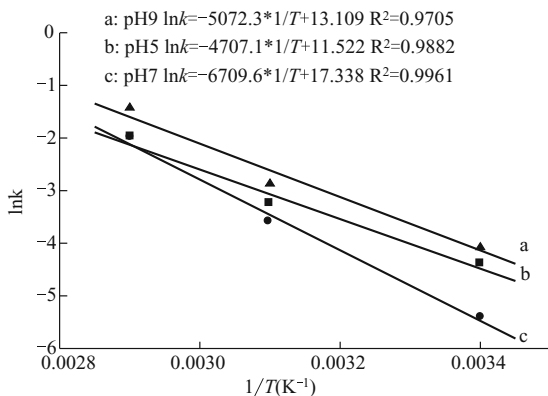
Fig 5.39 Relationship between temperature ($1/T$) and hydrolysis rate ($\ln k$) for Dufulin hydrolysis in the aqueous buffer solution with different pH values.

Table 5.38　k_{t+25}/k_t, activation energy (Ea), activation enthalpy (ΔH) and activation entropy (ΔS) of Dufulin hydroiysis in the aqueous buffer solution with different pH values at different temperatures

pH	Temp (℃)	25	50	75	Average
5	K	0.0120	0.0400	0.1301	—
	k_{t+25}/k_t	—	3.33	3.25	3.29
	Ea (kJ/mol)	38.990	39.534	38.879	39.134
	ΔH (kJ/mol)	36.490	36.834	35.979	36.434
	ΔS (J/mol·K)	−64.793	−63.856	−65.311	−64.653
7	K	0.0044	0.0278	0.1291	—
	k_{t+25}/k_t	—	6.32	4.64	5.48
	Ea (kJ/mol)	55.665	56.108	55.575	55.783
	ΔH (kJ/mol)	53.165	53.408	52.675	53.083
	ΔS (J/mol·K)	−17.206	−15.592	−17.419	−16.739
9	K	0.0177	0.0567	0.2353	—
	k_{t+25}/k_t	—	3.20	4.15	3.68
	Ea (kJ/mol)	41.920	42.855	41.731	42.169
	ΔH (kJ/mol)	39.420	40.155	38.831	39.469
	ΔS (J/mol·K)	−51.734	−50.679	−52.193	−51.535

Activation energy is the energy difference between the ground state and the transition state which decides the rate of reaction in a given chemical system. In other words, the greater the activation energy, the more slowly molecules would react as there is little likelihood of having effective molecular collision to acquire

the desired activation energy level. On the contrary, the lower the activation energy, the faster would be the reaction as most of the reactant molecules will have sufficient energy to reach the transition state. Dufulin hydrolysis activation energy has no significant correlation with temperature. Dufulin hydrolysis activation enthalpy also showed a similar trend as with activation energy. Activation entropy of hydrolysis is negative, which showed that not only the common nucleophilic substitution reaction between two molecules is prevalent, but also other factors may play important role in the process of Dufulin hydrolysis and metabolism.

(2) **Results of Hydrolysis test**

Photolysis in organic solvents. Dufulin in methanol and *n*-hexane solution can directly absorb light at λ≤300 nm. Electron transfer within different energy levels in Dufulin molecule takes palce with photochemical induction causing a rapid photochemical reaction. Photolysis-time dynamic curve of Dufulin is shown in Fig 5.40. Photolysis of Dufulin in methanol and *n*-hexane was quite fast and no Dufulin was detected after being exposed for 60 min. However, photolysis of Dufulin in acetone was relatively slow. Photolysis rates of Dufulin in methanol, *n*-hexane and acetone were 96.1%, 94.7% and 1.5% respectively when illuminated for 40 mins.
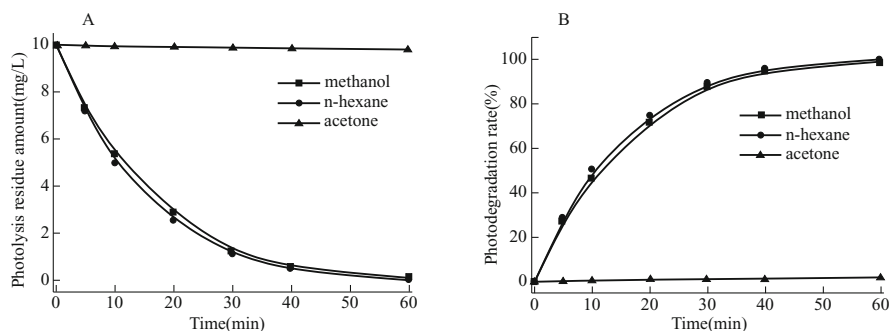
Fig 5.40   Photolysis dynamics curves of Dufulin in the different organic solvents (methanol, *n*-hexane and acetone) under the UV lights (A: residue amount-time relation, B photolysis rate-time relation)

It can be seen from Fig 5.40 that photolysis rate of Dufulin in the three tested solutions bears the following relation: *n*-hexane> methanol> acetone. The constant (*k*) for photolysis of Dufulin in acetone was calculated by direct fitting with first order dynamic equation, the equation of photolytic kinetics was $C_t=10.034 \cdot e^{-0.0032t}$ ($R^2=0.9898$) and the photodegradation half-life was 216.56 min.

Solvent polarity indexes of *n*-hexane, methanol and acetone are 0, 6.6 and 5.4 respectively (Polarity index=Measure of ability of solvent to interact as a proton donor, proton acceptor, or dipole.). There is no obvious relationship

between photolysis of Dufulin and solvent polarities. Solvent effects may be caused by the absorption from the solvent at the specified wavelength. Effects of various solvents on the absorbance characteristics of Dufulin solution are listed in Table 5.39.

Table 5.39 Solvent Effects on the absorbance of Dufulin solution

Illumination time (min)	Wavelength (nm)	Absorbance (%)		
		n-hexane	methanol	acetone
0	210	0.559	0.298	0.241
	230	0.853	0.441	<0
	254	0.259	0.120	0.785
	270	0.404	0.218	0.008
	310	<0	<0	0.083
	360	<0	<0	<0
60	210	0.258	0.755	1.258
	230	0.252	0.786	0.495
	254	0.108	0.233	<0
	270	0.010	0.290	<0
	310	0.051	0.042	0.019
	360	0.034	0.019	<0

Photolysis in buffer solutions. Photolysis dynamic curves of Dufulin in buffer solutions are shown in Fig 5.41. The results in Fig 5.41 showed that photolysis of Dufulin was evidently influenced by pH value of buffer solutions. Photolysis of Dufulin proceeded slowly in buffer solution of pH=5 and rapidly in buffer solution of both pH=7 and pH=9. The photodegradation rate constant (k) of Dufulin in aqueous buffer solutions was calculated by direct fitting with first order dynamic equation. The results are shown in Table 5.40.
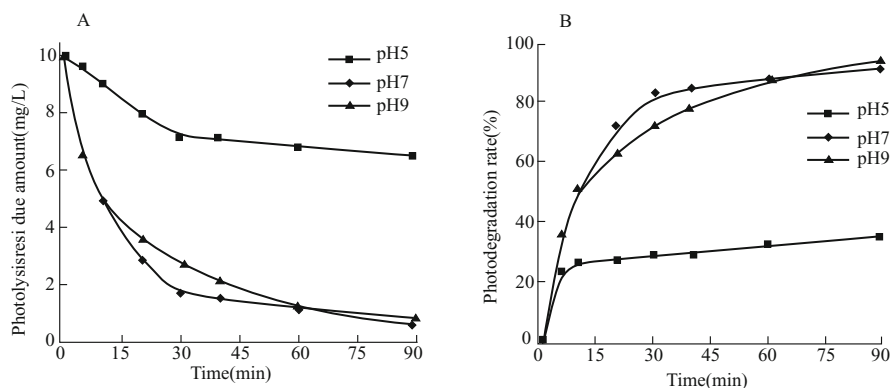
Fig 5.41 Photoiysis dynamics curves of Dufulin in the aqueous buffer solution with different pH values under the UV light (A: residue amount, B: photolysis rate)

Table 5.40   Photolysis kinetics of Dufulin in the aqueous buffer solution with different pH values under the UV light

Light source	pH	$C_t = C_0 \cdot e^{-kt}$	$K\,(\mathrm{d}^{-1})$	$T_{1/2}$ (min)	R^2
	5	$C_t = 10.672\,e^{-0.0665\,t}$	0.0665	10.42	0.9557
UV	7	$C_t = 13.066\,e^{-0.3595\,t}$	0.3595	1.93	0.9794
lamp	9	$C_t = 15.018\,e^{-0.3687\,t}$	0.3687	1.88	0.9721

The results showed that the photolysis dynamics of Dufulin in aqueous buffer solutions (pH=5, 7 and 9) could be described by direct fitting with the first order kinetics, and the correlation coefficients were 0.9557、0.9794 and 0.9721, respectively. The photodegradation rate constants (k) of Dufulin in buffer solutions (pH=5, 7, and 9) were 0.0665、0.3595 and 0.3687 respectively with ultraviolet lamp (30W, λ=253.7 nm), and the photolysis half-lives were 10.42 min, 1.93 min and 1.88 min respectively.

Photolysis in natural waters. Photolysis dynamic curves of Dufulin in natural solutions are shown in Fig 5.42. Although there is not much difference in the photolysis rate in pond water, river water and distilled water, it proceeded little faster in pond water.
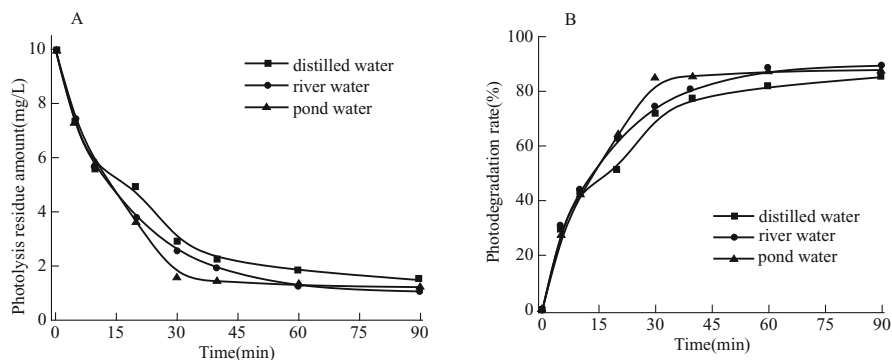
Fig 5.42   Photolysis dynamics curves of Dufulin in different natural waters (distilled water, river water and pond water) under the UV light (A indicates the residue amount and B the photodegradation rate)

It was presumed that the large number of other substances in river and pond water may result in a little faster photolysis compared to distilled water. The photolysis rate constant (k) of Dufulin in different water can be worked out with dynamic equation, the results are shown in Table 5.41.

The dynamic equation is quite appropriate to illustrate Dufulin photolysis dynamics, the correlation coefficients were 0.9864, 0.9925 and 0.9188 for distilled water, river water and pond water, respectively. At λ=253.7 nm, the photolysis half-lives were 2.04 min, 2.06 min and 2.49 min respectively.

Table 5.41   Photolysis kinetics of Dufulin in the different natural waters (distilled water, river water and pond water) under the UV light

Light source	Water	$C_t = C_0 \cdot e^{-kt}$	$K\,(d^{-1})$	$T_{1/2}$ (min)	R^2
UV lamp	Distilled water	$C_t = 12.905\,e^{-0.2787\,t}$	0.2787	2.49	0.9864
	River water	$C_t = 14.153\,e^{-0.3367\,t}$	0.3367	2.06	0.9925
	Pond water	$C_t = 13.384\,e^{-0.3393\,t}$	0.3393	2.04	0.9188

Effect of pH on photolysis of Dufulin in various aqueous solutions. Absorbance values at different wavelengths in various waters are listed in Table 5.42. The peak shapes, positions and the intensities of absorption are all affected to varying degree by various solution systems. Among them, the impact of buffer solution (pH=5) is the most obvious. In this solution, absorption band is shifted and the strongest absorption is reduced or disappeared (photomask). Buffer solution (pH=5) prevented light absorption by Dufulin and thus reduced the photolysis rate. In buffer solutions (pH=7 and pH=9), distilled water, river water and pond water show little difference and have practically no influence in terms of shifting of absorption band and photodegradation rate.

Table 5.42   Absorbance of Dufulin in the aqueous solutions

Illumination time (min)	Wavelength (nm)	Absorbance values					
		pH=5	pH=7	pH=9	Distilled water	River water	Pond water
0	210	< 0	0.035	0.648	0.118	0.076	0.074
	230	0.432	0.031	0.290	0.086	0.080	0.078
	254	0.627	< 0	0.073	0.027	0.030	0.029
	270	0.185	7.439	0.062	0.042	0.047	0.045
	310	< 0	< 0	0.003	< 0	0.005	0.004
	360	< 0	< 0	0	< 0	0.004	0.003
90	210	0.763	0.083	0.042	0.094	0.011	0.031
	230	0.127	0.061	0.053	0.066	0.058	0.035
	254	0.119	0.033	0.028	0.029	0.022	0.010
	270	0.549	0.032	0.029	0.027	0.022	0.013
	310	0.079	0.018	0.017	0.014	0.015	0.012
	360	0.029	0.005	0.005	0.002	0.009	0.001

5.1.9.4   Conclusions

Hydrochemical degradation of pesticides depends heavily on their persistence in the environment, and is an important index for studying the fate of pesticides and assessing residue level in aqueous systems. The results of hydrolysis showed that the degradation of Dufulin in water can be well fitted with the first order kinetic equation. The pH value and temperature displayed obvious impact on Dufulin hydrolysis rate. Half-lives of hydrolysis in the buffer solutions

of pH=5, 7 and 9 were 57.75 d, 157.5 d and 39.15 d, respectively. The rate of hydrolysis in alkaline conditions was faster than that in neutral and acidic conditions.

Temperature has strong influence on Dufulin hydrolysis, and the hydrolysis rate constant of Dufulin goes up with the temperature. With increase of temperature and alkalinity of the solution, Dufulin hydrolysis rate increased significantly. At 25℃, 50℃, 75℃, hydrolysis half-lives of Dufulin in buffer solution (pH=5) were 57.75 d, 17.33 d and 5.33 d, respectively. At pH=7 and 9, the corresponding values were 157.5 d, 24.9 d, 5.37 d; and 39.15 d, 12.22 d and 2.95 d, respectively. Dufulin hydrolysis activation energy and activation enthalpy have no significant correlation with temperature. Activation entropy of hydrolysis has a negative value which showed that not only the common nucleophilic substitution reaction between two molecules is prevalent, but also other factors may play important role in the process of Dufulin hydrolysis and metabolism. At the same temperature and under similar dark cultivation conditions, Dufulin hydrolysis rates were different in the pond water, river water and distilled water, the degradation rate showed an upward trend with elapse of time. Hydrolysis half-lives of Dufulin in pond water, river water and distilled water were 12.58 d, 14.68 d and 21.19 d respectively.

Based on the optimized HPLC methodology (HPLC-DAD), hydrolysis and photolysis studies of Dufulin in water were undertaken. The results showed that: (1) Hydrolysis rate of Dufulin in alkaline condition was faster than in neutral or acidic conditions and hydrolysis rate was directly proportional to the temperature. (2) Under the UV light (253.7 nm) irradiation, Dufulin degradation was faster in both natural water and organic solvents. The photolysis rate in organic solvents followed the order *n*-hexane> methanol> acetone, while in buffer solution a decreasing order with pH=9> pH=7> pH=5 was observed. Again, Dufulin hydrolysis was quicker in the pond water than in river water and redistilled water. Under the UV light (λ=253.7 nm), the half-lives of photolysis in buffer solutions of pH=5, 7 and 9 were 10.42 min, 1.93 min and 1.88 min, respectively. Photolysis half-lives in pond water, river water, and distilled water were 2.04 min, 2.06 min and 2.49 min respectively. It can be concluded that Dufulin is easily degradable by hydrolysis and susceptible to photolysis under natural environment.

As mentioned before, degradation of pesticides is closely related to their persistence in the environment. Consequently, it is an important index for the assessment of pesticide residue and degree of persistence in aqueous system. The longer half-life of the pesticide can cause extensive damage to the environment. In order to achieve effective prevention and treatment on plant diseases, persistency of pesticides should be taken into overall consideration. The study of environmental behavior (hydrolysis and photolysis) of Dufulin not only indicates residual characteristics and transformation of Dufulin in the water, but also provides the scientific basis for its safety evaluation under atmospheric conditions.

5.1.10　Systemic Behaviors

5.1.10.1　Introduction

Chirality is an important concept in synthetic agrochemicals. This is because enantioselectivity plays an important role not only in biological activities but also in the toxicity of targeted organism. Its significance has long been recognized by the differential behaviour in biological activity display by individual enantiopure isomers of natural and synthetic compounds[1−3]. A number of studies have shown that the biological activities such as toxicity[4−5], endocrine disruption[6], and fate in the environment[7−10] of chiral pesticides are greatly dependent on the nature of enantiomeric isomer. Therefore, we considered it worthwhile to study the enantiomeric selectivity of Dufulin for the development of safer and more effective new chiral antiviral agents. In the current work, we studied the systemic behaviors and enantiomeric selectivities of the two enantiomers of Dufulin in *Nicotiana tabacum*.

5.1.10.2　Materials and methods

Agilent 1100 and 1200 series apparatus equipped with a quaternary pump (Model G1311A); an autosampler (Model G1313A); a diode array and multiple wavelength detectors (DAD) (Model G1315B); micro vacuum degasser (Model G1379A); Agilent Eclipse XDB-C18 column (4.6 mm×150 mm, i.d.5 μm); Chiralpak IA column (250 mm×4.6 mm, i.d.5 μm) (Daicel Co.Japan); HP Chemstation software (Agilent Co., America); Ultrasonic tank (Beijing East Sunland Sci.& Techol.Ltd.China); Nitrogen blowing apparatus (ANPEL Sci.Instrument Co.China); Subminiature quantificational atomizer (Chendu Sci.Instrument Ltd.China) and commonly employed analytical instruments made in China.

Enantiomeric separation of Dufulin racemate to obtain pure individual isomers was carried out at our laboratory.[Racemate: white crystal; purity > 99.9%; mp, 147−148℃; ER=1:1. (*R*)-enantiomer: white crystal; purity > 99.5%; mp, 56.0−58.0℃; $[\alpha]_D^{25}$ =+84.63 (*c*0.01, methanol). *S*-enantiomer: white crystal; purity > 99.5%; mp 50.0−52.0℃; $[\alpha]_D^{25}$ =−83.29 (*c* 0.01, methanol)]. The chemical reagents and solvents *e.g.* petroleum ether (Zhi Yuan Chemical Reagents Ltd., China); acetone (Zunyi College Chemistry Reagent Factory, China); methanol (Zhen Xing Chemical Production First Factory, China); sodium bicarbonate (Fu Chen Chemistry Reagent Factory, China); sodium chloride and sodium sultranslocation (Jin Shan Chemical Reagents Ltd., China) were of A.R.grade and made in China.

Greenhouse Trials. For greenhouse trials, a trial scheme (Scheme 5.3) was established. According to the trial scheme, three groups of flowerpots (0.3 ft diameter×0.5 ft high) were placed on three shelves in greenhouse with adequate

space between each flowerpot to avoid cross pollution. All the flowerpots were filled with sterilized soil to which *Nicotiana tabacums* (K326) seeds were transplanted. Trickle hosing was laid on top of the soil for irrigation. The greenhouse temperature was maintained at 20℃ for most of the period. Besides natural light, artificial light was supplemented to provide sufficient illumination time for plant growth. This trial was conducted from April to November in 2007. When 8 to 10 leaves appeared, *Nicotiana* was sprayed with antiviral agents (Dufulin racemate, (*R*) isomer, or (*S*) isomer) using subminiature quantificational atomizer. During treatment, the flowerpot soil was covered by plastic film in order to reduce or eliminate contamination. In the first group, the leaves of *Nicotiana tabacums* were sprayed with Dufulin racemates. For the second and the third group, the leaves were treated with (*R*)-and (*S*)-enantiomer respectively. In addition, blank control was also set in the trial. Following the spray, treated leaves and untreated leaves, stems and roots were collected at various intervals (2 h, 1 d, 3 d, 5 d, 7 d, 14 d, 21 d, 30 d) and three plants were collected for every interval period in each group. All these samples were rinsed thoroughly with acetone to remove conglutinated Dufulin racemates or enantiomers on the surface of the leaves, stems and roots. Special attention was paid to the roots to ensure that all visible soil was rinsed off.

Enantiomertic selectivity on systemic behaviors of Dufulin in *Nicotiana tabacum*

↓

The *Nicotiana tabacum* was cultivated using sterilized soil

↓

| Racemate of Dufulin treat on the plant | *S*-enantiomer of Dufulin treat on the plant | *R*-enantiomer of Dufulin treat on the plant |

↓

The samples divided into leaves,stems and roots collected at different intervals (2h,1d,3d,5d,7d,14d,21d) after completing the above procedures

↓

All samples were rinsed thoroughly with acetone to ensure ultimate veracity of analyzed data

↓

Condtion tests (additive recovery rates;exactitude; veracity;chromatographic condition)

↓

Detection and analyses of Dufulin samples by HPLC

↓

The statistical analyses of figures and deduced conclusion

Scheme 5.3   Flow diagram of green house trial, sampling and analysis procedure for the investigation on the enantiomeric selectivity of Dufulin in *Nicotiana tabacum*

Sample Preparation. Around four grams of grinded samples were added into a 100 mL Erlenmeyer flask, and were extracted by 30.0 mL acetone for 20 min under ultrasonic agitation. The mixture was then filtered. The filtrate was mixed with 40.0 mL $NaHCO_3$-Na_2CO_3 buffer solution (pH=9.0) and 10.0 mL brine and then subjected to extraction by 30.0 mL petroleum-ether: acetone (9:1, *v/v*) for

three times. The organic parts were combined and dried with anhydrous sodium sulfate (Na_2SO_4), then filtered and evaporated on a rotary evaporator at 40℃. The residue was further dried by nitrogen flush. The dry products were dissolved in 5.0 mL methanol and filtered by a 0.4 μm filter membrane. This extraction procedure was adopted for all samples. The final samples were determined by HPLC to trace the concentration of the antiviral agents.

HPLC method. Agilent technologies model 1200 liquid chromatograph fitted with an ultraviolet (UV) 6000LP was used. Chromatographic separations were achieved on a Chiralpak IA column (250 mm×4.6 mm, i.d.5 μm) using mobile phase *n*-hexane/EtOH (90/10, *v/v*). Column temperature was maintained at room temperature. The injection volume was 10 μL, and the flow rate was 1.0 mL/min. The analysis was monitored at 230 nm. The retention times of (*R*)-and (*S*)-enantiomer were about 5.9 min and 6.8 min, respectively.

Qualitative Analysis. Qualitative analysis was carried out to identify the enantiomeric ratio (ER) of two enantioisomers in different plant tissues due to systemic behaviors. The result of qualitative analysis was followed by HPLC analysis on Chiralpak IA column and the representative chromatograms are presented in Fig 5.43.

Quantitative Analysis. Quantitative analysis was applied to trace the concentrations of Dufulin racemates and the enantiomers in different plant tissues after treating *Nicotiana tabacum*. An Agilent 1100 liquid chromatograph with an ultraviolet (UV) 6000LP was used. The chromatographic separation was achieved on an Agilent Eclipse XDB-C18 column (4.6 mm×150 mm, i.d.5 μm). Column temperature was maintained at 25℃ using a column heater. The HPLC solvent was a mixture of methanol/water (80:20, *v/v*). The injection volume was 10 μL, the flow rate was 1.0 mL/min and run time was 12.0 min. The analysis was performed at 270 nm, The retention time was about 5.2 min. The chromatograms are presented in Fig 5.44.
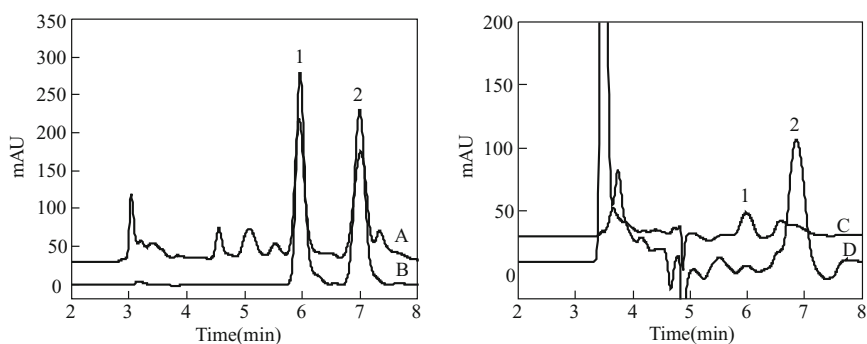
Fig 5.43   Chromatograms of sample recorded on HPLC-DAD with Chiralpak IA column in qualitative analysis: sample of racemate (A); racemic standard (B); sample of (*R*)-enantiomer (C); sample of (*S*)-enantiomer (D)
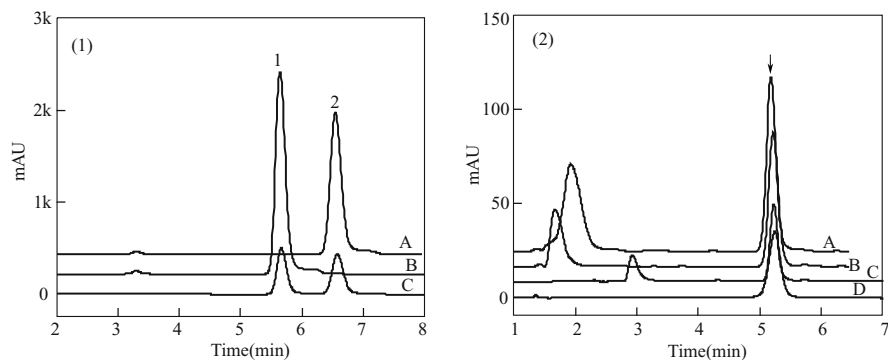
Fig 5.44 Chromatograms of analytical qualification on HPLC-DAD with different chromatographic columns: Qualitative analysis with Chiralpak IA column (1): (S)-enantiomer (A); (R)-enantiomer (B); racemate (C). Quantitative analysis with C18 column (2): (S)-enantiomer (A); (R)-enantiomer (B); racemate (C); standard (D)

5.1.10.3   Results and disccussion

Method Validation. Fortified recovery and precision of the analytical method were investigated. The fortified recoveries of Dufulin racemates and enantiomers were determined by the analysis of *Nicotiana tabacum* spiked at two levels (2.5 and 25.0 µg/g), as listed in Table 5.43. The recovery rates were calculated by standard calibration with calibration solutions (1.0, 10.0, 20.0, 50.0, 100.0, and 200.0 µg/mL). For Dufulin racemates, the linearity relationship of standard calibration is presented by means of the equation $A=23.76 \times C+3.95$ (A represents integral peak area and C represents concentration) and the relativity was 0.99999. For (R)-enantiomer, the corresponding equation is $A=22.60 \times C+10.76$ and the relativity was 0.99995. For (S)-enantiomer the linearity relationship is given by $A=22.42 \times C+1.58$ and the relativity was 0.99991. Average recoveries ($n=3$) were more than 80% for all levels ($P < 0.01$) with associated relative standard deviations (RSD) of $<8.5\%$. In general, the fortified recovery and precision were in accordance with the guidelines for analysis, suggesting the method was suitable for the concentration tracing of Dufulin racemate and the enantiomers.

Table 5.43   Overall Performance of the Analytical Method for Plant Tissues[*]

Plant Tissues	Spike level (µg/g)	Racemate		(R)-enantiomer		(S)-enantiomer	
		Recovery (%)	RSD (%)	Recovery (%)	RSD (%)	Recovery (%)	RSD (%)
Leaves	2.5	86.2±1.3	1.5	88.7±5.9	5.6	91.6±5.6	7.4
	25	97.2±3.0	2.5	91.3±1.2	1.6	88.6±2.4	2.6
Stems	2.5	93.6±2.4	3.4	85.0±3.0	3.0	87.1±7.7	7.0
	25	96.4±2.2	3.1	84.5±5.1	7.1	86.3±3.3	2.9
Roots	2.5	93.0±3.1	2.3	91.8±3.2	4.6	85.6±7.2	6.5
	25	96.4±4.4	4.6	95.1±6.0	8.5	89.9±1.3	1.8

*All results are expressed as mean±SD; $n=3$ for all groups ($P<0.01$).

Measurements and Analyses. The greenhouse trials were designed to investigate the enantiomeric selectivity in systemic behaviors of Dufulin racemate and the enantiomers. To avoid other contaminations, experiments were carried out with uncontaminated tools. The concentrations of Dufulin racemate and enantiomers under greenhouse conditions were traced by HPLC-DAD with C18 column to investigate systemic behaviors including uptake, distribution and translocation. The data for all collected samples are presented in Table 5.44.

Table 5.44 HPLC Analysis of Enantiomers of Dufulin in Plant Tissues[a]

Treated agent	Interval time	Treated leaves (μg/g)	Untreated leaves[b] (μg/g)	Stems (μg/g)	Roots (μg/g)	Whole plant[c] (μg/g)
Racemate	2 h	35.5±1.01	5.39±0.45	66.8±1.30	2.68±0.05	110.4±8.0
	1 d	75.5±1.15	11.2±0.40	16.0±0.20	4.09±0.21	106.9±5.4
	3 d	107.5±0.60	82.8±0.50	24.0±0.03	4.74±0.09	219.0±4.6
	5 d	128.8±2.10	53.2±0.13	36.6±0.41	1.64±0.05	220.2±6.7
	7 d	188.7±0.50	11.77±0.21	35.1±0.10	1.82±0.03	237.4±4.8
	14 d	69.6±0.21	8.85±0.05	17.2±0.20	1.96±0.05	97.6±9.7
	21 d	42.3±0.11	4.83±0.26	13.8±0.09	1.99±0.07	62.9±7.5
	30 d	7.09±0.81	2.57±0.50	7.53±1.53	<0.1	17.2±2.18
(R)-enanti-omer	2 h	59.9±4.12[b]	12.3±0.80	36.0±1.53	6.01±0.05	114.2±6.5
	1 d	64.0±0.41	1.30±0.30	2.34±0.14	1.19±0.02	68.83±0.9
	3 d	35.0±1.66	2.32±0.21	1.36±0.07	<0.1	38.68±1.9
	5 d	52.3±0.38	3.68±0.03	3.24±0.11	<0.1	59.22±1.5
	7 d	65.3±0.56	4.13±0.35	1.94±0.06	1.01±0.27	72.38±1.2
	14 d	51.3±1.58	10.3±0.15	5.39±0.07	3.73±0.16	70.72±2.0
	21 d	59.7±1.86	12.5±0.19	23.7±0.12	3.95±0.38	99.85±2.6
	30 d	9.10±0.24	3.04±0.05	11.5±0.48	1.81±0.31	25.45±1.1
(S)-enanti-omer	2 h	88.6±2.36	5.05±0.10	10.4±0.51	2.58±0.09	106.6±3.1
	1 d	43.5±4.59	3.44±0.06	10.5±0.23	2.20±0.33	59.64±5.2
	3 d	69.1±3.04	5.66±0.15	2.24±0.23	1.57±0.18	78.57±3.6
	5 d	77.7±1.88	3.06±0.14	7.23±0.10	<0.1	87.99±2.1
	7 d	107.0±3.16	7.64±0.21	9.08±0.33	2.90±0.19	126.6±3.9
	14 d	59.5±0.54	8.61±0.08	18.3±0.07	4.00±0.19	90.40±1.4
	21 d	57.3±0.33	4.46±0.31	51.9±0.19	5.80±0.08	119.5±3.9
	30 d	9.07±0.22	5.49±0.15	29.6±0.19	4.87±0.21	49.03±2.8

[a] The analytical methods are based on the results of Table 5.45, and all results are expressed as mean ±SD; n=3 for all groups; (P<0.01); [b] the untreated leaf tissues are fresh leaves without Dufulin treatment.[c] whole plants are integrated plant tissues including leaves, stems and roots.

It could be seen from Table 5.44 that the concentrations of Dufulin racemate and enantiomers in different plant tissues from 2 h to 30 d followed the order:

treated leaves > untreated leaves > stems > roots. The maximum uptake of Dufulin racemate and enantiomers was found in the leaves and stems by leaves-to-tissues route 7 days after spraying. The absorbable processes of Dufulin racemate and enantiomers are presented in Fig 5.45. Dufulin racemate and enantiomers were found to move into the plant tissues from its original treated leaves and the concentrations varied with different tissues at various intervals. For the systemic behaviors of racemate in *Nicotiana tabacum*, the ER was found to be 1:1 by qualitative analysis, and distributed in different plant tissues via systemic behaviors. The measured concentrations at 2 h were found to follow the order stems > leaves > roots and on the 7th day, this order was changed to leaves > stems > roots. Therefore, the uptake of Dufulin by the plant was primarily concentrated in the first week, and this process was affected by the plant growth. The concentration of Dufulin decreased by 26.5% after three weeks and this decline becomes more prominent after 21 d, mostly due to the plant degradation. The concentration of the racemate in different tissues indicated the significant systemic behavior of Dufulin in *Nicotiana tabacum*. According to plant growth characteristics and disease index, it is necessary to spray Dufulin for the second time after 21d for the effective protection of *Nicotiana tabacum*.
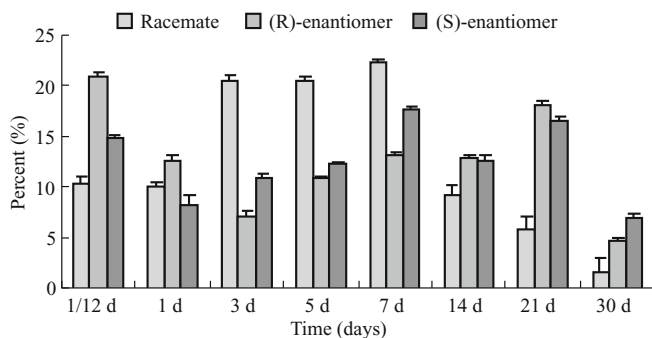
Fig 5.45   Absorbable processes of Dufulin and (*R*) or (*S*)-enantiomer in tobacco, percent (%) =whole plant at different period/treated agents

After spraying the plant with (*R*) or (*S*)-enantiomers of Dufulin, no ER change was found by qualitative analysis in tissues. The concentrations of (*R*) or (*S*)-enantiomer in different tissues are shown in Table 5.45. Similarly, the concentration changes can be attributed to the fact that their uptake and degradation are affected during the plant growth. Similar to that of Dufulin racemate, the growth of *Nicotiana tabacum* should help to increase uptake of the enantiomers, then transfer to the untreated leaves and roots via the stems. The tendency is not obvious for uptake distribution and translocation during 3 d to 7 d in different tissues. However, the effect of (*S*)-enantiomer from overall uptake and translocation process is more prominent than the (*R*)-enantiomer, probably due to the stereo structural feature of the enantiomer. In brief, we can conclude that the (*S*)-enantiomer acts prior to the (*R*)-enantiomer in terms of uptake, distribution and

translocation. Thus, we should focus on the development of (*S*)-enantiomer to further improve the antiviral activity. These experiments demonstrate that Dufulin racemate and enantiomers are systemic antiviral agents that function from leaves to tissues. After the uptake of Dufulin by the poisoned tobacco leaves, it is translocated to other untreated leaves and roots via stems. Moreover, different dynamic behaviors were found between Dufulin racemate and the enantiomers. The enantiomeric selectivity of systemic behaviors in *Nicotiana tabacum* was related with stereo structure of the antiviral agents.

5.1.10.4   Conclusions

Dufulin racemate and (*R*) or (*S*)-enantiomers are absorbed into plant tissues by systemic behavior, and then translocated into the whole plant tissues through stems. Dufulin racemate was kept in the racemic form (enantiomeric ratio=1:1) in plant tissues after treatment of the leaves. Moreover, after spraying the (*R*) or (*S*)-enantiomer, the stereo structure of the enantiomer was retained in plant tissues as detected by chiral HPLC analysis. Compared with the enantiomeric selectivity for pharmacokinetic process, the (*R*) or (*S*)-enantiomer is more quickly absorbed than the racemate, and rapidly transferred to other tissues. In brief, the systemic behavior of (*R*) or (*S*)-enantiomer is better than the racemate, and (*S*)-enantiomer is superior to (*R*)-enantiomer for systemic behavior.

This result can provide helpful information for the design and development of new chiral antiviral agents. However, the metabolic process and the nature of the products are still not clear. Also, in addition to greenhouse experiments, more investigations under field conditions are necessary.

References

1. Prelog V. Chirality in chemistry. *Science*. 1976, 193 (4247), 17-24.
2. Garay A S. Molecular chirality of life and intrinsic chirality of matter. *Nature*. 1978, 271, 186.
3. Inoue Y. Synthetic chemistry: light on chirality. *Nature*. 2005, 436, 1099-1100.
4. Liu W P, Gan J Y, Schlenk D, *et al*. Enantioselectivity in environmental safety of current chiral insecticides. *Proc. Natl. Acad. Sci. U.S.A.* 2005, 102, 701-706.
5. Liu W P, Gan J Y, Qin S J. Separation and aquatic toxicity of enantiomers of synthetic pyrethroid insecticides. *Chirality.* 2005, 17, 127-133.
6. Hayes T, Haston K, Tsui M, *et al*. Atrazine-induced hermaphroditism at 0.1 ppb in American leopard frogs (Rana pipiens), laboratory and field evidence. *Environ. Health Perspect.* 2003, 111, 568-575.
7. Lewis D L, Garrison A W, Wommack K E, *et al*. Influence of environmental changes on degradation of chiral pollutants in soils. *Nature*. 1999, 401, 898-901.
8. Kohler H P E, Angst W, Giger W, *et al*. Environmental fate of chiral pollutants the necessity of considering stereochemistry. *Chimia*. 1997, 51, 947-951.
9. Buser H R, Muller M D, Poiger T, *et al*. Environmental behavior of the chiral acetamide pesticide metalaxyl: Enantioselective degradation and chiral stability in soil. *Environ. Sci. Technol.* 2002, 36, 221-226.
10. Garrison A W. Probing the enantioselectivity of chiral pesticides. *Environ. Sci. Technol.* 2006, 40, 16-23.

5.2   GU188, 2-Cyanoacrylate Derivative,Candidate Antiviral Agent

2-Cyanoacrylate has been traditionally considered as a kind of herbicide that can target photosynthesis PSII system. The current research showed that this class of compounds also possessed anti-TMV activity, and one of these, GU188 (ethyl 3-nitroaniline-3-methylthio-2-cyanoacrylate), a typical cyanoacrylate and a new anti-plant virus agent, was discovered by Guizhou University in 2006. It was proved highly effective against TMV in both lab bioassay and the field trials. The curative effect of GU188 at the dosage of 100-300 g (a.i.) /ha on TMV infected disease is better than or close to the famous commercial anti-virus agent Ningnanmycin at the dosage of 90 g (a.i.) /ha. GU188 was proved to have lower toxicicty against mammals by the toxicological test in Chinese Center for Disease Control and Prevention, Institute for Occupational Health and Poison Control. In addition,ames test results conducted in Chinese Center for Inspection and Control of Pesticides Quality were found negative. Naturally, GU188, which has been assigned the intellectual property by the State Intellectual Property Office of China (ZL05100030417, Fig.5.4), and has good anti-TMV activity, is worth investigating for its potential to be employed as a candidate antiviral agent. The studies should involve the synthetic route optimization, indoor bioassays, outdoor bioassays, toxicity evaluation, and action mechanism. It was demonstrated that GU 188 is a potential anti-plant viral agent with high activity.

5.2.1   Synthesis

5.2.1.1   Introduction

As described in the second chapter, GU188 was found to be highly active against TMV. In order to synthesize more GU188 sample for field trial and finally for production at industrial scale, its synthetic route as well as the reaction conditions need to be optimized in lab scale. The brief synthetic route of GU188 is illustrated in Scheme 5.4. Different synthetic methods and the reaction parameters were also standardized. By using the optimized conditions, GU188 can be synthesized in 74% yield with 95% purity.

5.2.1.2   Materials and methods

Melting points were determined on a Buchi melting point apparatus and were uncorrected. The materials used for GU188 synthesis include ethyl 2-cyanoacetate, dimethyl sulfate, sodium ethoxide, 2-nitroaniline, sodium hydride, and some other common chemical reagents and solvents that are commercially available in the market.
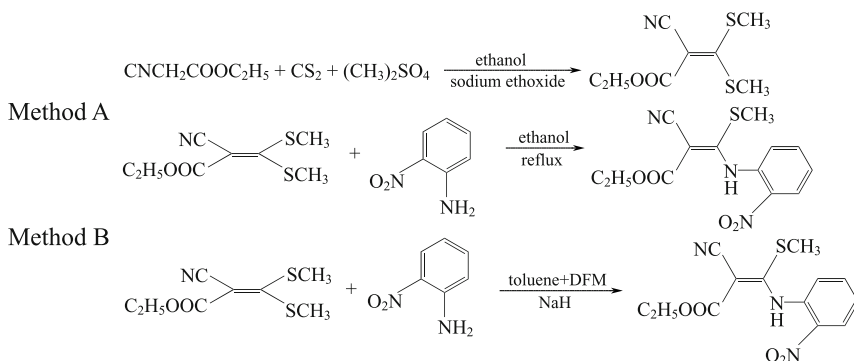
Scheme 5.4 Synthetic route to GU188

Preparation of the key intermediate Ethyl 2-cyano-3,3-dimethylthioacrylate. To a mixture of anhydrous ethanol (400 mL), ethyl cyanoacetate (34.0 g, 0.301 mol) and carbon disulfide (23.0 g, 0.303 mol) at 20℃,was added dropwise a solution of sodium ethoxide (38.48 g, 0.610 mol) in anhydrous ethanol (360 mL) over a period of 1 h. After adding the solution, the mixture was stirred for 8 h at room temperature. Then, dimethyl sulfate was added dropwise over 0.5 h and the reaction mixture was heated under reflux for 4 h. The solvent was removed under reduced pressure and then water (40 mL) was added and filtered. The residue was dried and recrystallized twice from ethanol to give a white solid (56.7 g), yield 86.8%; mp 58-59.5℃.

Preparation of the target compound GU188. To an oven-dried three-necked 500mL round-bottom flask fitted with a magnetic stirring bar and attached with a dry N_2 inlet, were added the intermediate 2-cyano-3, 3-dimethylthioacrylate (13.4 g, 0.062 mol), 60% sodium hydride (0.0868 g, 0.00217mol), DMF (110 mL) and toluene (110 mL). Then to the resulted mixture was added 2-nitroaniline (8.6 g, 0.062 mol) dissolved in 110 mL of DMF/toluene solvent mixture. The temperature was controlled below 10℃ and the mixture was then stirred at 20-25℃ for 20 h. The reaction progress was monitored by TLC. The mixture was poured into ice water (1000 mL) and separated. The aqueous phase was acidified with 10% HCl to pH 6-7, and filtered. The residue was dried and recrystallized from anhydrous ethanol to give a white solid, yield 86.1%, mp 171-174℃.

5.2.1.3　Results and discussion

As can be seen from Scheme 5.4, GU188 can be synthesized in two steps. The first step generates the important intermediate ethyl 2-cyano 3,3-dimethylthio-acrylate in 86% yield. For the second step, there are two possible methods and each method was investigated thoroughly. Method A is a reasonably good route that involves nontoxic solvents without the use of catalyst, but it has many drawbacks such as lower yield and longer reaction time. In order to overcome these problems, a series of reaction conditions were investigated and the results are listed in Table 5.45.

Table 5.45   The effect of different catalysts and catalyst amount on the yield

Reaction conditions	Reactant ratio (mol)	Reaction temp.	Reaction time	Yield (%)
Catalyst free	1:1	76-78℃	4h	74.1
Ionic liquid	1:1	r.t	10h	78.8
NaH	1:1	r.t	20h	81.3
Microwave irridation with NaH as cat.	1:1	78-80℃	25min	86.7
Ultrasonic irridation with NaH as cat.	1:1	r.t	1h	88.6

As shown in Table 5.45, the synthesis of GU188 was carried out in 88.6% yield at room temperature in the presence of NaH as catalyst by ultrasonic irradiation for 1 h. The reaction under microwave irradiation with NaH as catalyst also gives 86.7% yield in 20 min. For the reaction without any catalyst, GU188 was obtained in 74.1% yield in 4 h. Reaction carried out in ionic liquid afforded 78.8% yield in 10 h at room temperature, and with NaH as the catalyst, 81.3% yield was obtained in 20h. Therefore, under optimized conditions in lab scale, NaH was used as the catalyst in DMF/toluene mixture.

Besides NaH, several other catalysts were also screened. The catalytic efficacy of NaOH, NaOEt, and NaH was compared by employing fixed reactant ratio (1:1) at 20-25℃. The catalyst amount in all the experiments was 5mol% and the results are listed in Table 5.46. As shown in Table 5.46, NaH was proved to be a superior catalyst compared to C_2H_5ONa and NaOH and afforded a yield up to 84.1%.

Table 5.46   The effect of different catalysts on the yield

Experiment No.	Reactant ratio	Catalyst	Catalyst amount (mol)	Yield (%)
1	1:1	NaH	5%	84.1
2	1:1	C_2H_5ONa	5%	75.5
3	1:1	NaOH	5%	76.9

After selecting NaH as the catalyst, the effect of the amount of NaH was also investigated. The amount of NaH was varied from 0.5%, 2%, 3.5%, 5%, to 7.5%, and the results are listed in Table 5.47. As can be seen from Table 5.47, when the catalyst amount was 3.5%, the yield was 86.1%, however, the yield did not improve with further increase of catalyst amount.

Table 5.47   Effect of different catalyst amount on the yield of GU188

Entry	Reactant ratio	Catalyst amount (mol)	Yield (%)
1	1:1	0.5%	63.4
2	1:1	2%	77.1
3	1:1	3.5%	86.1
4	1:1	5%	84.5
5	1:1	7.5%	84.0

Next we also examined the effect of the reaction temperature on the yield. With the fixed reactant ratio (1:1), reaction time (20 h), and the amount of NaH (3.5%), the reaction temperature was varied from 0-5℃, 10-15℃, 20-25 ℃, 40-45℃, 60-100℃ to 118-120℃. It could be seen from Table 5.48 that when the reaction was carried out at 0-5℃ or 10-25℃, the yield was lower than that at 20-25℃. Interestingly, the yield was lowered when the reaction temperature was increased to 40-45℃, 60-100℃ and 118-120℃ (Table 5.48). It is likely that ethyl 3,3-dimethylthio-2-cyanoacrylate may get partially decomposed at higher temperature. Hence, the optimum temperature selected was 20-25℃.

Table 5.48　Effect of different catalyst amount on the yield of GU188

Entry	Reactant ratio	NaH amount (mol)	Reaction temp (℃)	yield (%)
1	1:1	3.5%	0-5	50.9
2	1:1	3.5%	10-15	75.3
3	1:1	3.5%	20-25	86.1
4	1:1	3.5%	40-45	85.3
5	1:1	3.5%	60-100	81.8
6	1:1	3.5%	118-120	75.2

The effect of reaction time on the yield was also investigated. With the fixed reactant ratio (1:1), and the amount of NaH (3.5%), the reaction time was varied from 5 h to 30 h. The results of different reaction time are listed in Table 5.49. It can be seen from Table 5.49 that when the reaction time was 5 or 10h, the yield was no more than 50%. The reaction yield attained its maximum value at 20 h and did not improve further when the reaction time was increased from 20 h (86.1%) to 30 h (85.6%). Thus the optimum reaction time chosen was 20 h.

Table 5.49　Effect of different reaction time on the yield of GU188

Entry	Reactant ratio	NaH amount (mol)	Reaction temp (℃)	Reaction time	Yield (%)
1	1:1	3.5%	20-25	5h	30.3
2	1:1	3.5%	20-25	10h	47.5
3	1:1	3.5%	20-25	15h	80.0
4	1:1	3.5%	20-25	20h	86.1
5	1:1	3.5%	20-25	25h	87.0
6	1:1	3.5%	20-25	30h	85.6

In order to check the reproducibility of the optimum reaction conditions, the optimal conditions were repeated for several times and the results are shown in Table 5.50. The optimum reaction conditions were established with a reactant ratio n (2-cyano 3, 3-dimethyl-thioacrylate) :n (2-aminoaniline) :NaH=1:1:0.035 (mol ratio) at 20-25℃ for 20 h.

Table 5.50   The reproducibility of the optimum reaction conditions

Entry	Yield (%)	Purity (%)	Entry	Yield (%)	Purity (%)
E1	86.11	95.78	E5	86.31	96.10
E2	86.00	95.45	E6	86.25	95.87
E3	86.43	95.60	E7	86.40	95.64
E4	86.26	95.35	E8	86.34	95.68

It can be seen from Table 5.50 that the reaction conditions are reliable and the yields are reproducible; GU188 could be obtained under the optimized conditions in >95.0% yield, and purity >86.0%. Based on these results, the technical parameters of the product standard are listed in Table 5.51.

Table 5.51   The main technical parameters of GU188 product

Index	Content (%)
GU188, % (m/m)	⩾95
Moisture, % (m/m)	⩽0.5
Acidity, % (m/m)	⩽0.5
Insoluble substance in methanol (m/m)	⩽1.0

***The development of* 30% *WP formulation*.** The method for preparation of 30% GU188 WP formulation in the lab is similar to the procedure described in Chapter 5.1.2.2. After the optimization of the synthetic techniques of GU188, its formulation preparation was carried out, and the optimum formulation of 30% GU188 WP is: LS (7%)+sodium lignosulphonate (3%)+GU188 (30%)+light calcium carbonate (60%).

5.2.1.4   Conclusions

The synthetic reaction conditions for GU188 were optimized. The optimum conditions are obtained with a reactant ratio n (2-cyano-3, 3-dimethylthioacry-late) :n (2-amino-aniline):n (NaH)=1:1:0.035 (mol ratio), at 20-25℃ for 20 h. Under the optimum conditions, the yield of GU188 could exceed 86% with 95% purity. The technology and the product quality are reliable and ideal for industrialization.

5.2.2   Analytical Method

5.2.2.1   Introduction

GU188 (ethyl 3-nitroaniline-3-methylthio-2-cyanoacrylate), a cyanoacrylate derivative and a candidate for new anti-plant virus agent, was discovered by Guizhou University in 2006. It was proved to be highly effective against TMV in both lab bioassay and under the field trials. In order to put it into practical use for large scale production, analytical methods and standards for the products need to be developed. Since GU188 and cyanoacrylate are somewhat polar and thermally unstable, analysis of the pesticides by the more traditional gas chromatographic

techniques appears a bit difficult. High-performance liquid chromatography (HPLC), capable to handle thermally unstable analytes with greater sensitivity and selectivity, has the potential for automation in pesticide analysis. Analytical method for GU188 to obtain optimal conditions for column dimensions, mobile phase compositions was investigated and the methodologies for the determination of GU188 by HPLC are introduced in this chapter. C18 column, mobile phase consisting of methanol+water=60+40 (v/v) and UV detector were used for the analysis. The results showed that the standard deviation of GU188 was 0.5, the average recovery was 101.5%, and the linear correlation was 0.9996.

5.2.2.2   Materials and methods

The materials used for GU188 analysis include GU188, common chemical reagents and solvents that are commercially available in the market.

Conditions:Agilent 1100 HPLC Eclipse XDB-C18 column-4.6×150 mm, temperature-25 ℃; flow rate-1.0 mL/min; λ-310 nm;injection volume-10 μL; mobile phase, methanol/water (60:40, v/v); retention time～7.3 min (Fig 5.46).
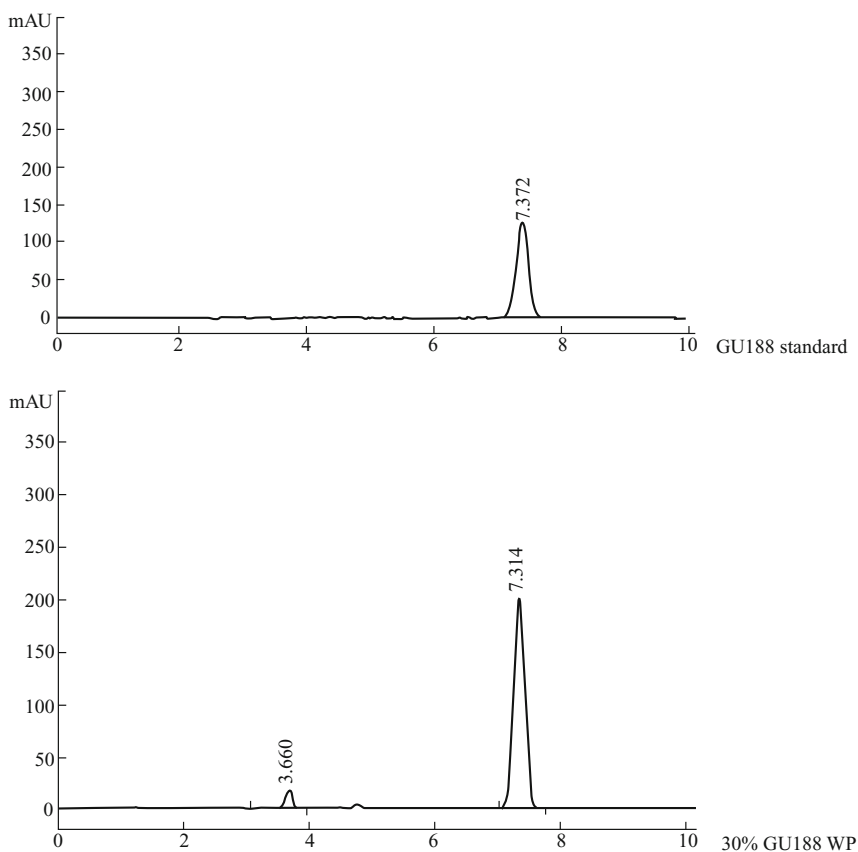
Fig 5.46   The chromatograms of GU188 standard and GU188 (30%, WP)

5.2.2.3   Results and discussion

Qualitative and quantitative analysis of GU188 and its formulation were tested by HPLC (Fig 5.46). The standard curve is shown in Fig 5.47.
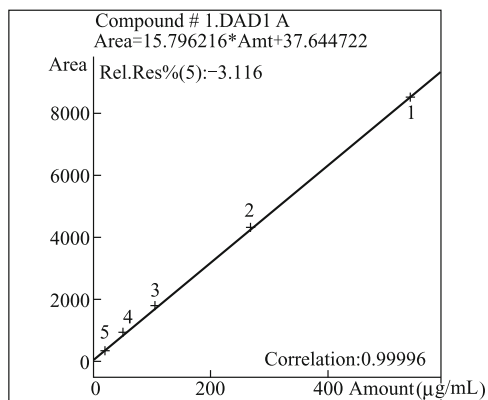
Fig 5.47   The standard curve of GU188 standard Standard equation: $Y=15.796X+37.645$, $r=0.99996$

The precision and accuracy tests were both conducted (Table 5.52 and Table 5.53). Relative standard deviation of peak area of GU188 ($n=5$) was 0.50% with satisfactory repeatability and reproducibility. The absolute recovery of GU188 was calculated by comparing peak area of the spiked analyte samples with the unextracted analyte of stock solution that was injected directly into an HPLC system. The average recovery of 101.5% indicates that the accuracy of method was satisfactory.

Table 5.52   The result of precision ($n=5$)

Entry	1	2	3	4	5	Average	RSD (%)
Peak area	1810.4	1812.2	1798.5	1819.7	1821.0	1812.4	0.50

Table 5.53   Accuracy data for GU188 in standard solution ($n=5$)

Entry	Actual amount (mg)	Experimental amount (mg)	Recovery (%)	Average recovery (%)
1	1.2500	1.2453	99.62	
2	1.2500	1.2794	102.4	
3	1.2500	1.2892	103.1	101.5
4	1.2500	1.2331	98.6	
5	1.2500	1.2998	104.0	

5.2.2.4   Conclusions

The analytical method for GU188 was established using HPLC method, the precision and accuracy of the method were satisfactory. The RSD of the method is

0.5%, and the average recovery was 101.5%. The method is stable and has good reproducibility.

5.2.3   Bioassays and Field Trials

5.2.3.1   Introduction

GU188 was found to have good anti-TMV bioactivity in the Preliminary bioassay. Then it was evaluated further both in lab bioassay and under field trial. In order to evaluate the field performance of GU188, a series of field trials were carried out from 2006 to 2008 in different areas of China which included Guizhou, Henan, Shandong andYunnan. All the field tests were approved by the pesticide administrative department of Ministry of Agriculture of China. Five field trials against TMV in tobacco and ToMV in tomato plant for registration were carried out in 2007. Six field trials against TMV and ToMV and CMV in tobacco, tomato and cucumber were carried out in 2008. The results demonstrated that the field efficacy of GU188 is better than or close to the commercial antiviral product agents Ningnanmycin and 20% Virus A WP.

5.2.3.2   Materials and methods

The materials and reagents used in field trials are as follows: 30% GU188 WP, 2% Ningnanmycin aqua, 20% Virus A WP. Among these experimental materials, 2% Ningnanmycin aqua and 20% Virus A WP were purchased from the market, the tested crops were tobacco, tomato and cucumber.

The method for evaluating anti-TMV bioassay in the lab is similar to the procedure described in Chapter 1.1.2.

The method for evaluating anti-TMV field efficacy of 30% GU188 WP is similar to the procedure described in Chapter 5.1.5.

5.2.3.3   Results and Discussion

GU188 has curative and protection activity for the bioassay indoors. The regression equation of GU188 for curative activity is $Y=-2.034X+6.7$. The EC_{50} of curative was determined as 29.45 μg/mL. The regression equation of Ningnamycin is $Y=2.4425+1.4724X$. The EC_{50} of curative was determined as 54.56 μg/mL, the curative activity of GU188 is better than the commercial standard Ningnamycin. The EC_{50} values of GU188 and Ningnamycin for protection activity against TMV were determined as 245.10 μg/mL and 239.0 μg/mL respectively which showed that the protection activity was close to the commercial standards. In 2006, the field trial of 30% GU188 WP was carried out in Guizhou, and the results are shown in Table 5.54. The test results show that the activity of GU188 against TMV at dosage of 100 g (a.i.) /ha was better than or close to 2% Ningnamycin at dosage of 90 g (a.i.) /ha, and much better than 20% virus A (WP).

Table 5.54 The results of field trial of GU188 in 2006

Place	30％GU188 WP[g (a.i.) /ha]			2% Ningnamycin[g (a.i.) /ha]	20% virus.A (WP) [g (a.i.) /ha]
	100	300	500	90	600
Guizhou	65.29	71.90	75.62	60.33	43.39

The five field trials for registration were conducted in 2007 and the results of 30% GU188 WP in 2007 are provided in Table 5.55. The test results show that the activity of GU188 against TMV at dosage of 100 a.i.g/ha was better than or close to 2% Ningnamycin at dosage of 90 g (a.i.) /ha (Guizhou, Henan and Yunnan). The activity of GU188 against ToMV in Tomato at dosage of 300, 500 g (a.i.) /ha was better than 2% Ningnamycin at dosage of 90 g (a.i.) /ha (Shandong and Henan), and close to 2% Ningnamycin at dosage of 100 g (a.i.) /ha.

Table 5.55 The results of field trial of GU188 in 2007   %

Place	Plant	Virus	Inhibition rate [g (a.i.) /ha]			Ningnamycin (300 mL/ha)
			100	300	500	
Guizhou	Tobacco	TMV	51.62	52.98	54.34	49.85
Henan	Tobacco	TMV	57.06	61.63	61.49	56.02
Yunnan	Tobacco	TMV	51.01	60.34	79.51	79.06
Shandong	Tomato	ToMV	42.27	51.04	58.68	45.78
Henan	Tomato	ToMV	49.01	52.31	59.14	46.92

The six field trials for registration were carried out in 2008 and the results of 30% GU188 WP in 2007 are given in Table 5.56. The test results show that the activity of GU188 against TMV at dosage of 300, 500 g (a.i.) /ha was better than or close to 2% Ningnamycin at dosage of 90 g (a.i.) /ha (Guizhou, Shandong, Henan and Yunnan). The activity of GU188 against CMV in Cucumber at dosage of 300, 500 g (a.i.) /ha was better than or close to 2% Ningnamycin at dosage of 90 g (a.i.) /ha (Shandong and Henan).

Table 5.56 The results of field trial of GU188 in 2008   %

Place	Plant	Virus	Inhibition rate [g (a.i.) /ha]			Ningnamycin (300 mL/ha)
			100	300	500	
Guizhou	Tobacco	TMV	45.37	52.90	54.53	48.51
Henan	Tobacco	TMV	34.33	51.64	56.65	54.27
Yunnan	Tobacco	TMV	16.84	59.02	74.25	59.12
Henan	Cucumber	CMV	32.51	47.80	58.00	52.11
Shandong	Tobacco	TMV	45.37	52.90	54.53	49.38
Shandong	Cucumber	CMV	25.75	46.13	53.64	51.31

5.2.3.4 Conclusions

The field trials demonstrated that the control effect of 30% GU188 WP in the

field was better than or close to the other commercial anti-plant viral product Ningnanmycin and obviously better than Virus A. Thus the prospect of GU188 as a new anti-plant viral agent is great and the future for its application is bright. The suggested dosages of 30% GU188 WP are 300-500 g (a.i.) /ha.

5.2.4   Toxicological Test

5.2.4.1   Introduction

According to the requirements of pesticide registration in China, in the context of health toxicity, new chemical entity needs to undergo toxicological evaluation. GU188 was tested for some necessary test items that are required for its temporary registration. All the tests were carried out by the toxicology test institute certified by the Ministry of Health, and the Ministry of Agriculture. The test results show that GU188 has lower acute toxicity and subchronical toxicological effects. The results of Ames test, microsome test and chromosome test were found negative.

5.2.4.2   Methods

The methods used in this part are the same as described in Chapter 5.1.4.

5.2.4.3   Results and discussion

According to the registration requirements for new pesticide, the health toxicity of GU188 as well as its 30% GU188 WP formulation was tested and the test results are shown in Table 5.57.

Table 5.57   Toxicological tests and results of GU188

Entry	Item	Result	Testing agency
1	Acute toxicity test	Acute Oral Toxicity, LD_{50}>5000 mg/kg w, low-toxic substance	Chinese Center for disease control and prevention
		Acute Skin Toxicity, LD_{50}>2000 mg/kg w, low-toxic substance	Chinese Center for disease control and prevention
2	Ames	Negative	Safty evaluation Center, Shenyang research institute of Chemical Industry.
3	Chromosome aberration of spermatocytes in mice test	Negative	Center for Chemical Toxicity Identification &Testing, Guiyang Medical University
4	Micronucleus tests of	Negative	Center for Chemical Toxicity Identification &Testing, Guiyang Medical University

It can be seen from Table 5.57 and Fig 5.48 that the acute oral LD_{50} value of GU188 in rat was more than 5000 mg/kg, the LD_{50} of skin toxicity on mice was more than 2000 mg/kg ($LD_{50} > 2000$ mg/kg). The test results of three kinds of mutagenic experiments were all negative. The subchronic acute oral toxicity test needs to be carried out. The pesticide has low toxicity and is safe to human being.

The result of acute oral toxicity and acute dermal toxicity test of GU188 are low,Ames test is Negative, chromosome aberration test of mouse spermatocyte and The mouse bone marrow polychromatic erythrocyte micronucleus test are negative.
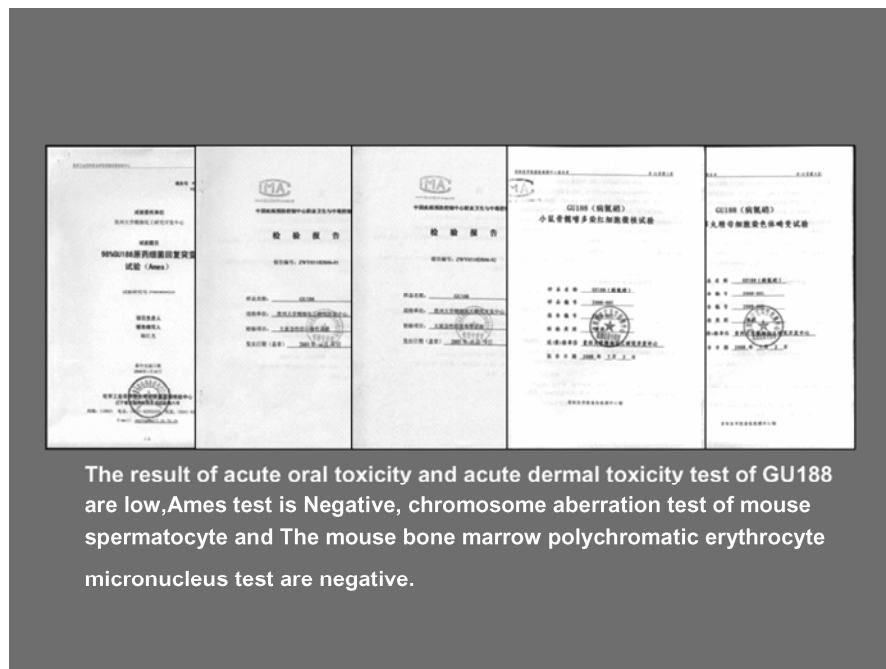
Fig 5.48   The test reports of oral toxicity, Ames, chromome aberration and erythrocyte micronucleus of GU188

5.2.4.4   Conclusions

All the health toxicity tests revealed that GU188 is a kind of low toxic chemical and is safe to mammals and human being. Efforts are currently underway for its industrialization.

5.2.5   Action Mechanism

5.2.5.1   Introduction

As mentioned before, GU188 is a new candidate anti-plant viral agent which was discovered by Center for R & D Fine Chemicals of Guizhou University. GU188 has good antiviral activities against the plant virus diseases caused by

TMV and CMV. Lab bioassay and field trial demonstrated that GU188 was associated with desirable anti-TMV activities. However, the mechanistic pathway through which GU188 acts to inhibit TMV is still uncertain. Thus, it is extremely necessary to figure out the action mode of GU188, which in turn may help researchers to understand the antiviral function process and lead to the quick discovery of new antiviral agents.

Extensive research was hereby conducted to elucidate the mechanism of action of GU188, especially on the gene level by activating the immune system of the plant.

5.2.5.2   Materials and Methods

The materials and methods used for the investigation of the mode of action of GU188 are basically similar to the procedure described in Chapter 5.1.8.

5.2.5.3   Results and Discussion

In order to study anti-TMV mechanism of GU188, based on the Arabidopsis genome oligonucleotide chip, gene expression of three kinds of treated tobacco leaves was detected. The results indicated that 260 effective gene expressions were valid when (A) leaves were inoculated only with TMV; 180 genes were found upregulated and 80 genes downregulated. When treated with TMV and GU188 (B), 175 effective gene expressions changed (55 upregulated and 120 downregulated). When treated only with GU188 (C), 83 effective gene expressions changed among which 10 were upregulated and 73 downregulated (Table 5.58, Table 5.59 and Table 5.60).

Table 5.58   96-time 13-week average of AT1G 39930 gene in chip A

Cy5	Cy3	Ratio	Cy5	Cy3	Ratio
30278.76693	47736.06673	0.513628	31101.37067	48130.39937	0.6367461
39198.92674	52460.78586	0.6146399	36979.9976	52516.54191	0.6506965
39308.82272	52528.66279	0.6068741	33695.23905	52518.15802	0.5957269
30394.31933	39190.0381	0.6516523	52855.92655	52550.48037	0.9625189
43786.27589	52500.38073	0.6947541	39969.81473	52559.36902	0.736265
26578.66622	32715.06386	0.7229728	40415.05506	51159.81138	0.6021146
30728.04756	40482.12393	0.6821738	37091.5097	52566.64155	0.5385817
28612.54993	35818.00921	0.7366562	40002.13707	50709.72269	0.7448848
34318.25229	52330.68841	0.5815459	26352.40979	45018.56538	0.5504302
31943.36782	44604.83934	0.6382952	30843.59995	44899.78076	0.7486747
46515.89812	52036.55505	0.7411681	30486.43802	49707.72992	0.6706177
37707.25041	48919.87271	0.6520053	41396.84636	52622.39759	0.7020055
41860.67205	48718.66609	0.7809731	35041.46482	52013.92941	0.6015516

Cy5	Cy3	Ratio	Cy5	Cy3	Ratio
25889.39216	33623.32183	0.7462052	33739.68228	46544.98823	0.6358695
26972.1908	36734.34776	0.5791112	32814.45508	46683.16627	0.6157973
30359.5728	39284.58096	0.6055347	44784.22836	52560.98513	0.8603409
34706.12046	50326.70287	0.5907874	29173.34265	40121.72976	0.742817
34943.68971	46433.47614	0.6454128	42252.58051	51248.69783	0.7747938
46269.44022	52537.55143	0.6840688	36064.46711	51853.93379	0.6500209
40423.94371	47700.51215	0.6656246	41161.70128	52563.40931	0.7045613
36638.18877	48199.89242	0.6684841	38982.36702	52512.50161	0.6664578
33002.73276	44885.2357	0.6552498	41191.59946	51028.90587	0.6845348
40107.1847	47495.26525	0.7459059	35007.52635	46256.51128	0.6494596
39400.13335	49498.44272	0.701996	44212.93087	51226.07219	0.6932477
38109.66364	52536.74337	0.6378311	34043.51234	47809.60007	0.575104
29829.48631	44802.00565	0.59522	43128.51612	52493.91626	0.8151255
31351.06081	47772.42938	0.533034	32272.24771	51465.25756	0.6333435
30419.36914	44372.92649	0.5624405	52876.93608	52519.77414	0.8866173
37544.83062	52560.98513	0.7328477	35509.33079	52607.04448	0.5958056
34149.36803	45288.45698	0.7797483	30367.65339	39514.87769	0.7256831
38670.45636	52563.40931	0.7658283	26240.08963	40595.25215	0.6135654
37186.05256	52222.40855	0.7452792	45454.91707	52546.44008	0.8039292
35287.11465	52539.97561	0.5368041	33802.71085	49895.19954	0.617628
28627.09498	44334.13968	0.5262923	41742.69548	52568.25766	0.6893752
36261.63343	52567.4496	0.6581618	36165.47444	52551.28843	0.6031812
35407.5154	48802.7042	0.6924612	48474.63237	52615.93312	0.8152926
35717.80993	49793.38414	0.6954444	38335.11201	52619.97342	0.67279
32867.78696	46110.25266	0.6960129	47905.75906	52586.84301	0.7445756
37883.40721	52453.51333	0.6336707	34132.3988	39047.01171	0.7429185
22198.1801	39644.16708	0.5291089	46213.68417	52600.58001	0.7944547
34477.43985	52501.99685	0.6121789	36417.58875	52523.81444	0.6227436
34918.6399	51166.27585	0.6369514	49087.14085	52563.40931	0.7711515
32024.17369	49563.89548	0.5431535	35715.38576	52557.7529	0.5749908
36204.26126	51331.92788	0.5873548	52668.45694	52612.70089	0.8331331
34277.84936	49300.46835	0.6875985	40986.35255	52535.12726	0.6849093
45265.02328	52639.36683	0.9430728	42238.84351	52585.22689	0.6917122
38351.27318	52501.99685	0.8004082	46376.10397	52586.84301	0.7438681
44172.52794	52577.14631	0.7570076	34874.19667	52507.65326	0.616925

Table 5.59   Analysis of the repeatabilty of AT1G29930 gene treatment

Treatments	Average	Standard deviation (σ)	Variance (CV)
A	0.5192	0.1110	0.2138
B	0.6779	0.0901	0.1329
C	0.4124	0.0556	0.1348
Mean	0.5365	0.0856	0.1605

Table 5.60   Statistics of three different simultaneous expressing gene

Items	A/B	A/C	B/C	Items	A/B	A/C	B/C
U2U2	2	4	5	U2D2	92	60	1
D2D2	1	2	64	SUM	123	69	70
D2U2	28	3	0				

Table 5.61   The statistics of differential expression gene among three treatments

Items	A	B	C	Items	A	B	C
U2	178	54	10	SUM	260	175	84
D2	82	121	74				

It can be inferred that most valid genes are upregulated genes in the treatment of TMV, which, after application of GU188, turn to downregulated genes. Inversely, most of the downregulated genes induced by TMV turn to the upregulated ones upon GU188 treatment. Similar tendency was revealed in the group treated only with GU188, but effective gene expressions were less than in treatment B group (TMV+GU188). All these data indicated that GU188 can totally or partially offset abnormal expression of the host induced by TMV, thereby leading to the conclusion that GU188 has much better curative efficiency than protection through activation of tobacco immune system.

The main mechanism of GU188 seems to correct or supress upregulated gene expressions (RNA synthesis related gene) caused by TMV, thereby inhibiting the reproduction of TMV (TMV can copy itself by making use of RNA) which is the key for GU188 to increase host resistance. TMV infection can upregulate the expression of the host cell protein, RNA synthesis and protein synthesis related gene expression and ubiquitin system. TMV interfered with the expression of hormone-related genes in the host. Prominent action was that the gene related to the synthesis of ethylene was upregulated while gibberellin related genes were downregulated, the photosynthesis related genes were downregulated and cell wall and cytoskeleton related genes were downregulated. The expressions of genes, such as heat shock proteins, reactive oxygen, were downregulated.

So we can conclude that the TMV caused signal transduction in plants should mainly be based on Calcineurin pathway as great differential gene expression was related to Calcineurin pathway. In addition, chip also detects the expression of DNA demethylation gene, miRNA gene, and the histone deacetylation gene, which maybe present in various levels to achieve the regulation of gene expression for the host. TMV may regulate the related gene in multiple levels (Fig 5.49-Fig 5.52).
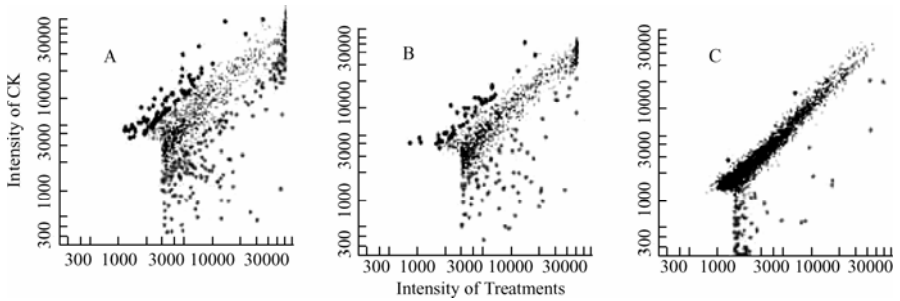
Fig 5.49   Scatter diagram of gene with effective expression (A) treatment of TMV (B) treatment of TMV and Dufulin, (C) treatment of Dufulin
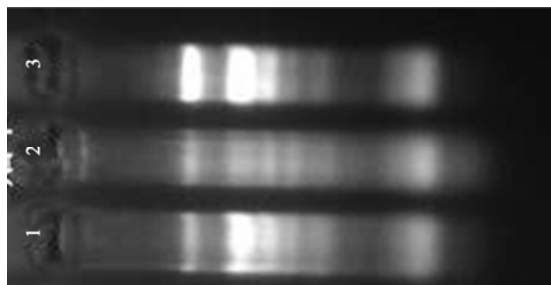
Fig 5.50   Electrophoresis of RNA denatured with formaldehyde
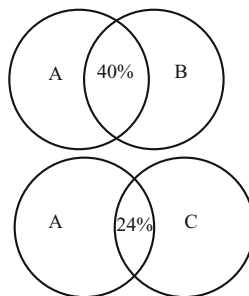
Fig 5.51   Differential expression of same gene in different treatment (A ＆ B; A ＆ C).
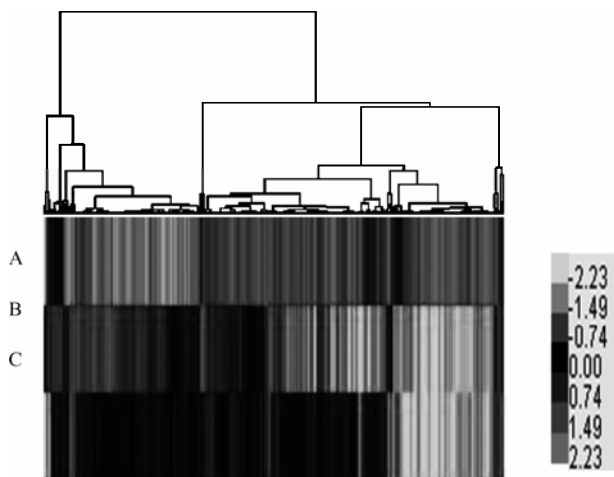
Fig 5.52   Cluster analysis among three treatments

5.2.5.4   Conclusions

GU188 can upregulate the tobacco genes which are downregulated upon infection with TMV, for upregulated genes treated with TMV, GU188 can downregulate them. The main mechanism of GU188 is to correct or suppress upregulated gene expressions (RNA synthesis related gene) caused by TMV, thus inhibiting the reproduction of TMV (TMV can copy itself by making use of RNA) which is the key for GU188 to increase host resistance. Thus, GU188 exerts its antiviral bioactivity by activating the immune system of the plant as a whole.

5.3   Studies on the Development of Novel Amino-oligosaccharide

5.3.1   Introduction

Oligosaccharins, a kind of agricultural chitooligosaccharides, obtained from deacetylation of chitin degradation by the enzyme prepared from glucosamine, are associated with a wide range of biological activities that include plant disease resistance, resilience, antifungal & antiviral. In this context, Jingtuling (5% amino-oligosaccharin aqueous solution) was developed to achieve efficient control over plant viral diseases.

In Beibu Gulf of South China Sea there exists a special bacteria BH#1 (*Bacillus* sp.) which can remove highly viscous amidocyanogen glycan restraint. BH#1 (*Bacillus* sp.) can be obtained by screening from the large amount of bacterium selected on the beach by following and adopting mutation screening of

modern biological technology. BH#1 (*Bacillus* sp.) has the following characteristics: 1) Highly active bacterial strain has fine transmissibility and shape that still keep high enzyme production ability with PDA culture medium passage for 5 years; 2) Easy to preserve, *e.g.*simple hermetic sealing can preserve for half a year without any loss of its working ability and still maintaining good enzyme production ability at room temperature 15-40℃; 3) Short enzyme-producing fermentation time. Generally, chitosan degradation enzyme can be prepared by cultivating at room temperature for 30 hours. The enzyme activity of unit fermentation liquid of this series of highly active degradation enzyme is 400 times larger than that by common degradation enzymes;4) Enzymolysis condition is generally mild and reaction conditions are easily obtained to gain different molecular weight range of target shell glycan.

In this process, a specific technology was adopted to overcome a key problem of bacteria inhibition by the chitosan of high viscosity. In this way, degradation bacteria vigorously grew and helped crude enzyme preparation that could be directly used in the enzymatic hydrolysis of chitosan. The technical process is highly efficient and cheap with a conversion rate of 99% and 99% yield of amino-oligosaccharin. The production cycle of enzyme normally takes 4-9 h (100 mL of crude enzyme is prepared for the hydrolysis of 1000 mL chitosan) and the oligosaccharins obtained are mainly composed of disaccharides instead of three to five polysaccharides.

5.3.2   Anti-TMV and Mechanism of Action

5.3.2.1   Anti-TMV bioassay

For determining the protective, curative, and inactive activities against TMV, extraction of enzyme and determination of enzyme activity for ascertaining mechanism, please refer to the description in previous chapters (5.1.8).

5.3.2.2   Mechanistic study

The indoor inhibitory effects of 0.5% aqua of amino-oligosaccharin against TMV and the defense related enzyme were attained.

As can be seen in Table 5.62 that 0.5% amino-oligosaccharin aqua exhibited low inactivation activity at the dosage of 6.25 μg/mL against TMV *in vivo* and the inhibition rate was only 11.8%. The *in vivo* inhibition rates based on the half leaf method for the curative and protective effects of 0.5% amino-oligosaccharin aqua were 43.6% and 58.5% respectively, which are comparable with the curative and protective effect of 2% Ningnanmycin aqua (500 μg/mL). Table 5.63 also showed that the protective effect of 0.5% amino-oligosaccharin aqua was better than its curative effect.

Table 5.62   The curative, protective and incurative effect of 0.5% amino-oligosaccharin aqua against TMV in tobacco *in vivo* (determination by half leaf method)

Medicaments	Inhibition (%)		
	C.E	P.E	I.E
0.5% amino Oligosaccharin aqua (6.25 µg/mL)	43.6	58.5	11.8
2% Ningnanmycin aqua (500 µg/mL)	48.7	60.0	89.1

Table 5.63   The protective effect of 0.5% amino Oligosaccharin aqua against TMV in tobacco *in vivo* (determination by whole leaf method)

Medicaments	Inhibition (%) (P.E)
0.5% amino Oligosaccharin aqua (6.25 µg/mL)	58.54
2% Ningnanmycin aqua (500 µg/mL)	71.21

5.3.2.3   Effects of 0.5% amino-oligosaccharin aqua on tobacco defense enzyme

As shown in Fig 5.53, the tobacco plants treated with Jingtuling exhibited higher PAL activity than with the control pure water treatment. PAL activity starts at a high level after 1 d treatment, and then kept declining until 7 d after treatment, but still maintaining higher value than the control. PAL activity treated by 2% Ningnanmycin aqua reached the highest value on the 3rd day, and then started to decline. The results indicate that tobacco plant pretreated with Jingtuling has higher PAL activity that helps it to develop greater defense, more resistance and is less susceptible to TMV infection.
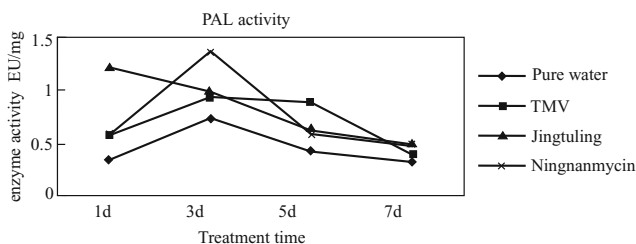
Fig 5.53   PAL activity changes of tobacco induced by 0.5% amino-oligosaccharin aqua

It can be seen from Fig 5.54 that POD activity of tobacco plant treated with Jingtuling began to rise gently in the first 5 days and then increased sharply to the highest level 7 d after treatment. On the other hand,for 2% Ningnanmycin aqua treatment, the POD activity of tobacco plant attained the highest value on the 5th day and then declined. POD activity of tobacco induced by Jingtuling was much higher than that of the commercial antiviral product Ningnanmycin.

As seen from Fig 5.55, SOD activity of Jingtuling treatment started at a higher value than the others on the first day, subsequently declined, and then increased again on the third day until finally the SOD activity was shown to attain a value appreciably higher than all the other treatments on the 7th day. The water
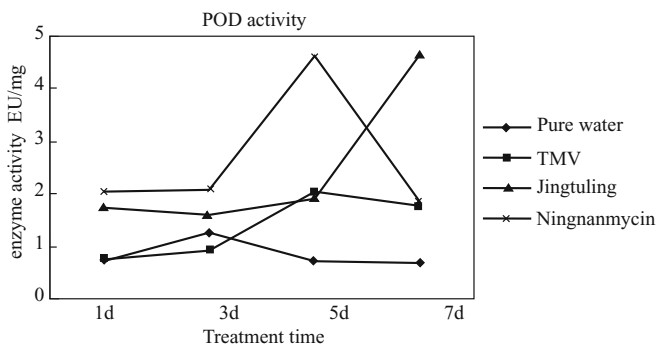
Fig 5.54   POD activity changes of tobacco induced by Jingtuling
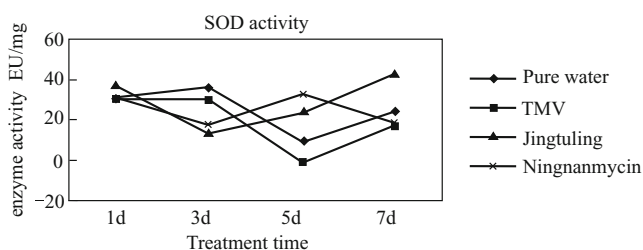
Fig 5.55   SOD activity changes of tobacco induced by 0.5% amino oligosaccharin aqua

treatment reached the highest value on the third day, and then followed a decline and increasing trend that matched with that treated by TMV.

In conclusion, the studies on anti-TMV activity of Jintuling, including protection, inactivation and curative effects, were conducted. The inhibitory effects obtained were 58.5%, 11.8%, and 43.65%, respectively. The mechanism of observed plant induced resistance by Jintuling could possibly be accounted by its binding to the receptor on plasma membrane. Oligosaccharides could increase activity of resistance related enzymes such as PAL, POD and SOD. It indicated that Jingtuling can act as an activator on the immune system of tobacco by inducing resistance of tobacco against TMV and thus improving the tobacco immune system.

5.3.3   Industrialization

As amino Oligosaccharins are water-soluble materials, we developed 0.5% aqua oligosaccharin (Jingtuling), amino-oligosaccharin aqua (1:8000) for our work. Based on a small trial, a pilot-plant equipped with 0.6-5 ton fermentor was established from which 15-60 tons 0.5% oligosaccharins aqua product

could be obtained with each batch of 36-42 production cycles. A construction with annual production capacity of 90 tons of Jingtulin raw powder and 5, 000 tons aqua was also set up. This unit is the first and the largest in terms of production. This pilot plant can also be used for refining crustacean enzyme preparation (Fig 5.56).
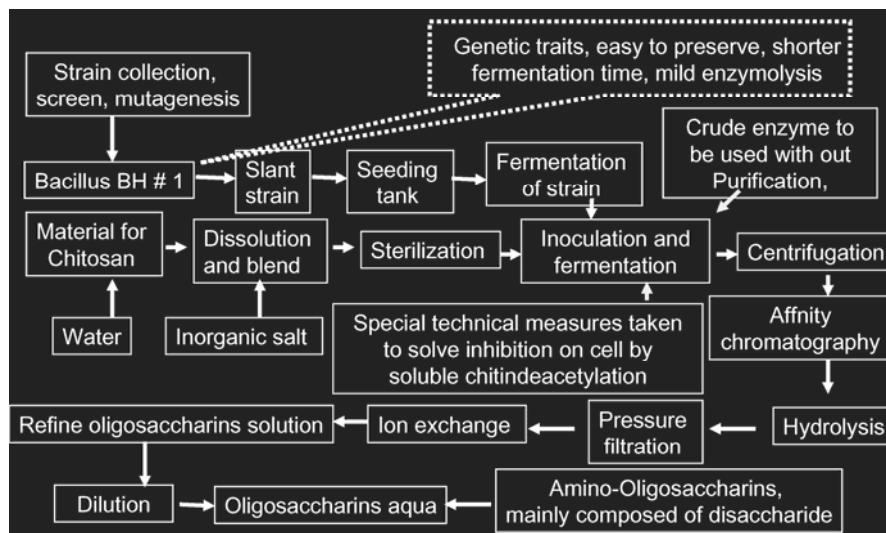
Fig 5.56   Production flow chart of biopesticide oligosaccharin (Jingtuling)

In the production of the water aqua of oligosaccharin, the key is to gain high activity and high degradation strain, adaptable to the source of different raw materials. The production is characterized by the use of deep fermentation technology. The prepared highly active oligosaccharide can maintain stable performance and possesses stable biological activities despite the source and origin of raw materials. The key of this technology is the strain fermentation, enzymatic reaction control and separation of active fragment preparation. Besides, high viscosity and solubility of chitosan can inhibit the growth of thallus. Generally, separation and purification of enzyme are required before executing enzymatic hydrolysis of chitosan.

Production and quality of 0.5% amino oligosaccharins biopesticide fulfill the product quality standards laid down by the enterprise Q/GFNY 002-2000. The product has obtained pesticide registration approved by the Ministry of Agriculture (LS 20021143, Fig 5.57) and received several awards including "new scientific research of Ministry of Agriculture", "the new technology products, the Guangxi Zhuang Autonomous Region" and other honors, and was recommended for the inclusion in "National Torch Technology Projects".

Fig 5.57   Production of biopesticide oligosaccharin (Jingtuling)

Index